

UNCLASSIFIED

AD NUMBER
AD911537
NEW LIMITATION CHANGE
TO Approved for public release, distribution unlimited
FROM Distribution: Further dissemination only as directed by Commander, Naval Air Systems Command, Attn: AIR-320, Department of the Navy, Washington, DC, 31 Jan 1973, or higher DoD authority.
AUTHORITY
USNASC Ltr, 8 Apr 1974

THIS PAGE IS UNCLASSIFIED

UNCLASSIFIED



HC144R1070

AD 911537

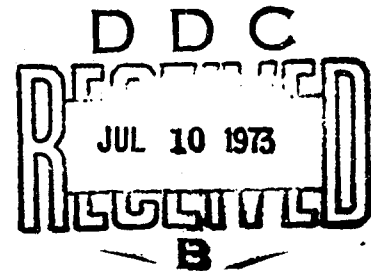
MODEL WIND TUNNEL TESTS OF A REVERSE VELOCITY ROTOR SYSTEM

FINAL REPORT
BY

J. R. Ewans
and
T. A. Krauss

Prepared for Naval Air Systems Command
Under Contract No. N00019-71-C-0506

BY



FAIRCHILD

Fairchild Republic Division Farmingdale, New York 11735

DISTRIBUTION LIMITED TO U. S. GOVERNMENT AGENCIES ONLY

TEST & EVALUATION

DATE: January 31, 1973

Other requests for this document must be referred to
Commander, Naval Air Systems Command, AIR-320,
Department of the Navy, Washington, D. C.

UNCLASSIFIED

UNCLASSIFIED



HC144R1070

MODEL WIND TUNNEL TESTS OF A
REVERSE VELOCITY ROTOR SYSTEM

FINAL REPORT

BY

J. R. Ewans
and
T. A. Krauss

Prepared for Naval Air Systems Command
Under Contract No. N00019-71-C-0506

BY

FAIRCHILD

Fairchild Republic Division Farmingdale, New York 11735,

DISTRIBUTION LIMITED TO U. S. GOVERNMENT AGENCIES ONLY
TEST & EVALUATION

DATE: JANUARY 31, 1973

Other requests for this document must be referred to
Commander, Naval Air Systems Command, AIR-320,
Department of the Navy, Washington, D. C.

UNCLASSIFIED

FAIRCHILD
REPUBLIC DIVISION

HC144R1070

The authors wish to acknowledge the work performed by staff at other organizations, namely, Naval Air Systems Command, National Aeronautics and Space Administration (Ames Research Center and Langley Research Center), Arnold Research Organization, and by their colleagues at Fairchild Republic.

HC144R1070

TABLE OF CONTENTS

<u>Section</u>		<u>Page</u>
	Summary	
1.	Introduction	1
1.1	The Reverse Velocity Rotor Concept	1
1.2	Previous Work	1
1.3	Purpose of Test	2
1.4	Description of Model and Test Rig	2
1.5	Test Procedures	7
1.6	Test Conditions	8
1.7	Scheduled Lift Coefficient	9
2.	Results - Performance	10
2.1	Aerodynamic Tares	10
2.2	Tabulated and Plotted Results	10
2.3	Rotor Lift	10
2.4	Rotor Lift-Drag Ratio	11
2.5	Rotor Torque	12
2.6	Accuracy	13
3.	Results - Rotor Control	14
3.1	Control Angle	14
3.2	Collective Control Power	14
3.3	Rotor Sensitivity	14
3.4	Control Phasing	15
3.5	Rotor Flapping	16
4.	Results - Rotor Blade Dynamics	17
4.1	Rotor Blade Resonances	17
4.2	Vibratory Flapwise Bending Stresses	18
5.	Theoretical Prediction of Rotor Performance and Comparison with Test Results	20
5.1	Airfoil Section Data	20
5.2	Performance Prediction	21
5.3	Comparison of Measured and Predicted Results	21
5.4	Effect of Reynolds Number on Rotor Performance	22

HC144R1070

TABLE OF CONTENTS (Cont'd)

<u>Section</u>		<u>Page</u>
5.5	Full Scale Rotor Performance	22
5.6	Comparison with Previous Performance Prediction	23
6.0	Conclusions and Recommendations	25
	References	27
	Tables	28
	Figures	33
 <u>Appendices</u>		
A	Airfoil Section Development	135
B	Rotor Test Results	143
C	Airfoil Tests	169
D	Airfoil Section Data	229

HC144R1070

SUMMARY

Contract No. N00019-71-C-0506 was awarded in July 1971 to Republic Aviation Division of Fairchild Hiller Corporation to cover the design, manufacture and test of a one-seventh scale reverse velocity rotor system with the goal of substantiating the results that had been predicted for this system in previous analytical studies. Additionally, two-dimensional wind tunnel tests were made on three airfoil sections of the model rotor blade to give data for comparison of the measured performance with that predicted.

The 8 ft diameter 4 bladed model rotor was provided with remote operation of the controls and shaft angle. The hydraulic drive system permitted both normal powered operation and braking of the rotor. Tests were conducted in the 12 ft pressure wind tunnel at NASA Ames during June and July 1972. The tests did not cover the whole range of conditions desired, but results were obtained at advance ratios from 0.3 to 2.46 and at tunnel speeds up to 350 knots.

Significant results of the tests were the freedom of the rotor from instability, and the ability to trim the rotor laterally and longitudinally under all conditions.

After allowance had been made for the effect of Reynolds number, the performance of the model rotor was found to be similar to that predicted in the previous analytical studies and to further predictions based on the two-dimensional model airfoil tests. The rotor response to control angle was greater than predicted at high advance ratios; however, the effective lift/drag ratios were generally in good agreement.

It is recommended that further tests be performed with this model to expand the envelope of test conditions, particularly to include testing with two-per-rev control angle input.

HC144R1070

LIST OF TABLES

		<u>Page</u>
1-I	Rotor Characteristics	28
2-I	Measured Effective Lift/Drag Ratios	29
2-II	Test Conditions for Zero Torque and 1g Lift Coefficient	30
5-I	Comparison of Rotor Characteristics - Phase I Study vs. Phase II Model	31
A-I	Airfoil Section Development - Input Parameters	138
A-II	Ordinates of Root Airfoil Section	139
A-III	Ordinates of Tip Airfoil Section	141
B	Tabulated Results of Rotor Tests	146
C-I	Location of Orifices in 18-inch Chord Airfoil Sections	170
C-II	Schedule of Airfoil Section Pressure Plotting Tests Made in Langley L. T. P. T.	171

HC144R1070

LIST OF FIGURES

	<u>Page</u>
1.1 Installation of Reverse Velocity Rotor Test Rig in NASA Ames 12 ft Pressure Tunnel	33
1.2 Three-Quarter Rear View of Reverse Velocity Rotor Test Rig (Fairing Removed)	34
1.3 Geometric Layout of Model	35
1.4 Model Rotor Airfoil Sections	36
1.5 Section Properties - 1/7 Scale Model RVR Rotor Blade	37
1.6 Section Properties - Scale Model RVR Rotor Blade (Cont'd)	38
1.7 Section Properties - Scale Model RVR Rotor Blade (Concluded)	39
1.8 Predicted and Measured Flapwise Stiffness - 1/7 Scale Model RVR Rotor Blade	40
1.9 Predicted and Measured Torsional Stiffness - 1/7 Scale Model RVR Rotor Blade	41
1.10 Natural Frequency Spectrum - 1/7 Scale Model RVR Rotor Blade	42
1.11 Control System	43
1.12 Control System Dimensions	44
1.13 Operating Envelope and Test Conditions - Reduced Pressure	45
1.14 Operating Envelope and Test Conditions - Atmospheric Pressure	46
1.15 Scheduled Rotor Lift Coefficient for 1g Level Flight	47
2.1 Hub Tare Corrections to Lift and Drag	48
2.2 Hub Tare Corrections to Lift	49
2.3 Hub Tare Corrections to Balance Pitching Moment Coefficient	50
2.4 Measured Rotor Performance - $\mu = .46$, runs 29 & 30	52
2.5 $\mu = .64$, runs 31 & 32	54
2.6 $\mu = .87$, runs 35 & 36	56
2.7 $\mu = .98$, run 41	58
2.8 $\mu = 1.15$, run 42	60
2.9 $\mu = 1.15$, run 45	62
2.10 $\mu = 1.40$, run 43	64
2.11 $\mu = 1.40$, run 46	66
2.12 $\mu = 1.66$, run 47	68

HC144R1070

LIST OF FIGURES (Cont'd)

	<u>Page</u>
2.13 Measured Rotor Performance - $\mu = 1.75$, run 44	70
2.14 $\mu = 2.16$, run 48	72
2.15 $\mu = 2.47$, run 49	74
2.16 $\mu = .29$, run 50	76
2.17 $\mu = .46$, run 51	78
2.18 $\mu = .57$, run 52	80
2.19 $\mu = .72$, run 57	82
2.20 $\mu = .82$, run 56	84
2.21 $\mu = .94$, run 55	86
2.22 $\mu = 1.00$, run 59	88
2.23 $\mu = 1.15$, run 54	90
2.24 $\mu = 1.50$, run 53	92
2.25 Rotor Lift Coefficient Ratio vs Advance Ratio	94
2.26 Rotor Lift Coefficient Ratio vs Advance Ratio	95
2.27 Maximum Effective Lift - Drag Ratio Achieved vs Advance Ratio	96
2.28 Effective Lift - Drag Ratio at 8 lb per sq ft Disc Loading	97
2.29 Effective Lift - Drag Ratio vs Rotor Lift Coefficient	98
2.30 Tip Path Plane Angle for Level Flight and Zero Torque vs Advance Ratio	99
3.1 Rotor Control - $\mu = .29$, run 50	100
3.2 $\mu = .46$, run 51	101
3.3 $\mu = .72$, run 57	102
3.4 $\mu = .94$, run 55	103
3.5 $\mu = 1.15$, run 54	104
3.6 $\mu = 1.45$, run 60	105
3.7 $\mu = 1.50$, run 53	106
3.8 $\mu = 1.40$, run 46	107
3.9 Collective Control Power at 5 Deg Tip Path Plane	108
3.10 Rotor Tip Path Plane Derivative with Respect to Control Axis Angle at Constant Rolling Moment	109

HR144R1070

LIST OF FIGURES (Cont'd)

	<u>Page</u>
3.11 Theoretical Phase Angle of Flapping Response to One-Per-Rev Cyclic Input in Hover	110
3.12 Rotor Flapping	111
4.1 Typical Traces of Flapwise Vibratory Moments Near Resonances - Outboard Station ~ .71R	112
4.2 Measured Vibratory Flapwise Bending Moments at Critical Stations	114
4.3 Typical Theoretical Spanwise Distributions of Vibratory Flapwise Bending Moment	115
4.4 Measured Vibratory Flapwise Bending Moments at Scheduled Flight Conditions	116
Comparison of Measured and Predicted Rotor Performance	
5.1 $\mu = .29$	117
5.2 $\mu = .29$	119
5.3 $\mu = .46$	120
5.4 $\mu = .57$	121
5.5 $\mu = .72$	122
5.6 $\mu = .82$	123
5.7 $\mu = .94$	124
5.8 $\mu = 1.15$	125
5.9 $\mu = 1.50$	126
5.10 $\mu = 1.66$	127
5.11 $\mu = 2.16$	128
5.12 $\mu = 2.47$	129
5.13 Comparison of Predicted and Measured Maximum Effective Lift/Drag Ratio	130
5.14 Effect of Reynolds Number on Predicted Maximum Effective Lift/Drag Ratio	131
5.15 Full Scale Maximum Effective Lift/Drag Ratio	132
5.16 Comparison of Full Scale Rotor Performance with Prediction of Phase I	133
5.17 Effect of Change of Delta-3 Lock Number and Altitude on Performance of Phase I Rotor	134

HC144R1070

LIST OF SYMBOLS

a	Linear lift curve slope
b	Number of blades
c	Rotor blade chord, inches
c_b, c_d, c_m	Airfoil section camber
C_d	Airfoil section drag coefficient
C_l	Airfoil section lift coefficient
C_m	Airfoil section moment coefficient
C_D or C_{D_R}	Rotor drag coefficient = $D/\pi \rho R^4 \Omega^2$
C_H	Rotor H - force coefficient = $H/\pi \rho R^4 \Omega^2$
C_L or C_{L_R}	Rotor lift coefficient = $L/\pi \rho R^4 \Omega^2$
C_M	Moment coefficient
C_Q	Rotor torque coefficient = $Q/\pi \rho R^5 \Omega^2$
C_T	Rotor thrust coefficient = $T/\pi \rho R^4 \Omega^2$
C_X	Coefficient of X force
C_Z	Coefficient of Z force
D	Rotor drag force in flight coordinate system, positive aft, lbs
D_E	Equivalent drag force of rotor, lbs
e_β	Spanwise offset of flapping hinge from centerline of rotation, feet
g	Acceleration due to gravity, ft/sec ²
H	Longitudinal component of rotor resultant force in shaft axis system, positive aft, lb
I_β	Blade mass moment of inertia about flap hinge, slug-ft ²
K_β	Angular spring rate about flapping hinge, in-lb/rad.
K_θ	Angular spring rate about blade pitch axis, in-lb/rad.

HC144R1070

L	Rotor lift, flight coordinate axis, lbs
M	Mach number
P_t	Wind tunnel total pressure
q	Dynamic pressure = $\frac{1}{2} \rho V^2$, lb/ft ²
Q	Steady rotor torque, ft-lb
r	Airfoil section radius
R	Rotor blade radius, ft
R or RN	Reynolds number
t	Airfoil maximum thickness, inches
T	Rotor thrust, shaft axis, positive up, lb
V	Forward velocity of aircraft, ft/sec
W	Aircraft gross weight, lb
x	Non-dimensional blade station from centerline of rotation
X	Rotor propulsive force, positive aft, lb
y	Non-dimensional blade distances normal to the blade chord
α	Local blade element aerodynamic angle of attack, degrees = $\theta - \phi$
α_{CA}	Control axis angle with respect to normal to flight velocity (= $\alpha_s + \theta_{1s}$)
α_s	Aft tilt angle of rotor shaft with respect to normal to flight velocity vector, deg
α_{TPP}	Inclination of rotor tip path plane to wind axis, positive aft
β	Blade flapping angle with respect to normal to shaft, positive up, deg
β_0	Rotor coning angle
β_{1c}	1st harmonic longitudinal flap angle
β_{1s}	1st harmonic lateral flap angle
γ	Blade Lock number = $\rho ac R^4 / I_\beta$

HC144R1070

δ_2	Pitch-flap coupling angle
θ	Blade pitch angle, positive nose up, deg
θ_0	Collective pitch angle at centerline of rotation, deg
θ_t	Blade linear built-in twist angle, deg
θ_{1c}	1st harmonic lateral cyclic pitch angle, deg
θ_{1s}	1st harmonic longitudinal cyclic pitch angle, deg
θ_{75}	Collective pitch angle at 75% blade radius = $\theta_0 + .75 \theta_t$, deg
μ	Rotor advance ratio = $V \cos \alpha_g / R \Omega$
ρ	Air density, slug/ft ³
σ	Rotor solidity ratio, = $bc/\pi R$
σ_β	Static moment of blade about flapping hinge, slug-ft
ψ	Blade azimuth angle measured in direction of rotation from aft position, deg
Ω	Rotor angular velocity, rad/sec

HC144R1070

1. INTRODUCTION

1.1 The Reverse Velocity Rotor Concept

Present day helicopters are speed limited due to three effects, namely stalling of the tip of the retreating blade, loss of lift due to reverse flow over the inboard part of the retreating blade and compressibility on the tip of the advancing blade.

The Reverse Velocity Rotor System is designed to remove these limitations and make possible cruising speeds up to 350 knots. At high forward speeds the rotor is slowed so that the flow on the retreating blade is reversed and lift is generated with a negative pitch angle making a positive angle of attack to the reverse flow. At the same time the velocity at the tip of the advancing blade is reduced so that compressibility effects are considerably reduced or avoided. Since the rotor blades are required to operate in reverse flow, a "reversible" airfoil section is used having a rounded trailing edge to give reasonable lift and drag characteristics in reverse flow.

In the region where appreciable mixed flow exists on the retreating blade (advance ratios from .4 to 1.0), a twice-per-revolution cyclic input of control angle to the rotor blades control system is utilized to control the lift distribution around the azimuth.

The three essential components of the reverse velocity concept are therefore:

- a) Reduced rotor rpm at high forward speed
- b) Rotor blade airfoil section suitable for reverse flow
- c) Higher harmonic feathering

Except in hover and low speed forward flight, the rotor of a RVR helicopter will operate in or near to an auto-rotative condition with auxiliary propulsion of the vehicle.

1.2 Previous Work

A theoretical feasibility study (designated Phase I) of the RVR rotor system was performed by Fairchild under contract from Naval Air Systems Command. The Phase I study covered rotor performance, rotor blade stability, rotor control, and preliminary design of RVR vehicles and is reported in Reference 1. It was concluded

HC144R1070

in this report that development of the system appeared feasible and that the achievable performance level would be satisfactory.

1.3 Purpose of Test

After review of the report, it was concluded that the next step was to confirm these conclusions by model tests in a high speed wind tunnel. This has been designated Phase II, and is the subject of this report.

The main goals of the Phase II test were:

1. Measurement of rotor lift at intermediate advance ratios and the effect of two per rev pitch
2. Measurement of rotor lift-drag ratio at high advance ratios

Other areas to be investigated were:

3. Rotor control characteristics
4. Rotor blade dynamic stability
5. Blade fatigue loads at high advance ratio
6. Windmilling characteristics

An additional requirement of the program was that the rotor blades would be approximately dynamically scaled models of those on a realistic RVR rotor. Because of the possibility of unforeseen rotor blade instabilities at high advance ratios, it was decided that use of a pressure tunnel was desirable; rotor characteristics could be initially determined at low tunnel pressure where instabilities are less likely due to the low Lock numbers in both the torsion and flapping modes. This led to the choice of the 12 foot pressure tunnel at the NASA Ames facility. It was also decided to make the rotor a 1/7 geometrically scaled model of the full scale design developed in Reference 1.

1.4 Description of Model and Test Rig

1.4.1 General

The rotor shaft bearings, the control system and the hydraulic drive system are all mounted on a baseplate carried on a NASA Ames 2.5 in dia. High Endurance Balance, which is in turn mounted in a Y-shaped support frame on a pedestal bolted to the

HC144R1070

floor of the tunnel. The support arm is pivoted on the pedestal so that the shaft angle can be varied in the range 5° forward to 15° aft using the wind tunnel incidence gear. The whole unit is enclosed in upper and lower fairings which give clearance for the blades and control system.

Figure 1.1 shows the installation in the NASA Ames 12 ft pressure tunnel. Figure 1.2 is a three-quarter rear view with fairing removed, showing the support frame, balance location, etc.

The whole of the airloads on the blades, hub, hub fairing and on the parts of the control system not shielded by the upper fairing are measured in six components on the balance, the geometric relationship being as shown in Figure 1.3.

1.4.2 Rotor Blades

Blade geometry is given in Table 1.I The rotor blades are of constant chord with a root cutout at 23 percent radius. The Fairchild developed reversible airfoil sections are a 1.5 percent cambered 6% thick section at the tip and a 3.5 percent cambered 18% thick section at the root, with linear taper from root to tip. The method of developing the airfoil sections is given in Appendix A. The airfoil sections at root, tip and mid-span are shown in Figure 1.4 and ordinates for these sections are given in Tables A-II and A-III. Pressure distribution and wake surveys tests were made on two-dimensional models of each of the sections in both forward and reverse flow in the 3 ft by 7 ft Low Turbulence Pressure Tunnel at NASA Langley, and are reported in Appendix C.

The construction of the blades consists of aluminum upper and lower skins with thickness variations chordwise and spanwise formed by chemical milling. A C-spar bonded to the skins over the full span at the chordwise change of thickness is machined integrally with the root end attachment. The skins are bonded to an aluminum wedge at the trailing edge and a bronze wedge at the leading edge which also serves as a balance weight. An aluminum honey-comb core is machined to the internal contour and serves as a shear tie between the upper and lower skins as well as a forming core for the bonding operation. Strain gages were bonded at three spanwise positions on two of the blades.

The rotor blade was designed with maximum torsional stiffness at minimum weight as a prime concern. The bonded metal structure was found to be the minimum cost and minimum risk approach to achieving this. The resulting blade Lock number was 2.3 at sea level which is much less than that of conventional helicopter rotor blades.

HC144R1070

The rotor shear center and pitch axis were placed at 27.5 percent chord and the section c.g. near 30 percent chord. This configuration was found to be near optimum from studies of flap-torsion dynamic instability at high advance ratio (See Section 4 of Reference 1). Plots of the rotor blade physical properties are shown in Figures 1.5, 1.6 and 1.7. A comparison of measured and theoretical spanwise variation of bending and torsional stiffness is given in Figures 1.8 and 1.9.

The natural frequency spectrum of the rotor blade modes in a vacuum are shown in Figure 1.10.

1.4.3 Rotor Hub

The rotor hub is a 4-bladed fully articulated type with provisions made for various values of delta-3 feedback; however, due to lack of time only a delta -3 angle of 26.5 degrees was used in this series of tests. The coincident flap and lag hinges are positioned at 6.5 percent of the blade radius.

Mechanical damping of the blades is provided about the drag hinge by rotary viscous dampers mounted above the rotor hub. The dampers provide a critical damping of approximately .20 about the lag hinge to minimize the potential of a ground resonance-type instability of the rotor mounted on the flexible balance.

A fiberglass fairing with cut-outs to permit blade flapping is mounted over the hub.

1.4.4 Control System

The control system consists of a conventional three-actuator-controlled swashplate to provide collective and one-per-rev pitch with the actuators set at 90°, 180° and 270°. The actuators are remotely operated with controls both for collective, longitudinal cyclic and lateral cyclic and for individual actuators.

Instead of operating the incidence rods directly, however, the swashplate outer-ring carries four levers which serve for the addition of the two-per-rev input to the swashplate motion. This system was based on the design work done in Section 5 of Reference 1, and is illustrated in Figures 1.11 and 1.12.

The two-per-rev motion is generated by a crank on a shaft driven at twice rotor rpm, then passed through a variable amplitude mechanism to a sleeve between the shaft and the one-per-rev swashplate. At the top of the sleeve is mounted a bearing which permits the non-rotating two-per-rev motion to be made

HC144R1070

rotating, and transferred, in the case of two blades directly to the mixing levers and in the case of the other two blades to rocker arms positioned on top of the hub and thence to the mixing levers.

Amplitude of the two-per-rev motion is controlled by a remotely operated D.C. actuator.

Because of the appreciable mass of the vertically oscillating sleeve, two weights are mounted near the base of the rotor shaft and connected to the sleeve through levers to balance out the oscillatory motion.

1.4.5 Drive System

The rotor is driven through a toothed belt by a hydraulic motor mounted on the baseplate; the belt passes around the hydraulic rotor drive pulley (21 teeth), the rotor shaft pulley (60 teeth) and the two-per-rev generator drive pulley (30 teeth). The ratio of hydraulic motor rpm to rotor shaft rpm is 2.857:1 and the ratio of the two-per-rev generator rpm to rotor shaft rpm is 2.0:1. When it is not required to operate the two-per-rev mechanism, a shorter belt can be fitted around the hydraulic motor drive pulley and the rotor shaft pulley only, and the two-per-rev sleeve locked in its central position. The phasing of the two-per-rev input to the main rotor shaft is accomplished by the relationship of the rotor and two-per-rev pulleys; phasing can readily be changed after slackening off the drive belt.

The hydraulic motor is driven by a self-contained hydraulic power pack located outside the wind tunnel shell, consisting of an electric motor, pumps, reservoir, filters, control and relief valves, etc. The power pack can be remotely controlled from the wind tunnel control room. Provision is made for controlled braking of the rotor to prevent overspeeding in the windmilling case, and also for automatic control of rotor speed.

Since the hydraulic motor is mounted on the metric part of the system, connection between it and the pedestal is through pressure-balanced swivel joints. It was not possible to measure any tare effects due to the load path across these swivels and pipes. The swivels also allow for the change of alignment of the hydraulic piping when the rotor shaft angle is altered.

HC144R1070

1.4.6 Instrumentation

The rotor blades were fitted with bending bridges measuring flapwise bending stress at 3 blade stations namely: .37, .51 and .71 radius, chosen as the most critical blade stations based on theoretical bending moment distributions calculated over the test spectrum. The gages were mounted internally so as not to affect the airfoil characteristics. Vibratory chordwise blade stresses were monitored by axial strain gage measurements on the lag damper rod linkage which is equivalent to monitoring the root vibratory moment. Though these stresses were monitored primarily as an indication of approaching instability, this moment in conjunction with theoretical chordwise vibratory moment distributions on the blade allowed for monitoring stresses at the critical span stations. Axial strain was measured on the pitch link for purposes of monitoring both control system stresses and blade torsional loads. Bending bridges mounted on flex beams which were deflected by cams were used for monitoring flap angle, lead-lag angle, and pitch angle at the blade root.

All of the above quantities were displayed on oscilloscopes which were triggered from a pulse at zero azimuth position on number 1 blade to indicate the phasing of the response on the scopes; this was of prime importance for efficient trimming of the rotor flapping at each test point. The dynamic information for each was also displayed on an oscillograph during the test as well as recorded on magnetic tape.

Transducers were used to measure hydraulic pressures at the input and output side of the hydraulic motor; this was intended for the purpose of correcting pressure tares; however, tests indicated that this was an insignificant correction.

The positions of the electric actuators which govern the swashplate motion and two-per-rev amplitude were measured using linear potentiometers of infinite resolution. These voltages were read in the control room using indicating millivolt potentiometers or "Imps". The pots were wired and calibrated in terms of collective pitch, longitudinal cyclic pitch, lateral cyclic pitch, and two-per-rev pitch amplitude.

Rotor speed was measured by the voltage output of a D. C. generator driven by the hydraulic motor. A second indication of rotor speed was obtained by using a magnetic pickup triggered by a 30 tooth gear on the rotor shaft; the output was directed to a counter which digitally displayed the RPM.

HC144R1070

The voltage output from the NASA balance gages was filtered through the "Imps" so that only the steady values remained; these were displayed in raw form on the "Imps" so that rolling moment at balance, rotor thrust, rotor drag and side force could be monitored during testing. The balance vibratory loads were also displayed on an oscillograph for monitoring of balance stresses and/or resonant conditions.

All the non-vibratory information i. e. , rotor speed, steady balance loads, control positions in terms of collective, longitudinal, lateral, and 2/rev amplitude, coning angle, and hydraulic pressures were automatically recorded at each test run on paper tape. The balance data was corrected for the primary interactions on a computer with overnight turn-around time. The rotor behavior was made visible in the control room by means of closed circuit television and the entire test was recorded on video tape.

1.5 Test Procedures

The tests were made in the NASA Ames, 12-foot Pressure Tunnel, a variable density, low turbulence wind tunnel, and covered the range of advance ratios from 0.4 to 2.5 at tunnel speeds from 100 to 350 knots. To develop familiarity with the operation and control of the model, initial tests were made at a tunnel total pressure of approximately 12 inches of mercury (density .0008 slugs per cu ft); later testing was at approximately atmospheric pressure (density .0020 slugs per cu ft).

The first series of tests was made with a dummy balance to explore the behavior of the rotor and the capability of controlling it at advance ratios from 0.14 up to 2.0. No problems were encountered, and the program was continued with a NASA Ames 2-1/2 inch two-plane Mark III balance; this was later replaced by a NASA Ames 2-1/2 inch two-plane high endurance balance. As a result of failures of balance bridges, not all the desired test data was obtained.

In general a run consisted of setting the tunnel pressure, tunnel Mach number, and rotor speed at constant values. The shaft angle was then varied from zero (perpendicular to the free stream velocity) to between 5 degrees forward and 12.5 degrees aft. At each shaft angle various settings of collective pitch were made; at each collective setting longitudinal and lateral cyclic pitch were adjusted to produce zero longitudinal flapping with respect to the shaft and zero rolling moment (the roll axis of the balance is located at approximately the C.G. axis with respect to the rotor center of a realistically scaled helicopter). Thus the shaft angle became the tip path plane angle. The

HC144R1070

rolling moment shown on the balance was accurately nulled while longitudinal flapping was kept to within one degree. When two-per-rev pitch was a variable, the same procedure as above was used except that for each collective setting the two-per-rev pitch amplitude was varied and the rotor trimmed as above for each two-per-rev setting.

As shaft angle was increased and/or the rotor controlled to flap backwards, auto-rotative conditions were reached. When the rotor torque was sufficient to overcome the friction of the control and drive systems and the hydraulic losses, the hydraulic braking control was brought into use to prevent overspeeding of the rotor and maintain the desired rpm. By this means testing was continued into the negative torque region.

After the operator had gained experience it was found possible, by operation of the lateral and longitudinal controls, to control rpm around the zero torque region, with the dump-valve opened to by-pass the hydraulic system.

In addition to the six-component balance data, rotor dynamic quantities were also recorded including azimuthal variations of blade lag and flapping motions, blade bending moments and the lag damping moments; these are considered in Section 4.

The usual tunnel corrections used to adjust data for the effects of wall interference have been applied to the data. These conventional wall corrections are expected to be satisfactory for rotor models operating at advance ratios above 0.3. No attempt has been made to account for aerodynamic interference from the model and support fairings.

1.6 Test Conditions

The relationship between wind tunnel speed, rotor rpm and advance ratio for the model rotor is shown in Figures 1.13 and 1.14. On these figures are indicated the values at which tests were made, designated by run number, for 0.40 atmosphere density and 1.0 atmosphere density respectively.

The maximum Reynolds number for the model and full scale blades occurs at the tip of the advancing blade, and has the following values:

full scale rotor blade,	19 million
model blade at approximately atmospheric pressure,	2.4 million
model blade at 40% atmosphere,	1.0 million

HC144R1070

1.7 Scheduled Lift Coefficient

The RVR concept requires the reduction of rotor speed as vehicle speed is increased, and the rotor lift coefficient for 1g level flight will therefore vary over the flight regime. Generally speaking, it is desirable to keep the rotor speed up to the limits of maximum rpm or of tip Mach number for advance ratios below unity and to reduce rotor rpm once reverse flow has been fully established over the retreating blade at advance ratios greater than one.

An optimum schedule of rotor rpm has yet to be established, but the following values were assumed for the purpose of interpreting the results of these tests: from the hover, 100% rpm until a tip Mach number of 0.92 is attained; then a progressive reduction of rpm maintaining this Mach number until the forward speed attains 300 knots at an advance ratio of about 1.0; then a reduction of rpm at 300 knots until tip Mach number equals 0.8 at an advance ratio of 1.2; at all higher speeds the tip Mach number is maintained at this value.

The model rotor was sized to carry a 1g scaled lift of 400 lbs corresponding to a disc loading of 8 lb per sq ft. This, in conjunction with the above velocity-rpm schedule, defines the lift coefficient versus advance ratio curve; thus the 1g lift condition can be related to advance ratio alone regardless of the velocity-rpm combination. Figure 1.15 shows this schedule of rotor lift coefficient as a function of advance ratio for this rotor system, assuming sea level standard conditions.

The scheduled velocity-rpm line is shown superimposed on plots of the test data runs in Figure 1.13 for the 40 percent atmosphere runs and Figure 1.14 for the one atmosphere runs. Note that for both tunnel density conditions considerable data was taken that is representative of the scheduled condition in which advance ratio and tip Mach number are both correctly represented.

HC144R1070

2. RESULTS - PERFORMANCE

2.1 Aerodynamic Tares

Aerodynamic tares were taken at each tunnel density tested by taking balance readings with rotor blades removed at various tunnel speeds, each time varying shaft angle and rotor speed. The latter had only a small effect on the tares, and an average value has been used in analysis. The tare corrections for force along the balance axis and at right angles to the balance axis and for pitching moment are shown in Figures 2.1, 2.2 and 2.3. Due to failure of the axial component of the balance, X-direction tares were not obtained at high density. The corresponding values from low density (Fig. 2.1) have therefore been used.

The drag tares and lift tares were found in some cases to be a large percentage of the total balance load. Torque tares were found to be negligible.

2.2 Tabulated and Plotted Results

The results for each data point, namely rotor lift, drag, and torque data corrected for weight and aerodynamic tares and the control angles used are presented in Appendix B of this report. For each setting of rotor shaft angle and collective pitch the lateral and longitudinal cyclic pitch were adjusted to produce zero rolling moment about the balance axis and approximately zero longitudinal flapping with respect to the shaft. Points which were not trimmed were identified by investigating the flapping oscillograph traces so that rotor tip path plane could be determined for each run.

For each significant run, rotor lift coefficient, effective lift/drag ratio, torque coefficient and drag coefficient have been plotted versus collective pitch for constant tip path plane angles in Figures 2.4 through 2.24.

2.3 Rotor Lift

For each advance ratio the 1g lift coefficient level obtained from Figure 1.15 has been indicated on the lift coefficient curves of Figures 2.4 through 2.24. The exact requirements for lifting ability of a high speed rotor system are not fully defined at this stage: for example the airflow over the fuselage, mast fairing and hub will provide appreciable lift on a high speed helicopter. However, if this is neglected, it will be seen that a requirement for 1.3g maneuver capability at a disc loading of 8 lb/sq ft

HC144R1070

at sea level standard conditions can be met or exceeded for all advance ratios outside the range of 0.7 to 1.5 without exceeding a tip path plane angle of ten degrees.

Rotor lift coefficient divided by the lift coefficient at 1g conditions was plotted as a function of advance ratio for constant values of control axis angle at constant tip path plane angles of 5 deg and 10 deg in Figures 2.25 and 2.26, respectively. The curves for both values of tip path plane show that for advance ratios below about 1.0, lower values of control axis angle produce more lift; beyond this advance ratio, lift increases with increase of control axis angle. For the 5° tip path plane case, the available lift is seen to drop below the 1g level over a wide range of advance ratios (from .5 to 1.4) for control axis variations between 0 and 7 degrees. When the tip path plane angle is increased to 10 degrees, a disc loading of 8 lb/sq ft can be achieved at all advance ratios.

Theoretical studies have verified this trend and have indicated that for approximately this same control axis range and tip path plane, the addition of moderate values of two-per-rev cosine phased pitch will increase the available lift in laterally trimmed flight to a minimum of 1.3g's over the full advance ratio range for this rotor.

It is noted that the lateral trim requirements were less than 6 degrees for all 1g conditions.

2.4 Rotor Lift-Drag Ratio

Rotor performance can be assessed by the parameter effective lift/drag ratio, defined by converting the total rotor power required into a force and adding to this the rotor drag (or subtracting the rotor propulsive force). In equation form:

$$L/D_E = L / \left(\frac{550 \text{ RHP}}{V} + D \right)$$

The effective lift-drag ratio of the rotor blades was computed by subtracting the aerodynamic hub tares from the measured rotor forces and moments and calculating the effective drag due to the combined effect of drag force and rotor torque. For those cases where the rotor torque was negative, i. e., the airloads were tending to speed up rotor, the torque was assumed to be transferred to a usable propulsive system (e. g., tail propeller) at 100 percent efficiency.

HC144R1070

It will be seen from Figures 2.4 through 2.24 that at low advance ratios ($\mu = .29$ Fig. 2.16) in the conventional helicopter range, rotor efficiency increases with decreasing tip path plane angle, i. e. , as the rotor moves into the propulsive region. Effective lift/drag ratios of 8 were measured, and this is maintained up to advance ratios of at least .46 (Fig. 2.17). In the range of intermediate advance ratios, effective lift/drag ratio falls off to a minimum of about 6 at an advance ratio near 0.8. At higher advance ratios the lift/drag ratio again increases, with a value of 8 at advance ratios of 1.0 through 1.4, and thereafter increasing to the order of 12 at advance ratios above 2.

The maximum achieved values of the effective lift/drag ratio are given in Table 2-I and plotted vs advance ratio in Figure 2.27. The lift coefficients corresponding to these maximum values may not be those for level flight at the assumed rotor disc loading of 8 lb per sq ft, and effective lift/drag ratios at the latter condition are also given in Table 2-I and plotted in Figure 2.28 for the range of advance ratios. Figure 2.29 shows the effect of lift coefficient in detail for an advance ratio of 1.5. In this case better cruise efficiency would have been obtained if a reduced disc loading had been selected. An alternative may be the use of small amounts of two-per-rev control which was shown in reference 1 to have a significant effect on the conditions under which best effective lift/drag ratio was obtained.

2.5 Rotor Torque

Although not essential to the RVR system it is desirable that when operating at reduced rpm the rotor should be in an auto-rotative condition at zero torque. At the same time, the lift must be appropriate to level flight and the rotor trimmed. From figures 2.4 through 2.24 the combination of collective control angle and tip path plane angle that meets these conditions can be determined, and figure 2.30 shows the tip path plane angle for zero torque and a lift coefficient corresponding to the scheduled combination of vehicle speed and rotor rpm for 8 lb/sq ft disk loading as a function of advance ratio. As was shown in figures 2.25 and 2.26, without using two-per-rev control large flapping angles would be required in the advance ratio range of 0.9 to 1.3. Outside this range, however, figure 2.30 shows that zero torque and the scheduled lift coefficient conditions can be met at practical tip path plane angles. At high advance ratios the necessary tip path plane angle decreases rapidly with increase of advance ratio.

HC144R1070

The use of two-per-rev control has been shown in Section 2.5 of reference 1 both to increase the lift available at intermediate advance ratios and to provide a control over torque.

2.6 Accuracy

The net value of the lift on the rotor blades is the difference between the total measured lift and the lift on the hub minus the weight of the model. The net value of the drag is the difference between the total measured drag and hub drag. The net values of both the lift and the drag are therefore the differences between two relatively large quantities, and are subject to magnification of any inaccuracies in measurement. In general, the plotted points for lift and effective lift/drag ratio (figures 2.4 through 2.24) show little scatter, but they may be subject to systematic errors, for example the effect of the rotor lift on the flow field around the hub and therefore on hub lift and drag.

HC144R1070

3. RESULTS - ROTOR CONTROL

3.1 Control Angle

Figures 3.1 through 3.8 show, for the range of advance ratios, the relationship between control angle, tip path plane and collective pitch with the rotor trimmed laterally at all times. With one exception results are given for the tests at atmospheric tunnel pressure only, since at the reduced tunnel pressure the Lock number is not representative of the full scale rotor. Figure 3.8, however, gives results for tests at low pressure at an advance ratio of 1.4 and may be compared with Figure 3.7 for atmospheric pressure and the same advance ratio.

3.2 Collective Control Power

The relationship between collective control angle and lift coefficient for a trimmed rotor at constant tip path plane can be derived from Figures 2.4 through 2.24. It will be seen that at low advance ratios lift increases with increasing collective pitch at constant tip path plane angle; as advance ratio is increased the slopes of the curves decrease until collective has no effect on lift at an advance ratio of 0.9. Beyond this advance ratio the rotor thrust is seen to decrease with increased collective pitch requiring negative values to achieve the required lift. Figure 3.9 shows a plot of the slope of the lift coefficient vs collective curve as a function of advance ratio for a 5 degree tip path plane. At the proposed high advance ratios corresponding to reverse velocity cruise flight ($\mu > 1.4$) collective may once again be a meaningful control but in the reverse sense than for low advance ratio flight.

3.3 Rotor Sensitivity

As rotor advance ratio is increased, it is well known that the rotor becomes increasingly sensitive to control inputs and gusts. Positive delta-3 (pitch-flap coupling) was determined from previous analytical studies to be effective in reducing this sensitivity and the rotor had provisions for incorporating delta-3 angles of 0, 26.5, and 45 degrees. For this test only the intermediate value of 26.5 degrees was used.

HC144R1070

Rotor sensitivity is shown in Figure 3.10 where the change in tip path plane angle per degree of control axis angle is plotted as a function of advance ratio. It is noted that this is not a pure derivative since lateral cyclic pitch was varied as required to retrim the rolling moment to zero. The curve shows that the derivative approaches unity at low advance ratios as expected for this moderate value of δ_3 . At RVR type advance ratios ($\mu > 1.2$) the derivative approaches 2.5 times the low advance ratio value. At higher advance ratios the sensitivity is seen to decrease.

This sensitivity increase is in good agreement with theoretical calculations. The square symbols show theoretical points calculated at various advance ratios for the model rotor. The decrease in sensitivity at high advance ratios is also as predicted by theory. The theoretical predictions calculated beyond the advance ratio range of the test indicate that the tip path plane sensitivity to control axis input continues to decrease so that at an advance ratio of 2.5 the derivative (at constant lateral flapping) reduces to .80 which is near the value at hover.

3.4 Control Phasing

The phasing between the maximum one-per-rev pitch amplitude and the maximum one-per-rev flapping amplitude is a function of the flapping frequency, flap aerodynamic damping and the δ_3 angle. The theoretical phase angle of the rotor at one atmosphere in hover as a function of δ_3 is shown in Figure 3.11. The low Lock number of the model blades provided relatively low critical damping ratios especially in the low density conditions. This coupled with the hinge offset effect on frequency resulted in the following phase angles calculated in hover:

45.7 degrees at one atmosphere density

30.9 degrees at 40% atmosphere density

These low values of phase angle resulted in a strong coupling of the conventional longitudinal and lateral controls. In the low density conditions the conventional longitudinal cyclic control was used primarily to trim rolling moment and the lateral control was used primarily to trim the fore and aft flapping. The control angles required for trim in the low density condition are thus not typical for full scale comparison unless significantly more δ_3 was used on the full scale rotor such that the phase angle calculated in hover approached 30 degrees. The one atmosphere runs should, however, be representative of full scale control.

HC144R1070

It should be noted that even with zero pitch-flap coupling the hinge offset effect produces a phase angle of 65 degrees. For practical values of delta-3 (0 to 45 degrees) the phase angle decreases approximately .7 degrees for every 1 degree increase in delta-3.

3.5 Rotor Flapping

Typical traces of rotor flapping at various advance ratios and near trimmed 1g lift coefficients are shown in Figure 3.12. Because of the low Lock number of the model rotor blades, the maximum coning angle encountered at these conditions is quite small. At the low advance ratio condition, the coning and all harmonics of flapping are seen to be negligible with the rotor trimmed normal to the shaft. At the .46 advance ratio, the flapping is seen to be primarily low amplitude and of two-per-rev frequency; coning angle is again almost negligible (less than one degree). At the intermediate advance ratio of .82 the flapping is again primarily two-per-rev though higher harmonics are becoming evident. Finally at the high advance ratio of 1.5 the higher harmonic content is more evident though the primary frequency is two-per-rev; the two-per-rev amplitude is near two degrees and the coning angle is approximately 2.5 degrees.

No detrimental effects of two-per-rev flapping were obvious though amplitudes near 2 degrees which appeared at the high advance ratios may cause local stalling conditions to occur. Since two-per-rev pitch is not required for lift generation at high advance ratios, this control may be useful in trimming out the two-per-rev flapping should it become desirable to do so.

HC144R1070

4. RESULTS - ROTOR BLADE DYNAMICS

4.1 Rotor Blade Resonances

Inherent in the RVR concept is a wide variation of rotor speed during operation from hover to cruise flight. In order to predetermine rotor speed ranges which would produce potentially high blade loads, the frequencies of the bending and torsion modes were calculated during the blade design stage using finite element theory including centrifugal stiffening. The results are shown in Figure 1.10. The flap bending modes were of major concern since these modes have frequencies near the low rotor harmonics where the aerodynamic excitation is relatively high.

During the tunnel test the blade flapwise frequencies were determined near each operating condition by varying the rotor speed at a given advance ratio and noting where the flapwise bending vibratory stresses reached a maximum value. The flapwise modes were found to occur at almost exactly the predicted values. Amplification of flapwise bending loads were noted in the following areas; examples of the flap bending moment traces near these conditions are given in Figure 4.1:

- 1670 rpm (100% rpm) A clear 5/rev frequency was noted in the bending traces which is near where the 3rd flap mode crosses 5/rev frequency.
- 1050 rpm (63% rpm) A clear 3/rev frequency was noted in the bending traces with high amplitude. This is the rpm where the theoretical 2nd flap mode crosses 3/rev.
- 680 rpm (41% rpm) At high advance ratio, a 10/rev low amplitude frequency was noted in the bending traces over a narrow rpm range. The theoretical 3rd flap mode is seen to cross 10/rev at this rpm. This was noted at low density conditions where the damping was small.
- 650 rpm (39% rpm) A 4/rev frequency of relatively high amplitude was noted which is near the rpm where the second flap mode crosses 4/rev.

No appreciable shift in these resonant rpms was noted as advance ratio was changed indicating that the aerodynamic effects even at advance ratios near 2.0 have small

HC144R1070

influence on the resonant frequencies. This is an important finding which allows the use of natural frequency spectra (assumed in a vacuum) to pinpoint areas of high blade loads for the complete advance ratio range.

Resonances of the 3rd flap mode with 6, 7, and 8 and 9/rev were not noted because the rpm band to excite these high frequencies is generally small and amplification is not expected unless the model test conditions were very near these points. Even when operating continually right on the high amplitude 1050 rpm at high advance ratio and high lift coefficient, the bending stresses were less than double the very conservative endurance limit placed on the dynamically scaled blades.

No resonances or amplification were noted in the chordwise vibratory stresses (as noted by the damper arm load) nor were any expected since the chordwise modes only cross integer rpm multiples above 9/rev in the operating range. (See Figure 1.10). No data on resonance of the torsional mode is available.

4.2 Vibratory Flapwise Bending Stresses

Vibratory bending stresses increase substantially with advance ratio due to the increased aerodynamic excitation caused by the complex flow field. To demonstrate this, data runs at 1g lift coefficient were chosen at a constant non-resonant rotor speed of 830 rpm. Thus, the effect of resonant amplification was held constant at various advance ratios. The vibratory bending moments at the 3 spanwise strain gage locations are shown in Figure 4.2. These are from the low density runs where there was sufficient data at constant rotor speed; thus, although the magnitude of the moments are not meaningful, the trend with advance ratio should be representative.

The curves show that as advance ratio is increased from that of present day helicopter limits ($\mu > .4$) to the high advance ratios required for RVR flight, the bending moments increase by a factor of over 3 for all gage locations. The bending moment is seen to at first increase most rapidly at the inboard station. At the high advance ratios the inboard moments level out and the center span bending moments also begin to do the same. The outboard moments however are seen to increase even more rapidly.

This trend is similar to that predicted by theoretical analysis. Figure 4.3 shows plots of typical estimated spanwise distributions of flapwise vibratory moment

HC144R1070

for a blade similar to the model rotor blades tested. Because the moments are calculated at different non-resonant rotor speeds and different air density than used in Figure 4.2, no scale is shown on the ordinate. The distributions show a rapid increase in bending moment as advance ratio is increased from .4 to .7 at the inboard end. At the 1.4 advance ratio condition the inboard moment (.37R) is seen to drop slightly, a small increase occurs in the center location (.51R) and very significant increase in the outboard moment. This may be due to the increasing amount of reverse flow on the outboard part of the span at the higher advance ratios.

To obtain realistic scaled rotor blade loads over the proposed advance ratio range, runs were selected near sea level atmosphere conditions so that aerodynamic jamping effects would be realistic. Data runs were also chosen near the scheduled rotor speed condition for each given advance ratio so that near resonant rpm effects would be represented. The moments at the center and outboard stations are shown in Figure 4.4; the inboard bending gage output was not available for all the conditions investigated and is not plotted.

The full scale moments show the near resonant condition at $\mu = 1.0$ (1170 rpm near 1/3 the frequency of the 2nd flap mode) produces more amplification in the outboard gage than the center gages (though this is not evident from the normalized mode moment shape).

HC144R1070

5. THEORETICAL PREDICTION OF ROTOR PERFORMANCE AND COMPARISON WITH TEST RESULTS

5.1 Airfoil Section Data

The airfoil sections at the root, mid-span and tip of the model rotor blades were tested in both forward and reverse flow over a range of Reynolds numbers at low Mach number in the Langley Low Turbulence Pressure Tunnel. The tests are described and the results given in Appendix C.

The approximate maximum Reynolds number values appropriate to the model and full scale conditions achieved on the tip of the advancing blade are as follows:

Model tests, average density .00086 slugs/ft ³ :	1.0 million
Model tests, average density .00212 slugs/ft ³ :	2.4 million
Full scale, sea level density .002378 slugs/ft ³ :	20 million

In the performance prediction program, to avoid the complication of tables of aerodynamic data dependent on Reynolds number as well as Mach number, aerodynamic data has been selected according to average Reynolds numbers appropriate to the condition in which the blade section is operating. For the comparison with the model test results, section drag coefficients, which have a greater effect on rotor performance at the higher rotor speeds and reduced angles of attack, were selected appropriate to the Reynolds number range of 1.0 to 2.0 million. The slope of the curve of section lift coefficient was found to vary only slightly with Reynolds number, and was obtained from data at 1 million. When blade sections are operating near maximum lift, they will be at reduced velocity and therefore at reduced Reynolds number - values appropriate to a Reynolds number of 0.4 million were selected.

For the prediction of full scale rotor performance it was indicated that there will be little or no variation of either lift or drag data above a Reynolds number of 12 million and data measured at this Reynolds number was therefore used.

After determining the data to be used at low Mach number and over the angle of attack range tested, it is necessary to extend it to cover all Mach numbers up to 0.92 and for the full angle of attack range of 360 degrees. This was done by the methods of reference 1, and using data from reference 2. The lift and drag coefficients so determined for the 6%, 12% and 18% sections are given in Appendix D.

HC144R1070

For the purpose of selecting the aerodynamic data to be used in the rotor performance prediction program, the rotor blade was divided into five equal spanwise units. The data for 6%, 12% and 18% sections was therefore interpolated on a linear basis to give data for 7.2%, 9.6%, 12%, 14.4% and 16.8% sections.

5.2 Performance Prediction

The Fairchild rotor performance computation program ("Aero") has been improved in detail, but is substantially as described in Appendix "B" of reference 1. For the purpose of comparisons with model tests, the "low Reynolds number data" as described in Section 5.1 was utilized, together with the geometric characteristics of the model rotor as given in Table 1-I. The air density, rpm, tunnel speed and speed of sound corresponding to the mean value of a particular run have been utilized, and the program run at a matrix of values of collective pitch angle and control angle, with the rotor balanced to be in lateral trim. Since previous work had shown that the effect of shaft angle with an articulated rotor was small, this was neglected.

The results of these calculations are plotted in Figures 5.1 through 5.12.

5.3 Comparison of Predicted and Measured Results

Initially, comparison was made between the values of tip path plane angle, rotor lift coefficient and equivalent lift/drag ratio measured and calculated at the same values of collective and longitudinal control angles, assuming the rotor to be trimmed laterally in both cases. There is good agreement at low advance ratios, (see figure 5.1) but not at intermediate and high advance ratios; this may be due to a number of factors, for example, changes in velocity and flow direction caused by the presence of the upper fairing. It was found that a better basis for comparison was equivalent lift/drag ratio versus rotor lift coefficient, and this has been used in Figures 5.2 through 5.12.

The maximum values of equivalent lift/drag ratio for both measured and predicted conditions obtained from Figures 5.2 through 5.12 have been plotted in Figure 5.13. Agreement is good in the advance ratio range of 0.5 to 1.0. One cause of the differences at lower and higher advance ratios may be that although in the case of the predicted data sufficient combinations of collective pitch and control angles were utilized to give certainty that the peak value had been obtained, the tests may not have been made at the conditions that would give a maximum. A further cause of difference is

HC144R1070

the aerodynamic data; while that at low Mach number had been based on comprehensive tests on the three airfoil sections at the Reynolds number conditions of the model rotor tests (data reported in Appendix C), the effects of Mach number were estimated. Comparing the measured and predicted values at an advance ratio of .45 where the advancing blade tip Mach number is .89 indicates that the extent of the drag rise on the tip section may have been over-estimated.

At higher advance ratios the amount of experimental data is limited and the results scattered; nevertheless it can be seen that the prediction method over-estimates rotor performance. This can be corrected by reducing the optional cut-off of maximum lift coefficient in radial flow which is an input to the prediction program.

5.4 Effect of Reynolds Number on Rotor Performance

The prediction of rotor performance was repeated for the same cases that were used in the comparison of the preceding paragraph, but using the full-scale Reynolds number data that were developed from the model airfoil section tests and presented in Appendix D, Figures D19 through D36. Again the span was divided into five sections with data corresponding to thickness-chord ratios of 16.8%, 14.4%, 12.0%, 9.6% and 7.2%. The values of maximum effective lift/drag ratio that were obtained are plotted in Figure 5.14 and compared with the corresponding values for low Reynolds number obtained from Figure 5.13.

It will be seen that at intermediate and high advance ratios the effect of Reynolds number is very considerable. This is due both to the reduction of drag of the airfoil section and the increase in lift at large angles of attack; the latter enables the rotor to operate at a smaller flapping angle for the same thrust.

5.5 Full Scale Rotor Performance

The best curve through the measured points (Table 2-I and Fig. 5.13) has been modified for the predicted effect of Reynolds number (Fig. 5.14) to give the expected full scale performance of a rotor having both the scaled-up physical characteristics and the aerodynamic sections of the model rotor. This is presented in Figure 5.15, which shows the maximum effective lift/drag ratio and the effective lift/drag ratio at a disk loading of 8 lb per sq ft.

HC144R1070

5.6 Comparison with Previous Performance Prediction

Figure 5.16 compares the performance now expected for a full scale reverse velocity rotor having the characteristics of the model rotor with the results obtained in previous predictions (Figure 2.38 of reference 1), corrected to be at zero two-per-rev. The characteristics of the two rotors are compared in Table 5-I. In the range of advance ratio from 0.6 to 1.6 the performance of the reference 1 rotor is slightly better. In order to investigate this further, the effect of specific differences between the rotors was predicted.

Performance runs were made with the physical dimensions and aerodynamic data of the rotor number 2 of Table 2-I of reference 1, which will be referred to as "1039" rotor, and with specific variations of characteristics. The results for the basic "1039" rotor operated with zero two-per-rev and a thrust of 20,000 lbs are given in Figure 5.16 for the eight cases considered in reference 1 as follows:

Case	Speed Knots	RPM	Advance Ratio	Fig. of Ref 1
1	250	91%	.66	2.29
2	250	80%	.75	2.30
3	250	60%	1.005	2.31
4	300	80%	.92	2.32
5	300	60%	1.21	2.33
6	300	50%	1.41	2.34
7	350	60%	1.407	2.35
8	350	50%	1.689	2.36

In each case the calculations were performed for three values of control angle and the results given for the optimum control angle.

The effect of individual changes to the following parameters was investigated for cases 2, 5, 6 and 8 of the above table.

- Delta 3, from zero to 26.5 degrees
- Lock number per blade from 6.0 to 3.0
- Atmospheric conditions, from 91.5°F and 3000 ft to standard sea level conditions (59°F) changing density from .001998 slugs/ft³ to .002378 slugs/ft³ and the speed of sound from 1150 ft/sec to 1117 ft/sec. (Note that a change of density also changes the Lock number.)

HC144R1070

The results are shown in Figure 5.17. As might be expected, the purely geometrical change of delta-3 has no effect on rotor performance. Both the reduction in altitude and the increase of blade inertia cause a significant improvement in rotor performance, with the exception that at 350 knots the increase of Mach number on the tip of the advancing blade causes a loss of performance. The combined effect of all three changes is also shown in Figure 5.17.

It would appear from this that the cause of differences in performance shown in Figure 5.16 must be due to differences in the aerodynamic data.

HC144R1070

6. CONCLUSIONS AND RECOMMENDATIONS

The tests conducted on a model 8 ft diameter 4-blade rotor with reversible airfoil sections demonstrated that it could be operated satisfactorily at advance ratios up to 2.5 and speeds up to 350 knots. Control was maintained throughout by conventional controls, both in power, in free auto-rotation and in the braking modes. Operation was free of dynamic instability.

Two-dimensional tests were performed over a range of Reynolds numbers on the root, mid-span and tip airfoil sections of the rotor blades to give data for the prediction of the rotor performance using the Fairchild rotor performance program. When using airfoil data appropriate to the Reynolds number of the model tests, there was generally good agreement between measured and predicted effective lift/drag ratio. With data appropriate to full-scale Reynolds numbers, a substantial improvement in effective lift/drag ratio was predicted. It appears from this and from the results of the estimates made of other changes in rotor characteristics that the overall rotor performance is sensitive to the properties of the airfoil sections selected for the blade.

It is recommended that further tests be conducted with this model to more completely cover the range of test conditions, and to include testing with two-per-rev blade pitch angle input. A comprehensive study of the effect of airfoil section on rotor performance leading to the selection of optimum rotor blade sections along the span is considered an essential step before proceeding to the development of a full scale rotor.

FAIRCHILD
REPUBLIC DIVISION

HC144R1070

This page intentionally left blank.

HC144R1070

REFERENCES

1. Staff of Fairchild Republic Division, Analytical Study of the Reverse Velocity Rotor System, Fairchild HC122R1039, October 1971.
2. W. H. Tanner, Charts fo. Estimating Rotary Wing Performance in Hover and at High Forward Speeds, NASA CR-114, November 1964.

HC144R1070

TABLE 1-I. ROTOR CHARACTERISTICS

Item	Value
Scaled Vehicle Gross Weight	400 lb
Disk Loading	8.0 lb/sq ft
Solidity	.133
Hover Tip Speed	700 ft/sec
Number of Blades	4
Rotor Radius	48.36 in.
Blade Chord (Constant)	5.0 in.
Blade Linear Twist	0
Root Cutoff/Blade Radius	.23
Flapping Inertia per Blade	2972 lb/in. ²
Flapping Moment per Blade	132 lb/in.
Torsional Inertia per Blade	5.0 lb/in. ²
Lock Number (sea level atmosphere)	2.3
Lag Hinge Offset/Rotor Radius	.065
Pitch Flap Coupling Angle - Delta-3	26.5 deg*

* Other values available were not used during this test program.

HC144R1070

TABLE 2-I. MEASURED EFFECTIVE LIFT-DRAG RATIOS
(See Figures 2.27 and 2.28)

Figure No.	Advance Ratio	Maximum L/D_E		At Disc Loading = 8 lb/sq ft	
		L/D_E	At α_{TPP}	L/D_E	At α_{TPP}
<u>Low Density</u>					
2.4	.46	6.4	5°	5.9	5°
2.5	.64	4.2	5°	3.3	5°
2.6	.87	8	10°	Not achieved	
2.7	.98	7.8	7.5°	7.0	9°
2.8	1.15	7.8	5°	7.0	8°
2.9	1.15	6.5	7.5°	6.5	7.5°
2.10	1.40	7.7	5°	7.6	7°
2.11	1.40	8.2	7.5°	8.0	7°
2.12	1.66	9.8	0	9.5	2.5°
2.13	1.75	27	5°	23	5°
2.14	2.16	18	0	18	0
2.15	2.47	12.5	0	12.5	0
<u>High Density</u>					
2.16	.29	7.8	-2°	7.8	-4°
2.17	.46	8.2	5°	8	4°
2.18	.57	7.4	0	6.8	5°
2.19	.72	5.8	5°	5.8	8°
2.20	.82	5.6	5° & 10°	5.4	8°
2.21	.94	7.2	5°	7.0	8°
2.22	1.00	No drag results			
2.23	1.15	7.0	5°	Not achieved	
2.24	1.50	10.6	0°	9.2	2°

HC144R1070

**TABLE 2-II. TEST CONDITIONS FOR ZERO TORQUE
AND 1G LIFT-COEFFICIENT**

Figure Number	Run Number	Pressure (in. Hg.)	μ	θ_o (deg)	α_{TPP} (deg)
2.6	35/36	12	.87	2	13
2.10	43	12	1.40	3.5	11
2.12	47	12	1.66	2	8.5
2.13	44	12	1.75	1	6
2.14	48	12	2.16	0.5	2
2.16	50	30	.29	1.5	8
2.17	51	30	.46	2.9	7
2.18	52	30	.57	4.5	6
2.19	57	30	.72	4	7.5
2.20	56	30	.82	5	9

HC144R1070

**TABLE 5-I COMPARISON OF ROTOR CHARACTERISTICS
PHASE I STUDY VS. PHASE II MODEL**

Characteristic	Phase I Study	Phase II Model
Radius - inches	338	48.38
Chord - inches	35.2	5.00
Root cutout - non dim.	.150	.232
Root airfoil thickness ratio - non dim.	.150	.180
Tip airfoil thickness ratio - non dim.	.060	.060
Twist angle - deg.	0	0
Number of blades	4	4
Solidity - non dim.	.133	.133
Normal tip speed - ft/sec	700	700
Normal disk loading - lb/sq ft	8	8
Flap hinge offset* - non dim.	0	.065
Flapping inertia per blade lb/in ²	16.54x10 ⁶	2972
Flapping moment lb/in	75,000	132
Flapping root spring, non dim.	2.48x10 ⁶	0
Lock number per blade	6.0	2.3
Delta - 3 - degrees	0	26.5
Flap frequency at normal tip speed - non dim.	1.05	1.07
Aerodynamic data assumptions:		
Number of spanwise stations	2	5
Thickness - chord ratio at stations	12%	16.8%
	7%	14.4%
		12.0%
		9.6%
		7.2%
Maximum lift coefficient in radial flow option	3.5	2.5
Atmospheric conditions:		
Altitude - feet	3000	Sea level
Temperature - °F	91.5	59
Density - slugs/ft ³	.001998	.002378
Speed of sound - ft/sec	1150	1117

* The Phase I rotor was hingeless simulated by a flapping spring at a zero offset hinge. The Phase II rotor is fully articulated.

FAIRCHILD
REPUBLIC DIVISION

HC144R1070

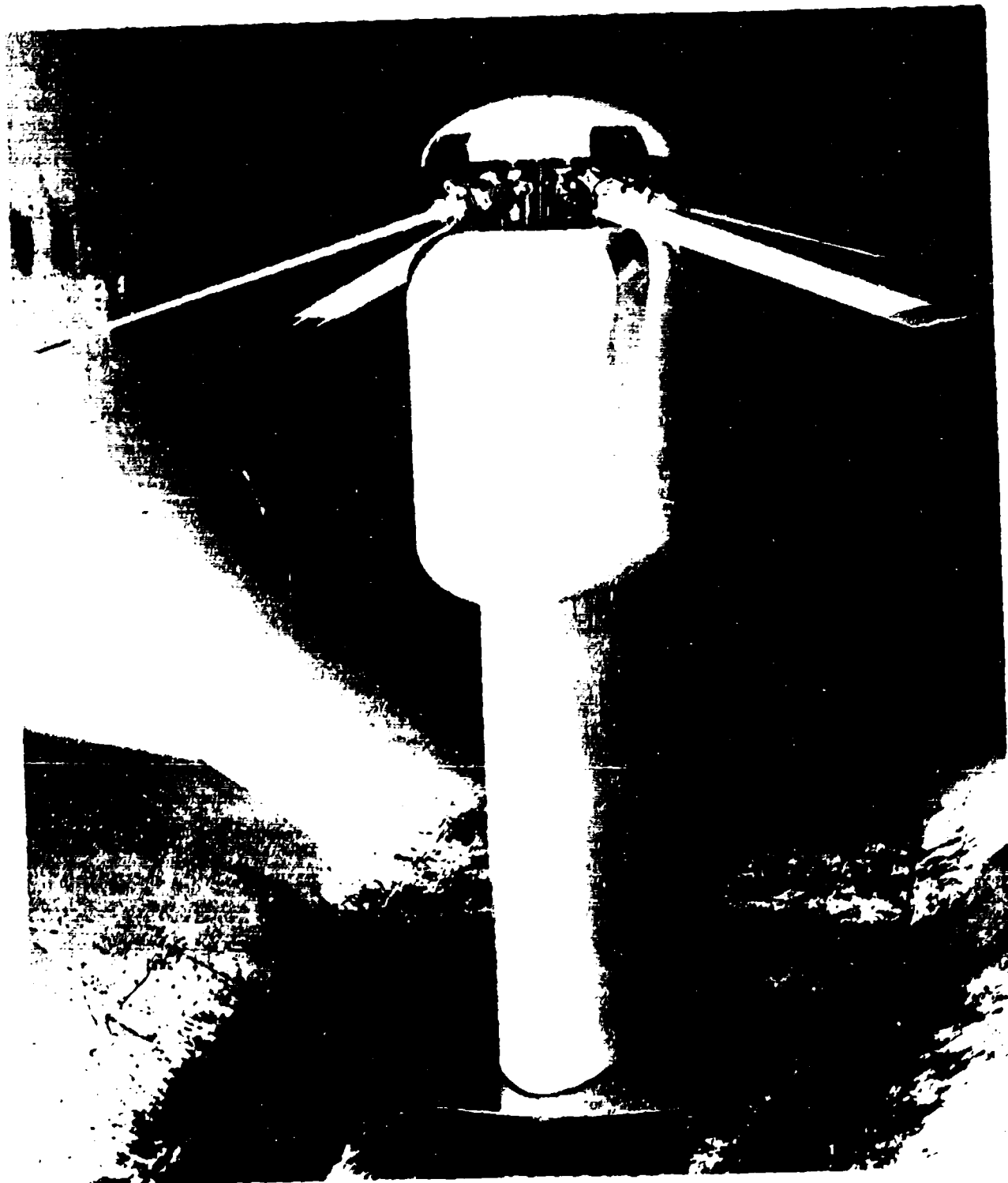
This page intentionally left blank.

FAIRCHILD
AERONAUTICAL DIVISION

HC144R1070

Figure 1.1

INSTALLATION OF REVERSE VELOCITY ROTOR TEST RIG
IN NASA AMES 12 FT PRESSURE TUNNEL

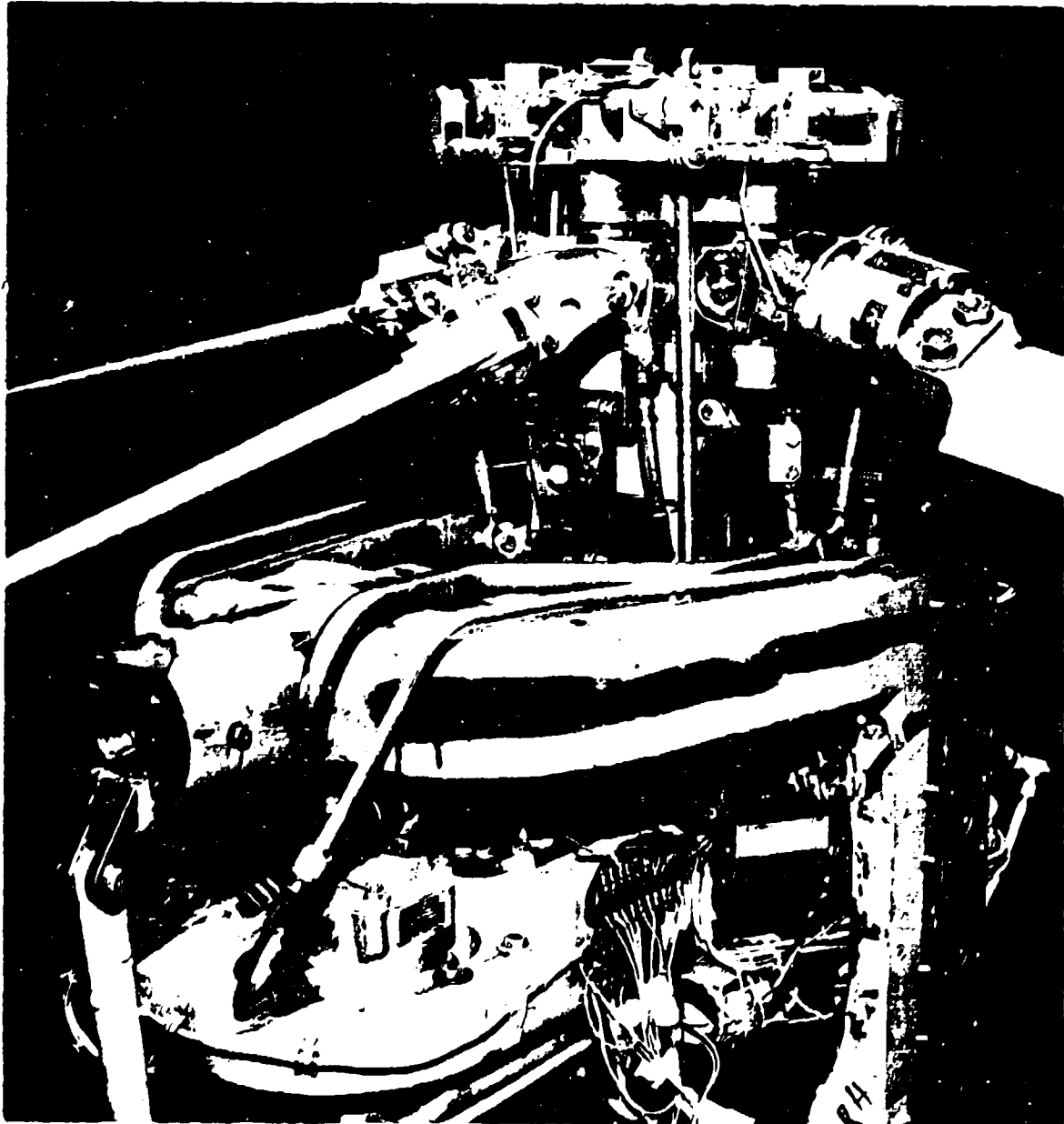


FAIRCHILD
HELICOPTER DIVISION

HC144R1070

Figure 1.2

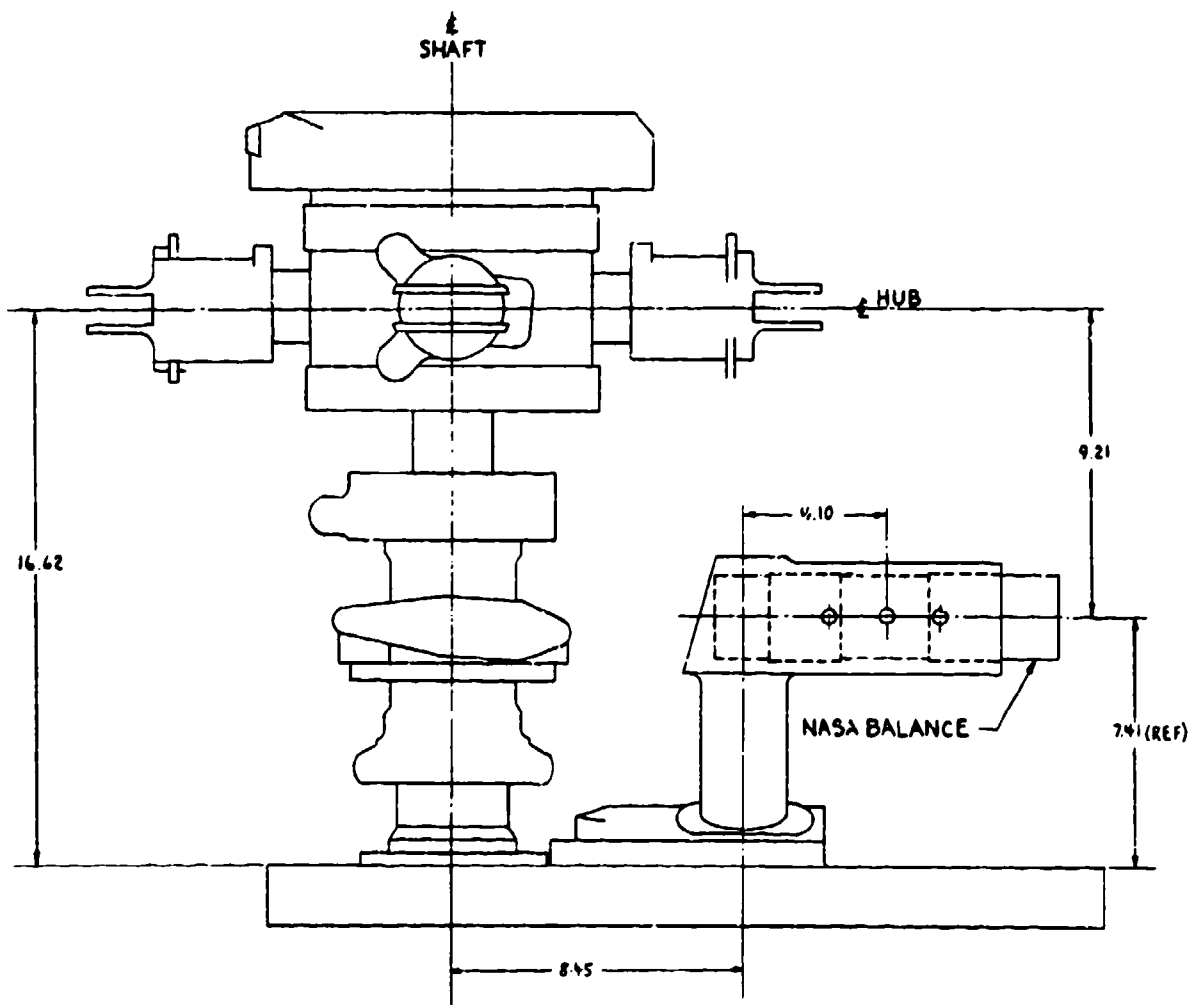
THREE-QUARTER REAR VIEW OF REVERSE VELOCITY ROTOR TEST RIG
(Fairing Removed)



HC144R1070

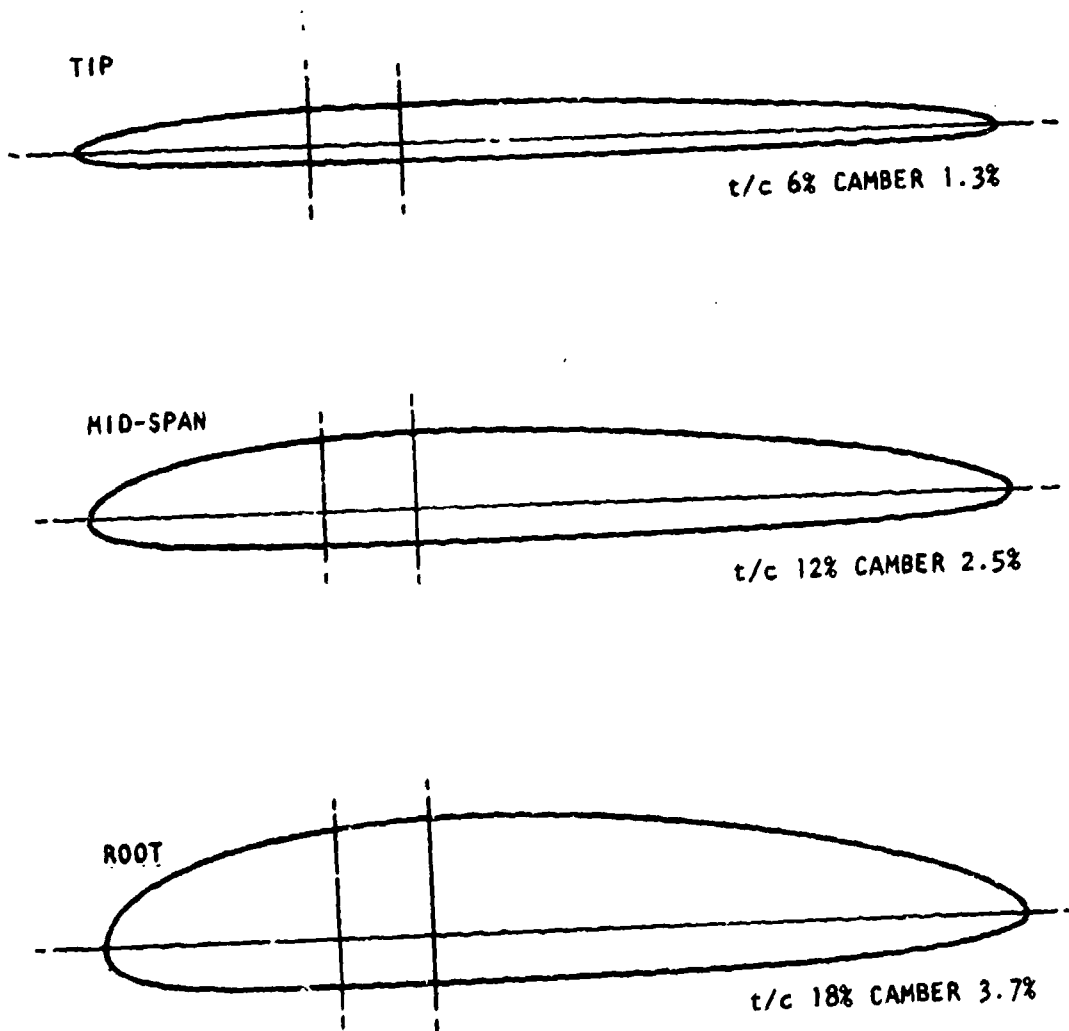
Figure 1.3

REVERSE VELOCITY ROTOR TEST RIG - GEOMETRIC LAYOUT



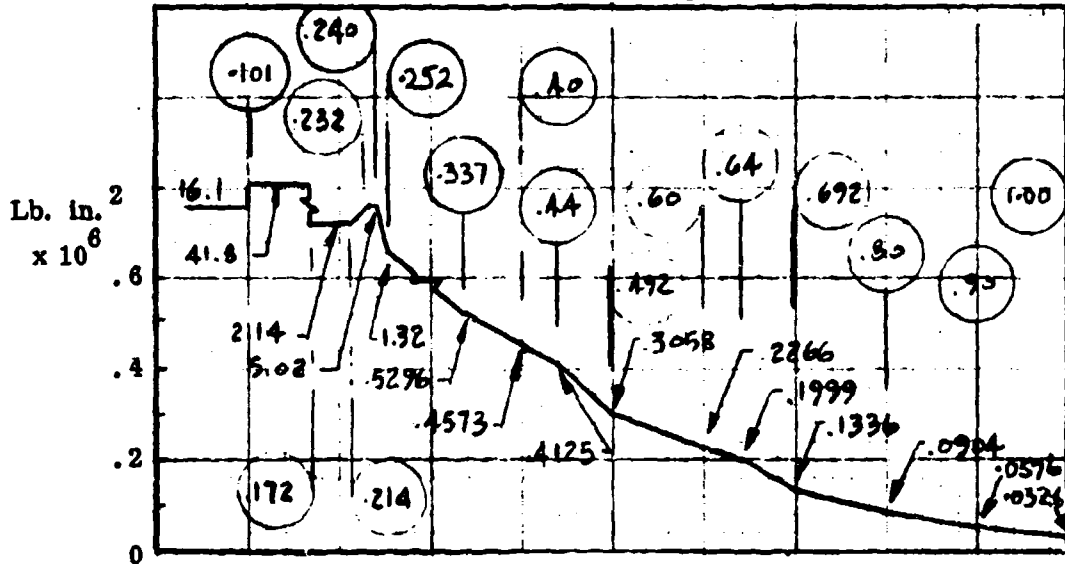
HC144R1070

MODEL ROTOR AIRFOIL SECTIONS

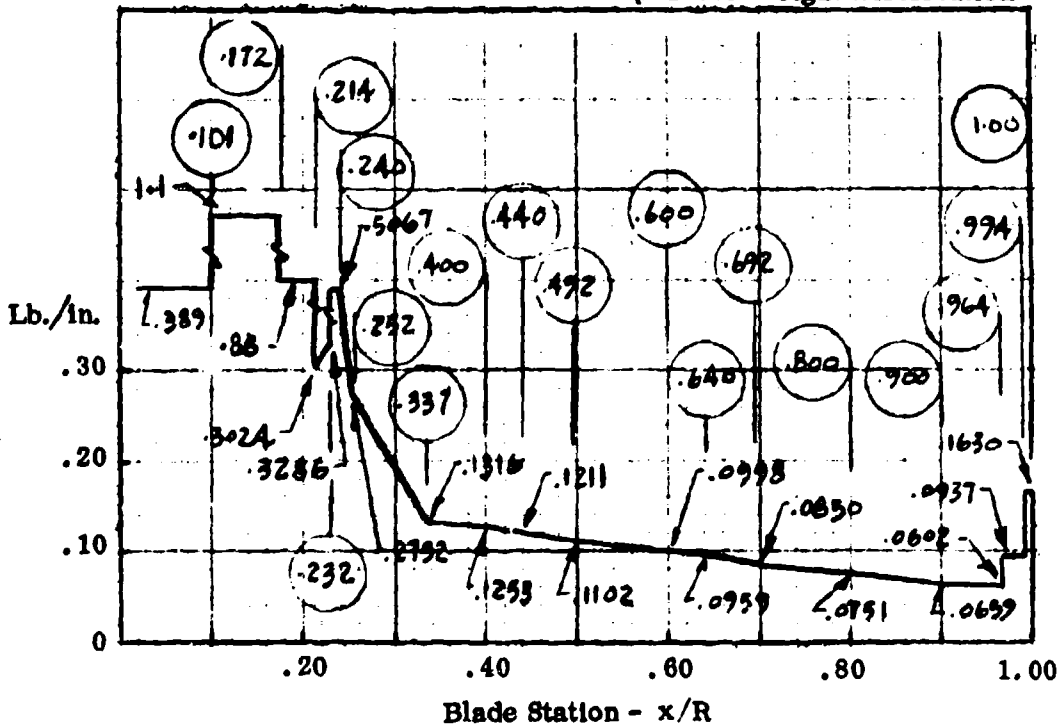


**SECTION PROPERTIES - 1/7 SCALE MODEL
RVR ROTOR BLADE**

Flapwise Stiffness Distribution

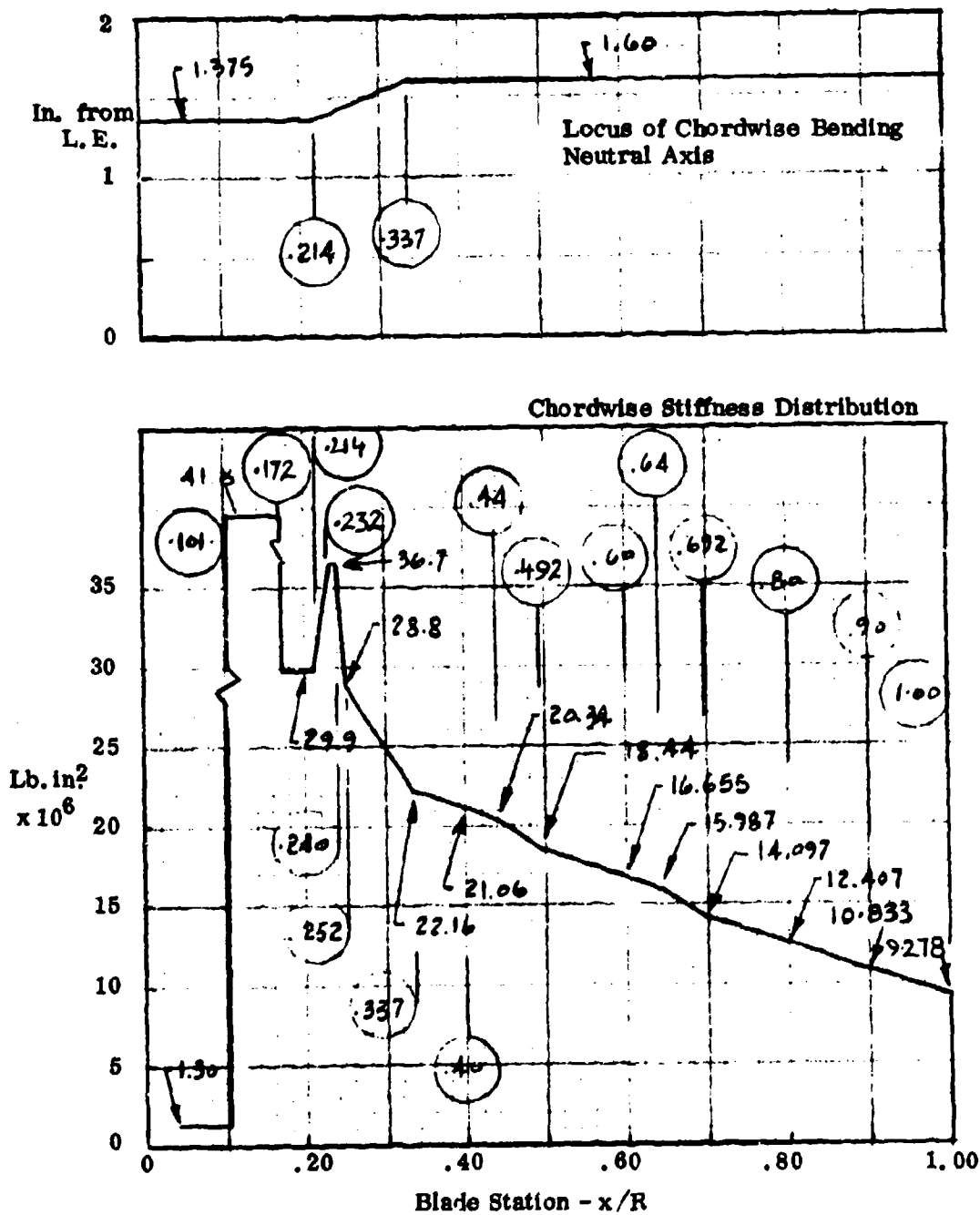


Spanwise Weight Distribution



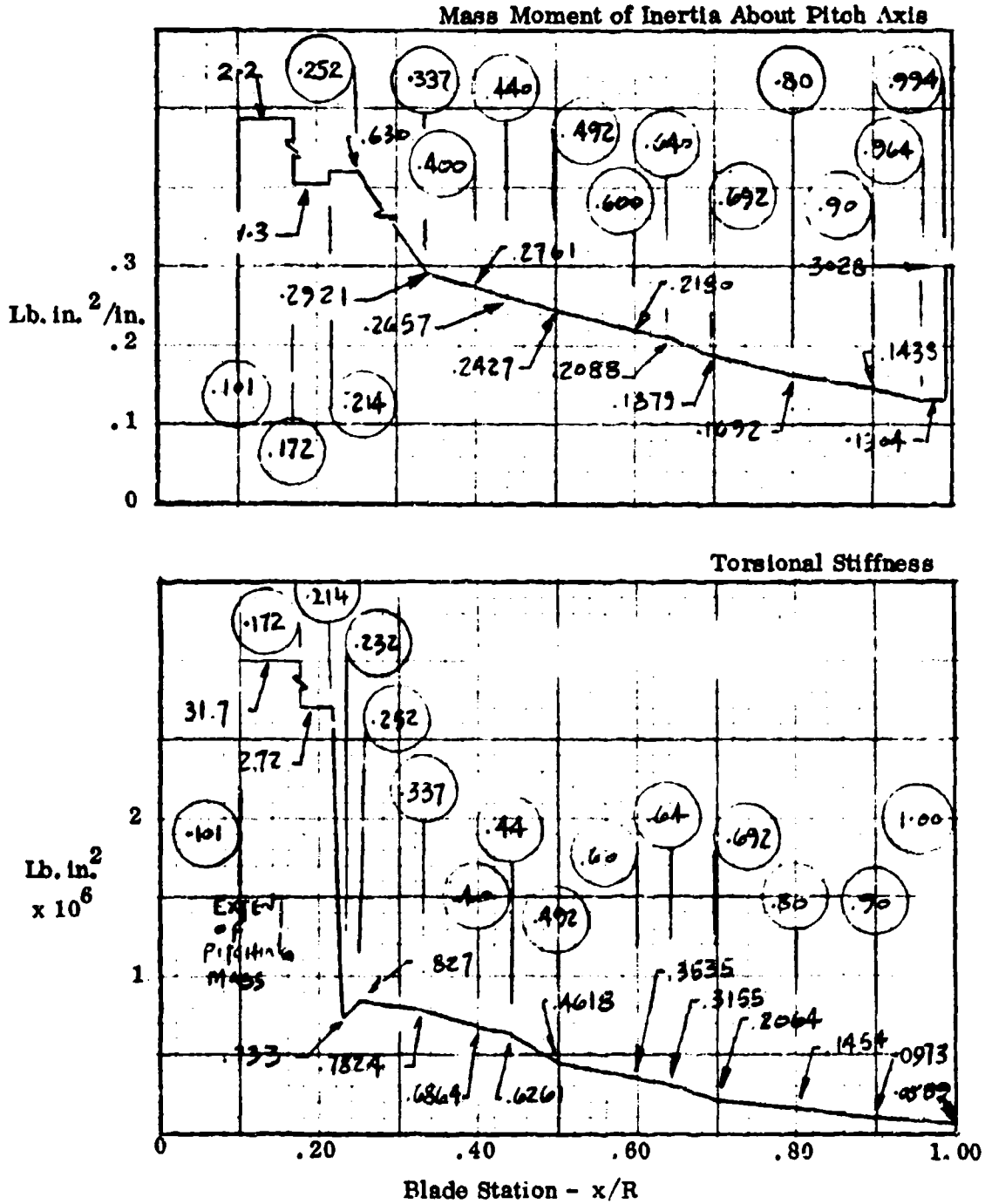
HC144R1070

**SECTION PROPERTIES - SCALE MODEL
RVR ROTOR BLADE (CONTINUED)**



HC144R1070

**SECTION PROPERTIES - SCALE MODEL
RVR ROTOR BLADE (CONCLUDED)**

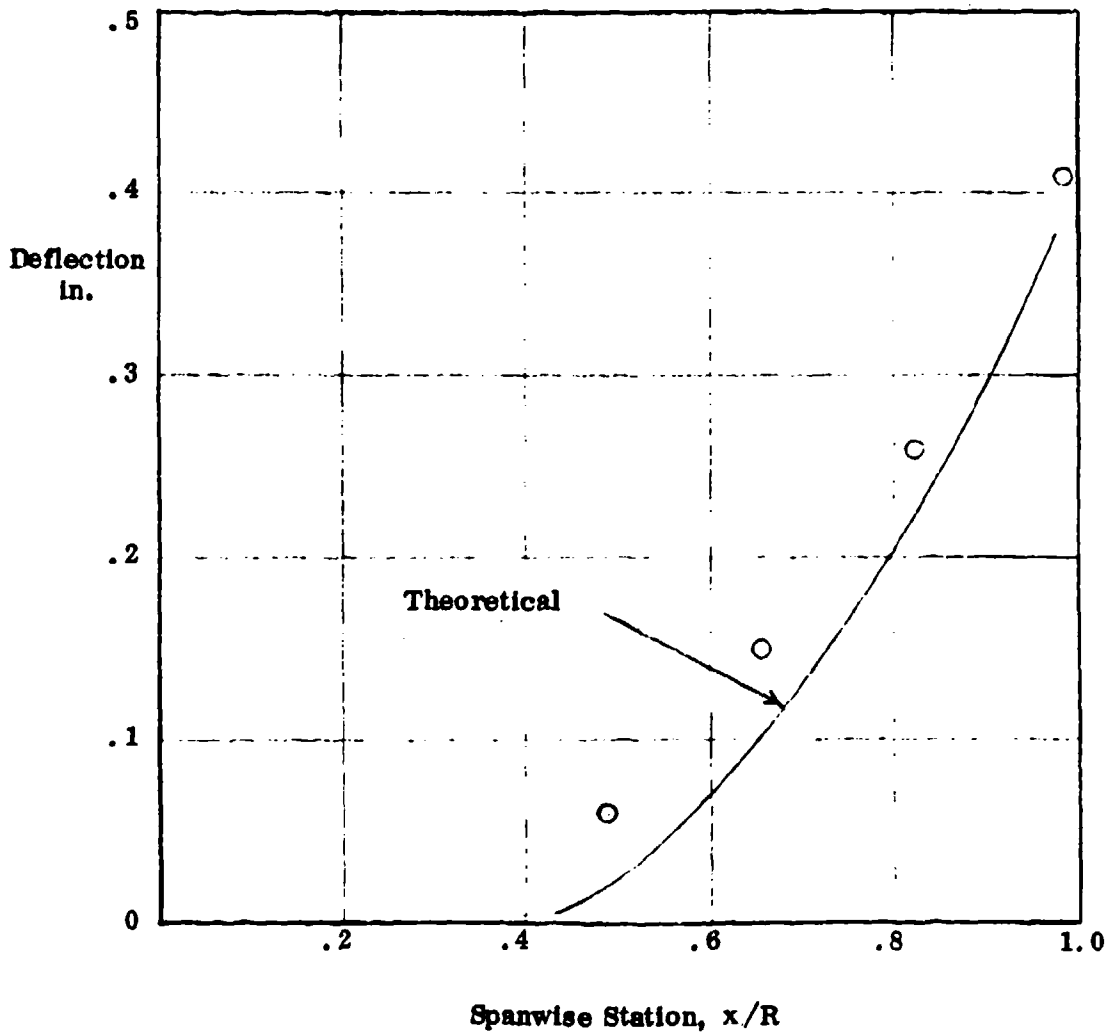


HC144R1070

**PREDICTED AND MEASURED FLAPWISE STIFFNESS
1/7 SCALE MODEL RVR ROTOR BLADE**

Deflection with 10 lbs load applied at .95 radius

○ = Measured, qualification blade

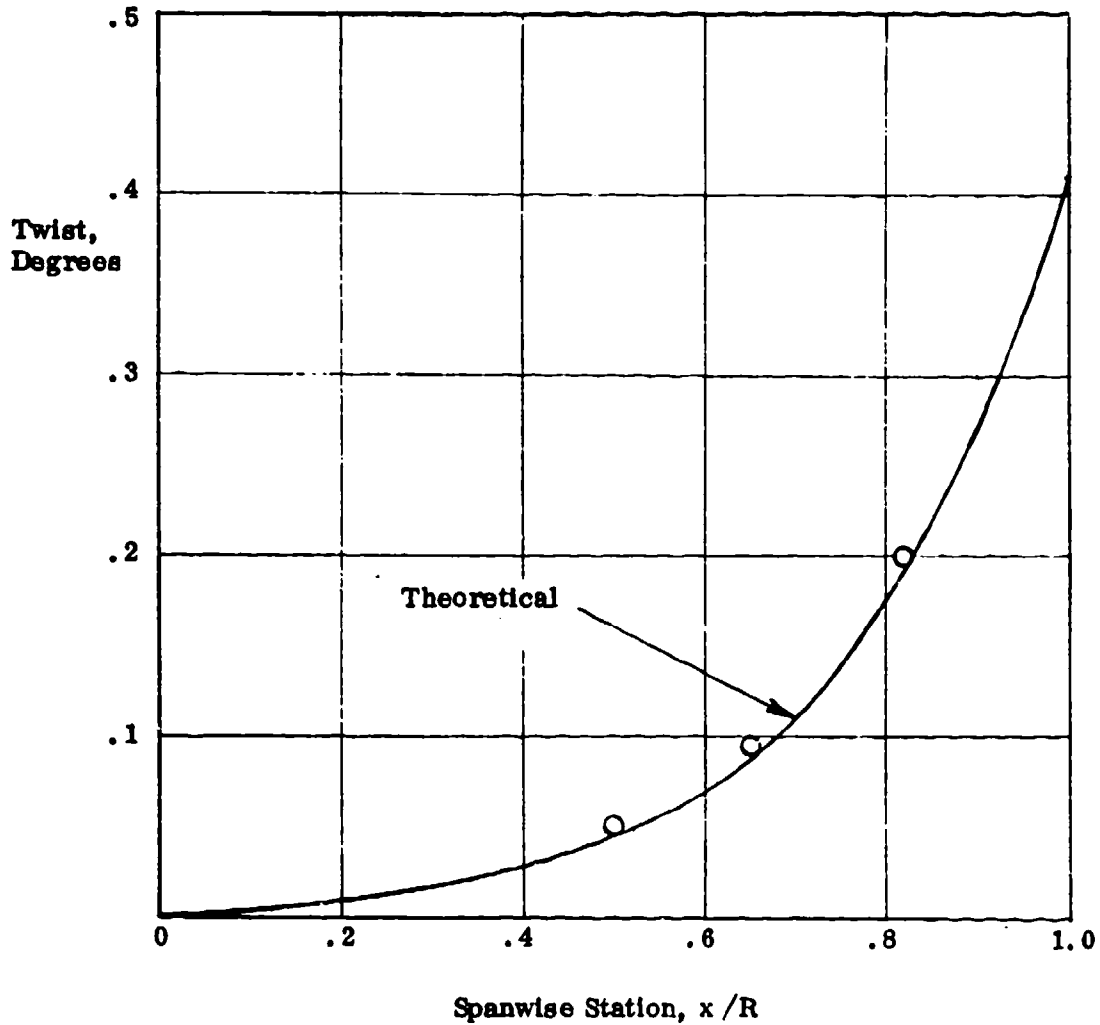


HC144R1070

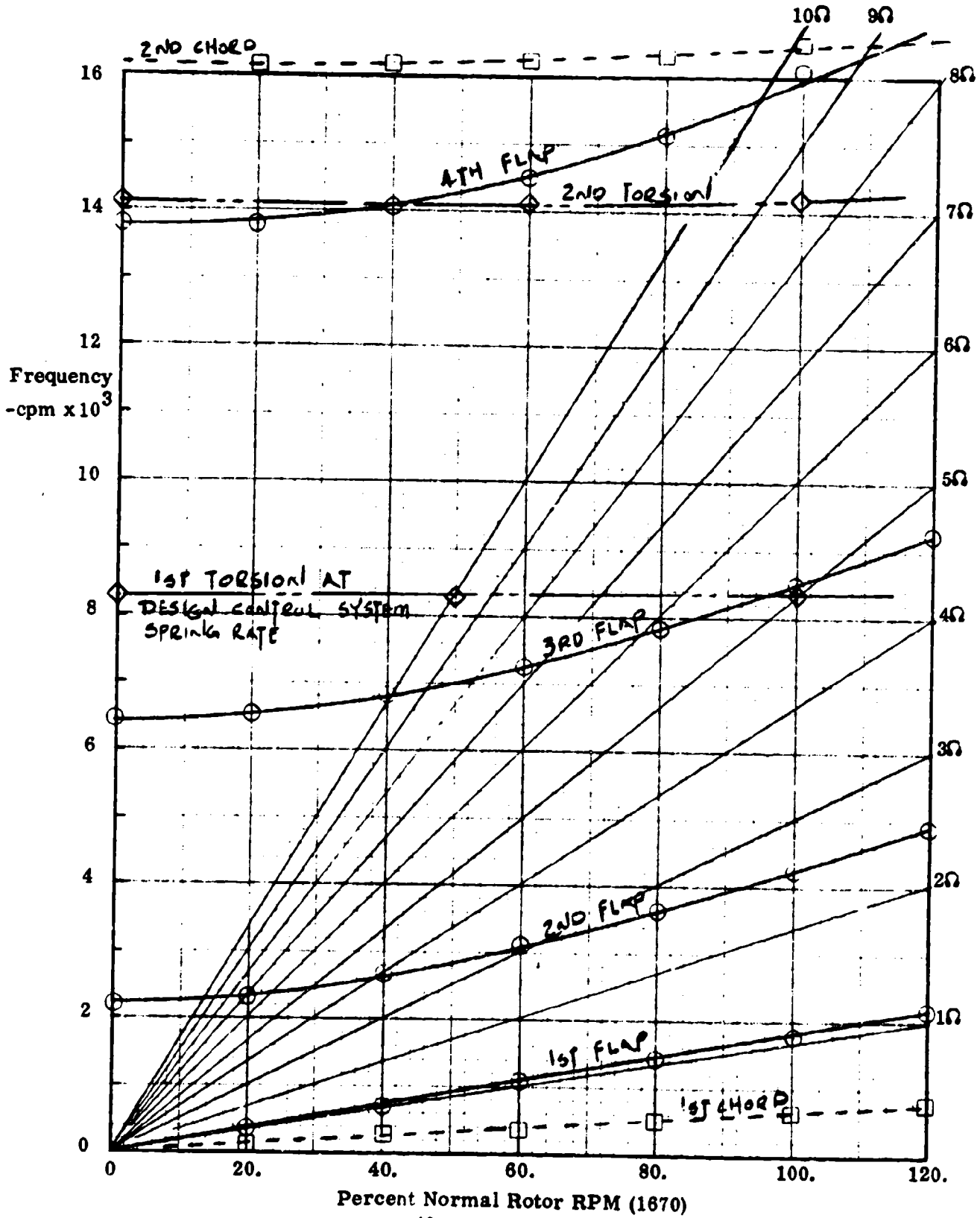
**PREDICTED AND MEASURED TORSIONAL STIFFNESS
1/7 SCALE MODEL RVR ROTOR BLADE**

Deflection with 100 in. lb. torque applied at .95 radius

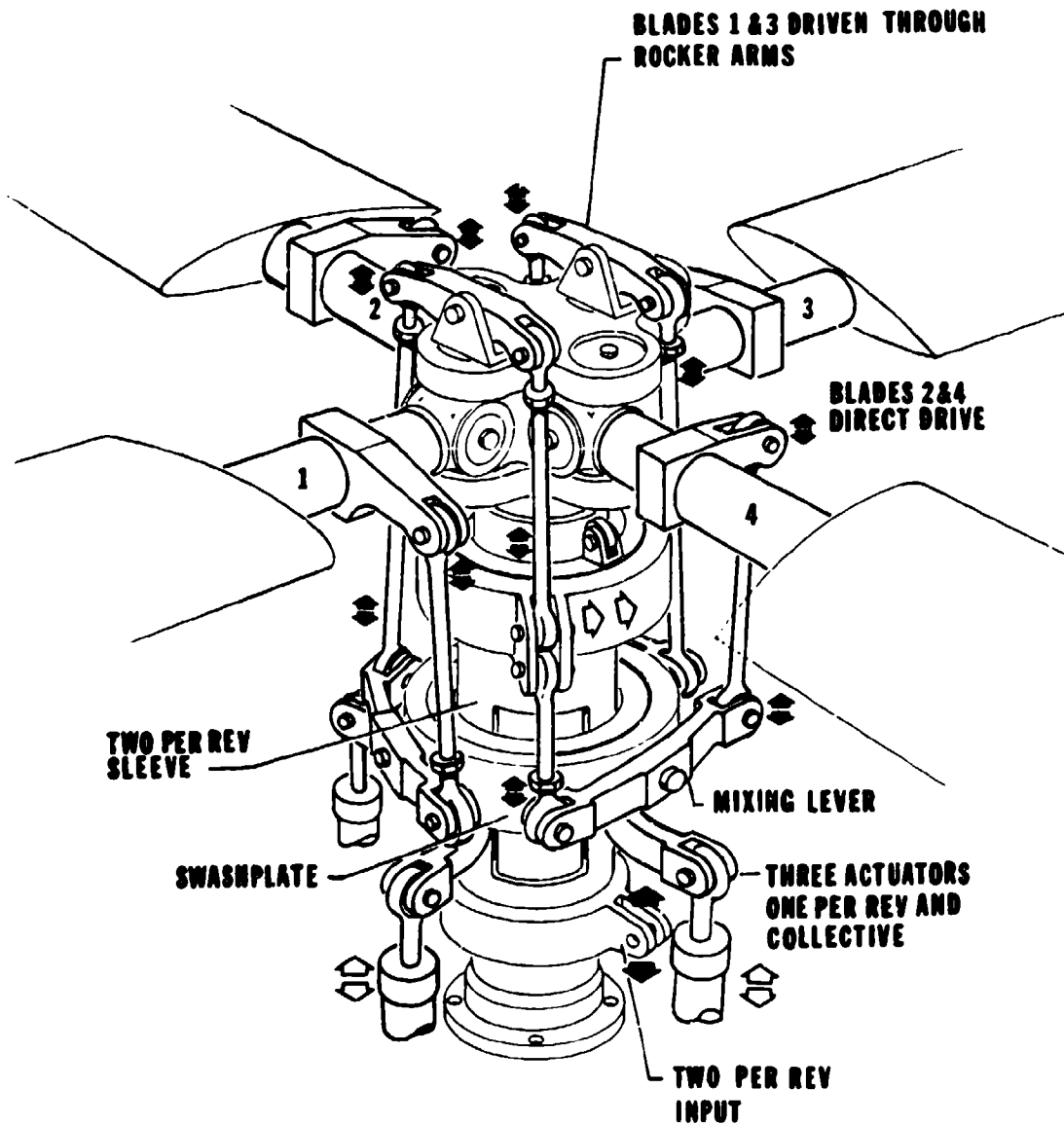
○ = Measured, qualification blade



NATURAL FREQUENCY SPECTRUM - 1/7 SCALE MODEL
RVR ROTOR BLADE



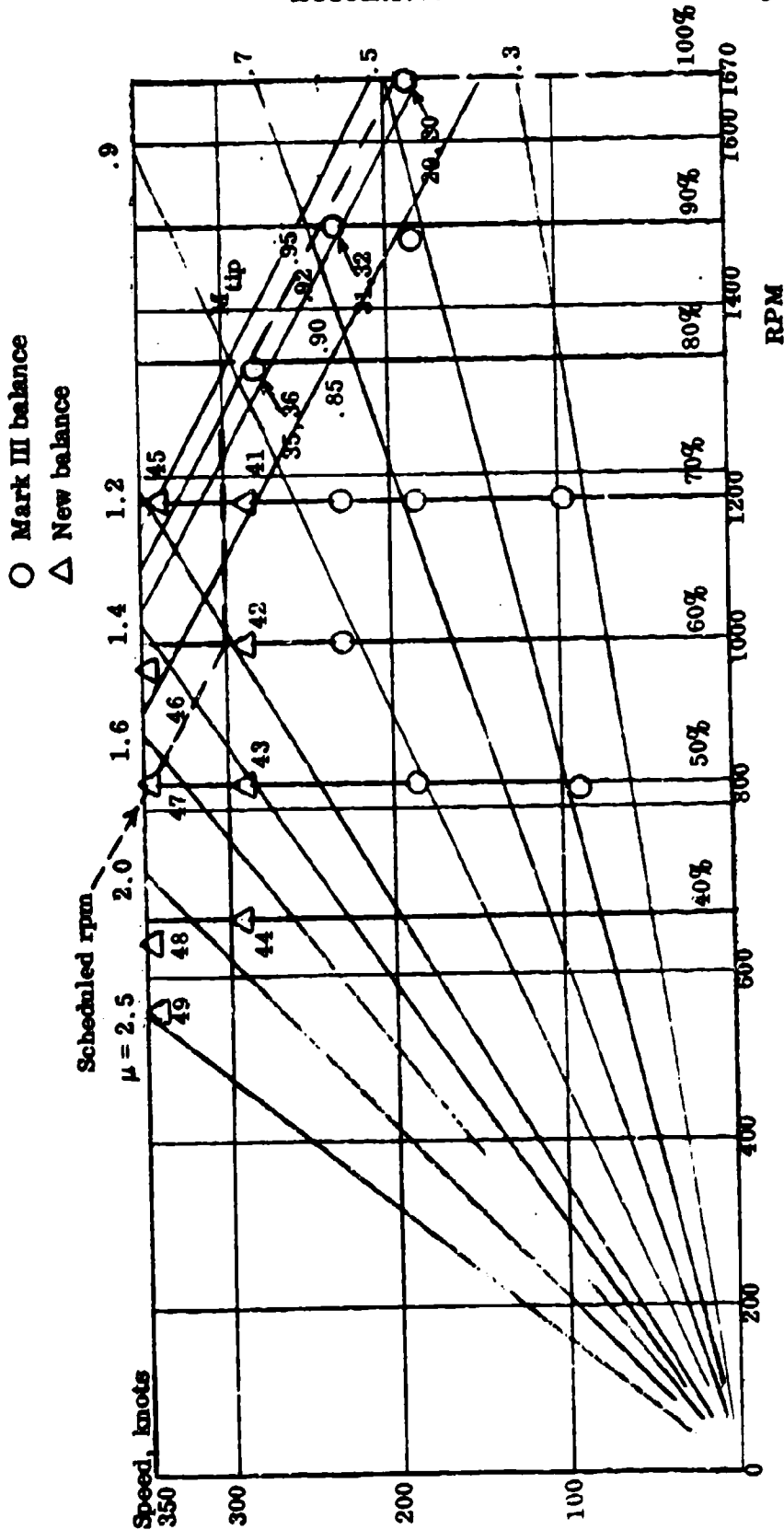
CONTROL SYSTEM 1/7 SCALE R.V.R MODEL



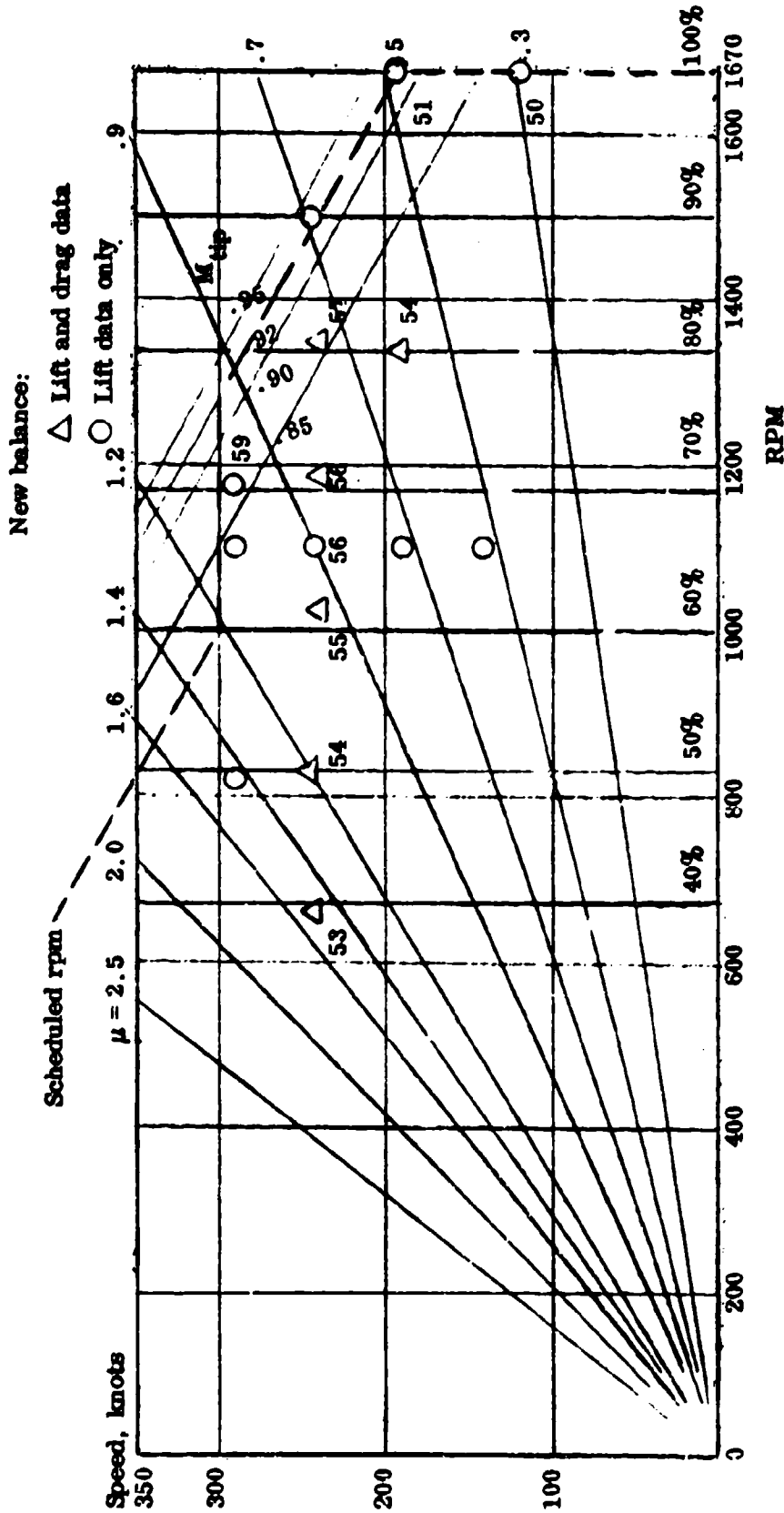
HC144R1070

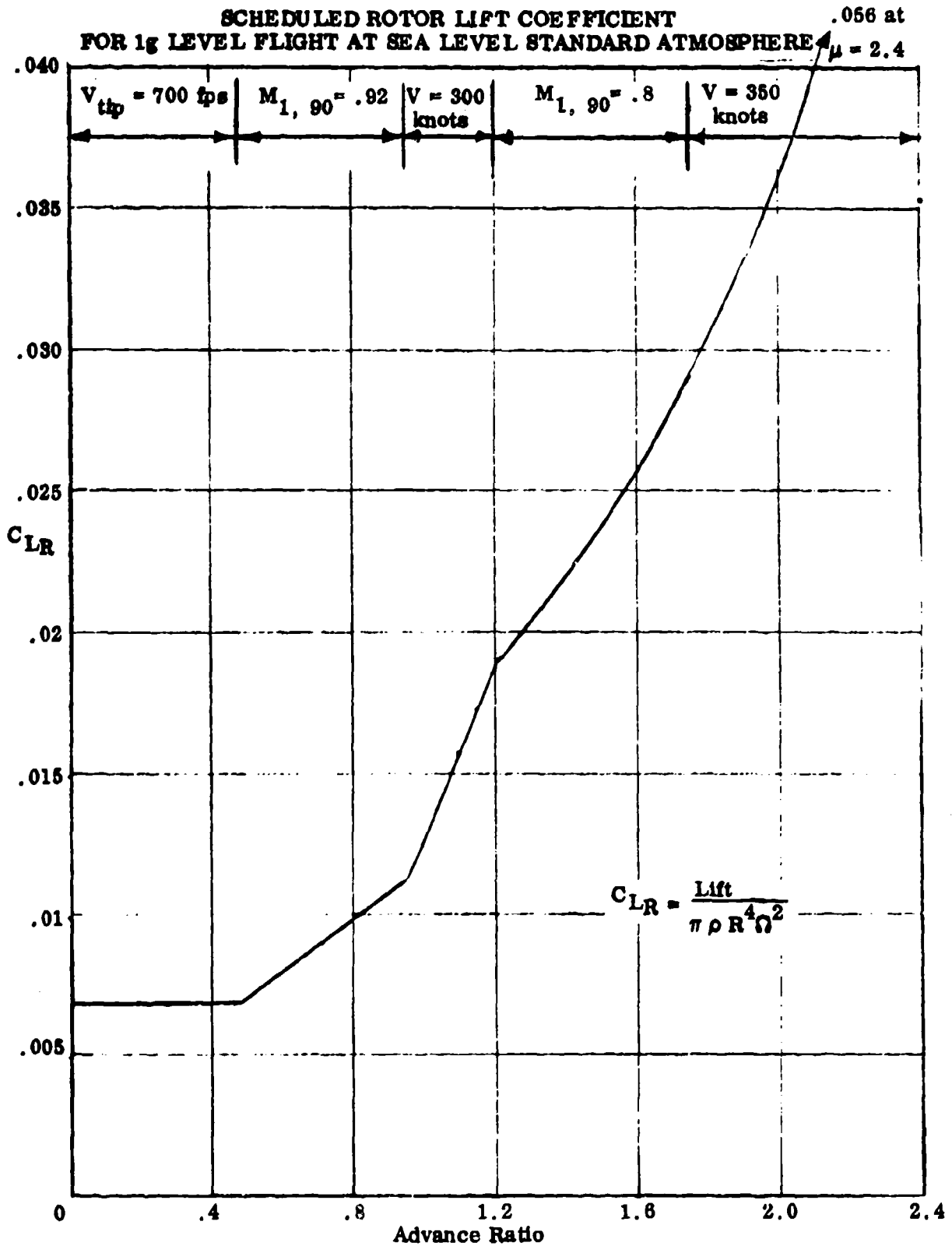
Figure 1.13

OPERATING ENVELOPE AND TEST CONDITIONS - REDUCED PRESSURE

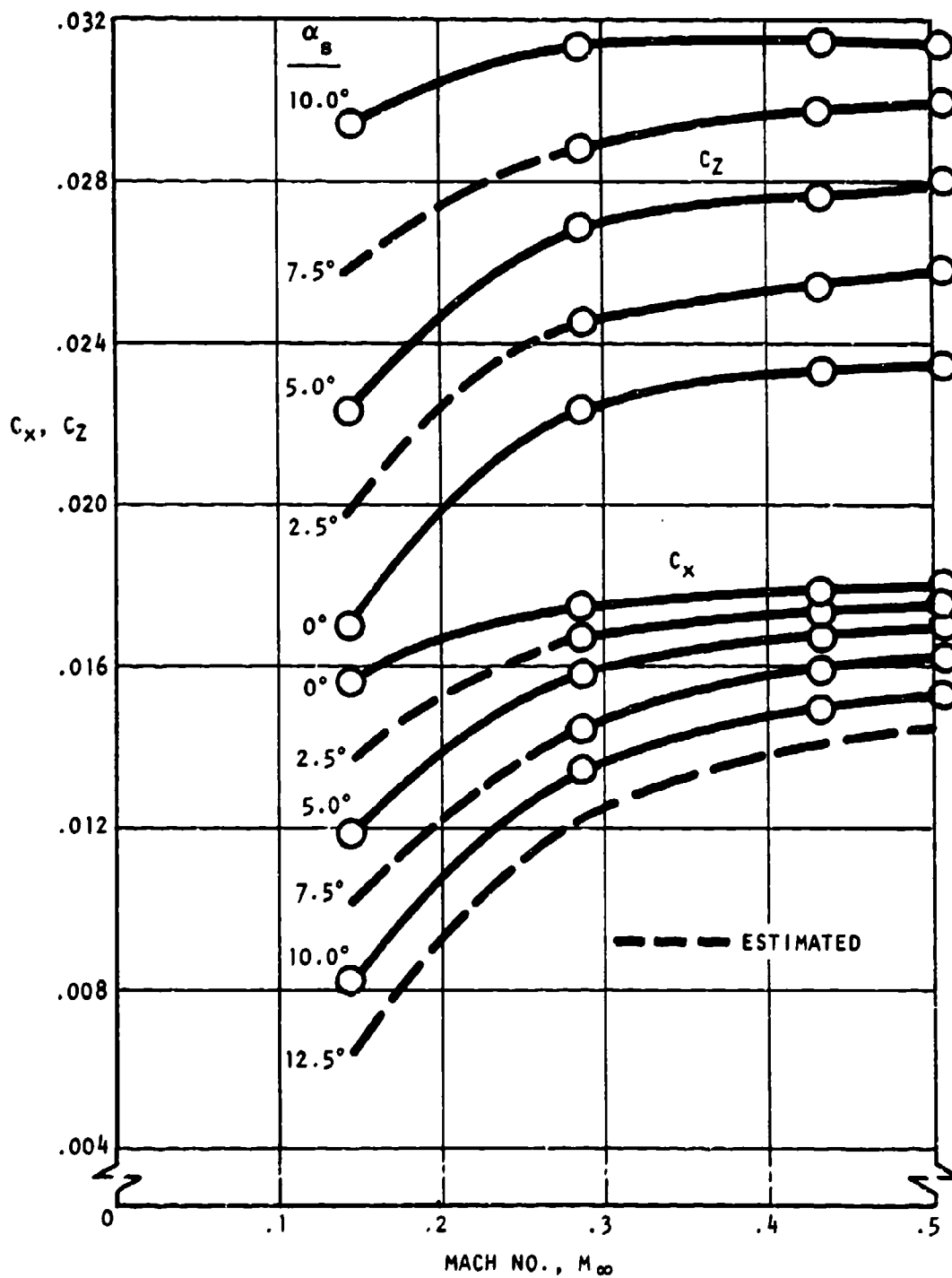


OPERATING ENVELOPE AND TEST CONDITIONS - ATMOSPHERIC PRESSURE

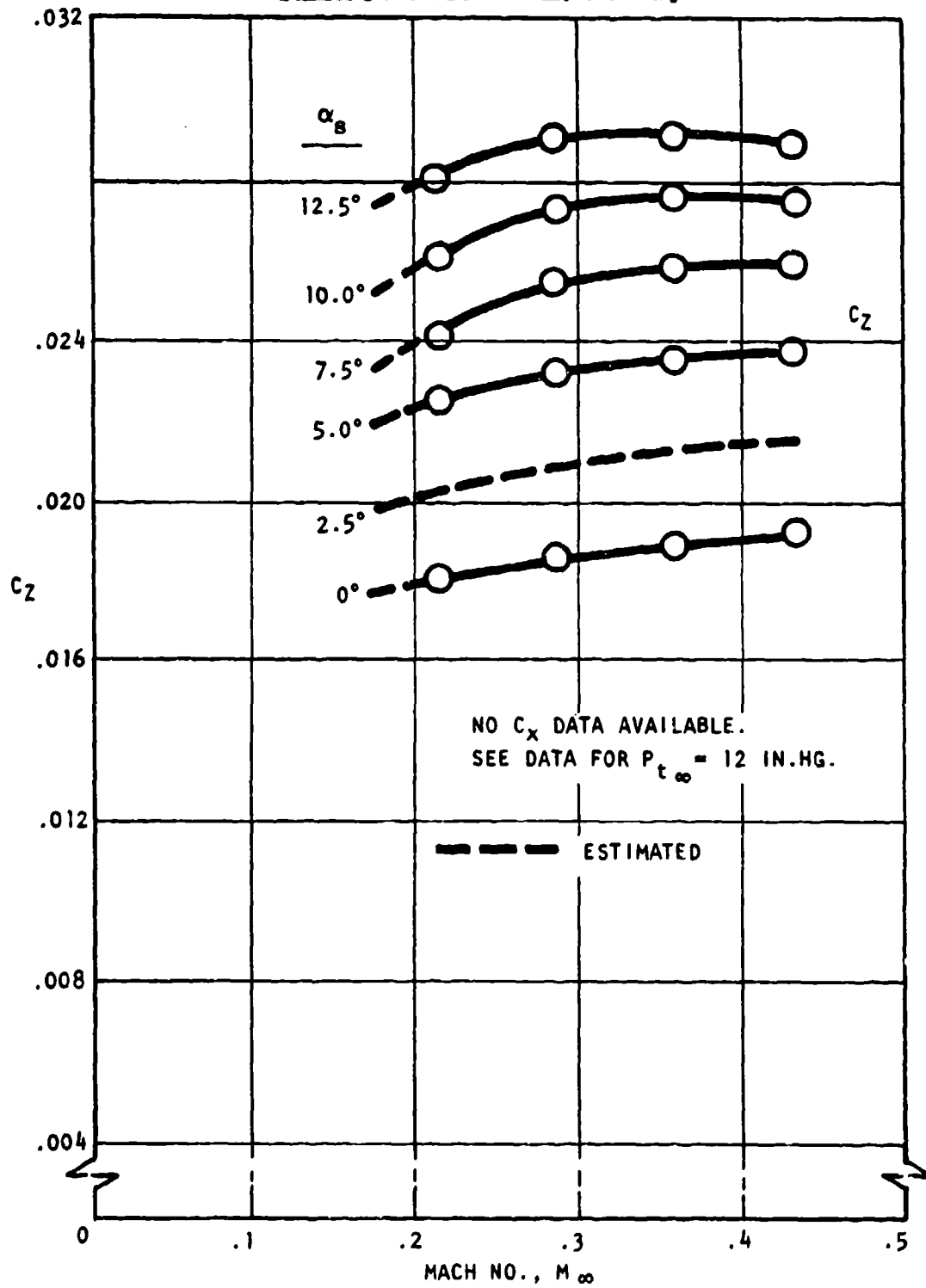




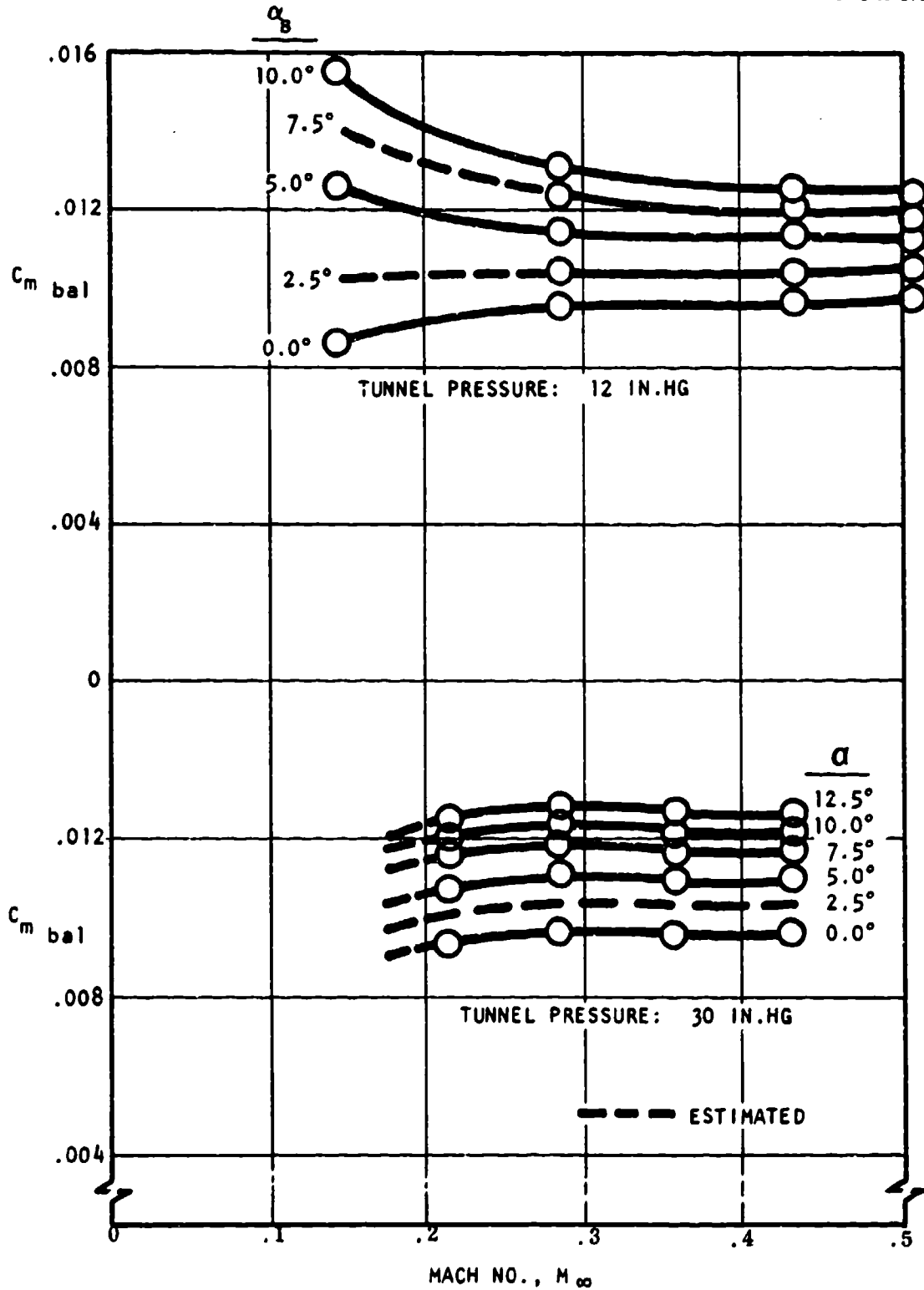
HUB TARE CORRECTIONS TO NORMAL AND AXIAL FORCE COEFFICIENTS
Tunnel Pressure - 12 in. Mercury



HUB TARE CORRECTIONS TO NORMAL FORCE COEFFICIENT
Tunnel Pressure - 30 in. Mercury



HUB TARE CORRECTIONS TO BALANCE PITCHING MOMENT COEFFICIENT



FAIRCHILD
REPUBLIC DIVISION

HC144R1070

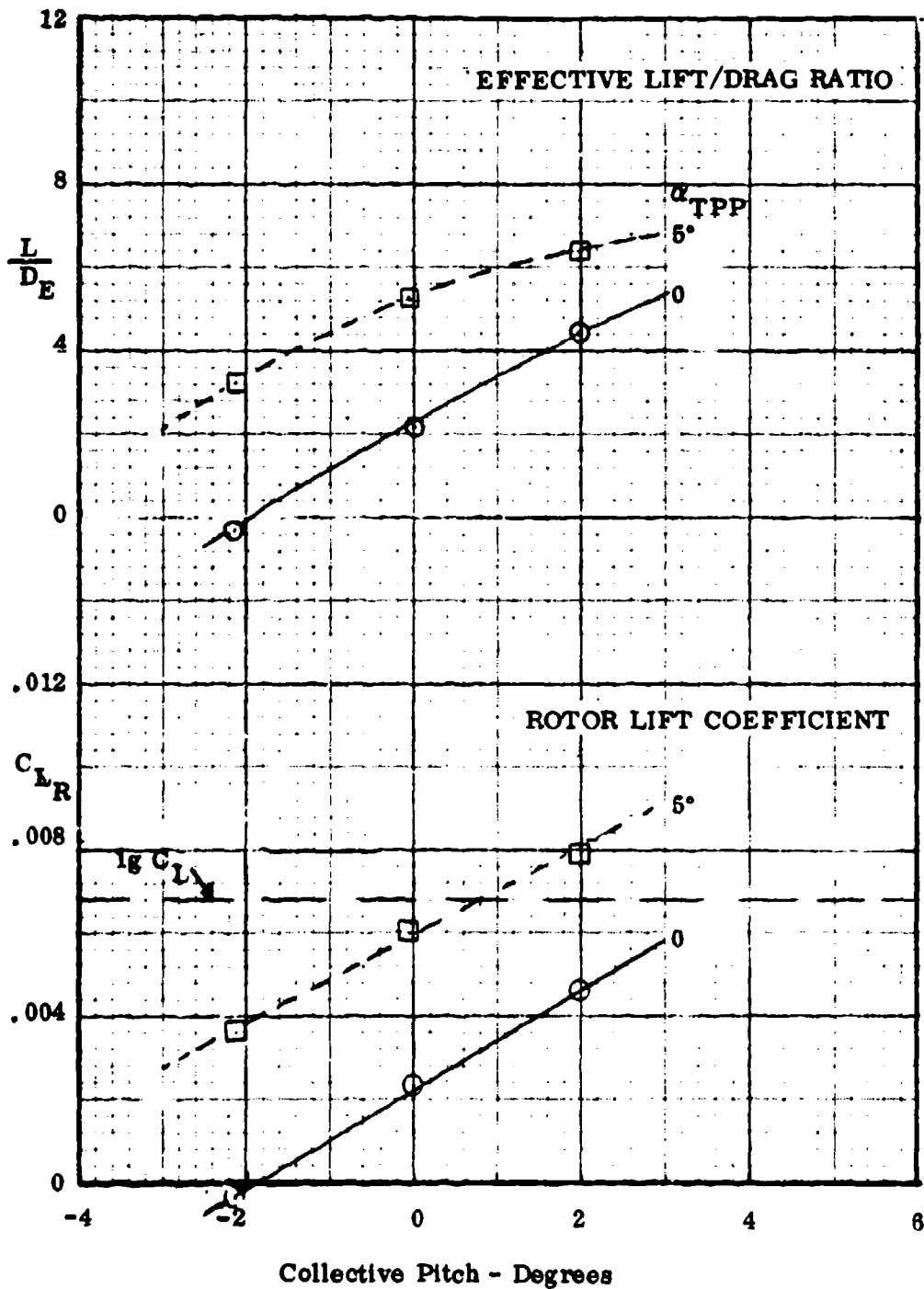
This page intentionally left blank.

HC144R1070

Figure 2.4A

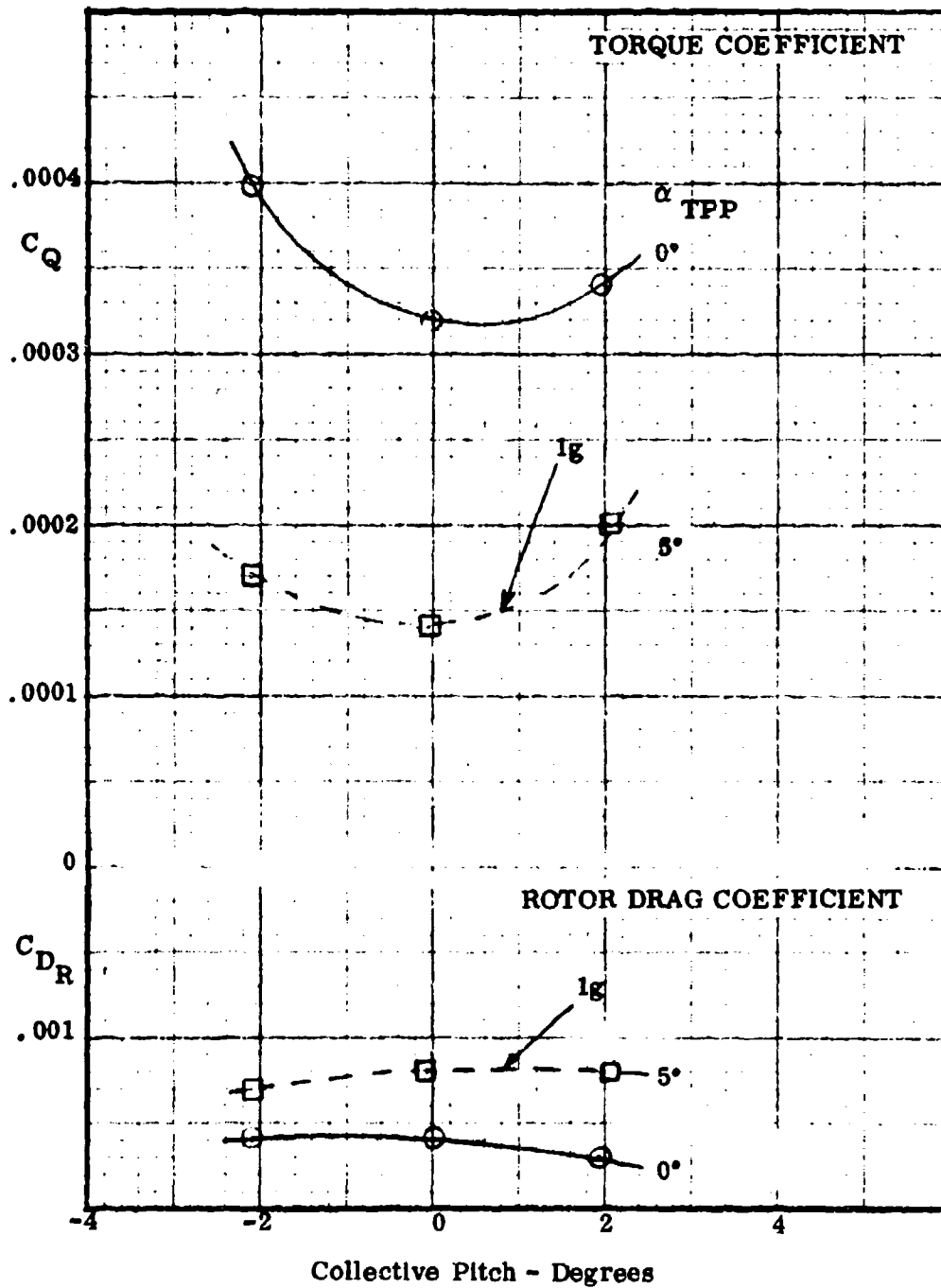
MEASURED ROTOR PERFORMANCE

$\mu = .46$, 1670 r.p.m., 187 knots, $M_{1,90} = .89$, $\rho = .00090$, runs 29&30



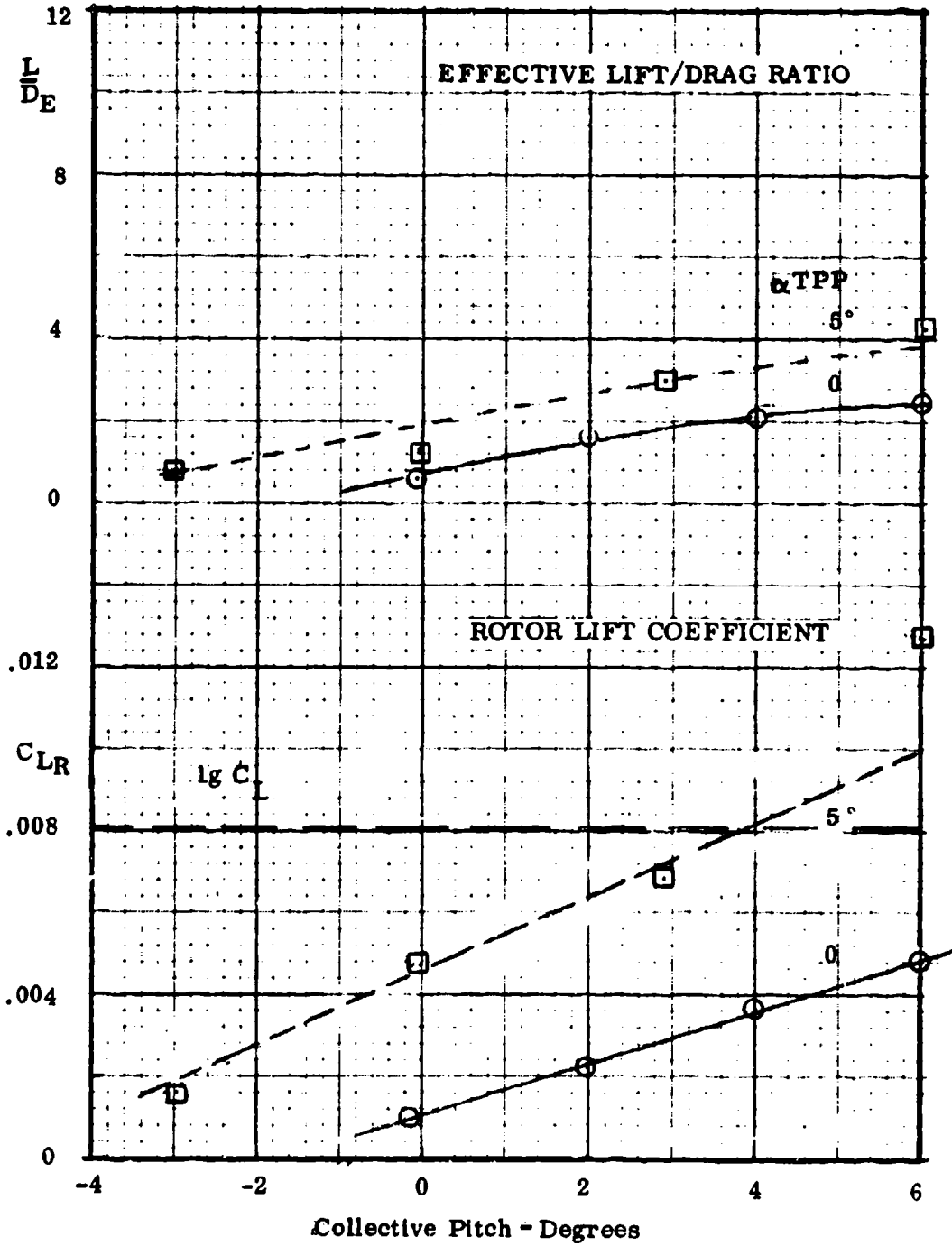
MEASURED ROTOR PERFORMANCE

$\mu = .46$, 1670 r.p.m., 187 knots, $M_{1,50} = .89$, $\rho = .00090$, runs 29&30



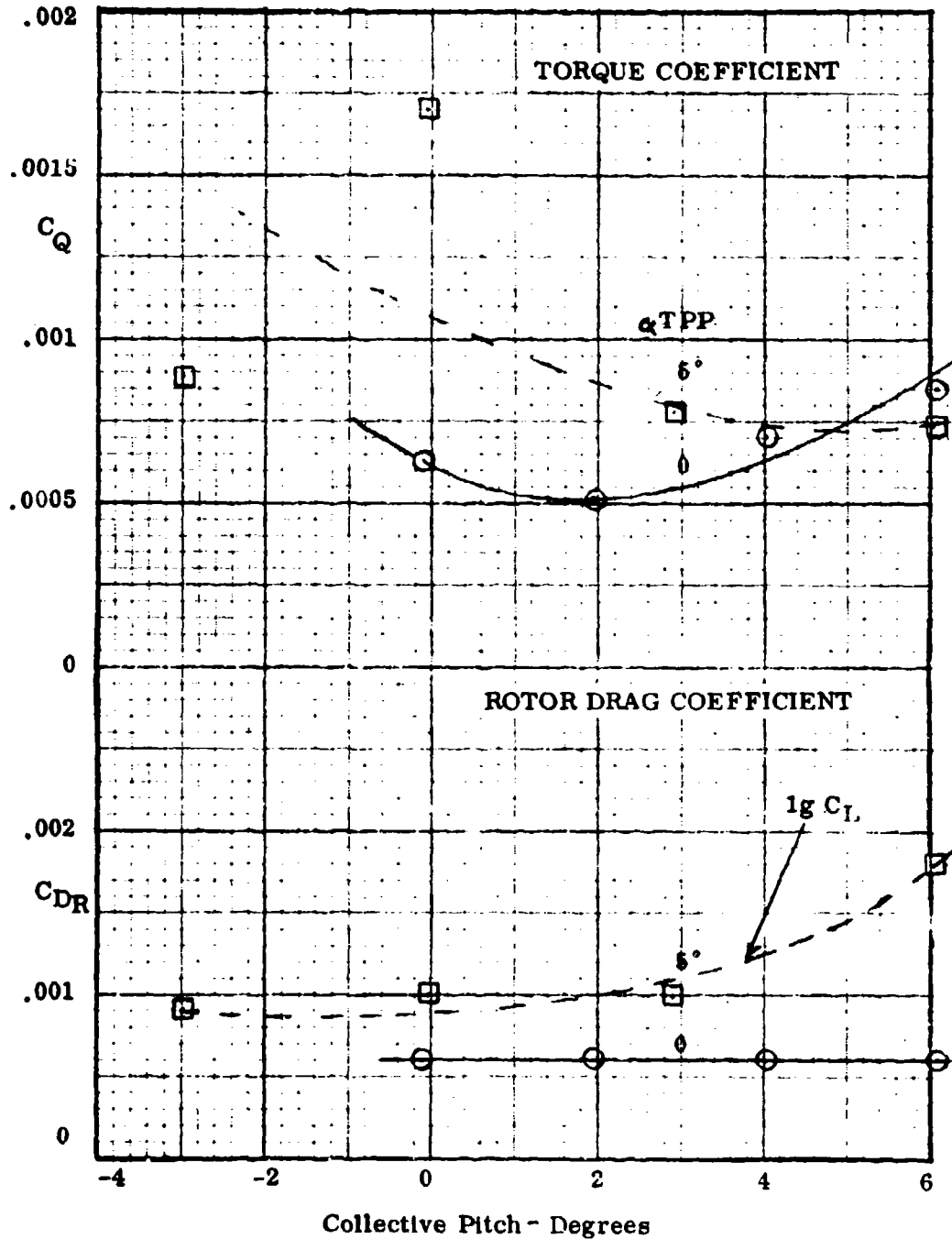
MEASURED ROTOR PERFORMANCE

$\mu = .64$, 1500 r.p.m., 230 knots, $M_{1,90} = .90$, $\rho = .00089$, runs 31 & 32



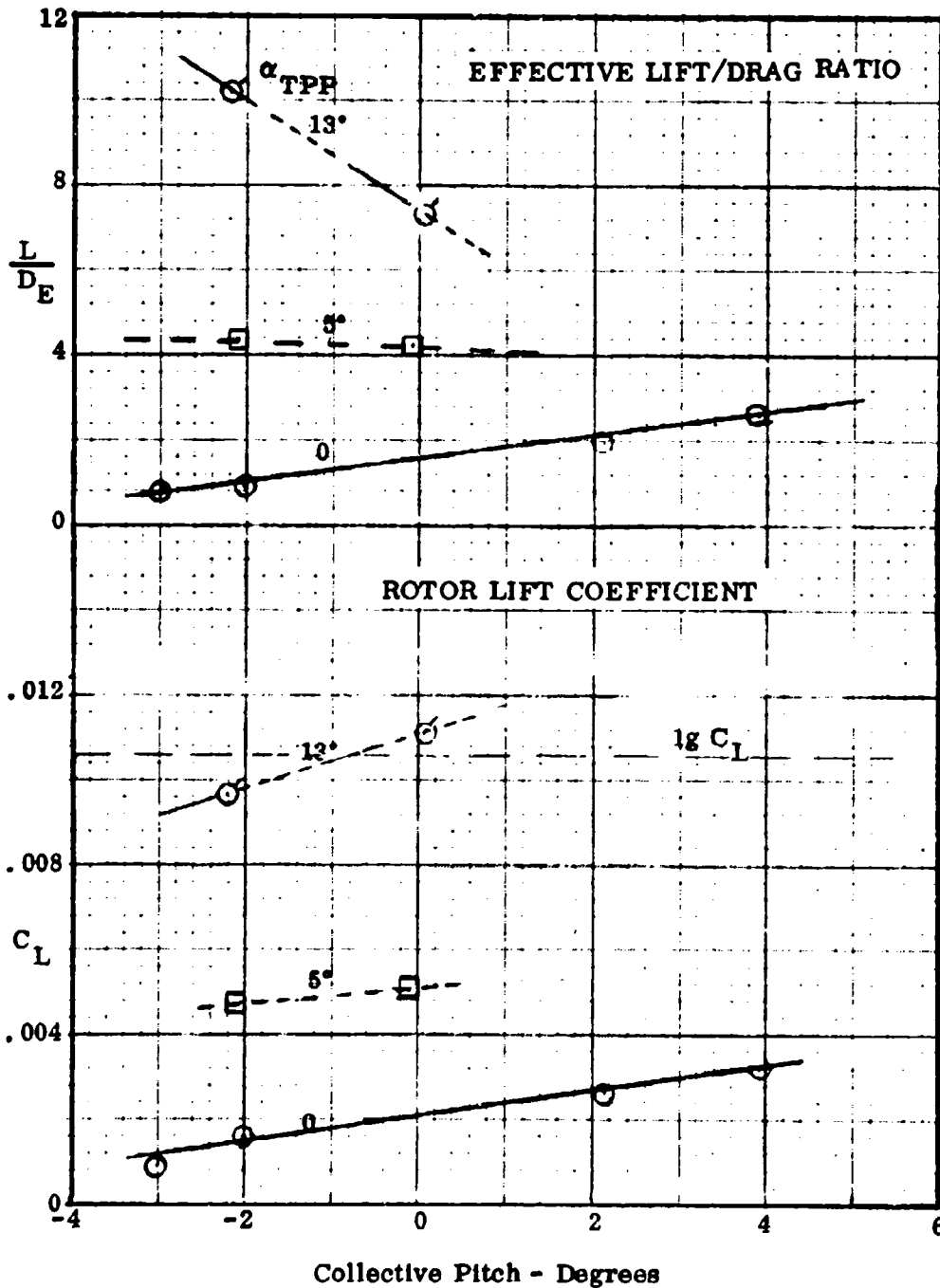
MEASURED ROTOR PERFORMANCE

$\mu = .64$, 1500 r.p.m., 230 knots, $M_{1,90} = .90$, $\rho = .00089$, runs 31 & 32



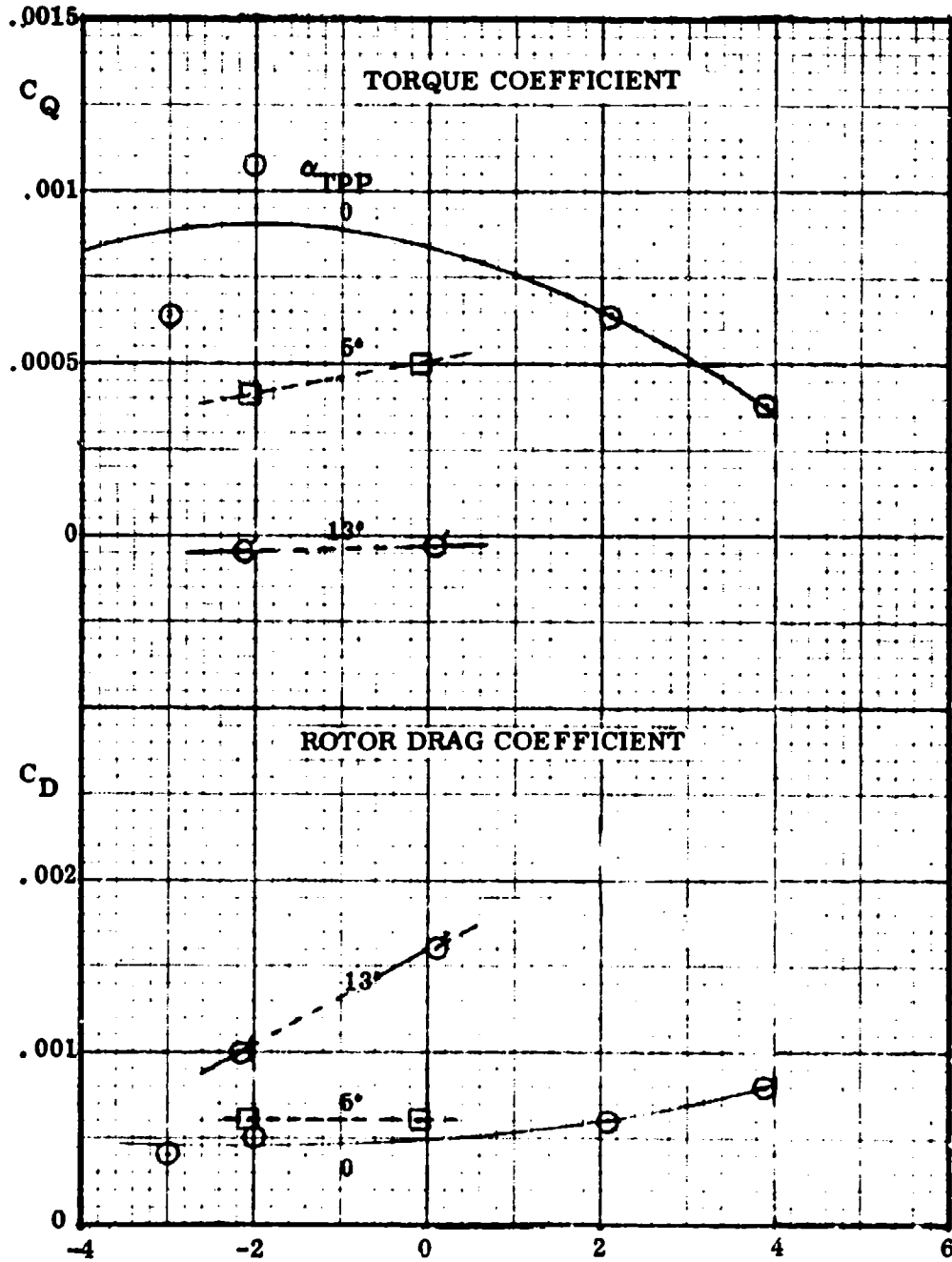
MEASURED ROTOR PERFORMANCE

$\mu = .87$, 1330 r.p.m., 281 knots, $M_{1,90} = .92$, $\rho = .00086$, runs 35&36



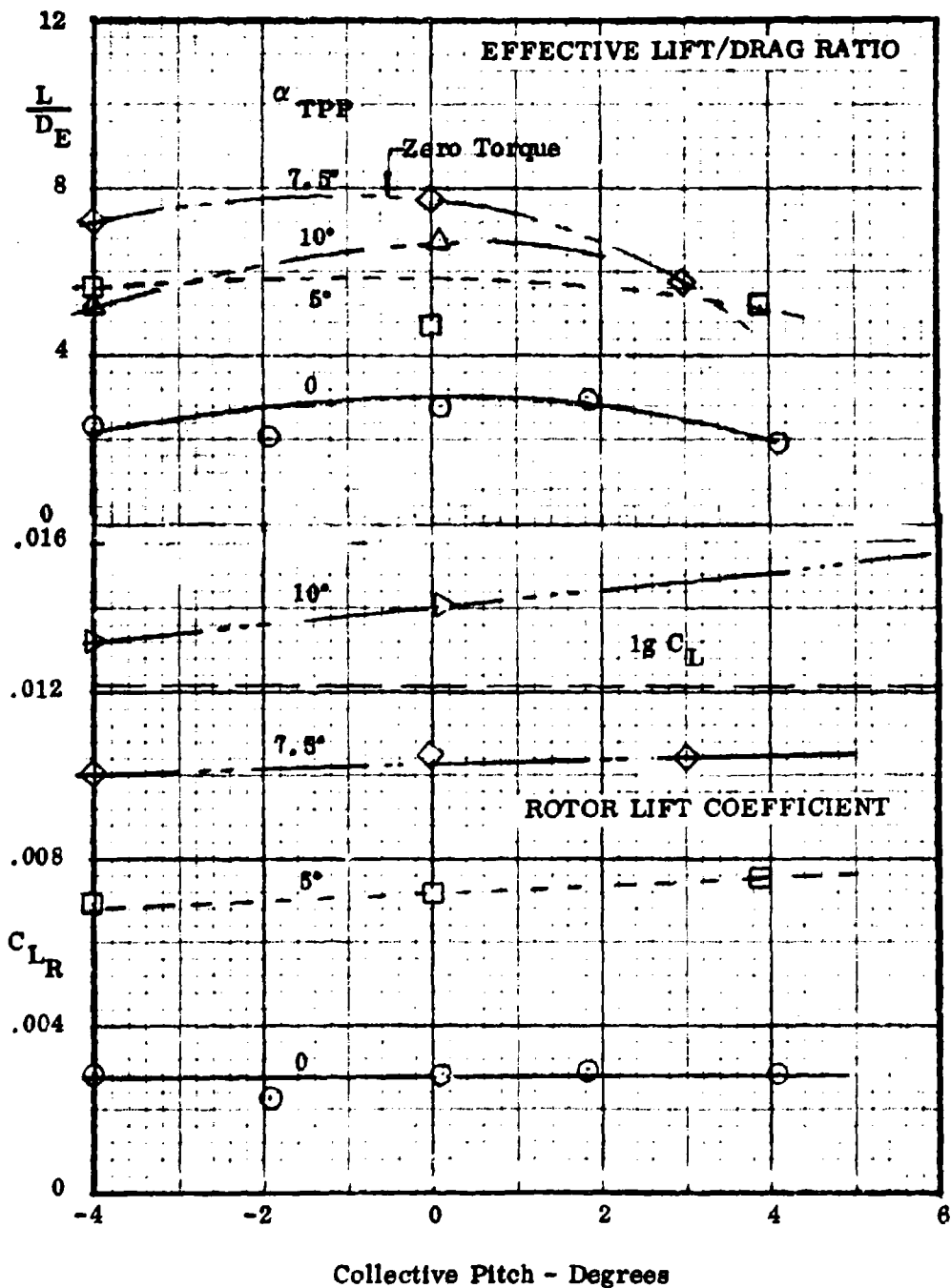
MEASURED ROTOR PERFORMANCE

$\mu = .87$, 1330 r.p.m., 281 knots, $M_{1,90} = .92$, $\rho = .00086$, runs 35&36



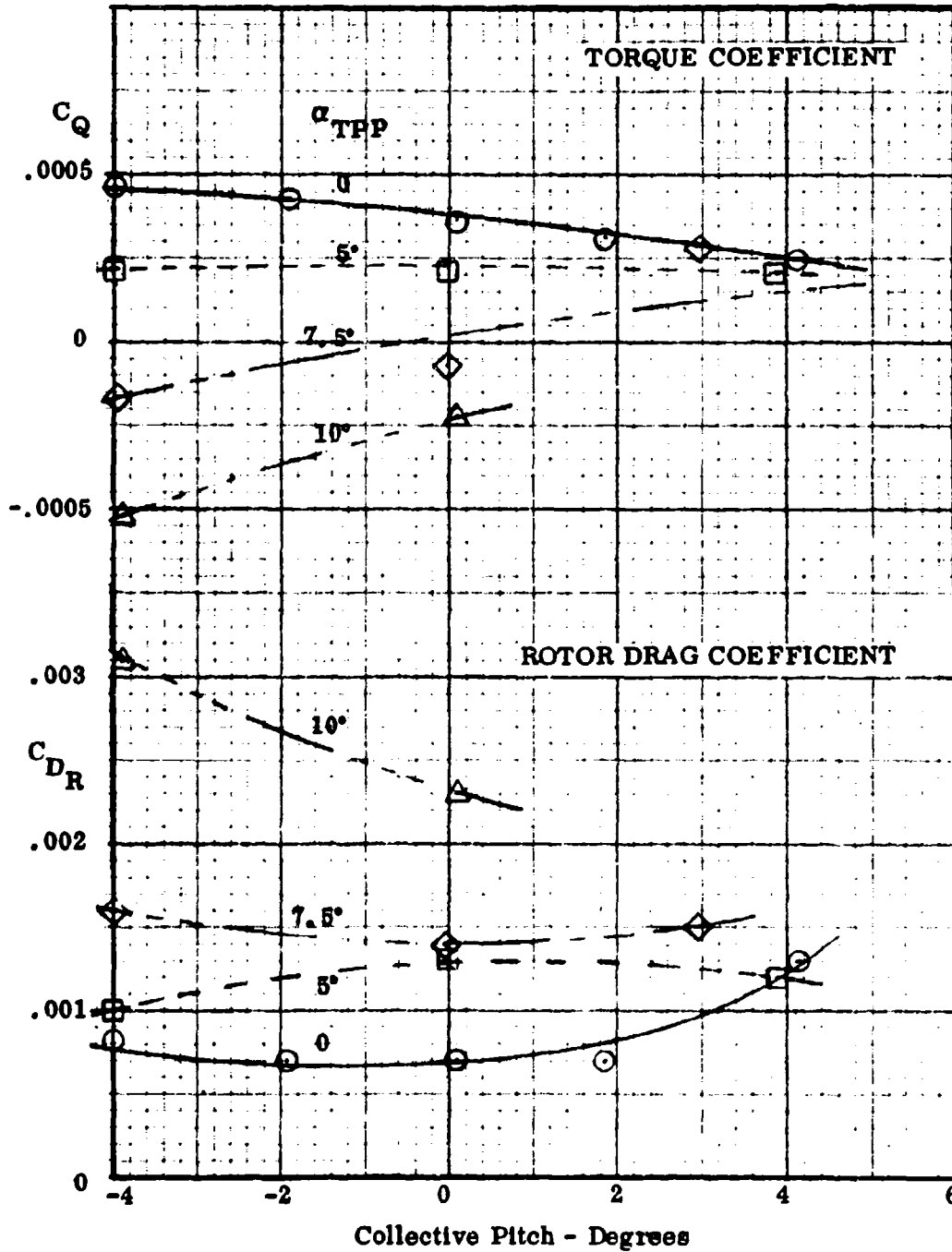
MEASURED ROTOR PERFORMANCE

$\mu = .98$, 1170 r.p.m., 288 knots, $M_{1,90} = .84$, $\rho = .00087$, run 41



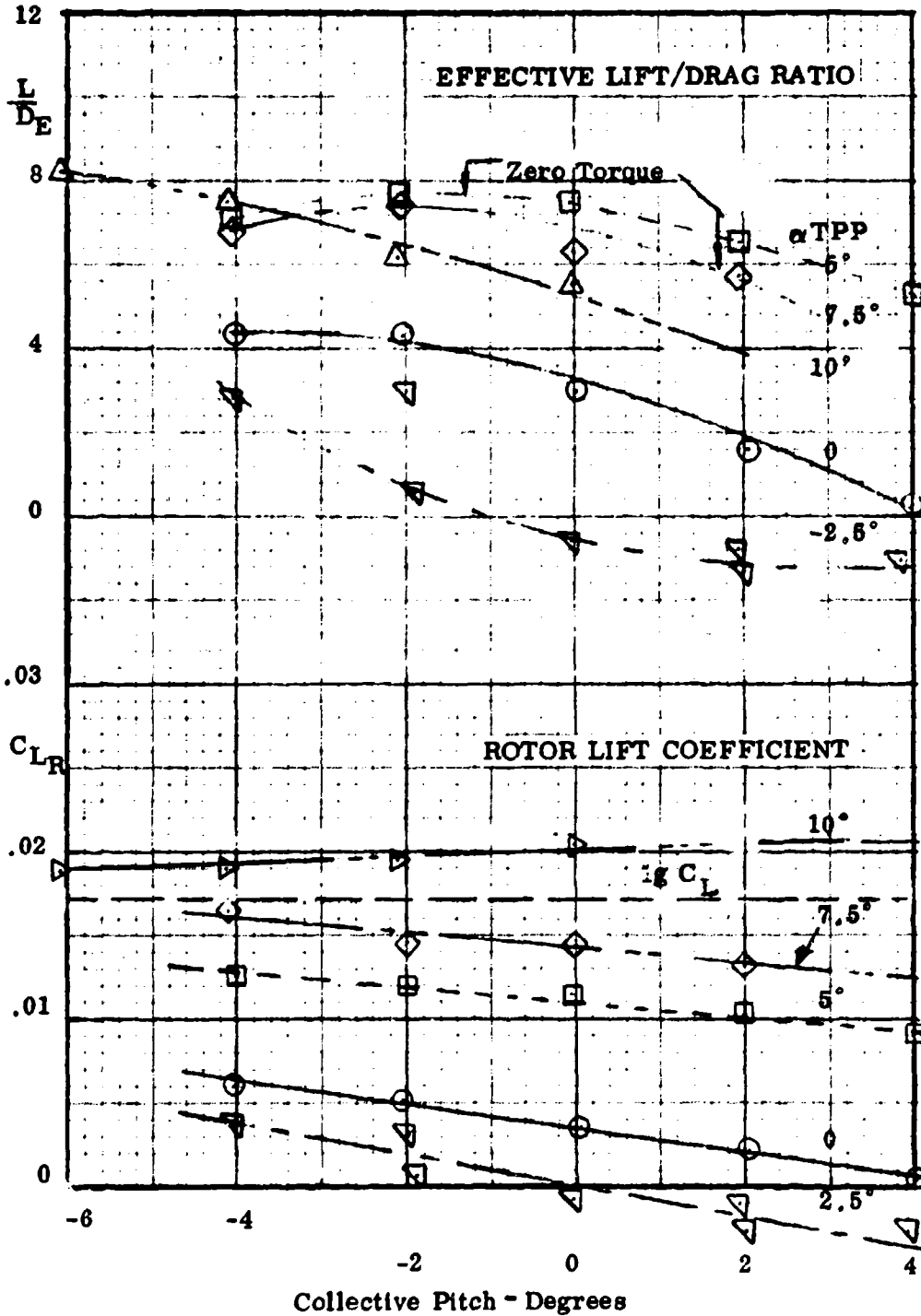
MEASURED ROTOR PERFORMANCE

$\mu = .98$, 1170 r.p.m., 288 knots, $M_{1,90} = .84$, $\rho = .00087$, run 41



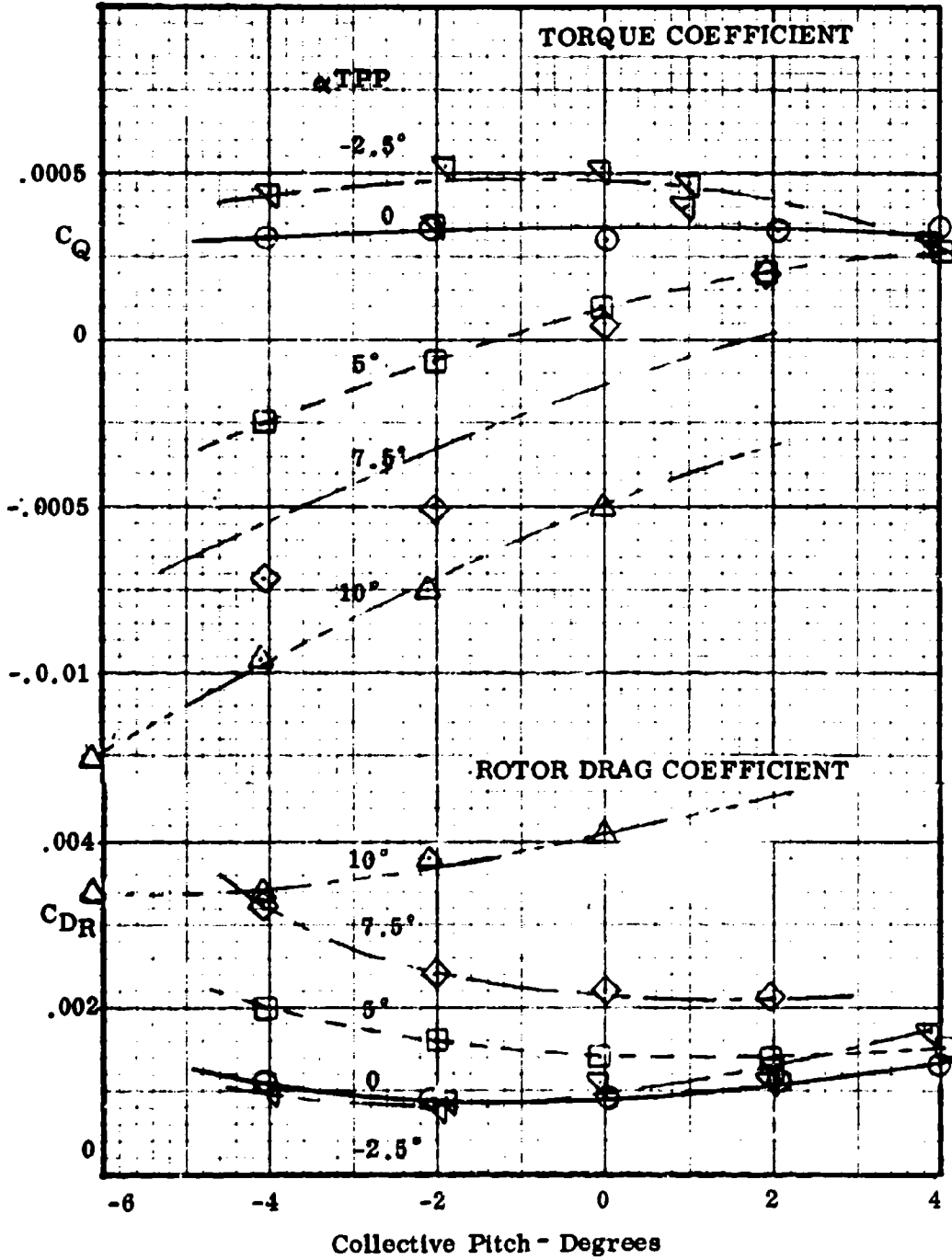
MEASURED ROTOR PERFORMANCE

$\mu = 1.15$, 1000 r.p.m., 287 knots, $M_{1,90} = .79$, $\rho = .00085$, run 42



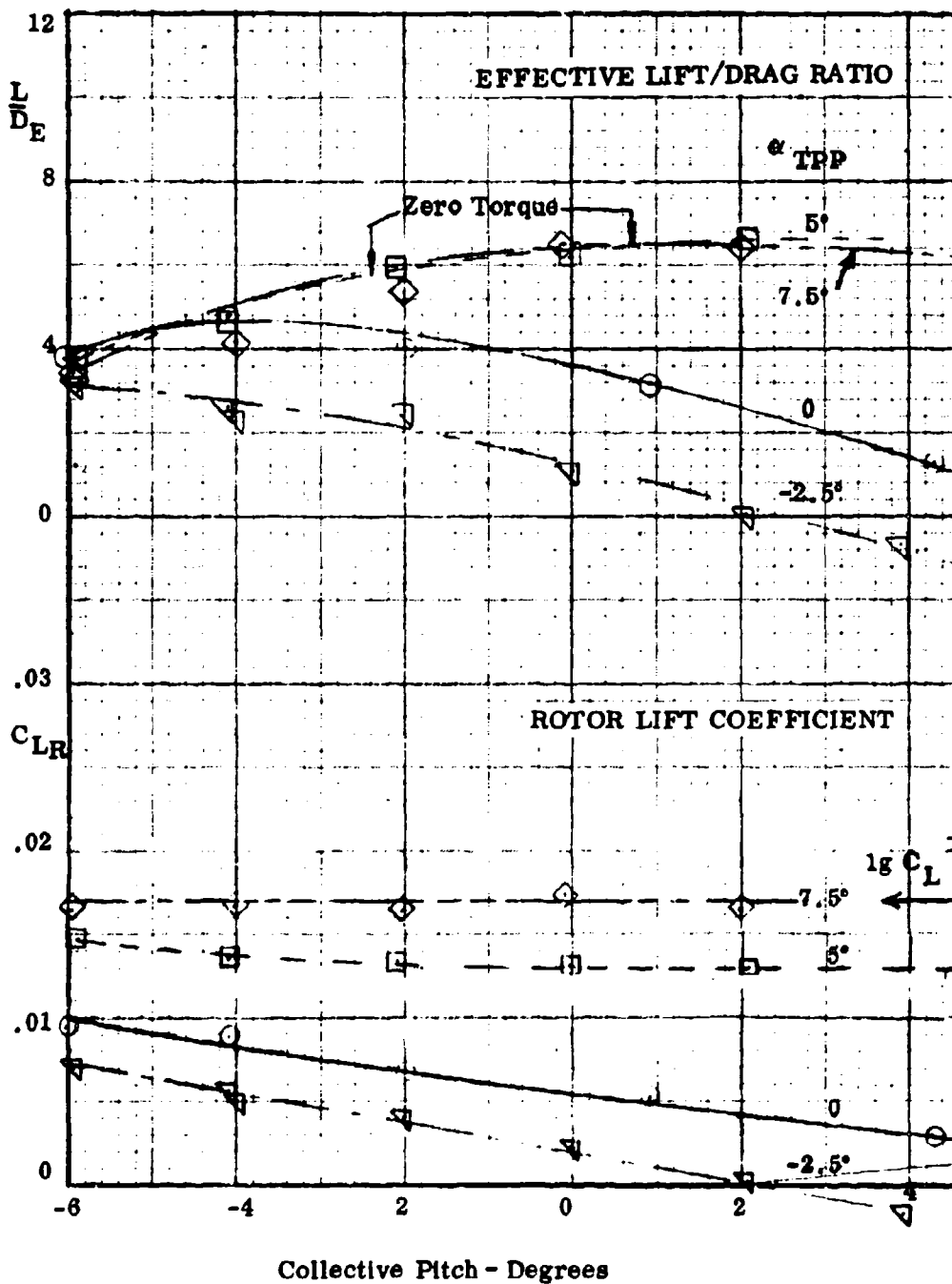
MEASURED ROTOR PERFORMANCE

$\mu = 1.15$, 1000 r.p.m., 287 knots, $M_{1,90} = .79$, $\rho = .00085$, run 42



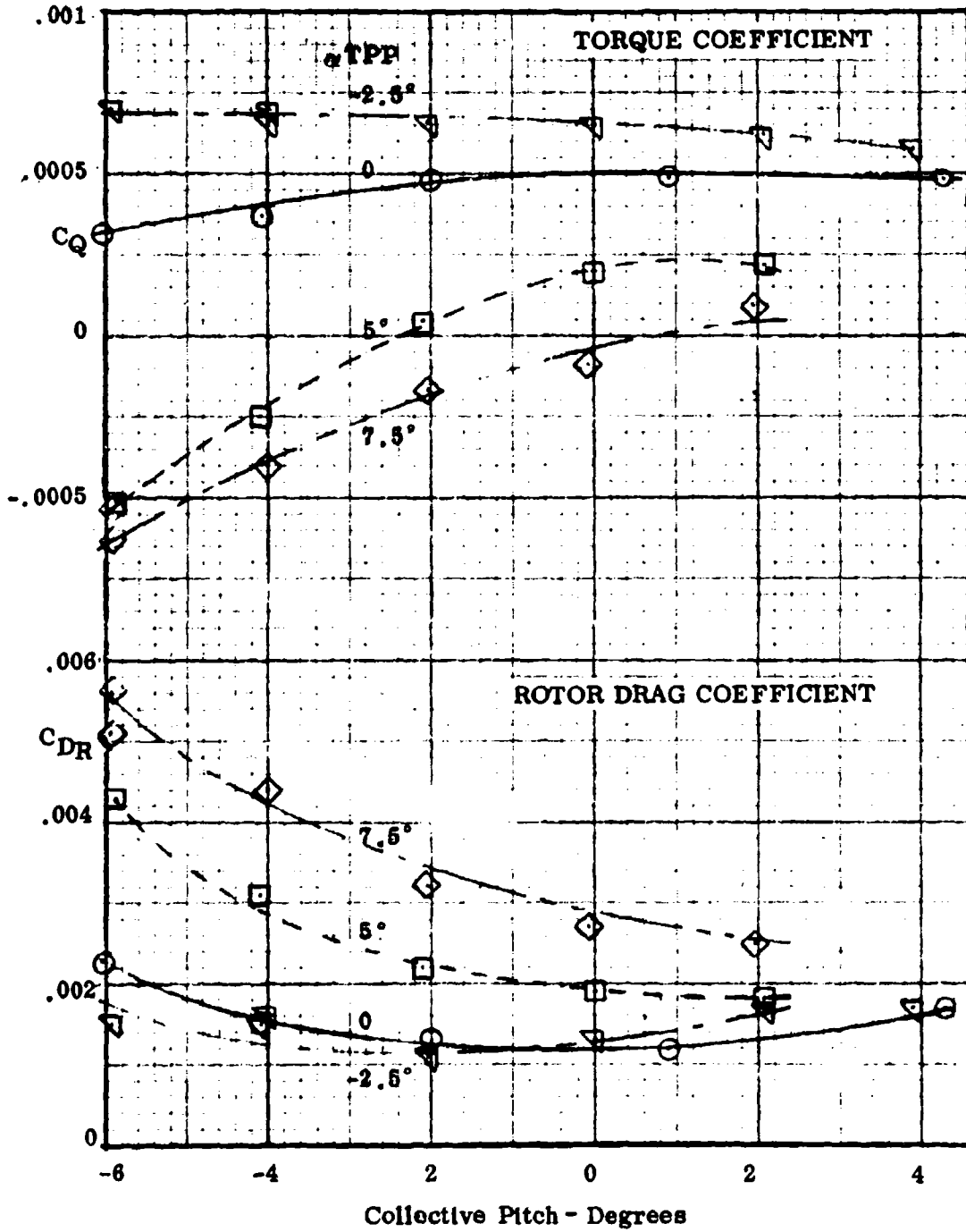
MEASURED ROTOR PERFORMANCE

$\mu = 1.15$, 1167 r.p.m., 350 knots, $M_{1,90} = .93$, $\rho = .00084$, run 45



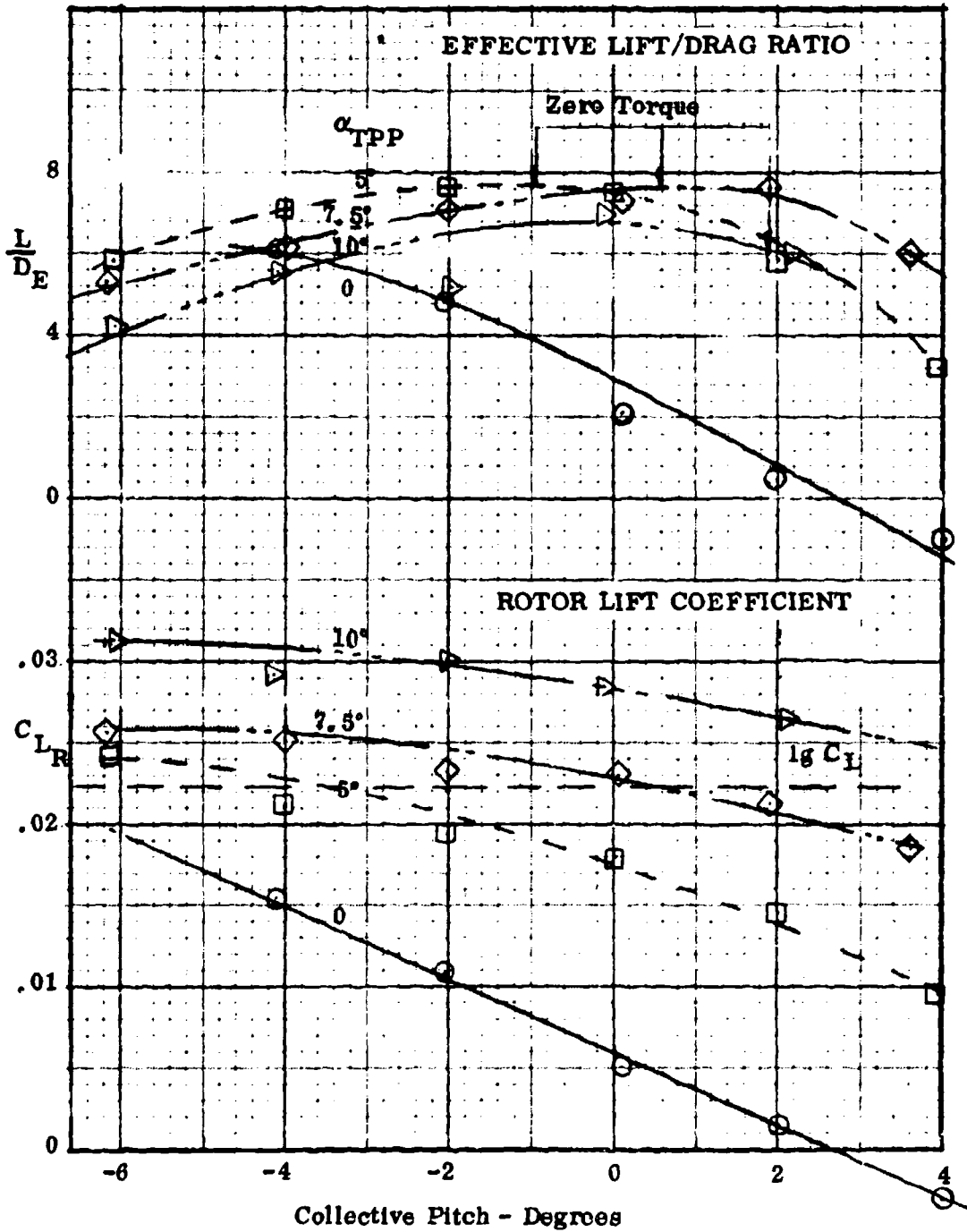
MEASURED ROTOR PERFORMANCE

$\mu = 1.15$, 1167 r.p.m., 350 knots, $M_{1, 90} = .93$, $\rho = .00084$, run 45



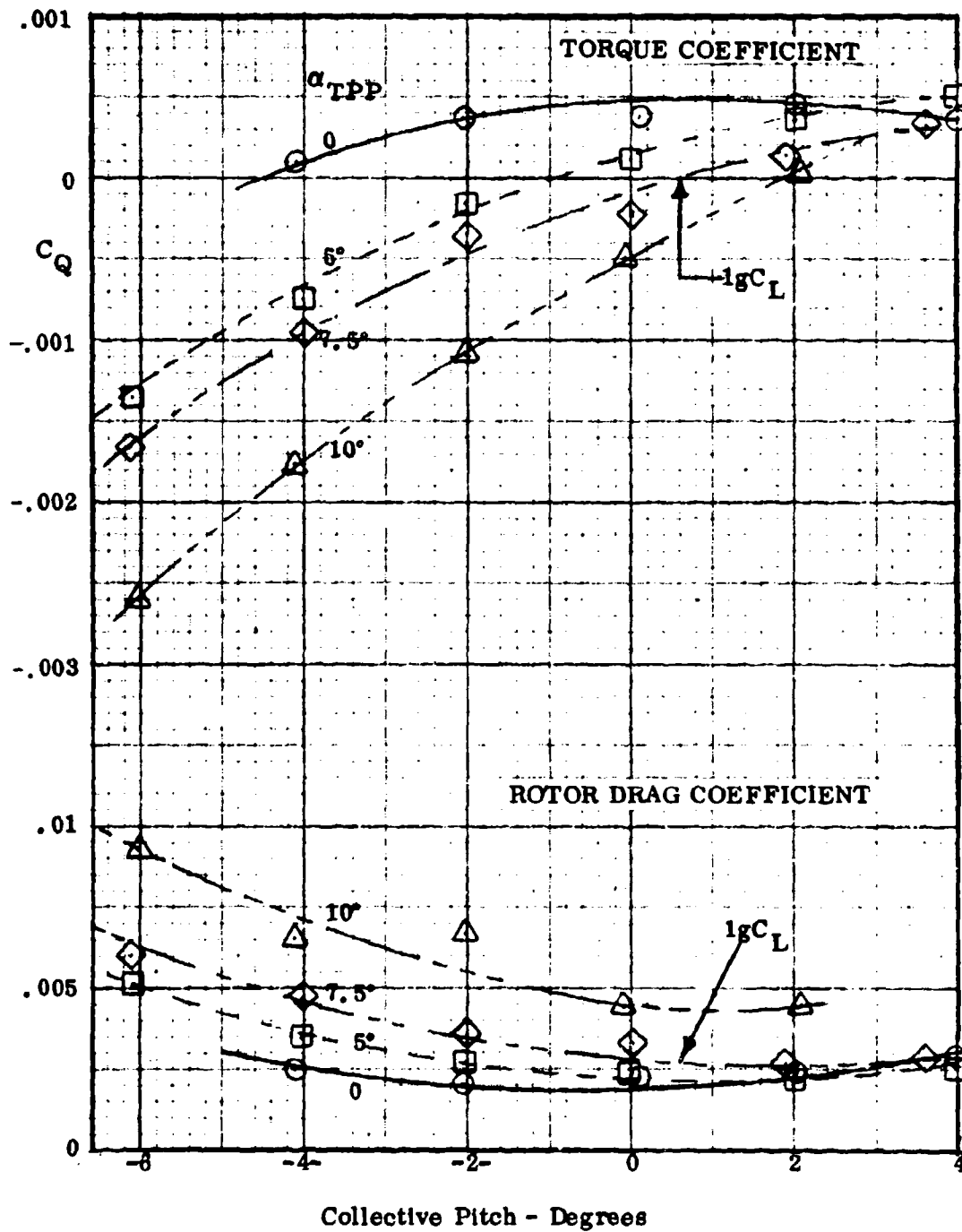
MEASURED ROTOR PERFORMANCE

$\mu = 1.40$, 833 r.p.m., 290 knots, $M_{1,90} = .73$, $\rho = .00085$, run 43



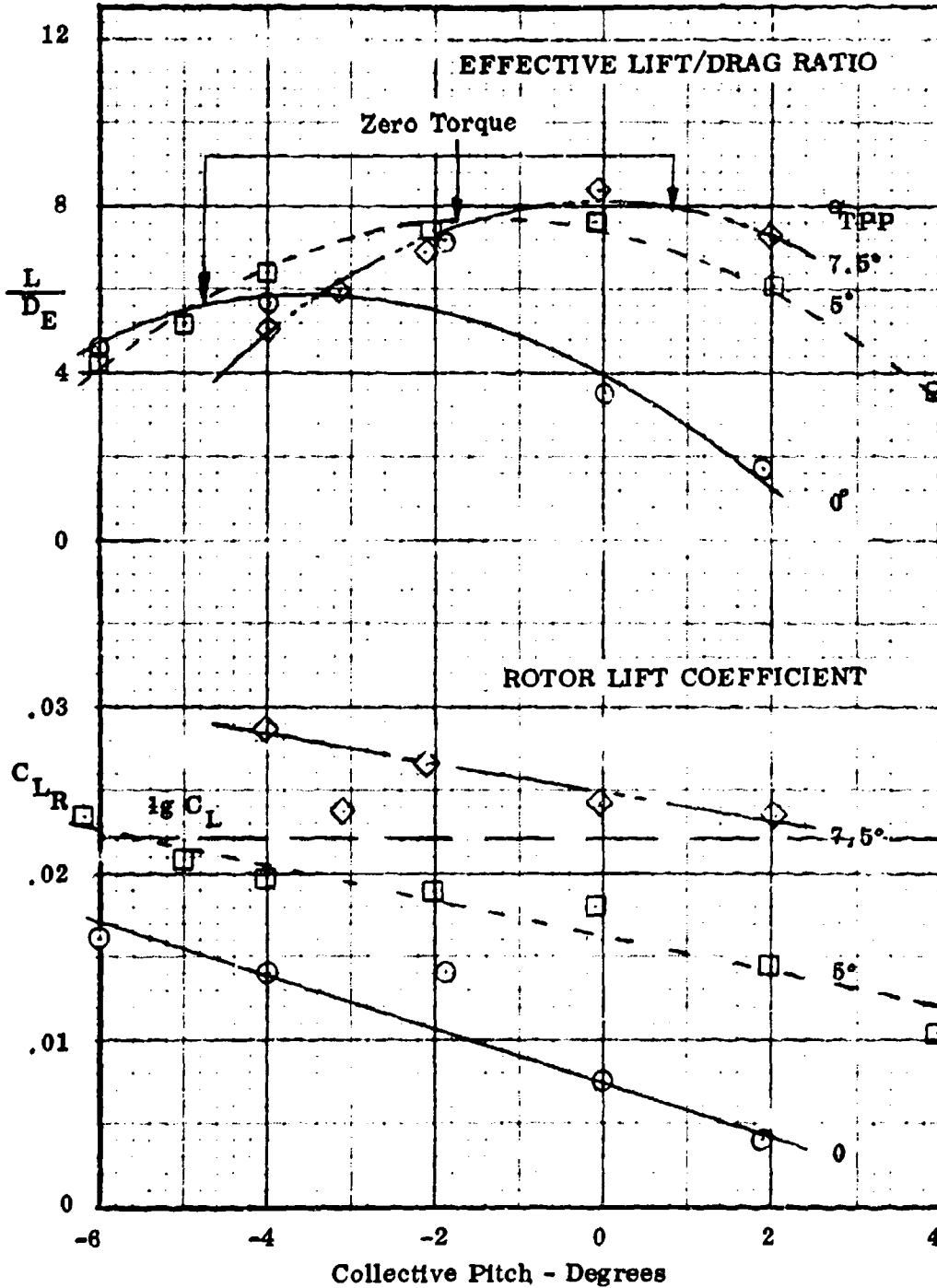
MEASURED ROTOR PERFORMANCE

$\mu = 1.40$, 833 r.p.m., 290 knots, $M_{1, 90} = .73$, $\rho = .00085$, run 43



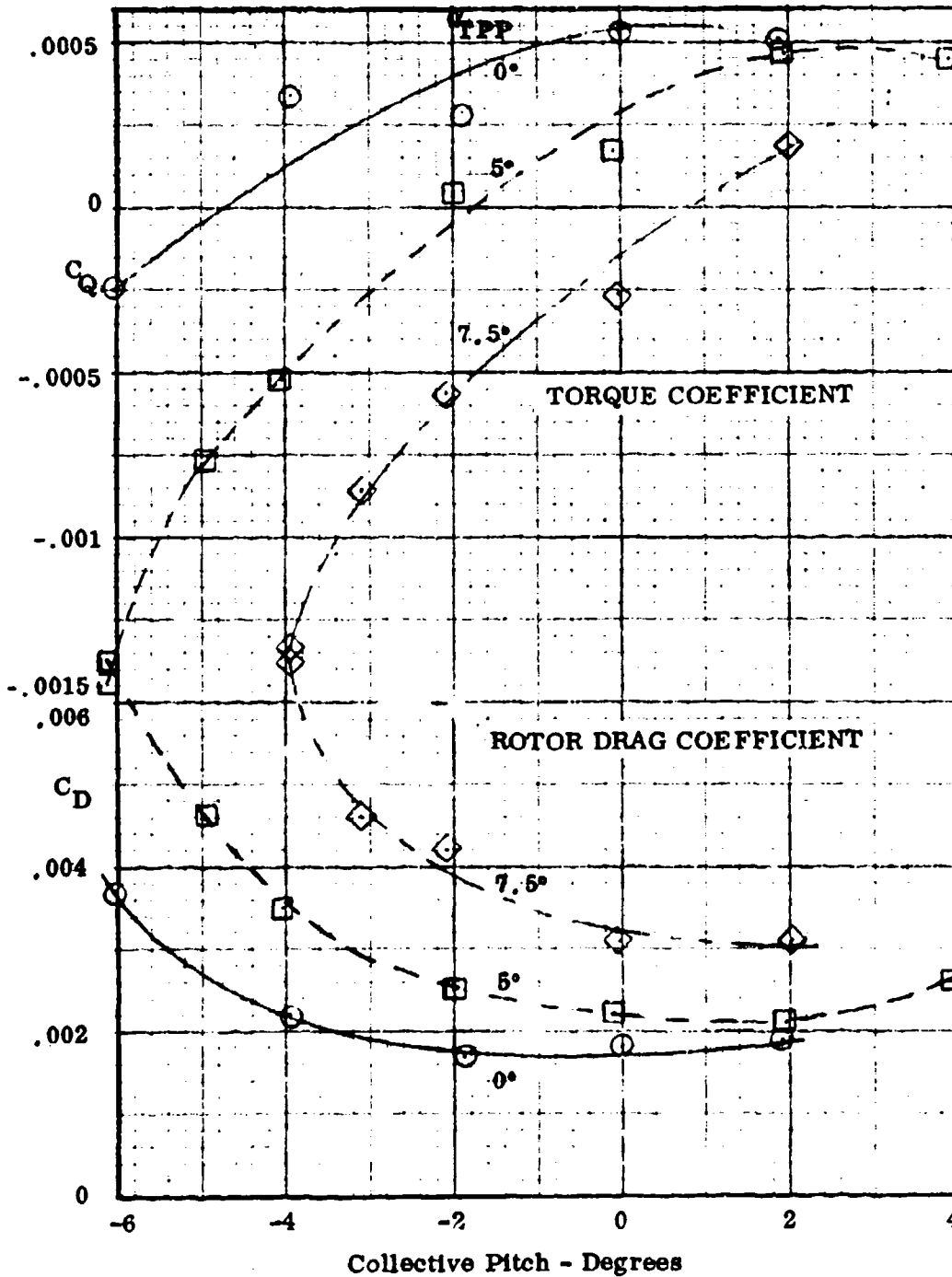
MEASURED ROTOR PERFORMANCE

$\mu = 1.40$, 970 r.p.m., 345 knots, $M_{1, 90} = .86$, $\rho = .00084$, run 46



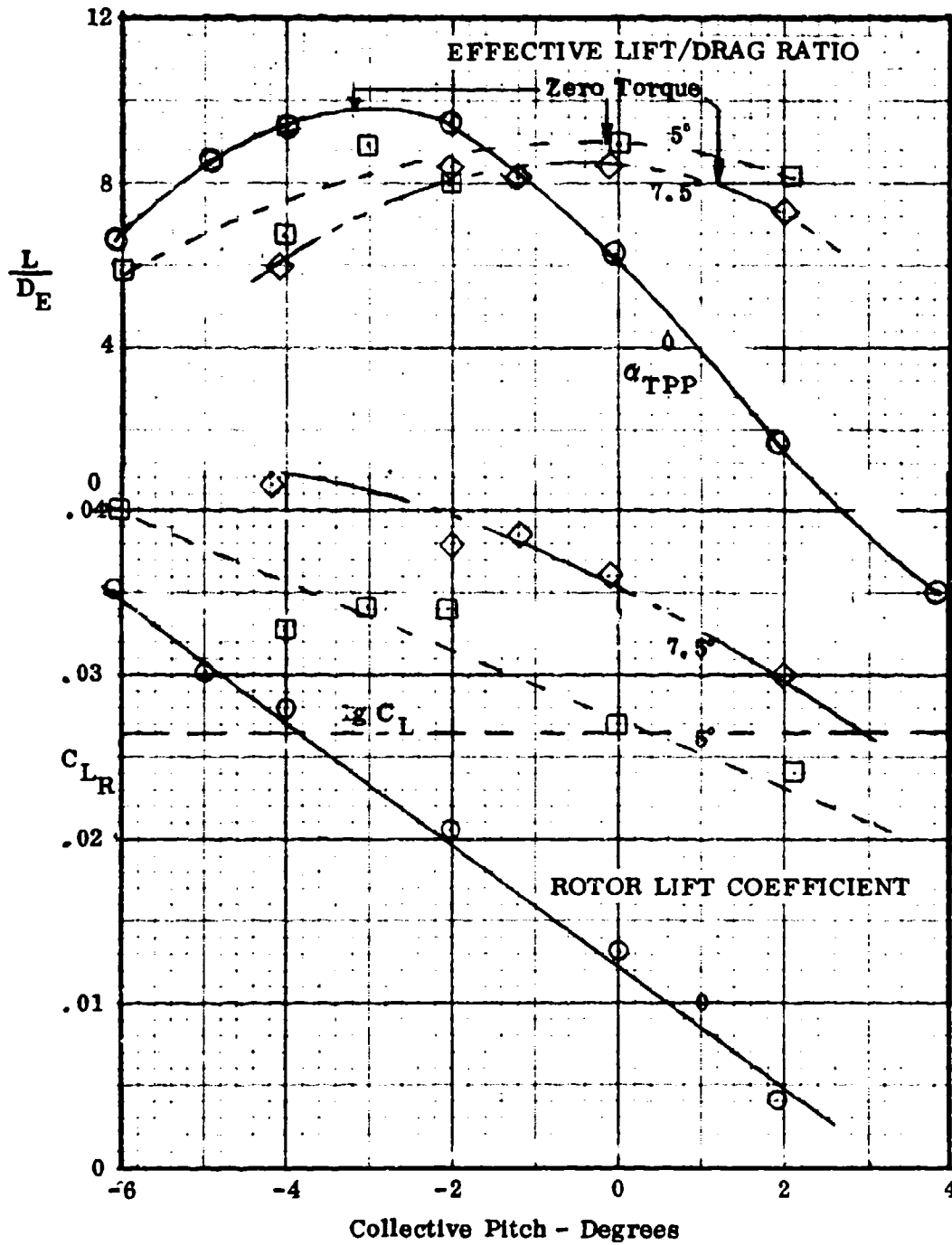
MEASURED ROTOR PERFORMANCE

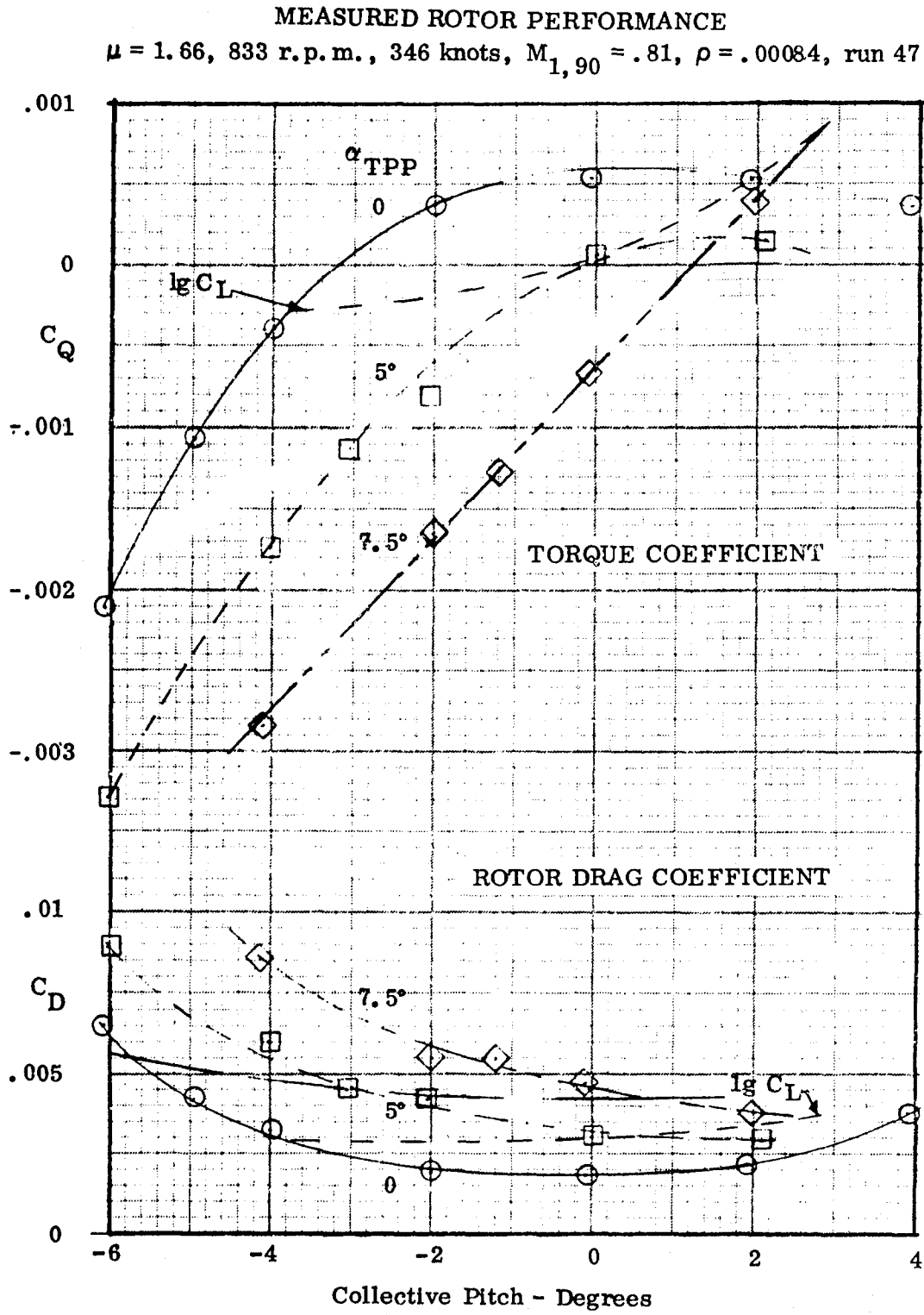
$\mu = 1.40$, 970 r.p.m., 345 knots, $M_{1, 90} = .86$, $\rho = .00084$, run 46



MEASURED ROTOR PERFORMANCE

$\mu = 1.66$, 833 r.p.m., 346 knots, $M_{1,90} = .81$, $\rho = .00084$, run 47



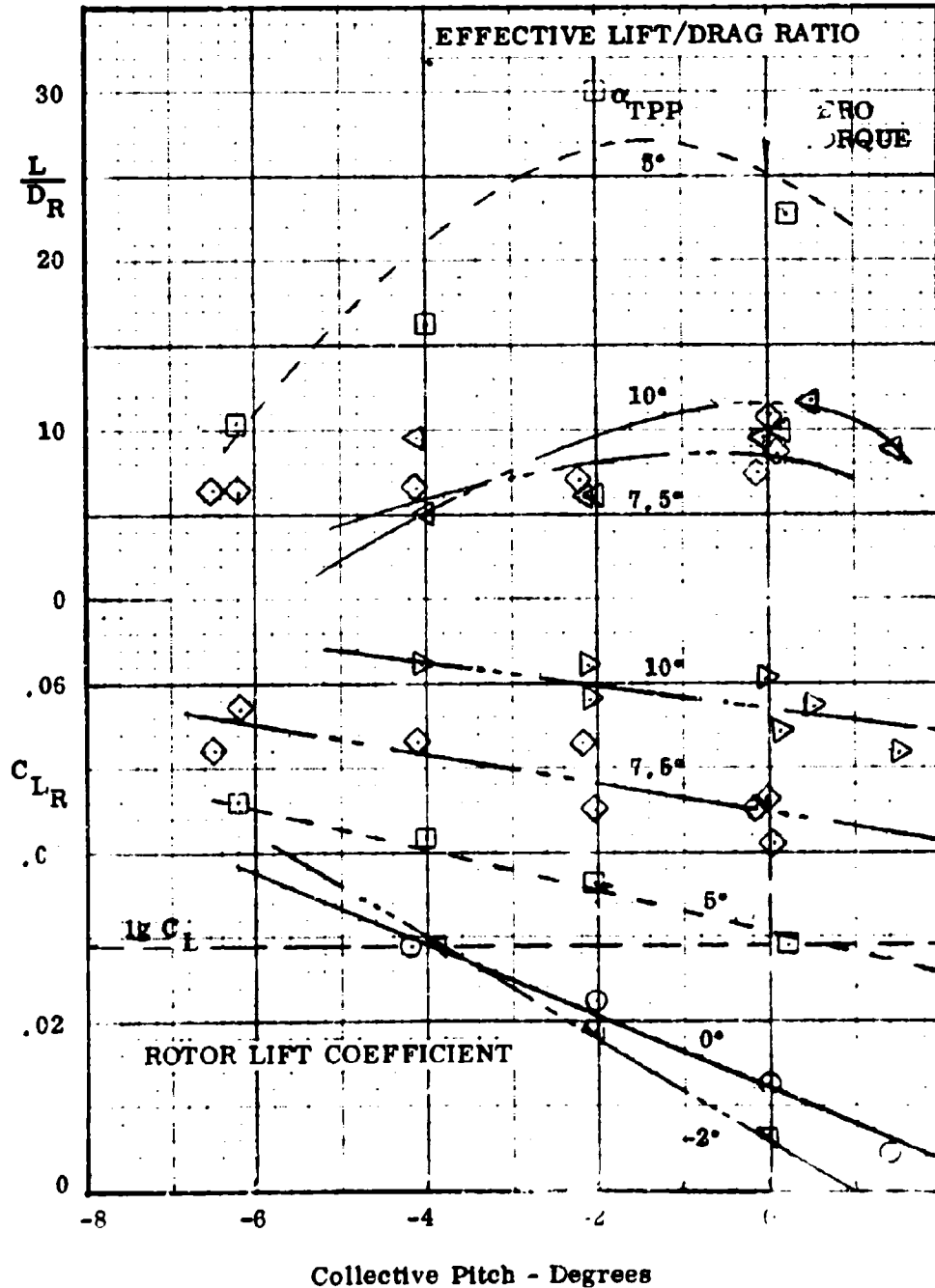


HC144R1070

Figure 2.13A

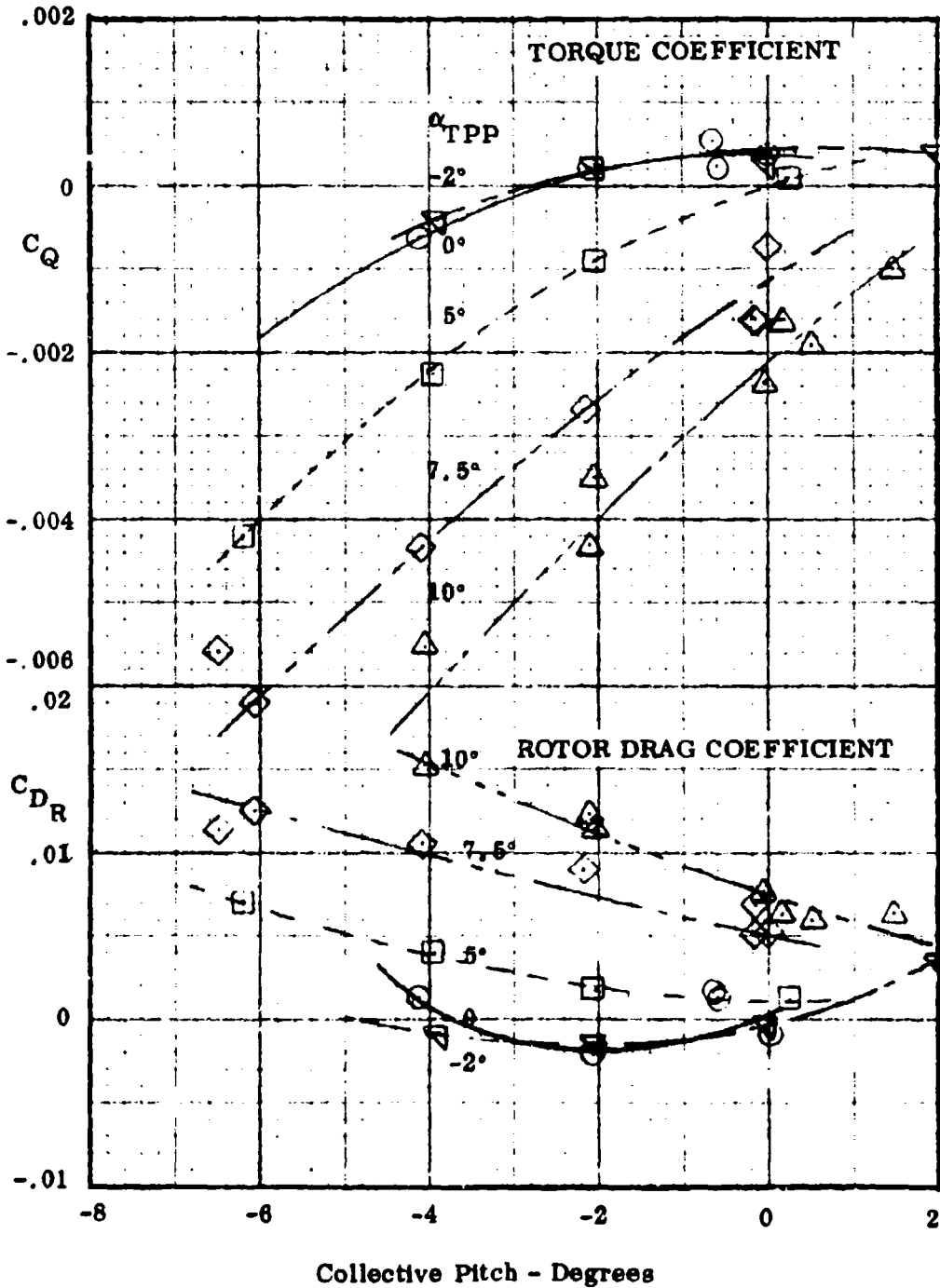
MEASURED ROTOR PERFORMANCE

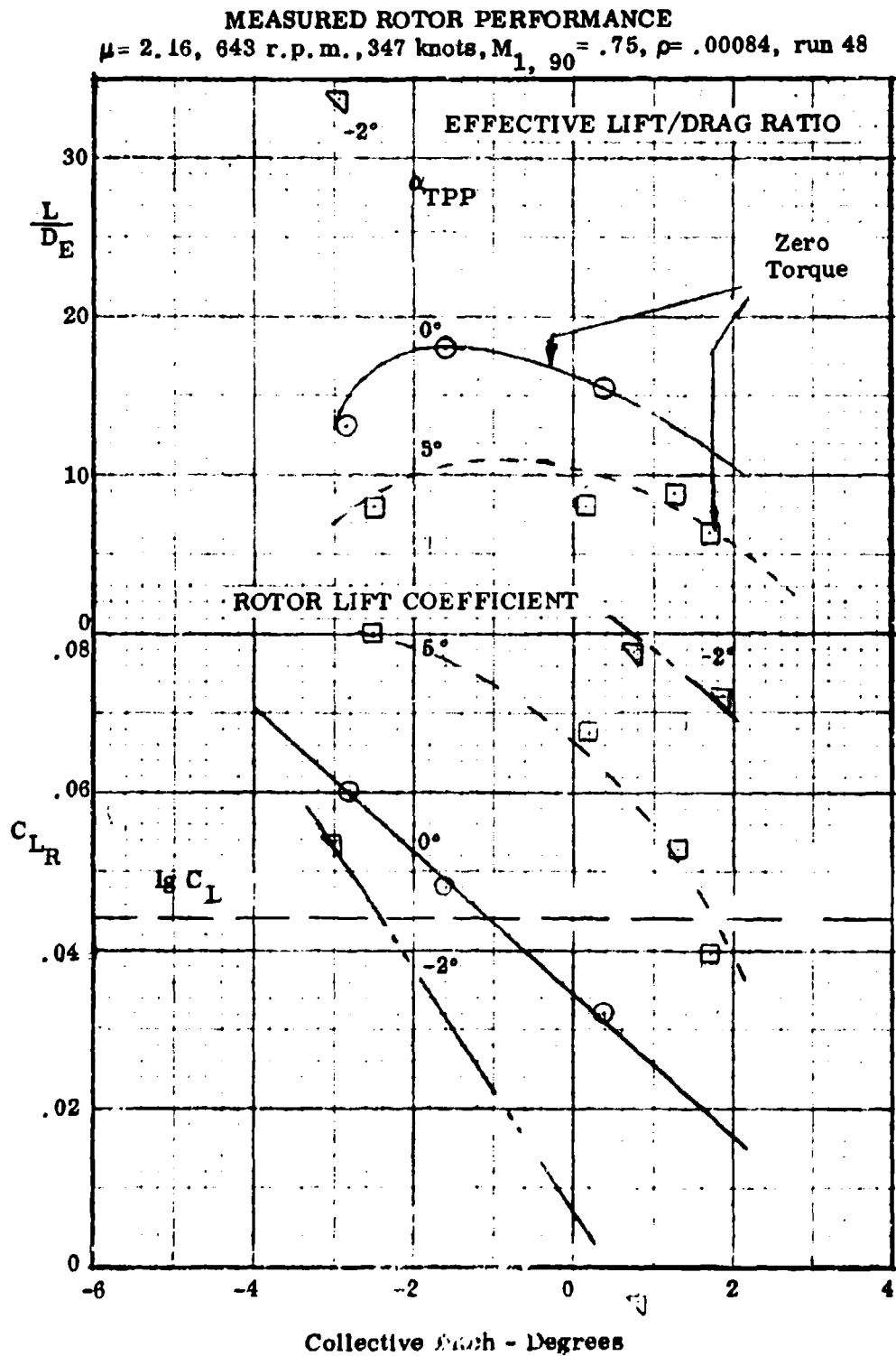
$\mu=1.75$, 656 r.p.m., 292 knots, $M_{1, 90} = .67$, $\rho = .00085$, run 44



MEASURED ROTOR PERFORMANCE

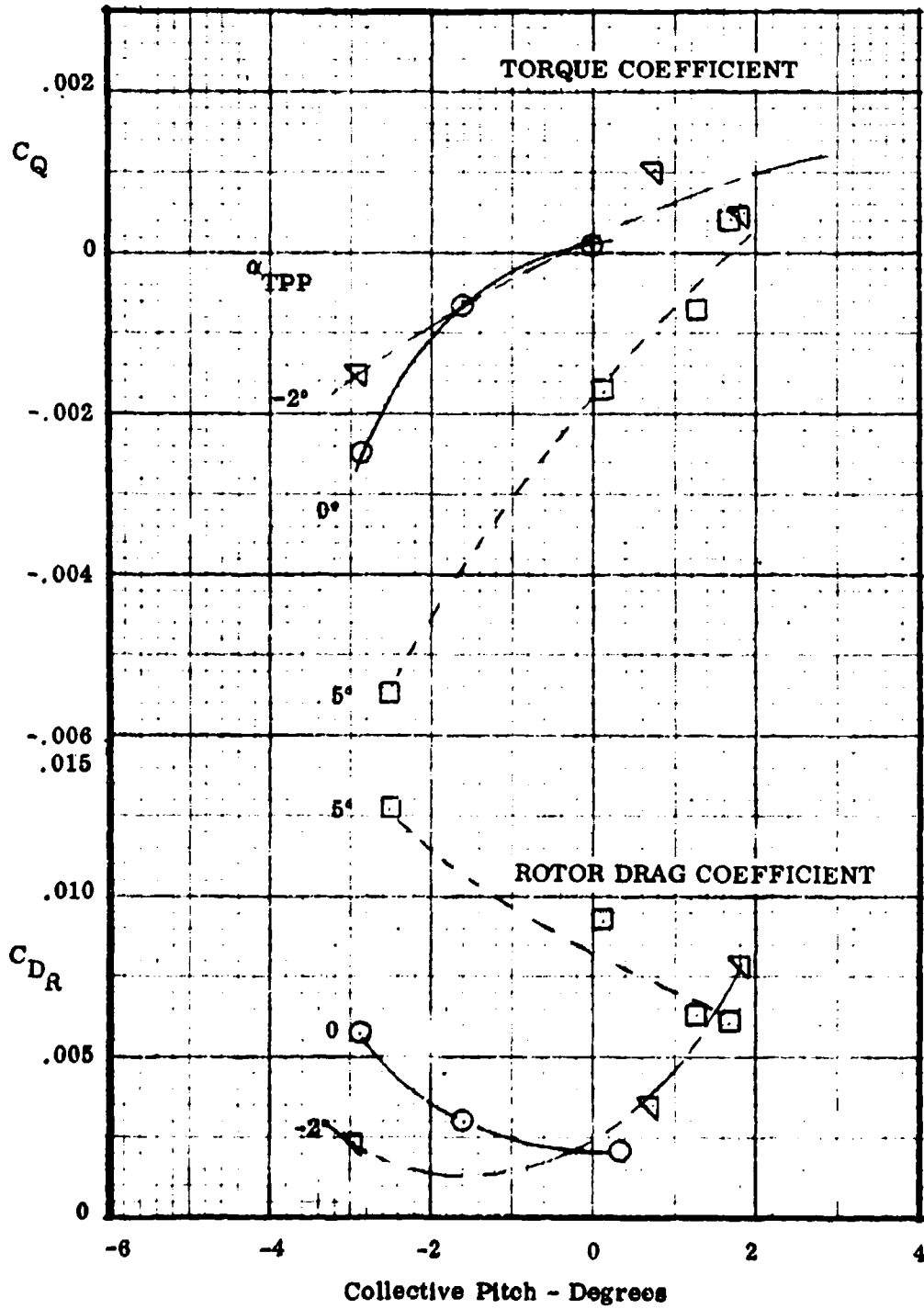
$\mu = 1.75$, 656 r.p.m., 292 knots, $M_{1, 90} = .67$, $\rho = .00085$, run 44





MEASURED ROTOR PERFORMANCE

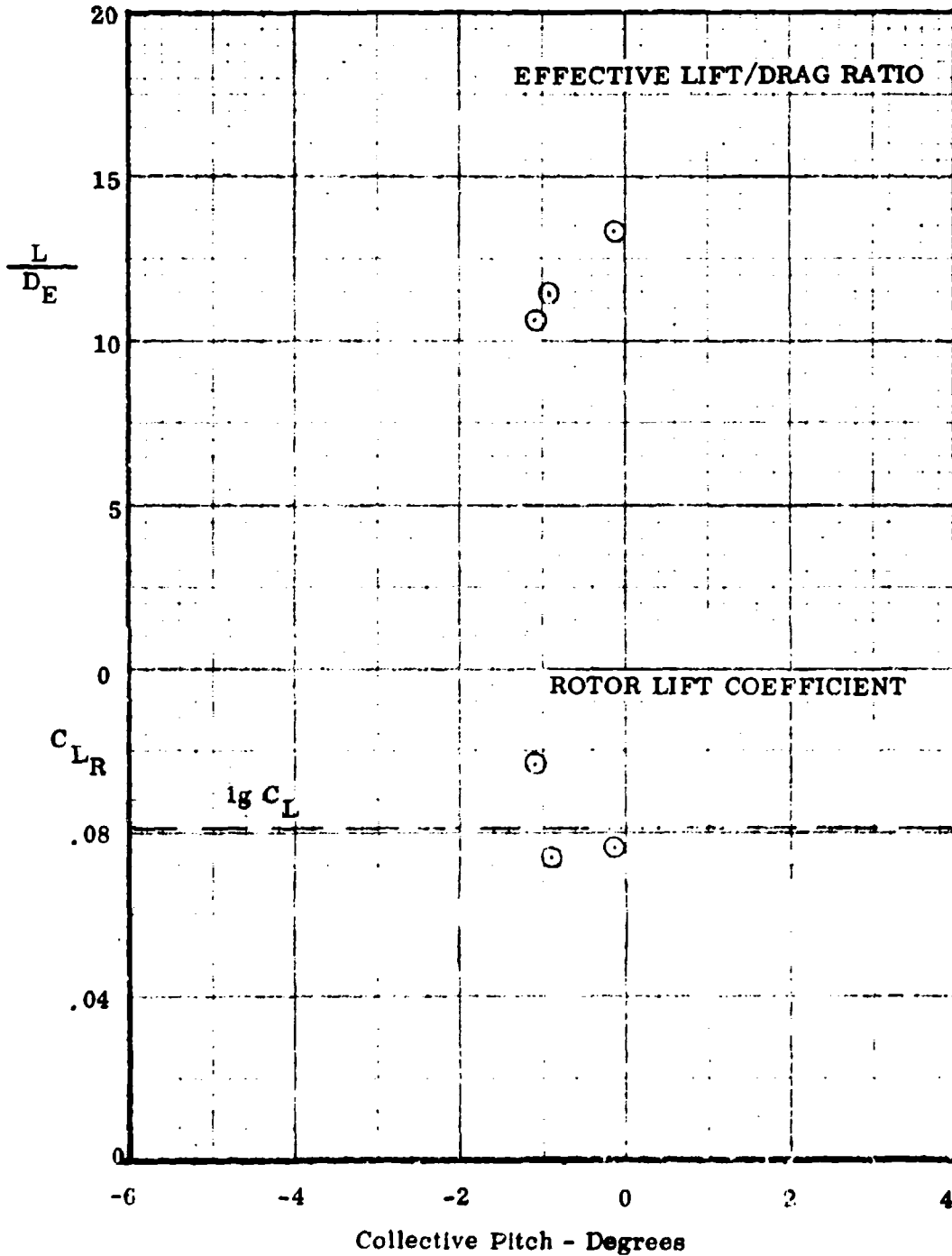
$\mu = 2.16$, 643 r.p.m., 347 knots, $M_{1, 90} = .75$, $\rho = .00084$, run 48



MEASURED ROTOR PERFORMANCE

$\mu = 2.47$, 560 r.p.m., 350 knots, $M_{1, 90} = .72$, $\rho = .00084$, run 49

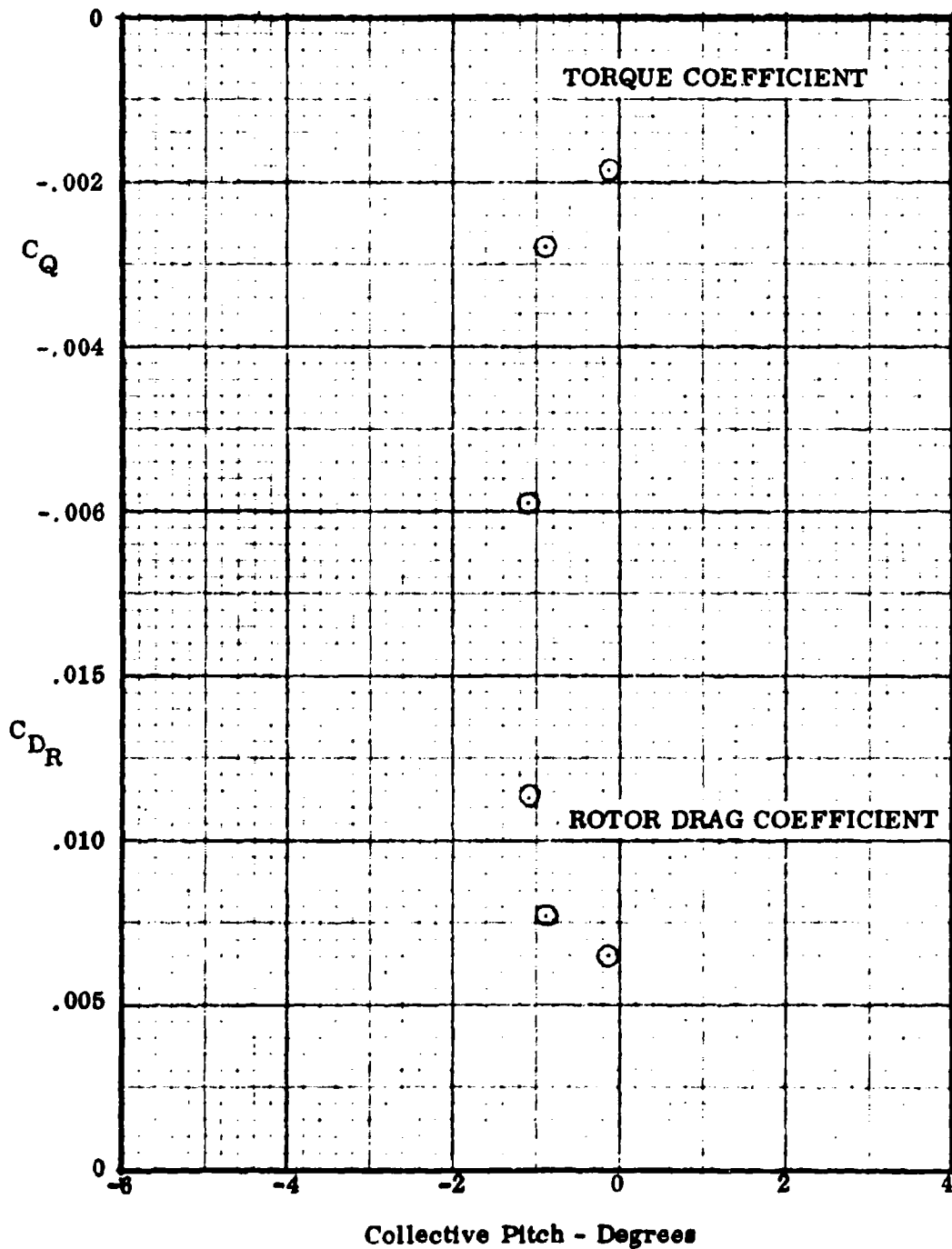
$\alpha_{TPP} = 0$



MEASURED ROTOR PERFORMANCE

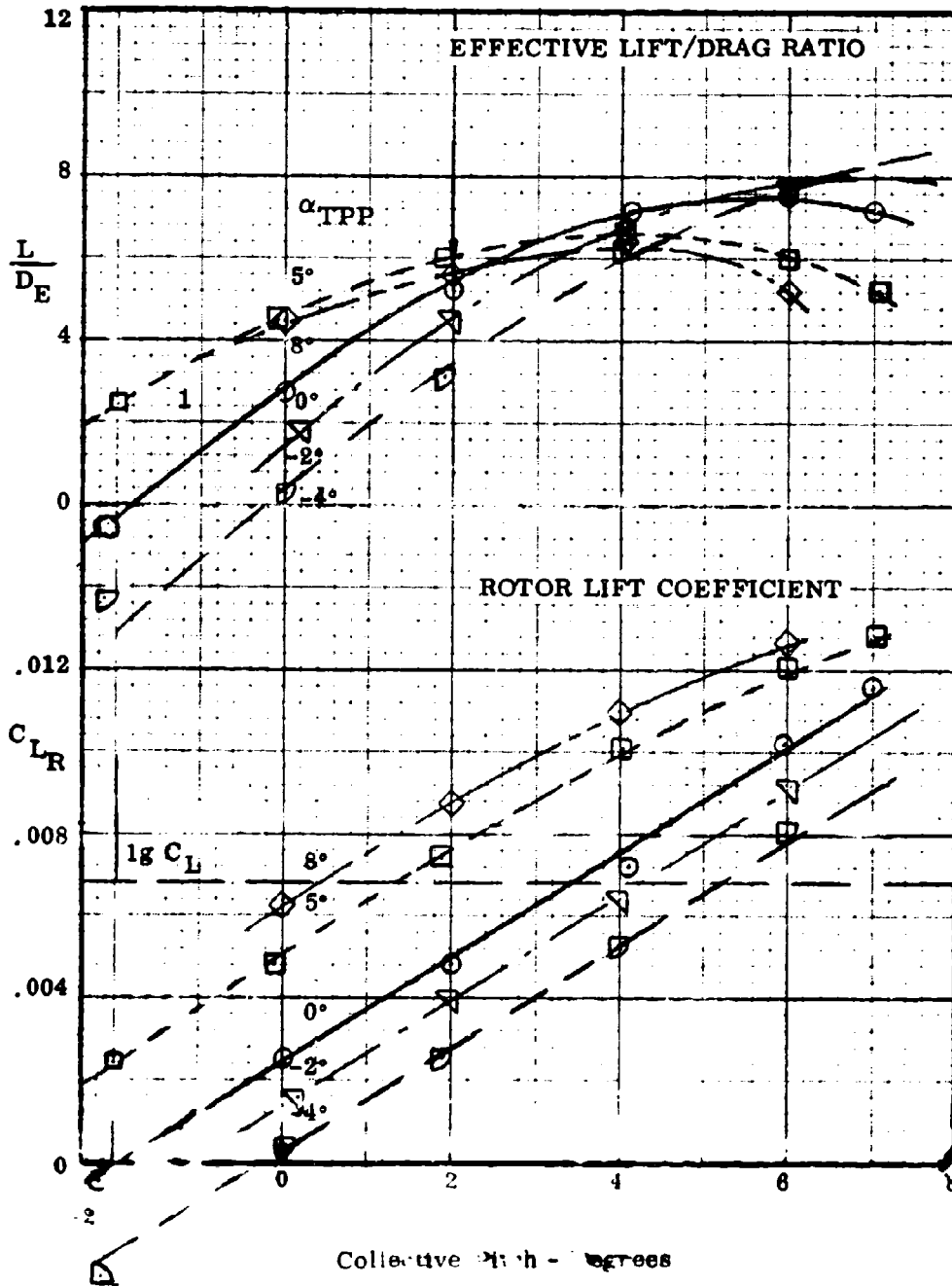
$\mu = 2.47$, 560 r.p.m., 350 knots, $M_{1, 90} = .72$, $\rho = .00084$, run 49

$\alpha_{TPP} = 0$



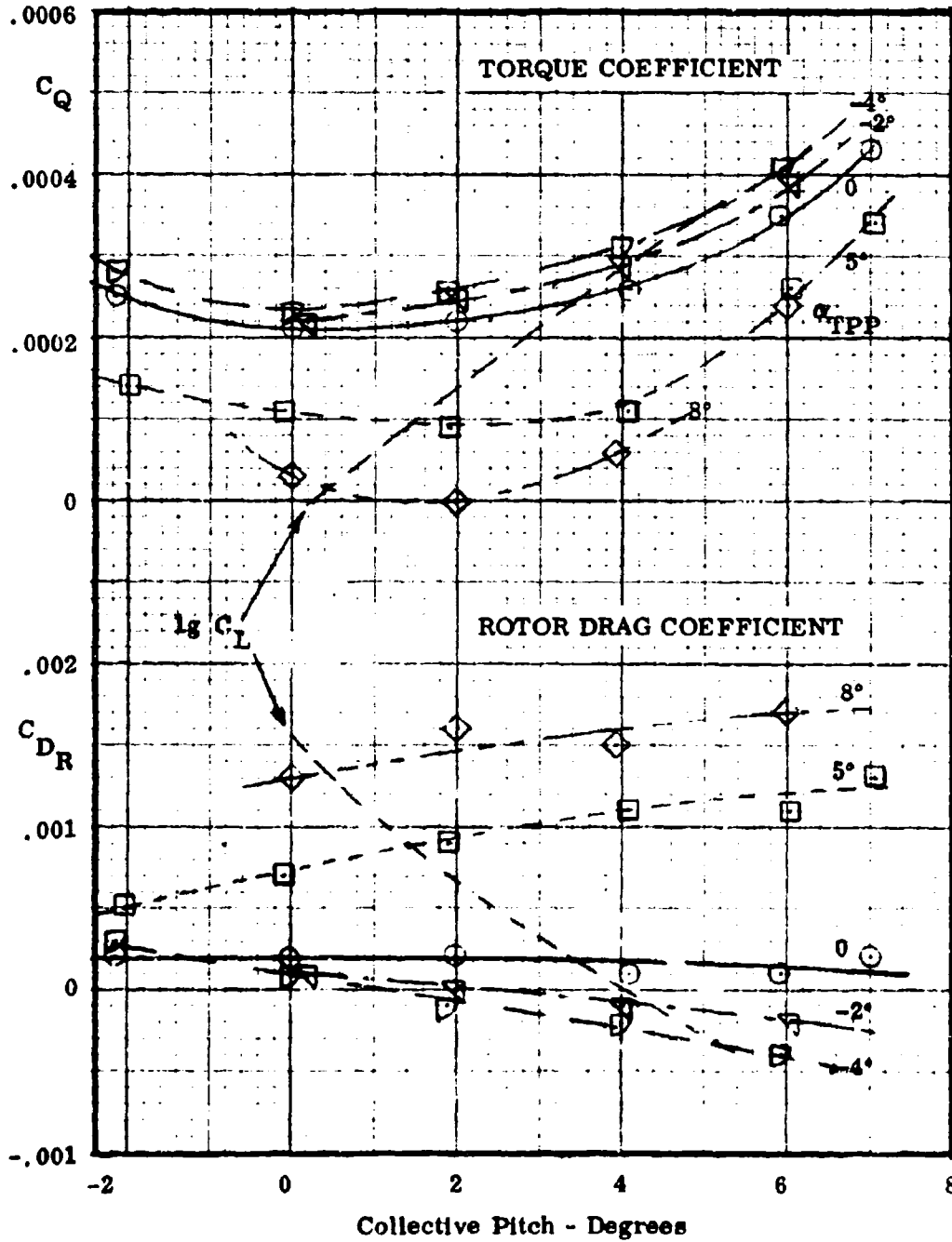
MEASURED ROTOR PERFORMANCE

$\mu = .29$, 1670 r.p.m, 121 knots, $M_1, 90 = .79$, $\rho = .0023$, run 50



MEASURED ROTOR PERFORMANCE

$\mu = .29$, 1670 r.p.m., 121 Knots, $M_{1, 90} = .79$, $\rho = .0023$, run 50

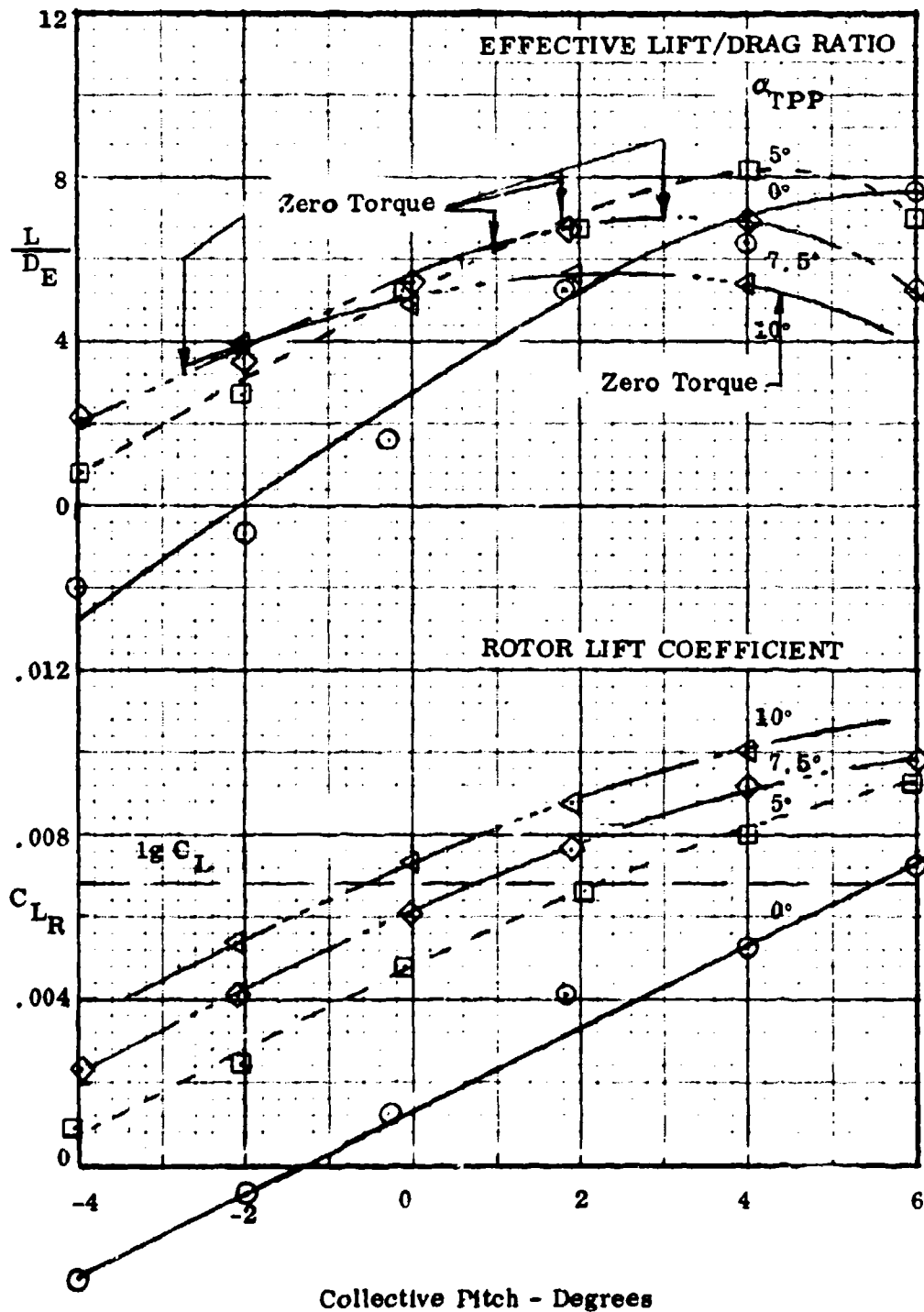


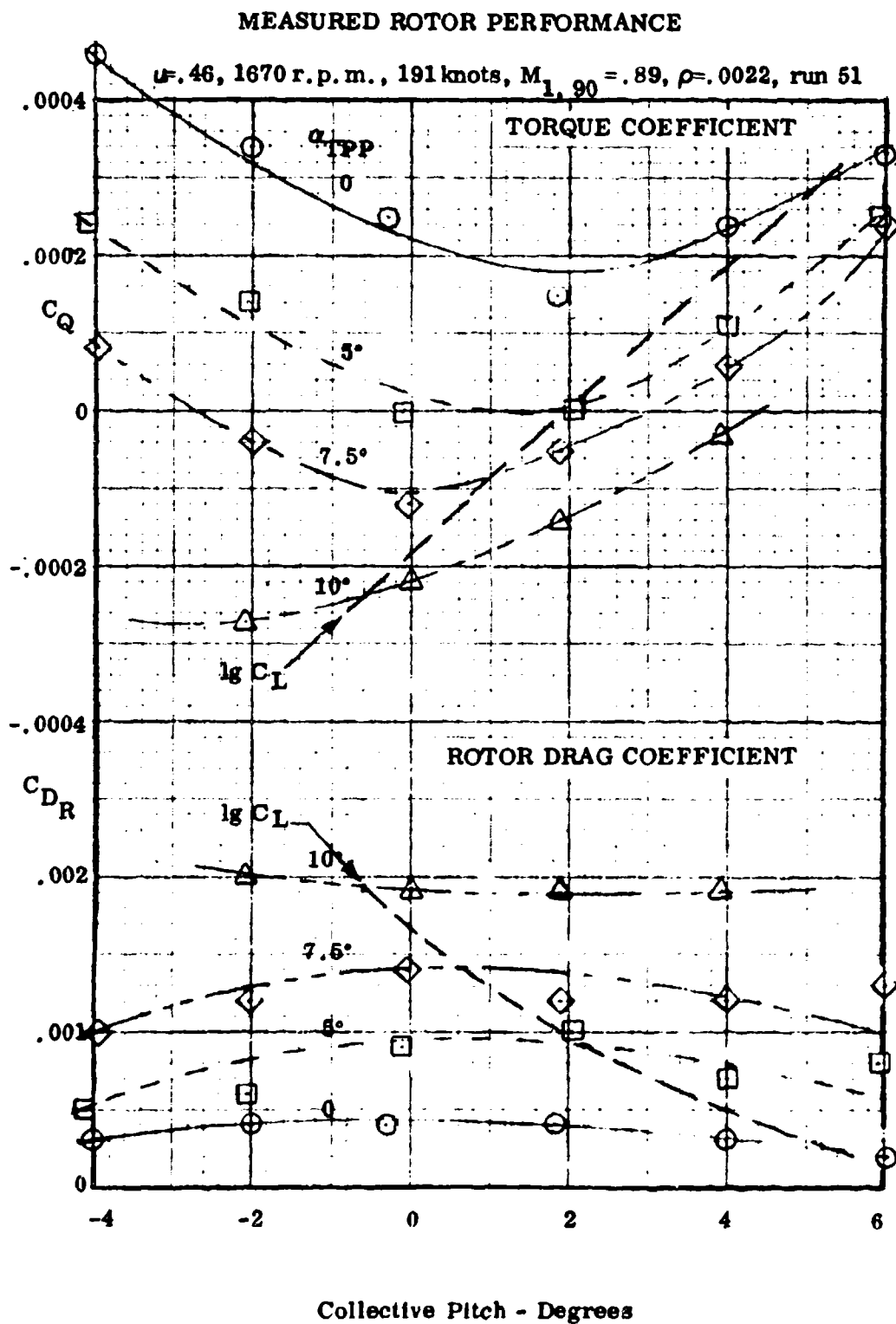
HC144R1070

Figure 2.17A

MEASURED ROTOR PERFORMANCE

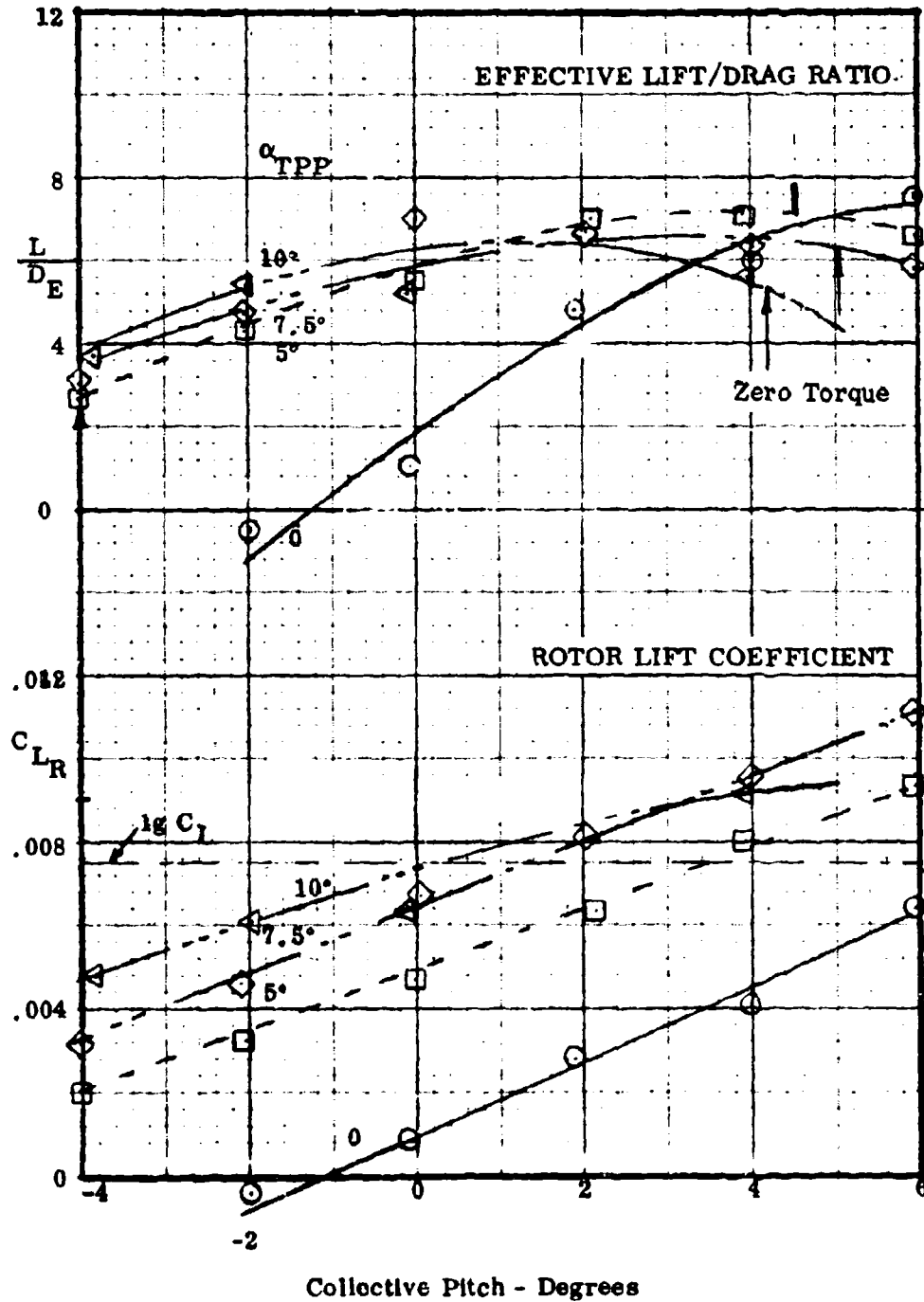
$\mu = .46$, 1670 r.p.m., 191 knots, $M_{1, 90} = .89$, $\rho = .0022$, run 51





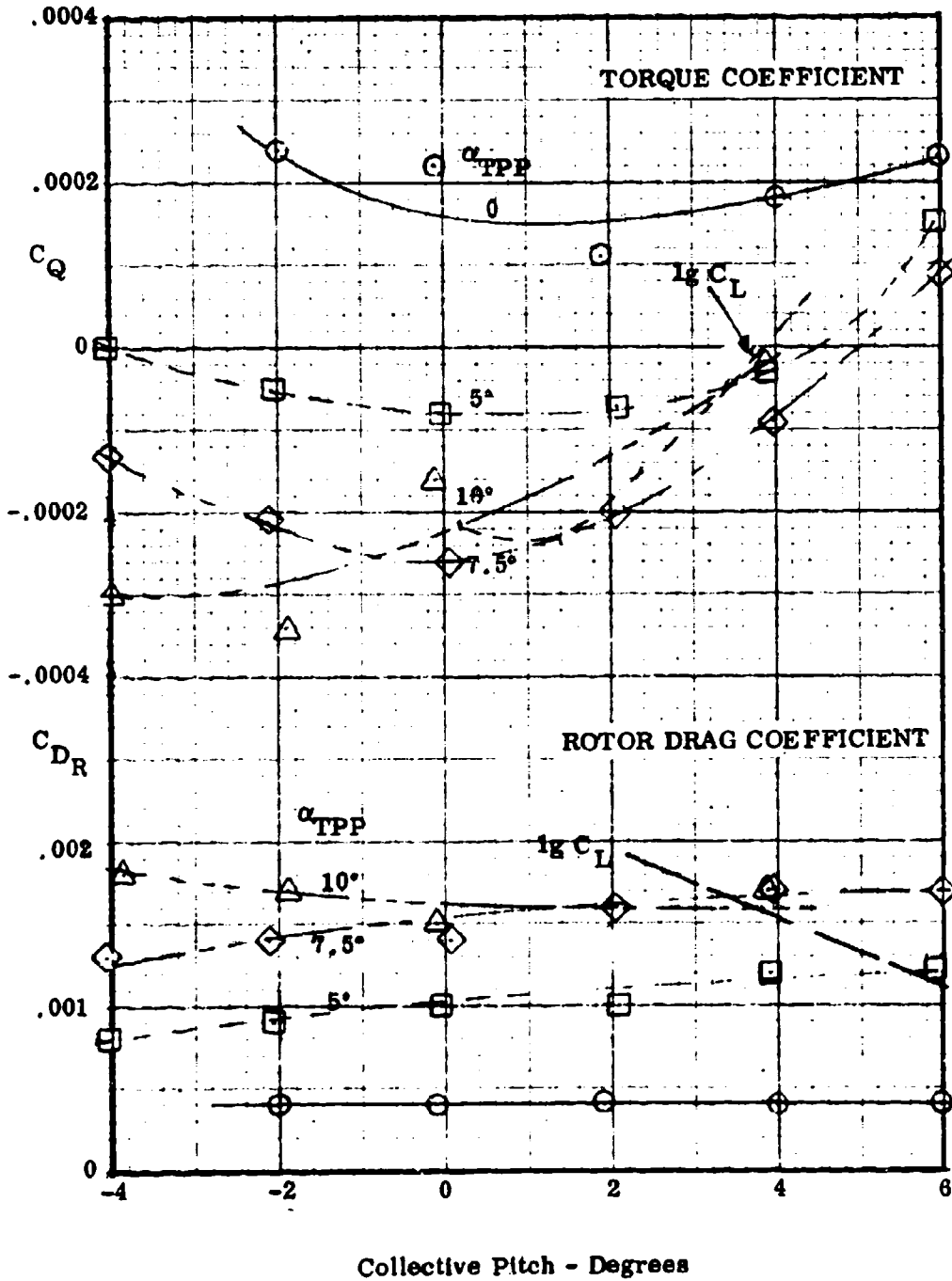
MEASURED ROTOR PERFORMANCE

$\mu = .57$, 1330 r.p.m., 192 knots, $M_{1, 90} = .76$, $\rho = .0022$, run 52



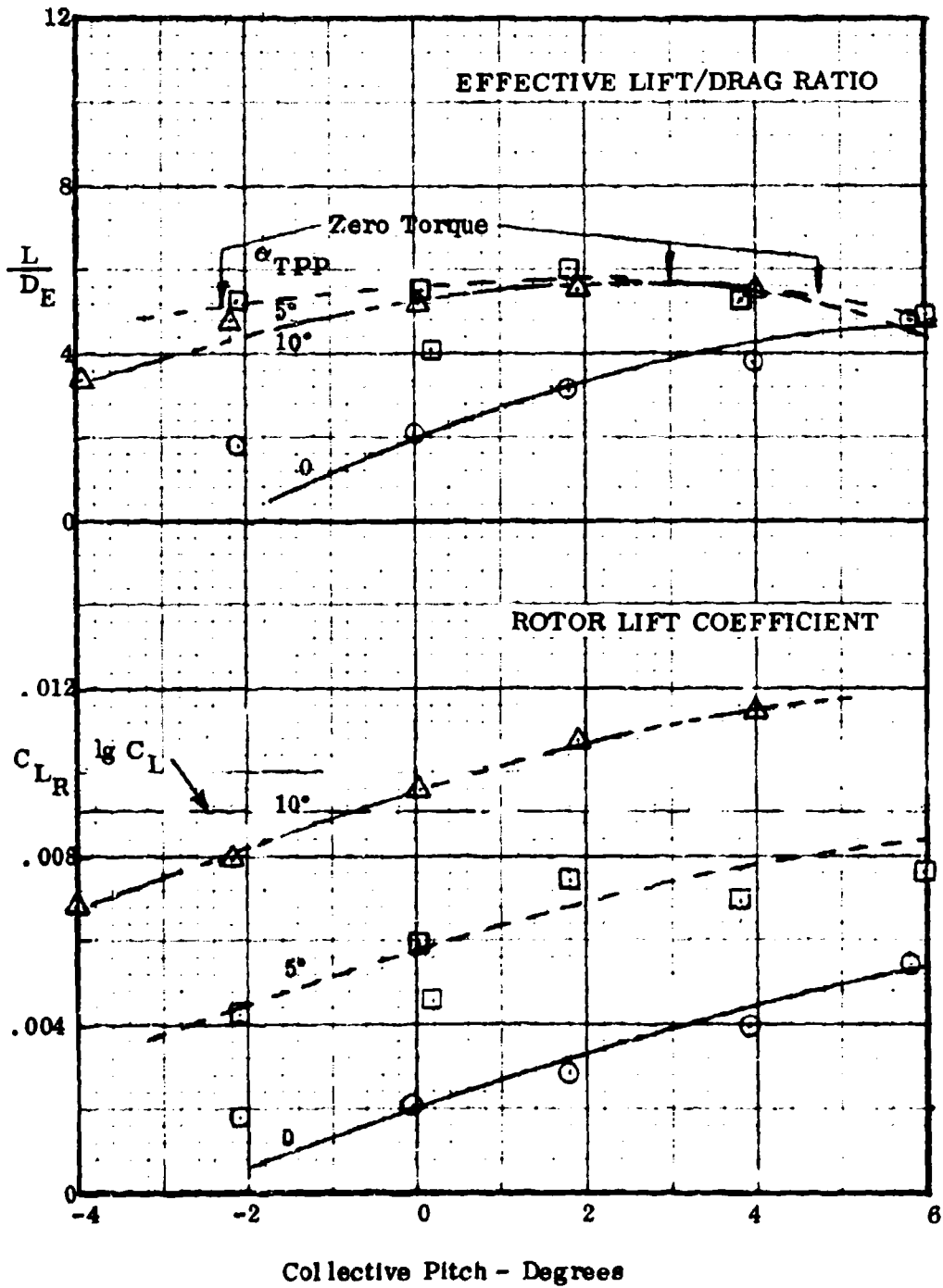
MEASURED ROTOR PERFORMANCE

$\mu = .57$, 1330 r.p.m., 192 knots, $M_{1, 90} = .76$, $\rho = .0022$, run 52



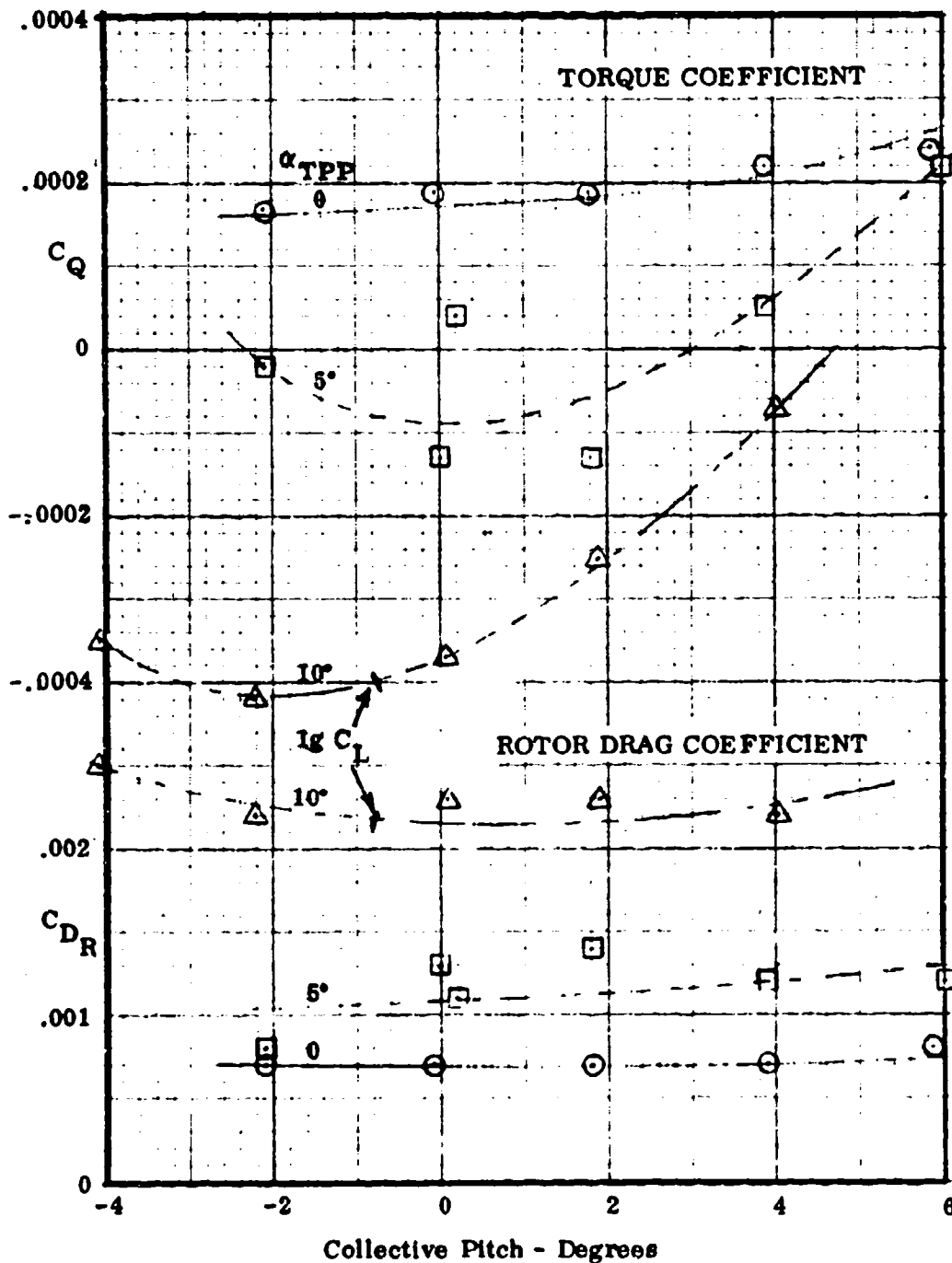
MEASURED ROTOR PERFORMANCE

$\mu = .72$, 1350 r.p.m., 243 knots, $M_{1,90} = .61$, $\rho = .0021$, run 57



MEASURED ROTOR PERFORMANCE

$\mu = .72$, 1350 r.p.m., 243 knots, $M_{1,90} = .61$, $\rho = .0021$, run 57

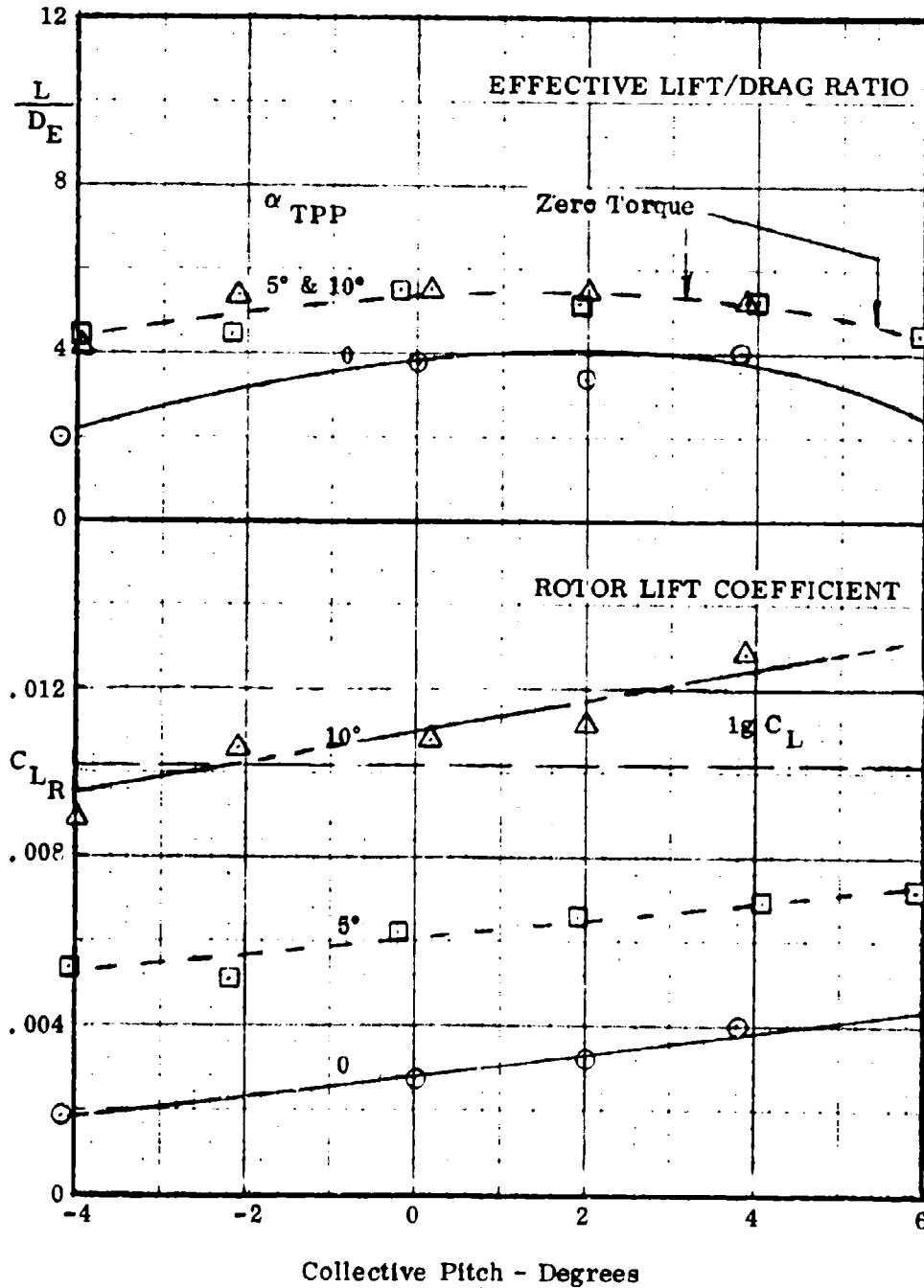


HC144R1070

Figure 2.20A

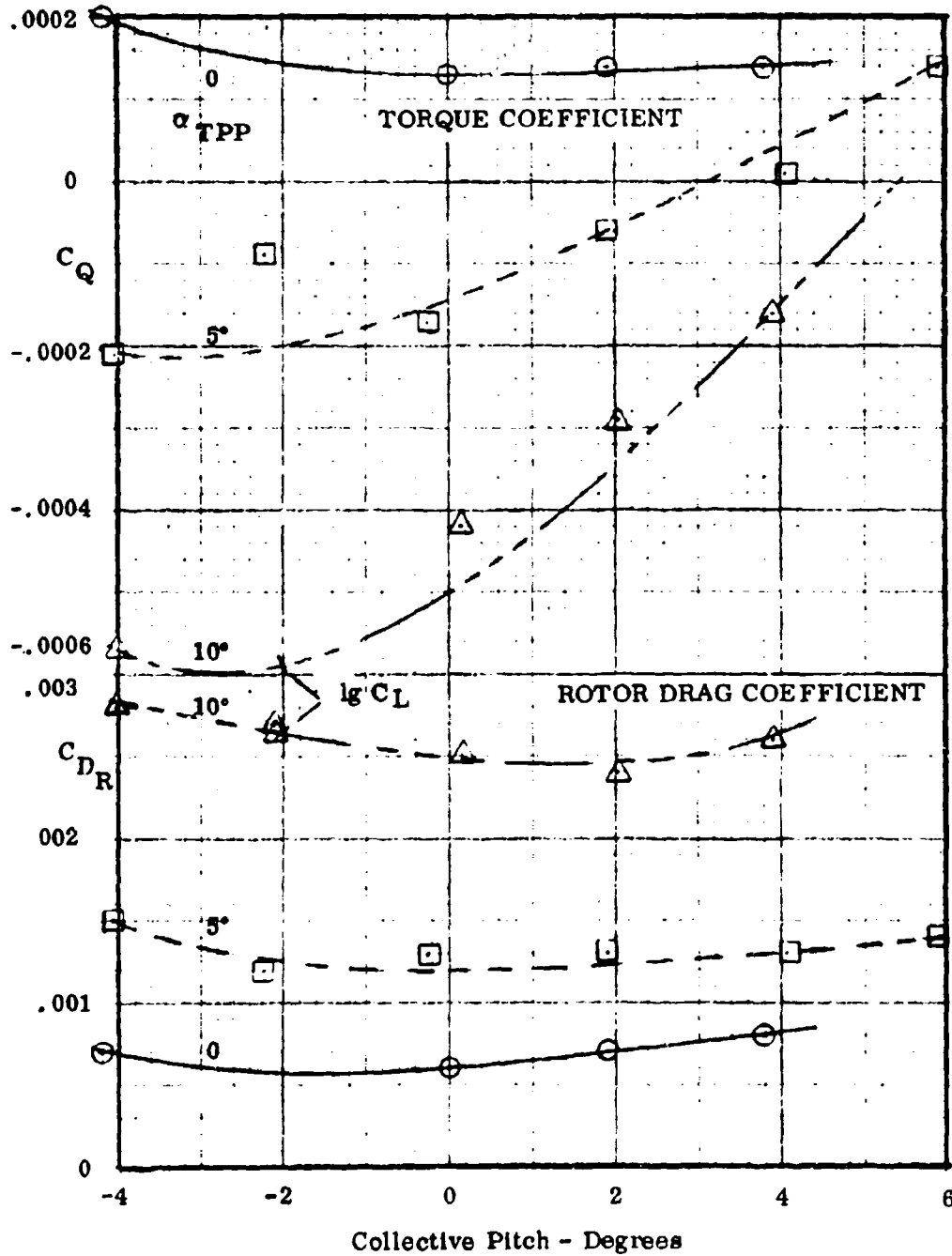
MEASURED ROTOR PERFORMANCE

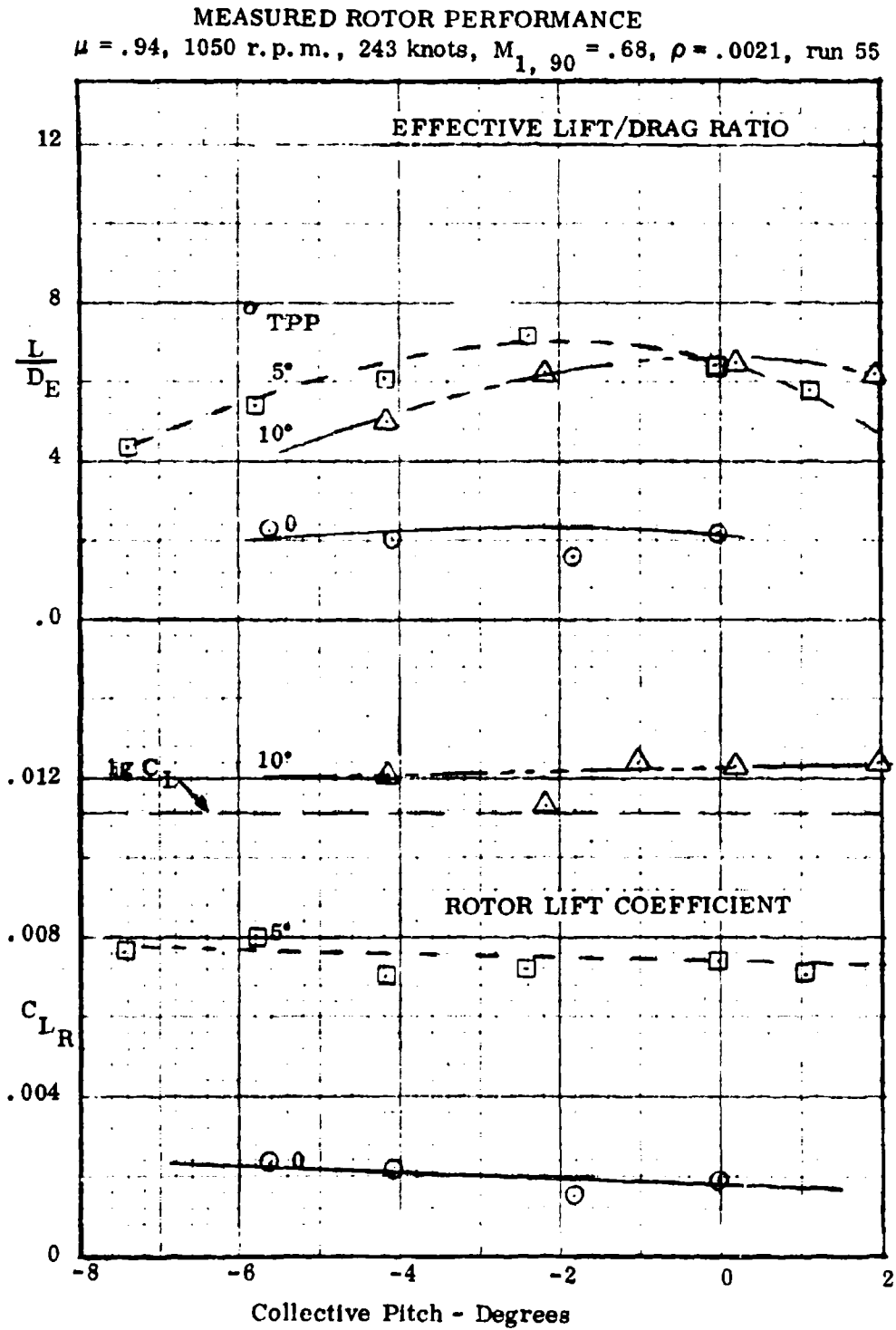
$\mu = .82$, 1170 r.p.m., 243 knots, $M_{1,90} = .65$, $\rho = .0021$, run 56



MEASURED ROTOR PERFORMANCE

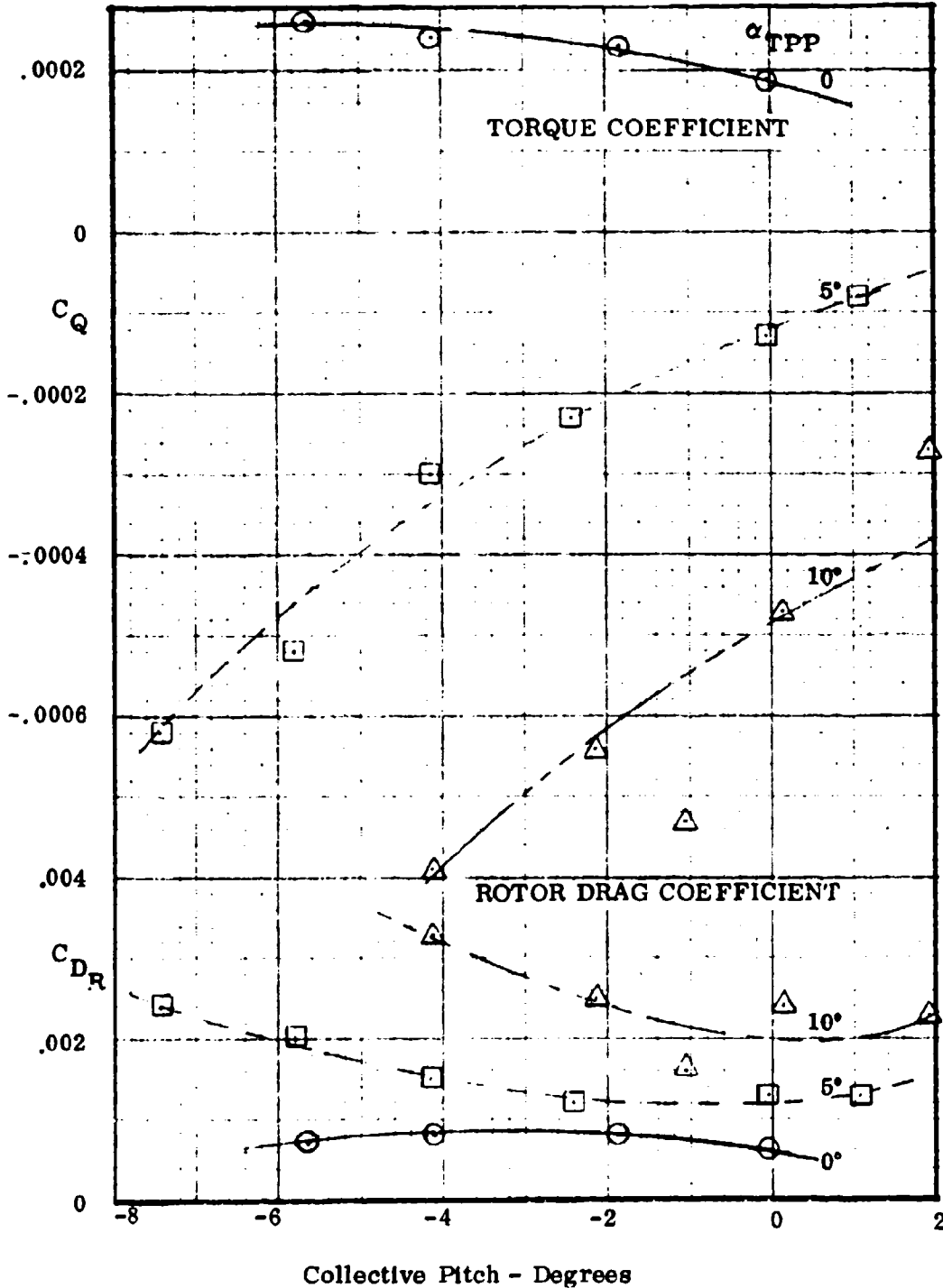
$u = .82$, 1170 r.p.m., 243 knots, $M_{1,90} = .65$, $\rho = .0021$, run 56





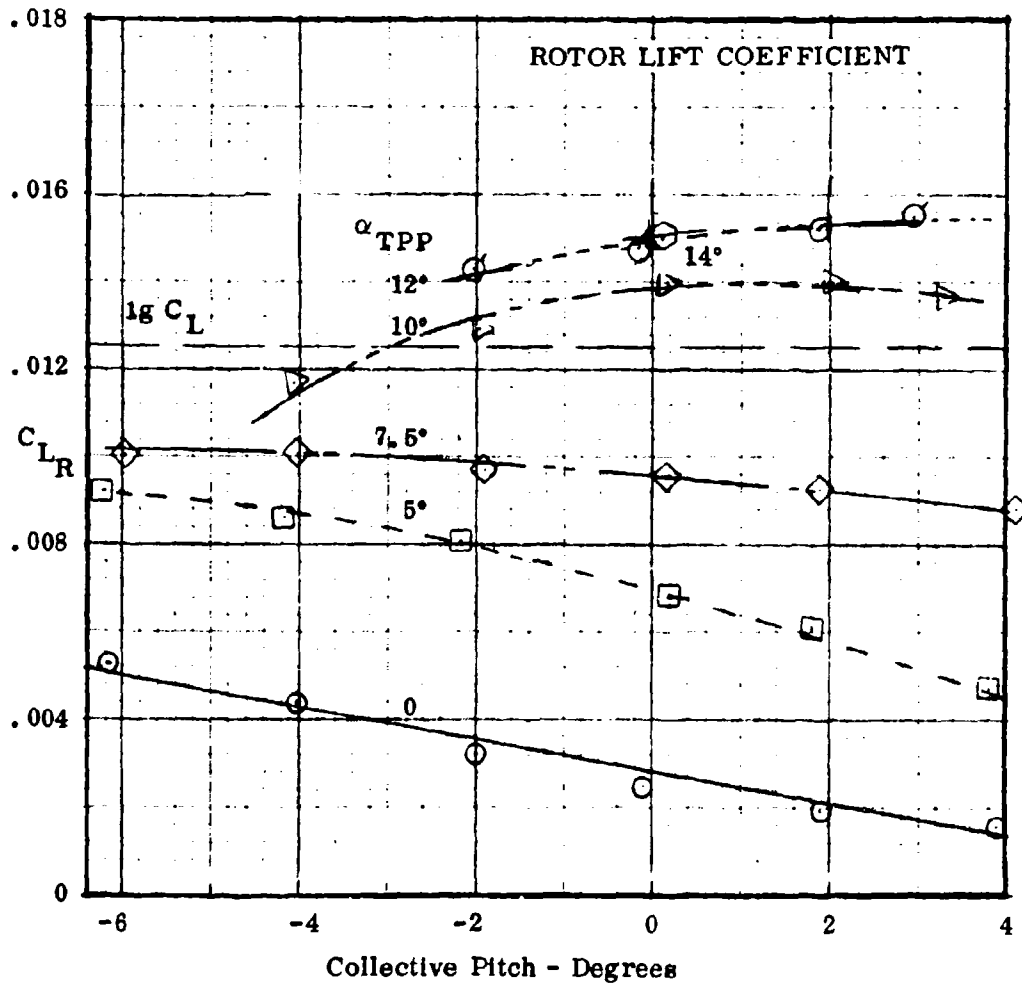
MEASURED ROTOR PERFORMANCE

$\mu = .94$, 1050 r.p.m., 243 knots, $M_{1,90} = .68$, $\rho = .0021$, run 55



MEASURED ROTOR PERFORMANCE

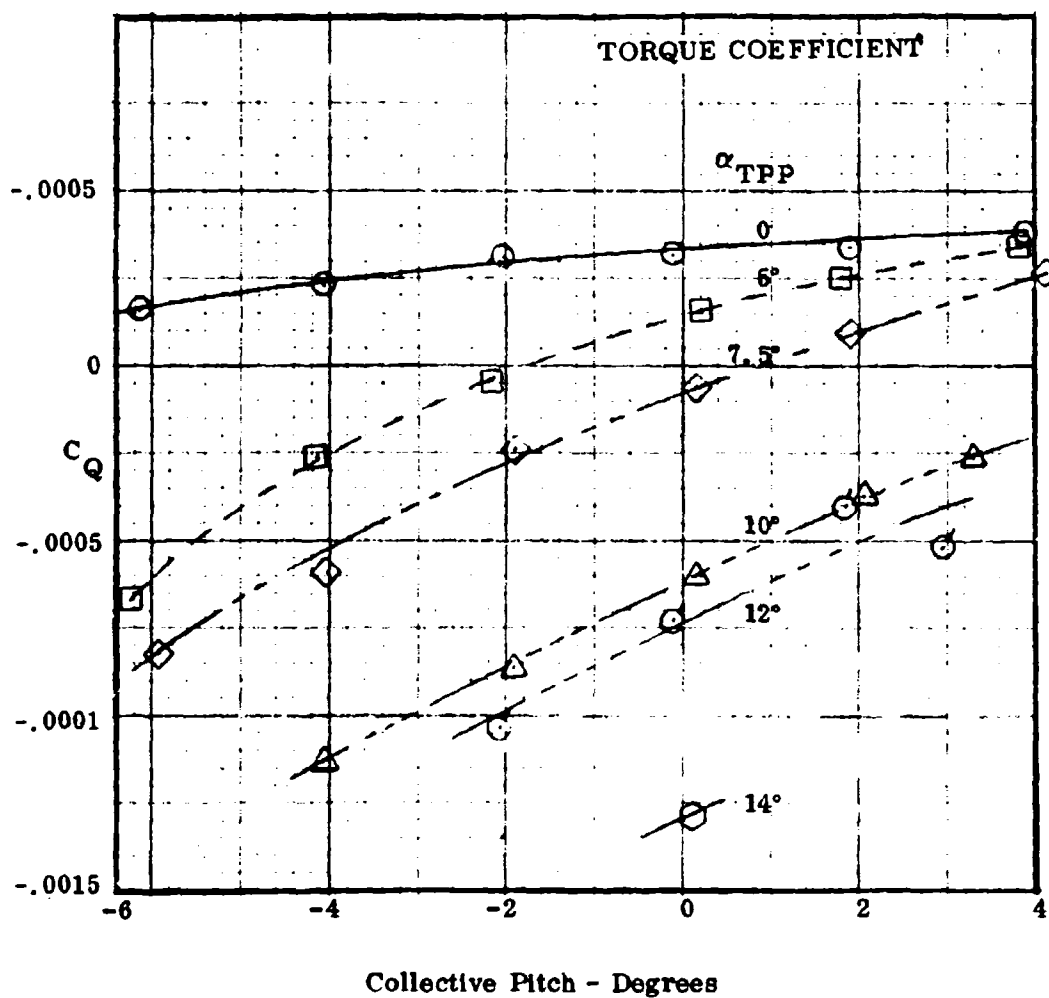
$\mu = 1.60$, 1170 r.p.m., 295 knots, $M_{1,90} = .85$, $\rho = .0020$, run 59



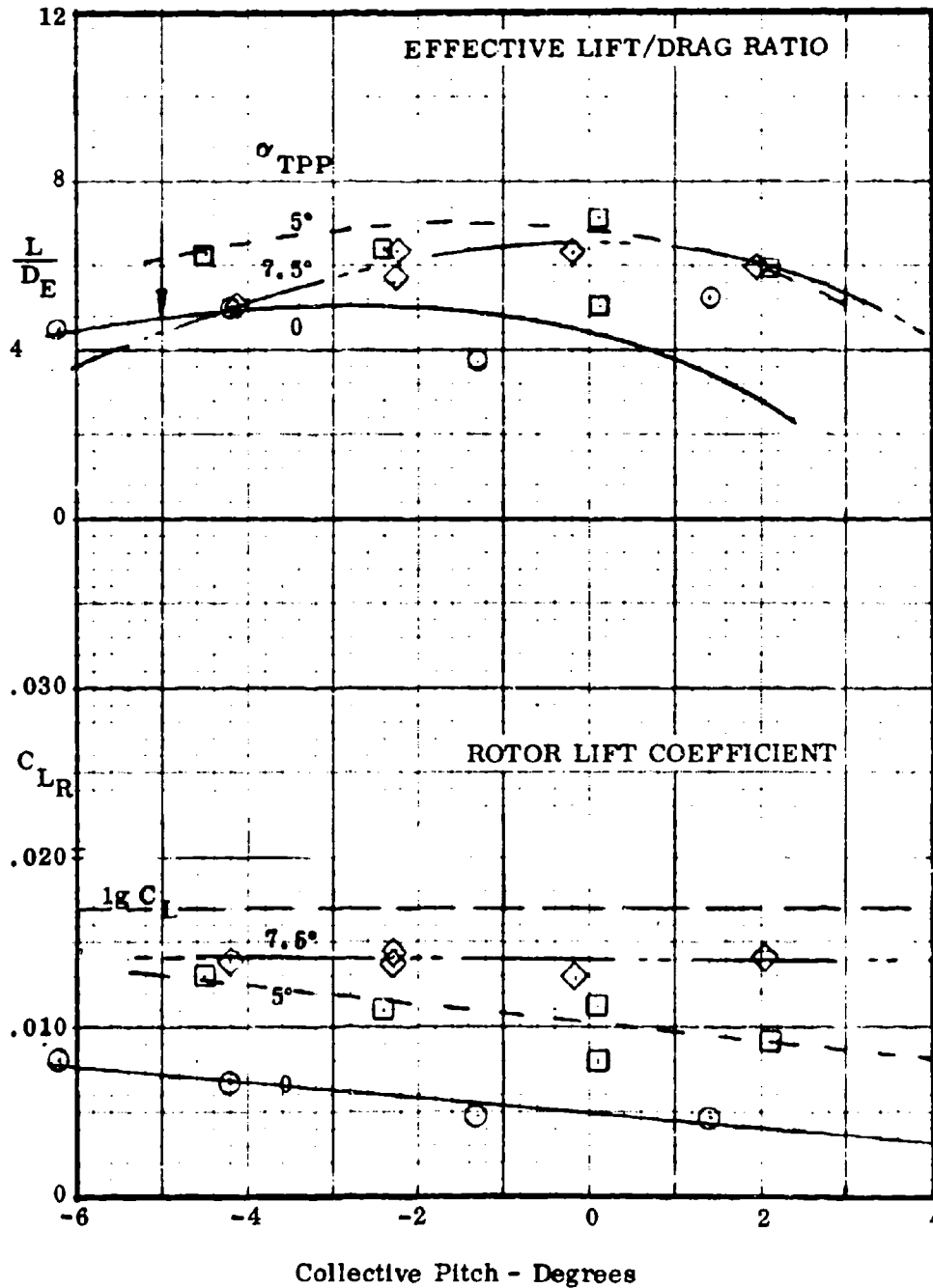
MEASURED ROTOR PERFORMANCE

$\mu = 1.00$, 1170 r.p.m., 295 knots, $M_{1,90} = .85$, $\rho = .0020$, run 59

(Drag data not available)

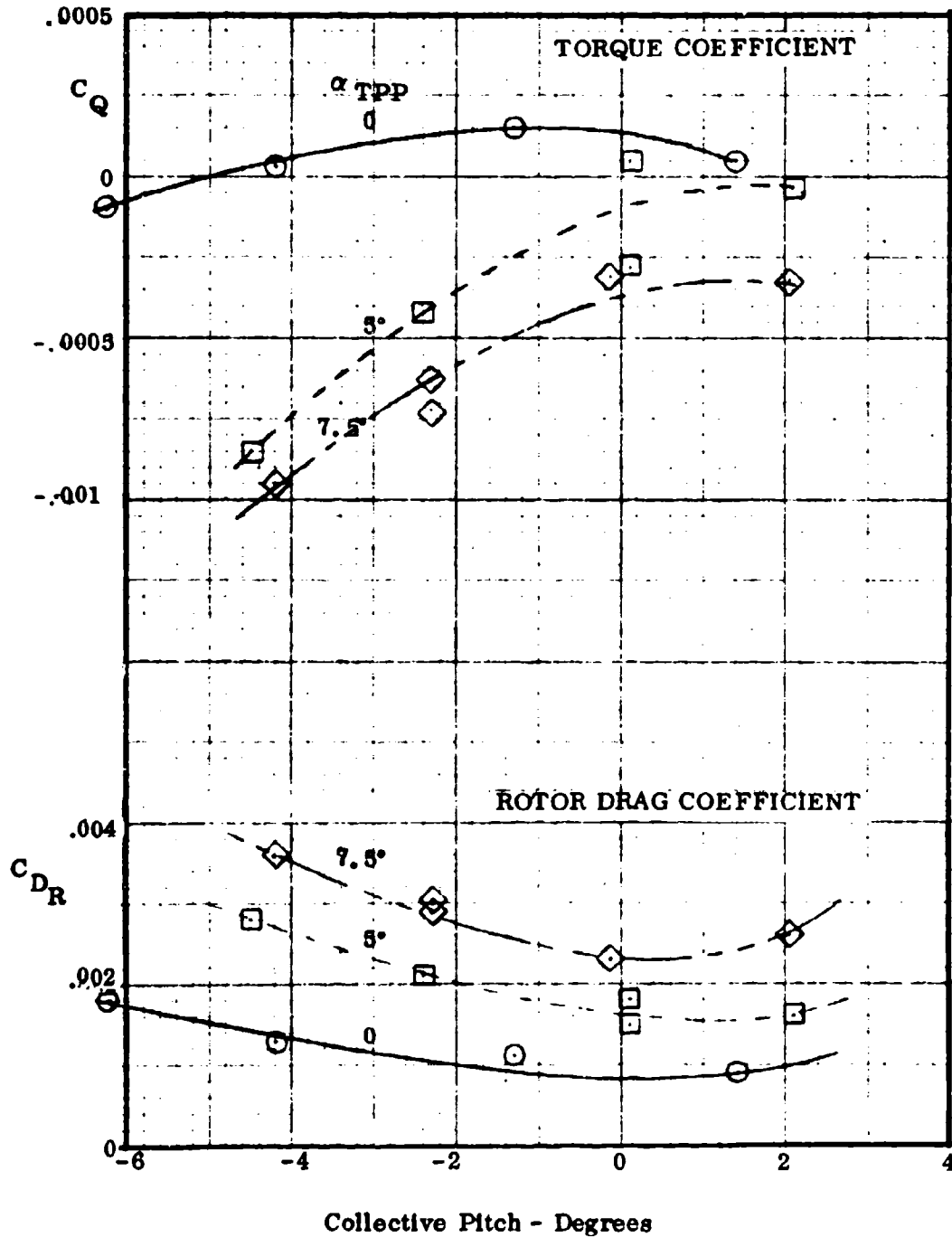


MEASURED ROTOR PERFORMANCE
 $\mu = 1.15$, 833 r.p.m., 239 knots, $M_{1,90} = .66$, $\rho = .0021$, run 54



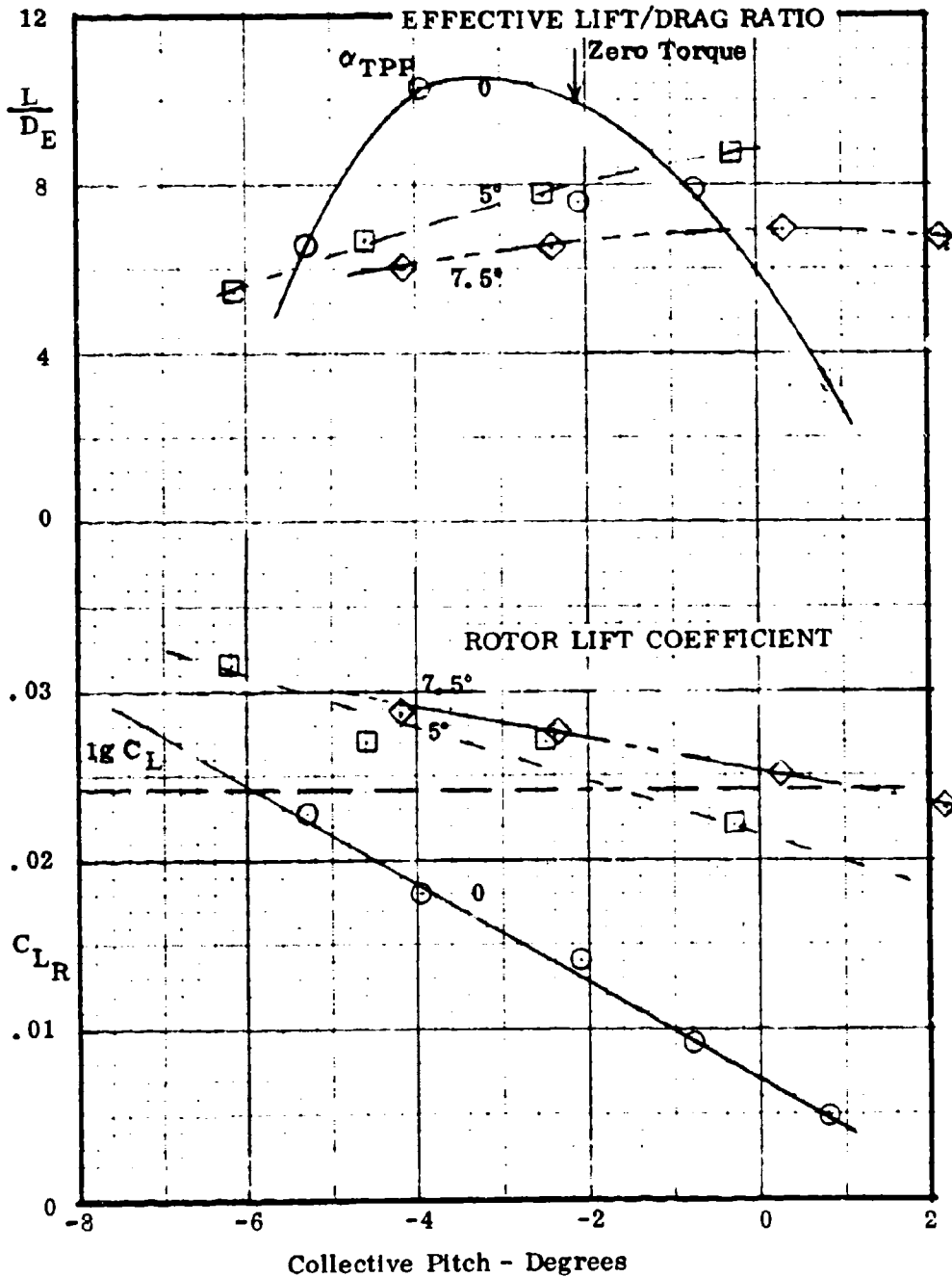
MEASURED ROTOR PERFORMANCE

$u = 1.15$, 833 r.p.m., 239 knots, $M_{1,90} = .66$, $\rho = .0021$, run 54

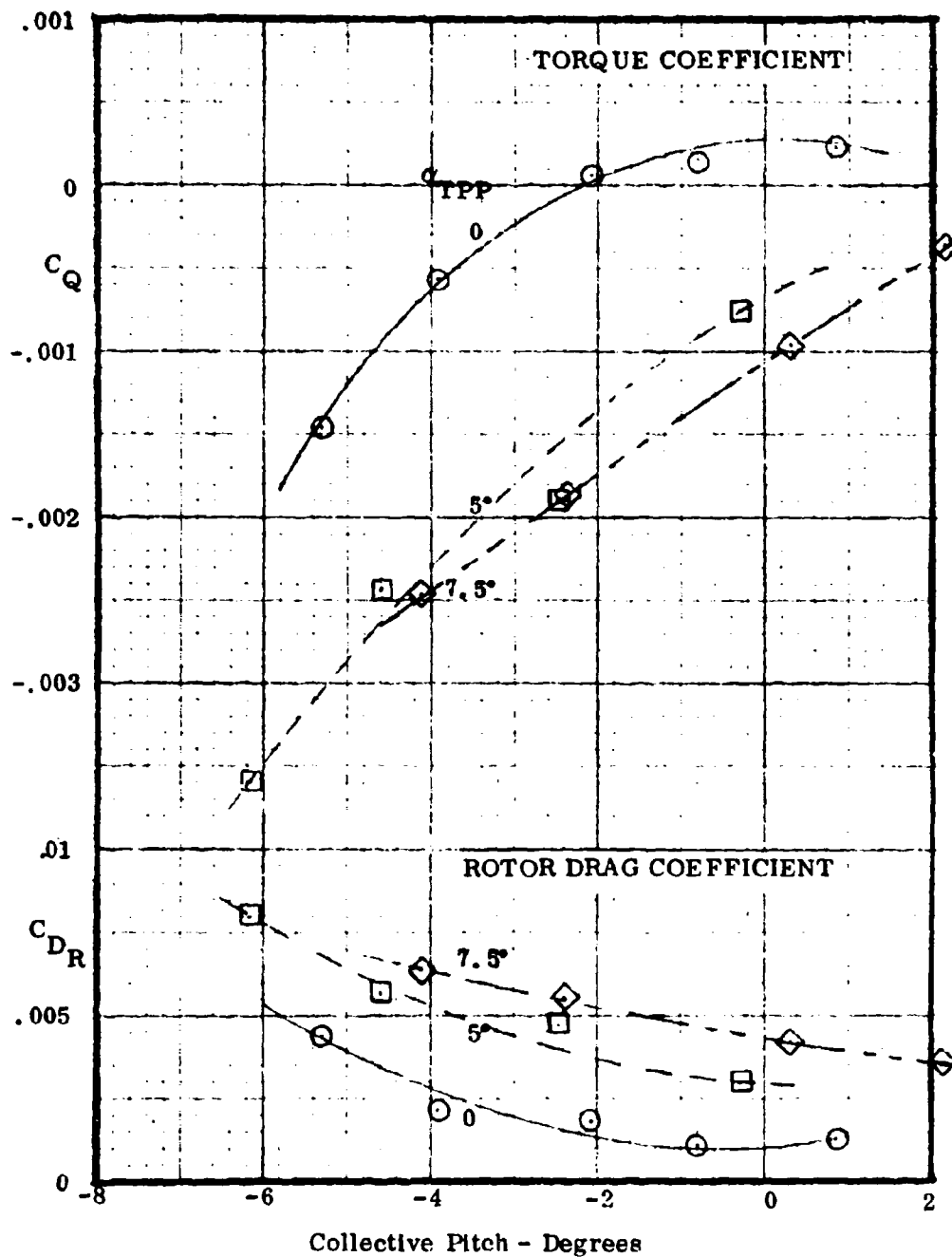


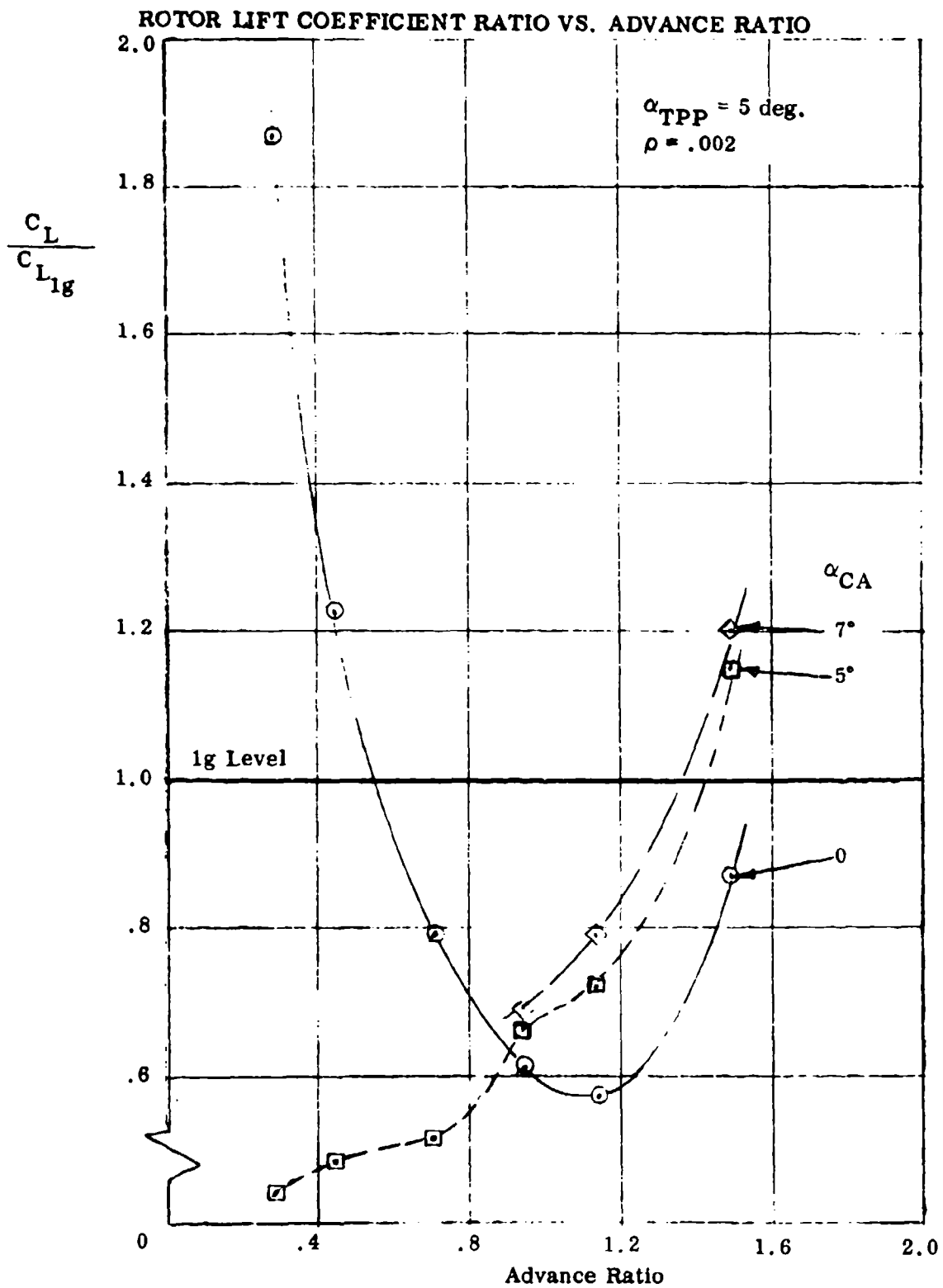
MEASURED ROTOR PERFORMANCE

$\mu = 1.50$, 660 r.p.m., 243 knots, $M_{1,90} = .59$, $\rho = .0021$, run 53

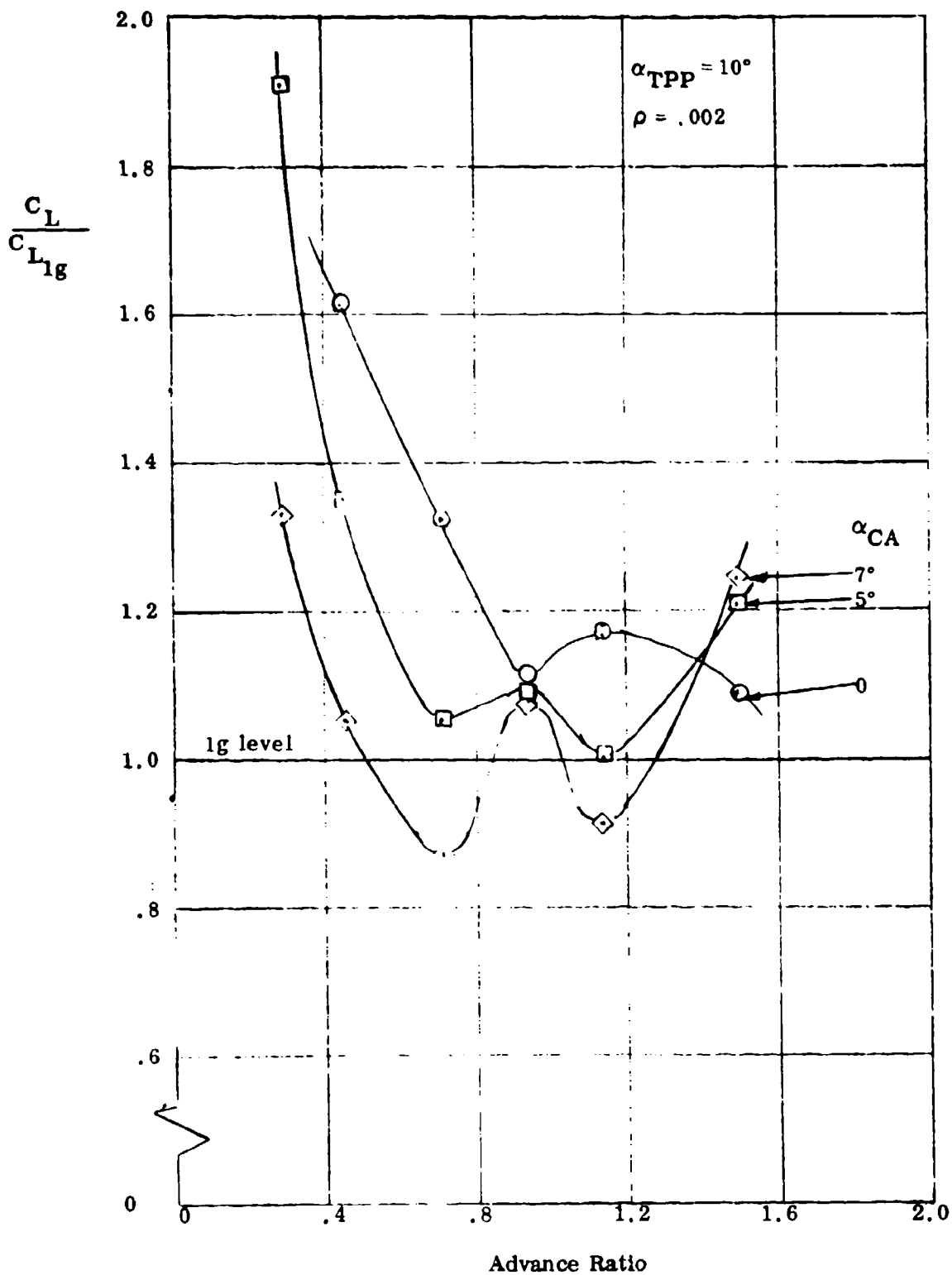


MEASURED ROTOR PERFORMANCE
 $\mu = 1.50$, 660 r.p.m., 243 knots, $M_{1,90} = .59$, $\rho = .0021$, run 53



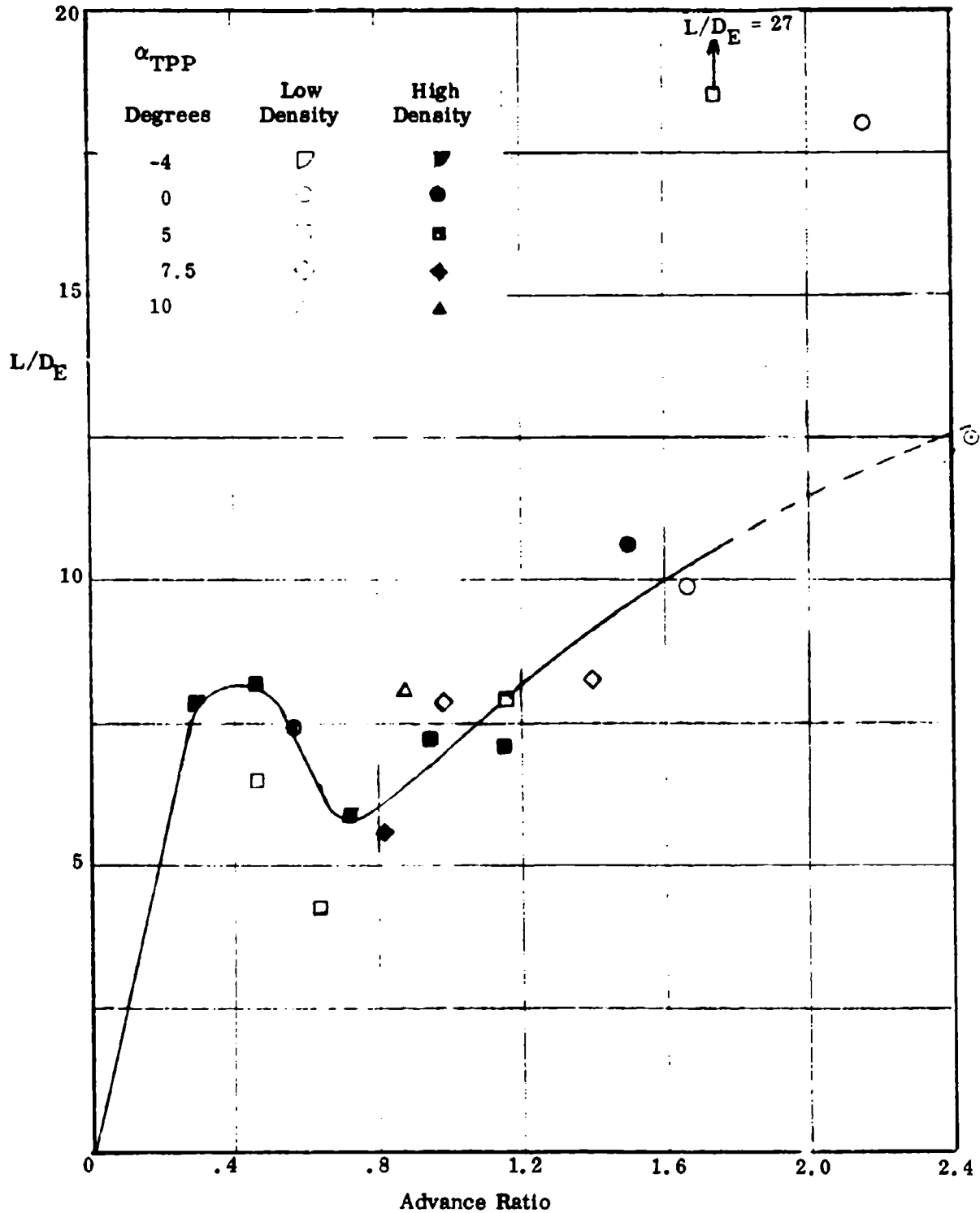


ROTOR LIFT COEFFICIENT RATIO VS. ADVANCE RATIO

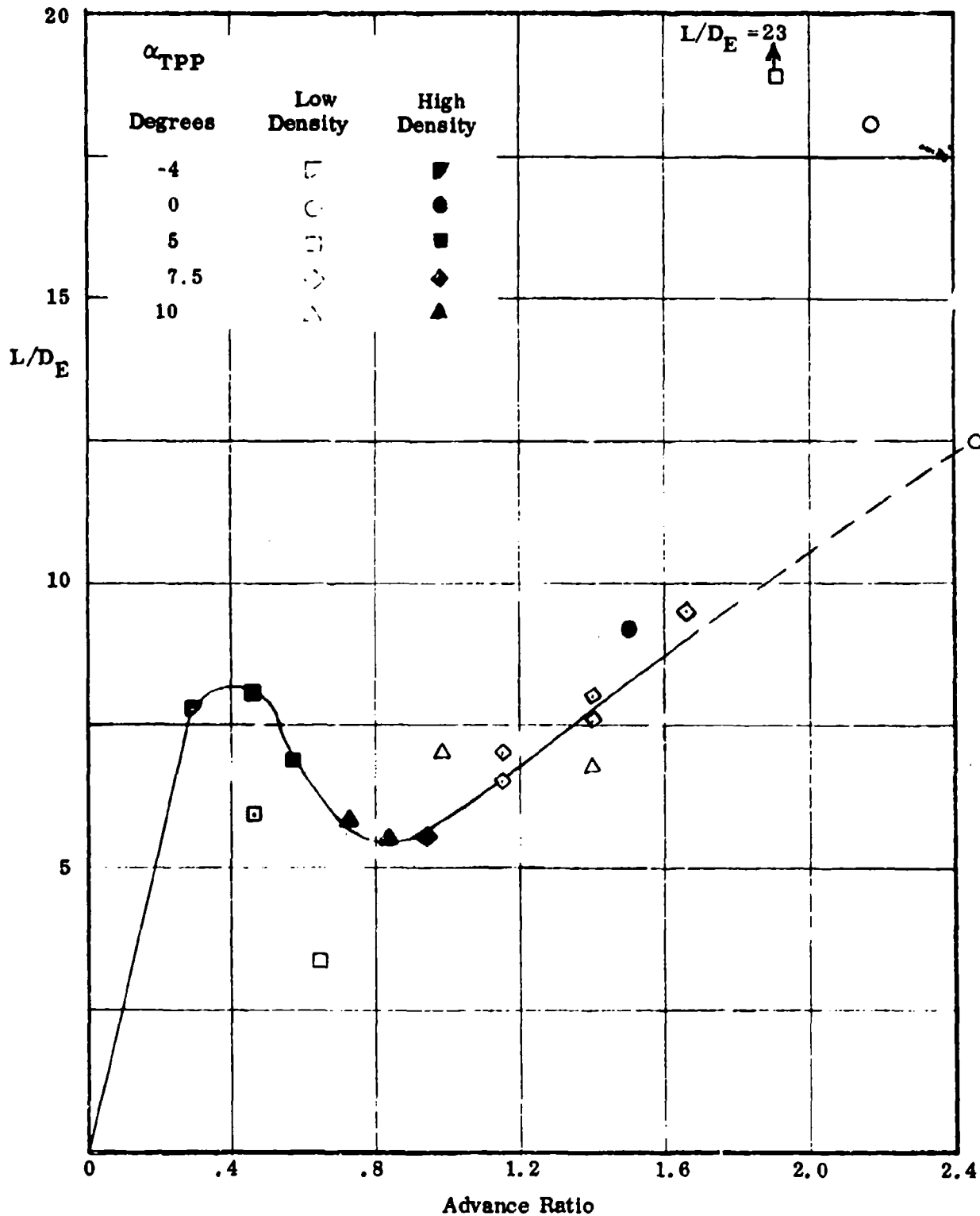


HC144R1070

**MAXIMUM EFFECTIVE LIFT - DRAG RATIO MEASURED
VS ADVANCE RATIO**

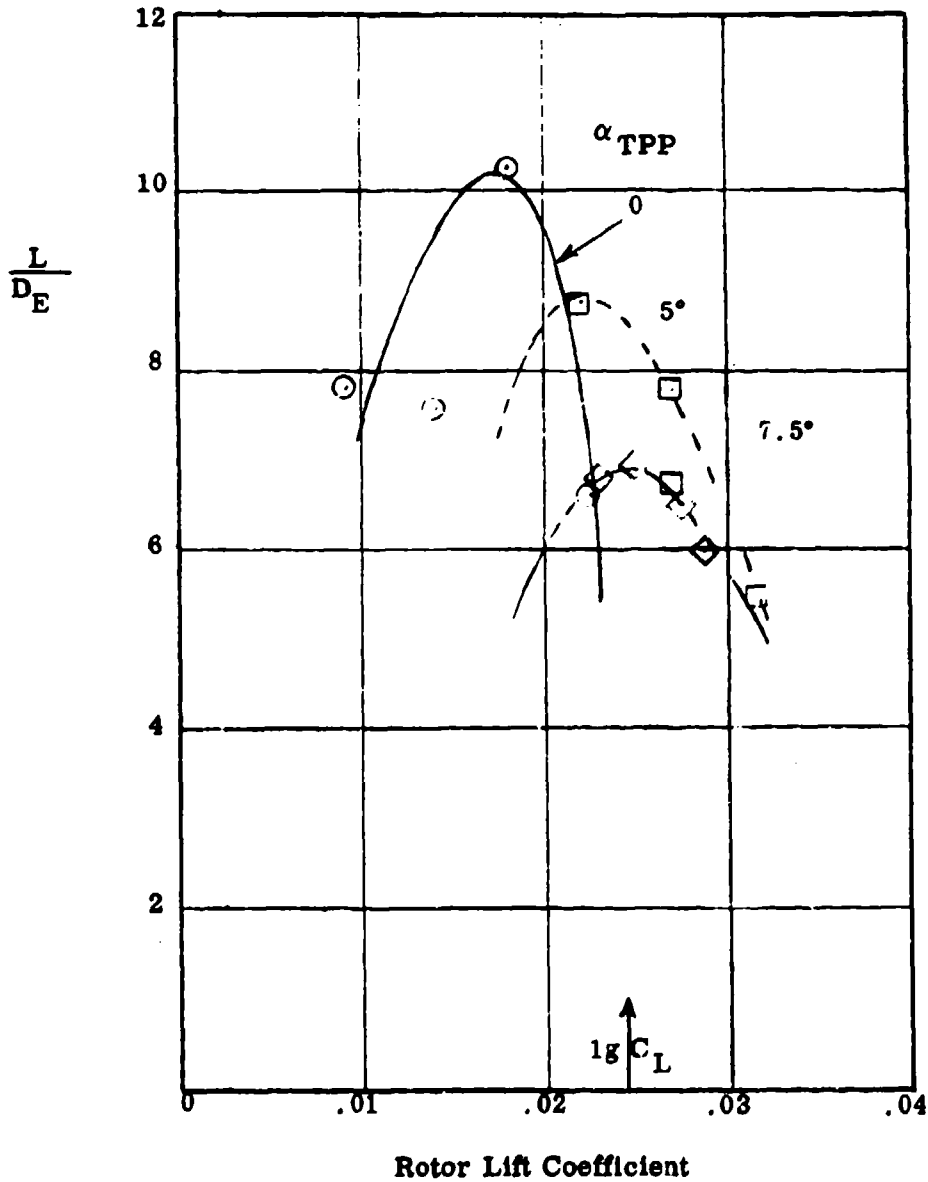


MEASURED EFFECTIVE LIFT - DRAG RATIO AT 8 LB. PER SQ. FT.
DISC LOADING VS ADVANCE RATIO

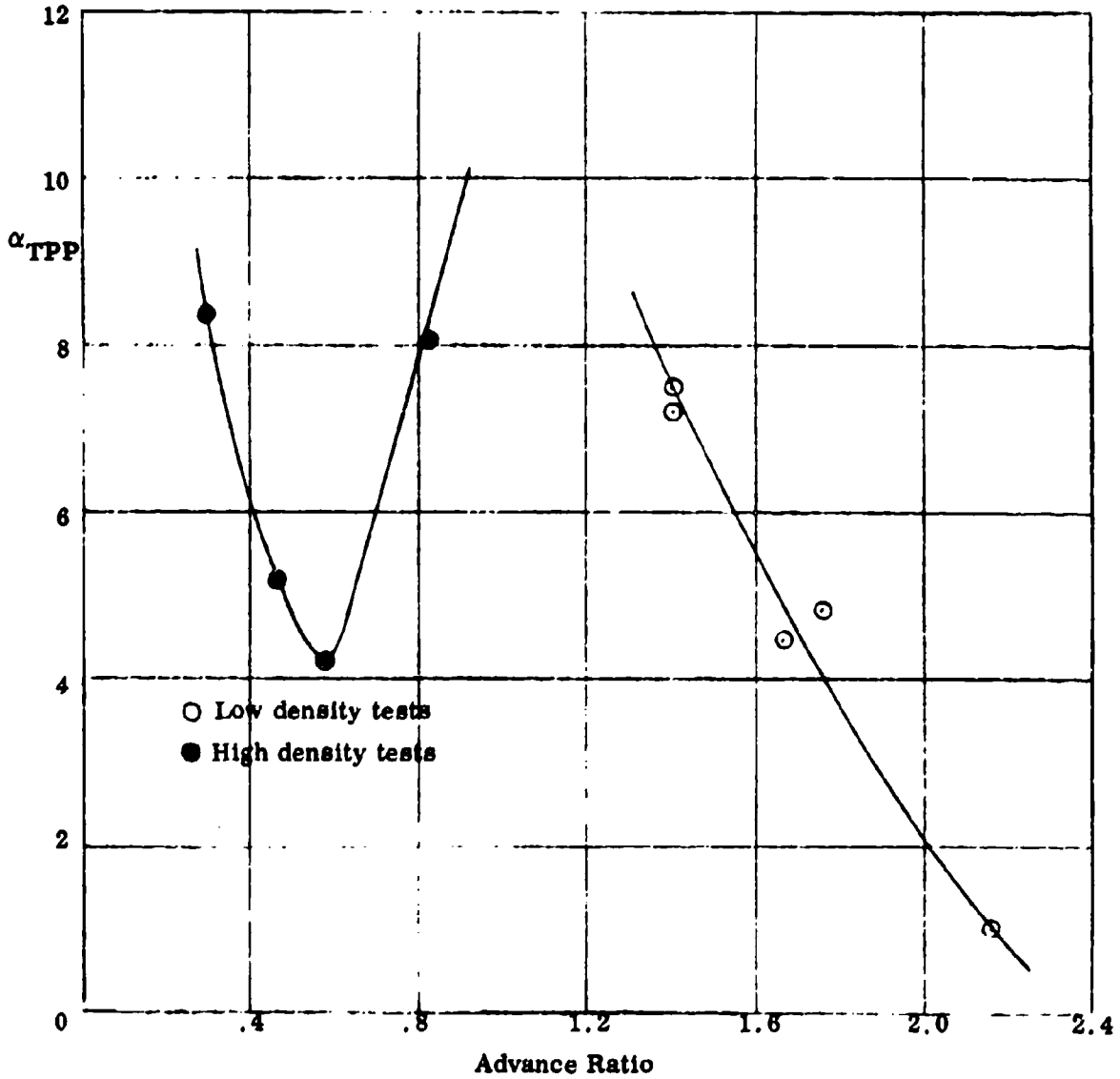


**EFFECTIVE LIFT-DRAG RATIO VS
ROTOR LIFT COEFFICIENT**

$\mu = 1.50$, 660 rpm, 243 knots, $M_{1,90} = .59$, $\rho = .002$, Run 53.



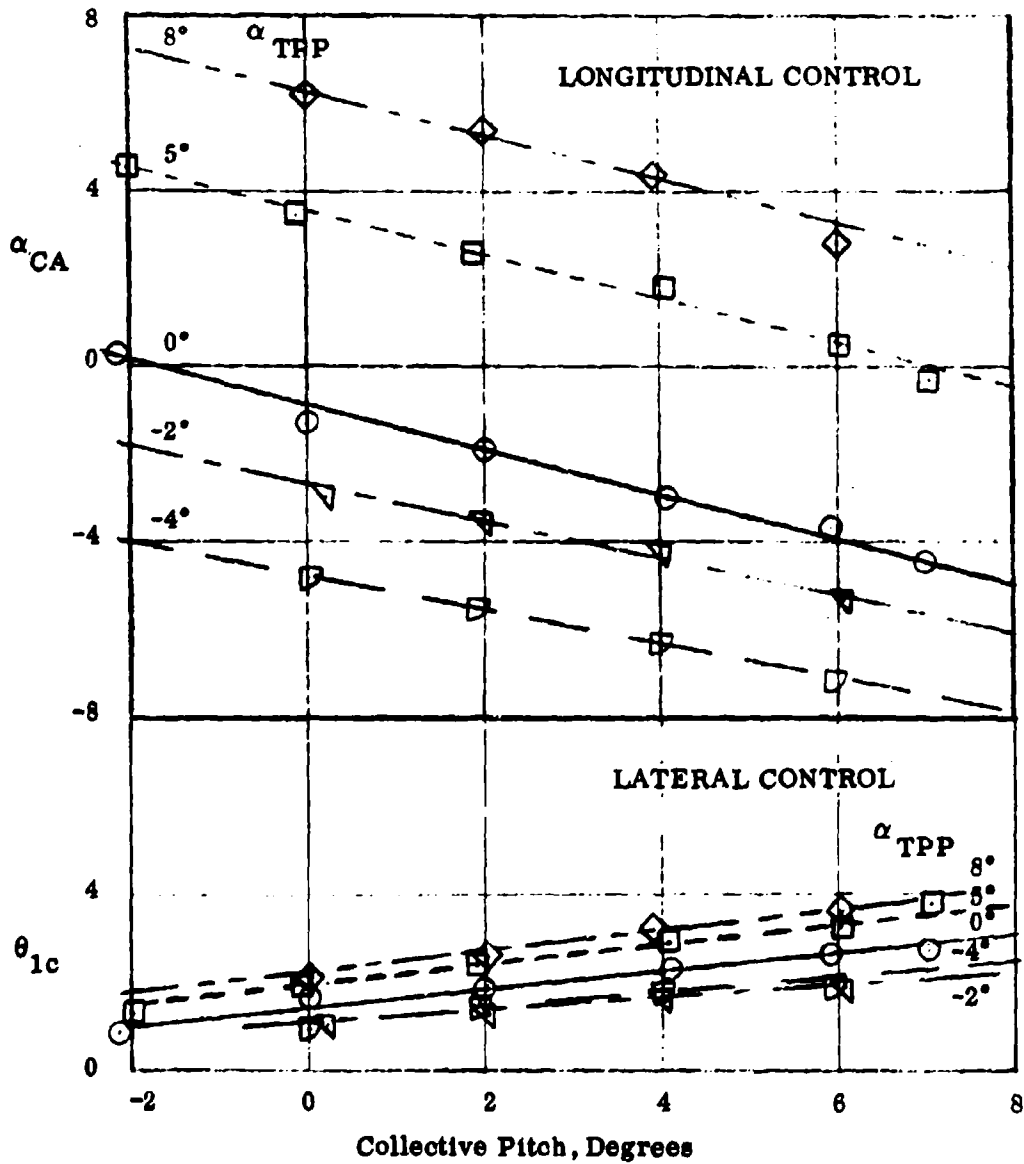
**TIP PATH PLANE ANGLE FOR LEVEL FLIGHT
AND ZERO TORQUE VS ADVANCE RATIO**



ROTOR CONTROL

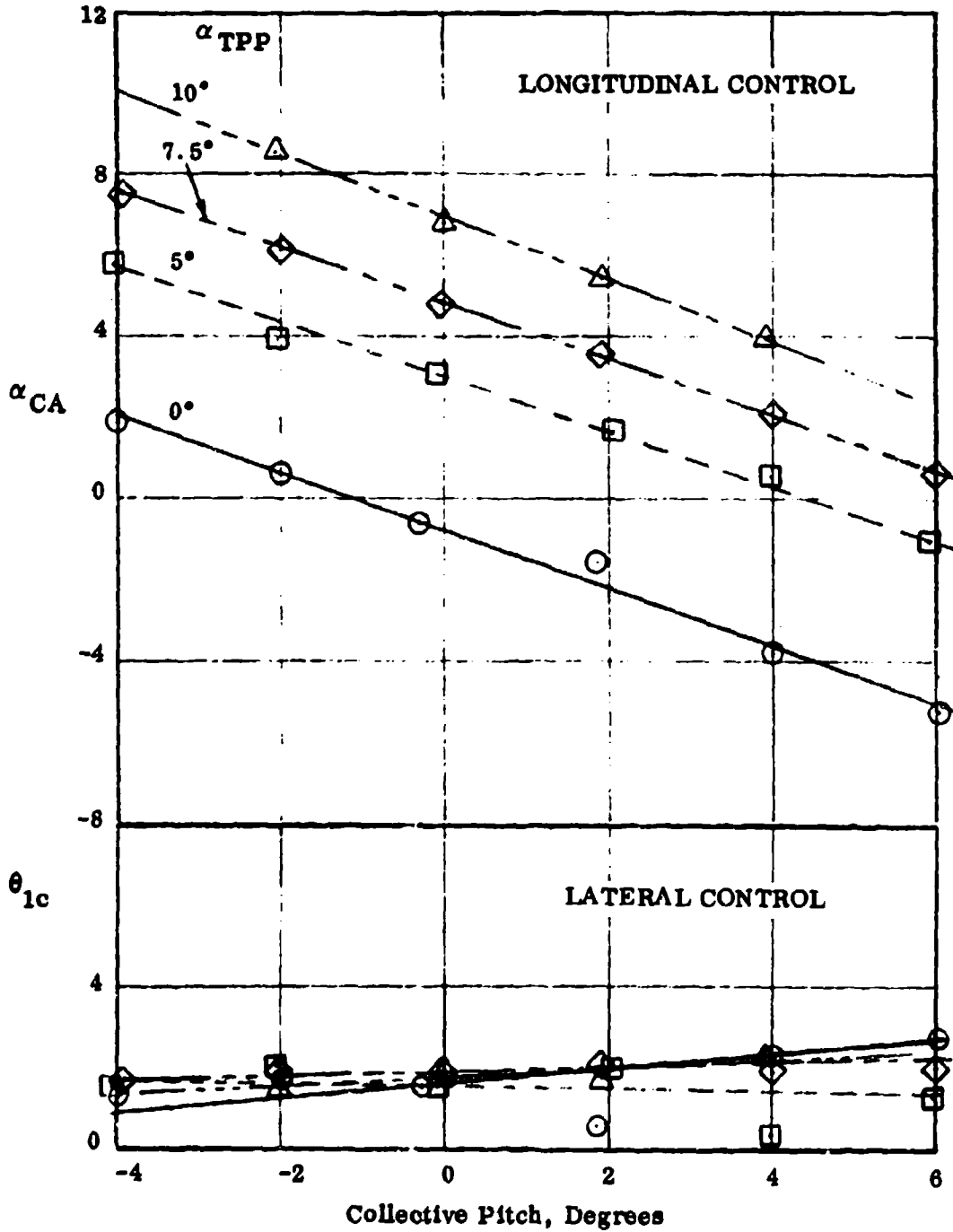
$\mu = .29$, 1670 r.p.m., 121 knots, $M_{1,90} = .79$, $D = .0023$, run 50

(Rotor trimmed laterally and longitudinally)



ROTOR CONTROL

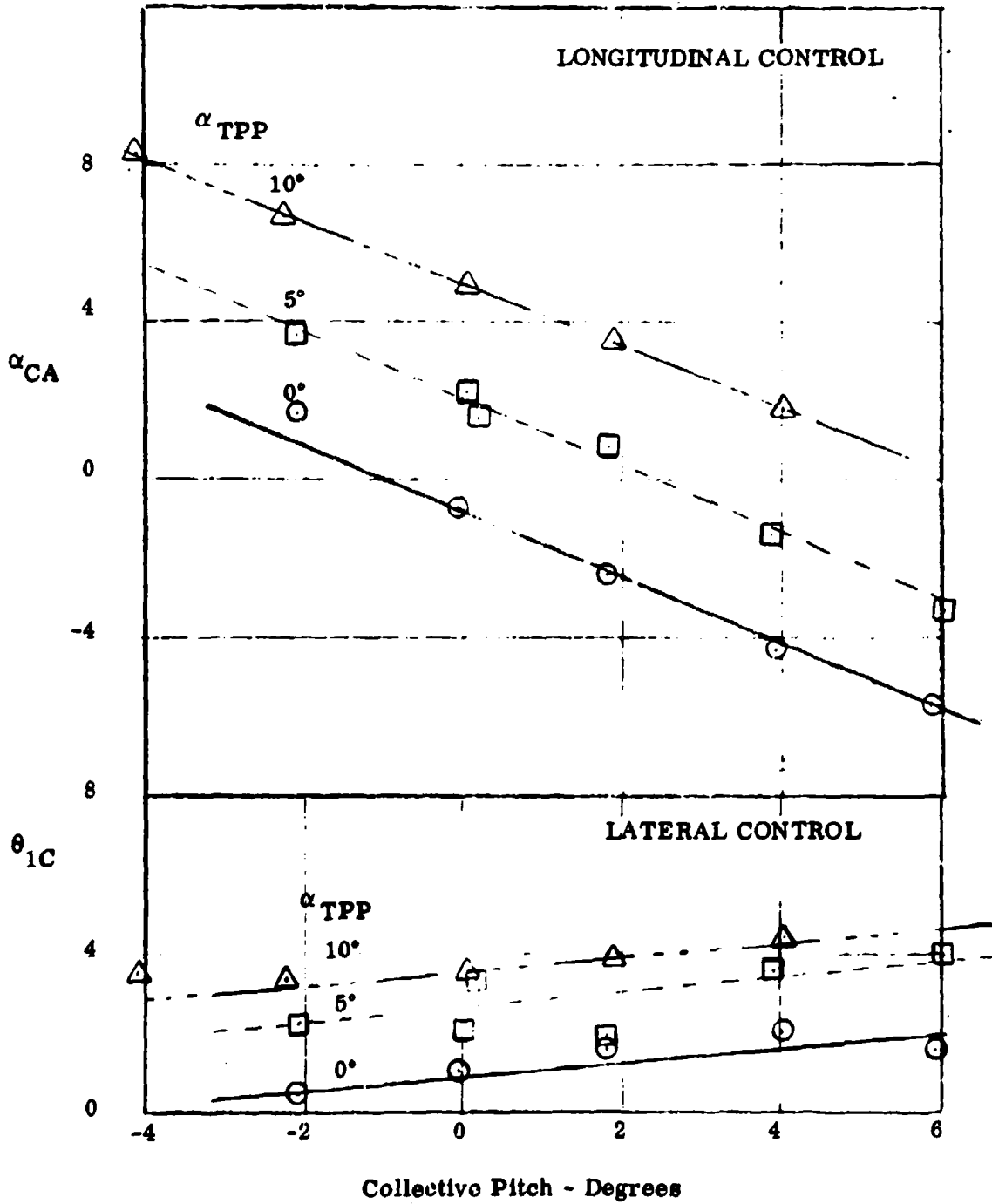
$\mu = .46$, 1670 r.p.m., 191 knots, $M_{1,90} = .89$, $\rho = .0022$, run 51



ROTOR CONTROL

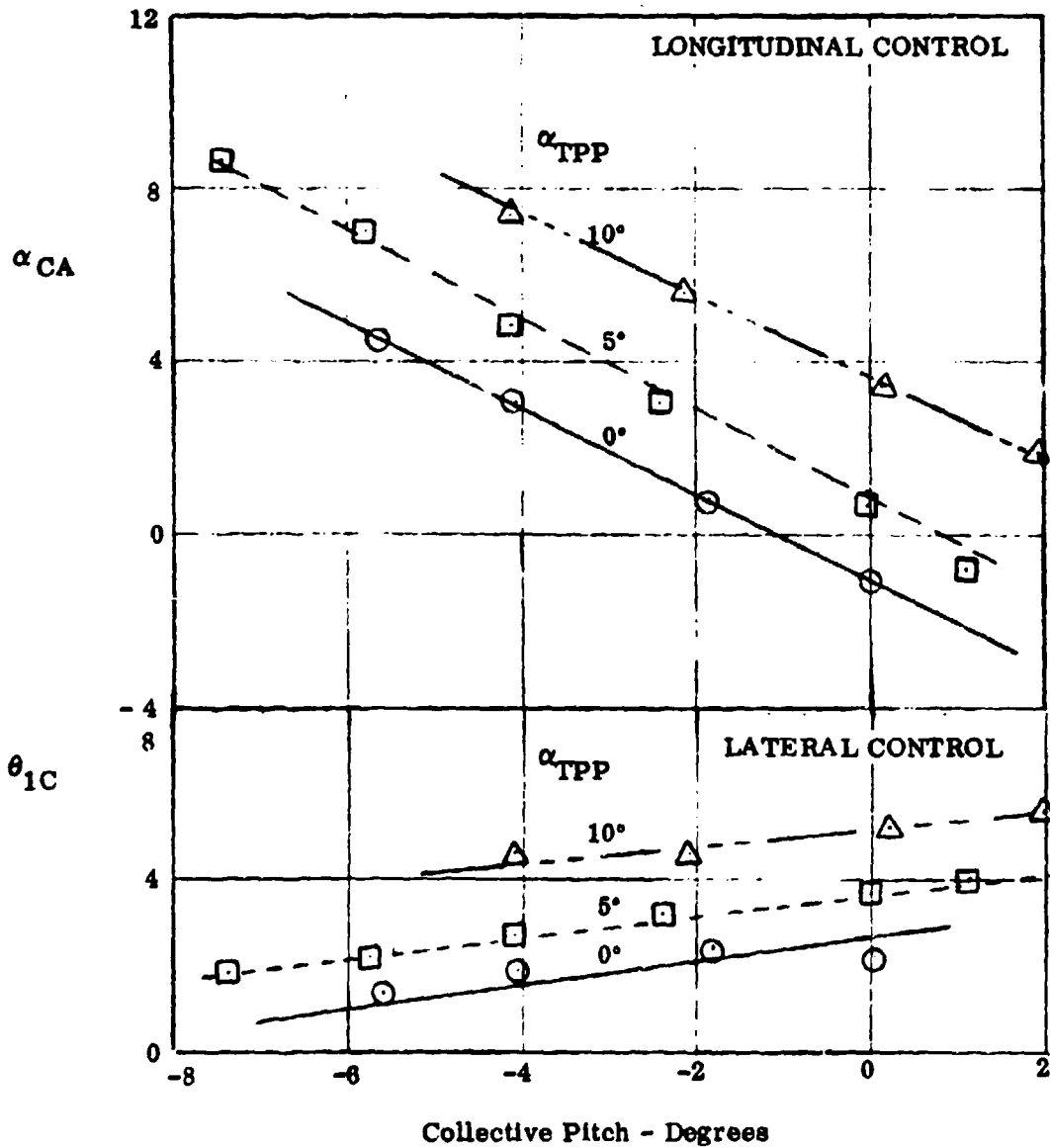
$\mu = .72$, 1350 rpm, 243 knots, $M_{1,90} = .61$, $\rho = .0021$, Run 57

(Rotor trimmed laterally and longitudinally)



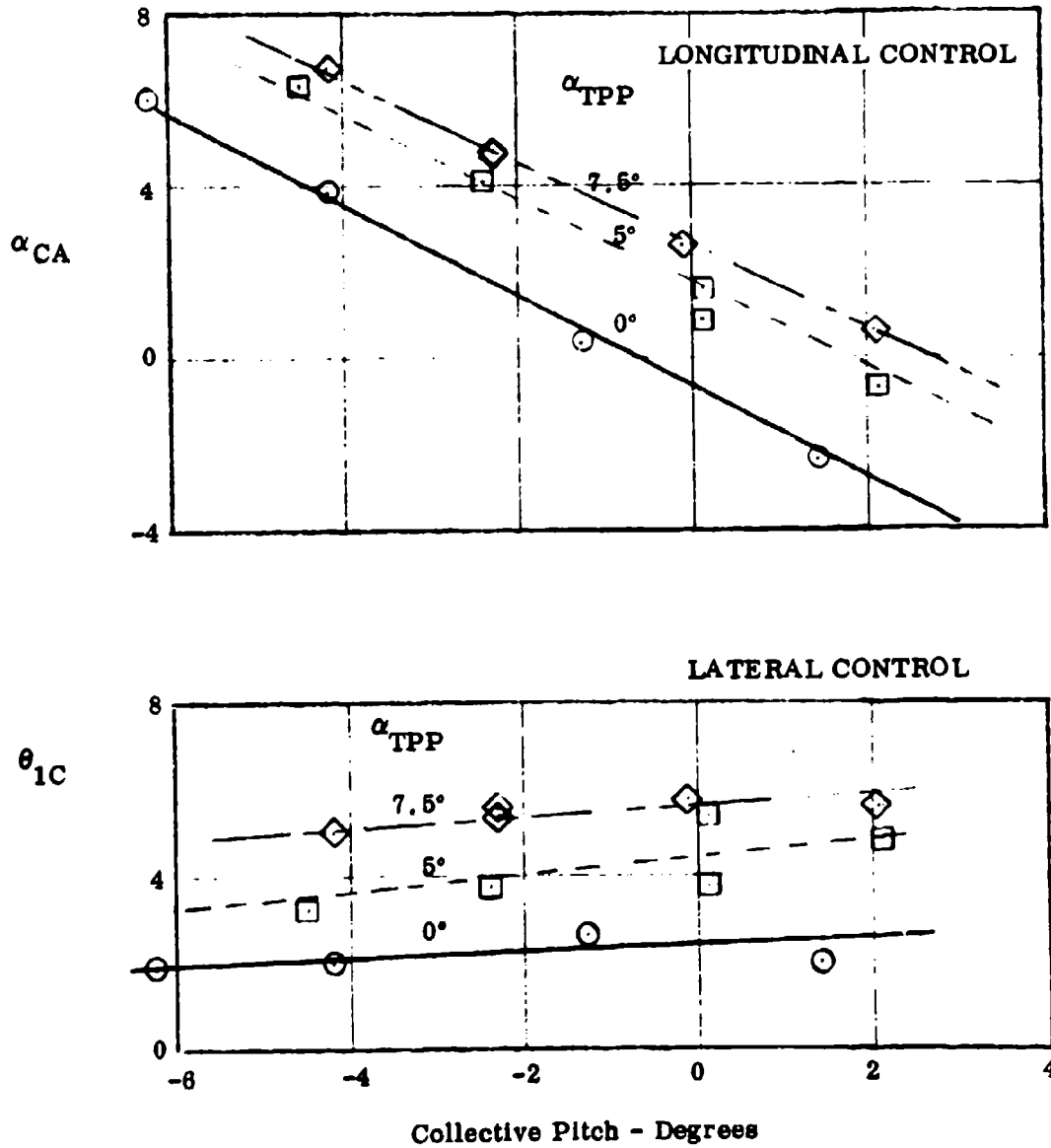
ROTOR CONTROL

$\mu = .94$, 1060 r.p.m., 243 knots, $M_{1.90} = .68$, $\rho = .0021$, Run 55



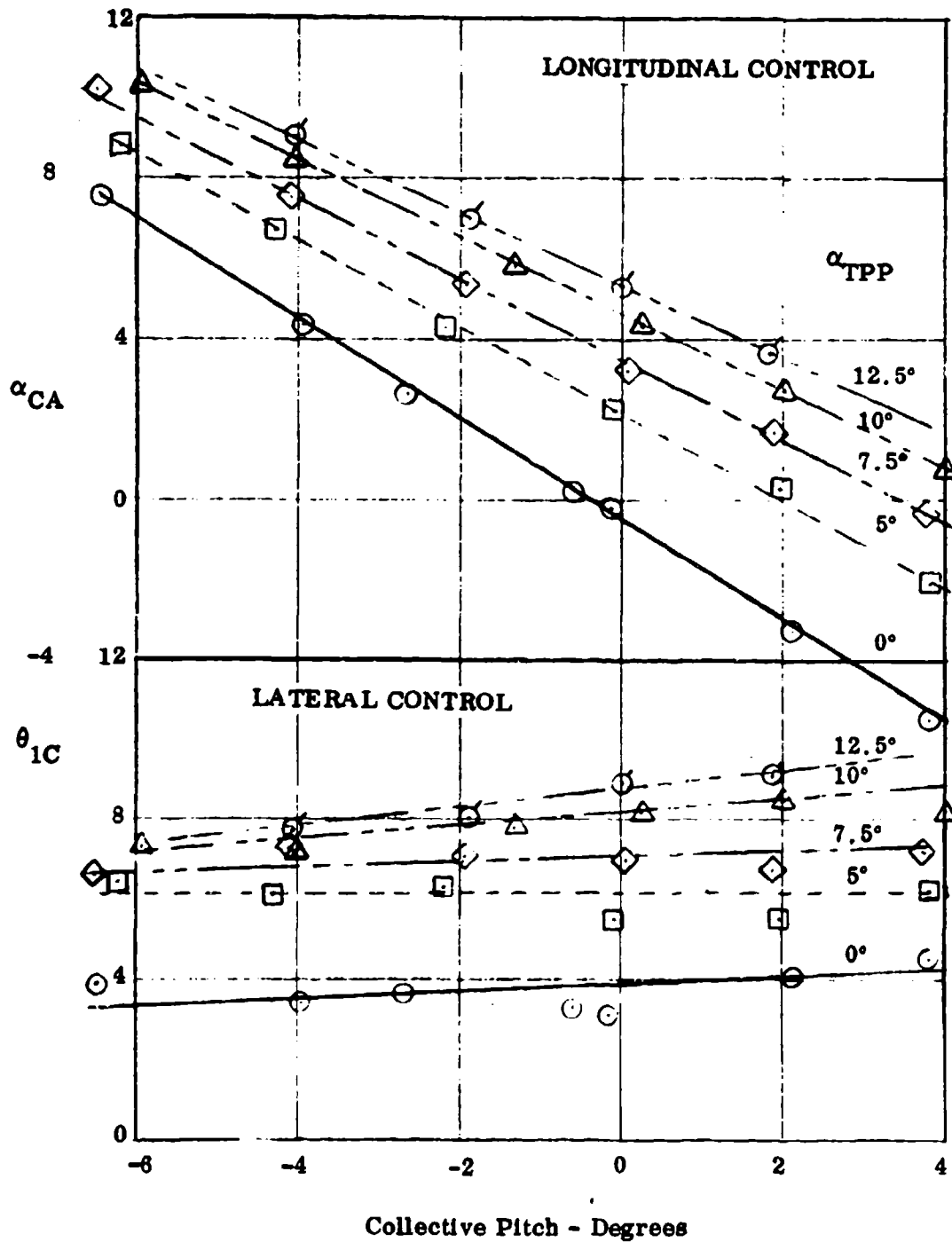
ROTOR CONTROL

$\mu = 1.15$, 833 r.p.m., 239 knots, $M_{1,90} = .66$, $\rho = .0021$, Run 54



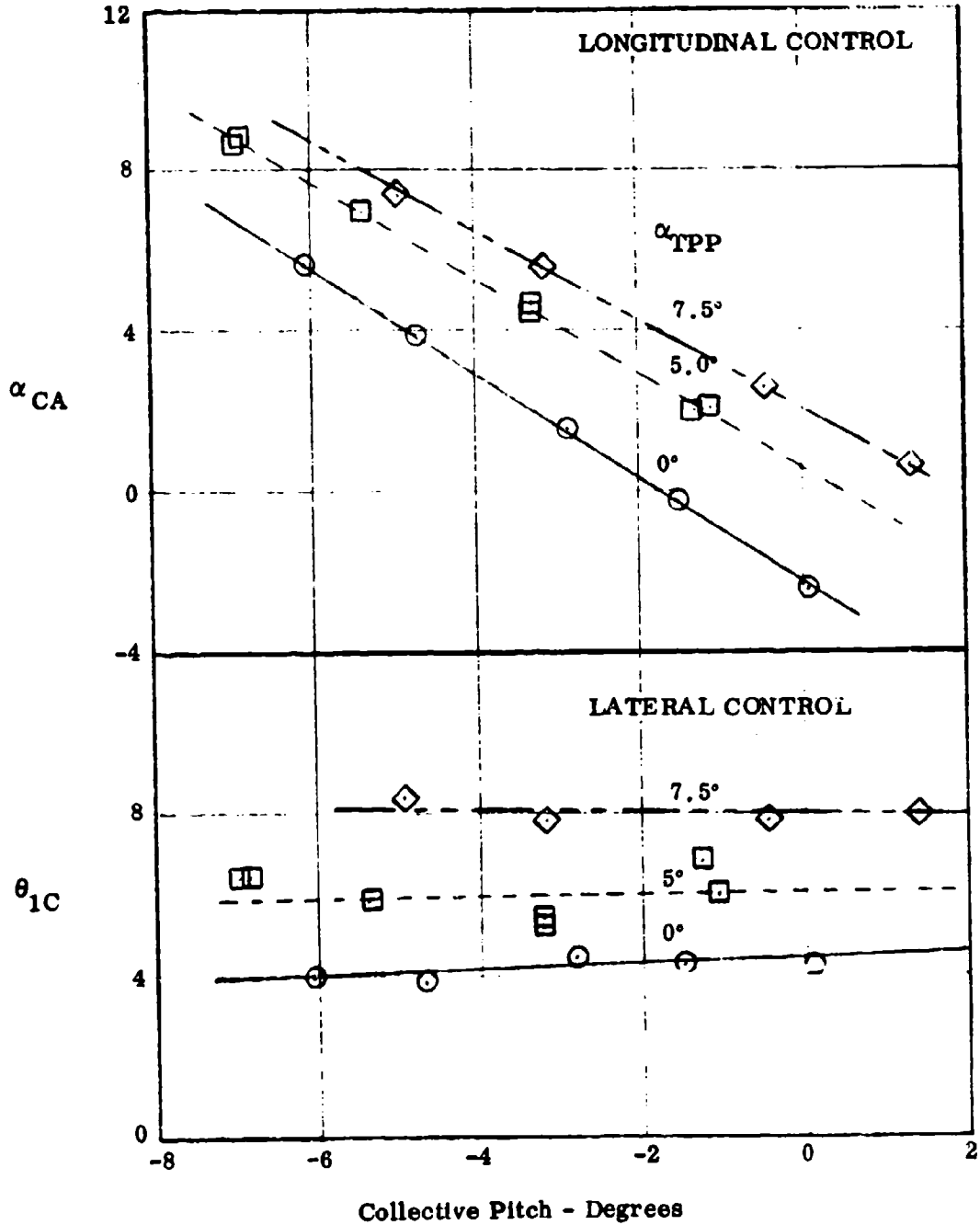
ROTOR CONTROL

$\mu = 1.45$, 820 r.p.m., 293 knots, $M_{1.90} = .75$, $\rho = .00205$, Run 60



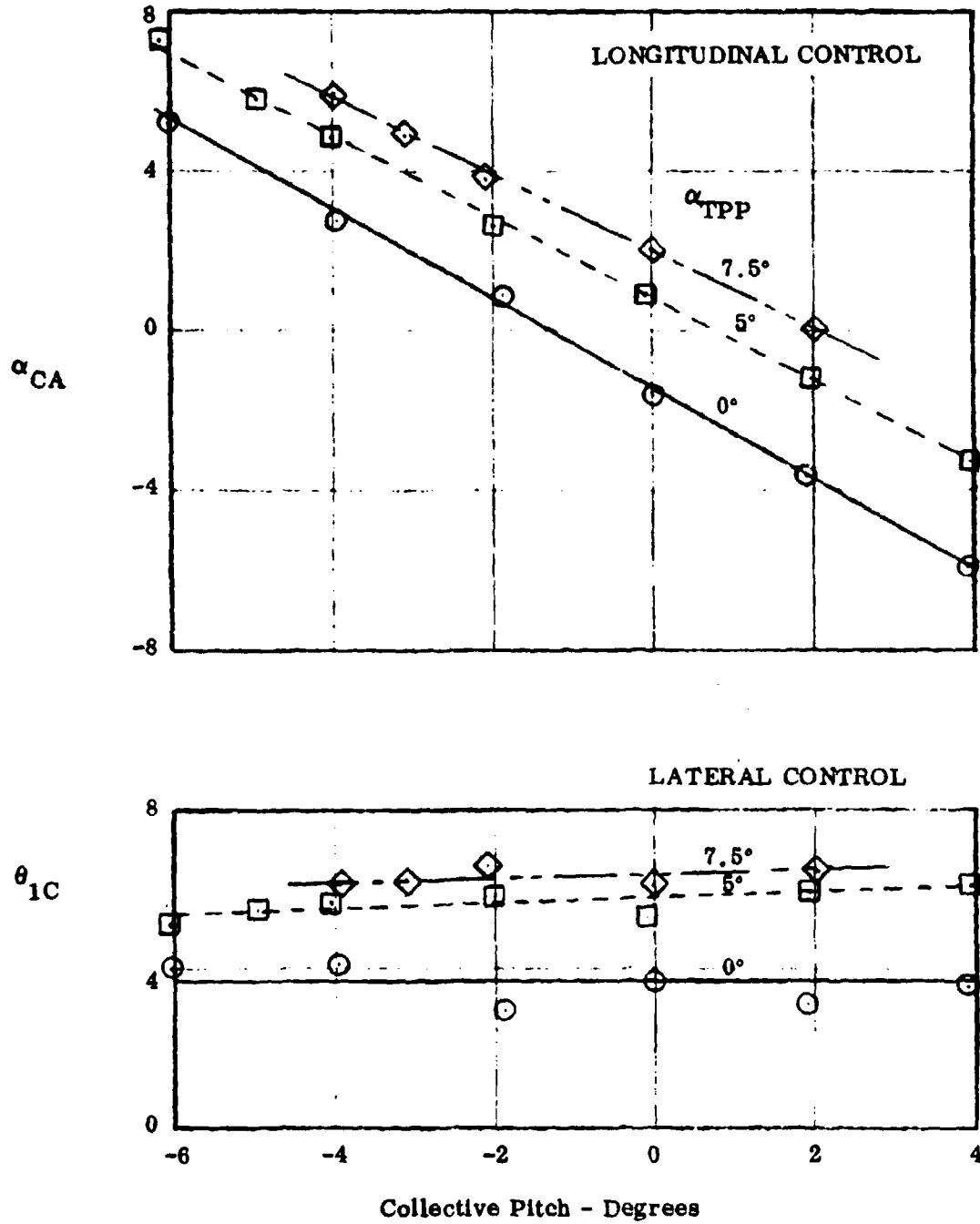
ROTOR CONTROL

$\mu = 1.50$, 680 r.p.m., 243 knots, $M_{1,00} = .59$, $\rho = .0021$, Run 53



ROTOR CONTROL

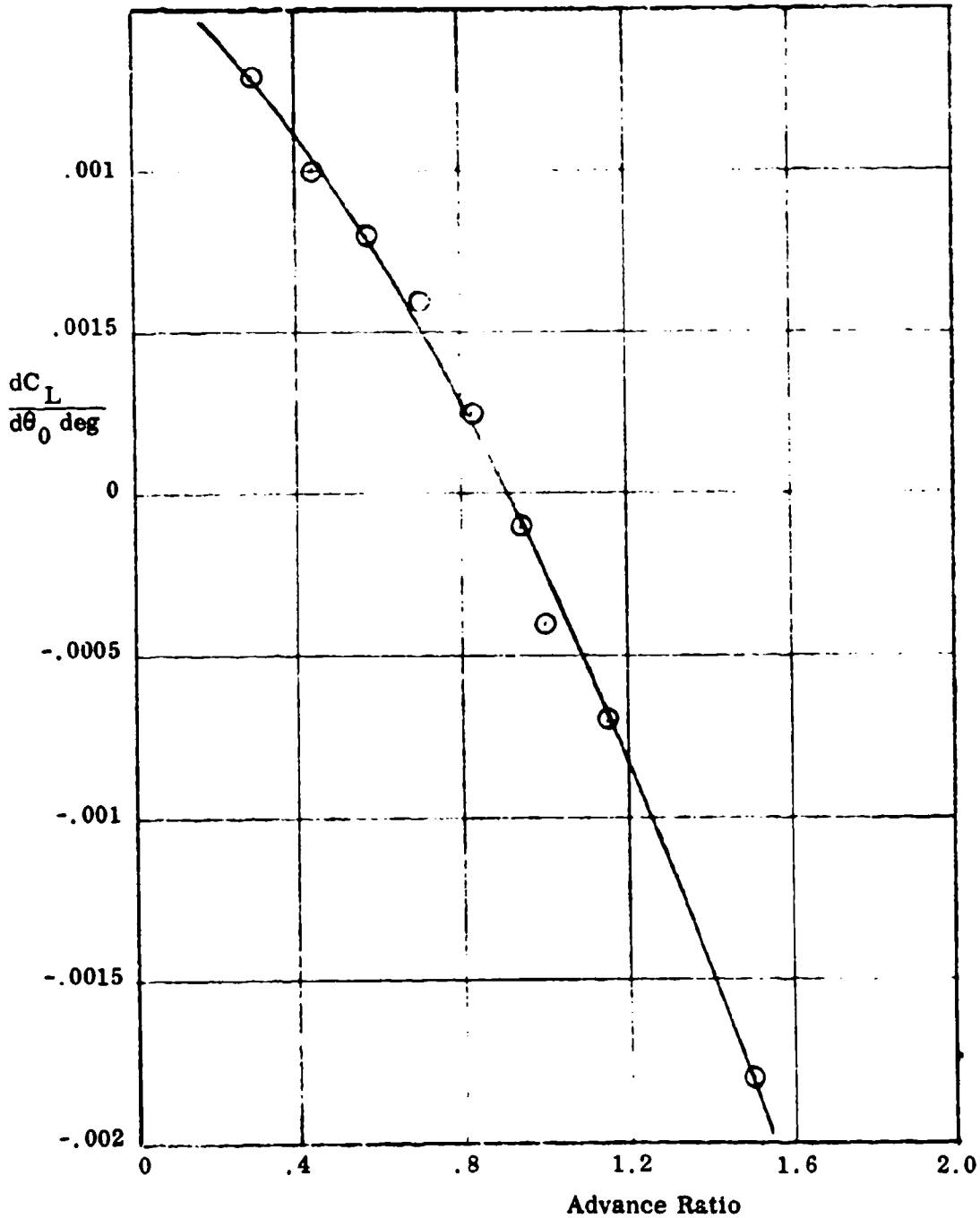
$\mu = 1.40$, 970 r.p.m., 345 knots, $M_{1,90} = .86$, $\rho = .00084$, Run 46



**COLLECTIVE CONTROL POWER AT 5 DEG
TIP PATH PLANE**

(Rotor Trimmed Laterally and Longitudinally)

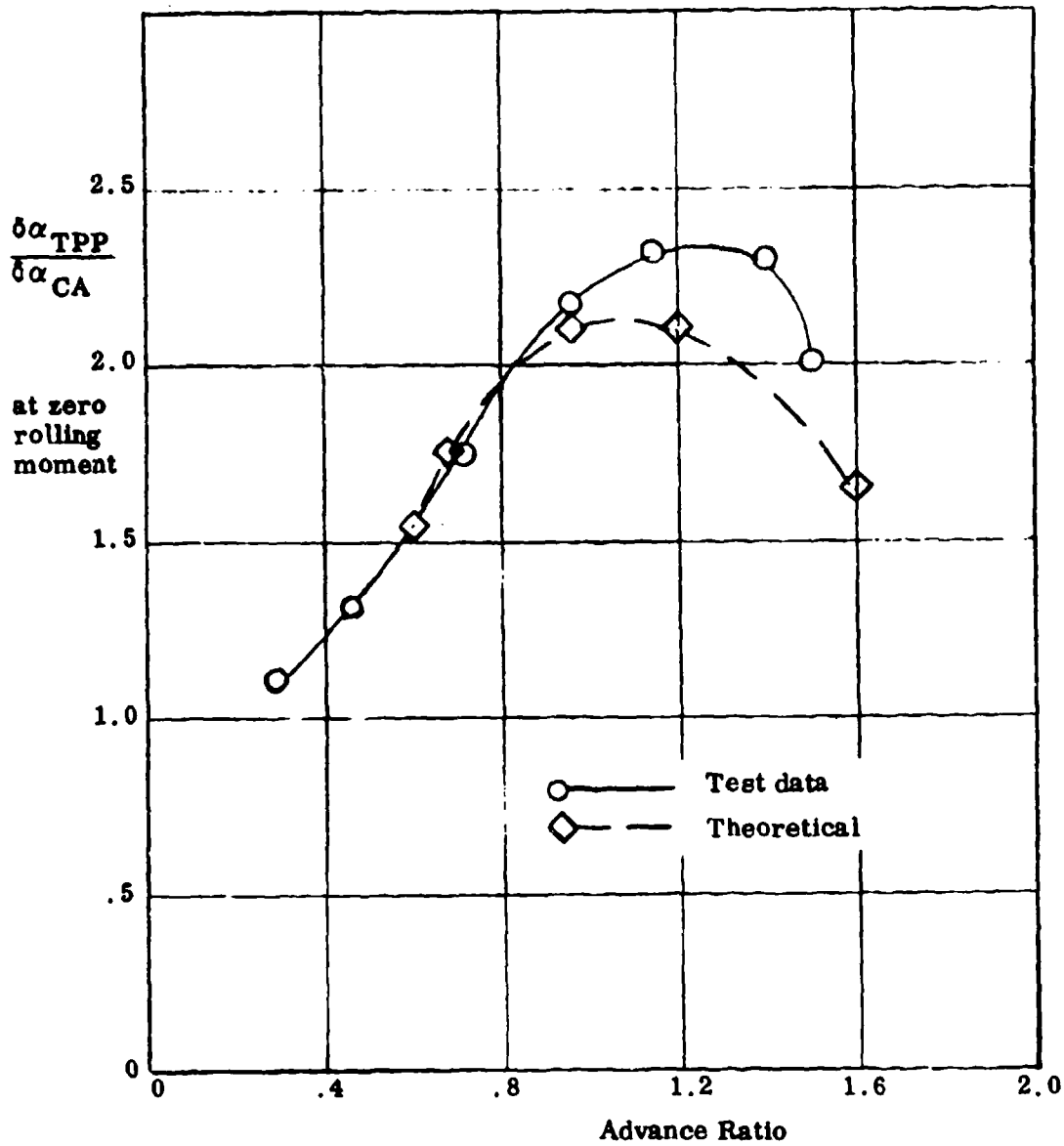
$$\rho = .002 \text{ slugs/ft}^3$$



**ROTOR TIP PATH PLANE DERIVATIVE WITH RESPECT TO
CONTROL AXIS ANGLE AT CONSTANT ROLLING MOMENT**

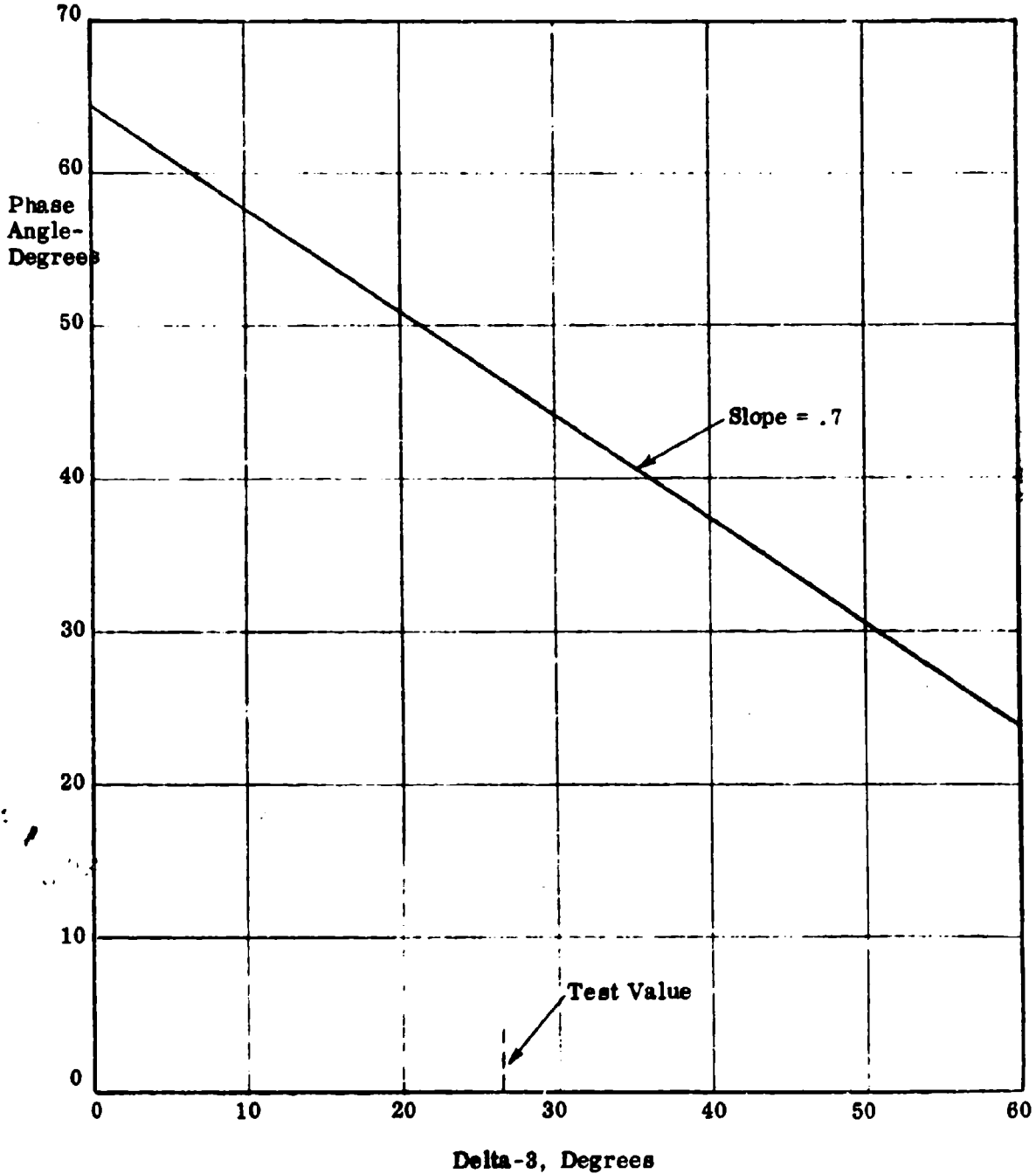
(Lateral Control Adjusted to Keep Rolling Moment
Zero During Variations in Control Axis Angle)

$$\rho = .0020 \text{ slugs/ft}^3$$



**THEORETICAL PHASE ANGLE OF FLAPPING RESPONSE
TO ONE-PER-REV CYCLIC INPUT IN HOVER**

$\rho = .002378 \text{ slugs/ft}^3$



HC144R1070

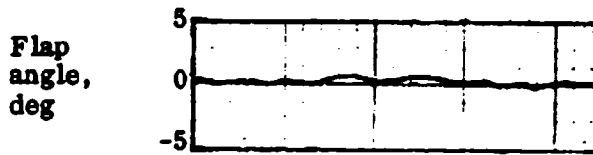
Figure 3.12

ROTOR FLAPPING

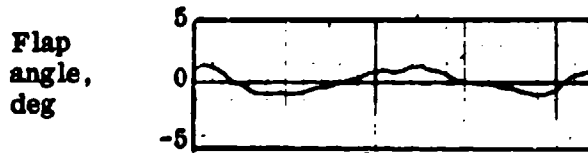
Trimmed 1g conditions, $\rho = .002$

Traces shown are one rotor revolution from
0° to 360° azimuth

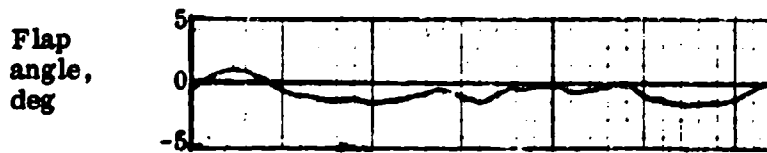
$\mu = .29$ $C_L = .0081$ Run 50



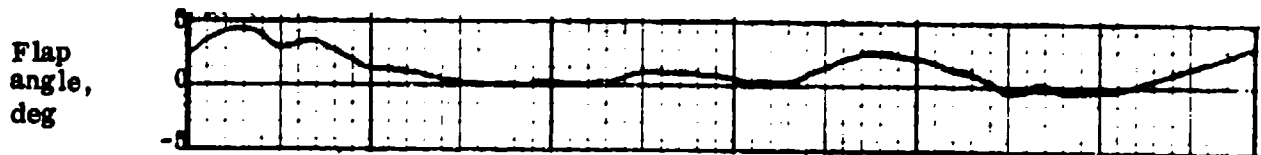
$\mu = .46$ $C_L = .0079$ Run 51



$\mu = .82$ $C_L = .0116$ Run 56

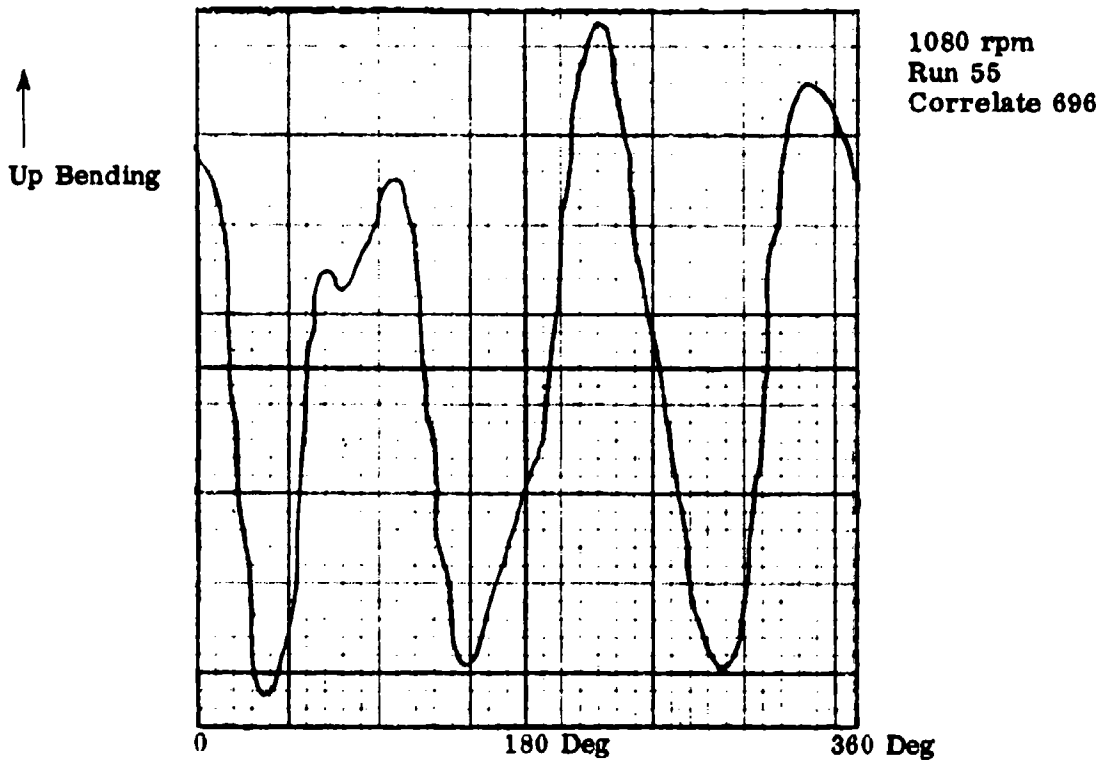


$\mu = 1.5$ $C_L = .029$ Run 53

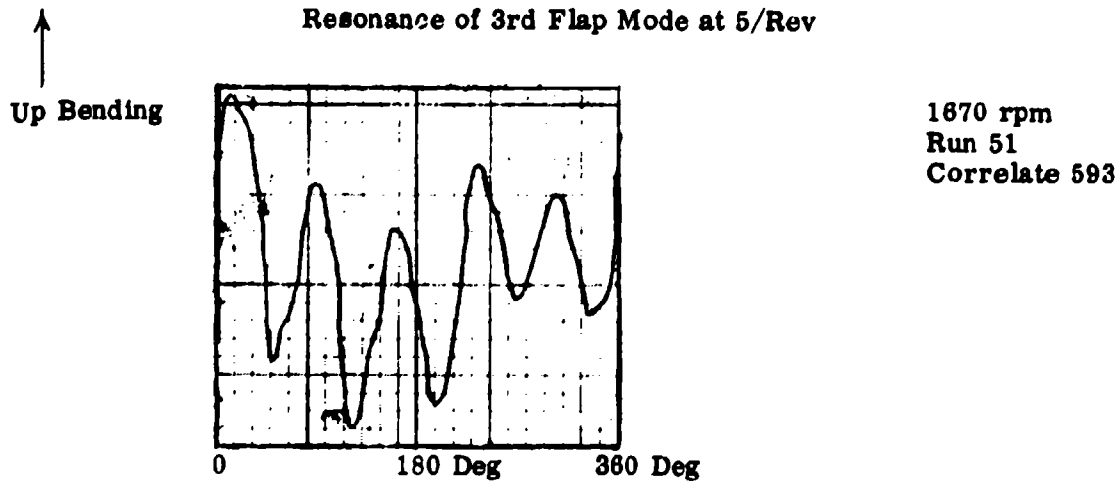


**TYPICAL TRACES OF FLAPWISE VIBRATORY MOMENTS
NEAR RESONANCES - OUTBOARD STATION ~ .71R**

Resonance of 2nd Flap Mode at 3/Rev



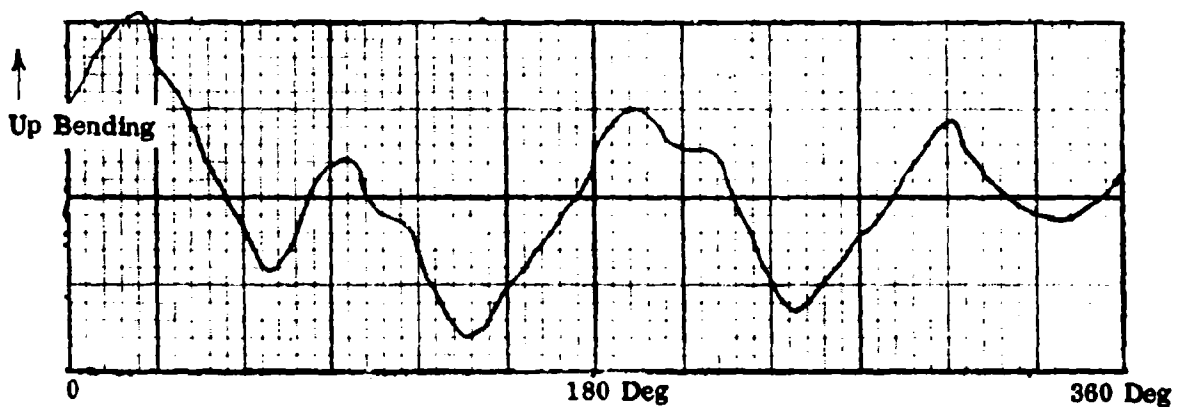
Resonance of 3rd Flap Mode at 5/Rev



**TYPICAL TRACES OF FLAPWISE VIBRATORY MOMENTS
NEAR RESONANCES - OUTBOARD STATION ~ .71R**

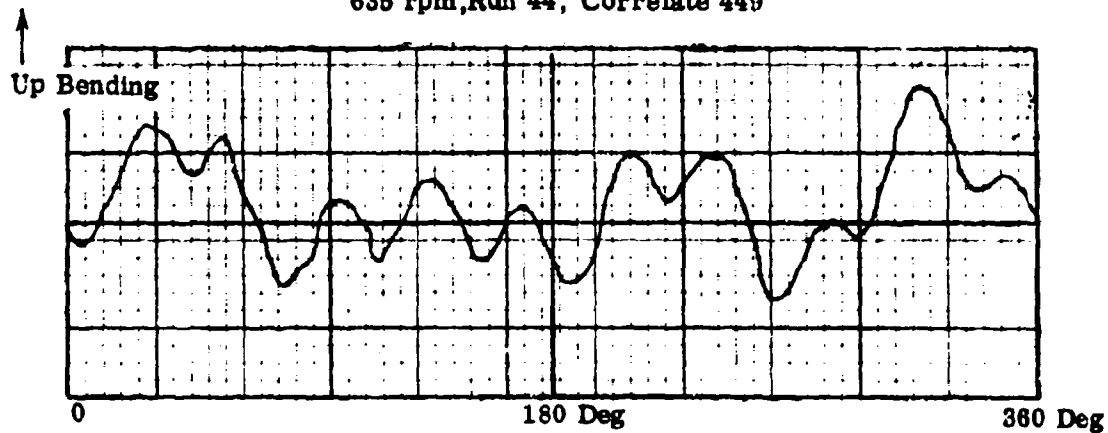
Resonance of 2nd Flap Mode at 4/Rev

667 rpm, Run 53, Correlate 661



Resonance of 3rd Flap Mode at 10/Rev

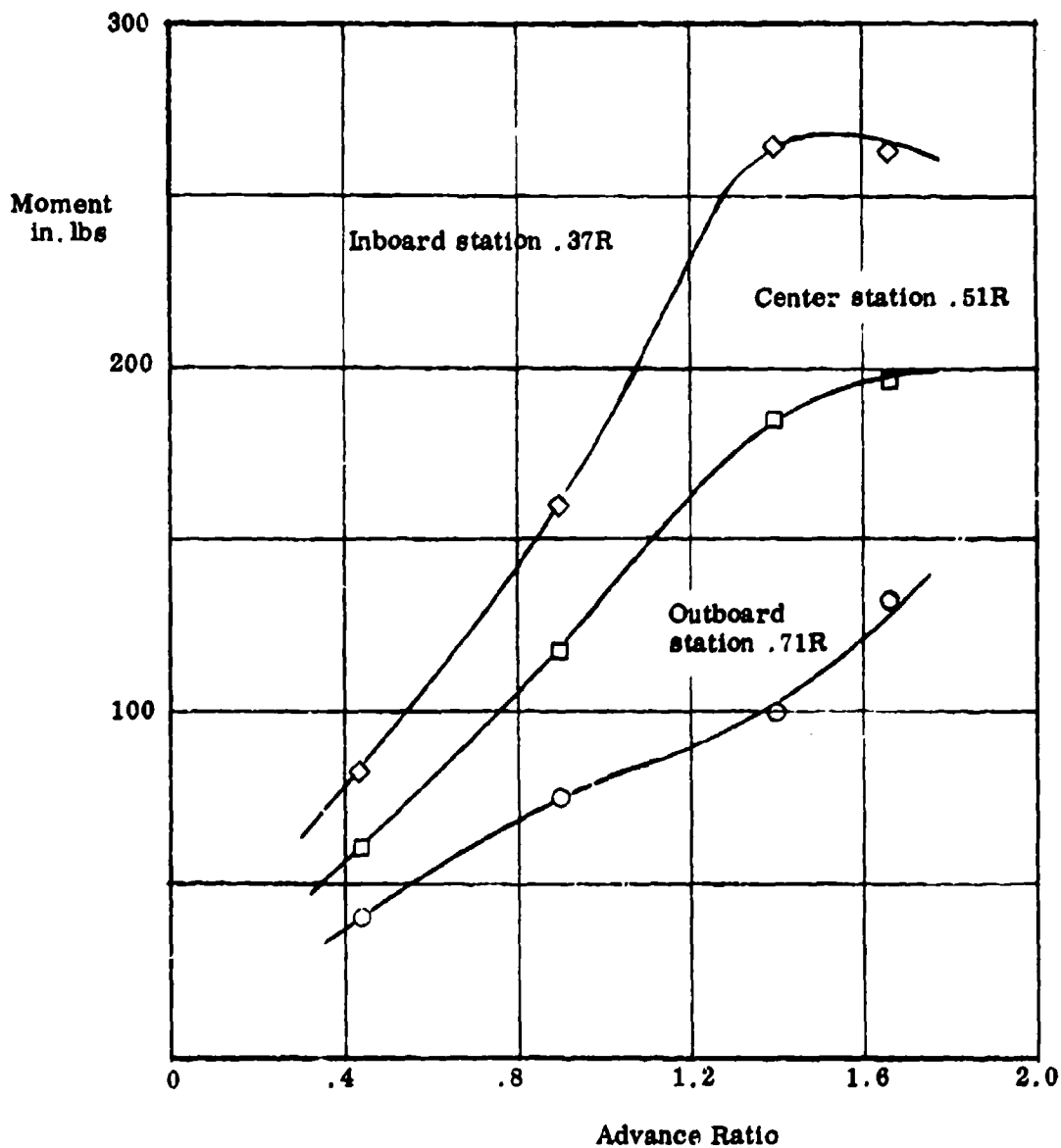
635 rpm, Run 44, Correlate 449



**MEASURED VIBRATORY FLAPWISE BENDING MOMENTS
AT CRITICAL STATIONS**

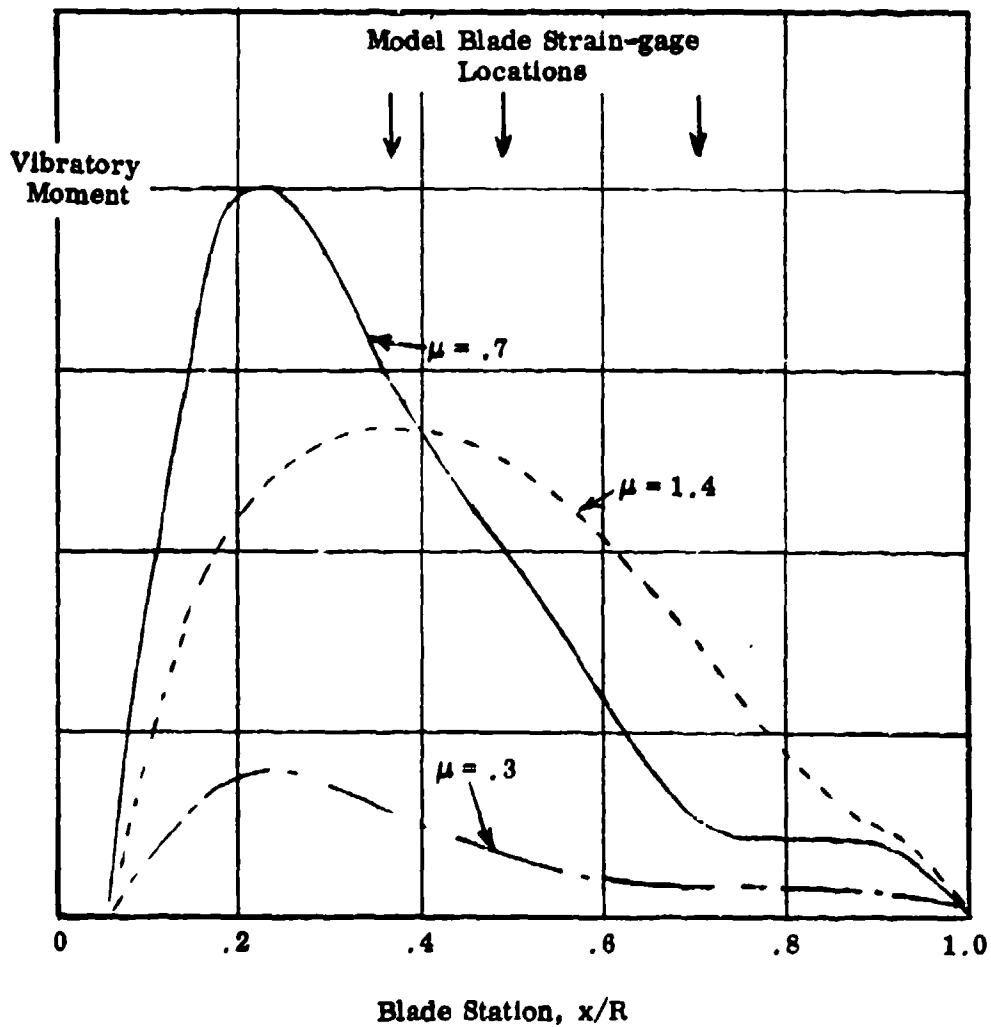
(One half peak-to-peak values)

1g Lift coefficients, 830 rpm, $\rho = .0008 \text{ slugs/ft}^3$



TYPICAL THEORETICAL SPANWISE DISTRIBUTIONS
OF VIBRATORY FLAPWISE BENDING MOMENT

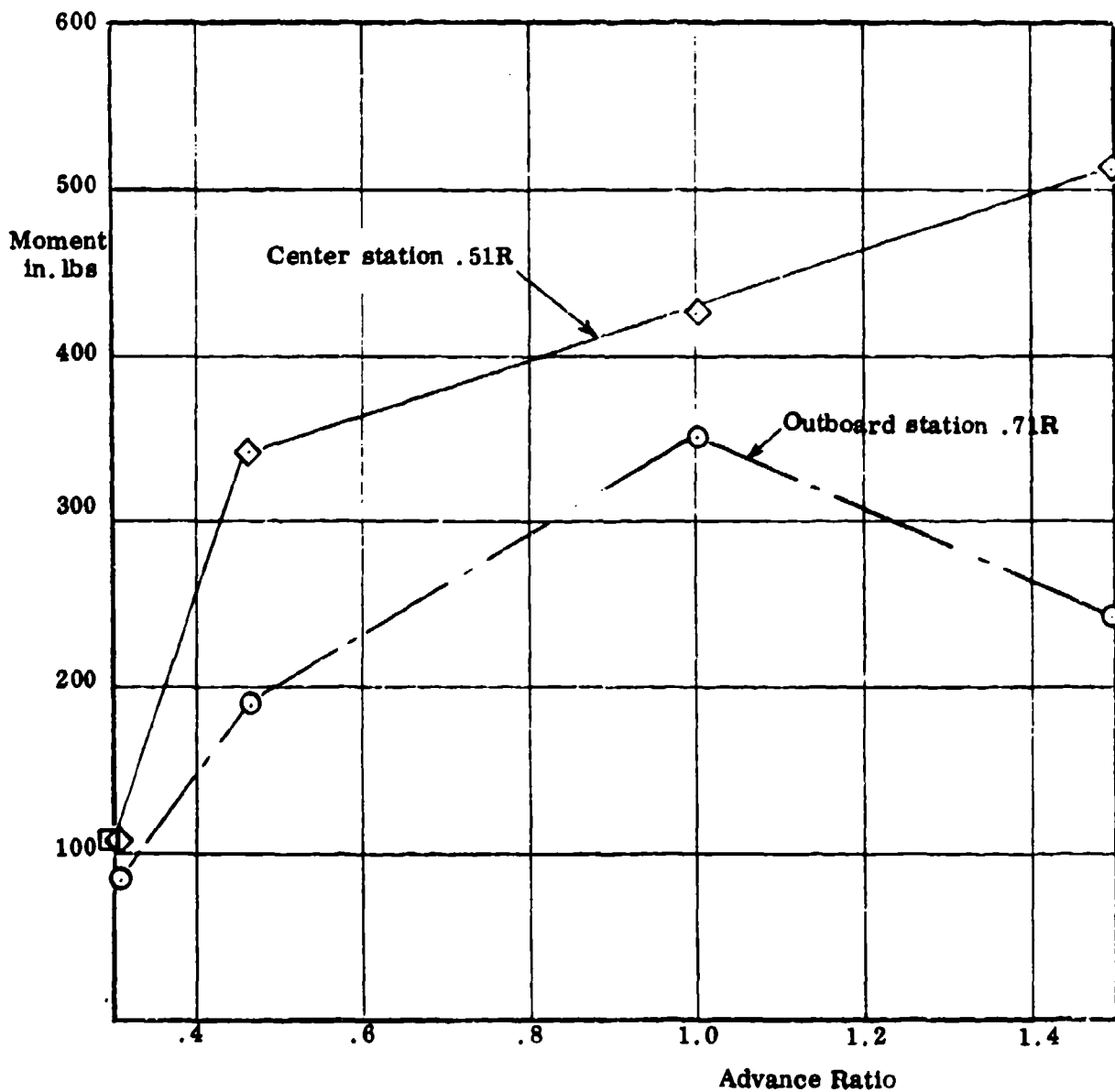
At 1g Lift Coefficients. Non-resonant r.p.m.



**MEASURED VIBRATORY FLAPWISE BENDING MOMENTS
AT SCHEDULED FLIGHT CONDITIONS**

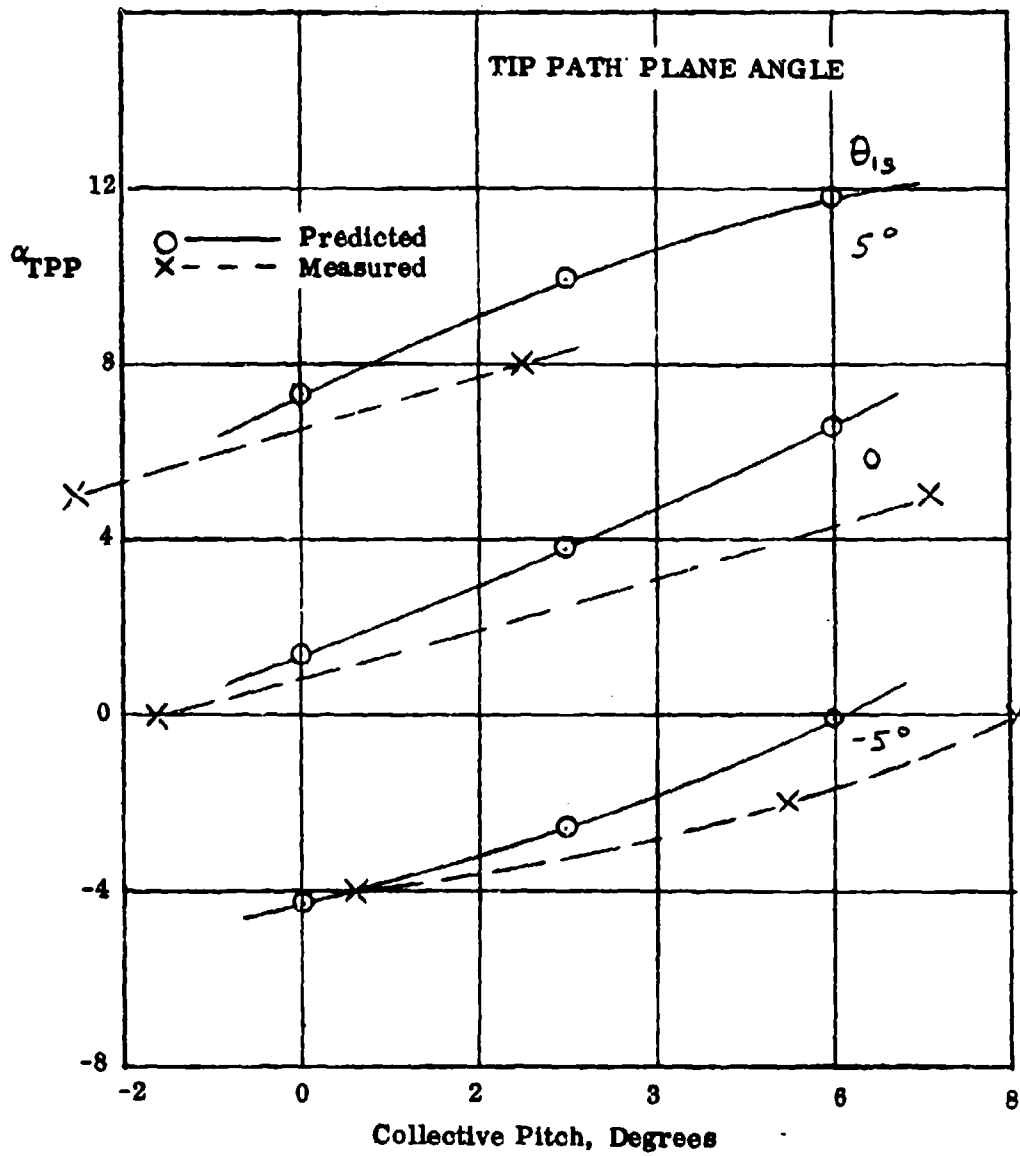
(One half peak-to-peak values)

$$\rho = .002 \text{ slugs/ft}^3$$



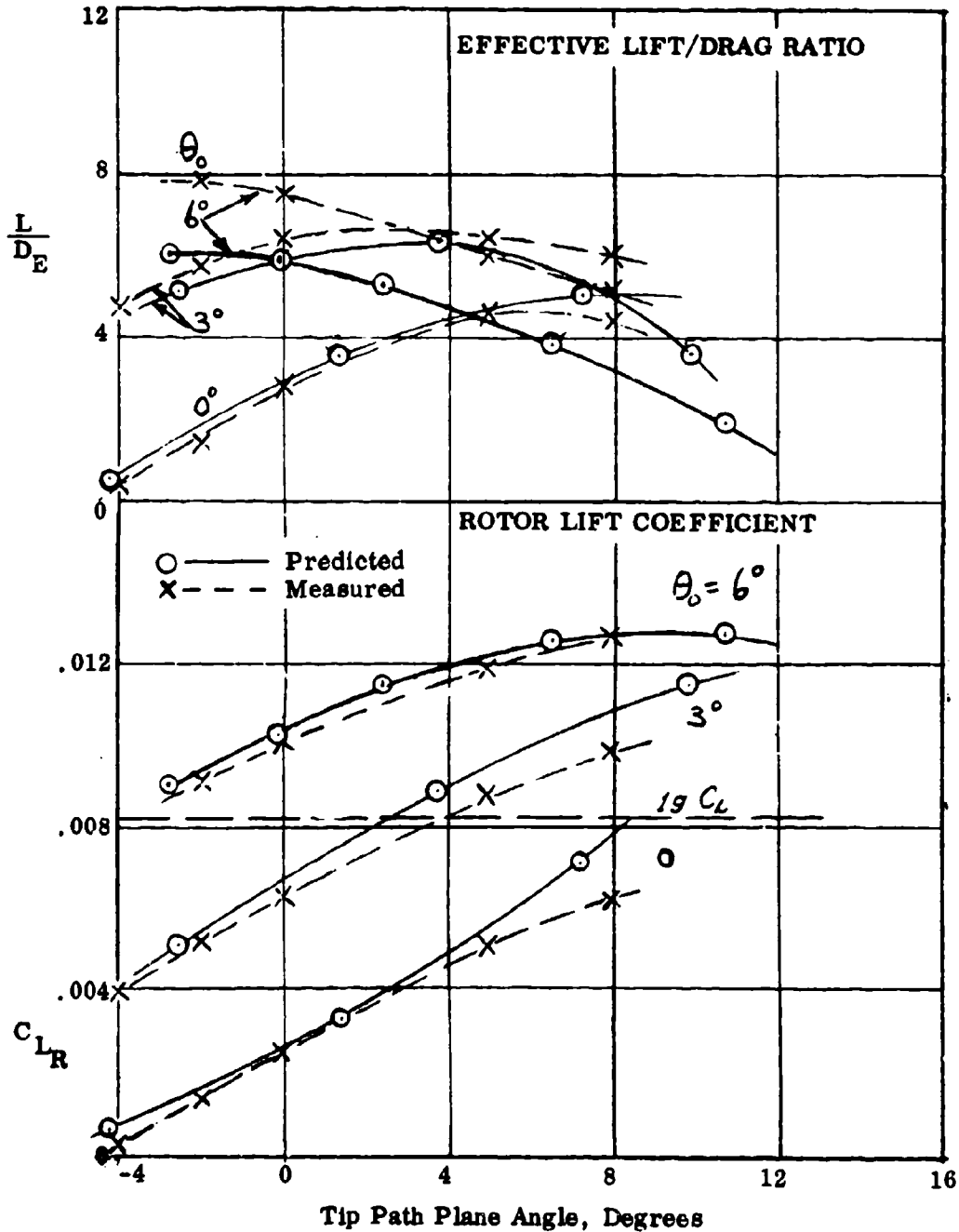
COMPARISON OF PREDICTED AND MEASURED ROTOR PERFORMANCE

$\mu = .29$, 1670 r.p.m, 121 knots, $M_{1, 90} = .79$, $\rho = .0023$, run 50



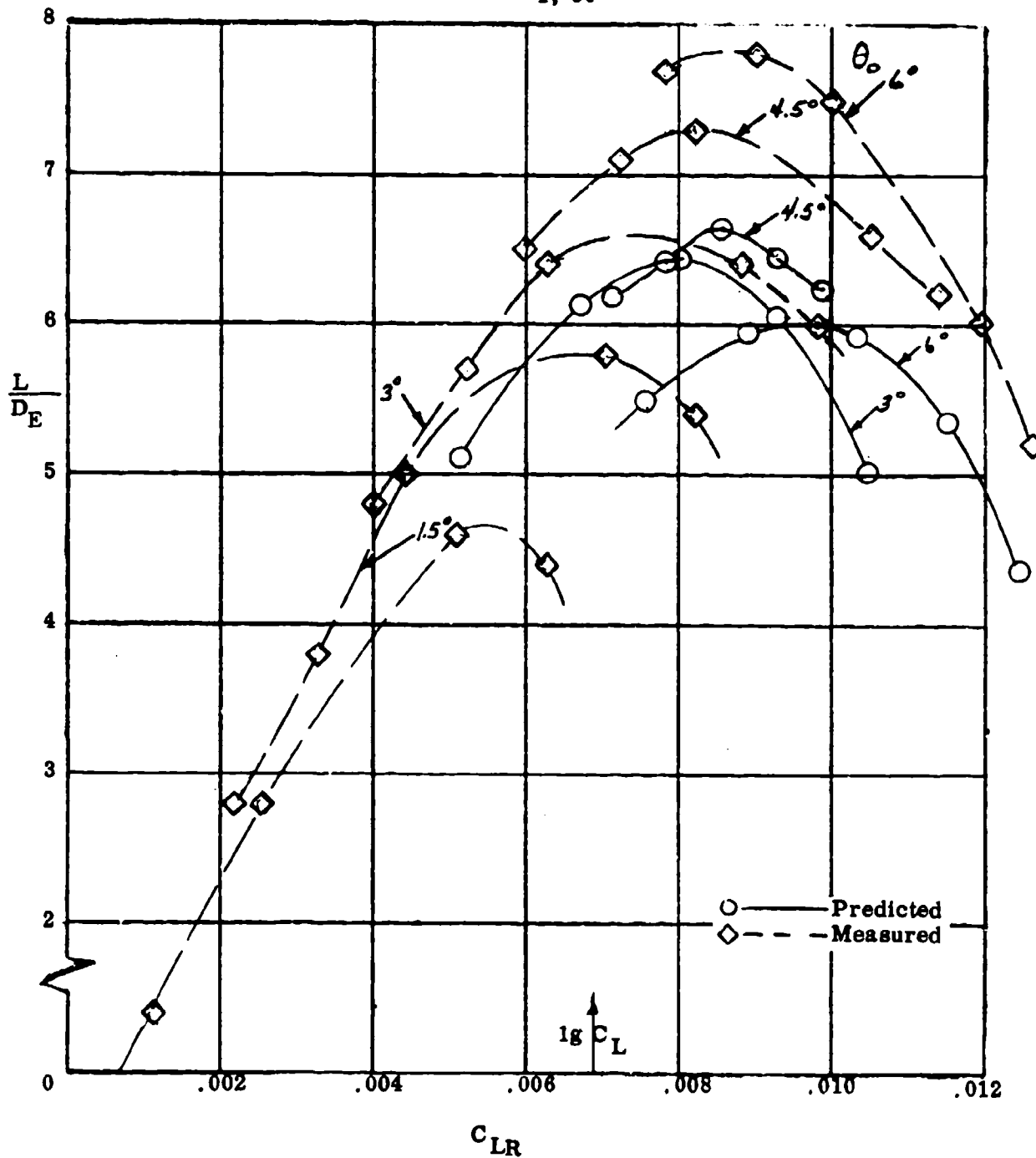
COMPARISON OF PREDICTED AND MEASURED ROTOR PERFORMANCE

$\mu = .29$, 1670 r.p.m., 121 Knots, $M_{1, 90} = .79$, $\rho = .0023$, run 50

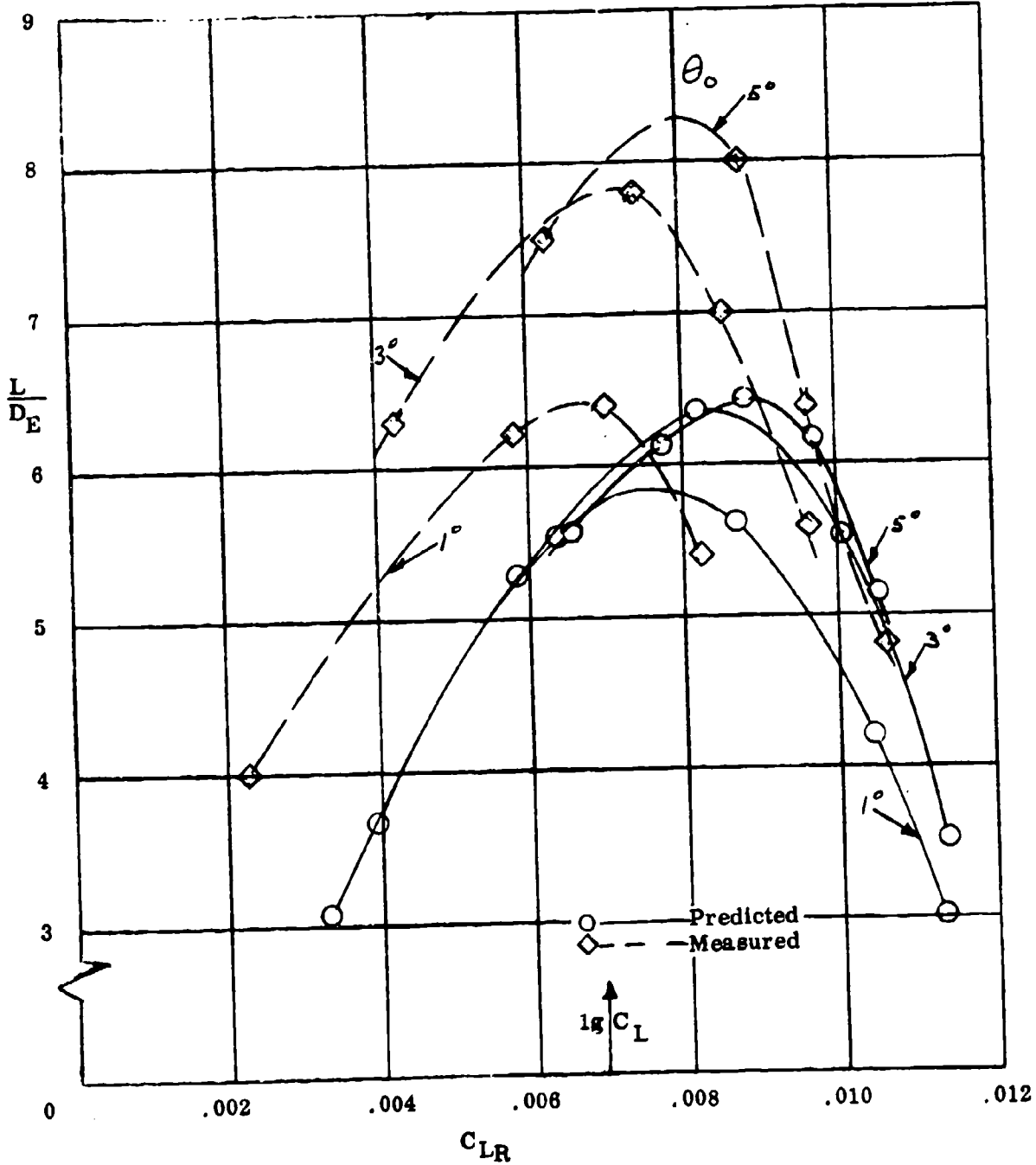


COMPARISON OF PREDICTED AND MEASURED ROTOR PERFORMANCE

$\mu = .29$, 1670 r.p.m., 121 Knots, $M_{1, 90} = .79$, $\rho = .0023$, run 50

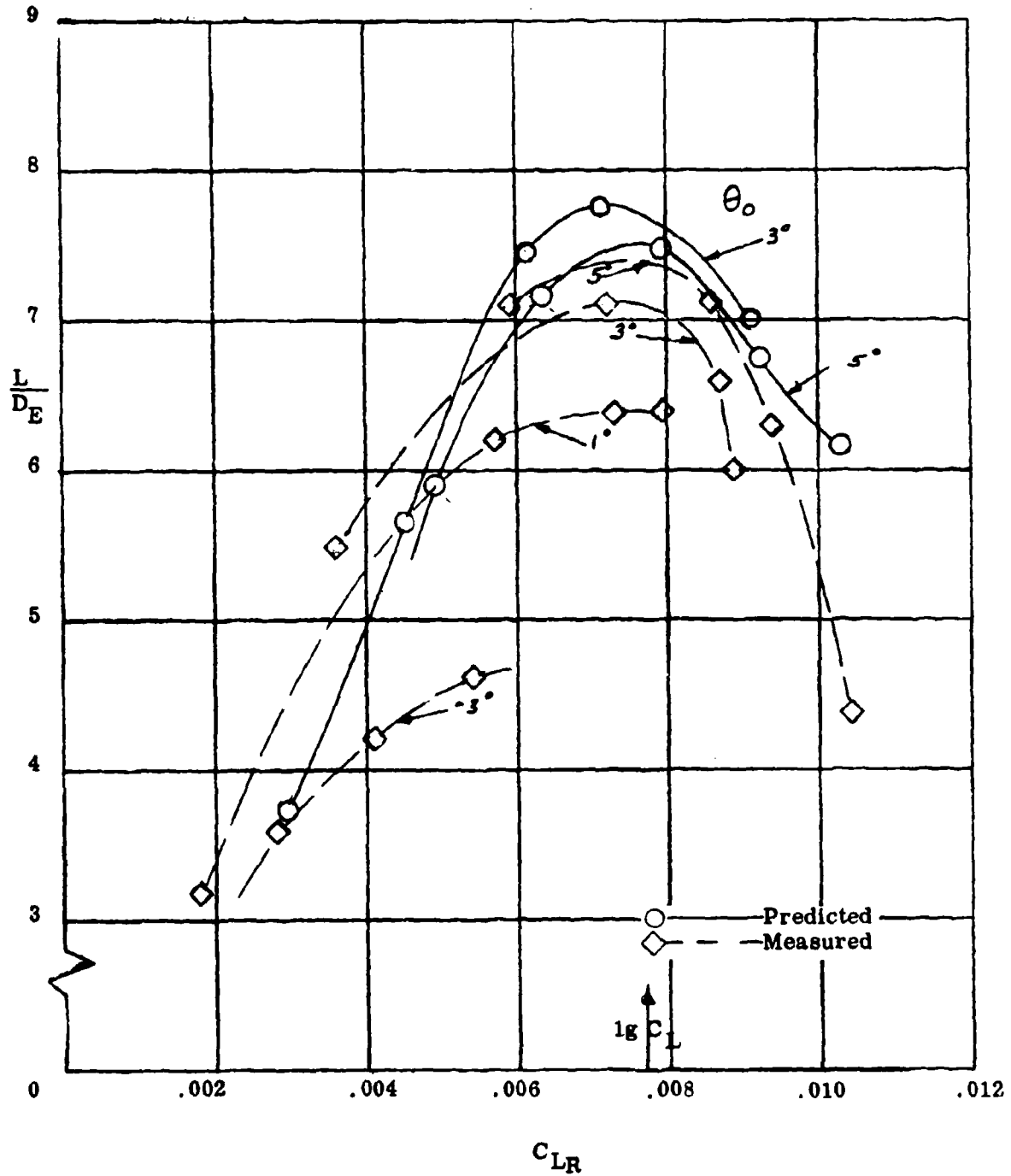


COMPARISON OF PREDICTED AND MEASURED ROTOR PERFORMANCE
 $\mu = .46$, 1670 r.p.m., 191 knots, $M_{1,90} = .89$, $\rho = .0022$, run 51

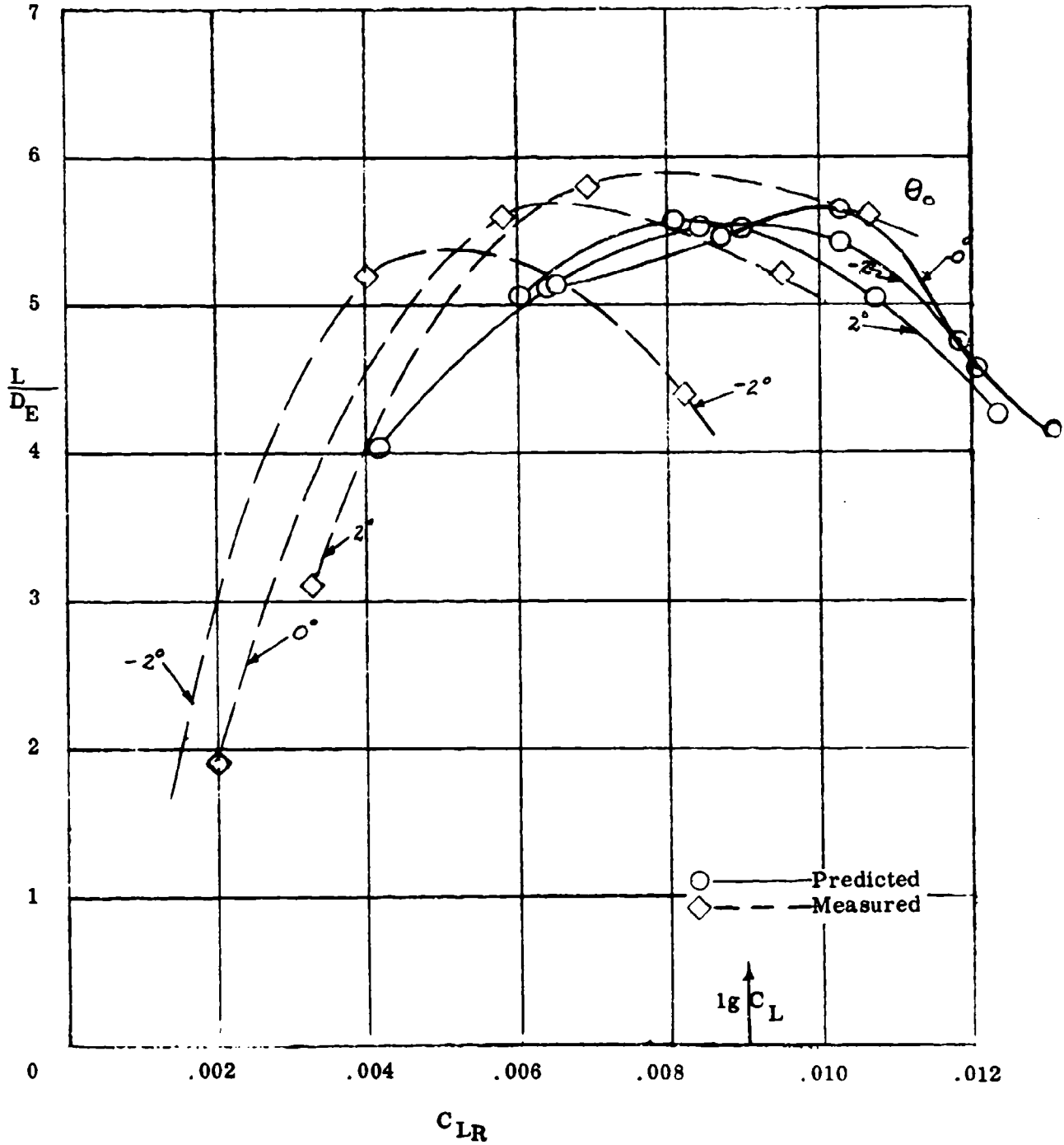


COMPARISON OF PREDICTED AND MEASURED ROTOR PERFORMANCE

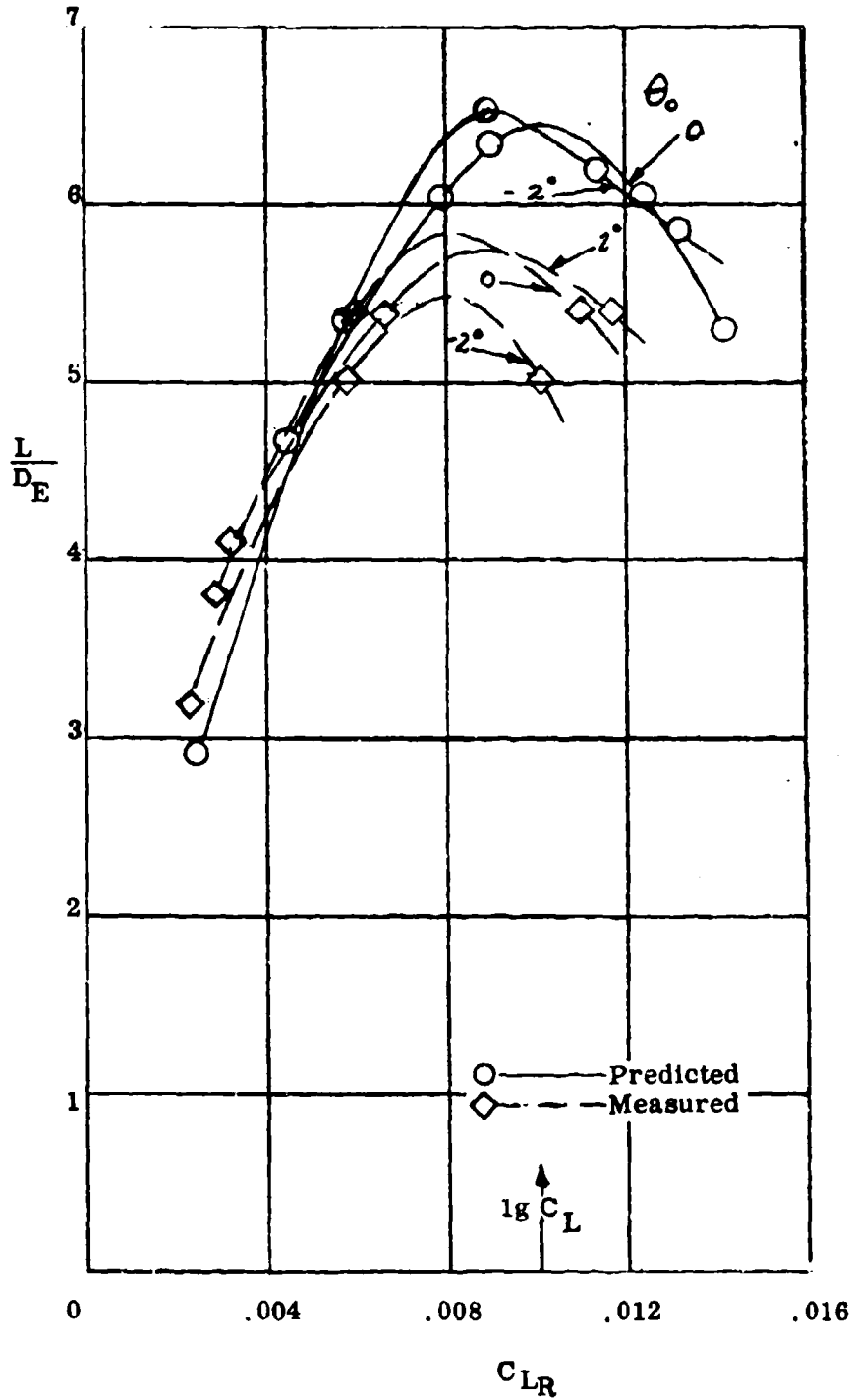
$\mu = .57$, 1330 r.p.m., 192 knots, $M_{1, 90} = .76$, $\rho = .0022$, run 52



COMPARISON OF PREDICTED AND MEASURED ROTOR PERFORMANCE
 $\mu = .72$, 1350 r.p.m., 243 knots, $M_{1, 90} = .61$, $\rho = .0021$, run 57

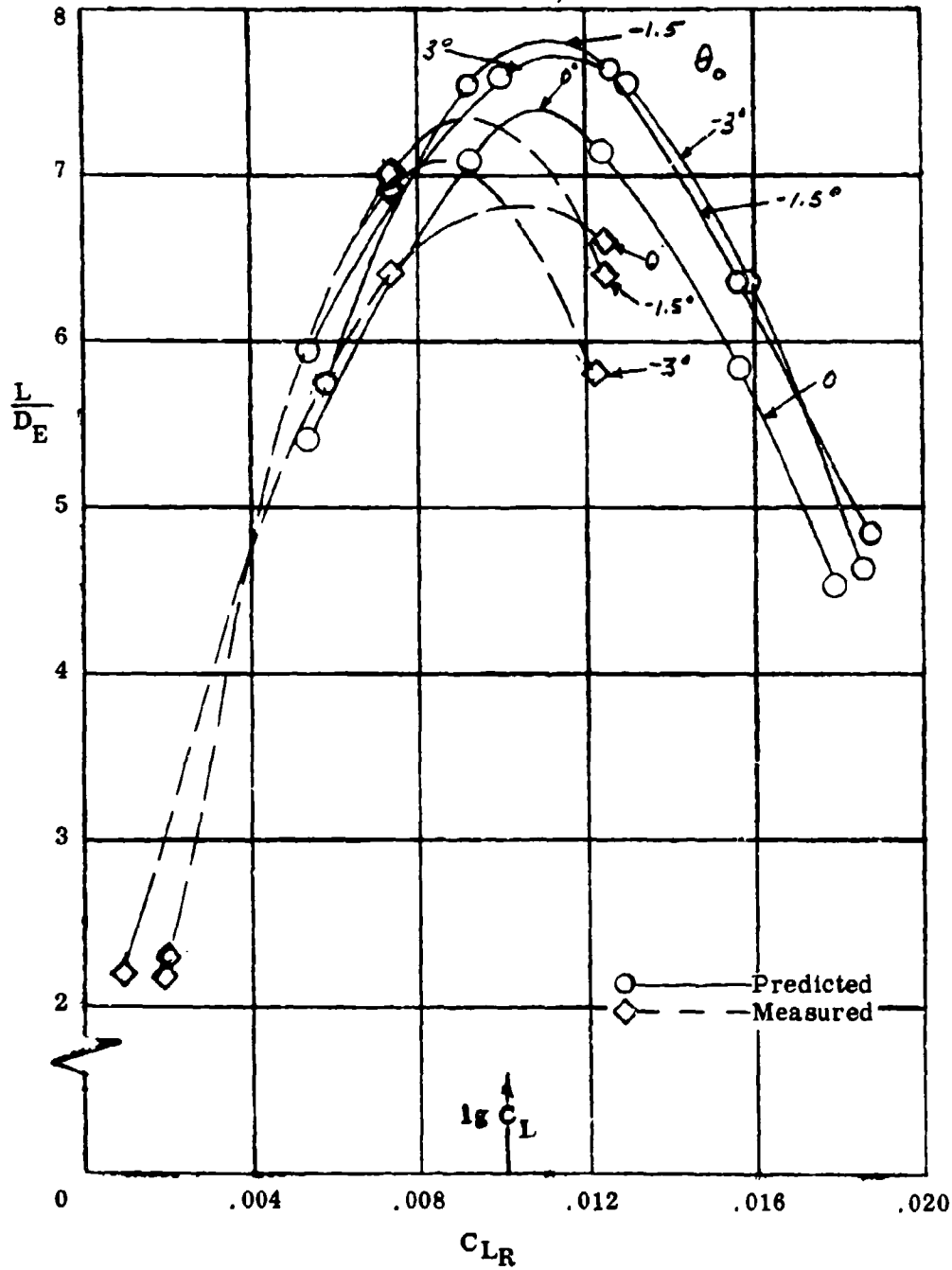


COMPARISON OF PREDICTED AND MEASURED ROTOR PERFORMANCE
 $\mu = .82$, 1170 r.p.m., 243 knots, $M_{1, 90} = .65$, $\rho = .0021$, run 56



COMPARISON OF PREDICTED AND MEASURED ROTOR PERFORMANCE

$\mu = .94$, 1050 r.p.m., 243 knots, $M_{1,90} = .68$, $\rho = .0021$, run 55

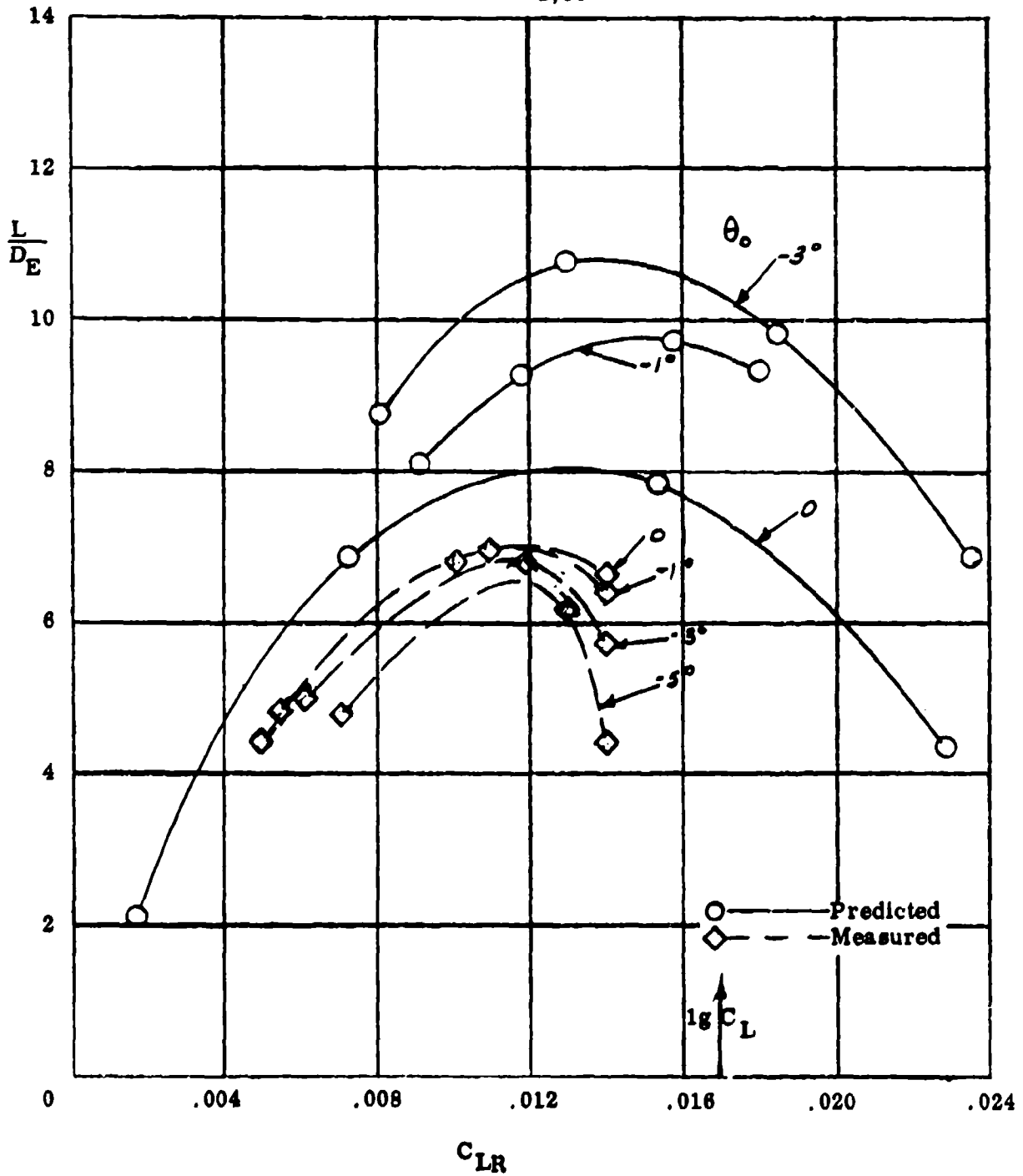


HC144R1070

Figure 5.8

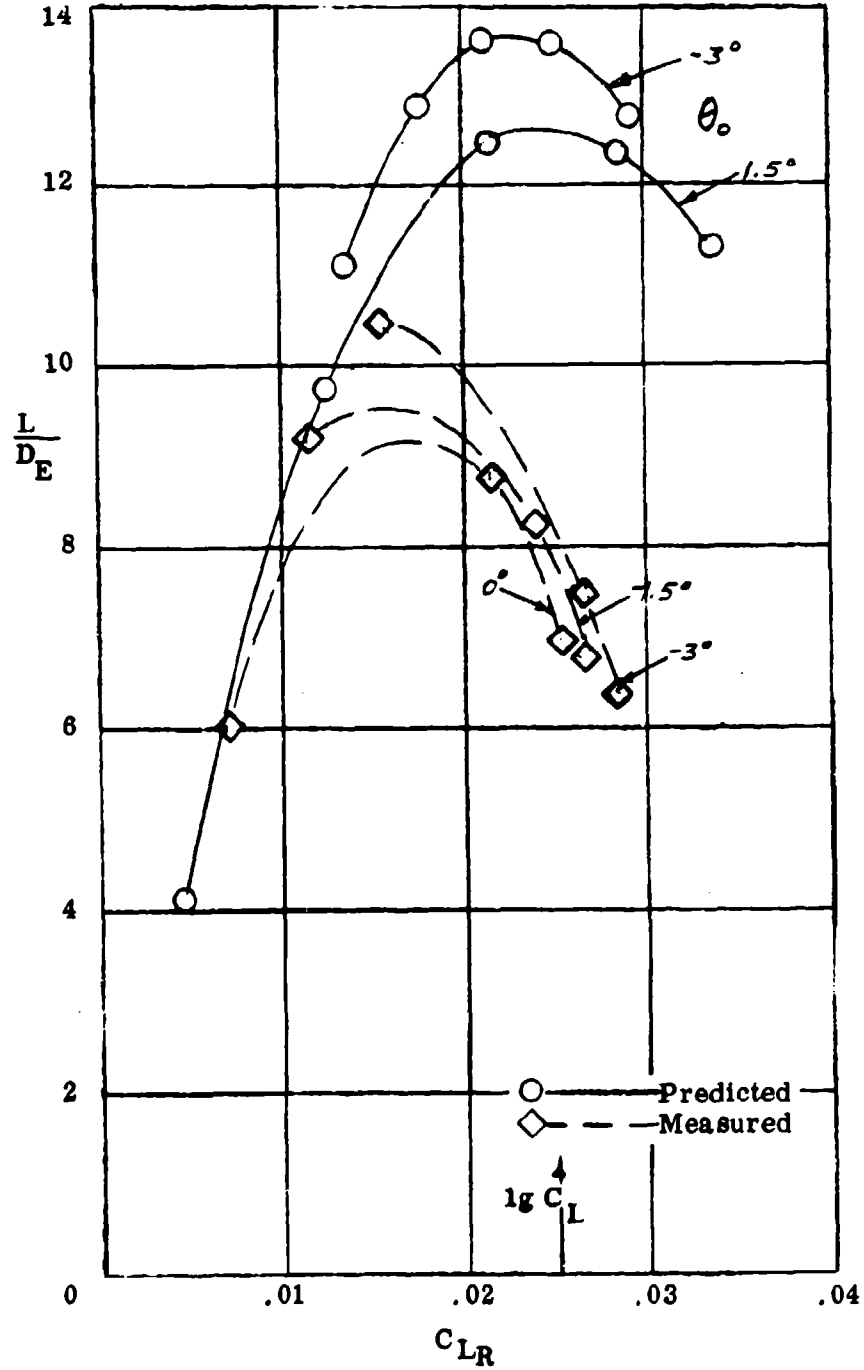
COMPARISON OF PREDICTED AND MEASURED ROTOR PERFORMANCE

$\mu = 1.15$, 833 r.p.m., 239 knots, $M_{1,90} = .66$, $\rho = .0021$, run 54

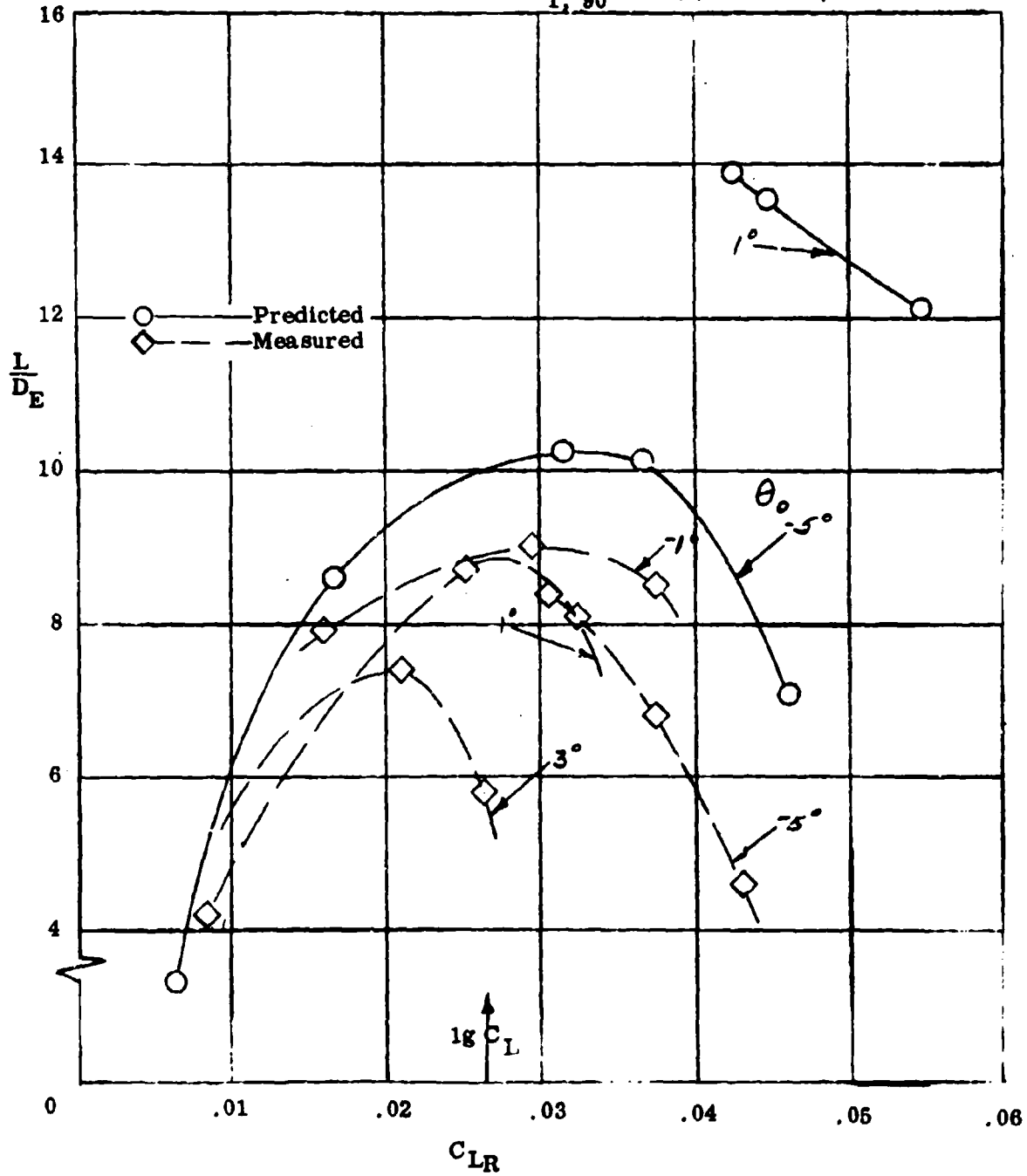


COMPARISON OF PREDICTED AND MEASURED ROTOR PERFORMANCE

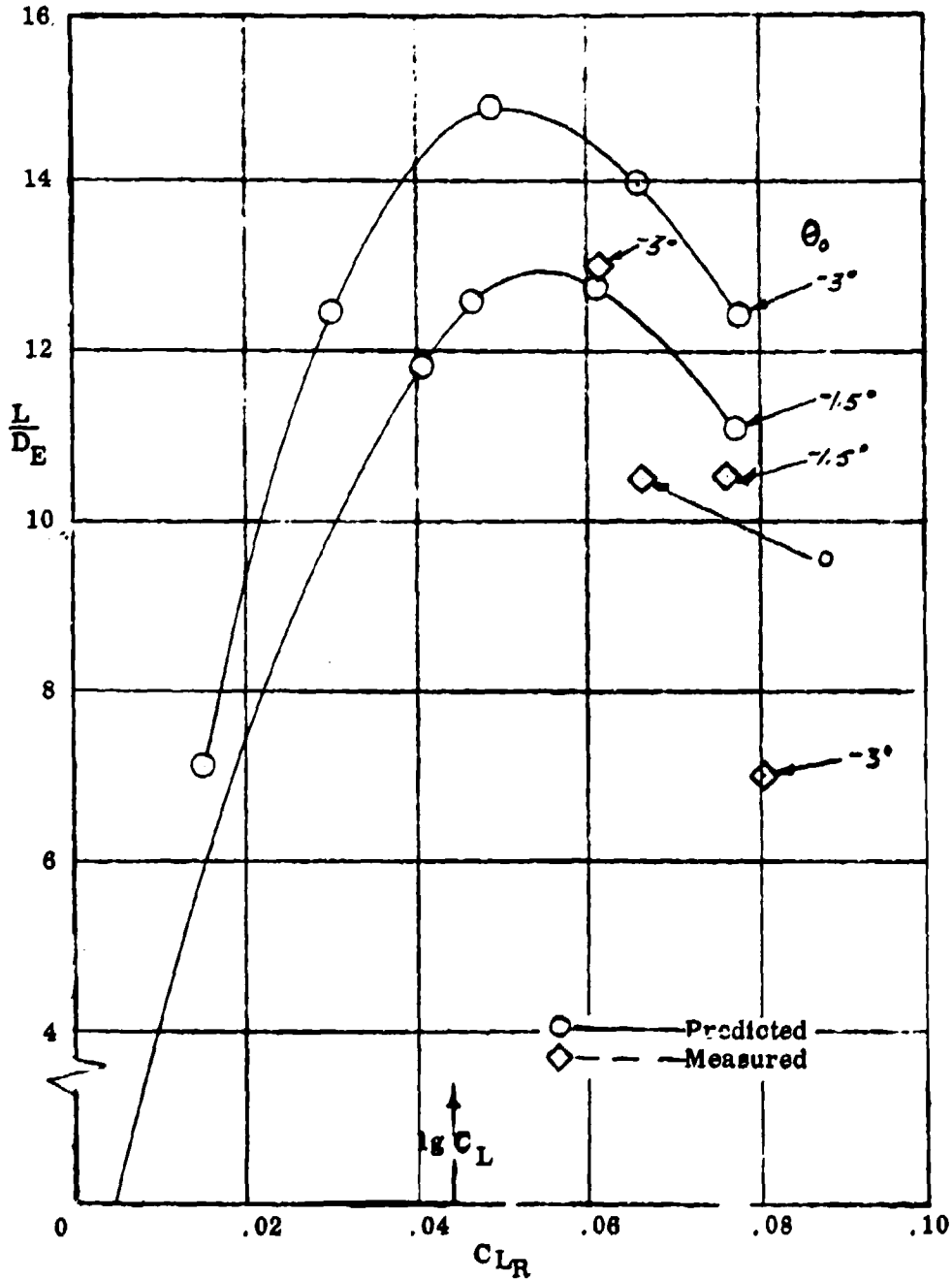
$\mu = 1.50$, 660 r.p.m., 243 knots, $M_{1,90} = .59$, $\rho = .0021$, run 53



COMPARISON OF PREDICTED AND MEASURED ROTOR PERFORMANCE
 $\mu = 1.66$, 833 r.p.m., 346 knots, $M_{1, 90} = .81$, $\rho = .00084$, run 47

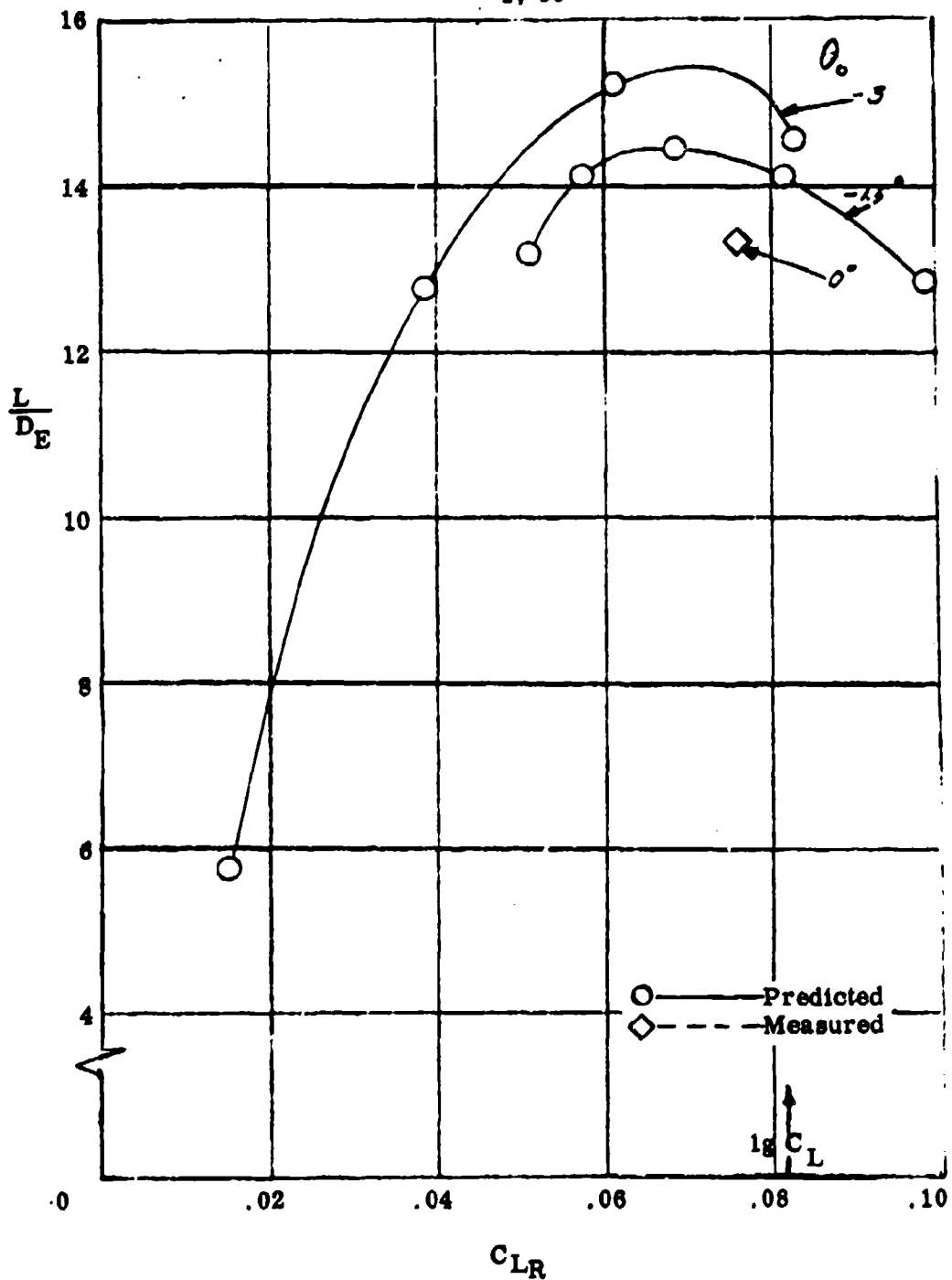


COMPARISON OF PREDICTED AND MEASURED ROTOR PERFORMANCE
 $\mu = 2.16$, 643 r.p.m., 347 knots, $M_{1, 90} = .75$, $\rho = .00084$, run 48

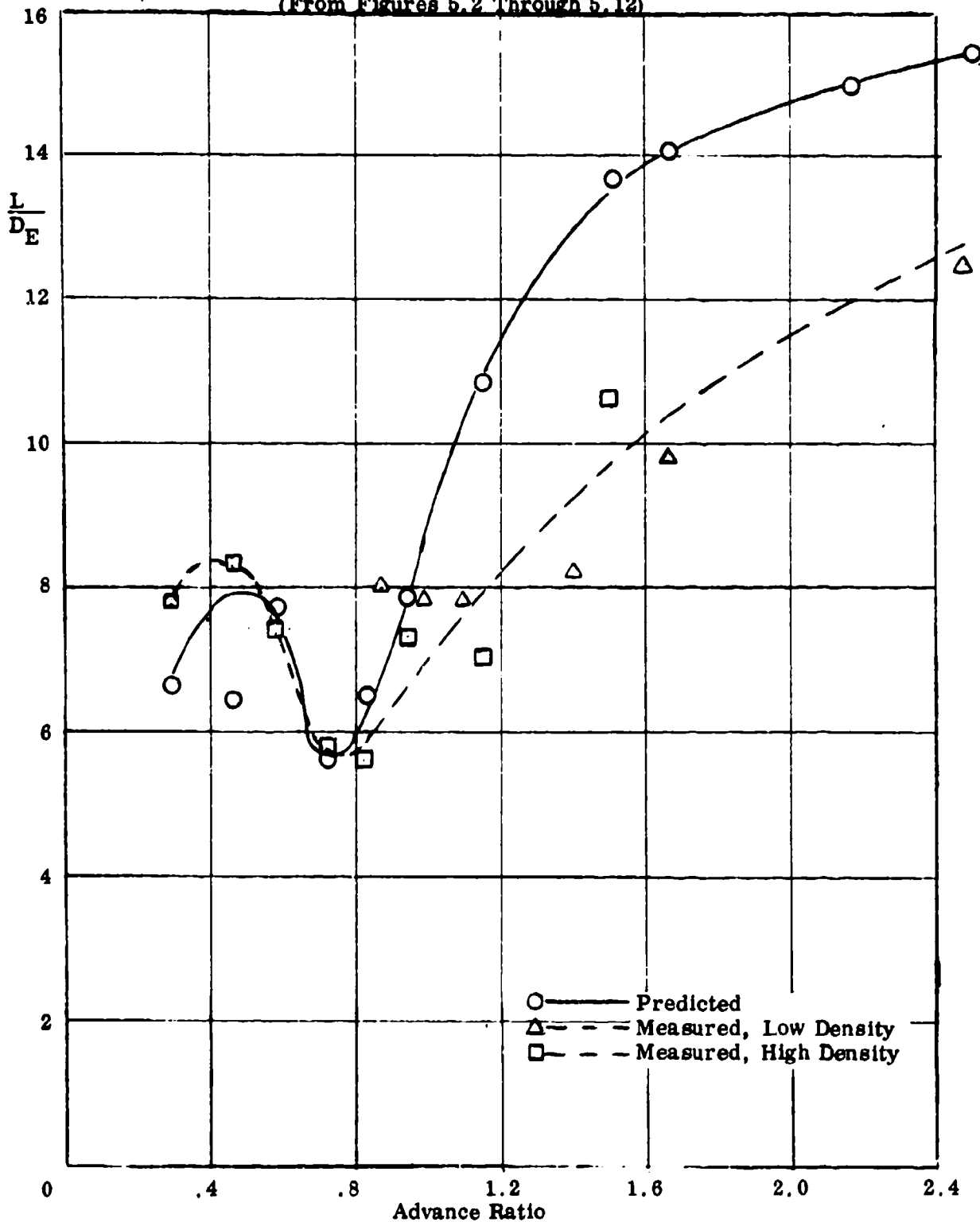


COMPARISON OF PREDICTED AND MEASURED ROTOR PERFORMANCE

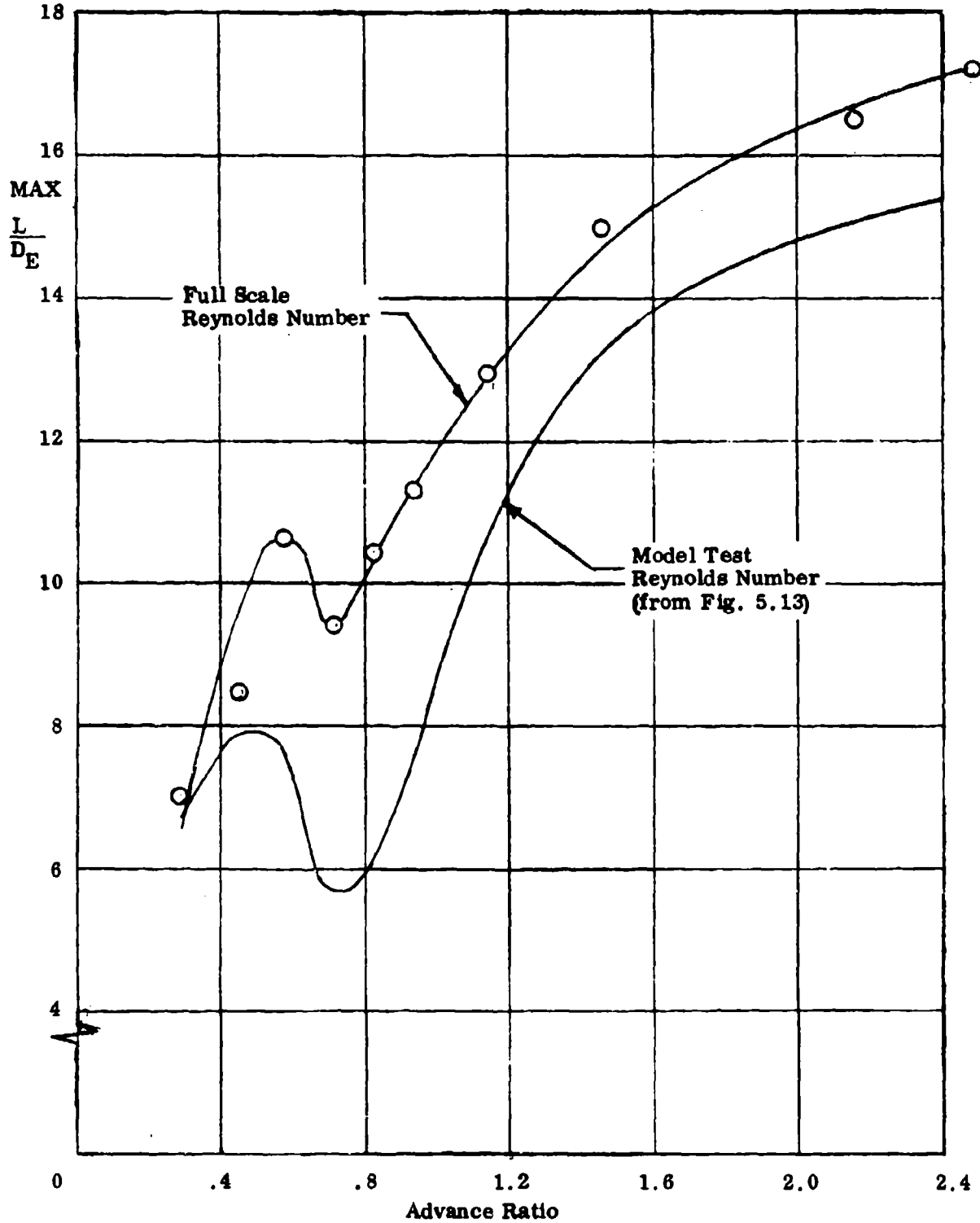
$\mu = 2.47$, 560 r.p.m., 350 knots, $M_1, 90^\circ = .72$, $\rho = .00084$, run 49



COMPARISON OF MEASURED AND PREDICTED MAXIMUM EFFECTIVE
LIFT/DRAG RATIO - ADVANCE RATIOS 0.3 TO 2.5
(From Figures 5.2 Through 5.12)



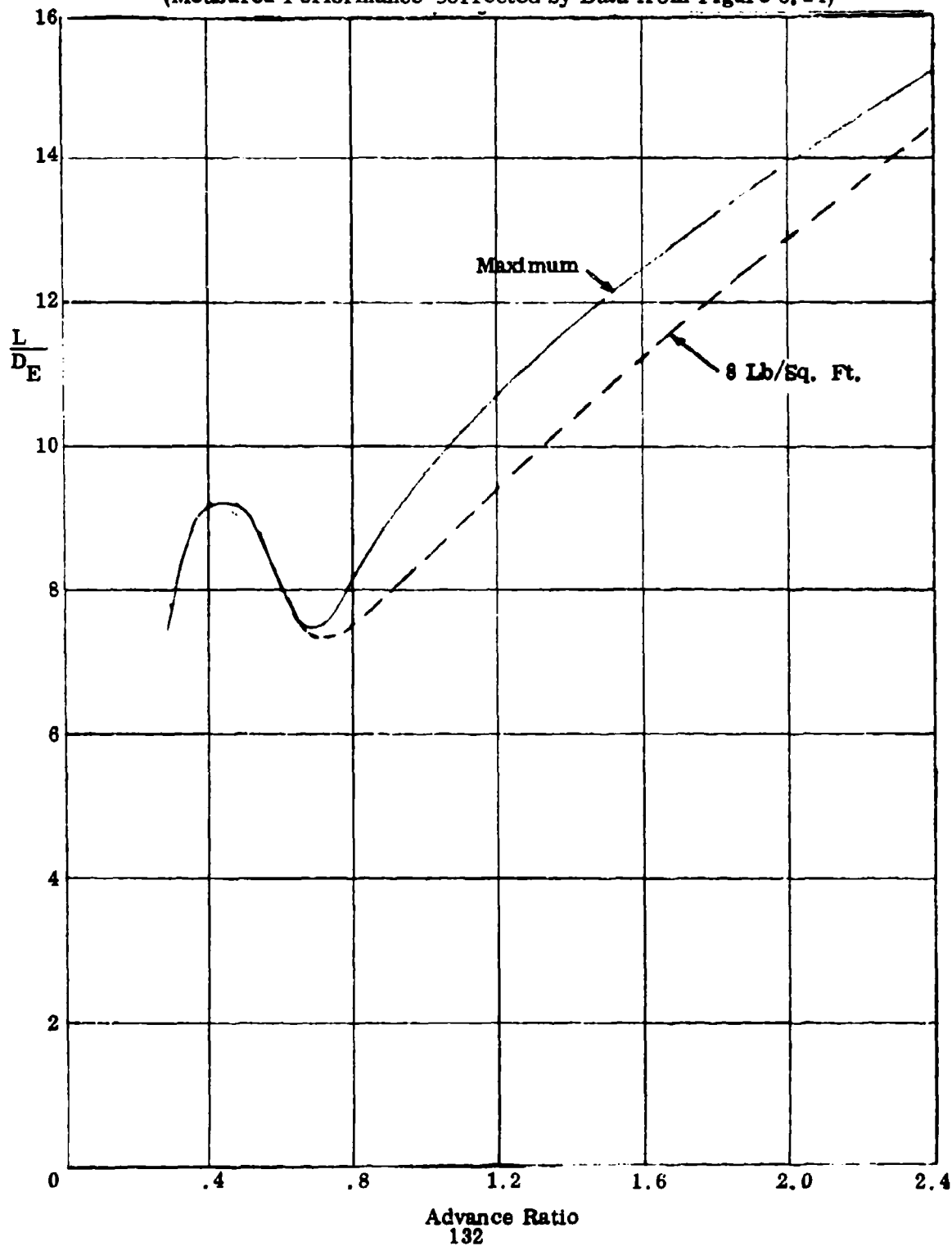
EFFECT OF REYNOLDS NUMBER ON PREDICTED
ROTOR PERFORMANCE - MODEL ROTOR, 18% TO 6%



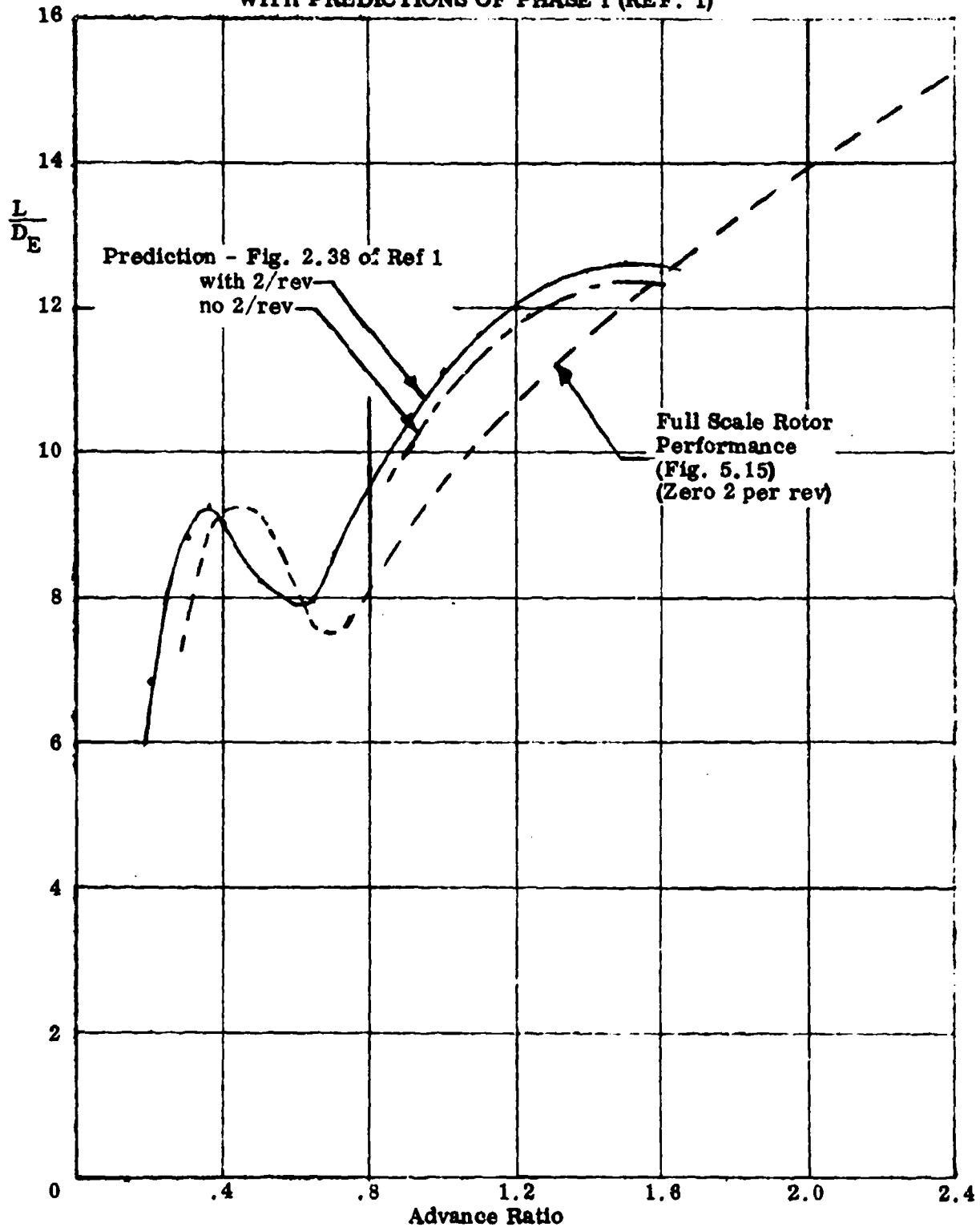
HC144R1070

Figure 5.16

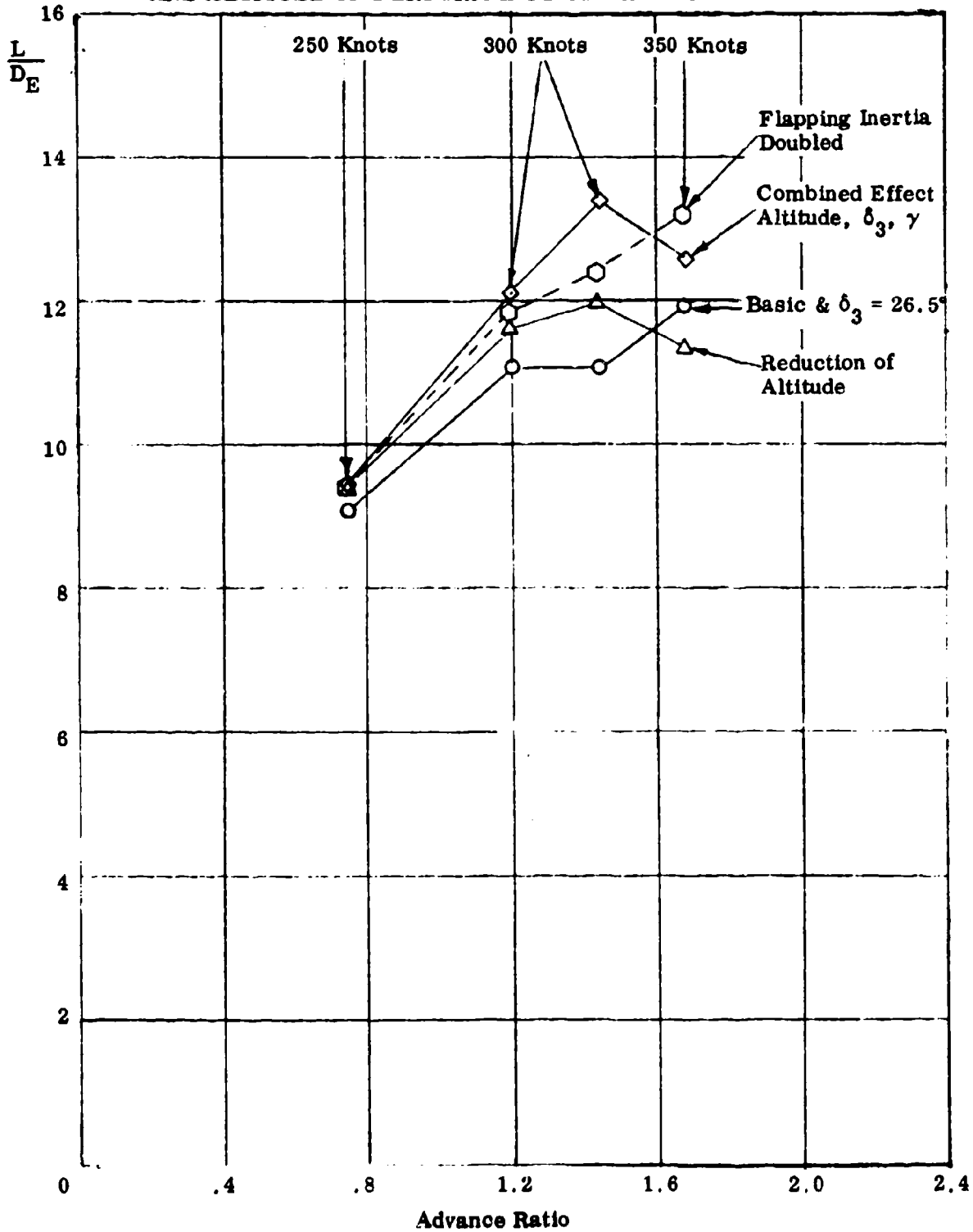
**FULL-SCALE EFFECTIVE LIFT - DRAG RATIO -
MAXIMUM AND AT 8 LB. PER SQ. FT. DISK LOADING**
(Measured Performance Corrected by Data from Figure 5, 14)



COMPARISON OF FULL-SCALE ROTOR PERFORMANCE
WITH PREDICTIONS OF PHASE I (REF. 1)



EFFECT OF CHANGE OF DELTA-3, LOCK NUMBER
AND ALTITUDE ON PERFORMANCE OF PHASE I ROTOR



HC144R1070

APPENDIX A
AIRFOIL SECTION DEVELOPMENT

A1 General

The airfoil sections used in the blade design have been completely defined on a mathematical basis, that is, they are derived from separate equations defining the camber line ordinates and thickness distribution. These equations have been coded in Fairchild Republic digital computer program RAD T620279, and can be used to generate a wide variety of airfoil shapes with either rounded trailing-edge thickness distributions suitable for the RVR concept or conventional sharp trailing edge forms.

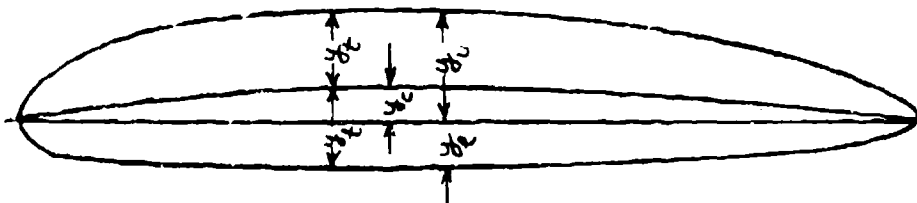
A2 Mathematical Airfoil Definition

A2.1 Surface Ordinates

The upper and lower surface ordinates, y_u and y_l , respectively are determined from the following relations (see sketch)

$$y_u = y_c + y_t \quad (1)$$

$$y_l = y_c - y_t \quad (2)$$



where y_c and y_t denote the mathematical camber line and thickness distribution function respectively, described next.

A2.2 Thickness Distribution

Two separate functions are used to generate the thickness distribution: one equation is used forward of the maximum thickness location; and another for the portion aft of that location. Thus for the fore section, that is, for $0 \leq x \leq x_t$ (where x_t location, in fraction of chord, of maximum thickness)

$$y_t = b_0 \sqrt{x} + b_1 + b_2 x^2 \quad (3)$$

HC144R1070

and for the aft section i. e., for $x_t \leq x \leq 1.0$

$$y_t = c_0 \sqrt{1-x} + c_1 (1-x) + c_2 (1-x)^2 + c_3 (1-x)^3 \quad (4)$$

It is to be noted that these functions representing the fore and aft sections of the thickness distribution are constrained to have the same value of the second derivative at the "join", which is taken to be the station, $x = x_t$, at which the thickness is maximum. This ensures that the curvature of the thickness distribution is continuous along the length of the airfoil.

It should also be noted that the coordinates x and y_t appearing here are dimensionless, that is to say, they have been normalized with respect to the chord length, c .

The coefficients of the various terms in equations (1) and (2) above are dependent upon the following geometric parameters:

x_t = chordwise location of maximum thickness

r_{le} = leading edge radius (fraction of chord)

t_m = semi-maximum thickness ratio

r_{te} = trailing edge semi-thickness

A2.2 Camber line

The camber line function y_c is given by two curves, one for the camber line portion forward of the maximum camber location, and one for the portion aft of this location. Thus, for $x \leq x_c$ (where $x_c = \text{max camber location fraction of chord}$):

$$y_c = a_1 x + a_2 x^2 + a_3 x^3 \quad (5)$$

and for $x \geq x_c$

$$y_c = d_1 (1-x) + d_2 (1-x)^2 + d_3 (1-x)^3 + d_4 (1-x)^4 \quad (6)$$

The coefficients in the equations (5) and (6) are determined by the following geometric parameters, together with the requirement that the second derivative (and hence the camber line curvature) be continuous at the join of the fore and aft section camber lines:

HC144R1070

- x_c = chordwise location of maximum camber
- c_m = maximum camber, fraction of chord
- c_b = slope of camber line at leading edge
- c_e = slope of camber line at trailing edge

A3 Sections Developed for the Model

For all sections used on the blade the maximum thickness and maximum camber are both located at 40% chord: For the root section of the rotor an 18% thick section with 3.7% camber was selected. The tip section is of 6% thickness with 1.3% camber. This reduced camber in the tip section was dictated by manufacturing considerations, in that avoidance of concavity on the under surface of the blade led to a significant reduction of cost. Use of 1.3% camber at the tip eliminated the concavity that would have resulted had a 2-1/2% camber been used along the entire blade. Consequently, the section at the semi-span station is of 12% thickness with 2.5% camber.

Tabulated ordinates for the root (18%) and tip (6%) sections are given in tables A-I and A-II, and the sections are illustrated in Figure 1.4 of the main report.

It is noted that the sections selected for the rotor differ slightly from the modified 0012 section tested previously (Ref. 1). The difference in geometry is restricted to the region of the trailing region and consists primarily of a slight thickening and a better shaped round trailing edge based on the above mentioned mathematical approach which is described briefly below. These changes were expected to yield an improvement in maximum lift coefficients for both forward and reverse flow, as well as improved transonic aerodynamic characteristics.

HC144R1070

TABLE A-1. AIRFOIL SECTION DEVELOPMENT -
INPUT PARAMETERS

Input Parameters	Root Section	Tip Section
Max Camber Location, x_c	.400000	.400000
Max Thickness Location, x_t	.400000	.400000
Trailing Edge Semi-Thickness	0	0
Trailing Edge Semi-Angle	0	0
Max Semi-Thickness, t_m	.090000	.030000
Max Camber, c_m	.037000	.013000
Slope of Camber Line at Trailing Edge, c_e	.148000	.052000
Slope of Camber Line at Leading Edge, c_b	.222000	.078000
Leading Edge Radius, R_L	.039487	.004387
Trailing Edge Radius, R_T	.010000	.002870

HC144R1070

Copy available to DDC does not
permit fully legible reproduction

TABLE A-II. ORDINATES OF ROOT AIRFOIL SECTION
18 Percent Thick, 3.7 Percent Camber

	x	y _u	y _l	y _c	y _t	2y _t
1	0.0	0.0	0.0	0.0	0.0	0.0
2	0.005000	0.019998	-0.017559	0.001100	0.018790	0.037577
3	0.010000	0.028115	-0.023790	0.002179	0.025937	0.051873
4	0.015000	0.034476	-0.027937	0.003237	0.031169	0.062338
5	0.020000	0.039485	-0.031175	0.004275	0.035410	0.070820
6	0.025000	0.043317	-0.033723	0.005293	0.038917	0.077634
7	0.030000	0.046465	-0.035882	0.006297	0.042173	0.084347
8	0.035000	0.049258	-0.037719	0.007270	0.044988	0.089977
9	0.040000	0.051769	-0.039204	0.008229	0.047533	0.095067
10	0.045000	0.053925	-0.040469	0.009168	0.049957	0.099714
11	0.050000	0.055794	-0.041508	0.010088	0.051996	0.103992
12	0.055000	0.057466	-0.042387	0.010989	0.053977	0.107954
13	0.060000	0.058992	-0.043199	0.011871	0.055921	0.111641
14	0.065000	0.060379	-0.044010	0.012735	0.057845	0.115169
15	0.070000	0.061742	-0.044832	0.013580	0.059762	0.118524
16	0.075000	0.063100	-0.045678	0.014406	0.061664	0.121768
17	0.080000	0.064453	-0.046549	0.015214	0.063550	0.124900
18	0.085000	0.065802	-0.047443	0.016005	0.065428	0.127955
19	0.090000	0.067147	-0.048367	0.016777	0.067298	0.129929
20	0.095000	0.068487	-0.049324	0.017532	0.069165	0.131971
21	0.100000	0.069821	-0.050317	0.018284	0.071026	0.134022
22	0.105000	0.071150	-0.051343	0.019029	0.072883	0.136080
23	0.110000	0.072473	-0.052408	0.019766	0.074736	0.142334
24	0.115000	0.073793	-0.053512	0.020493	0.076585	0.146115
25	0.120000	0.075108	-0.054654	0.021216	0.078428	0.149400
26	0.125000	0.076418	-0.055837	0.021935	0.080265	0.152410
27	0.130000	0.077723	-0.057063	0.022651	0.082097	0.155178
28	0.135000	0.079023	-0.058333	0.023364	0.083925	0.157717
29	0.140000	0.080318	-0.059648	0.024073	0.085748	0.160056
30	0.145000	0.081608	-0.061009	0.024779	0.087566	0.162208
31	0.150000	0.082893	-0.062417	0.025481	0.089378	0.164187
32	0.155000	0.084173	-0.063873	0.026180	0.091183	0.165905
33	0.160000	0.085448	-0.065378	0.026876	0.092982	0.167376
34	0.165000	0.086718	-0.066933	0.027569	0.094775	0.168607
35	0.170000	0.087983	-0.068548	0.028259	0.096562	0.169608
36	0.175000	0.089243	-0.070224	0.028946	0.098343	0.170480
37	0.180000	0.090498	-0.071959	0.029630	0.100118	0.171224
38	0.185000	0.091748	-0.073754	0.030311	0.101887	0.171843
39	0.190000	0.092993	-0.075609	0.030989	0.103650	0.172338
40	0.195000	0.094233	-0.077524	0.031664	0.105407	0.172708
41	0.200000	0.095468	-0.079499	0.032336	0.107158	0.172955
42	0.205000	0.096698	-0.081534	0.033005	0.108903	0.173080
43	0.210000	0.097923	-0.083629	0.033671	0.110642	0.173085
44	0.215000	0.099143	-0.085784	0.034334	0.112375	0.172960
45	0.220000	0.100358	-0.088009	0.034994	0.114102	0.172705
46	0.225000	0.101568	-0.090304	0.035651	0.115823	0.172320
47	0.230000	0.102773	-0.092669	0.036305	0.117538	0.171805
48	0.235000	0.103973	-0.095104	0.036956	0.119247	0.171160
49	0.240000	0.105168	-0.097609	0.037604	0.120950	0.170385
50	0.245000	0.106358	-0.100184	0.038249	0.122647	0.169480
51	0.250000	0.107543	-0.102829	0.038891	0.124338	0.168445
52	0.255000	0.108723	-0.105544	0.039530	0.126023	0.167270
53	0.260000	0.109898	-0.108329	0.040166	0.127702	0.165955
54	0.265000	0.111068	-0.111184	0.040800	0.129375	0.164500
55	0.270000	0.112233	-0.114109	0.041431	0.131042	0.162905
56	0.275000	0.113393	-0.117104	0.042059	0.132703	0.161170
57	0.280000	0.114548	-0.120269	0.042684	0.134358	0.159305
58	0.285000	0.115698	-0.123504	0.043306	0.136007	0.157310
59	0.290000	0.116843	-0.126809	0.043925	0.137650	0.155185
60	0.295000	0.117983	-0.130284	0.044541	0.139287	0.152920
61	0.300000	0.119118	-0.133929	0.045154	0.140918	0.150525

Copy available to DDC does not
permit fully legible reproduction

HC144R1070

TABLE A-II (Continued)

	x	y _u	y _l	y _c	y _t	2y _t
62	0.510000	0.123749	-0.052668	0.035541	0.088209	0.174418
63	0.520000	0.123148	-0.049282	0.035283	0.087865	0.175730
64	0.530000	0.122498	-0.045248	0.035008	0.087490	0.174979
65	0.540000	0.121799	-0.04052368	0.034715	0.087083	0.174167
66	0.550000	0.121051	-0.035224	0.034406	0.086646	0.173291
67	0.560000	0.120246	-0.029297	0.034079	0.086176	0.172382
68	0.570000	0.119412	-0.022937	0.033737	0.085675	0.171349
69	0.580000	0.118519	-0.0161762	0.033379	0.085140	0.170281
70	0.590000	0.117578	-0.0091569	0.033004	0.084574	0.169147
71	0.600000	0.116588	-0.0019369	0.032615	0.083974	0.167947
72	0.610000	0.115550	-0.0041130	0.032210	0.083340	0.166680
73	0.620000	0.114462	-0.0056883	0.031784	0.082673	0.165345
74	0.630000	0.113324	-0.006617	0.031354	0.081971	0.163941
75	0.640000	0.112136	-0.0069331	0.030902	0.081234	0.162468
76	0.650000	0.110897	-0.0066225	0.030436	0.080461	0.160923
77	0.660000	0.109606	-0.005699	0.029954	0.079653	0.159305
78	0.670000	0.108263	-0.0049351	0.029456	0.078807	0.157614
79	0.680000	0.106866	-0.0043082	0.028942	0.077924	0.155848
80	0.690000	0.105415	-0.0038591	0.028412	0.077003	0.154006
81	0.700000	0.103908	-0.0034777	0.027866	0.076043	0.152085
82	0.710000	0.102344	-0.0031741	0.027302	0.075042	0.150084
83	0.720000	0.100721	-0.0029279	0.026721	0.074000	0.148001
84	0.730000	0.099039	-0.0027294	0.026122	0.072916	0.145833
85	0.740000	0.097294	-0.0025684	0.025505	0.071789	0.143578
86	0.750000	0.095488	-0.0024374	0.024869	0.070617	0.141234
87	0.760000	0.093611	-0.0023366	0.024213	0.069398	0.138797
88	0.770000	0.091668	-0.0022595	0.023537	0.068132	0.136264
89	0.780000	0.089654	-0.0022039	0.022839	0.066815	0.133630
90	0.790000	0.087566	-0.0021682	0.022120	0.065447	0.130893
91	0.800000	0.085401	-0.0021506	0.021378	0.064024	0.128047
92	0.810000	0.083156	-0.00214931	0.020612	0.062543	0.125087
93	0.820000	0.080825	-0.0021611	0.019822	0.061003	0.122006
94	0.830000	0.078405	-0.00218397	0.019006	0.059399	0.118798
95	0.840000	0.075891	-0.0022239	0.018163	0.057727	0.115485
96	0.850000	0.073276	-0.0022769	0.017291	0.055983	0.111965
97	0.860000	0.070558	-0.00234767	0.016394	0.054161	0.108322
98	0.870000	0.067719	-0.00243181	0.015465	0.052254	0.104598
99	0.880000	0.064759	-0.00252575	0.014504	0.050268	0.100809
100	0.890000	0.061664	-0.0026343	0.013511	0.048183	0.096937
101	0.900000	0.058427	-0.00275255	0.012483	0.045998	0.091877
102	0.910000	0.055046	-0.00288431	0.011324	0.043784	0.086567
103	0.920000	0.051505	-0.00303174	0.010042	0.041559	0.080919
104	0.930000	0.047800	-0.00319497	0.0086375	0.039326	0.078473
105	0.940000	0.043923	-0.00337379	0.0071121	0.037093	0.074220
106	0.950000	0.039880	-0.00356739	0.0054756	0.034979	0.079588
107	0.960000	0.035676	-0.00377555	0.0038182	0.032876	0.076875
108	0.970000	0.031328	-0.00400831	0.0021508	0.030783	0.074060
109	0.980000	0.026856	-0.0042659	0.0004704	0.028704	0.071129
110	0.990000	0.022263	-0.00454835	0.000000	0.026634	0.068069
111	0.995000	0.017546	-0.00485544	0.000000	0.024572	0.064864
112	0.999000	0.012704	-0.00518723	0.000000	0.022519	0.061492
113	0.999500	0.007736	-0.00554372	0.000000	0.020474	0.057927
114	0.999750	0.002641	-0.00592591	0.000000	0.018437	0.054131
115	0.999875	0.000000	-0.00633391	0.000000	0.016408	0.050096
116	0.9999375	0.000000	-0.00676772	0.000000	0.014386	0.045829
117	0.99996875	0.000000	-0.00722835	0.000000	0.012371	0.041342
118	0.999984375	0.000000	-0.00771580	0.000000	0.010361	0.036722
119	0.9999921875	0.000000	-0.00823007	0.000000	0.008356	0.032091
120	0.99999609375	0.000000	-0.00878117	0.000000	0.006356	0.027512
121	0.999998046875	0.000000	-0.00936920	0.000000	0.004361	0.023012

HC144R1070

TABLE A-III. ORDINATES OF TIP AIRFOIL SECTION
6 Percent Thick, 1.3 Percent Camber

	x	y _u	y _t	y _c	y _t	2y _t
1	0.0	0.0	0.0	0.0	0.0	0.0
2	0.005000	0.006449	-0.005877	0.000346	0.006743	0.012486
3	0.010000	0.009411	-0.007890	0.000765	0.009644	0.017221
4	0.015000	0.011527	-0.009252	0.001137	0.010390	0.020779
5	0.020000	0.013305	-0.010301	0.001502	0.011180	0.023607
6	0.025000	0.014865	-0.011146	0.001860	0.013006	0.026011
7	0.030000	0.016264	-0.011847	0.002211	0.014054	0.028116
8	0.035000	0.017550	-0.012442	0.002554	0.014996	0.029992
9	0.040000	0.018736	-0.012953	0.002891	0.015844	0.031689
10	0.045000	0.019940	-0.013395	0.003221	0.016619	0.033238
11	0.050000	0.020977	-0.013787	0.003545	0.017337	0.034664
12	0.055000	0.021953	-0.014131	0.003861	0.017992	0.035985
13	0.060000	0.022774	-0.014434	0.004171	0.018607	0.037214
14	0.065000	0.023655	-0.014707	0.004474	0.019182	0.038363
15	0.070000	0.024492	-0.014949	0.004771	0.019721	0.039441
16	0.075000	0.025290	-0.015166	0.005062	0.020224	0.040456
17	0.080000	0.026052	-0.015361	0.005346	0.020707	0.041413
18	0.085000	0.026782	-0.015536	0.005623	0.021159	0.042318
19	0.090000	0.027483	-0.015694	0.005895	0.021584	0.043176
20	0.095000	0.028155	-0.015835	0.006160	0.021995	0.043990
21	0.100000	0.028801	-0.015963	0.006414	0.022382	0.044764
22	0.110000	0.030020	-0.016183	0.006691	0.023101	0.046203
23	0.120000	0.031159	-0.016381	0.006944	0.023754	0.047511
24	0.130000	0.032200	-0.016558	0.007187	0.024353	0.048706
25	0.140000	0.033176	-0.016714	0.007424	0.024900	0.049800
26	0.150000	0.034085	-0.016794	0.007654	0.025402	0.050803
27	0.160000	0.034931	-0.016794	0.007869	0.025862	0.051725
28	0.170000	0.035719	-0.016554	0.008043	0.026284	0.052572
29	0.180000	0.036451	-0.016901	0.008177	0.026676	0.053352
30	0.190000	0.037132	-0.016937	0.008298	0.027035	0.054069
31	0.200000	0.037764	-0.016944	0.008400	0.027364	0.054729
32	0.210000	0.038350	-0.016945	0.008483	0.027668	0.055335
33	0.220000	0.038893	-0.016999	0.008547	0.027945	0.055897
34	0.230000	0.039393	-0.017009	0.008592	0.028201	0.056402
35	0.240000	0.039854	-0.017015	0.008619	0.028435	0.056864
36	0.250000	0.040277	-0.017019	0.008629	0.028644	0.057295
37	0.260000	0.040663	-0.017020	0.008622	0.028841	0.057693
38	0.270000	0.041015	-0.017020	0.008598	0.029017	0.058034
39	0.280000	0.041333	-0.017018	0.008554	0.029176	0.058331
40	0.290000	0.041620	-0.017016	0.008492	0.029318	0.058586
41	0.300000	0.041876	-0.017013	0.008413	0.029444	0.058804
42	0.310000	0.042103	-0.017011	0.008316	0.029557	0.058983
43	0.320000	0.042301	-0.017008	0.008204	0.029655	0.059130
44	0.330000	0.042473	-0.017006	0.008073	0.029739	0.059259
45	0.340000	0.042618	-0.017004	0.007927	0.029811	0.059362
46	0.350000	0.042734	-0.017003	0.007768	0.029871	0.059441
47	0.360000	0.042823	-0.017001	0.007597	0.029918	0.059506
48	0.370000	0.042895	-0.017001	0.007414	0.029955	0.059559
49	0.380000	0.042940	-0.017000	0.007218	0.029980	0.059590
50	0.390000	0.042990	-0.017000	0.007005	0.029995	0.059600
51	0.400000	0.043000	-0.017000	0.006770	0.030000	0.059600
52	0.410000	0.042990	-0.017000	0.006515	0.029995	0.059590
53	0.420000	0.042967	-0.017000	0.006241	0.029981	0.059572
54	0.430000	0.042915	-0.016999	0.005948	0.029957	0.059544
55	0.440000	0.042850	-0.016995	0.005636	0.029924	0.059508
56	0.450000	0.042764	-0.016993	0.005304	0.029882	0.059463
57	0.460000	0.042654	-0.016993	0.004954	0.029830	0.059401
58	0.470000	0.042527	-0.016994	0.004587	0.029770	0.059324
59	0.480000	0.042380	-0.016994	0.004204	0.029701	0.059243
60	0.490000	0.042222	-0.016996	0.003804	0.029624	0.059158
61	0.500000	0.042100	-0.016997	0.003387	0.029538	0.059076

HC144R1070

TABLE A-III (Continued)

	x	y _u	y _l	y _c	y _t	2y _t
62	0.410000	0.041731	-0.016996	0.012487	0.029444	0.058887
63	0.420000	0.041734	-0.016944	0.012397	0.029341	0.058682
64	0.430000	0.041930	-0.016930	0.012300	0.029230	0.058460
65	0.440000	0.041304	-0.016914	0.012197	0.029111	0.058222
66	0.450000	0.041077	-0.016896	0.012088	0.028994	0.057968
67	0.460000	0.040823	-0.016875	0.011974	0.028849	0.057708
68	0.470000	0.040552	-0.016852	0.011854	0.028706	0.057442
69	0.480000	0.040282	-0.016827	0.011728	0.028555	0.057110
70	0.490000	0.039992	-0.016800	0.011596	0.028396	0.056792
71	0.500000	0.039684	-0.016770	0.011459	0.028229	0.056458
72	0.510000	0.039371	-0.016737	0.011317	0.028054	0.056109
73	0.520000	0.039041	-0.016702	0.011169	0.027872	0.055743
74	0.530000	0.038697	-0.016665	0.011016	0.027684	0.055362
75	0.540000	0.038340	-0.016626	0.010858	0.027492	0.054964
76	0.550000	0.037962	-0.016582	0.010694	0.027295	0.054550
77	0.560000	0.037564	-0.016536	0.010524	0.027090	0.054120
78	0.570000	0.037146	-0.016487	0.010349	0.026876	0.053673
79	0.580000	0.036711	-0.016435	0.010169	0.026654	0.053208
80	0.590000	0.036268	-0.016381	0.009984	0.026423	0.052727
81	0.600000	0.035808	-0.016323	0.009794	0.026183	0.052227
82	0.610000	0.035347	-0.016261	0.009593	0.025934	0.051708
83	0.620000	0.034874	-0.016195	0.009389	0.025676	0.051170
84	0.630000	0.034404	+0.016124	0.009178	0.025409	0.050612
85	0.640000	0.033927	-0.016055	0.008961	0.025136	0.050032
86	0.650000	0.033453	-0.015978	0.008738	0.024856	0.049431
87	0.660000	0.032981	-0.015894	0.008507	0.024563	0.048807
88	0.670000	0.032518	-0.015809	0.008270	0.024259	0.048157
89	0.680000	0.032055	-0.015716	0.008028	0.023941	0.047482
90	0.690000	0.031581	-0.015617	0.007772	0.023609	0.046778
91	0.700000	0.031103	-0.015511	0.007511	0.023262	0.046048
92	0.710000	0.030621	-0.015397	0.007242	0.022899	0.045278
93	0.720000	0.029703	-0.015274	0.006964	0.022519	0.044467
94	0.730000	0.028746	-0.015140	0.006678	0.022118	0.043626
95	0.740000	0.027758	-0.014994	0.006382	0.021696	0.042752
96	0.750000	0.026747	-0.014835	0.006076	0.021251	0.041822
97	0.760000	0.025719	-0.014665	0.005760	0.020784	0.040838
98	0.770000	0.024673	-0.014484	0.005434	0.020296	0.039798
99	0.780000	0.023609	-0.014297	0.005096	0.019783	0.038708
100	0.790000	0.022546	-0.014102	0.004747	0.019249	0.037568
101	0.800000	0.021497	-0.013795	0.004386	0.018691	0.036372
102	0.805000	0.021497	-0.013572	0.004201	0.017773	0.035548
103	0.810000	0.021433	-0.013409	0.004013	0.017420	0.034940
104	0.815000	0.020971	-0.013211	0.003821	0.017052	0.034105
105	0.820000	0.020291	-0.013041	0.003626	0.016667	0.033135
106	0.825000	0.019491	-0.012816	0.003429	0.016264	0.032427
107	0.830000	0.018669	-0.012611	0.003226	0.015833	0.031674
108	0.835000	0.017812	-0.012370	0.003021	0.015391	0.030781
109	0.840000	0.017774	-0.012104	0.002812	0.014918	0.029832
110	0.845000	0.017011	-0.011812	0.002600	0.014412	0.028823
111	0.850000	0.016256	-0.011499	0.002384	0.013873	0.027748
112	0.855000	0.015488	-0.011130	0.002164	0.013294	0.026588
113	0.860000	0.014608	-0.010799	0.001940	0.012668	0.025336
114	0.865000	0.013697	-0.010273	0.001712	0.011988	0.023970
115	0.870000	0.012712	-0.009752	0.001480	0.011272	0.022464
116	0.875000	0.011534	-0.009146	0.001244	0.010540	0.020780
117	0.880000	0.010478	-0.008483	0.001004	0.009777	0.018960
118	0.885000	0.009362	-0.007783	0.000760	0.008963	0.016986
119	0.890000	0.007424	-0.006802	0.000511	0.008091	0.013975
120	0.895000	0.005270	-0.004755	0.000258	0.006801	0.010025
121	0.900000	0.000000	-0.000000	0.000000	0.000000	0.000000

HC144R1070

APPENDIX B
ROTOR TEST RESULTS

Results are reproduced from NASA provided print-out. They have been corrected for tare. See Section 2.1.

HC144R1070

KEY TO ABBREVIATIONS - ROTOR TEST RESULTS

M	M_∞	free-stream Mach number
R	R	Reynolds number, millions per foot
PT	P_{t_∞}	free-stream total pressure, lb per sq ft
Q	q_∞	free-stream dynamic pressure, lb per sq ft
TT	T_{t_∞}	free-stream total temperature, °F
RHO	$\rho \times 100$	free-stream density, slugs/ft ³
GAMA	γ	blade lock number $\rho_\infty (a) (c) (b^4) / I_\beta$
PHI	φ_2	two-per-rev phasing, degrees
DEL 3	δ_3	flapping hinge cant, degrees
CORR		data correlation number
THEZ	θ_0	collective pitch, degrees
THEC	θ_{1c}	cyclic pitch (cosine), degrees
THES	θ_{1s}	cyclic pitch (sine), degrees
ALFA	α	angle of attack of model reference axis, degrees
V	V_∞	free-stream velocity, ft/sec
VTIP	ΩR	tip speed, RPM ($\pi/30$) (b), ft/sec
MU	μ	advance ratio, $V_\infty (\cos \alpha) / \Omega R$
LAMB	λ	inflow ratio, $-\mu (\tan \alpha) + 0.5 C_{T^*} / (\lambda^2 + \mu^2)^{1/2}$
CZ	C_N	normal-force coefficient, normal force/ $q_\infty S$
CX	C_A	axial-force coefficient, axial force/ $q_\infty S$
CPM	C_m	pitching-moment coefficient, pitching moment/ $q_\infty S c$
CRM	C_l	rolling-moment coefficient, rolling moment/ $q_\infty s b$
CL	C_L	lift coefficient, lift/ $q_\infty S$

HC144R1070

KEY TO ABBREVIATIONS - ROTOR TEST RESULTS (Cont'd)

CD	C_D	drag coefficient, $\text{drag}/q_\infty S$
CT	C_T	thrust coefficient, $\frac{1}{2} C_N (V_\infty / \Omega R)^2$
CH	C_H	in-plane force coefficient, $\frac{1}{2} C_A (V_\infty / \Omega R)^2$
CQ	C_q	torque coefficient, $10 \times \frac{1}{2} C_n (V_\infty / \Omega R)^2$
CLR	C_{LR}	rotor lift coefficient, $\frac{1}{2} C_L (V_\infty / \Omega R)^2$
CDR	C_{DR}	rotor drag coefficient, $\frac{1}{2} C_D (V_\infty / \Omega R)^2$
LOD	$(L/D)_R$	rotor lift-to-drag ratio, $C_{LR} / [C_q (\Omega R / V_\infty) + C_{DR}]$
DL	DL	disc loading, $C_L q_\infty$, lb/ft^2
CRB	C_{Bal}	balance axis rolling-moment coefficient, $\text{balance rolling-moment}/q_\infty S b$

HC144R1070

APPENDIX B. ROTOR TEST RESULTS
TARES - RUNS 37, 38

RUN	L	TN	TST	P	DATE	TIME	M	R	PT	Q	TT	RHO	GAMA	PHI	DEL3
37	1	12	614	1	0626	1603	0.143	0.412	0888.	012.5	068.9	0.069	00.81	000.0	26.00
CORR THEZ THEC THES ALFA V VTIP CZ CX CPM CRM CL CD															
296	00.02	00.10	00.05	00.04	160.7	281.5	.0167	.0159	.0020	.0005	.0166	.0153			
297	00.01	00.23	00.03	00.04	161.3	420.6	.0177	.0165	.0011	.0007	.0176	.0165			
298	00.07	00.18	00.07	00.03	161.9	562.1	.0158	.0139	.0021	.0008	.0158	.0139			
299	00.17	00.28	00.06	00.03	161.9	702.0	.0174	.0168	.0010	.0010	.0174	.0168			
300	00.01	00.04	00.04	05.01	162.0	278.1	.0247	.0135	.0048	.0014	.0234	.0156			
301	00.06	00.05	00.07	05.01	162.0	419.7	.0226	.0130	.0045	.0015	.0213	.0149			
302	00.16	00.15	00.06	05.00	162.0	560.5	.0211	.0098	.0054	.0017	.0201	.0116			
303	00.11	00.25	00.07	05.00	162.0	700.4	.0204	.0110	.0053	.0018	.0193	.0127			
304	00.04	00.18	00.06	10.05	161.6	279.8	.0310	.0090	.0061	.0025	.0289	.0143			
305	00.09	00.15	00.06	10.03	161.6	418.9	.0288	.0074	.0070	.0029	.0271	.0124			
306	00.12	00.12	00.08	10.05	161.6	562.1	.0274	.0068	.0074	.0029	.0288	.0120			
307	00.17	00.24	00.07	10.03	162.1	699.5	.0308	.0092	.0070	.0030	.0258	.0139			
308	00.01	00.03	00.06	10.06	162.1	000.0	.0330	.0101	.0068	.0025	.0307	.0158			
309	00.00	00.13	00.07	05.06	161.7	000.0	.0334	.0120	.0075	.0007	.0323	.0149			
310	00.01	00.01	00.06	00.00	162.1	000.0	.0254	.0197	.0003	.0001	.0254	.0197			

RUN	L	TN	TST	P	DATE	TIME	M	K	PT	Q	TT	RHO	GAMA	PHI	DEL3
38	1	12	614	1	0626	1620	0.286	0.798	0899.	048.7	076.5	0.0938	00.79	000.0	26.00
CORR THEZ THEC THES ALFA V VTIP CZ CX CPM CRM CL CD															
311	00.03	00.11	00.07	00.01	322.3	277.3	.0230	.0171	.0008	.0001	.0230	.0171			
312	00.05	00.09	00.06	00.01	322.9	416.4	.0222	.0179	.0007	.0002	.0222	.0179			
313	00.14	00.21	00.07	00.01	323.2	560.5	.0221	.0170	.0010	.0003	.0221	.0170			
314	00.12	00.19	00.08	00.01	323.2	697.0	.0220	.0173	.0008	.0004	.0220	.0173			
315	00.00	00.13	00.03	02.49	323.1	278.1	.0255	.0171	.0012	.0002	.0247	.0182			
316	00.10	00.07	00.06	02.50	323.4	416.4	.0250	.0171	.0012	.0003	.0242	.0182			
317	00.08	00.17	00.06	02.49	323.0	561.3	.0245	.0161	.0015	.0004	.0238	.0172			
318	00.09	00.13	00.08	02.49	323.1	700.4	.0236	.0163	.0015	.0005	.0229	.0173			
319	00.06	00.06	00.06	05.01	322.9	280.6	.0269	.0158	.0018	.0003	.0255	.0181			
320	00.18	00.13	00.06	04.99	323.2	419.7	.0268	.0171	.0018	.0004	.0252	.0193			
321	00.12	00.01	00.08	05.00	322.9	560.5	.0276	.0148	.0021	.0005	.0262	.0171			
322	00.12	00.22	00.06	05.00	322.9	700.4	.0263	.0152	.0020	.0006	.0249	.0175			
323	00.06	00.01	00.06	07.47	322.7	279.8	.0283	.0150	.0028	.0005	.0261	.0185			
324	00.11	00.12	00.07	07.47	323.0	416.4	.0289	.0151	.0024	.0006	.0267	.0188			
325	00.12	00.09	00.07	07.47	323.5	598.8	.0288	.0140	.0028	.0007	.0268	.0176			
326	00.11	00.21	00.09	07.48	323.4	698.7	.0290	.0147	.0024	.0008	.0269	.0183			
327	00.02	00.06	00.08	09.98	323.4	277.3	.0315	.0132	.0029	.0006	.0297	.0185			
328	00.04	00.01	00.08	09.97	323.2	422.2	.0316	.0150	.0027	.0008	.0295	.0203			
329	00.13	00.04	00.07	09.98	323.2	561.3	.0315	.0129	.0032	.0009	.0288	.0182			
330	00.13	00.23	00.07	09.98	323.2	698.7	.0314	.0134	.0030	.0010	.0286	.0187			

HC144R1070

APPENDIX B. ROTOR TEST RESULTS (Continued)
RUNS 29, 30, 31, 32

RUN	L	TN	TST	P	DATE	TIME	M	R	PT	G	TT	RHO	GAMA	PHI	DEL3
29	1	12	514	1	0621	1001	0.292	0.776	0645.	047.5	069.1	.0893	00.75	000.0	26.00
CORR THEZ THEC THES ALFA V VTIP MU LAMB CZ CX CPM															
299	00.00	00.00	01.57	03.81	05.00	326.3	697.9	0.466	0.0343	.0550	.0028	.0016			
298	02.00	00.00	01.37	05.18	05.05	327.6	697.9	0.468	0.0329	.0719	.0013	.0044			
295	02.12	00.00	01.09	02.21	04.93	322.5	703.7	0.457	0.0355	.0345	.0037	.0028			

RUN	L	TN	TST	P	DATE	TIME	M	R	PT	G	TT	RHO	GAMA	PHI	DEL3
30	1	12	514	1	0021	1007	0.287	0.762	0647.	046.0	071.4	.0893	00.75	000.0	26.00
CORR THEZ THEC THES ALFA V VTIP MU LAMB CZ CX CPM															
297	00.00	00.00	01.49	02.87	-00.05	321.2	697.9	0.460	0.0029	.0219	.0035	-0.0002			
298	01.94	00.00	02.33	03.92	00.21	321.0	699.5	0.459	0.0033	.0434	.0027	-0.0036			
299	02.10	00.00	01.91	01.18	00.05	320.4	701.2	0.457	0.0009	-0.0038	.0035	-0.0040			

RUN	L	TN	TST	P	DATE	TIME	M	R	PT	G	TT	RHO	GAMA	PHI	DEL3
31	1	12	514	1	0021	1010	0.358	0.934	0656.	070.5	076.4	.0875	00.73	000.0	26.00
CORR THEZ THEC THES ALFA V VTIP MU LAMB CZ CX CPM															
240	00.10	00.00	02.34	02.82	-00.05	401.3	626.6	0.640	0.0014	.0050	.0030	-0.0030			
241	01.96	00.00	02.37	04.27	-00.03	401.2	628.3	0.639	0.0021	.0109	.0031	-0.0014			
242	04.03	00.00	02.44	05.97	-00.01	401.9	630.0	0.638	0.0029	.0177	.0030	-0.0008			
243	06.05	00.00	02.79	07.52	00.01	401.9	630.0	0.638	0.0036	.0235	.0028	-0.0012			
244	09.71	00.00	02.96	06.27	00.04	402.4	633.3	0.635	0.0048	.0334	.0040	.0114			
245	05.69	00.00	04.02	05.30	00.07	403.0	630.0	0.640	0.0060	.0426	.0046	.0210			
246	05.86	00.00	08.79	04.48	00.07	401.9	630.0	0.637	0.0057	.0403	.0166	.0346			
247	00.41	00.00	02.65	00.99	-00.02	403.7	630.0	0.641	0.0026	.0150	.0041	.0139			
248	00.05	00.00	05.66	00.04	00.02	403.7	630.0	0.641	0.0040	.0259	.0034	.0243			

RUN	L	TN	TST	P	DATE	TIME	M	R	PT	G	TT	RHO	GAMA	PHI	DEL3
32	1	12	514	1	0021	1037	0.358	0.931	0669.	071.4	083.4	.0875	00.73	000.0	26.00
CORR THEZ THEC THES ALFA V VTIP MU LAMB CZ CX CPM															
249	00.04	00.00	02.49	04.56	05.10	404.0	627.5	0.641	0.0535	.0229	.0028	-0.0012			
250	02.90	00.00	02.46	06.64	05.13	404.3	628.3	0.641	0.0523	.0330	.0021	.0004			
251	06.03	00.00	01.90	07.64	05.22	403.0	627.5	0.640	0.0484	.0621	.0030	.0179			
252	03.13	00.00	01.60	01.90	05.06	404.9	626.6	0.644	0.0545	.0152	.0035	.0007			
253	03.15	00.00	03.71	00.10	05.11	404.0	629.2	0.640	0.0523	.0304	.0050	.0184			
254	02.99	00.00	04.99	02.68	05.05	403.9	622.5	0.646	0.0558	.0078	.0036	-0.0110			
255	02.84	00.00	08.61	03.85	05.01	404.6	623.3	0.647	0.0568	.0013	.0032	-0.0243			

Copy available to DDC does not permit fully legible reproduction

HC144R1070

Copy available to DDC does not
permit fully legible reproduction

CRM	CL	CD	CT	CH	CO	CLR	CDR	LOD	DL	CRB	CORR
.0001	.0543	.0076	.0060	.0003	.0014	.0060	.0008	05.91	02.99	.0001	233
.0005	.0715	.0076	.0079	.0001	.0020	.0079	.0008	06.27	03.43	.0003	234
.0001	.0341	.0066	.0036	.0004	.0017	.0036	.0007	03.35	01.58	.0001	235

CRM	CL	CD	CT	CH	CO	CLR	CDR	LOD	DL	CRB	CORR
.0002	.0219	.0035	.0023	.0004	.0032	.0023	.0004	02.18	01.01	.0002	237
.0001	.0434	.0028	.0046	.0003	.0034	.0046	.0003	04.43	01.99	.0001	238
.0001	.0038	.0035	.0004	.0004	.0040	.0004	.0004	00.32	00.18	.0001	239

CRM	CL	CD	CT	CH	CO	CLR	CDR	LOD	DL	CRB	CORR
.0001	.0050	.0030	.0010	.0006	.0063	.0010	.0006	00.64	00.35	.0001	240
.0001	.0109	.0031	.0022	.0006	.0052	.0022	.0006	01.53	00.77	.0001	241
.0001	.0177	.0030	.0036	.0006	.0070	.0036	.0006	02.12	01.25	.0001	242
.0002	.0235	.0028	.0048	.0006	.0085	.0048	.0006	02.51	01.66	.0002	243
.0001	.0334	.0041	.0067	.0008	.0048	.0067	.0008	04.25	02.36	.0001	244
.0002	.0426	.0047	.0087	.0009	.0063	.0087	.0010	04.50	03.03	.0002	245
.0004	.0403	.0166	.0082	.0034	.0118	.0082	.0034	01.97	02.85	.0004	246
.0001	.0150	.0041	.0031	.0008	.0024	.0031	.0008	02.52	01.07	.0001	247
.0002	.0259	.0034	.0053	.0011	.0022	.0053	.0011	03.65	01.85	.0002	248

CRM	CL	CD	CT	CH	CO	CLR	CDR	LOD	DL	CRB	CORR
.0001	.0226	.0049	.0047	.0006	.0170	.0047	.0010	01.28	01.61	.0001	249
.0002	.0327	.0050	.0060	.0004	.0078	.0060	.0010	03.01	02.34	.0002	250
.0005	.0615	.0087	.0128	.0006	.0074	.0127	.0010	04.32	04.38	.0005	251
.0001	.0148	.0048	.0032	.0007	.0063	.0031	.0010	01.56	01.06	.0001	252
.0001	.0298	.0076	.0063	.0010	.0004	.0061	.0016	04.07	02.13	.0001	253
.0000	.0075	.0043	.0017	.0008	.0064	.0016	.0009	00.83	00.53	.0000	254
.0004	.0015	.0031	.0003	.0007	.0128	.0003	.0007	00.12	00.11	.0004	255

HC144R1070

APPENDIX B. ROTOR TEST RESULTS (Continued)
RUNS 35, 36, 41

RUN	L	TN	TST	P	DATE	TIME	M	R	PT	Q	TT	RHO	GAMA	PHI	DEL3
35	1	12	614	1	0621	1248	0.433	1.108	0898.	103.7	093.2	.0863	00.72	000.0	26.00
CORR THEZ THEC THES ALFA V VTIP MU LAMB CZ CX CPM															
276	00.01	00.12	01.95	-00.07	490.0	559.6	0.876	.0026	.0067	.0012	.0034				
277	02.11	00.53	03.72	-00.07	489.9	557.9	0.878	.0026	.0068	.0017	.0036				
278	03.90	00.20	05.20	-00.06	490.3	561.3	0.874	.0028	.0084	.0021	.0046				
279	02.01	00.10	00.11	-00.08	491.1	562.1	0.874	.0021	.0061	.0014	.0030				
280	02.94	00.94	01.95	-00.03	492.0	559.6	0.879	.0049	.0203	.0035	.0253				
281	02.99	00.02	01.02	-00.09	493.5	565.5	0.873	.0018	.0023	.0012	.0041				

RUN	L	TN	TST	P	DATE	TIME	M	R	PT	Q	TT	RHO	GAMA	PHI	DEL3
36	1	12	614	1	0621	1313	0.434	1.105	0907.	105.1	099.5	.0862	00.72	000.0	26.00
CORR THEZ THEC THES ALFA V VTIP MU LAMB CZ CX CPM															
282	00.09	02.13	04.40	05.00	493.9	563.0	0.874	-.0736	.0130	.0004	.0017				
283	00.02	05.08	05.04	04.99	493.3	562.1	0.874	-.0740	.0105	.0005	-.0059				
284	00.05	03.94	02.71	05.07	492.7	563.8	0.870	-.0708	.0294	.0015	.0145				
285	02.07	01.77	02.62	05.01	492.8	562.1	0.873	-.0788	.0125	.0005	.0015				
286	02.18	05.62	00.54	05.06	492.3	559.6	0.876	-.0720	.0253	.0004	.0187				
287	02.00	06.29	03.61	04.94	493.0	563.8	0.871	-.0762	-.0040	.0013	-.0070				

RUN	L	TN	TST	P	DATE	TIME	M	R	PT	Q	TT	RHO	GAMA	PHI	DEL3
41	1	12	614	1	0626	2206	0.434	1.129	0883.	102.1	078.1	.0872	00.73	000.0	26.00
CORR THEZ THEC THES ALFA V VTIP MU LAMB CZ CX CPM															
379	00.08	02.37	02.20	-00.12	483.9	490.1	0.987	.0035	.0060	.0014	.0006				
380	01.94	02.32	00.55	-00.12	484.5	490.9	0.987	.0033	.0048	.0015	.0004				
381	03.99	02.28	01.62	-00.11	484.8	490.9	0.988	.0034	.0058	.0017	.0005				
382	01.85	01.90	03.72	-00.11	485.9	490.1	0.991	.0035	.0061	.0014	.0018				
383	04.13	01.93	05.82	-00.11	485.1	489.3	0.991	.0034	.0058	.0026	.0020				
384	04.00	03.79	01.06	04.89	486.1	489.3	0.990	-.0812	.0140	.0009	-.0010				
385	03.88	03.85	07.69	04.90	487.0	490.9	0.988	-.0809	.0153	.0012	.0009				
386	00.03	03.98	04.65	04.89	487.0	491.8	0.987	-.0808	.0149	.0015	.0007				
387	00.04	04.00	05.61	07.48	487.7	494.3	0.978	-.1231	.0218	.0001	.0009				
388	03.98	04.06	02.26	07.49	487.6	491.8	0.983	-.1242	.0206	.0005	-.0001				
389	02.96	05.03	08.32	07.48	487.9	490.1	0.987	-.1244	.0212	.0003	.0004				
390	00.07	04.79	06.94	09.96	488.7	491.8	0.979	-.1647	.0289	-.0004	.0006				
391	04.93	04.49	03.49	09.96	487.8	490.9	0.979	-.1650	.0274	.0015	-.0002				

FAIRCHILD
A PUBLIC DIVISION

HC144R1070

CRM	CL	CD	CT	CH	CG	CLR	CDR	LOD	DL	CRB	CORR
.0000	.0067	.0012	.0026	.0005	.0044	.0026	.0004	02.68	00.69	.0000	276
.0000	.0068	.0017	.0026	.0006	.0064	.0026	.0006	01.92	00.70	.0000	277
-.0001	.0084	.0021	.0032	.0008	.0038	.0032	.0008	02.58	00.87	.0001	278
-.0000	.0041	.0014	.0016	.0005	.0108	.0016	.0005	00.89	00.43	.0000	279
-.0002	.0203	.0035	.0078	.0014	.0100	.0078	.0014	03.13	02.11	.0002	280
.0001	.0023	.0011	.0009	.0004	.0064	.0009	.0004	00.75	00.24	.0001	281

CRM	CL	CD	CT	CH	CG	CLR	CDR	LOD	DL	CRB	CORR
.0000	.0129	.0016	.0050	.0002	.0050	.0050	.0006	04.24	01.36	.0000	282
.0001	.0104	.0014	.0040	.0002	.0252	.0040	.0005	01.17	01.09	.0001	283
.0001	.0292	.0041	.0112	.0006	.0003	.0111	.0016	07.28	03.05	.0001	284
-.0000	.0124	.0016	.0048	.0002	.0041	.0047	.0006	04.35	01.29	.0000	285
.0000	.0252	.0026	.0098	.0002	.0005	.0097	.0010	10.22	02.63	.0000	286
.0000	.0041	.0009	.0015	.0005	.0094	.0016	.0004	01.08	00.43	.0000	287

CRM	CL	CD	CT	CH	CG	CLR	CDR	LOD	DL	CRB	CORR
-.0004	.0060	.0014	.0029	.0007	.0037	.0029	.0007	02.71	00.61	.0004	379
-.0003	.0048	.0014	.0023	.0007	.0043	.0023	.0007	02.04	00.49	.0003	380
-.0003	.0088	.0017	.0029	.0008	.0047	.0029	.0008	02.20	00.60	.0003	381
-.0003	.0061	.0014	.0030	.0007	.0031	.0030	.0007	03.05	00.63	.0003	382
-.0003	.0058	.0025	.0028	.0013	.0025	.0026	.0013	01.89	00.59	.0003	383
-.0003	.0139	.0021	.0069	.0003	.0021	.0069	.0010	05.48	01.43	.0003	384
-.0006	.0152	.0025	.0075	.0006	.0021	.0075	.0012	05.17	01.56	.0006	385
-.0003	.0147	.0027	.0073	.0007	.0022	.0072	.0013	04.63	01.52	.0003	386
-.0003	.0216	.0030	.0106	.0001	.0007	.0105	.0014	07.65	02.23	.0003	387
-.0006	.0204	.0032	.0101	.0003	.0017	.0100	.0016	07.10	02.11	.0006	388
-.0006	.0210	.0031	.0105	.0002	.0029	.0104	.0015	05.73	02.17	.0006	389
-.0007	.0285	.0046	.0142	.0002	.0022	.0141	.0023	06.79	02.96	.0007	390
-.0006	.0267	.0063	.0135	.0008	.0052	.0132	.0031	05.15	02.77	.0006	391

HC144R1070

APPENDIX B. ROTOR TEST RESULTS (Continued)
RUNS 42, 43

RUN L TN TST P DATE TIME M R PT G TT RHO GAMA PHI DELS
42 1 12 614 1 0627 0854 0.432 1.090 0858. 098.7 079.9 .0845 00.71 000.0 26.00

CORR	THEZ	THEC	THES	ALFA	V	VTIP	MU	LAMB	CZ	CX	CPM
397	00.03-02.15	02.03	-00.12	483.1	419.7	1.151	.0040	.0038	.0014	.0009	
398	02.06-02.70	04.05	-00.13	482.7	419.7	1.150	.0035	.0035	.0016	.0007	
399	04.01-03.15	06.05	-00.15	483.2	418.0	1.156	.0031	.0007	.0019	.0003	
400	02.06-01.82	00.11	-00.11	483.4	420.6	1.149	.0045	.0077	.0014	.0012	
401	04.04-01.84	02.22	-00.11	484.8	423.1	1.146	.0048	.0091	.0017	.0015	
402	00.05-02.51	00.89	-02.53	485.6	419.7	1.156	.0506	.0013	.0015	-.0006	
403	02.00-02.98	03.14	-02.54	485.8	420.6	1.154	.0501	.0039	.0018	-.0010	
404	01.96-01.74	02.77	-02.53	485.9	421.4	1.152	.0503	.0019	.0016	.0007	
405	03.87-02.01	04.82	-02.54	486.0	418.0	1.161	.0503	.0040	.0024	.0005	
406	01.99-00.64	02.04	-02.51	485.2	421.4	1.150	.0517	.0047	.0014	.0028	
407	01.88-02.38	01.27	-02.52	484.6	417.2	1.160	.0514	.0012	.0014	.0001	
408	04.02-00.88	03.94	-02.50	487.4	420.6	1.158	.0523	.0058	.0018	.0022	
409	00.05-03.84	04.30	04.98	488.6	419.7	1.160	.0961	.0169	.0006	.0007	
410	01.95-04.20	06.39	04.96	486.1	420.6	1.151	.0955	.0154	.0008	.0003	
411	04.04-04.38	08.34	04.96	488.8	420.6	1.158	.0967	.0133	.0010	.0005	
412	02.03-03.29	02.60	04.97	489.2	425.6	1.145	.0944	.0183	.0009	.0010	
413	04.05-03.05	00.56	04.96	489.2	419.7	1.161	.0953	.0189	.0013	.0010	
414	00.01-03.57	03.92	07.44	488.9	417.2	1.162	.1455	.0210	.0005	-.0008	
415	01.96-03.90	07.68	07.44	488.4	420.6	1.151	.1446	.0198	.0006	-.0010	
416	02.03-03.47	03.88	07.45	489.2	446.5	1.086	.1354	.0242	.0009	.0017	
417	04.07-03.91	01.94	07.45	489.6	421.4	1.152	.1434	.0248	.0015	.0016	
418	00.01-04.71	05.80	07.45	489.3	416.4	1.165	.1457	.0227	.0003	.0007	
419	00.02-03.24	07.01	10.02	488.5	419.7	1.146	.1935	.0308	.0007	.0008	
420	02.10-03.13	05.32	10.02	488.9	423.9	1.136	.1919	.0302	.0005	.0007	
421	04.09-03.30	03.44	10.02	488.9	426.4	1.129	.1910	.0294	.0000	.0005	
422	06.14-03.15	01.41	10.01	489.6	423.9	1.137	.1924	.0287	.0001	.0005	
423	00.05-06.11	07.14	10.01	490.1	424.7	1.136	.1924	.0286	.0014	-.0000	

RUN L TN TST P DATE TIME M R PT G TT RHO GAMA PHI DELS
43 1 12 614 1 0627 0940 0.434 1.088 0861. 102.1 093.5 .0846 00.71 000.0 26.00

CORR	THEZ	THEC	THES	ALFA	V	VTIP	MU	LAMB	CZ	CX	CPM
424	00.08-04.07	02.11	-00.07	491.1	350.2	1.403	.0036	.0052	.0022	-.0007	
425	02.05-03.36	00.58	-00.05	489.2	350.2	1.397	.0051	.0111	.0020	.0004	
426	04.09-03.05	03.15	-00.04	490.8	346.8	1.415	.0065	.0195	.0025	.0014	
427	02.03-03.96	04.35	-00.09	491.7	350.2	1.404	.0027	.0015	.0024	-.0006	
428	04.02-04.20	06.98	-00.10	491.7	362.7	1.356	.0012	.0035	.0031	-.0012	
429	00.00-05.41	04.32	05.02	491.0	350.2	1.397	.1182	.0184	.0007	-.0003	
430	02.02-05.85	06.56	05.01	491.4	351.0	1.394	.1171	.0149	.0010	-.0006	
431	03.98-06.57	08.75	05.00	491.4	346.8	1.412	.1201	.0097	.0018	-.0013	
432	02.02-05.26	02.50	05.03	490.8	351.9	1.389	.1153	.0203	.0010	-.0000	
433	04.02-04.94	00.38	05.03	491.2	351.0	1.394	.1150	.0219	.0017	.0004	
434	06.10-05.07	01.99	05.04	490.2	349.3	1.398	.1145	.0247	.0030	.0004	
435	00.03-06.05	05.70	07.46	490.8	349.3	1.393	.1741	.0237	.0003	.0001	
436	01.88-06.67	07.54	07.46	491.6	346.8	1.405	.1763	.0214	.0001	-.0003	
437	03.62-06.64	09.26	07.46	490.9	351.9	1.383	.1744	.0191	.0004	-.0004	
438	02.01-06.73	03.81	07.47	490.6	351.9	1.382	.1729	.0242	.0005	-.0007	
439	04.03-06.93	01.87	07.47	490.5	347.7	1.399	.1744	.0256	.0014	-.0008	
440	06.14-06.59	00.34	07.47	491.3	351.0	1.388	.1727	.0266	.0027	-.0002	
441	00.07-07.67	07.04	09.93	490.9	346.8	1.394	.2338	.0287	.0005	-.0003	
442	02.07-07.93	08.92	09.92	491.1	351.9	1.375	.2309	.0275	.0002	-.0008	
443	02.02-07.58	05.27	09.94	490.9	346.8	1.394	.2334	.0308	.0014	-.0008	
444	04.13-07.29	03.09	09.93	490.3	355.2	1.359	.2272	.0315	.0015	-.0004	
445	06.02-06.97	00.85	09.94	490.3	349.3	1.382	.2306	.0329	.0038	.0001	

HC144R1070

Copy available to DDC, declassified
permut fully legible reproduction

CRM	CL	CD	CT	CH	CO	CLR	CDR	LOD	DL	CRB	CORR
.0004	.0053	.0014	.0035	.0009	.0030	.0035	.0009	03.00	00.53	.0004	397
.0004	.0033	.0016	.0022	.0011	.0033	.0022	.0011	01.62	00.33	.0004	398
.0004	.0007	.0019	.0004	.0013	.0034	.0004	.0013	00.28	00.07	.0004	399
.0005	.0077	.0013	.0051	.0009	.0033	.0051	.0009	04.35	00.76	.0005	400
.0005	.0091	.0017	.0060	.0011	.0031	.0060	.0011	04.38	00.90	.0005	401
.0003	.0013	.0016	.0009	.0010	.0051	.0009	.0011	00.57	00.13	.0003	402
.0003	.0038	.0019	.0026	.0012	.0047	.0025	.0013	01.48	00.38	.0003	403
.0004	.0018	.0017	.0013	.0011	.0040	.0012	.0011	00.81	00.18	.0004	404
.0004	.0039	.0026	.0027	.0016	.0030	.0026	.0017	01.31	00.38	.0004	405
.0005	.0047	.0012	.0031	.0009	.0035	.0031	.0008	02.95	00.47	.0005	406
.0004	.0012	.0014	.0008	.0010	.0052	.0008	.0009	00.60	00.12	.0004	407
.0005	.0059	.0015	.0039	.0012	.0044	.0039	.0010	02.85	00.59	.0005	408
.0007	.0168	.0021	.0115	.0004	.0010	.0114	.0014	07.53	01.69	.0007	409
.0006	.0152	.0021	.0103	.0005	.0020	.0102	.0014	06.48	01.52	.0006	410
.0005	.0131	.0022	.0090	.0007	.0026	.0089	.0015	05.27	01.32	.0005	411
.0006	.0161	.0024	.0121	.0006	.0007	.0120	.0016	07.70	01.83	.0006	412
.0006	.0187	.0029	.0129	.0009	.0025	.0127	.0020	07.17	01.89	.0006	413
.0006	.0208	.0032	.0144	.0003	.0005	.0143	.0022	06.32	02.10	.0006	414
.0005	.0196	.0032	.0134	.0004	.0020	.0132	.0021	05.73	01.98	.0005	415
.0006	.0239	.0040	.0145	.0005	.0050	.0144	.0024	07.42	02.42	.0006	416
.0006	.0244	.0047	.0168	.0010	.0072	.0165	.0032	06.43	02.48	.0006	417
.0006	.0226	.0026	.0157	.0002	.0009	.0156	.0018	09.03	02.28	.0006	418
.0007	.0302	.0061	.0208	.0005	.0050	.0204	.0041	05.56	03.04	.0007	419
.0006	.0296	.0058	.0201	.0004	.0075	.0197	.0038	06.17	03.00	.0006	420
.0006	.0289	.0051	.0193	.0000	.0096	.0190	.0034	07.51	02.92	.0006	421
.0005	.0282	.0051	.0191	.0001	.0128	.0188	.0034	08.28	02.86	.0005	422
.0006	.0284	.0036	.0191	.0009	.0037	.0189	.0024	09.11	02.89	.0006	423

CRM	CL	CD	CT	CH	CO	CLR	CDR	LOD	DL	CRB	CORR
.0004	.0052	.0022	.0051	.0022	.0038	.0051	.0022	02.09	00.53	.0004	424
.0005	.0111	.0020	.0109	.0020	.0037	.0109	.0020	04.90	01.13	.0005	425
.0006	.0155	.0024	.0155	.0025	.0010	.0155	.0025	06.14	01.58	.0006	426
.0004	.0015	.0024	.0015	.0024	.0045	.0015	.0024	00.54	00.15	.0004	427
.0003	.0035	.0031	.0032	.0028	.0037	.0032	.0028	01.04	00.36	.0003	428
.0005	.0182	.0023	.0180	.0007	.0012	.0179	.0023	07.50	01.86	.0005	429
.0005	.0147	.0023	.0146	.0009	.0036	.0144	.0022	05.87	01.51	.0005	430
.0004	.0095	.0026	.0097	.0018	.0049	.0096	.0026	03.23	00.97	.0004	431
.0005	.0201	.0028	.0197	.0010	.0016	.0196	.0027	07.64	02.05	.0005	432
.0004	.0216	.0036	.0214	.0017	.0075	.0212	.0035	07.06	02.21	.0004	433
.0006	.0243	.0052	.0243	.0030	.0135	.0240	.0051	05.81	02.48	.0006	434
.0006	.0235	.0033	.0234	.0003	.0022	.0232	.0033	07.37	02.40	.0006	435
.0006	.0212	.0027	.0215	.0001	.0013	.0213	.0027	07.67	02.17	.0006	436
.0006	.0189	.0029	.0186	.0004	.0032	.0184	.0028	05.98	01.93	.0006	437
.0007	.0239	.0037	.0235	.0005	.0044	.0232	.0036	07.11	02.44	.0007	438
.0007	.0252	.0047	.0255	.0014	.0095	.0251	.0047	06.24	02.57	.0007	439
.0005	.0260	.0061	.0260	.0026	.0166	.0255	.0060	05.31	02.66	.0005	440
.0006	.0283	.0044	.0287	.0005	.0050	.0284	.0044	06.97	02.90	.0006	441
.0007	.0271	.0046	.0268	.0002	.0004	.0264	.0044	05.91	02.77	.0007	442
.0006	.0301	.0067	.0308	.0014	.0108	.0301	.0067	05.10	03.07	.0006	443
.0005	.0308	.0069	.0300	.0014	.0171	.0293	.0066	05.47	03.14	.0005	444
.0007	.0318	.0094	.0324	.0038	.0260	.0313	.0093	04.21	03.24	.0007	445

HC144R1070

APPENDIX B. ROTOR TEST RESULTS (Continued)
RUNS 44, 45

RUN L TN TST P DATE TIME M R PT G TT RHO GAMA PHI DELS
44 1 12 614 1 0527 1048 0.434 1.097 0886. 102.7 093.0 .0853 00.72 000.0 26.00

CORR	THEZ	THEC	THES	ALFA	V	VTIP	MU	LAMB	CZ	CX	CPM
446	00.10-06.28	00.63	-00.00	490.6	213.6	2.297	.0097	.0168-.0021	.0019		
447	00.03-04.47	01.89	00.08	490.1	282.3	1.736	.0012	.0082-.0006	.0002		
448	02.03-04.73	00.91	00.10	490.6	282.3	1.738	.0034	.0148-.0014	.0008		
449	02.05-06.56	00.57	00.09	489.8	279.8	1.750	.0022	.0110-.0019	-.0008		
450	04.13-06.10	03.98	00.11	491.2	283.2	1.735	.0050	.0194-.0008	.0005		
451	01.36-05.43	03.84	00.05	490.8	281.5	1.743	.0016	.0004-.0011	-.0011		
452	01.39-03.16	03.83	00.07	492.6	284.8	1.730	.0008	.0031-.0009	.0006		
453	00.23-07.24	04.50	04.98	491.8	284.8	1.720	.1415	.0196-.0009	-.0001		
454	02.03-07.01	01.90	05.00	491.8	281.5	1.741	.1417	.0240-.0009	.0003		
455	03.97-06.74	00.33	05.01	492.3	280.6	1.747	.1412	.0271-.0001	.0014		
456	06.21-06.78	03.23	05.02	492.5	284.0	1.727	.1384	.0309-.0019	.0021		
457	00.15-06.69	04.92	07.54	493.0	284.8	1.716	.2136	.0312-.0006	.0023		
458	00.02-06.79	05.94	07.53	494.8	283.2	1.732	.2170	.0271-.0002	.0009		
459	00.17-06.61	04.92	07.53	494.1	285.7	1.715	.2133	.0308-.0006	.0010		
460	02.18-08.22	03.06	07.54	494.4	267.2	1.834	.2282	.0315-.0011	.0008		
461	04.08-07.96	00.71	07.56	494.0	278.1	1.761	.2184	.0344-.0022	.0019		
462	06.16-07.48	01.71	07.57	493.4	274.8	1.780	.2202	.0363-.0031	.0028		
463	06.50-08.41	02.14	07.56	493.6	283.2	1.728	.2142	.0348-.0029	.0017		
464	01.47-09.16	07.92	10.06	493.2	277.3	1.751	.2961	.0327-.0017	.0011		
465	00.04-08.76	06.21	10.06	493.5	268.9	1.807	.3041	.0360-.0018	.0018		
466	00.15-09.97	06.86	10.05	494.7	272.3	1.789	.3021	.0330-.0020	.0013		
467	00.50-08.82	06.97	10.06	495.2	271.4	1.796	.3029	.0342-.0025	.0018		
468	02.09-09.25	03.92	10.08	494.5	274.8	1.772	.2973	.0392-.0008	.0024		
469	02.04-09.54	04.13	10.07	494.4	272.3	1.788	.3010	.0360-.0007	.0011		
470	04.05-09.29	01.94	10.07	494.2	272.3	1.787	.2997	.0388-.0025	.0017		
471	00.00-02.86	00.03	-02.51	494.5	274.8	1.798	.0807	.0040-.0000	.0009		
472	03.86-04.10	05.82	-02.47	494.7	273.9	1.804	.0857	.0178-.0003	.0018		
473	02.02-04.11	03.10	-02.48	494.9	274.8	1.799	.0833	.0116-.0006	.0011		
474	01.98-03.28	03.31	-02.55	495.1	273.9	1.806	.0768	.0082-.0017	-.0004		

RUN L TN TST P DATE TIME M R PT G TT RHO GAMA PHI DELS
45 1 12 614 1 0627 1258 0.507 1.260 0913. 137.9 100.2 .0838 00.70 000.0 26.00

CORR	THEZ	THEC	THES	ALFA	V	VTIP	MU	LAMB	CZ	CX	CPM
475	00.93-02.60	02.06	-00.03	573.6	501.8	1.143	.0029	.0078-.0018	.0000		
476	04.30-02.55	05.45	-00.04	575.0	498.5	1.154	.0021	.0042-.0026	.0000		
477	02.03-02.14	01.51	-00.01	574.1	493.4	1.164	.0039	.0127-.0016	.0013		
478	01.99-02.24	00.91	-00.02	574.6	490.9	1.170	.0034	.0100-.0019	.0008		
479	04.08-01.56	03.33	-00.01	574.4	495.1	1.160	.0040	.0133-.0023	.0017		
480	06.05-01.98	05.57	-00.01	574.5	496.0	1.158	.0042	.0142-.0034	.0014		
481	00.01-03.29	03.55	04.95	576.9	493.4	1.165	.0953	.0193-.0012	.0010		
482	02.06-02.94	05.37	04.96	576.7	496.0	1.158	.0949	.0193-.0010	.0019		
483	02.10-03.13	01.80	04.96	576.3	493.4	1.164	.0952	.0198-.0015	.0009		
484	04.10-02.71	00.36	04.97	576.6	496.8	1.156	.0946	.0204-.0029	.0016		
485	05.91-02.44	02.62	04.97	577.5	496.8	1.158	.0941	.0224-.0045	.0021		
486	00.07-03.89	04.85	07.53	578.9	497.6	1.153	.1448	.0259-.0007	.0012		
487	01.97-04.17	06.62	07.53	578.4	511.0	1.122	.1411	.0257-.0005	.0011		
488	02.04-04.60	03.30	07.52	579.1	491.8	1.167	.1470	.0240-.0019	.0002		
489	04.01-04.16	01.24	07.53	578.6	496.0	1.157	.1455	.0253-.0032	.0001		
490	05.93-04.73	00.65	07.52	578.3	490.1	1.170	.1474	.0243-.0042	-.0007		
491	04.04-05.30	00.23	07.53	578.6	490.9	1.169	.1464	.0272-.0037	.0004		
492	01.92-05.84	01.13	07.54	578.7	493.4	1.163	.1448	.0319-.0020	.0019		
493	05.94-04.26	00.73	07.52	577.7	490.9	1.171	.1473	.0241-.0049	.0002		
494	00.00-01.89	00.26	-02.46	580.6	493.4	1.173	.0914	.0029-.0020	.0001		
495	02.06-02.11	02.05	-02.47	581.1	493.4	1.177	.0908	.0000-.0024	-.0003		
496	03.92-02.33	04.08	-02.48	581.2	493.4	1.177	.0902	.0024-.0023	-.0010		
497	02.03-01.97	02.54	-02.45	580.5	491.8	1.179	.0522	.0057-.0018	.0004		
498	03.98-02.03	04.38	-02.45	580.2	491.8	1.179	.0525	.0071-.0026	-.0000		
499	04.11-01.98	04.64	-02.44	580.7	495.1	1.172	.0523	.0080-.0026	.0002		
500	05.95-01.76	00.73	-02.44	580.9	496.0	1.170	.0527	.0100-.0027	.0007		
501	00.01-03.97	02.90	02.71	582.7	423.1	1.376	.0601	.0147-.0009	.0003		

HC144R1070

CRM	CL	CD	CT	CH	CO	CLR	CDR	LOD	DL	CRB	CORR
-.0006	.0168	.0021	.0444	.0055	.0017	.0444	.0055	07.92	01.73	.0006	446
-.0004	.0082	.0006	.0124	.0009	.0041	.0124	.0009	18.99	00.84	.0004	447
-.0002	.0148	.0014	.0224	.0021	.0021	.0224	.0021	11.55	01.52	.0002	448
-.0004	.0110	.0019	.0169	.0029	.0049	.0169	.0029	06.54	01.13	.0004	449
-.0006	.0194	.0008	.0292	.0012	.0063	.0292	.0012	32.74	02.00	.0006	450
-.0004	.0004	.0011	.0007	.0017	.0059	.0007	.0017	00.33	00.04	.0004	451
-.0006	.0031	.0009	.0046	.0013	.0023	.0046	.0013	03.25	00.32	.0006	452
-.0005	.0196	.0008	.0292	.0013	.0010	.0292	.0012	22.71	02.02	.0005	453
-.0005	.0240	.0012	.0366	.0014	.0090	.0366	.0018	29.08	02.48	.0005	454
-.0006	.0270	.0025	.0417	.0002	.0226	.0415	.0039	16.15	02.79	.0006	455
-.0004	.0906	.0046	.0465	.0029	.0421	.0461	.0070	10.13	03.17	.0004	456
-.0007	.0310	.0035	.0468	.0010	.0159	.0465	.0052	10.88	03.22	.0007	457
-.0001	.0269	.0034	.0414	.0003	.0069	.0411	.0052	08.61	02.81	.0001	458
-.0006	.0305	.0046	.0461	.0009	.0158	.0456	.0069	07.62	03.18	.0006	459
-.0005	.0311	.0053	.0539	.0019	.0268	.0532	.0090	07.04	03.24	.0005	460
-.0006	.0338	.0067	.0542	.0035	.0434	.0533	.0106	06.54	03.52	.0006	461
-.0007	.0356	.0078	.0565	.0049	.0621	.0573	.0126	06.28	03.70	.0007	462
-.0006	.0342	.0075	.0529	.0044	.0578	.0519	.0114	06.45	03.55	.0006	463
-.0007	.0325	.0040	.0518	.0027	.0100	.0514	.0064	08.80	03.38	.0007	464
-.0007	.0358	.0045	.0606	.0030	.0235	.0602	.0076	09.92	03.72	.0007	465
-.0004	.0329	.0038	.0545	.0032	.0162	.0543	.0063	10.00	03.44	.0004	466
-.0006	.0341	.0035	.0569	.0041	.0191	.0568	.0059	11.76	03.58	.0006	467
-.0007	.0385	.0076	.0635	.0012	.0429	.0623	.0123	06.26	04.02	.0007	468
-.0007	.0353	.0070	.0593	.0012	.0350	.0582	.0115	06.06	03.69	.0007	469
-.0007	.0378	.0093	.0639	.0042	.0553	.0622	.0153	05.09	03.94	.0007	470
-.0004	.0040	.0002	.0064	.0000	.0026	.0064	.0003	54.22	00.41	.0004	471
-.0005	.0178	.0005	.0290	.0005	.0041	.0290	.0008	28.44	01.86	.0005	472
-.0005	.0116	.0011	.0188	.0009	.0025	.0188	.0017	11.67	01.21	.0005	473
-.0003	.0081	.0020	.0134	.0027	.0038	.0132	.0033	03.77	00.85	.0003	474

CRM	CL	CD	CT	CH	CO	CLR	CDR	LOD	DL	CRB	CORR
-.0005	.0078	.0018	.0051	.0012	.0049	.0051	.0012	03.12	01.07	.0005	475
-.0004	.0042	.0026	.0028	.0017	.0049	.0028	.0017	01.29	00.58	.0004	476
-.0011	.0127	.0016	.0086	.0011	.0043	.0086	.0011	05.80	01.76	.0011	477
-.0004	.0100	.0019	.0069	.0013	.0049	.0069	.0013	04.00	01.39	.0004	478
-.0005	.0133	.0023	.0089	.0015	.0037	.0089	.0015	04.82	01.83	.0005	479
-.0005	.0142	.0034	.0095	.0023	.0032	.0095	.0023	03.75	01.96	.0005	480
-.0006	.0191	.0028	.0132	.0008	.0020	.0131	.0019	06.18	02.66	.0006	481
-.0006	.0191	.0026	.0130	.0006	.0022	.0129	.0018	06.61	02.66	.0006	482
-.0004	.0196	.0032	.0135	.0010	.0025	.0134	.0022	05.93	02.73	.0004	483
-.0006	.0201	.0046	.0138	.0019	.0025	.0136	.0031	04.68	02.80	.0006	484
-.0006	.0219	.0064	.0151	.0030	.0051	.0148	.0043	03.80	03.05	.0006	485
-.0006	.0256	.0040	.0175	.0004	.0009	.0173	.0027	06.92	03.58	.0006	486
-.0006	.0254	.0038	.0164	.0003	.0009	.0163	.0025	06.44	03.55	.0006	487
-.0006	.0236	.0046	.0166	.0010	.0017	.0164	.0032	05.38	03.30	.0006	488
-.0005	.0247	.0065	.0172	.0022	.0040	.0168	.0044	04.14	03.45	.0005	489
-.0005	.0235	.0074	.0169	.0030	.0054	.0164	.0051	03.49	03.29	.0005	490
-.0024	.0265	.0073	.0189	.0026	.0076	.0184	.0050	04.19	03.70	.0024	491
-.0043	.0313	.0062	.0219	.0014	.0104	.0215	.0042	06.41	04.39	.0043	492
-.0005	.0232	.0080	.0168	.0034	.0063	.0162	.0056	03.20	03.26	.0005	493
-.0003	.0030	.0019	.0020	.0014	.0065	.0021	.0013	01.13	00.42	.0003	494
-.0003	.0001	.0024	.0000	.0017	.0062	.0001	.0017	00.04	00.02	.0004	495
-.0003	.0023	.0024	.0017	.0016	.0058	.0016	.0017	00.74	00.32	.0003	496
-.0004	.0098	.0015	.0040	.0012	.0066	.0040	.0011	02.50	00.82	.0004	497
-.0002	.0072	.0023	.0049	.0018	.0070	.0050	.0016	02.30	01.01	.0002	498
-.0004	.0081	.0023	.0055	.0018	.0066	.0056	.0015	02.63	01.14	.0004	499
-.0004	.0101	.0023	.0069	.0018	.0070	.0070	.0015	03.24	01.43	.0004	500
-.0004	.0146	.0016	.0139	.0009	.0023	.0139	.0015	08.19	02.07	.0004	501

HC144R1070

APPENDIX B. ROTOR TEST RESULTS (Continued)
RUNS 46, 47, 48

RUN L TN TST P DATE TIME H R PT Q TT RHO GAMA PHI DELB
46 1 12 514 1 0627 1334 0.509 1.252 0934. 141.6 114.1 .0836 00.70 000.0 26.00

CORR	THEZ	THEC	TRES	ALFA	V	VTIP	QU	LAMB	CZ	CX	CPM
502	00.00-03.77	01.63	-00.01	582.1	431.3	1.451	.0028	.0071	.0017	-.0006	
503	01.92-03.07	03.66	-00.03	582.8	399.6	1.458	.0020	.0037	.0018	-.0000	
504	03.93-03.85	03.92	-00.03	582.9	421.3	1.453	.0009	.0019	.0027	-.0005	
505	01.89-02.95	00.82	00.01	582.4	399.6	1.457	.0045	.0131	.0016	.0007	
506	03.96-04.11	02.77	00.01	582.3	410.5	1.419	.0047	.0139	.0022	-.0006	
507	06.03-03.98	05.23	00.01	582.4	410.5	1.419	.0053	.0160	.0037	.0004	
508	00.09-03.32	04.10	04.97	582.6	417.2	1.591	-.1146	.0184	.0057	-.0004	
509	01.90-05.93	06.22	04.95	583.0	407.2	1.427	-.1184	.0144	.0058	-.0010	
510	03.94-06.06	06.31	04.95	583.0	408.0	1.424	-.1197	.0104	.0017	-.0013	
511	02.00-05.82	02.30	04.98	582.3	411.3	1.410	-.1163	.0199	.0009	-.0009	
512	04.04-05.68	00.14	04.97	582.2	427.3	1.357	-.1108	.0215	.0019	-.0004	
513	06.14-05.09	02.20	04.99	583.5	413.0	1.407	-.1144	.0241	.0044	.0002	
514	04.95-05.47	00.61	04.99	584.2	426.1	1.360	-.1109	.0227	.0030	-.0004	
515	03.12-06.21	02.50	07.48	584.1	423.1	1.369	-.1710	.0253	.0016	-.0003	
516	03.96-06.08	01.50	07.50	584.5	401.3	1.444	-.1800	.0278	.0025	-.0003	
517	02.08-06.59	03.74	07.46	584.6	397.9	1.457	-.1820	.0250	.0006	-.0007	
518	00.03-06.12	05.40	07.47	585.4	413.9	1.402	-.1754	.0244	.0001	-.0003	
519	02.02-06.45	07.50	07.47	586.1	400.4	1.451	-.1821	.0222	.0000	-.0005	

RUN L TN TST P DATE TIME H R PT Q TT RHO GAMA PHI DELB
47 1 12 514 1 0627 1402 0.509 1.253 0942. 143.4 118.5 .0837 00.70 000.0 26.00

CORR	THEZ	THEC	TRES	ALFA	V	VTIP	QU	LAMB	CZ	CX	CPM
520	00.05-04.36	01.32	-00.01	585.4	351.2	1.672	.0042	.0094	.0013	-.0004	
521	01.92-03.73	03.85	-00.02	584.7	352.7	1.658	.0019	.0029	.0015	-.0002	
522	03.92-04.39	06.53	-00.06	586.0	351.0	1.669	-.0008	.0058	.0028	-.0011	
523	02.02-04.84	01.02	00.02	585.6	351.9	1.664	.0057	.0148	.0014	-.0006	
524	03.99-04.14	03.50	00.03	585.1	351.0	1.667	.0074	.0200	.0023	.0005	
525	06.06-03.97	06.30	00.05	584.2	346.0	1.688	.0090	.0246	.0046	.0017	
526	04.97-04.20	04.80	00.04	584.5	354.4	1.650	.0079	.0221	.0031	.0010	
527	00.01-05.52	04.09	04.97	584.5	351.9	1.655	-.1356	.0198	.0005	-.0004	
528	02.08-05.88	06.20	04.96	585.0	346.5	1.672	-.1379	.0172	.0006	.0001	
529	02.04-06.40	01.70	05.00	585.1	348.5	1.673	-.1362	.0243	.0012	.0003	
530	04.03-05.91	00.34	04.99	585.1	373.6	1.560	-.1257	.0270	.0025	.0009	
531	06.03-05.43	02.81	05.00	585.5	353.5	1.650	-.1320	.0297	.0039	.0016	
532	03.05-06.19	00.91	04.95	585.6	351.9	1.658	-.1342	.0249	.0011	.0002	
533	01.21-06.81	04.00	07.46	585.7	352.7	1.647	-.2041	.0281	.0003	.0007	
534	04.13-06.39	00.81	07.43	585.8	356.0	1.631	-.2014	.0313	.0023	.0016	
535	01.90-06.82	03.20	07.47	586.2	358.6	1.616	-.1999	.0290	.0004	.0009	
536	00.11-07.34	05.15	07.46	586.2	353.5	1.644	-.2043	.0265	.0000	.0001	
537	01.96-08.41	07.50	07.44	587.0	349.3	1.666	-.2080	.0211	.0000	-.0014	

RUN L TN TST P DATE TIME H R PT Q TT RHO GAMA PHI DELB
48 1 12 514 1 0627 1433 0.509 1.254 0949. 144.3 121.2 .0839 00.70 000.0 26.00

CORR	THEZ	THEC	TRES	ALFA	V	VTIP	QU	LAMB	CZ	CX	CPM
538	00.38-04.94	01.10	00.00	586.4	285.7	2.053	.0078	.0153	.0010	.0008	
539	01.61-06.60	01.73	00.02	585.8	269.8	2.175	.0104	.0203	.0013	.0003	
540	02.85-05.53	03.37	00.03	585.7	270.6	2.164	.0127	.0256	.0024	.0015	
541	01.27-09.87	04.42	04.93	586.2	279.0	2.094	-.1678	.0240	.0008	.0003	
542	01.70-09.05	05.83	04.91	587.0	273.1	2.142	-.1748	.0174	.0012	-.0009	
543	02.53-07.02	00.13	04.96	585.6	268.1	2.176	-.1703	.0340	.0024	.0028	
544	00.17-07.59	03.34	04.94	586.5	269.0	2.166	-.1717	.0287	.0014	.0011	
545	00.77-04.04	01.62	02.07	587.3	267.2	2.196	.0754	.0019	.0014	-.0008	
546	01.84-04.51	04.17	02.11	586.5	270.6	2.166	.0725	.0136	.0028	-.0522	
547	02.95-05.56	05.31	01.99	586.8	267.2	2.194	.0882	.0222	.0017	.0015	

FAIRCHILD
REPUBLIC DIVISION

HC144R1070

Copy available to DDC does not
permit fully legible reproduction

CRM	CL	CO	CT	CH	CC	CLR	CDR	LOD	DL	CRB	CORR
-.0003	.0071	.0017	.0075	.0018	.0053	.0075	.0018	03.53	01.01	.0003	502
-.0003	.0037	.0018	.0040	.0019	.0051	.0040	.0019	01.73	00.53	.0003	503
-.0004	.0019	.0027	.0020	.0028	.0043	.0020	.0026	00.64	00.27	.0004	504
-.0005	.0131	.0016	.0139	.0017	.0029	.0139	.0017	07.17	01.85	.0005	505
-.0004	.0139	.0022	.0140	.0022	.0034	.0140	.0022	09.74	01.97	.0004	506
-.0005	.0160	.0037	.0161	.0037	.0025	.0161	.0037	04.58	02.26	.0005	507
-.0005	.0163	.0022	.0160	.0028	.0017	.0179	.0022	07.72	02.60	.0005	508
-.0005	.0143	.0020	.0146	.0020	.0047	.0146	.0021	06.08	02.03	.0005	509
-.0005	.0102	.0026	.0106	.0017	.0045	.0104	.0026	03.91	01.45	.0005	510
-.0005	.0188	.0025	.0190	.0029	.0004	.0188	.0025	07.35	02.66	.0005	511
-.0007	.0213	.0037	.0200	.0017	.0052	.0157	.0035	06.42	03.01	.0007	512
-.0004	.0236	.0065	.0240	.0044	.0144	.0236	.0065	04.33	03.36	.0004	513
-.0005	.0223	.0050	.0211	.0028	.0077	.0208	.0046	05.12	03.19	.0005	514
-.0005	.0249	.0049	.0241	.0015	.0086	.0237	.0046	05.92	03.55	.0005	515
-.0005	.0272	.0061	.0294	.0027	.0134	.0286	.0065	05.15	03.89	.0005	516
-.0005	.0247	.0039	.0269	.0007	.0056	.0266	.0042	06.98	03.53	.0005	517
-.0006	.0242	.0031	.0244	.0001	.0026	.0242	.0031	08.32	03.47	.0006	518
-.0005	.0220	.0029	.0236	.0000	.0019	.0236	.0031	07.25	03.16	.0005	519

CRM	CL	CO	CT	CH	CC	CLR	CDR	LOD	DL	CRB	CORR
-.0005	.0094	.0013	.0132	.0013	.0053	.0132	.0016	06.30	01.35	.0005	520
-.0004	.0029	.0015	.0040	.0021	.0052	.0040	.0021	01.63	00.41	.0004	521
-.0003	.0058	.0028	.0081	.0028	.0036	.0081	.0036	01.99	00.83	.0003	522
-.0005	.0148	.0014	.0205	.0019	.0030	.0205	.0019	09.48	02.12	.0005	523
-.0004	.0200	.0023	.0276	.0032	.0039	.0279	.0032	09.45	02.87	.0004	524
-.0006	.0246	.0046	.0350	.0045	.0211	.0350	.0065	06.61	03.51	.0006	525
-.0006	.0220	.0031	.0300	.0042	.0106	.0300	.0042	08.47	03.16	.0006	526
-.0005	.0197	.0022	.0273	.0006	.0006	.0271	.0030	08.93	02.81	.0005	527
-.0005	.0171	.0020	.0242	.0006	.0015	.0241	.0029	08.13	02.45	.0005	528
-.0006	.0241	.0034	.0342	.0016	.0081	.0339	.0047	07.98	03.46	.0006	529
-.0005	.0267	.0049	.0331	.0031	.0173	.0327	.0060	08.75	03.83	.0005	530
-.0006	.0292	.0065	.0407	.0023	.0028	.0471	.0029	05.83	04.20	.0006	531
-.0005	.0247	.0023	.0344	.0015	.0112	.0342	.0045	08.91	03.55	.0005	532
-.0006	.0279	.0040	.0368	.0005	.0127	.0364	.0055	08.13	04.01	.0006	533
-.0006	.0307	.0064	.0423	.0021	.0284	.0416	.0066	08.04	04.42	.0006	534
-.0006	.0287	.0042	.0325	.0005	.0165	.0321	.0055	08.41	04.11	.0006	535
-.0005	.0263	.0034	.0365	.0001	.0068	.0362	.0047	08.46	03.79	.0005	536
-.0005	.0209	.0027	.0296	.0001	.0041	.0296	.0038	07.30	03.02	.0005	537

CRM	CL	CO	CT	CH	CC	CLR	CDR	LOD	DL	CRB	CORR
-.0005	.0153	.0010	.0322	.0020	.0008	.0322	.0020	15.43	02.21	.0005	538
-.0005	.0203	.0013	.0480	.0037	.0065	.0470	.0030	17.96	02.93	.0005	539
-.0004	.0256	.0024	.0600	.0057	.0252	.0600	.0057	13.14	03.69	.0004	540
-.0009	.0239	.0024	.0531	.0017	.0072	.0527	.0063	08.89	03.45	.0009	541
-.0006	.0172	.0026	.0401	.0027	.0042	.0357	.0061	06.31	02.49	.0006	542
-.0004	.0337	.0053	.0412	.0056	.0054	.0874	.0126	07.99	04.86	.0004	543
-.0006	.0285	.0039	.0679	.0034	.0170	.0674	.0092	07.98	04.12	.0006	544
-.0004	.0018	.0014	.0046	.0033	.0102	.0044	.0035	01.12	00.27	.0004	545
-.0002	.0135	.0034	.0320	.0067	.0046	.0318	.0079	03.93	01.96	.0002	546
-.0006	.0222	.0009	.0534	.0041	.0147	.0525	.0023	33.76	03.21	.0006	547

HC144R1070

APPENDIX B. ROTOR TEST RESULTS (Continued)
RUNS 49, 50

RUN	L	TN	TST	P	DATE	TIME	M	R	PT	Q	TT	RHO	GAMA	PHI	DELS
49	1	12	614	1	0627	1905	0.508	1.254	0953	144.5	122.7	.0841	00.71	000.0	26.00
CORR THEZ THEC THES ALFA V VTIP MU LAMB CZ CX CPM															
548	00	93	06.64	01.98	00.13	586.2	244.6	2.396	.0099	.0259	.0026	.0016			
549	01	12	06.97	02.82	00.16	586.4	231.2	2.536	.0121	.0300	.0034	.0030			
550	00	17	06.96	00.98	00.13	586.7	237.1	2.475	.0097	.0250	.0021	.0013			

RUN	L	TN	TST	P	DATE	TIME	M	R	PT	Q	TT	RHO	GAMA	PHI	DELS
50	1	12	614	1	0627	2022	0.182	1.229	2123	048.0	074.3	.2279	01.91	000.0	26.00
CORR THEZ THEC THES ALFA V VTIP MU LAMB CZ CX CPM															
555	00	01	01.75	01.34	00.06	205.2	702.0	0.292	.0039	.0574	.0044	-.0037			
556	02	00	01.93	01.86	00.26	205.1	701.2	0.292	.0070	.1133	.0039	-.0005			
557	04	08	02.30	02.77	00.45	202.7	699.5	0.290	.0102	.1730	.0015	.0026			
558	05	04	02.60	03.70	00.68	204.5	702.0	0.291	.0141	.2409	.0005	.0026			
559	07	01	02.69	04.40	00.72	205.5	681.9	0.301	.0152	.2525	.0010	.0020			
560	02	17	00.91	00.24	-00.18	205.5	699.5	0.294	.0000	.0125	.0044	.0017			
561	00	23	01.16	01.03	-02.40	205.3	701.2	0.293	.0149	.0360	.0040	.0003			
562	02	02	01.32	01.55	-02.21	204.4	702.0	0.291	.0180	.0932	.0043	.0030			
563	04	01	01.64	02.34	-02.00	203.4	702.0	0.290	.0212	.1543	.0038	.0048			
564	06	05	01.95	03.32	-01.77	204.1	701.2	0.291	.0248	.2181	.0029	.0059			
565	00	00	01.01	00.80	-03.92	205.7	702.9	0.292	.0205	.0068	.0026	-.0004			
566	01	01	01.49	01.47	-03.74	205.5	701.2	0.292	.0235	.0599	.0027	.0009			
567	03	09	01.73	02.31	-03.51	204.3	699.5	0.291	.0269	.1247	.0025	.0026			
568	05	04	02.00	03.18	-03.29	202.3	699.5	0.289	.0305	.1935	.0025	.0043			
569	02	17	00.12	01.24	-04.17	205.0	700.4	0.292	.0164	.0661	.0016	.0062			
570	00	10	02.04	01.47	05.40	204.0	702.9	0.289	.0187	.1178	.0063	-.0003			
571	01	08	02.40	02.38	05.60	204.4	702.0	0.290	.0156	.1759	.0047	.0002			
572	04	06	02.90	03.15	05.81	202.9	699.5	0.289	.0118	.2406	.0016	.0011			
573	06	03	03.33	04.50	05.96	205.6	702.9	0.291	.0097	.2809	.0033	.0000			
574	07	06	03.81	05.34	06.02	204.5	698.7	0.291	.0087	.2998	.0010	.0028			
575	02	03	01.37	00.44	05.20	205.3	702.0	0.291	.0224	.0567	.0055	.0019			
576	00	01	02.21	01.80	07.91	204.7	700.4	0.289	.0294	.1475	.0098	-.0015			
577	02	00	02.77	02.63	08.11	205.3	697.9	0.291	.0264	.2042	.0071	-.0004			
578	03	04	03.20	03.65	08.28	206.8	699.5	0.293	.0236	.2551	.0025	.0006			
579	06	01	03.57	05.17	08.41	206.2	699.5	0.292	.0214	.2925	.0045	-.0014			
580	01	00	07.72	02.76	00.24	204.4	701.2	0.291	.0043	.0764	.0007	-.0018			
581	02	02	04.11	02.84	00.30	205.3	704.6	0.291	.0052	.0920	.0002	-.0191			
582	01	08	00.02	02.81	00.35	205.1	702.9	0.292	.0061	.1084	.0039	.0072			
583	02	40	03.63	03.08	00.30	205.0	702.0	0.292	.0052	.0919	.0063	.0020			
584	02	56	02.37	03.96	00.25	205.9	702.0	0.293	.0044	.0771	.0015	-.0239			
585	01	32	01.56	00.18	00.33	205.5	703.7	0.292	.0060	.1047	.0057	.0110			
586	01	09	01.64	00.11	00.42	204.3	703.7	0.290	.0073	.1297	.0062	.0124			
587	01	00	01.58	02.66	00.49	205.7	702.9	0.293	.0083	.1476	.0092	.0254			

FAIRCHILD
REPUBLIC DIVISION

HC144R1070

CRM	CL	CD	CT	CH	CQ	CLR	CDR	LOD	DL	CRB	CORR
-.0006	.0259	.0027	.0743	.0075	.0278	.0743	.0077	11.42	03.74	.0006	548
-.0005	.0300	.0035	.0966	.0111	.0392	.0966	.0113	10.71	04.35	.0005	549
-.0006	.0250	.0021	.0765	.0063	.0186	.0765	.0065	13.34	03.62	.0006	550

*Copy available to DDC does not
permit fully legible reproduction*

CRM	CL	CD	CT	CH	CQ	CLR	CDR	LOD	DL	CRB	CORR
-.0004	.0574	.0045	.0025	.0002	.0021	.0025	.0002	02.68	02.75	.0004	555
-.0011	.1133	.0044	.0048	.0002	.0022	.0048	.0002	05.23	05.43	.0011	556
-.0016	.1720	.0028	.0073	.0001	.0026	.0073	.0001	07.11	08.09	.0016	557
-.0019	.2409	.0033	.0102	.0000	.0035	.0102	.0001	07.56	11.47	.0019	558
-.0021	.2924	.0041	.0115	.0000	.0043	.0115	.0002	07.15	12.12	.0021	559
-.0004	.0125	.0045	.0005	.0002	.0025	.0005	.0002	00.51	00.60	.0005	560
-.0008	.0361	.0024	.0015	.0002	.0022	.0015	.0001	01.78	01.73	.0008	561
-.0012	.0933	.0007	.0040	.0002	.0025	.0040	.0000	04.51	04.43	.0012	562
-.0015	.1543	.0016	.0065	.0002	.0029	.0065	.0001	06.92	07.26	.0015	563
-.0020	.2181	.0038	.0092	.0001	.0039	.0092	.0002	07.80	10.34	.0020	564
-.0003	.0370	.0022	.0003	.0001	.0023	.0003	.0001	00.34	00.34	.0003	565
-.0008	.0599	.0012	.0026	.0001	.0026	.0026	.0001	03.12	02.88	.0008	566
-.0014	.1246	.0051	.0053	.0001	.0031	.0053	.0002	06.18	05.92	.0014	567
-.0019	.1933	.0066	.0081	.0001	.0041	.0081	.0004	07.58	09.00	.0019	568
-.0000	.0658	.0064	.0028	.0001	.0028	.0028	.0003	02.29	03.15	.0001	569
-.0015	.1167	.0173	.0050	.0003	.0011	.0049	.0007	04.47	05.52	.0015	570
-.0016	.1746	.0218	.0075	.0002	.0009	.0074	.0009	05.98	08.30	.0016	571
-.0022	.2392	.0259	.0101	.0001	.0011	.0101	.0011	06.79	11.21	.0022	572
-.0021	.2798	.0259	.0120	.0001	.0026	.0120	.0011	05.99	13.45	.0020	573
-.0020	.2982	.0305	.0128	.0000	.0034	.0128	.0013	05.17	14.20	.0019	574
-.0010	.0559	.0107	.0024	.0002	.0014	.0024	.0005	02.52	02.68	.0010	575
-.0017	.1448	.0300	.0063	.0004	.0003	.0062	.0013	04.51	06.90	.0017	576
-.0015	.2012	.0359	.0088	.0003	.0003	.0087	.0016	05.55	09.65	.0015	577
-.0014	.2528	.0343	.0111	.0001	.0006	.0110	.0015	06.55	12.30	.0014	578
-.0021	.2901	.0383	.0127	.0002	.0024	.0126	.0017	05.12	14.03	.0020	579
-.0192	.0764	.0004	.0032	.0000	.0031	.0032	.0000	03.12	03.63	.0192	580
-.0024	.0920	.0007	.0039	.0000	.0025	.0039	.0000	04.40	04.41	.0024	581
.0103	.1084	.0046	.0046	.0002	.0022	.0046	.0002	04.86	05.19	.0103	582
.0244	.0920	.0059	.0039	.0003	.0030	.0039	.0003	04.95	04.40	.0245	583
.0197	.0771	.0012	.0033	.0001	.0035	.0033	.0001	02.92	03.72	.0197	584
-.0004	.1047	.0063	.0045	.0002	.0015	.0045	.0003	05.64	05.03	.0003	585
-.0098	.1296	.0071	.0055	.0003	.0015	.0055	.0003	06.66	06.16	.0098	586
-.0212	.1476	.0105	.0063	.0004	.0008	.0063	.0005	08.74	07.11	.0212	587

HC144R1070

APPENDIX B. ROTOR TEST RESULTS (Continued)
RUNS 51, 52

RUN	L	TH	TST	P	DATE	TIME	H	R	PT	Q	TT	RHO	GAMA	PHI	DELS
51	1	12	614	1	0527	2119	0.286	1.874	2121.	115.0	078.8	.2204	01.85	000.0	26.00
CORR THEZ THEC THES ALFA V VTIP MU LAMB CZ CX CPM															
588	00.32	01.55	00.77	00.02	323.1	697.9	0.463	.0013	.0125	.0033	-.0007				
589	01.84	00.63	01.59	00.11	323.4	699.5	0.462	.0035	.0386	.0040	.0040				
590	04.00	02.29	03.75	00.15	323.3	698.7	0.463	.0045	.0496	.0027	-.0019				
591	06.03	02.75	05.25	00.21	324.0	699.5	0.463	.0062	.0680	.0020	-.0020				
592	02.01	01.71	00.62	00.04	323.4	702.0	0.461	.0005	.0068	.0034	-.0019				
593	04.02	01.29	01.85	00.10	323.1	700.4	0.461	.0021	.0250	.0028	-.0029				
594	00.08	01.58	01.94	05.03	323.4	699.5	0.461	.0352	.0457	.0046	.0016				
595	02.04	02.02	03.32	05.08	323.4	700.4	0.460	.0337	.0622	.0037	.0012				
596	03.96	00.78	04.43	05.13	323.5	700.4	0.460	.0325	.0756	.0001	.0071				
597	05.94	01.32	06.06	05.17	323.5	697.9	0.462	.0316	.0872	.0003	.0063				
598	02.05	02.13	01.07	04.95	323.9	703.7	0.459	.0369	.0242	.0039	-.0022				
599	04.06	01.55	00.77	04.90	324.0	700.4	0.461	.0385	.0085	.0043	-.0009				
600	00.04	01.85	02.66	07.58	323.4	702.9	0.456	.0539	.0587	.0055	.0013				
601	01.86	02.05	03.92	07.63	324.1	701.2	0.458	.0529	.0731	.0020	.0026				
602	04.00	01.89	05.37	07.66	324.7	702.9	0.458	.0518	.0863	.0004	.0040				
603	06.00	01.98	06.66	07.71	323.1	714.6	0.448	.0497	.0967	.0000	.0045				
604	02.02	02.01	01.37	07.50	324.4	702.9	0.458	.0557	.0400	.0064	-.0004				
605	03.57	01.74	00.02	07.43	324.1	701.2	0.458	.0573	.0230	.0062	-.0006				
606	00.01	01.91	03.20	10.08	323.6	707.9	0.450	.0717	.0725	.0058	.0016				
607	01.59	01.81	04.54	10.10	323.6	701.2	0.454	.0714	.0831	.0031	.0041				
608	03.93	02.32	06.06	10.17	323.8	703.7	0.453	.0701	.0968	.0012	.0033				
609	02.07	01.63	01.46	10.02	324.1	699.5	0.456	.0744	.0532	.0093	.0027				

RUN	L	TH	TST	P	DATE	TIME	H	R	PT	Q	TT	RHO	GAMA	PHI	DELS
52	1	12	614	1	0627	2203	0.282	1.952	2122.	115.1	083.9	.2164	01.83	000.0	26.00
CORR THEZ THEC THES ALFA V VTIP MU LAMB CZ CX CPM															
610	00.11	01.98	01.02	00.07	324.7	565.5	0.574	.0014	.0047	.0021	-.0003				
611	01.86	01.19	02.02	00.03	324.4	563.8	0.575	.0028	.0171	.0024	.0033				
612	03.99	02.12	04.15	00.01	324.4	560.5	0.579	.0036	.0246	.0022	.0015				
613	05.98	01.66	05.26	00.04	324.6	563.0	0.577	.0051	.0385	.0027	.0037				
614	01.98	01.23	00.95	00.09	323.6	563.0	0.575	.0005	.0023	.0022	.0019				
615	00.04	01.97	02.55	05.04	323.6	565.5	0.570	.0461	.0293	.0035	.0022				
616	02.07	02.15	04.05	05.06	324.2	562.1	0.574	.0454	.0383	.0028	.0027				
617	03.90	02.13	05.26	05.10	323.7	562.1	0.574	.0442	.0486	.0028	.0039				
618	05.94	03.17	07.05	05.13	324.2	563.8	0.573	.0432	.0571	.0020	.0019				
619	02.06	01.42	00.95	05.01	324.1	567.2	0.569	.0470	.0204	.0035	.0027				
620	04.04	01.02	00.93	04.97	324.0	564.6	0.572	.0479	.0126	.0036	.0038				
621	06.14	00.60	02.84	04.94	323.6	563.0	0.573	.0489	.0043	.0036	.0038				
622	07.03	00.11	00.33	04.99	323.8	562.1	0.574	.0480	.0148	.0079	.0137				
623	01.03	00.63	00.12	05.05	324.7	559.6	0.578	.0461	.0345	.0051	.0113				
624	01.01	01.27	00.21	05.03	324.7	611.6	0.529	.0420	.0359	.0021	.0138				
625	00.54	01.60	00.03	05.06	324.4	645.9	0.500	.0396	.0372	.0022	.0152				
626	00.41	01.35	00.13	05.08	324.0	674.4	0.479	.0375	.0426	.0037	.0157				
627	01.12	00.87	00.02	05.04	324.6	559.6	0.578	.0460	.0346	.0050	.0111				
628	00.05	02.25	03.36	07.66	324.5	563.8	0.570	.0708	.0410	.0030	.0030				
629	00.04	02.75	04.82	07.70	324.2	563.0	0.571	.0700	.0494	.0028	.0026				
630	09.95	03.25	06.23	07.72	324.3	563.0	0.571	.0691	.0580	.0023	.0019				
631	06.00	03.66	07.82	07.77	324.0	565.5	0.568	.0677	.0678	.0014	.0018				
632	01.98	03.95	05.29	07.68	323.5	565.5	0.567	.0702	.0435	.0025	-.0014				
633	02.13	02.23	01.92	07.43	324.0	570.5	0.563	.0712	.0295	.0045	.0018				
634	04.05	01.80	00.25	07.60	324.2	565.5	0.568	.0730	.0200	.0053	.0017				
635	05.92	01.81	01.21	07.53	324.1	563.0	0.571	.0742	.0114	.0047	.0007				
636	00.65	01.01	02.38	07.67	324.2	559.6	0.574	.0715	.0398	.0048	.0060				
637	00.12	04.70	05.03	09.90	324.9	565.5	0.566	.0931	.0395	.0023	-.0042				
638	03.87	05.70	07.85	09.93	324.5	564.6	0.566	.0910	.0562	.0005	-.0051				
639	03.85	02.37	01.22	09.87	324.3	566.3	0.564	.0938	.0309	.0061	.0013				
640	01.93	02.75	02.80	09.90	324.6	567.2	0.564	.0929	.0384	.0039	.0012				

FAIRCHILD
REPUBLIC DIVISION

HC144R1070

CPII	CL	CD	CT	CH	CO	CLR	CDR	LOD	DL	CRB	CORR
.0004	.0125	.0035	.0013	.0004	.0025	.0013	.0004	01.48	01.44	.0004	598
.0008	.0386	.0041	.0041	.0004	.0015	.0041	.0004	05.32	04.44	.0008	599
.0006	.0496	.0023	.0053	.0003	.0024	.0053	.0003	06.41	05.71	.0006	590
.0007	.0680	.0022	.0073	.0002	.0033	.0073	.0002	07.73	07.55	.0007	591
.0003	.0068	.0034	.0007	.0004	.0036	.0007	.0004	00.66	00.78	.0003	592
.0001	.0250	.0028	.0027	.0003	.0046	.0027	.0003	02.04	02.87	.0001	593
.0008	.0451	.0036	.0044	.0005	.0000	.0048	.0004	05.29	05.18	.0008	594
.0009	.0617	.0092	.0066	.0004	.0000	.0036	.0010	06.71	07.08	.0009	595
.0010	.0753	.0069	.0081	.0000	.0011	.0020	.0007	08.18	08.65	.0010	596
.0010	.0869	.0076	.0094	.0000	.0025	.0063	.0008	06.93	09.98	.0010	597
.0006	.0238	.0059	.0026	.0004	.0014	.0025	.0006	02.69	02.73	.0006	598
.0006	.0081	.0050	.0009	.0003	.0024	.0029	.0005	00.83	00.93	.0006	599
.0008	.0575	.0132	.0062	.0006	.0012	.0051	.0014	05.37	06.60	.0008	600
.0010	.0722	.0117	.0078	.0002	.0005	.0077	.0012	06.79	06.32	.0010	601
.0010	.0896	.0111	.0092	.0000	.0006	.0041	.0012	06.93	09.88	.0010	602
.0010	.0958	.0129	.0099	.0000	.0024	.0098	.0013	05.26	10.97	.0010	603
.0007	.0388	.0116	.0043	.0007	.0004	.0041	.0012	03.56	04.47	.0007	604
.0006	.0220	.0091	.0025	.0007	.0008	.0023	.0010	02.06	02.53	.0006	605
.0008	.0704	.0184	.0076	.0006	.0022	.0074	.0019	05.07	08.07	.0008	606
.0011	.0813	.0176	.0069	.0003	.0014	.0047	.0019	05.48	09.31	.0011	607
.0009	.0951	.0182	.0103	.0001	.0003	.0101	.0019	05.37	10.90	.0009	608
.0009	.0508	.0104	.0057	.0010	.0027	.0054	.0020	03.90	05.83	.0009	609

CRM	CL	CD	CT	CH	CO	CLR	CDR	LOD	DL	CRB	CORR
.0004	.0047	.0021	.0006	.0004	.0022	.0008	.0004	01.06	00.54	.0004	610
.0007	.0171	.0024	.0026	.0004	.0011	.0008	.0004	04.78	01.97	.0007	611
.0005	.0246	.0022	.0041	.0004	.0018	.0010	.0004	05.96	02.82	.0005	612
.0007	.0385	.0027	.0064	.0004	.0023	.0064	.0004	07.52	04.43	.0007	613
.0004	.0023	.0022	.0004	.0004	.0024	.0004	.0004	00.49	00.26	.0004	614
.0007	.0289	.0061	.0046	.0006	.0008	.0047	.0010	05.56	03.31	.0007	615
.0006	.0379	.0062	.0064	.0005	.0007	.0063	.0010	06.98	04.35	.0006	616
.0009	.0482	.0071	.0051	.0005	.0003	.0040	.0012	07.07	05.51	.0009	617
.0006	.0567	.0071	.0094	.0003	.0015	.0044	.0012	06.58	06.50	.0006	618
.0006	.0200	.0053	.0033	.0005	.0005	.0033	.0009	04.27	02.30	.0006	619
.0006	.0124	.0047	.0021	.0006	.0000	.0000	.0008	02.65	01.41	.0006	620
.0005	.0140	.0039	.0007	.0006	.0014	.0007	.0006	00.73	00.45	.0005	621
.0071	.0141	.0091	.0025	.0013	.0024	.0023	.0015	02.12	01.61	.0071	622
.0009	.0339	.0081	.0056	.0006	.0037	.0067	.0014	07.85	03.40	.0009	623
.0009	.0355	.0052	.0051	.0003	.0032	.0050	.0007	36.80	04.09	.0009	624
.0009	.0369	.0055	.0047	.0003	.0028	.0047	.0007	36.82	04.23	.0009	625
.0009	.0421	.0074	.0049	.0004	.0023	.0049	.0009	12.82	04.82	.0009	626
.0009	.0360	.0081	.0058	.0006	.0037	.0047	.0014	08.01	03.91	.0009	627
.0007	.0402	.0085	.0066	.0005	.0026	.0047	.0014	07.02	04.62	.0007	628
.0007	.0486	.0094	.0082	.0005	.0020	.0051	.0016	06.69	05.57	.0007	629
.0009	.0571	.0100	.0096	.0004	.0009	.005	.0017	06.32	06.55	.0009	630
.0006	.0670	.0105	.0111	.0002	.0009	.0110	.0017	05.82	07.67	.0006	631
.0006	.0427	.0083	.0071	.0004	.0010	.0070	.0014	05.93	04.68	.0006	632
.0008	.0286	.0084	.0046	.0007	.0021	.0046	.0014	04.71	03.27	.0008	633
.0006	.0192	.0079	.0033	.0009	.0013	.0031	.0013	02.94	02.20	.0006	634
.0006	.0106	.0067	.0019	.0006	.0004	.0018	.0010	01.62	01.22	.0006	635
.0007	.0388	.0100	.0067	.0008	.0036	.0045	.0017	06.32	04.45	.0007	636
.0006	.0386	.0091	.0065	.0004	.0016	.0044	.0015	05.22	04.44	.0006	637
.0006	.0553	.0102	.0093	.0001	.0002	.0001	.0017	05.58	06.34	.0006	638
.0006	.0294	.0113	.0051	.0010	.0030	.0048	.0018	03.64	03.37	.0006	639
.0006	.0371	.0104	.0063	.0006	.0034	.0041	.0017	05.45	04.27	.0006	640

Copy available to DDC does not
permit fully legible reproduction

HC144R1070

APPENDIX B. ROTOR TEST RESULTS (Continued)

RUNS 53, 54, 55

RUN	L	TN	TST	P	DATE	TIME	M	R	PT	Q	TT	RHO	GAMA	PHI	DELS
53	1	12	514	1	0628	1525	0.358	2.200	2120.	174.1	096.9	.2084	01.75	000.0	26.00
CORR THEZ THEC THES ALFA V VTIP MU LAMB CZ CX CPM															
647	00	77	04	16	00	35	00	00	408.7	284.8	1.435	.0032	.0089	.0010	-.0001
648	02	07	04	44	01	52	00	01	408.7	275.6	1.483	.0043	.0128	.0016	-.0001
649	03	94	03	79	03	91	00	02	408.4	278.1	1.468	.0054	.0186	.0025	.0013
650	00	85	04	21	02	51	-00	01	409.1	277.3	1.475	.0019	.0044	.0012	-.0002
651	03	29	03	92	05	64	00	04	409.3	267.2	1.531	.0064	.0195	.0037	.0014
652	00	69	06	64	02	97	04	96	408.9	267.2	1.525	-.1258	.0188	.0006	-.0001
659	00	29	05	85	02	87	05	08	402.7	273.1	1.469	-.1230	.0204	.0010	.0010
660	02	47	05	39	00	60	05	09	402.5	306.6	1.308	-.1088	.0282	.0017	.0015
661	02	47	05	23	00	43	05	10	402.5	266.4	1.505	-.1253	.0298	.0020	.0017
662	04	61	05	94	01	91	05	10	403.1	273.1	1.470	-.1219	.0292	.0030	.0015
663	06	09	06	38	03	85	05	10	403.0	278.1	1.443	-.1192	.0264	.0042	.0018
664	06	18	06	37	03	68	05	10	403.0	258.9	1.551	-.1282	.0264	.0043	.0017
665	00	28	07	79	04	95	07	40	404.2	262.2	1.529	-.1902	.0213	.0008	.0000
666	02	41	07	77	01	99	07	40	404.2	271.4	1.477	-.1825	.0251	.0017	.0006
667	04	14	08	29	00	19	07	42	404.5	277.3	1.447	-.1784	.0273	.0025	.0004
668	02	14	07	97	06	90	07	39	405.4	262.2	1.533	-.1915	.0194	.0009	-.0001

RUN	L	TN	TST	P	DATE	TIME	M	R	PT	Q	TT	RHO	GAMA	PHI	DELS
54	1	12	514	1	0628	2215	0.358	2.245	2120.	173.7	087.6	.2120	01.78	000.0	26.00
CORR THEZ THEC THES ALFA V VTIP MU LAMB CZ CX CPM															
669	01	30	02	66	00	32	-00	12	404.8	350.2	1.156	.0046	.0072	.0017	.0004
670	04	20	02	00	03	84	-00	11	405.0	360.2	1.124	.0052	.0106	.0021	.0014
671	06	25	01	93	06	04	-00	10	405.7	353.5	1.148	.0054	.0120	.0028	.0015
672	01	42	02	04	02	38	-00	02	405.9	355.2	1.143	.0024	.0072	.0013	.0013
673	00	09	03	81	03	43	04	93	405.6	355.2	1.138	-.0931	.0174	.0019	.0009
674	02	39	03	75	00	95	04	93	405.6	364.4	1.109	-.0907	.0178	.0016	.0008
675	04	51	03	24	01	31	04	93	405.8	351.9	1.149	-.0934	.0198	.0025	.0016
676	00	10	05	45	04	10	04	91	406.3	353.5	1.145	-.0950	.0120	.0013	-.0013
677	02	08	04	85	05	70	04	92	407.3	356.0	1.140	-.0941	.0139	.0012	-.0002
678	00	13	05	81	04	92	07	34	407.1	358.6	1.126	-.1394	.0200	.0010	-.0006
679	02	29	05	36	02	72	07	36	406.8	351.0	1.149	-.1423	.0214	.0016	.0001
680	02	33	05	68	02	79	07	34	406.9	351.0	1.150	-.1421	.0206	.0018	-.0002
681	04	22	05	03	00	78	07	36	407.3	363.6	1.111	-.1373	.0224	.0029	.0004
682	02	04	05	59	06	90	07	34	407.9	351.9	1.150	-.1420	.0211	.0012	.0001

RUN	L	TN	TST	P	DATE	TIME	M	R	PT	Q	TT	RHO	GAMA	PHI	DELS
55	1	12	514	1	0628	2238	0.358	2.209	2120.	173.7	094.5	.2093	01.76	000.0	26.00
CORR THEZ THEC THES ALFA V VTIP MU LAMB CZ CX CPM															
683	01	84	02	98	00	82	-00	09	407.3	433.1	0.940	.0023	.0034	.0017	.0001
684	04	10	01	89	03	10	-00	08	407.6	437.3	0.932	.0025	.0051	.0019	.0007
685	05	64	01	36	04	53	-00	08	407.5	452.4	0.901	.0026	.0056	.0018	.0007
686	00	04	02	24	01	14	-00	09	408.5	432.3	0.945	.0025	.0041	.0015	.0003
692	01	07	04	01	05	41	05	00	418.4	431.4	0.966	-.0808	.0152	.0014	.0001
693	00	05	03	70	04	28	05	01	418.6	429.8	0.970	-.0812	.0157	.0019	.0002
694	02	43	03	21	01	94	05	00	418.8	442.3	0.943	-.0787	.0162	.0014	.0007
695	04	17	02	70	00	18	05	01	419.0	452.4	0.923	-.0771	.0166	.0020	.0011
696	05	80	02	16	01	99	05	02	419.3	453.2	0.922	-.0765	.0190	.0031	.0021
697	07	43	01	84	03	69	05	01	419.7	459.9	0.909	-.0755	.0187	.0042	.0022
698	00	14	05	23	06	52	09	96	409.8	434.0	0.930	-.1567	.0280	.0005	-.0003
699	01	93	05	52	08	10	09	98	409.4	429.8	0.938	-.1584	.0277	.0002	-.0006
700	02	16	04	56	04	39	09	97	409.3	442.3	0.912	-.1541	.0269	.0012	.0001
701	04	14	04	61	02	59	09	97	410.9	424.7	0.953	-.1610	.0268	.0024	-.0005
702	01	06	00	82	01	59	05	00	410.5	426.1	0.955	-.0771	.0271	.0012	.0073

FAIRCHILD
REPUBLIC DIVISION

HC144R1070

CRM	CL	CD	CT	CH	CO	CLR	CDR	LOD	DL	CRB	CORR
-.0004	.0089	.0010	.0092	.0011	.0015	.0092	.0011	07.85	01.59-	.0004	647
-.0005	.0128	.0017	.0140	.0018	.0008	.0140	.0018	07.95	02.22-	.0005	648
-.0008	.0166	.0020	.0179	.0021	.0057	.0179	.0021	10.32	02.88-	.0008	649
-.0004	.0044	.0012	.0048	.0013	.0022	.0048	.0013	03.25	00.76-	.0004	650
-.0004	.0195	.0028	.0228	.0044	.0146	.0228	.0044	06.62	03.39-	.0004	651
-.0005	.0167	.0021	.0197	.0007	.0030	.0196	.0024	08.76	02.90-	.0005	652
-.0005	.0203	.0028	.0222	.0011	.0076	.0220	.0030	08.75	03.54-	.0005	659
-.0005	.0230	.0038	.0205	.0015	.0122	.0198	.0032	08.53	04.00-	.0005	660
-.0005	.0236	.0041	.0272	.0023	.0190	.0269	.0047	07.78	04.10-	.0005	661
-.0005	.0249	.0052	.0275	.0033	.0243	.0271	.0057	06.71	04.33-	.0005	662
-.0006	.0259	.0065	.0277	.0044	.0316	.0272	.0068	05.84	04.50-	.0006	663
-.0005	.0260	.0066	.0320	.0052	.0358	.0315	.0080	05.48	04.51-	.0005	664
-.0005	.0211	.0036	.0254	.0010	.0097	.0250	.0042	06.94	03.67-	.0005	665
-.0006	.0247	.0050	.0279	.0019	.0184	.0274	.0055	06.49	04.30-	.0006	666
-.0006	.0267	.0060	.0290	.0027	.0247	.0284	.0064	06.00	04.65-	.0006	667
-.0006	.0191	.0030	.0231	.0006	.0035	.0229	.0036	06.78	03.34-	.0006	668

CRM	CL	CD	CT	CH	CO	CLR	CDR	LOD	DL	CRB	CORR
-.0005	.0072	.0017	.0048	.0011	.0015	.0048	.0011	03.83	01.26-	.0005	669
-.0005	.0106	.0021	.0067	.0013	.0003	.0067	.0013	04.94	01.83-	.0005	670
-.0005	.0120	.0028	.0079	.0018	.0010	.0079	.0018	04.57	02.10-	.0005	671
-.0004	.0072	.0013	.0047	.0009	.0005	.0047	.0009	03.26	01.26-	.0004	672
-.0005	.0172	.0028	.0113	.0008	.0028	.0112	.0018	07.13	02.99-	.0005	673
-.0005	.0176	.0033	.0110	.0011	.0042	.0109	.0021	06.44	03.05-	.0005	674
-.0005	.0195	.0042	.0132	.0017	.0085	.0130	.0028	06.26	03.39-	.0005	675
-.0004	.0118	.0023	.0079	.0008	.0010	.0078	.0015	04.90	02.06-	.0004	676
-.0005	.0138	.0024	.0091	.0008	.0003	.0090	.0016	05.90	02.40-	.0005	677
-.0005	.0197	.0035	.0129	.0006	.0031	.0127	.0023	06.34	03.44-	.0005	678
-.0005	.0210	.0043	.0144	.0011	.0072	.0141	.0029	06.17	03.66-	.0005	679
-.0005	.0202	.0044	.0138	.0012	.0063	.0136	.0030	05.62	03.51-	.0005	680
-.0005	.0219	.0057	.0141	.0018	.0095	.0137	.0036	05.01	03.81-	.0005	681
-.0005	.0208	.0038	.0142	.0008	.0032	.0140	.0026	06.04	03.63-	.0005	682

CRM	CL	CD	CT	CH	CO	CLR	CDR	LOD	DL	CRB	CORR
-.0004	.0034	.0017	.0015	.0008	.0023	.0015	.0008	01.50	00.59-	.0004	683
-.0005	.0051	.0019	.0022	.0008	.0024	.0022	.0008	02.02	00.89-	.0005	684
-.0004	.0056	.0018	.0023	.0007	.0026	.0023	.0007	02.20	00.98-	.0004	685
-.0004	.0041	.0014	.0019	.0006	.0019	.0019	.0006	02.20	00.72-	.0004	686
-.0005	.0151	.0028	.0072	.0007	.0008	.0071	.0013	03.83	02.76-	.0005	692
-.0005	.0156	.0027	.0075	.0006	.0013	.0074	.0013	06.43	02.84-	.0005	693
-.0005	.0160	.0028	.0072	.0006	.0023	.0072	.0012	07.16	02.92-	.0005	694
-.0005	.0163	.0034	.0071	.0009	.0030	.0070	.0015	06.14	02.98-	.0005	695
-.0009	.0187	.0048	.0081	.0013	.0052	.0080	.0020	05.40	03.41-	.0009	696
-.0005	.0182	.0058	.0078	.0017	.0062	.0076	.0024	04.36	03.33-	.0005	697
-.0005	.0275	.0055	.0125	.0002	.0047	.0123	.0024	06.53	04.78-	.0005	698
-.0006	.0273	.0050	.0126	.0001	.0027	.0124	.0023	06.24	04.74-	.0006	699
-.0006	.0263	.0058	.0115	.0005	.0064	.0113	.0025	06.23	04.58-	.0006	700
-.0005	.0260	.0070	.0125	.0011	.0079	.0121	.0033	04.98	04.53-	.0005	701
-.0006	.0269	.0036	.0124	.0006	.0073	.0123	.0014	14.03	04.68-	.0006	702

FAIRCHILD
REPUBLIC DIVISION

HC144R1070

APPENDIX B. ROTOR TEST RESULTS (Continued)
RUNS 56, 57

RUN L TN TST P DATE TIME M R PT G TT RHO GAMA PHI DEL3
56 1 12 614 1 0629 1540 0.359 2.181 2115. 174.2 100.3 .2065 01.73 000.0 26.00

CORR	THEZ	THEC	THES	ALFA	V	VTIP	MU	LAMB	CZ	CX	CPM
703	02.00	02.02	00.57	-00.05	410.7	499.3	0.823	.0008	.0004	.0024	.0018
704	00.03	01.20	01.03	-00.02	410.5	498.5	0.824	.0019	.0080	.0017	.0021
705	01.94	01.53	02.93	-00.02	410.5	493.4	0.832	.0021	.0089	.0021	.0017
706	01.41	03.60	00.32	00.02	410.7	496.8	0.827	.0036	.0186	.0006	.0122
707	03.78	01.43	04.57	-00.01	410.8	490.9	0.837	.0025	.0114	.0024	.0022
708	04.20	00.71	03.29	-00.02	410.9	495.1	0.830	.0014	.0055	.0021	.0023
709	00.25	02.43	02.97	04.93	410.8	491.8	0.832	.0081	.0181	.0023	.0015
710	01.89	03.09	05.05	04.93	410.9	491.8	0.832	.0078	.0191	.0022	.0008
711	04.06	03.57	07.08	04.94	411.2	495.1	0.827	.0072	.0203	.0020	.0005
712	05.89	04.11	06.70	04.95	410.8	500.1	0.818	.0063	.0218	.0024	.0001
713	02.23	02.57	01.46	04.92	411.0	493.4	0.830	.0084	.0149	.0023	.0008
714	04.05	01.70	00.80	04.93	410.6	494.3	0.828	.0080	.0160	.0029	.0023
715	00.14	04.31	05.81	09.99	411.3	494.3	0.819	.1377	.0319	.0016	.0001
716	02.02	04.61	07.34	10.00	411.0	501.0	0.809	.1357	.0336	.0013	.0000
717	03.90	04.61	08.82	10.01	411.0	490.9	0.824	.1376	.0374	.0010	.0006
718	02.10	03.34	03.62	09.99	411.1	492.6	0.822	.1382	.0312	.0025	.0019
719	04.04	03.78	02.22	09.97	411.3	492.6	0.822	.1390	.0267	.0036	.0001

RUN L TN TST P DATE TIME M R PT G TT RHO GAMA PHI DEL3
57 1 12 614 1 0629 1558 0.359 2.173 2115. 174.3 102.0 .2059 01.73 000.0 26.00

CORR	THEZ	THEC	THES	ALFA	V	VTIP	MU	LAMB	CZ	CX	CPM
720	00.06	01.14	00.73	-00.02	411.4	566.3	0.726	.0016	.0076	.0026	.0016
721	01.78	01.62	02.40	-00.01	412.7	565.5	0.730	.0021	.0108	.0025	.0010
722	03.92	01.98	04.34	-00.00	413.5	567.2	0.729	.0027	.0146	.0027	.0006
723	03.86	01.47	05.70	00.02	411.8	563.0	0.730	.0034	.0204	.0031	.0023
724	08.03	02.46	07.86	00.02	411.7	568.0	0.725	.0039	.0231	.0031	.0009
725	02.10	00.46	01.71	-00.02	411.1	565.5	0.727	.0014	.0066	.0027	.0020
726	00.18	03.28	03.42	04.99	411.1	564.6	0.725	.0002	.0175	.0025	.0012
727	00.04	02.05	02.73	05.00	411.2	569.7	0.719	.0588	.0231	.0028	.0010
728	01.82	01.93	04.14	05.03	412.5	566.3	0.726	.0587	.0281	.0029	.0025
729	03.86	03.57	06.36	05.02	411.8	570.5	0.719	.0584	.0268	.0024	.0003
730	05.98	03.96	08.32	05.03	411.5	568.8	0.721	.0581	.0293	.0022	.0007
731	02.11	02.20	01.27	04.99	411.5	566.3	0.724	.0602	.0162	.0017	.0011
732	00.06	03.54	05.00	09.99	410.5	563.8	0.717	.1195	.0369	.0023	.0007
733	01.88	03.81	06.48	09.99	412.7	564.6	0.720	.1193	.0408	.0014	.0005
734	04.02	04.43	08.22	10.00	412.0	565.5	0.717	.1186	.0437	.0006	.0004
735	02.25	03.34	03.29	09.95	412.4	560.5	0.725	.1216	.0303	.0030	.0002
736	04.10	03.47	01.74	09.95	412.6	563.0	0.722	.1218	.0266	.0047	.0005

FAIRCHILD
REPUBLIC DIVISION

HC144R1070

CRM	CL	CD	CT	CH	CO	CLR	CDR	LOD	DL	CRB	CORR
.0004	.0004	.0024	.0001	.0008	.0024	.0001	.0008	00.12	00.07-	.0004	703
.0006	.0080	.0017	.0027	.0006	.0013	.0027	.0006	03.76	01.40-	.0006	704
.0005	.0089	.0021	.0091	.0007	.0014	.0031	.0007	03.43	01.55-	.0005	705
.0007	.0186	.0006	.0064	.0002	.0022	.0064	.0002	13.27	03.24-	.0007	706
.0005	.0114	.0024	.0040	.0008	.0014	.0040	.0008	03.93	01.99-	.0005	707
.0005	.0055	.0021	.0019	.0007	.0020	.0019	.0007	01.99	00.96-	.0005	708
.0007	.0178	.0038	.0063	.0008	.0017	.0062	.0019	05.53	03.11-	.0007	709
.0005	.0188	.0038	.0067	.0008	.0006	.0066	.0013	05.15	03.27-	.0005	710
.0008	.0202	.0038	.0071	.0007	.0001	.0070	.0013	05.33	03.53-	.0008	711
.0005	.0215	.0042	.0073	.0008	.0014	.0072	.0014	04.54	03.74-	.0005	712
.0005	.0147	.0035	.0052	.0008	.0009	.0051	.0012	04.55	02.56-	.0005	713
.0005	.0157	.0043	.0055	.0010	.0021	.0054	.0015	04.41	02.73-	.0005	714
.0006	.0311	.0071	.0110	.0006	.0042	.0108	.0025	05.48	03.43-	.0006	715
.0006	.0329	.0071	.0113	.0004	.0029	.0111	.0024	05.43	03.73-	.0006	716
.0006	.0367	.0075	.0131	.0003	.0016	.0129	.0026	05.28	06.38-	.0006	717
.0006	.0303	.0079	.0109	.0009	.0047	.0106	.0027	05.45	03.28-	.0006	718
.0005	.0256	.0081	.0093	.0012	.0037	.0089	.0028	04.15	04.47-	.0005	719

CRM	CL	CD	CT	CH	CO	CLR	CDR	LOD	DL	CRB	CORR
.0004	.0076	.0026	.0020	.0007	.0019	.0020	.0007	02.09	01.32-	.0004	720
.0005	.0108	.0023	.0029	.0007	.0019	.0029	.0007	03.11	01.90-	.0005	721
.0005	.0146	.0027	.0039	.0007	.0022	.0039	.0007	03.78	02.56-	.0005	722
.0005	.0204	.0031	.0054	.0008	.0024	.0054	.0008	04.72	03.56-	.0005	723
.0005	.0231	.0031	.0061	.0008	.0041	.0061	.0008	04.39	04.04-	.0005	724
.0005	.0066	.0027	.0018	.0007	.0017	.0018	.0007	01.82	01.15-	.0005	725
.0004	.0172	.0040	.0046	.0007	.0004	.0046	.0011	04.08	02.99-	.0004	726
.0006	.0228	.0048	.0060	.0007	.0013	.0059	.0013	05.50	03.96-	.0006	727
.0006	.0278	.0054	.0075	.0008	.0013	.0074	.0014	05.94	04.86-	.0006	728
.0006	.0263	.0047	.0070	.0006	.0005	.0069	.0012	05.33	04.62-	.0006	729
.0005	.0290	.0048	.0077	.0006	.0022	.0076	.0012	04.88	05.04-	.0005	730
.0005	.0160	.0031	.0043	.0005	.0002	.0042	.0008	05.31	02.79-	.0005	731
.0006	.0360	.0086	.0098	.0006	.0037	.0095	.0023	05.34	06.23-	.0006	732
.0006	.0399	.0085	.0109	.0004	.0025	.0107	.0023	05.55	06.99-	.0006	733
.0007	.0429	.0082	.0116	.0002	.0007	.0114	.0022	05.48	07.48-	.0007	734
.0007	.0293	.0082	.0082	.0008	.0042	.0079	.0022	04.85	05.11-	.0007	735
.0005	.0254	.0082	.0071	.0013	.0035	.0068	.0025	03.42	04.63-	.0005	736

FAIRCHILD
REPUBLIC DIVISION

HC144R1070

CRM	CL	CD	CT	CH	CO	CLR	CDR	LCD	DL	CRB	CORR
-.0003	.0051	.0049	.0026	.0025	.0032	.0026	.0025	00.91	01.23-	.0003	752
-.0003	.0037	.0044	.0019	.0022	.0034	.0019	.0022	00.72	00.90-	.0003	753
-.0003	.0030	.0043	.0015	.0022	.0030	.0015	.0022	00.60	00.74-	.0003	754
-.0003	.0063	.0054	.0032	.0027	.0031	.0032	.0027	01.05	01.54-	.0003	755
-.0004	.0086	.0066	.0044	.0033	.0023	.0044	.0033	01.23	02.13-	.0004	756
-.0004	.0106	.0078	.0053	.0040	.0016	.0053	.0040	01.30	02.57-	.0004	757
-.0004	.0133	.0065	.0071	.0027	.0016	.0068	.0034	01.94	03.23-	.0004	758
-.0004	.0119	.0058	.0064	.0025	.0025	.0061	.0030	01.89	02.89-	.0004	759
-.0002	.0092	.0050	.0049	.0022	.0034	.0047	.0026	01.62	02.25-	.0002	760
-.0004	.0158	.0081	.0085	.0034-	.0004	.0081	.0042	01.98	03.83-	.0004	761
-.0004	.0170	.0100	.0090	.0043-	.0026	.0086	.0031	01.80	04.11-	.0004	762
-.0005	.0180	.0129	.0097	.0057-	.0067	.0092	.0065	01.56	04.37-	.0005	763
-.0004	.0163	.0088	.0100	.0033-	.0006	.0095	.0045	02.13	04.49-	.0004	764
-.0004	.0179	.0080	.0097	.0029	.0009	.0093	.0042	02.18	04.36-	.0004	765
-.0004	.0172	.0075	.0092	.0027	.0026	.0088	.0038	02.13	04.18-	.0004	766
-.0004	.0190	.0100	.0103	.0038-	.0024	.0097	.0051	02.00	04.60-	.0004	767
-.0006	.0196	.0121	.0108	.0049-	.0059	.0101	.0062	01.78	04.77-	.0006	768
-.0004	.0196	.0146	.0109	.0061-	.0077	.0100	.0075	01.50	04.76-	.0004	769
-.0004	.0268	.0123	.0148	.0039-	.0060	.0139	.0064	02.40	06.52-	.0004	770
-.0004	.0270	.0114	.0148	.0034-	.0037	.0140	.0059	02.53	06.58-	.0004	771
-.0005	.0265	.0106	.0144	.0030-	.0026	.0137	.0055	02.62	06.45-	.0005	772
-.0003	.0252	.0139	.0139	.0047-	.0086	.0129	.0071	02.06	06.12-	.0003	773
-.0003	.0228	.0149	.0128	.0055-	.0113	.0117	.0076	01.79	05.53-	.0003	774
-.0004	.0289	.0143	.0160	.0041-	.0073	.0148	.0073	02.25	07.01-	.0004	775
-.0004	.0294	.0126	.0162	.0032-	.0040	.0152	.0065	02.49	07.15-	.0004	776
-.0004	.0301	.0118	.0164	.0027-	.0052	.0155	.0061	02.79	07.29-	.0004	777
-.0003	.0279	.0154	.0156	.0047-	.0103	.0143	.0079	02.09	06.73-	.0003	778
-.0003	.0295	.0112	.0159	.0019-	.0128	.0150	.0057	03.38	07.08-	.0003	779

CRM	CL	CD	CT	CH	CO	CLR	CDR	LCD	DL	CRB	CORR
-.0004			.0101		.0004					-.0004	794
-.0003			.0022		.0034					-.0003	795
-.0003			.0045		.0034					-.0003	796
-.0004			.0125		-.0009					-.0004	797
-.0004			.0158		-.0062					-.0004	798
-.0003			.0159		-.0168					-.0003	799
-.0004			.0108		.0007					-.0004	800
-.0004			.0183		-.0064					-.0004	801
-.0005			.0163		-.0033					-.0005	802
-.0004			.0111		.0009					-.0004	803
-.0004			.0172		-.0076					-.0004	804
-.0004			.0185		-.0163					-.0004	805
-.0003			.0197		-.0233					-.0003	806
-.0003			.0107		-.0082					-.0003	807
-.0004			.0196		-.0071					-.0004	808
-.0004			.0158		-.0020					-.0004	809
-.0004			.0217		-.0148					-.0004	810
-.0004			.0221		-.0207					-.0004	811
-.0003			.0223		-.0316					-.0003	812
-.0004			.0241		-.0136					-.0004	813
-.0004			.0252		-.0084					-.0004	814
-.0003			.0247		-.0044					-.0003	815
-.0004			.0247		-.0175					-.0004	816
-.0004			.0251		-.0236					-.0004	817
-.0004			.0253		-.0328					-.0004	818
-.0004			.0299		-.0143					-.0004	819
-.0004			.0205		-.0106					-.0004	820
-.0003			.0292		-.0231					-.0003	821
-.0006			.0286		-.0313					-.0006	822

HC144R1070

This page intentionally left blank.

HC144R1070

APPENDIX C AIRFOIL TESTS

C1 Models

To provide a basis for the prediction of rotor performance, three 18-inch chord airfoil models were constructed to the ordinates of the root (18% thick), mid-span (12% thick) and tip (6% thick) rotor blade airfoil sections. The 12% and 18% models were constructed in aluminum and the 6% model in steel. The models were fitted with orifices for pressure measurements at the stations shown in Table C-1.

C2 Wind Tunnel and Test Procedure

Pressure plotting tests were conducted in the 3 ft by 7-1/2 ft Low Turbulence Pressure Tunnel at NASA Langley Research Center during August 1972. Each model was tested with flow in both the forward and the reverse direction over the range of angles of attack from -10° to $+24^{\circ}$, with the model rotating about 50% chord. Pressures were measured at the orifices detailed in Table C-1 and on a 96 port rake 33 inches downstream of the trailing edge of the model.

C3 Test Conditions

The tests were intended to cover both the low Reynolds numbers appropriate to the model rotor tests and the high Reynolds numbers experienced on the blades of a full scale helicopter. The conditions tested are shown in Table C-2. Most tests were made with the models smooth, but some tests at the lower Reynolds numbers were made with grit added to the surface in the leading edge area to induce transition. Number 80 grit was used in a band one-tenth inch wide at 5% chord (.9 in. aft of the leading edge).

C4 Results

Lift coefficient, drag coefficient and moment coefficient were obtained from the measured pressures by NASA Langley using the conventional computational methods, and are plotted in figures C1 through C28. Table C-2 provides a key to these figures.

**REPRODUCED FROM
BEST AVAILABLE COPY**

HC144R1070

TABLE C-1. LOCATION OF ORIFICES IN 18-INCH
CHORD AIRFOIL SECTIONS
(UPPER AND LOWER SURFACES)

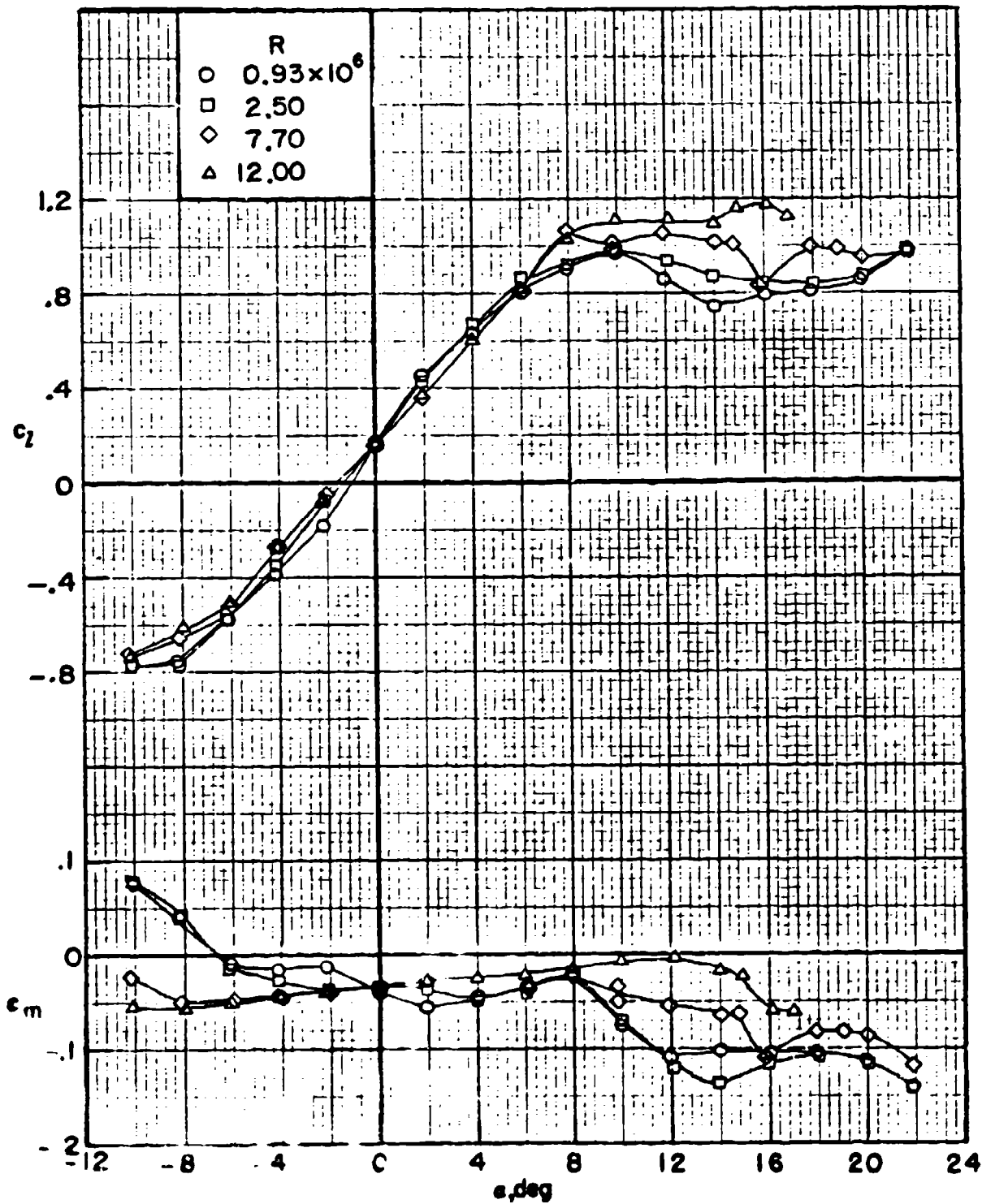
Percentage Chord	Inches from Leading Edge
0	0
.3	.054
.6	.108
1.2	.162
1.6	.282
2.0	.360
2.5	.450
3.75	.675
5.0	.900
7.5	1.350
10.0	1.800
15.0	2.700
20.0	3.600
25.0	4.500
30.0	5.400
40.0	7.200
50.0	9.000
60.0	10.800
70.0	12.600
75.0	13.500
80.0	14.400
85.0	15.300
90.0	16.200
92.5	16.650
95.0	17.100
96.25	17.325
97.5	17.550
98.0	17.640
98.5	17.730
99.0	17.820
99.5	17.910
100.0	18.000
1/3 Span	5.400
	12.600
2/3 Span	5.400
	12.600

HC144R1070

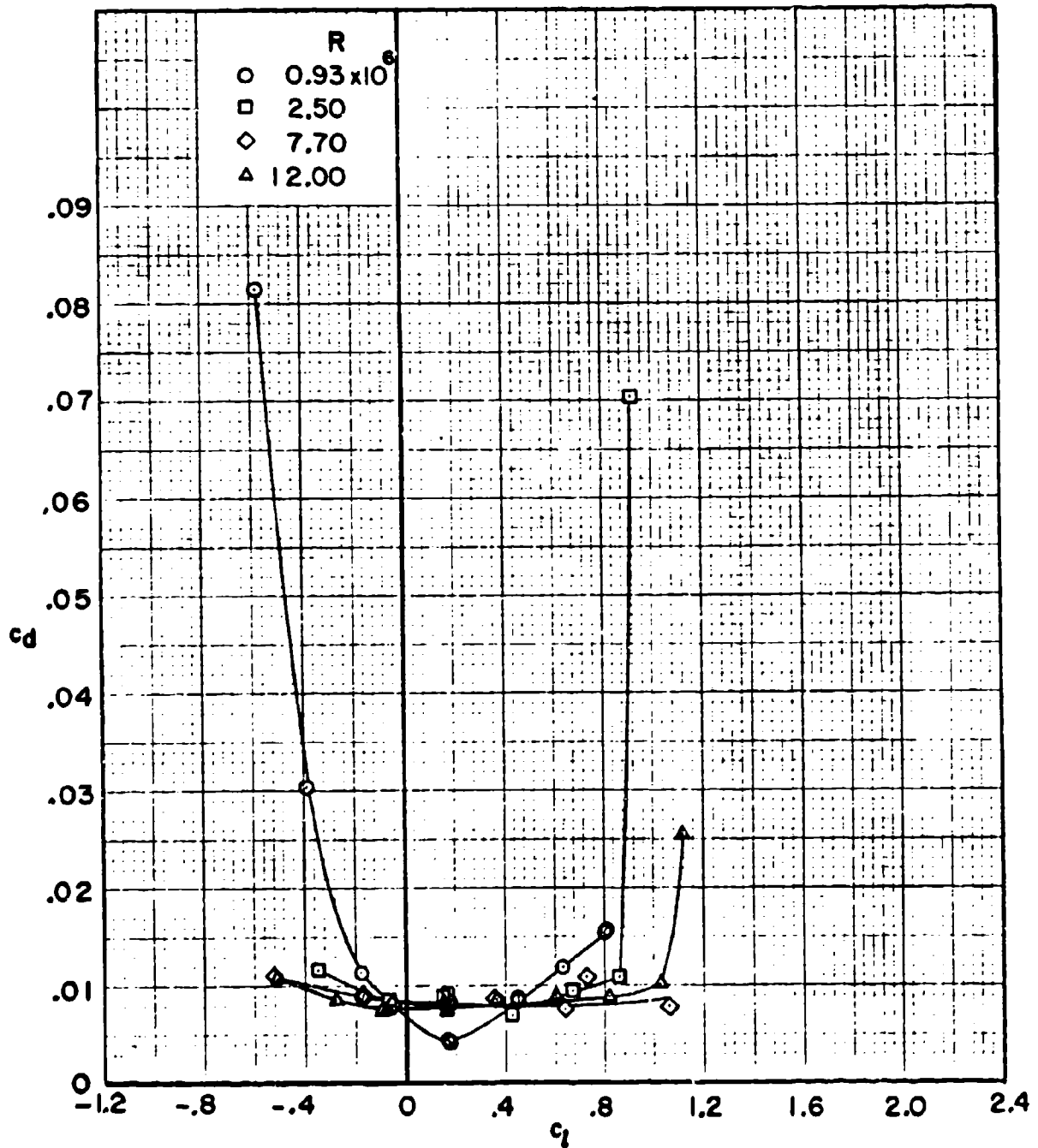
TABLE C-2. SCHEDULE OF AIRFOIL SECTION PRESSURE PLOTTING TESTS MADE IN LANGLEY LTPT

Reynolds Number (million)	M	Grit	Figure Number					
			6%		12%		18%	
			Forward	Reverse	Forward	Reverse	Forward	Reverse
.93-.95	.26	off	1	5	10	15	20	24
2.5-2.6	.26	off	1	5	10	15	20	24
7.6-7.7	.26	off	1	5	10	15	20	24
11.65-12.0	.26	off	1	-	10	-	20	-
.93-.96	.26	on	2	6	11	16	21	25
2.5-2.6	.26	on	3	7	12	17	22	26
7.6-7.7	.26	on	-	8	-	18	-	27
11.65	.26	on	-	-	13	-	-	-
2.26-2.6	.16	off	4	9	14	19	23	28
2.26=2.6	.35	off	4	9	14	19	23	28

TWO-DIMENSIONAL SECTION CHARACTERISTICS OF A 6-PERCENT RVR AIRFOIL WITH LEADING EDGE FORWARD. $M = 0.26$; MODEL SMOOTH

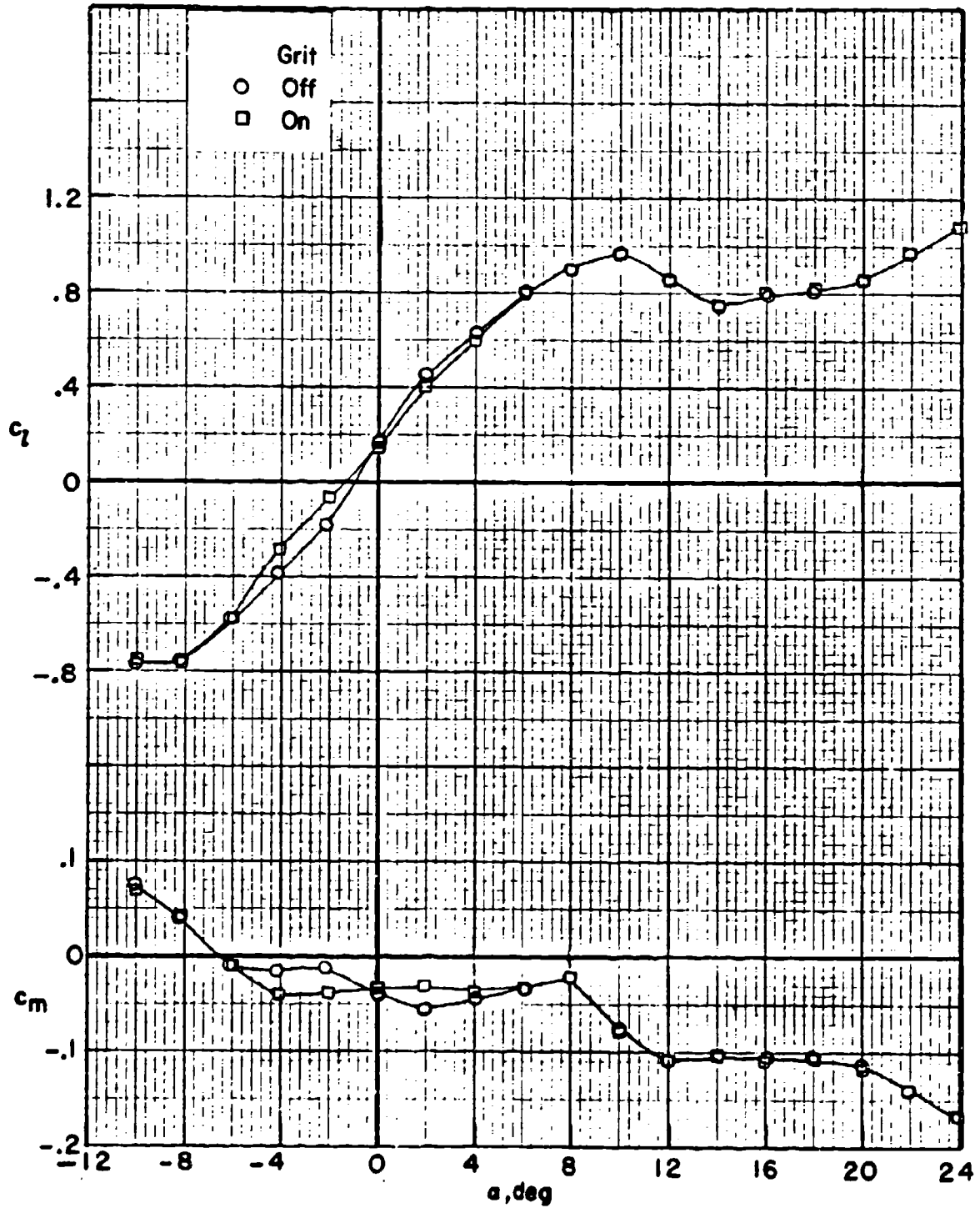


TWO-DIMENSIONAL SECTION CHARACTERISTICS OF A 6-PERCENT RVR AIRFOIL WITH LEADING EDGE FORWARD. $M = 0.26$; MODEL SMOOTH



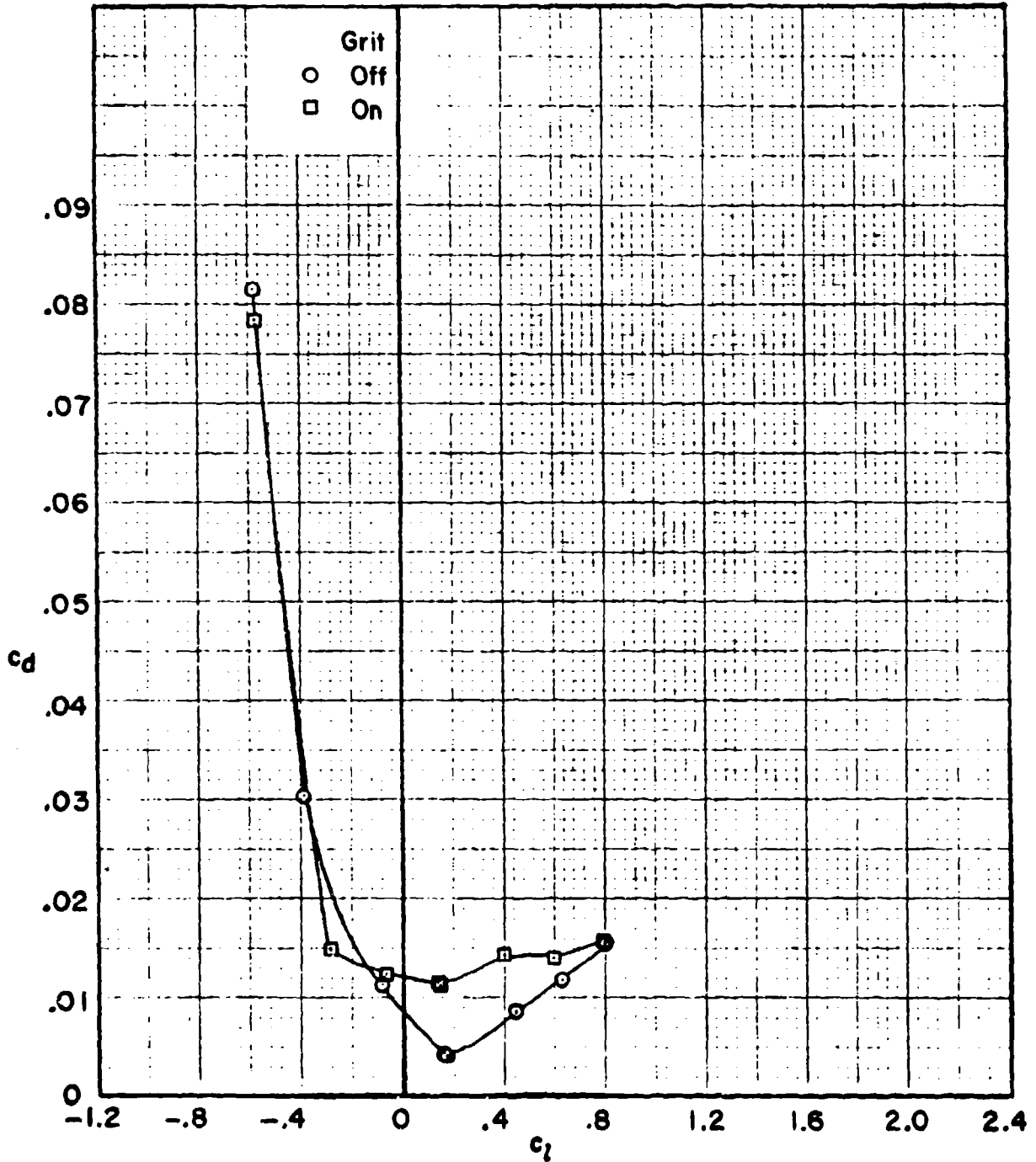
HC144R1070

**TWO-DIMENSIONAL SECTION CHARACTERISTICS OF A 6-PERCENT RVR
AIRFOIL WITH LEADING EDGE FORWARD. $M=0.26$; $R=0.93 \times 10^6$**



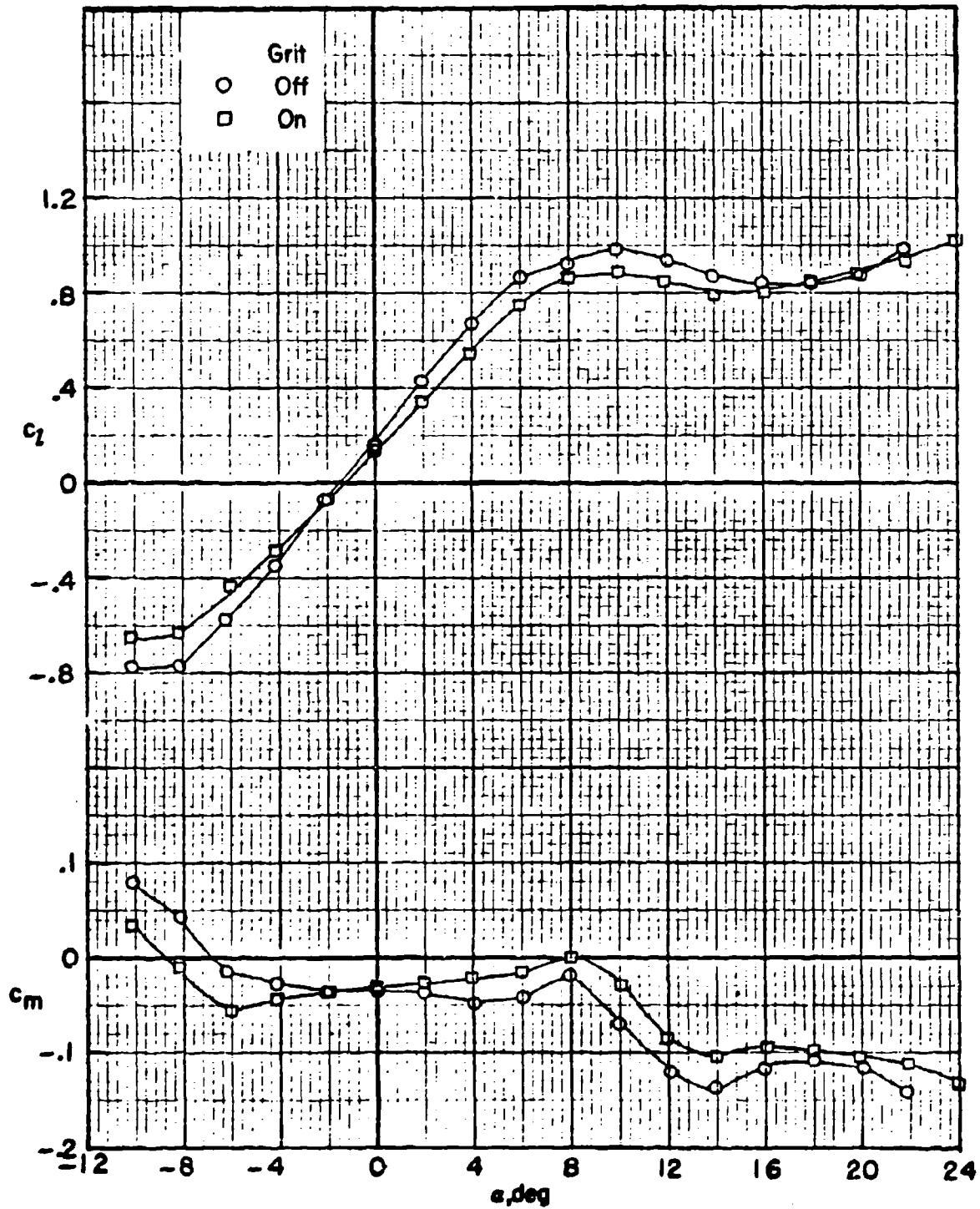
HC144R1070

TWO-DIMENSIONAL SECTION CHARACTERISTICS OF A 6-PERCENT RVR
AIRFOIL WITH LEADING EDGE FORWARD. $M = 0.26$; $R = 0.93 \times 10^6$



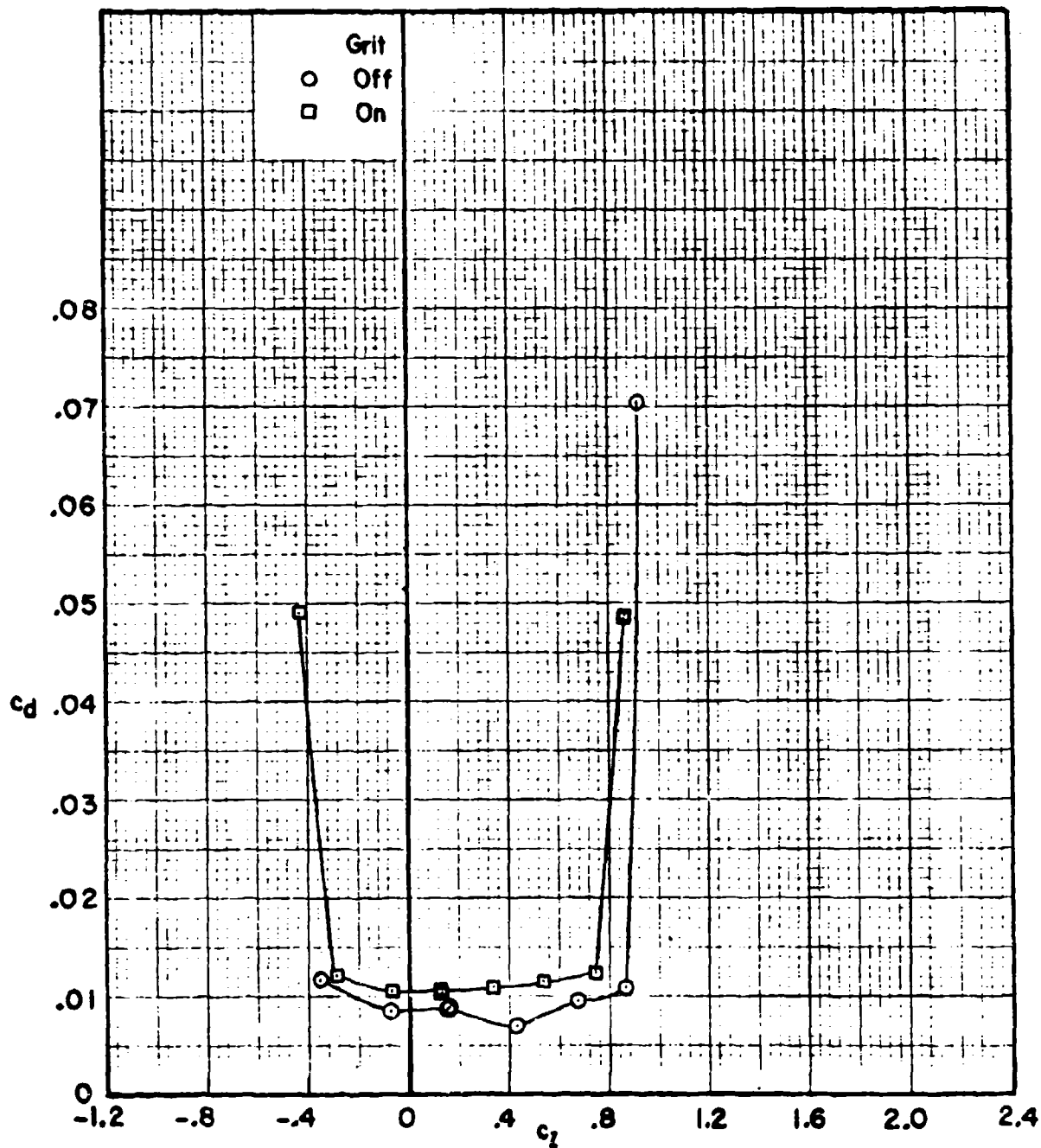
HC144R1070

TWO-DIMENSIONAL SECTION CHARACTERISTICS OF A 6-PERCENT RVR
AIRFOIL WITH LEADING EDGE FORWARD. $M=0.26$; $R=2.60 \times 10^6$



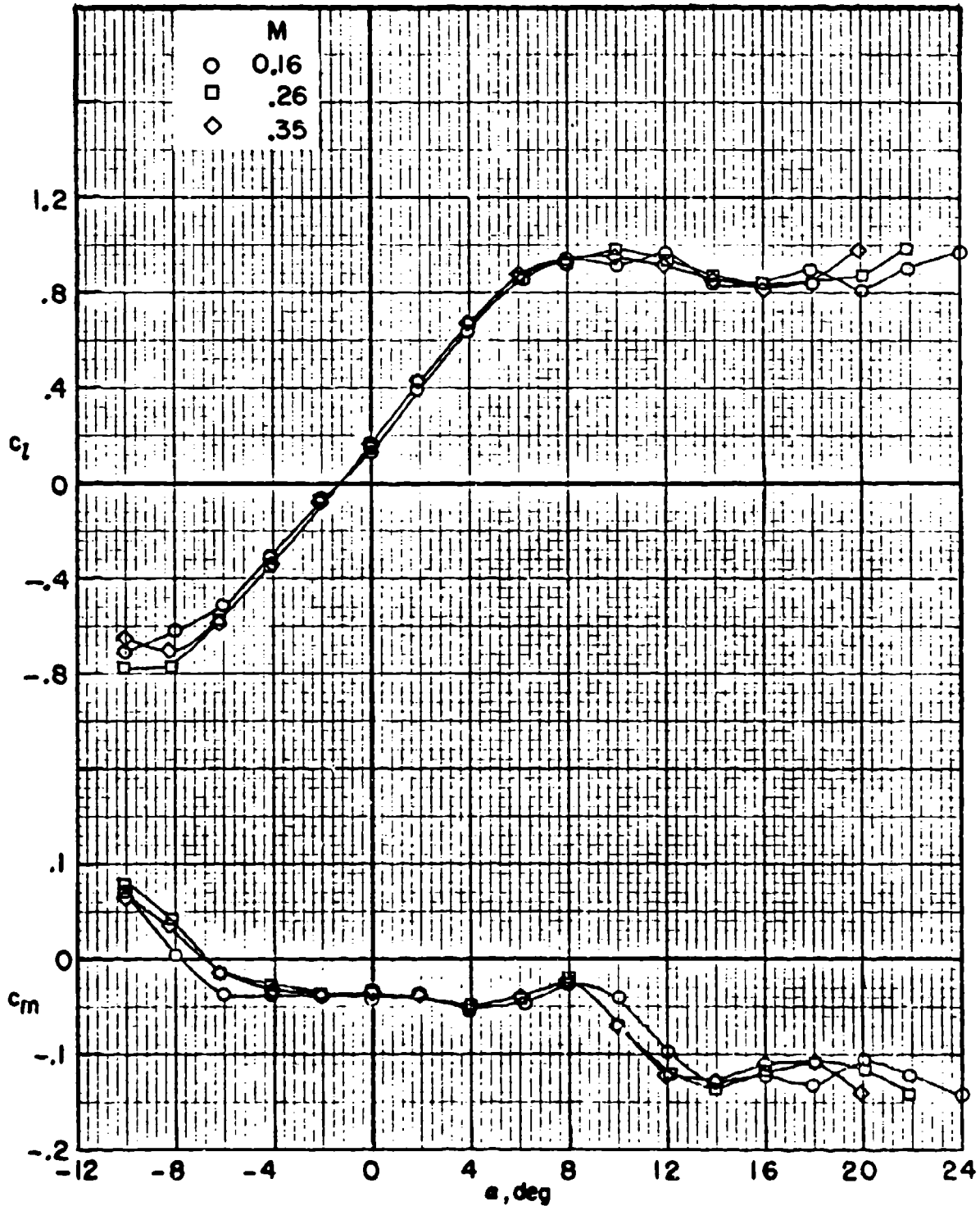
HC144R1070

TWO-DIMENSIONAL SECTION CHARACTERISTICS OF A 6-PERCENT BVR
AIRFOIL WITH LEADING EDGE FORWARD. $M = 0.26$; $R = 2.60 \times 10^6$



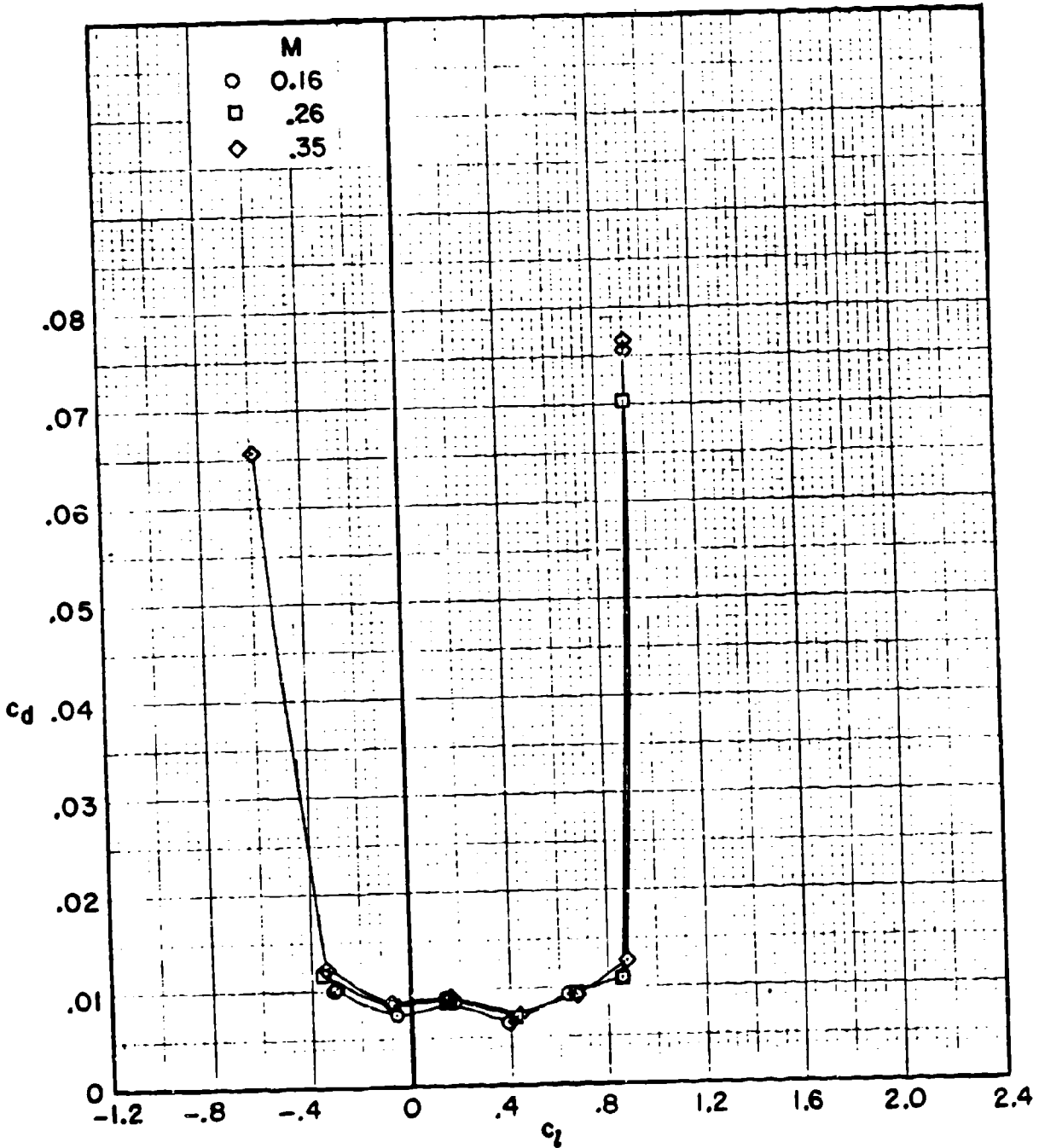
HC144R1070

TWO-DIMENSIONAL SECTION CHARACTERISTICS OF A 6-PERCENT RVR
AIRFOIL WITH LEADING EDGE FORWARD. $R = 2.6 \times 10^6$, MODEL SMOOTH

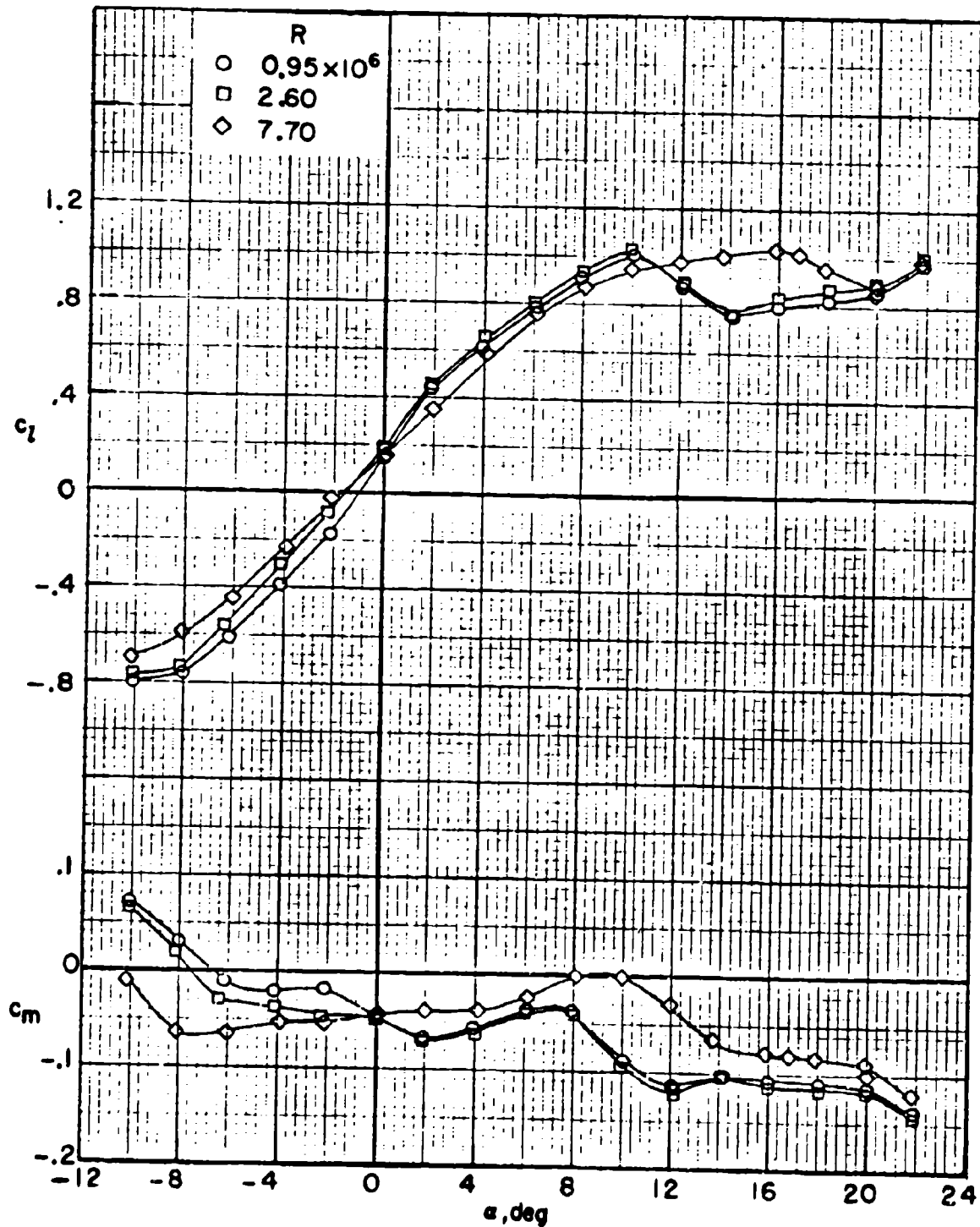


HC144R1070

TWO DIMENSIONAL SECTION CHARACTERISTICS OF A 6-PERCENT RVR
AIRFOIL WITH LEADING EDGE FORWARD. $R = 2.6 \times 10^6$, MODEL SMOOTH

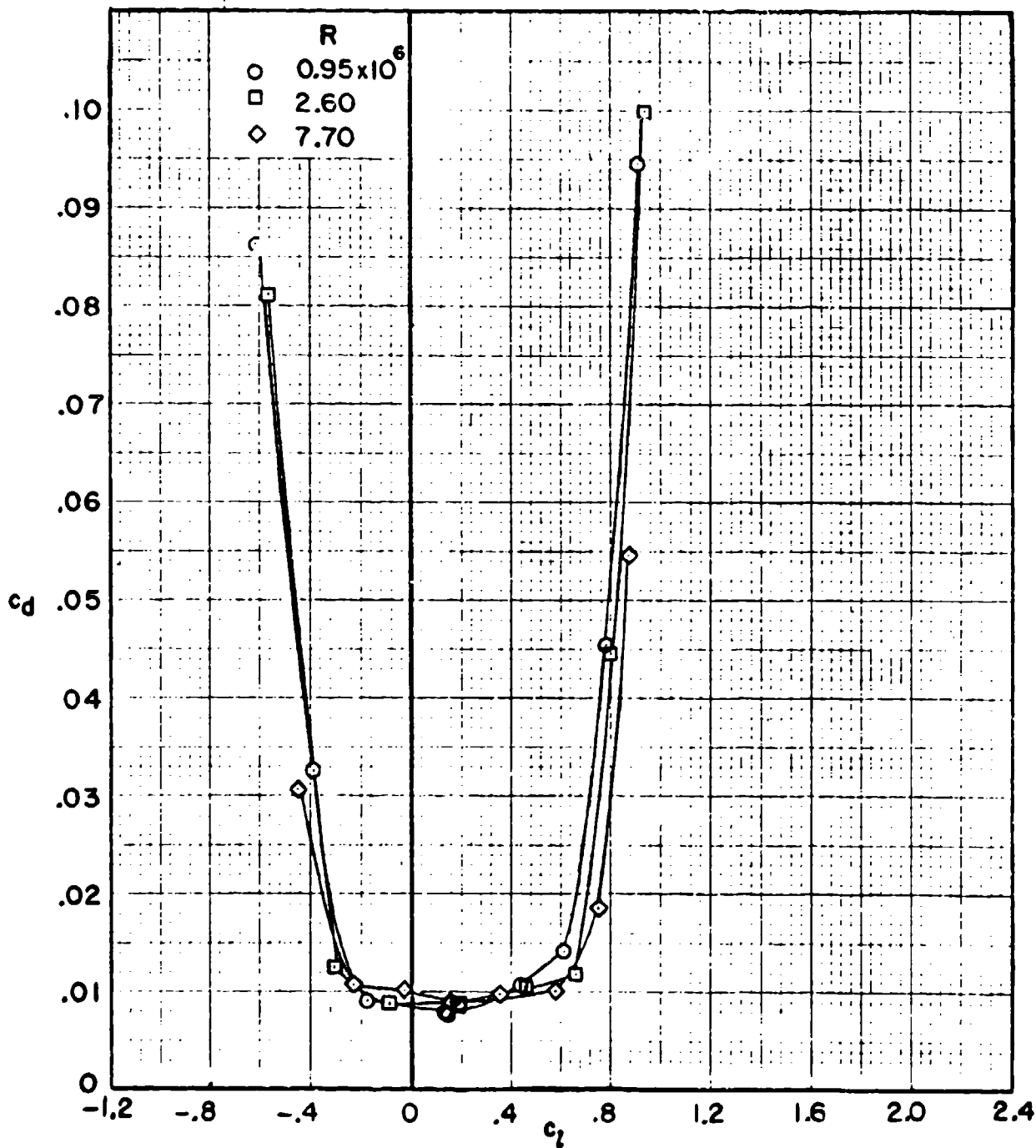


TWO-DIMENSIONAL SECTION CHARACTERISTICS OF A 6-PERCENT RVR AIRFOIL WITH TRAILING EDGE FORWARD. $M = 0.26$; MODEL SMOOTH



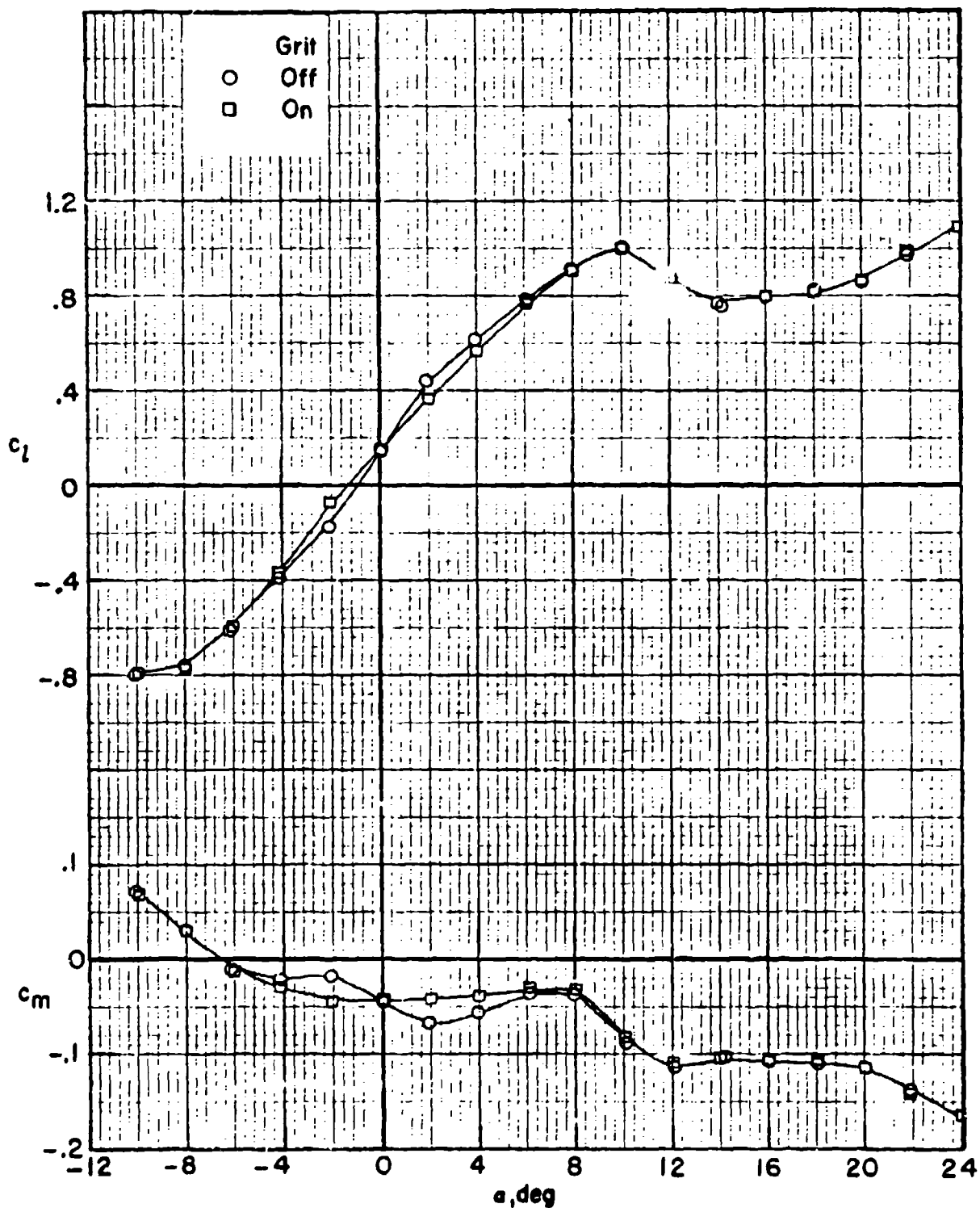
HC144R1070

TWO-DIMENSIONAL SECTION CHARACTERISTIC OF A 6-PERCENT RVR AIRFOIL WITH TRAILING EDGE FORWARD. $M = 0.26$; MODEL SMOOTH



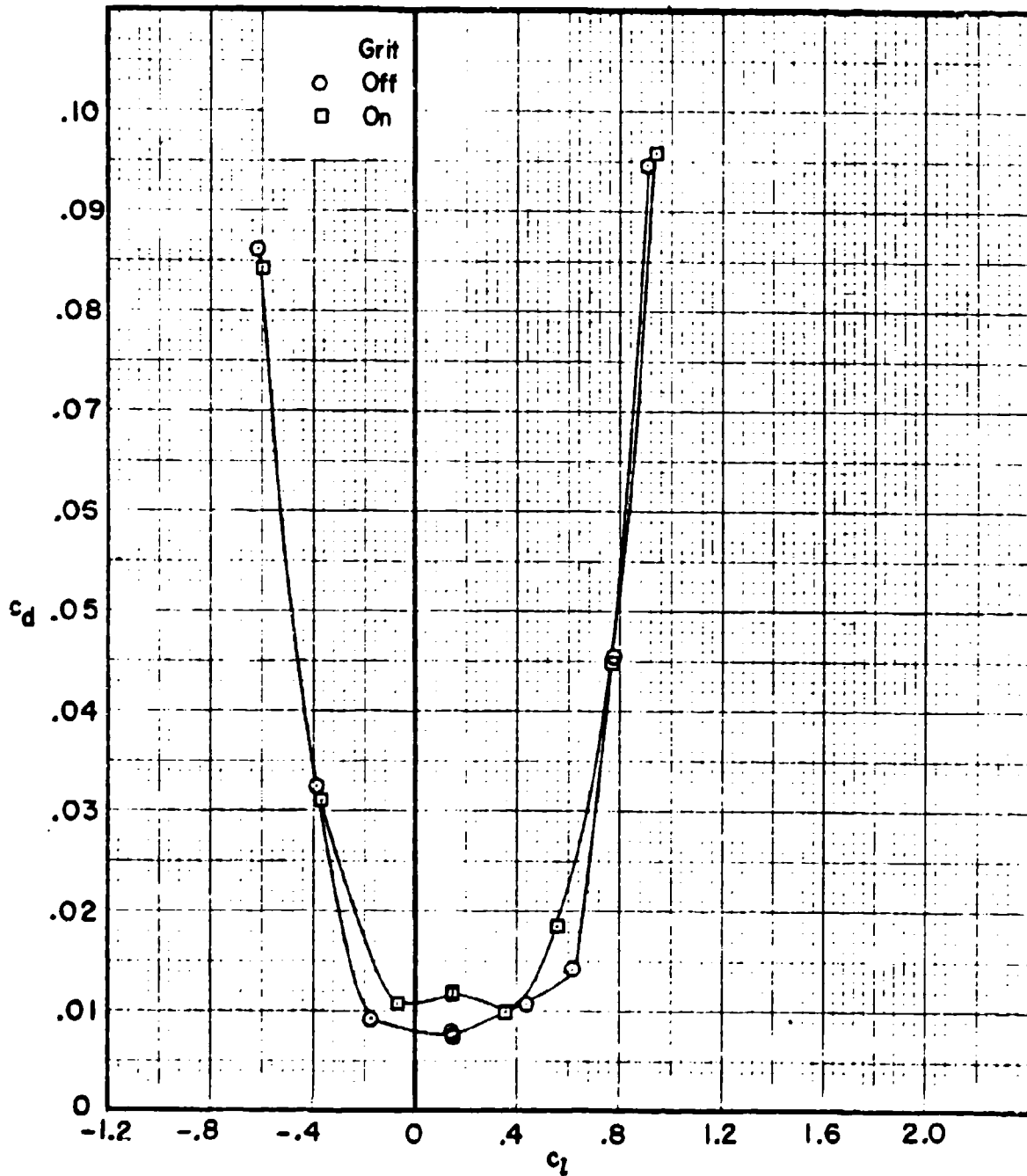
HC 144R1070

TWO-DIMENSIONAL SECTION CHARACTERISTICS OF A 6-PERCENT RVR
AIRFOIL WITH TRAILING EDGE FORWARD. $M = 0.26$; $R = 0.93 \times 10^6$



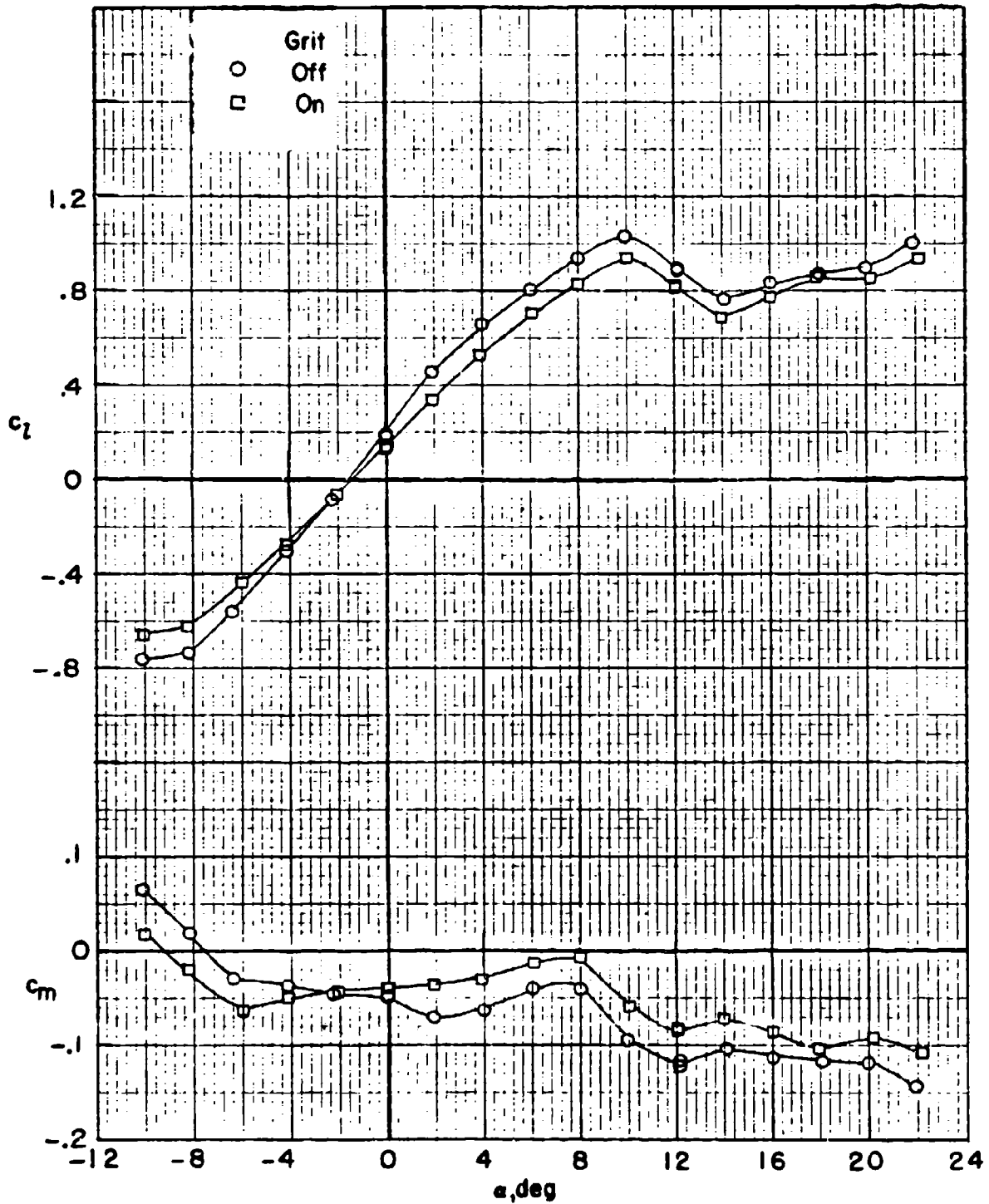
HC144R1070

TWO-DIMENSIONAL SECTION CHARACTERISTICS OF A 6-PERCENT RVR
AIRFOIL WITH TRAILING EDGE FORWARD. $M = 0.26$; $R = 0.93 \times 10^6$



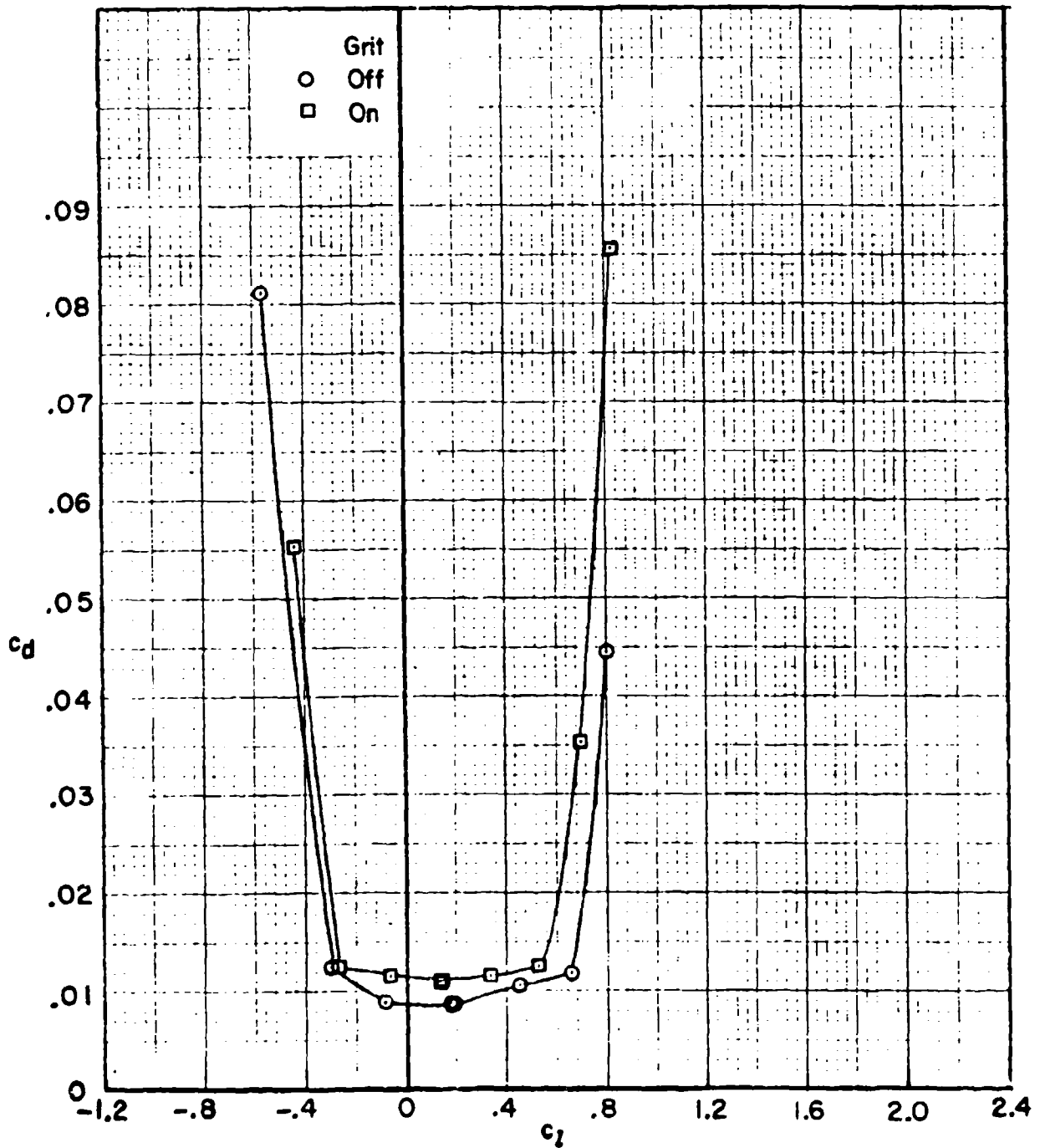
HC144R1070

**TWO-DIMENSIONAL SECTION CHARACTERISTICS OF A 6-PERCENT RVR
 AIRFOIL WITH TRAILING EDGE FORWARD. $M = 0.26$; $R = 2.60 \times 10^6$**



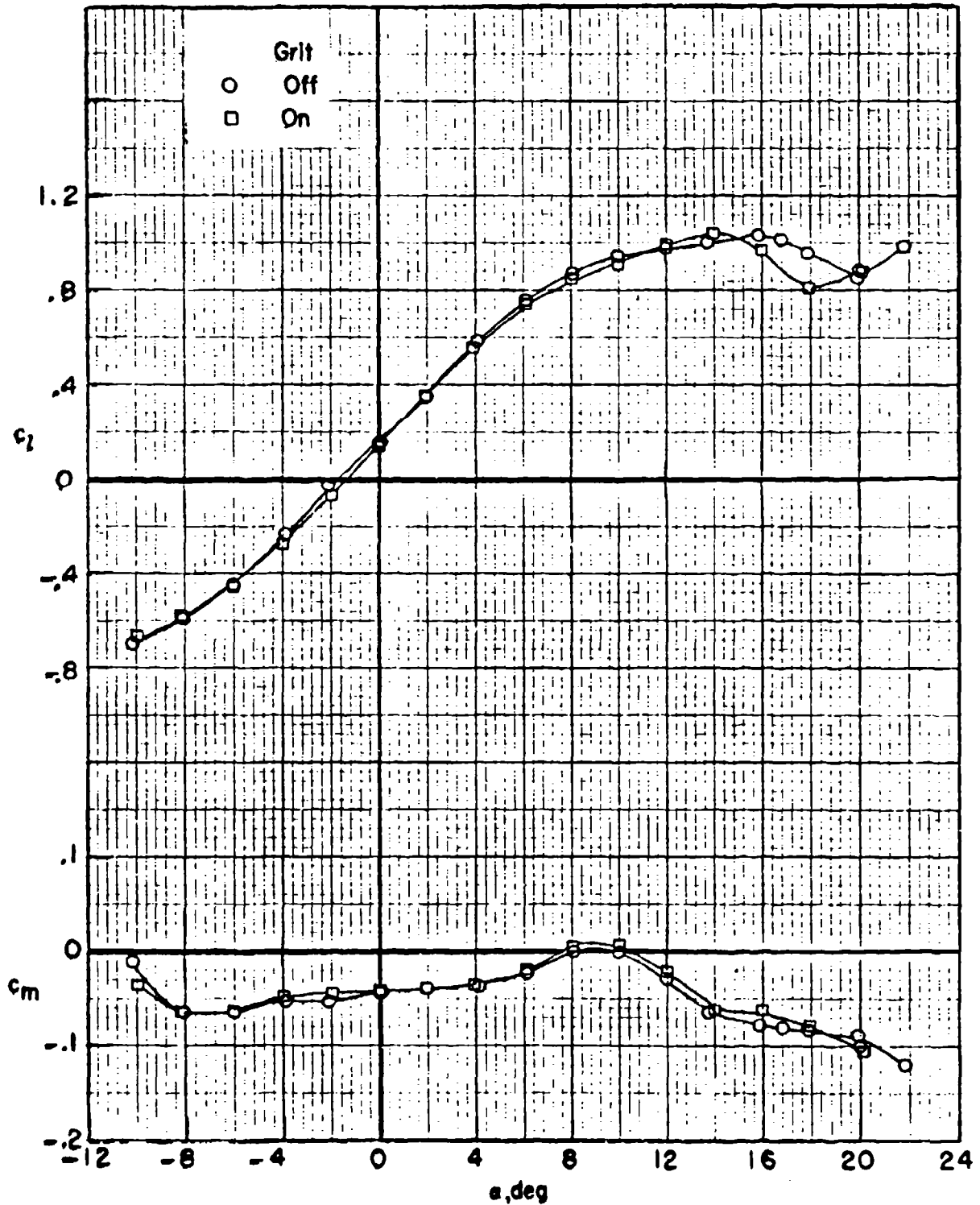
HC144R1070

TWO-DIMENSIONAL SECTION CHARACTERISTICS OF A 6-PERCENT RVR
AIRFOIL WITH TRAILING EDGE FORWARD. $M = 0.26$; $R = 2.60 \times 10^6$



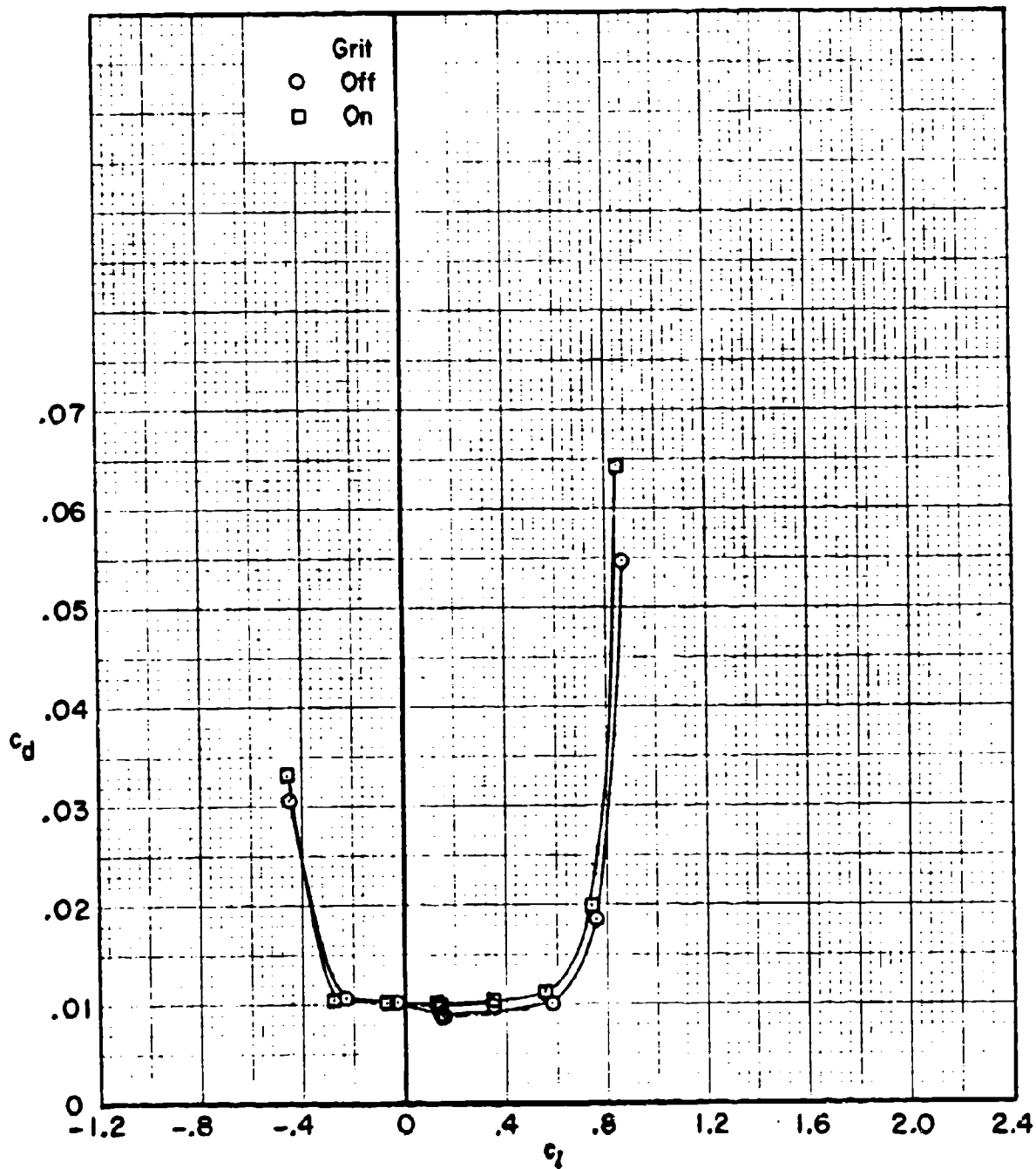
HC144R1070

TWO-DIMENSIONAL SECTION CHARACTERISTICS OF A 6 PERCENT RVR
AIRFOIL WITH TRAILING EDGE FORWARD. $M = 0.26$; $R = 7.7 \times 10^6$



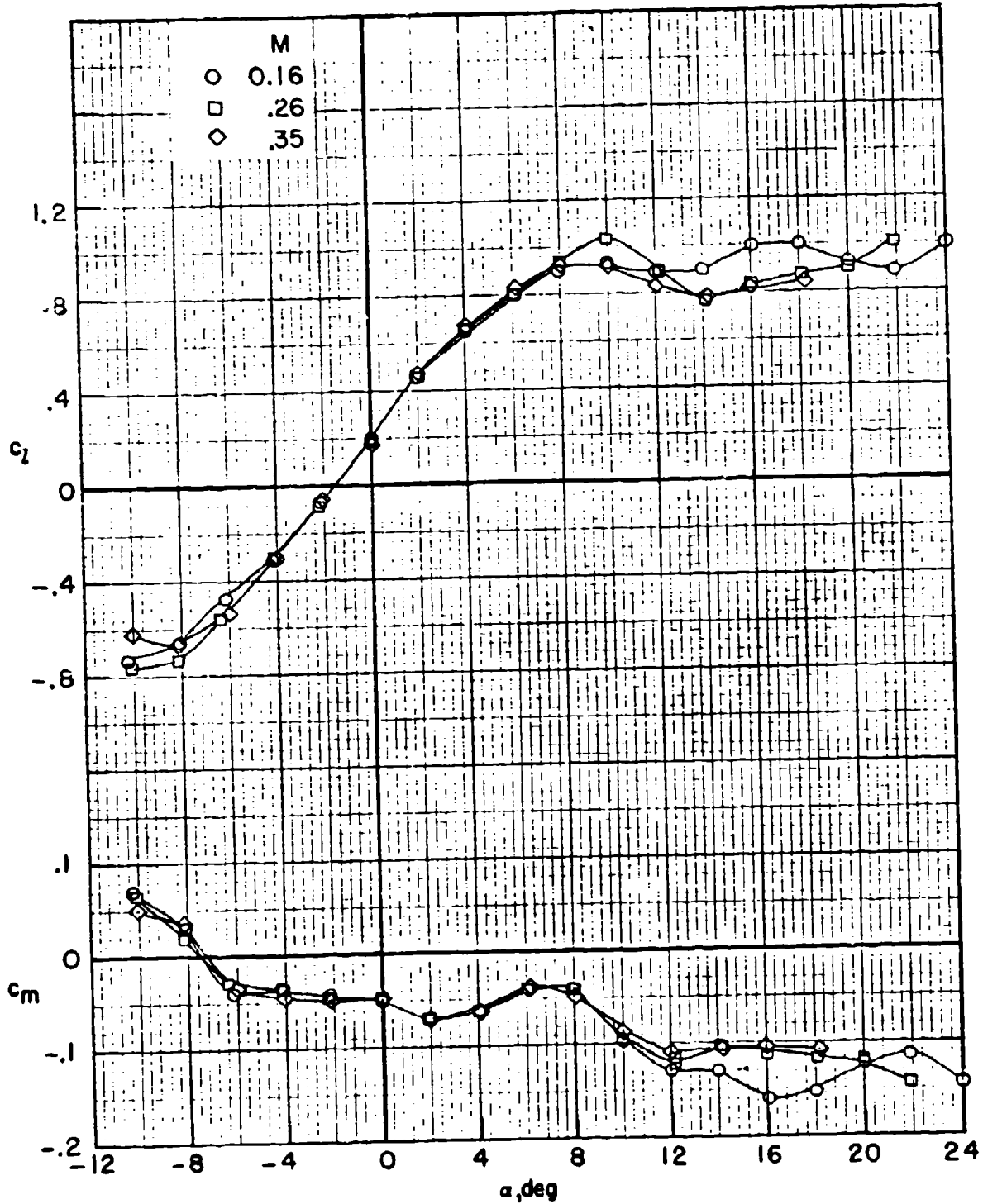
HC144R1070

TWO-DIMENSIONAL SECTION CHARACTERISTICS OF A 6 PERCENT RVR
AIRFOIL WITH TRAILING EDGE FORWARD. $M = 0.26$; $R = 7.7 \times 10^6$



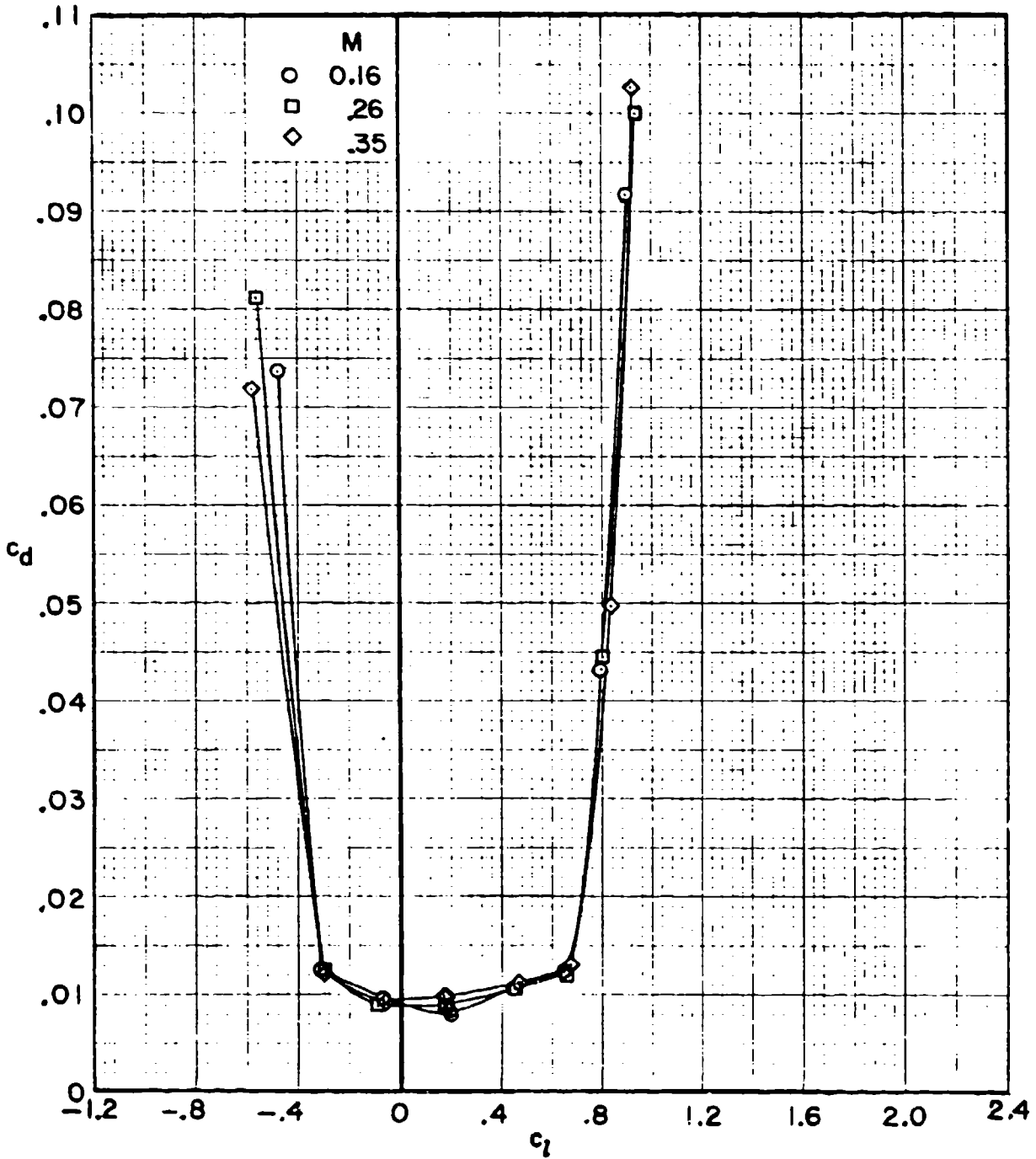
HC144R1070

TWO-DIMENSIONAL SECTION CHARACTERISTICS OF A 6-PERCENT RVR
 AIRFOIL WITH TRAILING EDGE FORWARD. $R = 2.60 \times 10^6$; MODEL SMOOTH



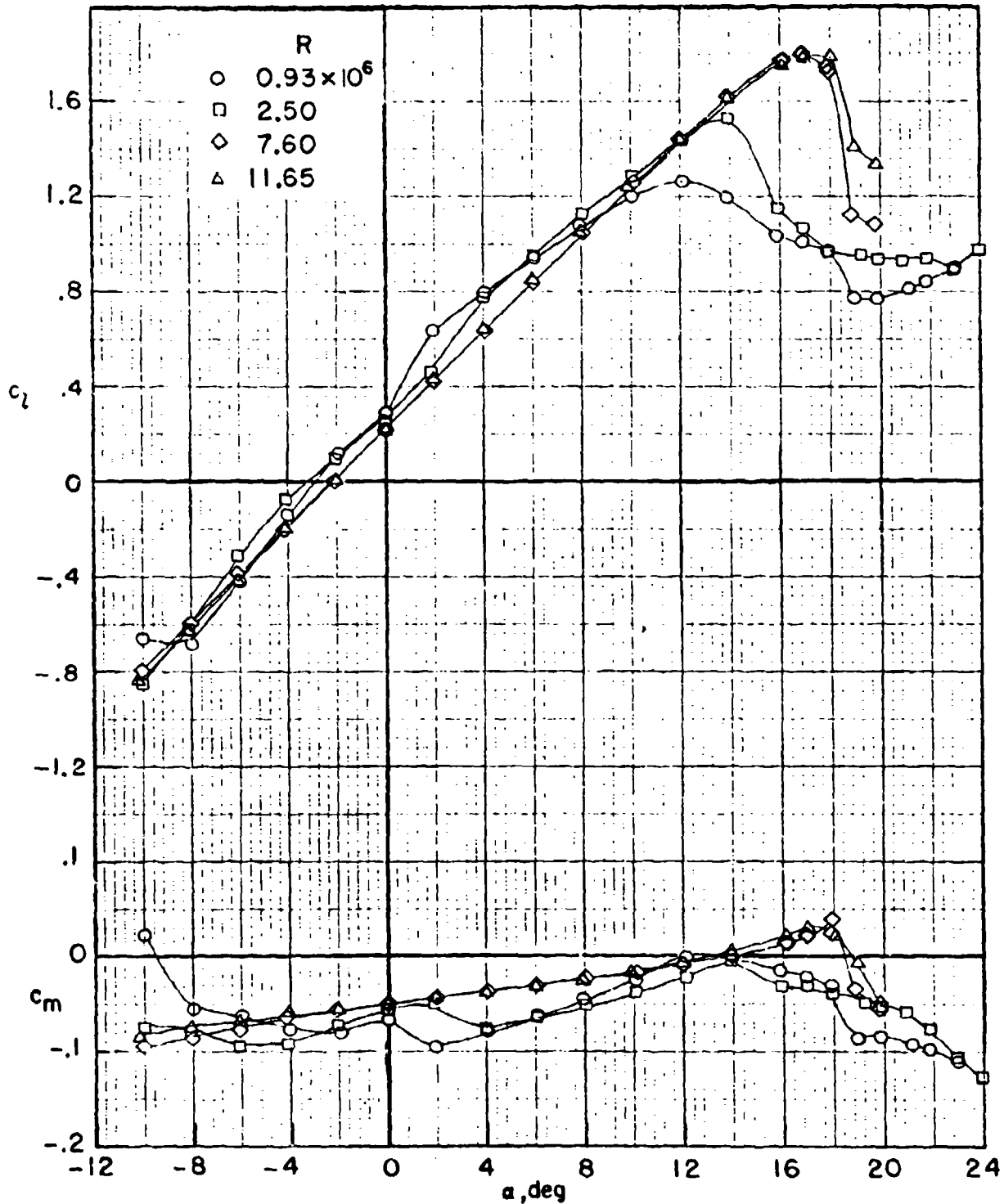
HC144R1070

**TWO-DIMENSIONAL SECTION CHARACTERISTICS OF A 6-PERCENT RVR
AIRFOIL WITH TRAILING EDGE FORWARD. $R = 2.60 \times 10^5$; MODEL SMOOTH**

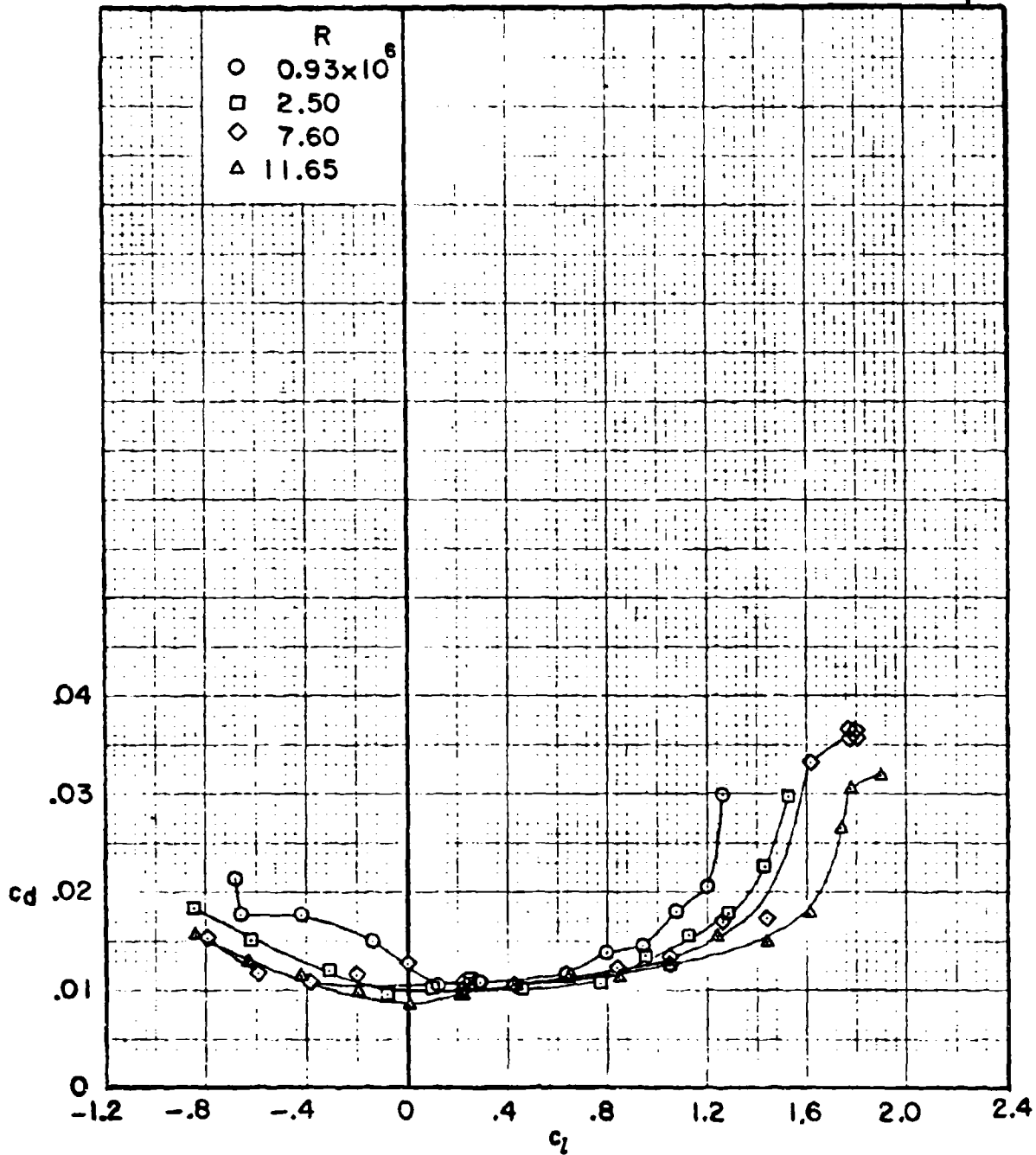


HC144R1070

TWO-DIMENSIONAL SECTION CHARACTERISTICS OF A 12-PERCENT RVR
 AIRFOIL WITH LEADING EDGE FORWARD. $M = 0.26$; MODEL SMOOTH

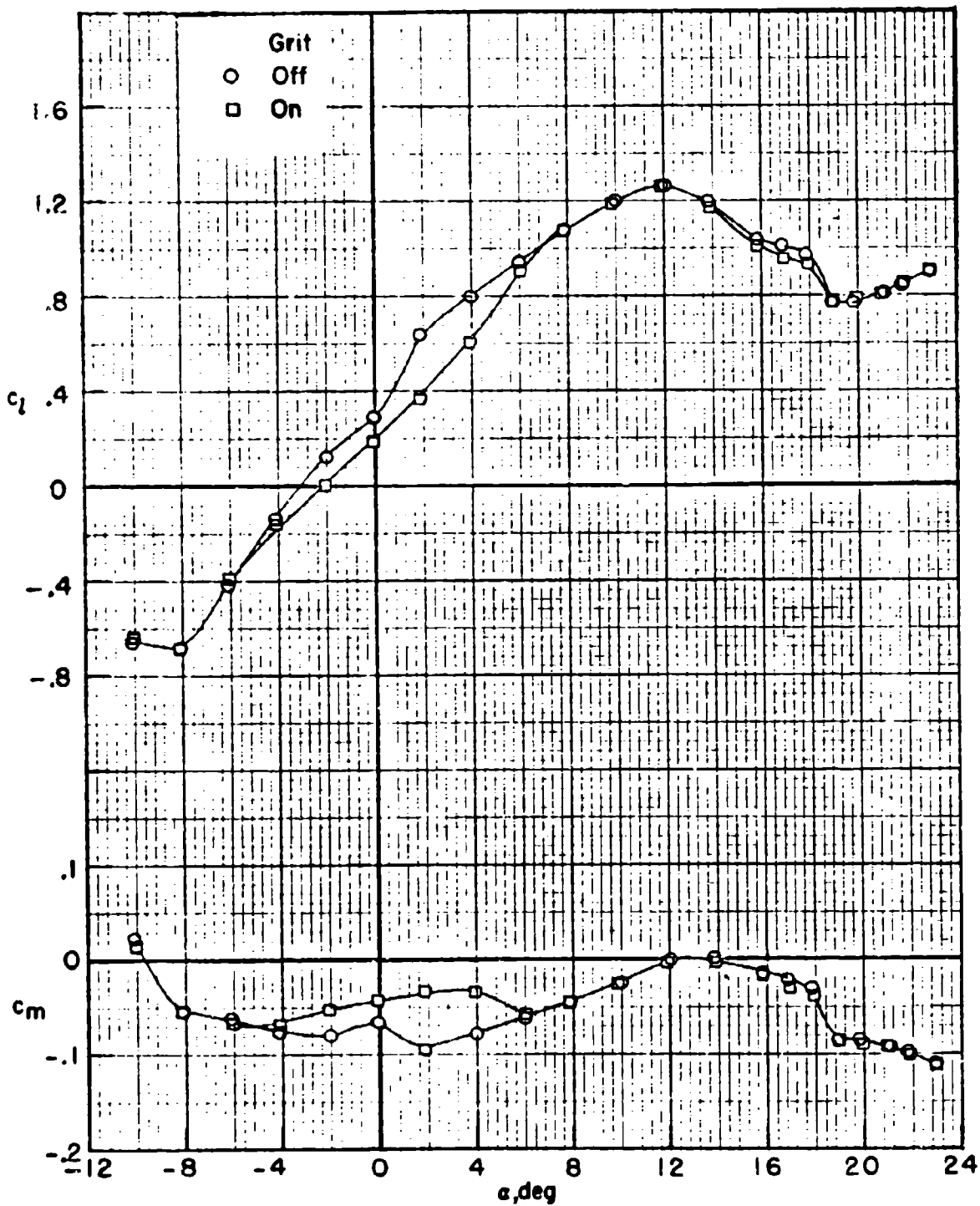


TWO-DIMENSIONAL SECTION CHARACTERISTICS OF A 12-PERCENT RVR AIRFOIL WITH LEADING EDGE FORWARD. $M = 0.26$; MODEL SMOOTH



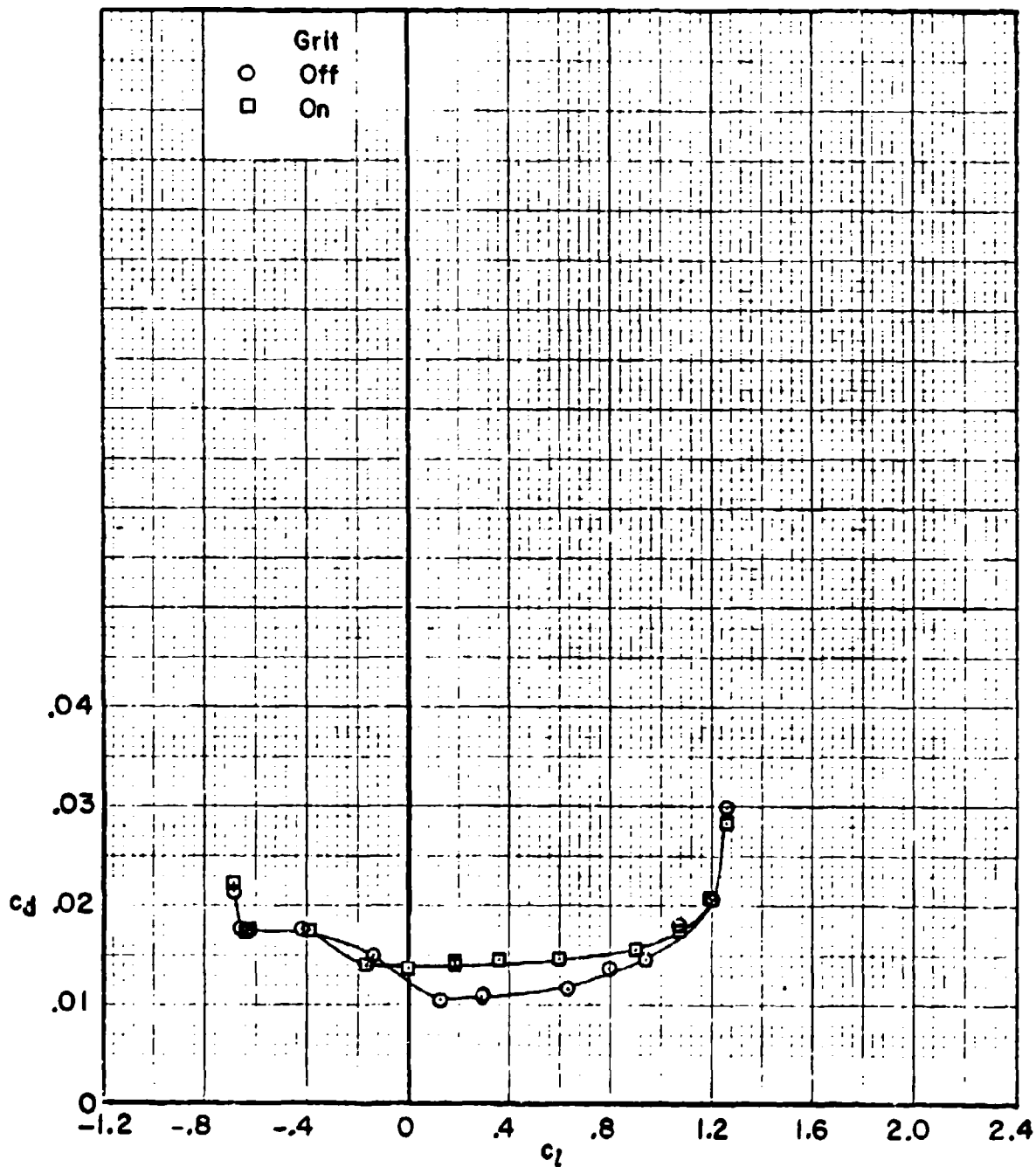
HC144R1070

TWO-DIMENSIONAL SECTION CHARACTERISTICS OF A 12-PERCENT RVR
 AIRFOIL WITH LEADING EDGE FORWARD. $M = 0.26$; $R = 0.93 \times 10^6$



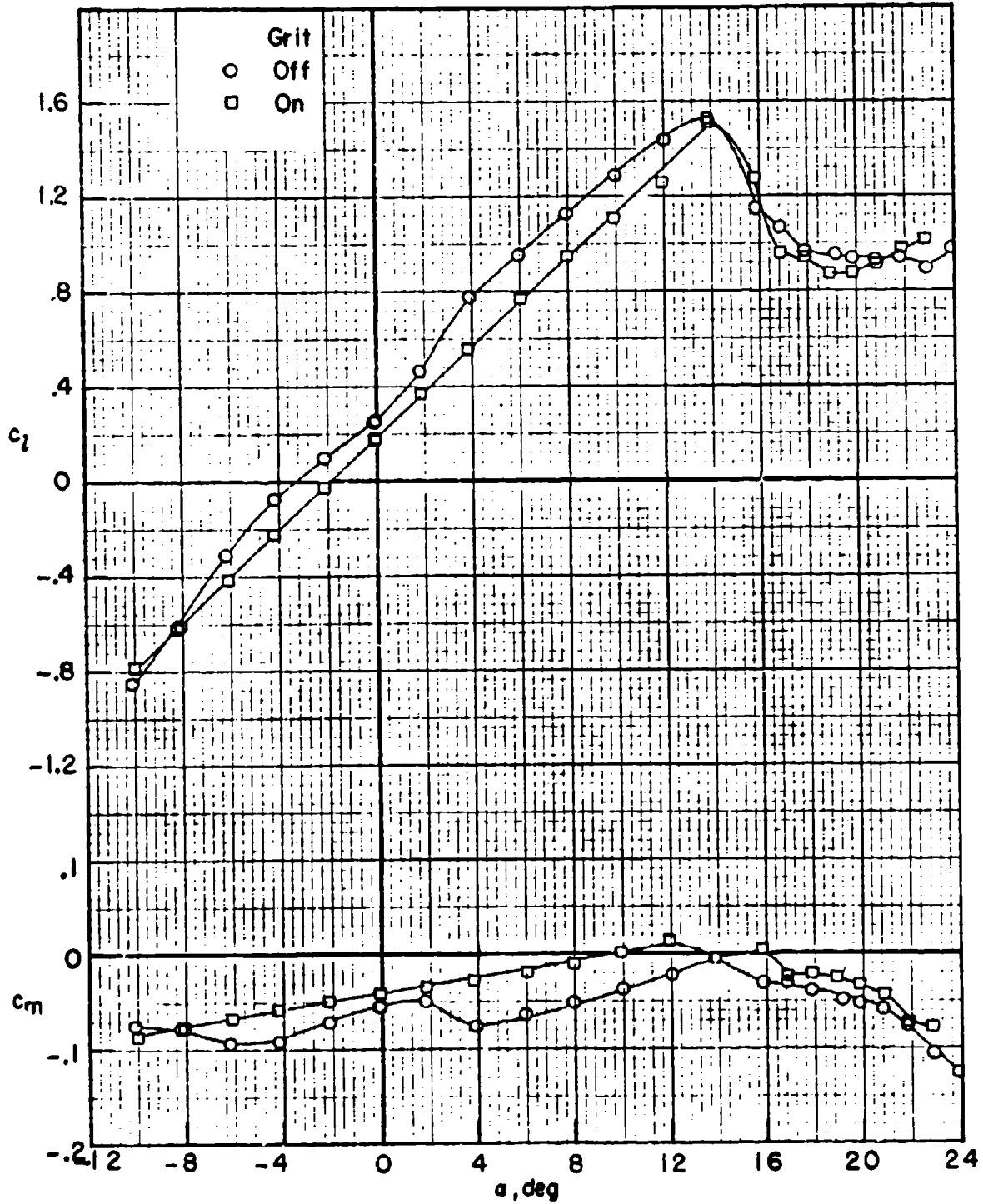
HC144R1070

**TWO-DIMENSIONAL SECTION CHARACTERISTICS OF A 12-PERCENT RVR
AIRFOIL WITH LEADING EDGE FORWARD. $M = 0.26$; $R = 0.93 \times 10^6$**



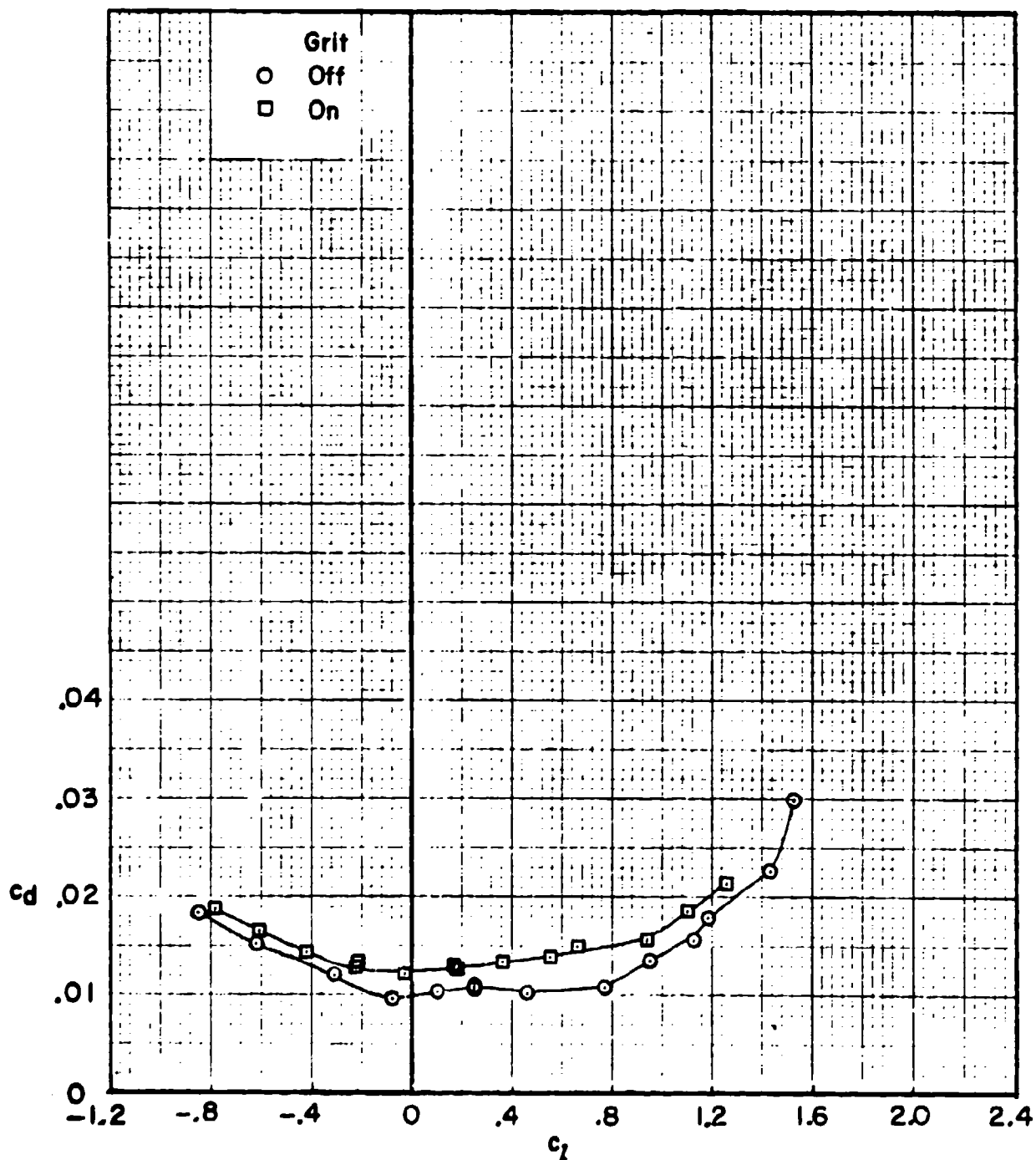
HC144R1070

TWO-DIMENSIONAL SECTION CHARACTERISTICS OF A 12-PERCENT RVR
AIRFOIL WITH LEADING EDGE FORWARD. $M = 0.26$; $R = 2.5 \times 10^6$



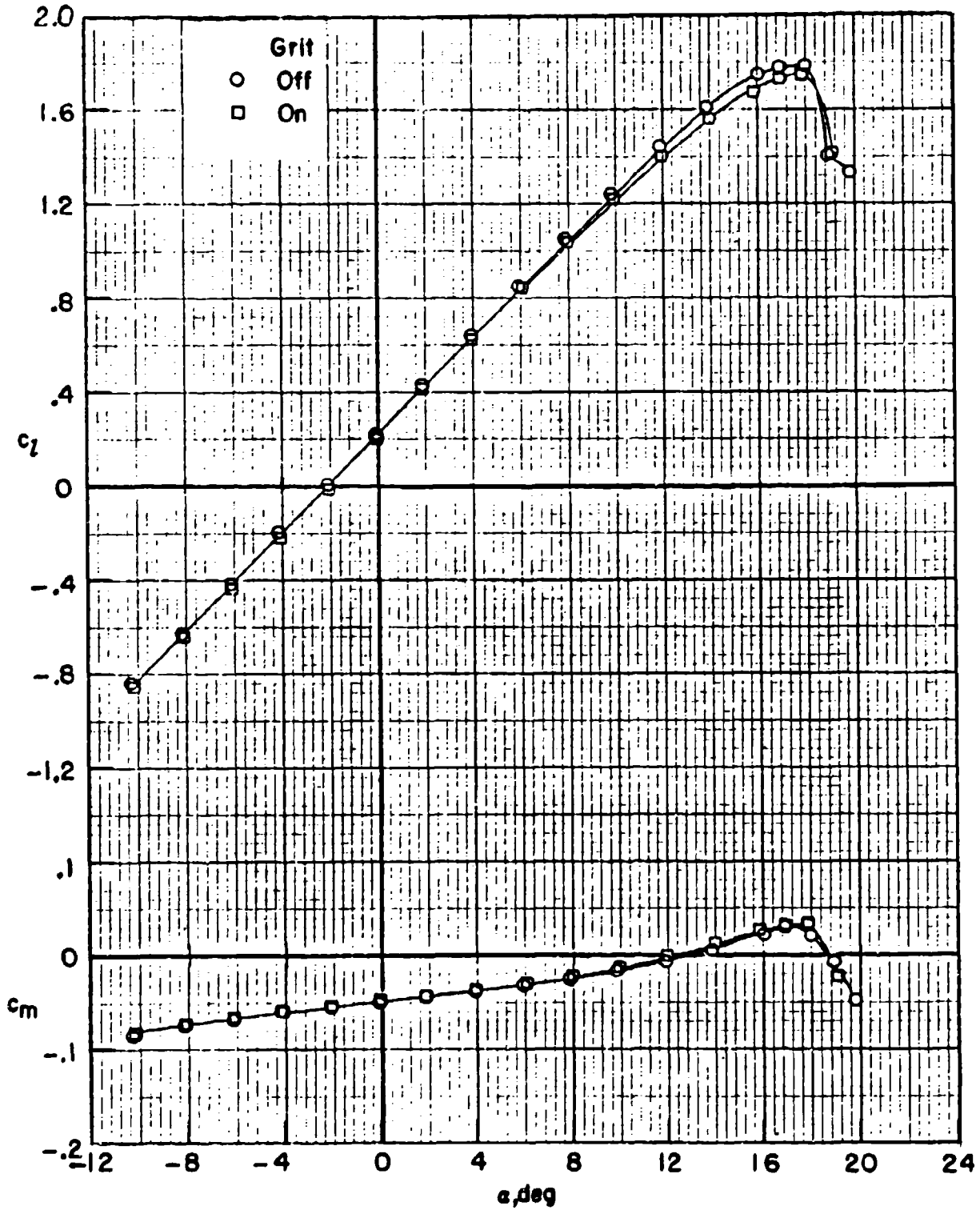
HC144R1070

TWO-DIMENSIONAL SECTION CHARACTERISTICS OF A 12-PERCENT RVR
AIRFOIL WITH LEADING EDGE FORWARD. $M = 0.26$; $R = 2.5 \times 10^6$



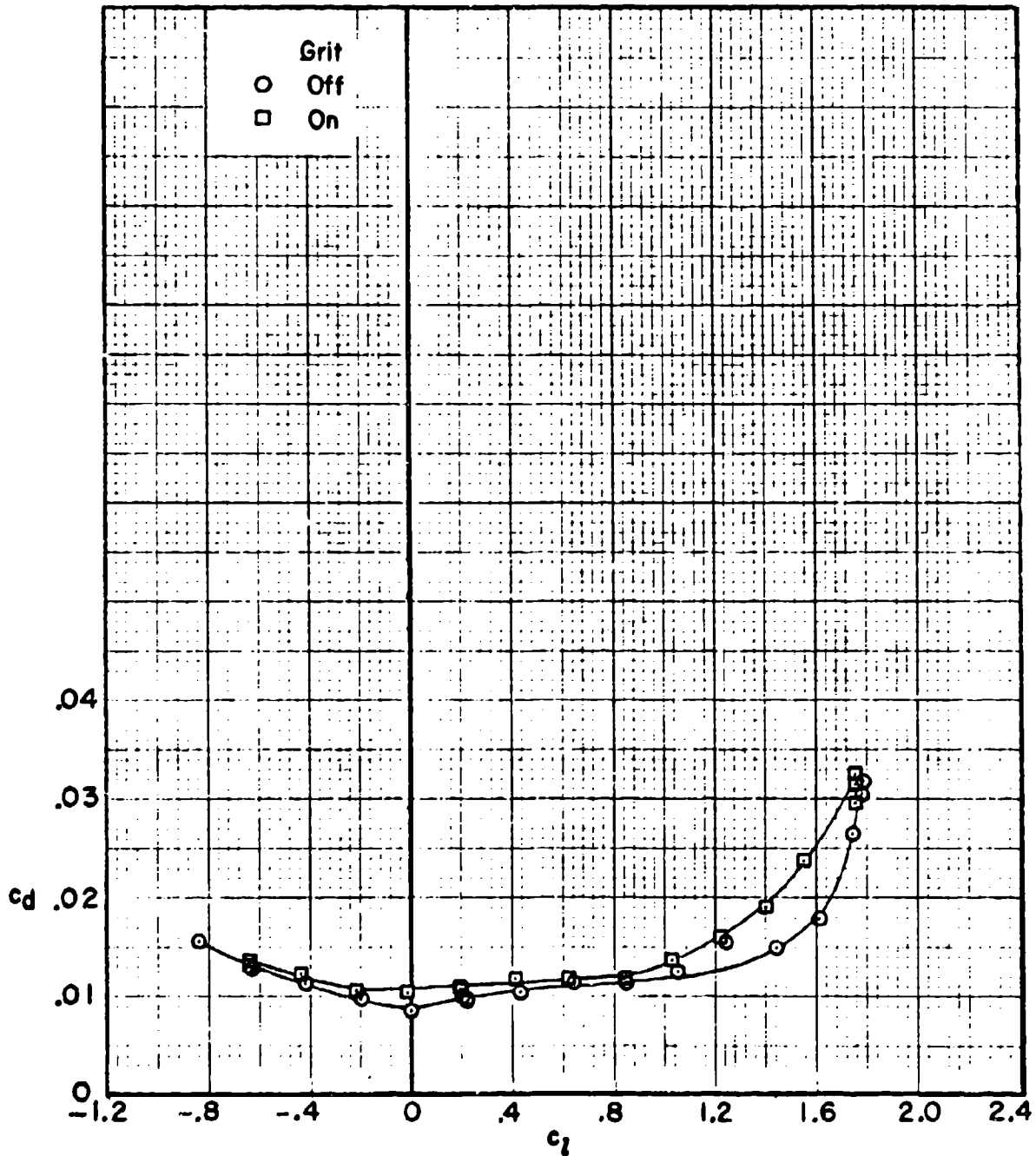
HC144R1070

TWO-DIMENSIONAL SECTION CHARACTERISTICS OF A 12-PERCENT RVR
AIRFOIL WITH LEADING EDGE FORWARD. $M = 0.26$; $R = 11.65 \times 10^6$



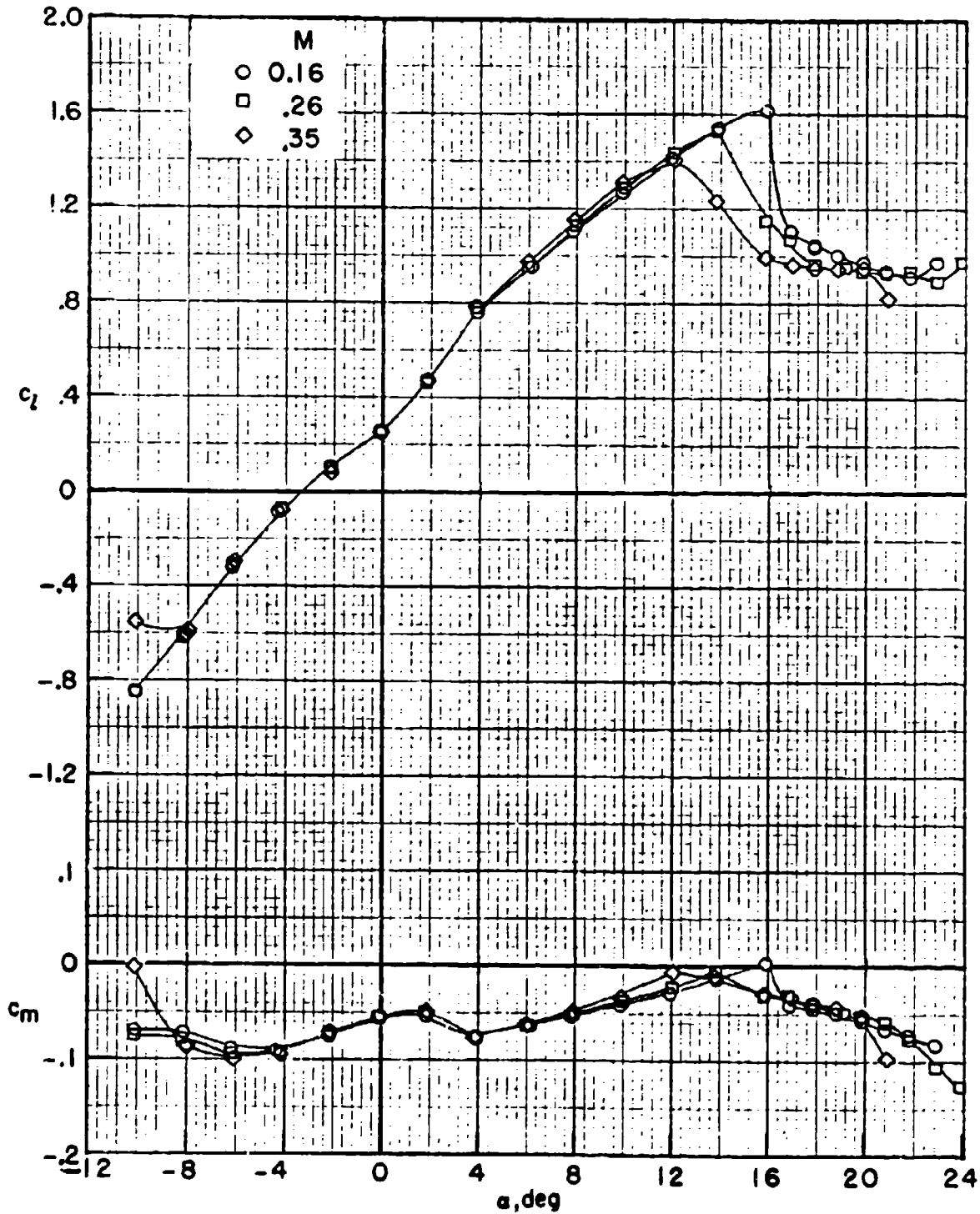
HC144R1070

**TWO-DIMENSIONAL SECTION CHARACTERISTICS OF A 12-PERCENT RVR
AIRFOIL WITH LEADING EDGE FORWARD. $M = 0.26$; $R = 11.65 \times 10^6$**



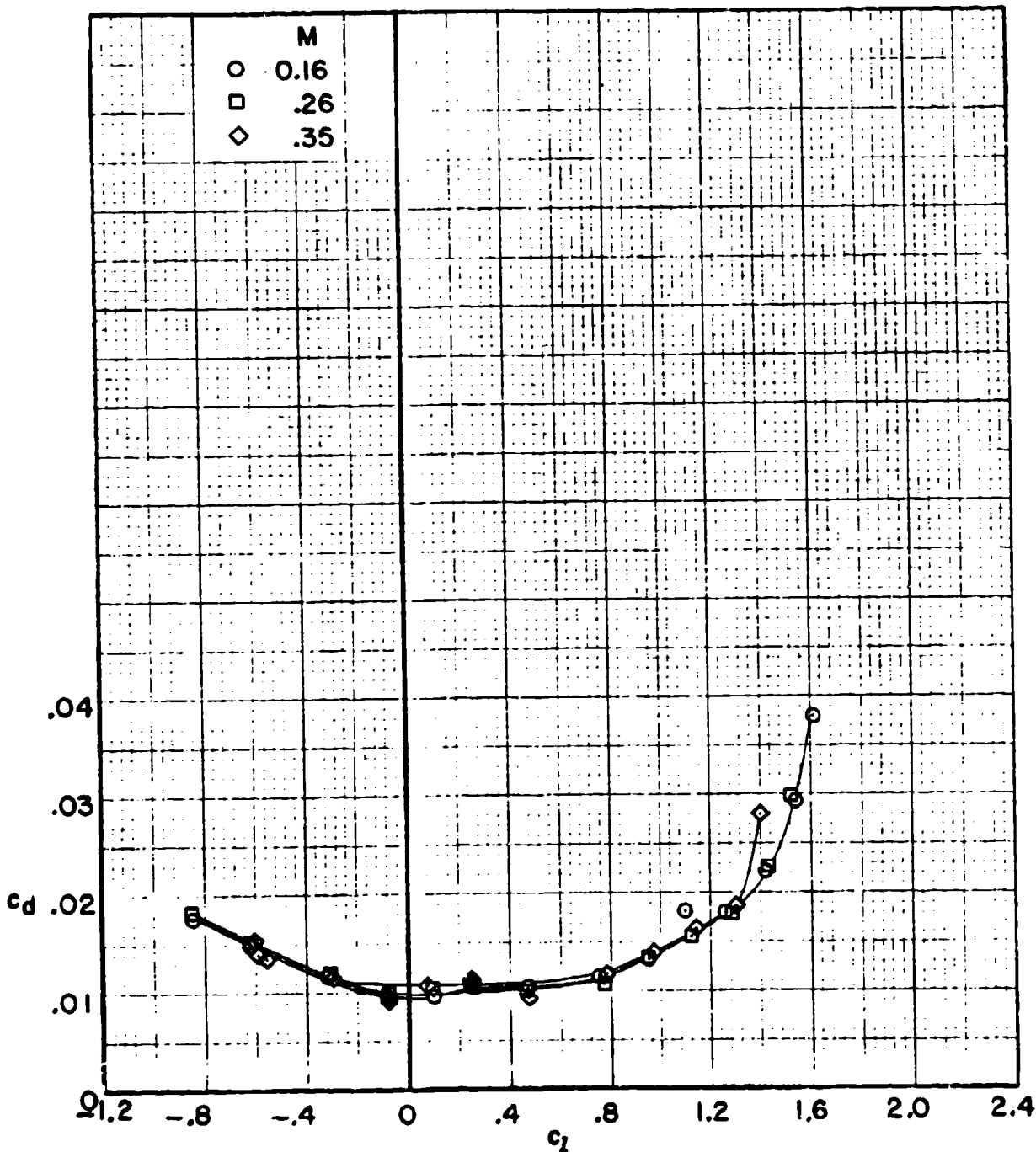
HC144R1070

TWO-DIMENSIONAL SECTION CHARACTERISTICS OF A 12-PERCENT RVR AIRFOIL WITH LEADING EDGE FORWARD. $R = 2.50 \times 10^6$; MODEL SMOOTH

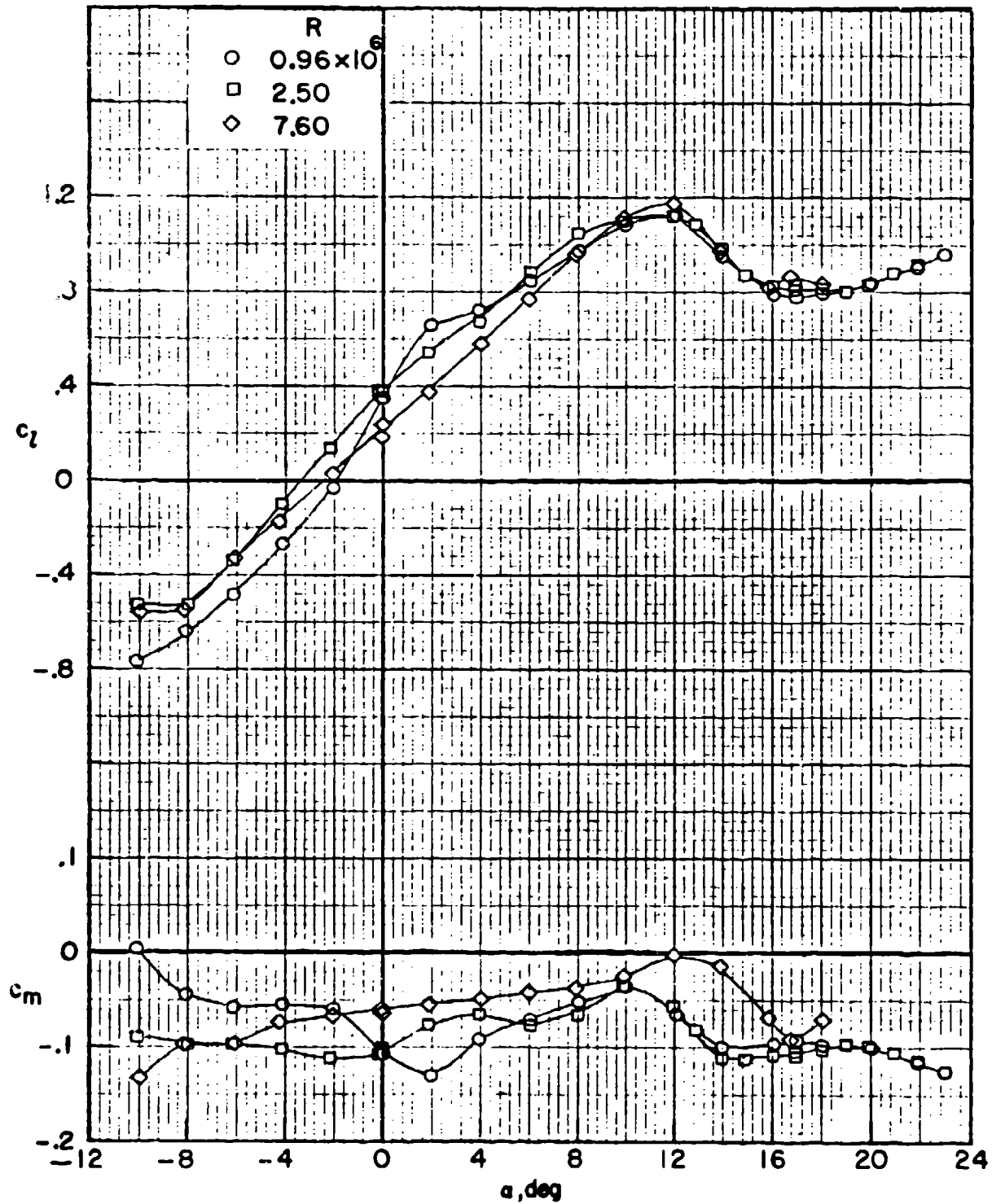


HC144R1070

TWO-DIMENSIONAL SECTION CHARACTERISTICS OF A 12-PERCENT RVR AIRFOIL WITH LEADING EDGE FORWARD. $R = 2.50 \times 10^6$; MODEL SMOOTH

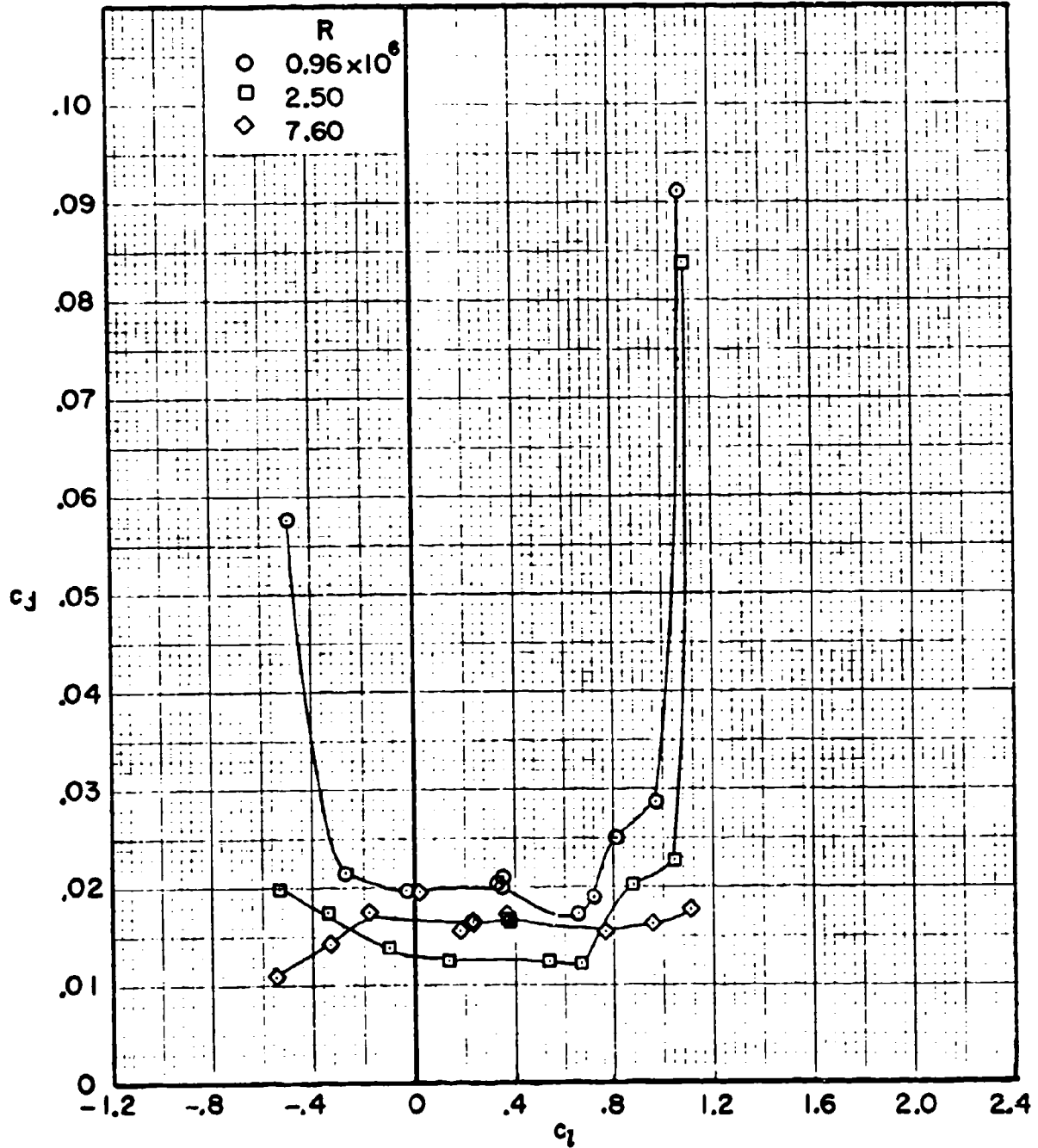


TWO-DIMENSIONAL SECTION CHARACTERISTICS OF A 12-PERCENT RVR
AIRFOIL WITH TRAILING EDGE FORWARD. $M = 0.26$; MODEL SMOOTH



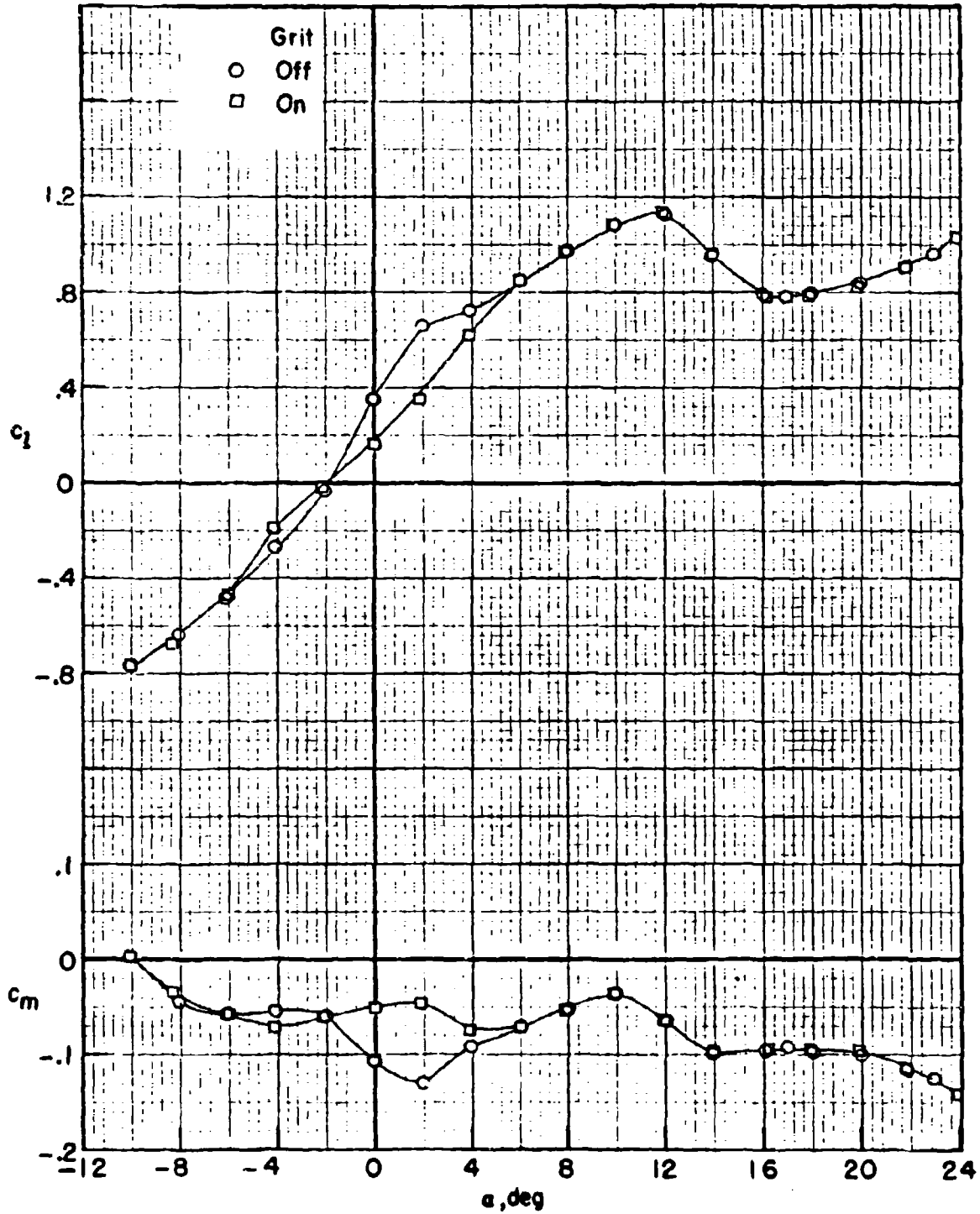
HC144R1070

TWO-DIMENSIONAL SECTION CHARACTERISTICS OF A 12-PERCENT RVR AIRFOIL WITH TRAILING EDGE FORWARD. $M = 0.26$; MODEL SMOOTH



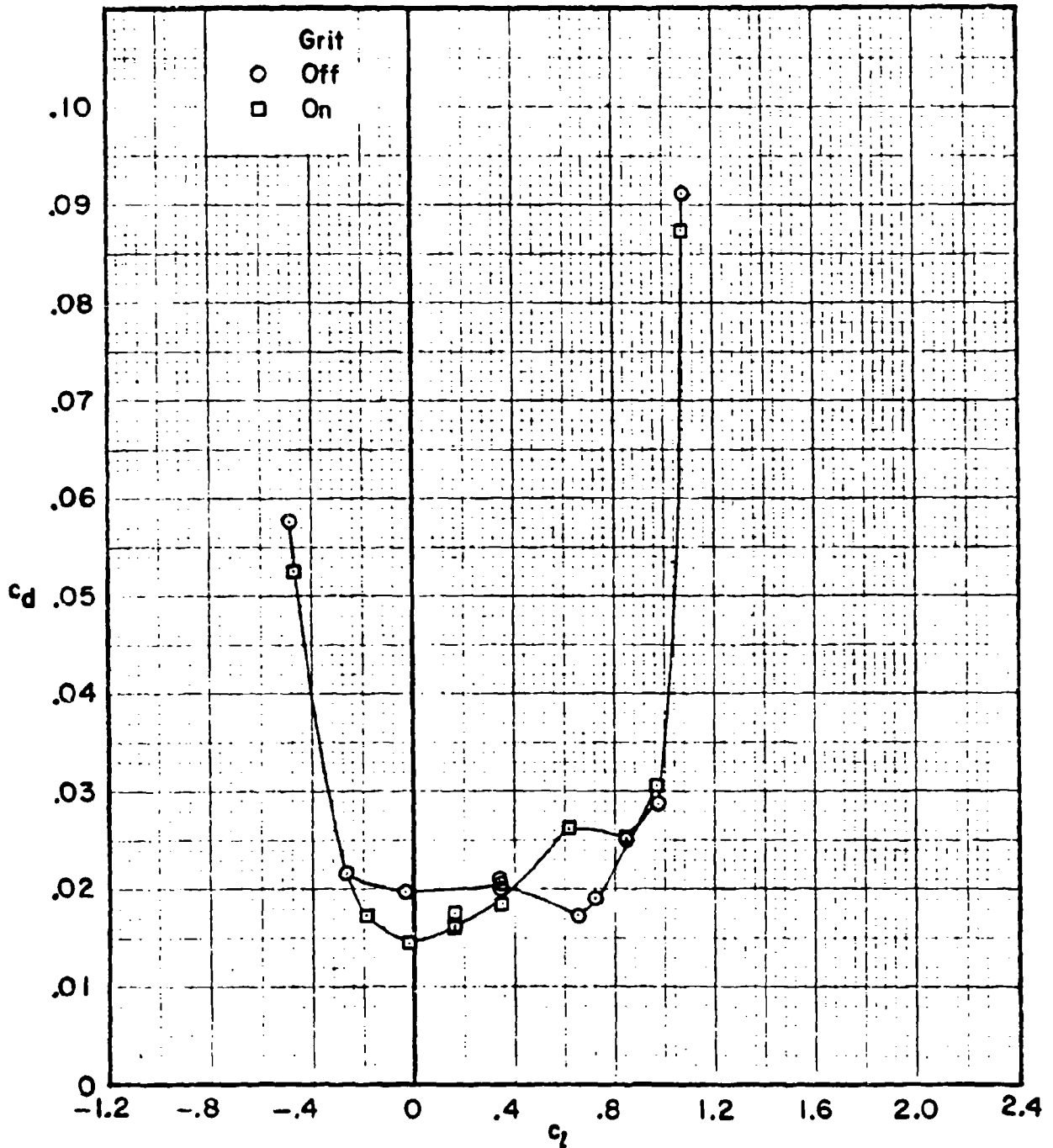
HC144R1070

**TWO-DIMENSIONAL SECTION CHARACTERISTICS OF A 12-PERCENT RVR
AIRFOIL WITH TRAILING EDGE FORWARD. $M = 0.26$; $R = 0.96 \times 10^6$**



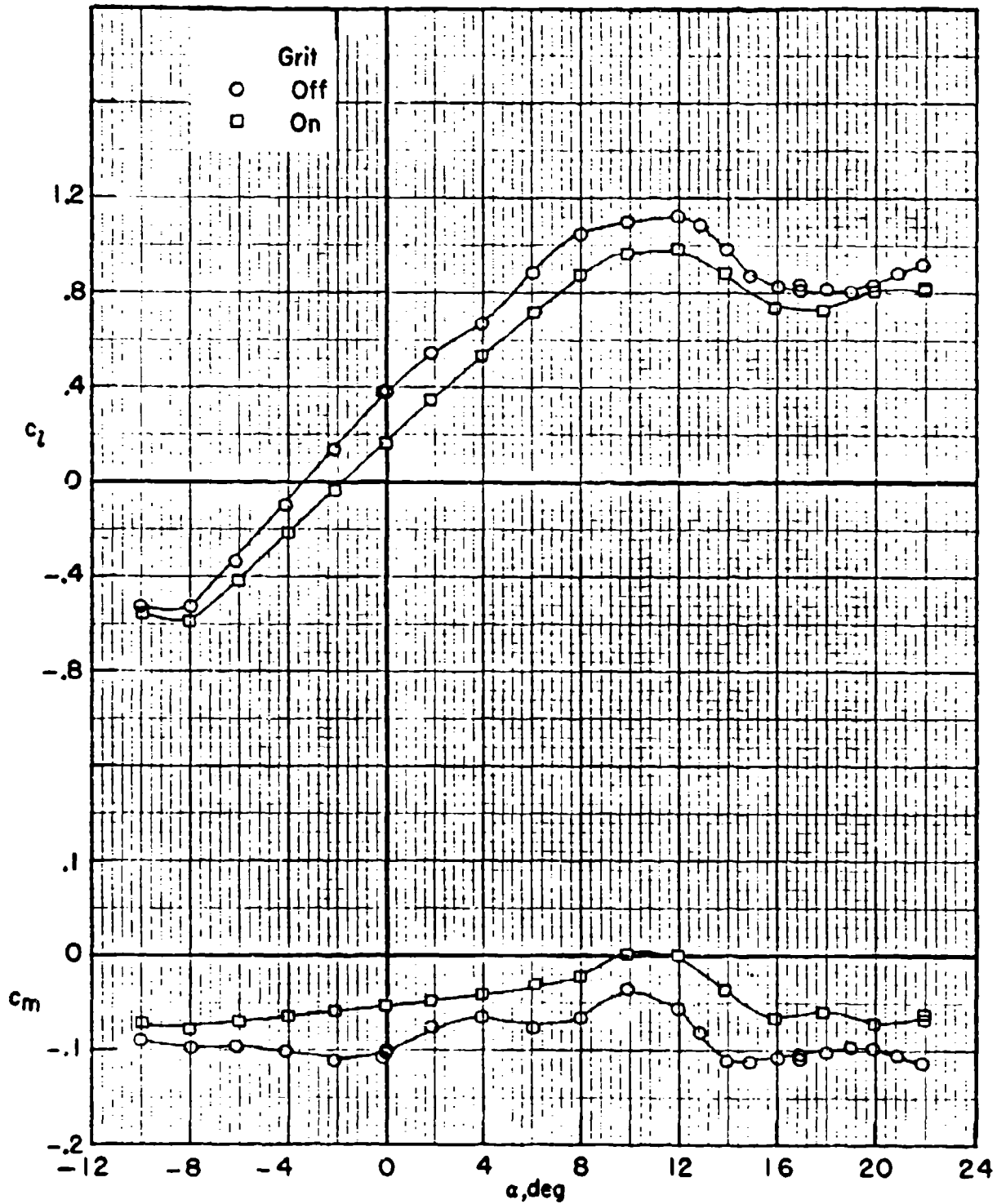
HC144R1070

**TWO-DIMENSIONAL SECTION CHARACTERISTICS OF A 12-PERCENT RVR
AIRFOIL WITH TRAILING EDGE FORWARD. $M = 0.26$; $R = 0.96 \times 10^6$**



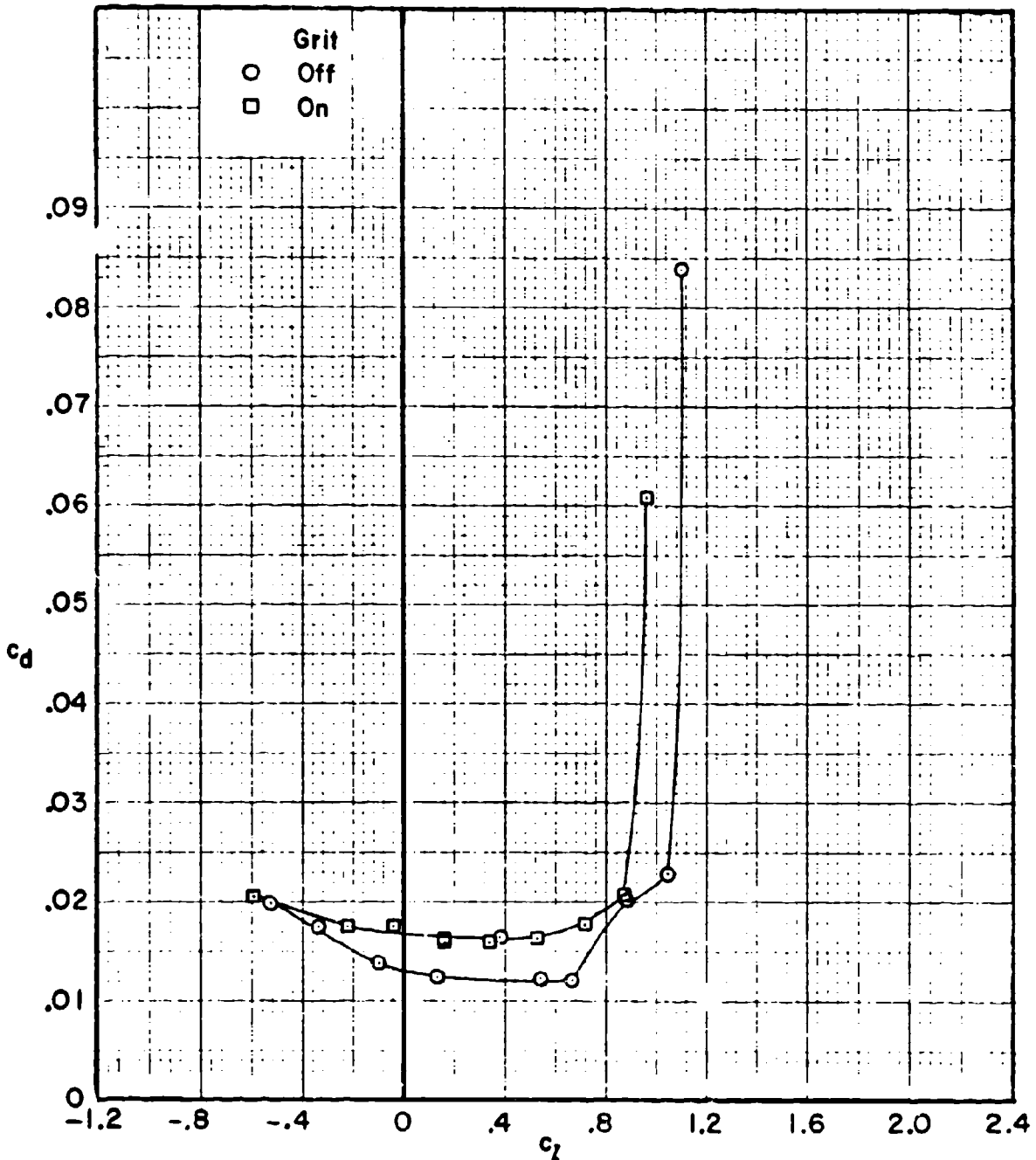
HC144R1070

TWO-DIMENSIONAL SECTION CHARACTERISTICS OF A 12-PERCENT RVR
AIRFOIL WITH TRAILING EDGE FORWARD. $M = 0.26$; $R = 2.50 \times 10^6$



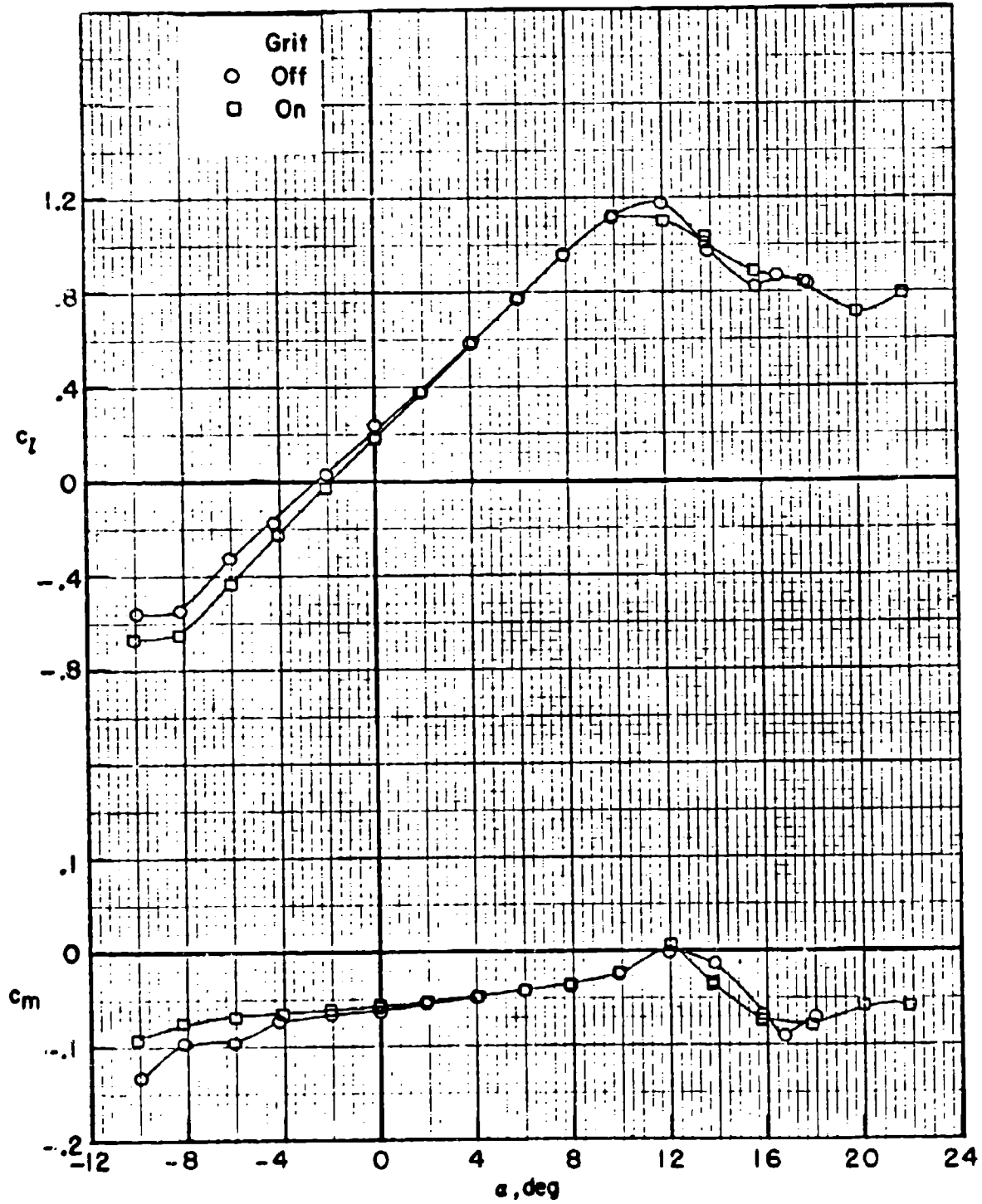
HC144R1070

**TWO-DIMENSIONAL SECTION CHARACTERISTICS OF A 12-PERCENT RVR
AIRFOIL WITH TRAILING EDGE FORWARD. $M = 0.26$; $R = 2.50 \times 10^6$**



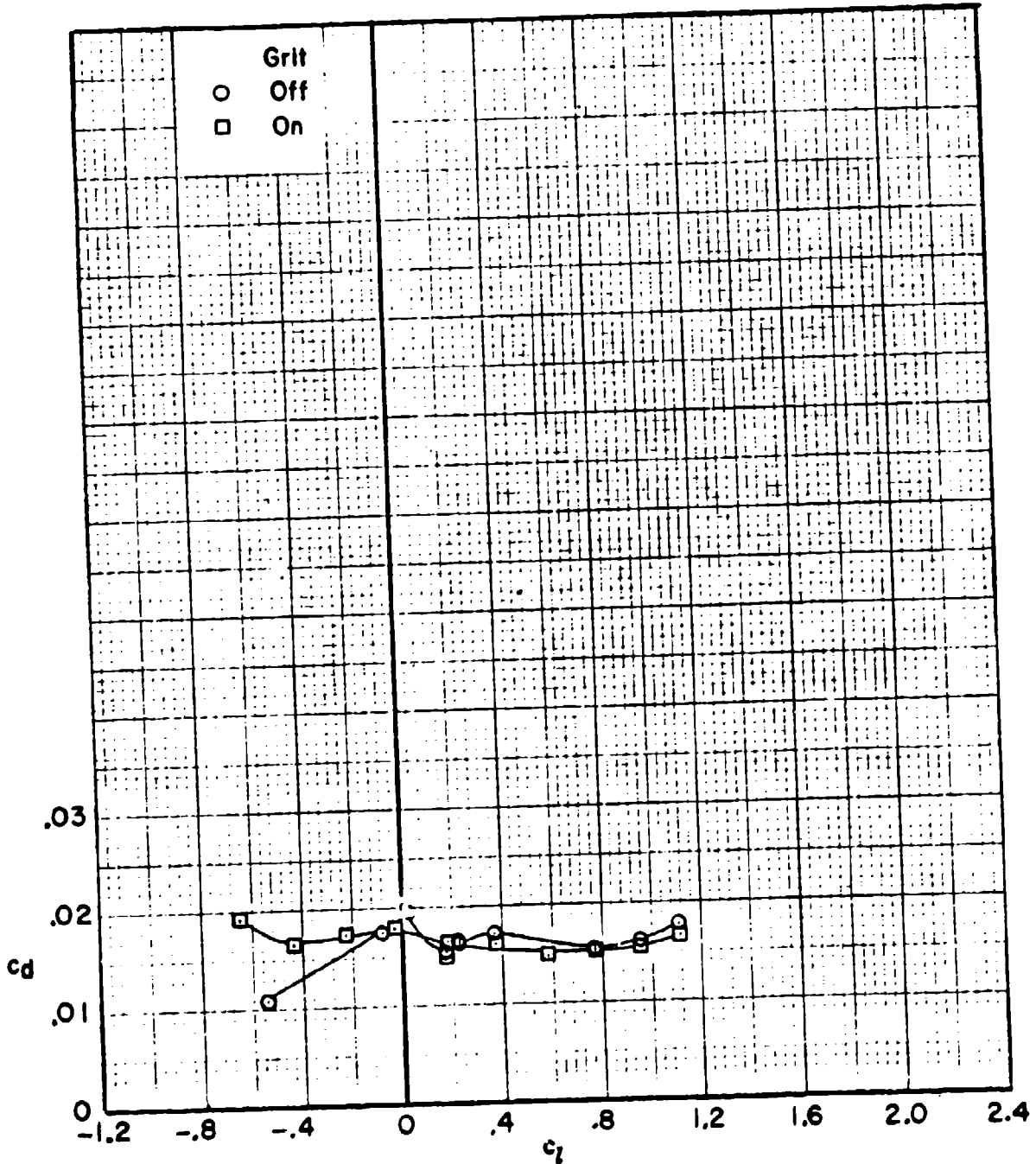
HC144R1070

TWO-DIMENSIONAL SECTION CHARACTERISTICS OF A 12-PERCENT BVR
AIRFOIL WITH TRAILING EDGE FORWARD. $M = 0.26$; $R = 7.60 \times 10^6$



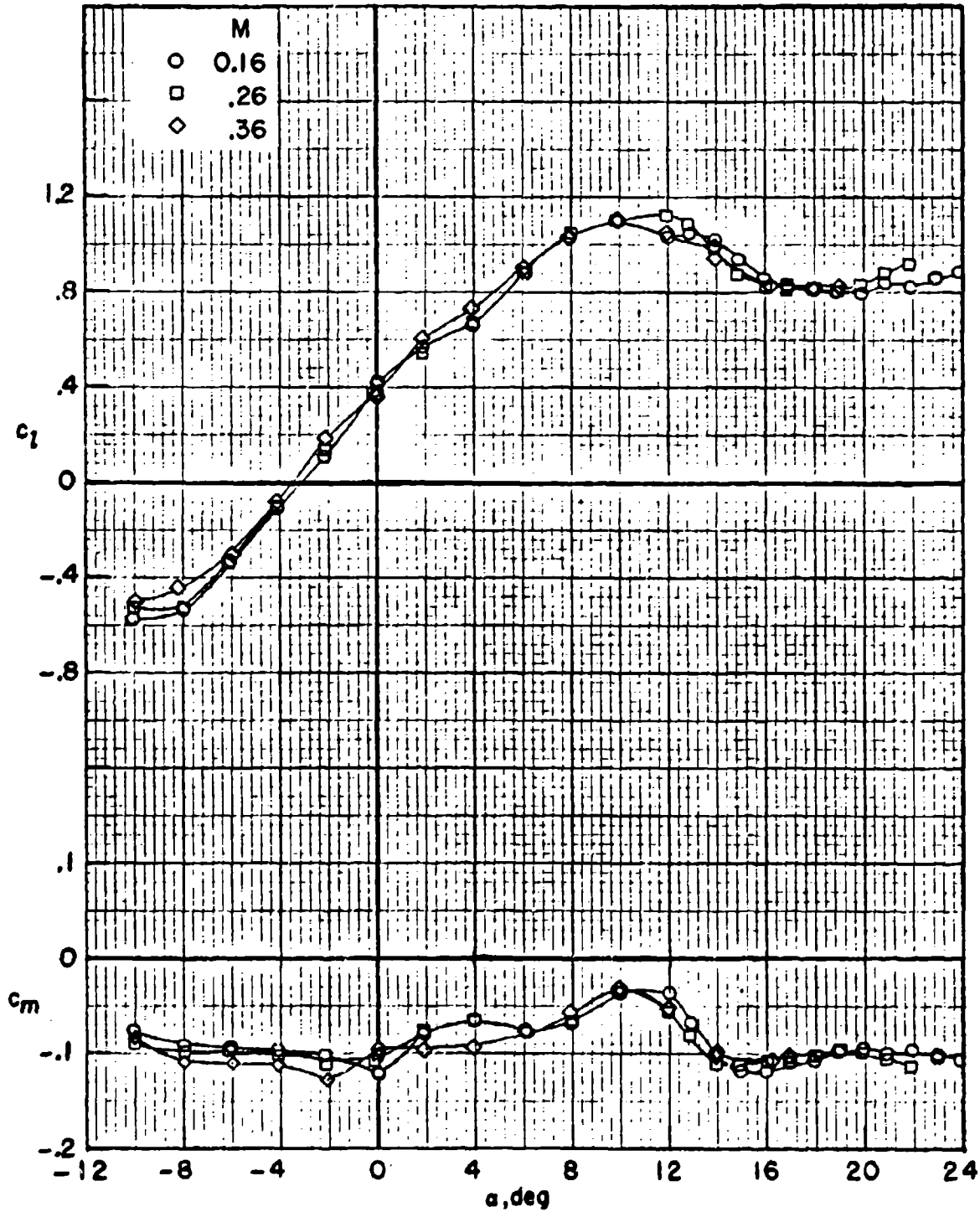
HC144R1070

TWO-DIMENSIONAL SECTION CHARACTERISTICS OF A 12-PERCENT RVR
AIRFOIL WITH TRAILING EDGE FORWARD. $M = 0.28$; $R = 7.60 \times 10^6$



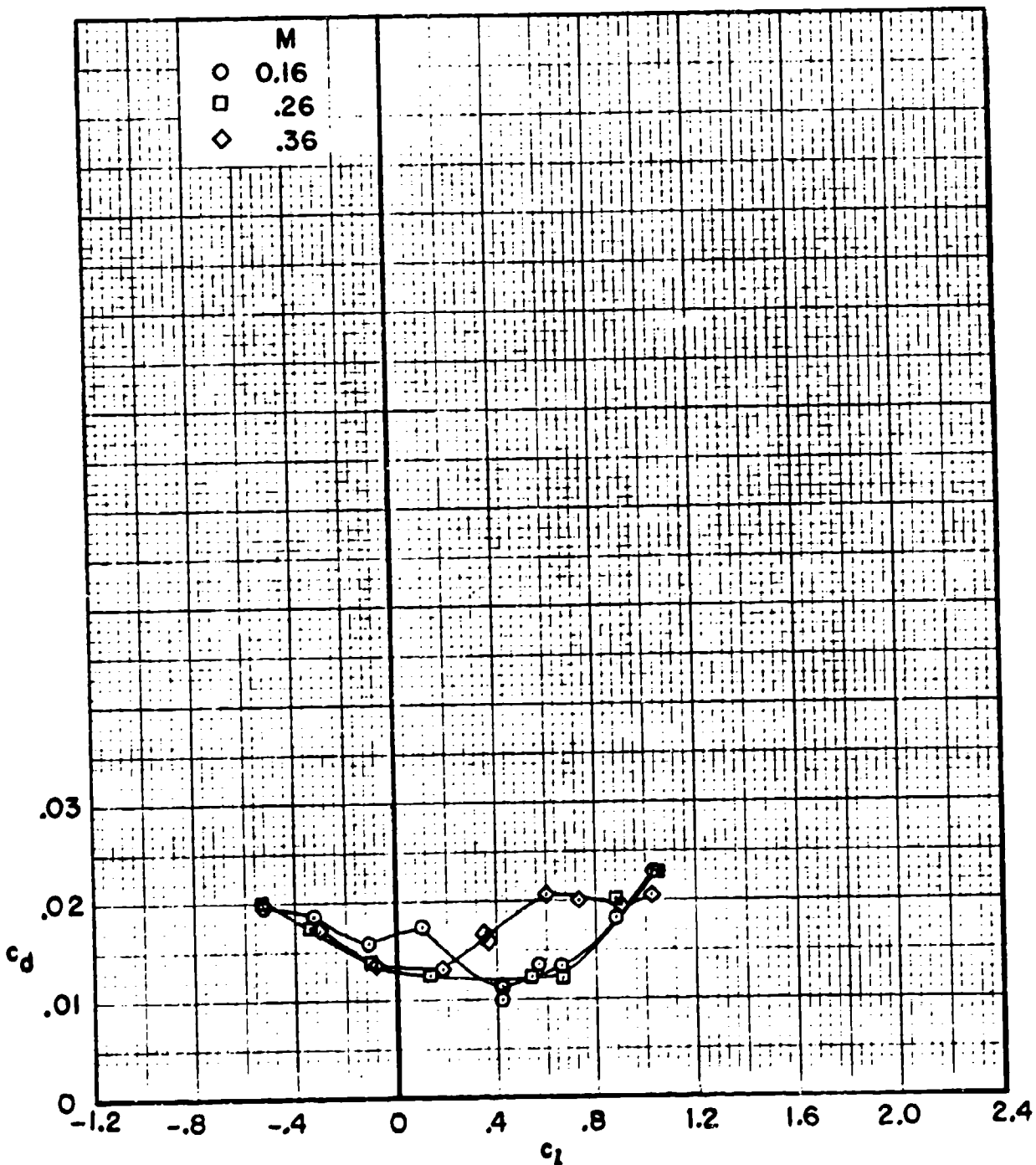
HC144R1070

TWO-DIMENSIONAL SECTION CHARACTERISTICS OF A 12-PERCENT RVR
AIRFOIL WITH TRAILING EDGE FORWARD. $R = 2.56 \times 10^6$; MODEL SMOOTH



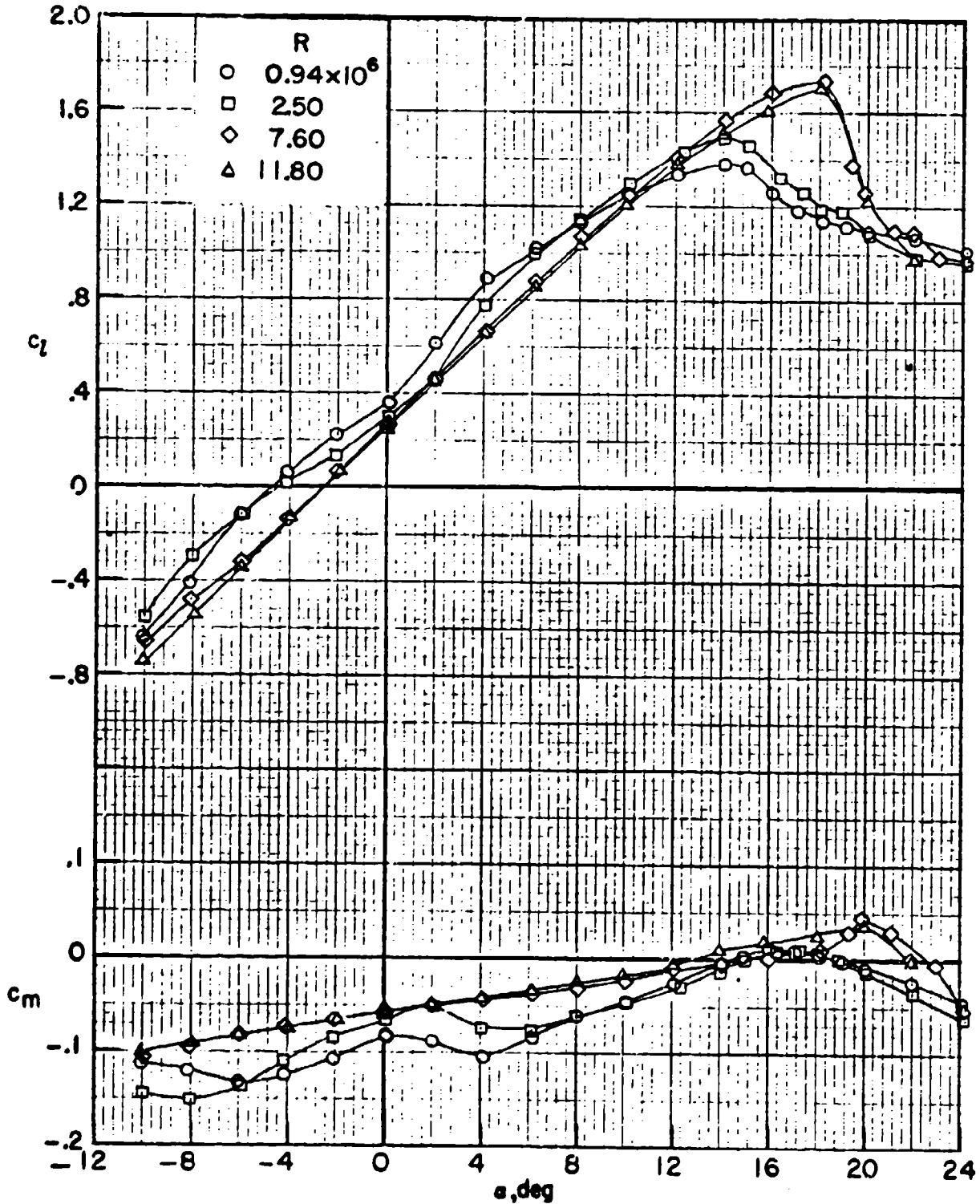
HC144R1070

TWO-DIMENSIONAL SECTION CHARACTERISTICS OF A 12-PERCENT RVR AIRFOIL WITH TRAILING EDGE FORWARD. $R = 2.56 \times 10^6$; MODEL SMOOTH



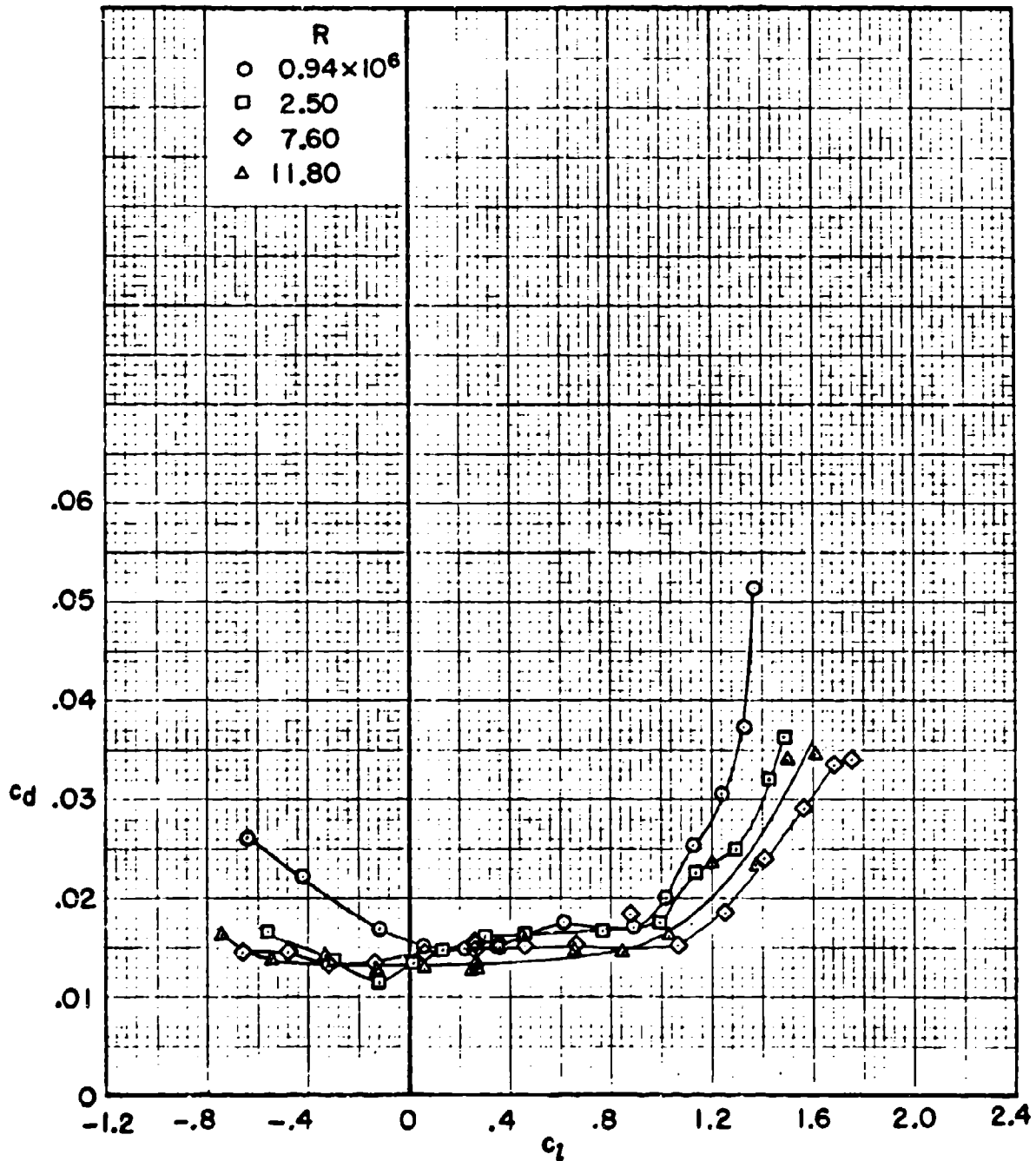
HC144R1070

TWO-DIMENSIONAL SECTION CHARACTERISTICS OF AN 18-PERCENT RVR AIRFOIL WITH LEADING EDGE FORWARD. $M = 0.26$; MODEL SMOOTH



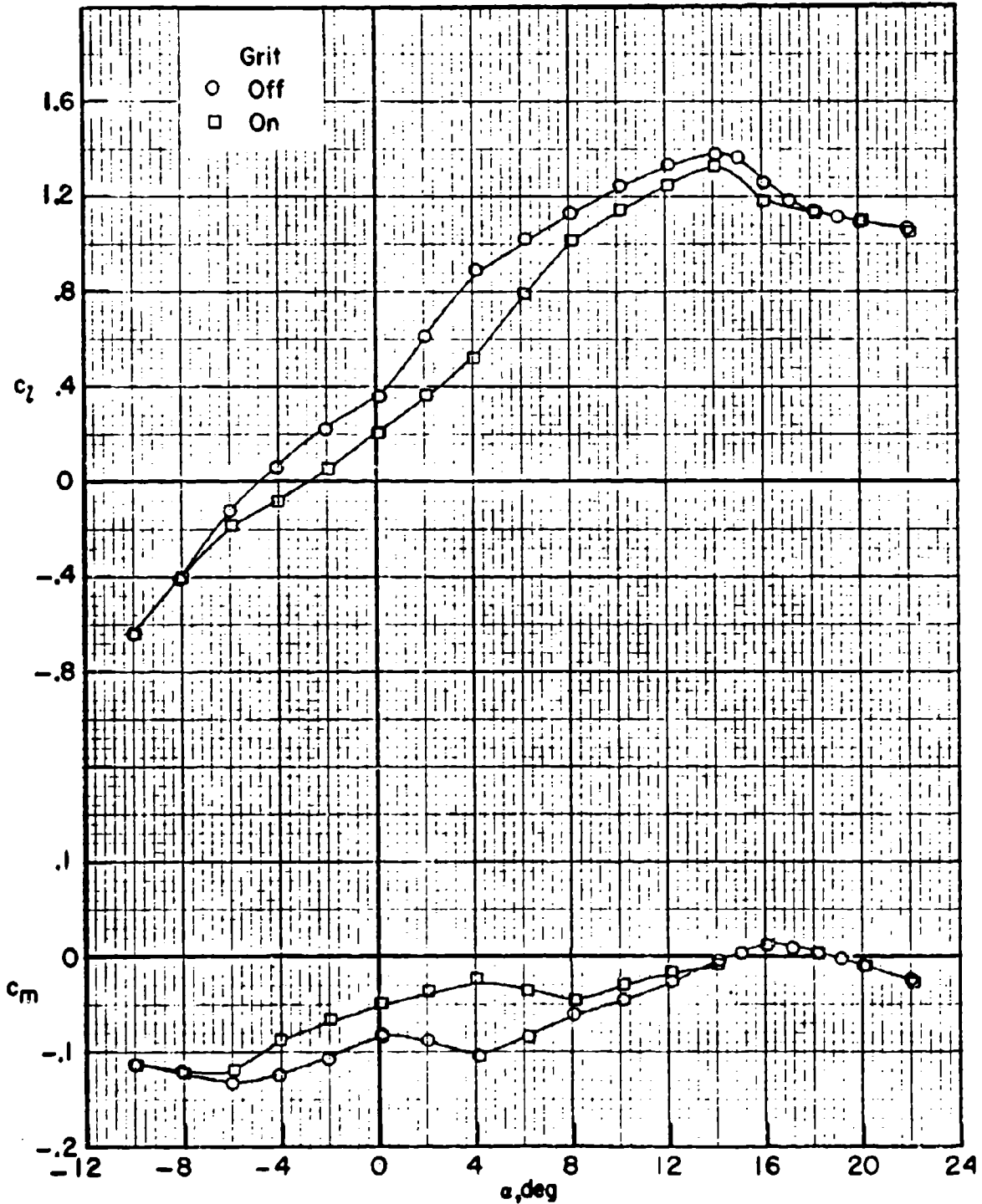
HC144R1070

TWO-DIMENSIONAL SECTION CHARACTERISTICS OF AN 18-PERCENT RVR AIRFOIL WITH LEADING EDGE FORWARD. $M = 0.26$; MODEL SMOOTH



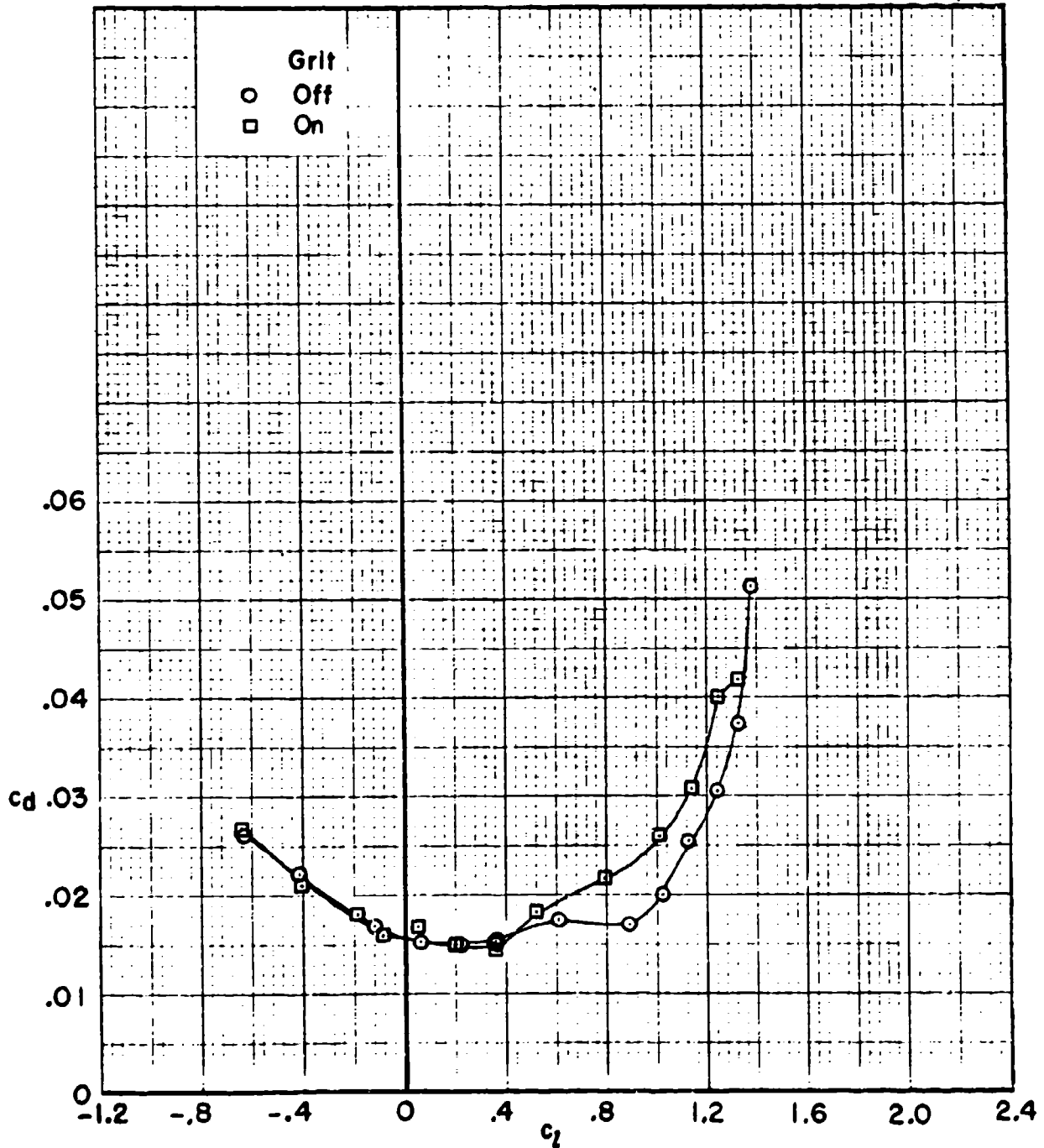
HC144R1070

TWO-DIMENSIONAL SECTION CHARACTERISTICS OF AN 18-PERCENT RVR AIRFOIL WITH LEADING EDGE FORWARD. $M = 0.26$; $R = 0.94 \times 10^6$



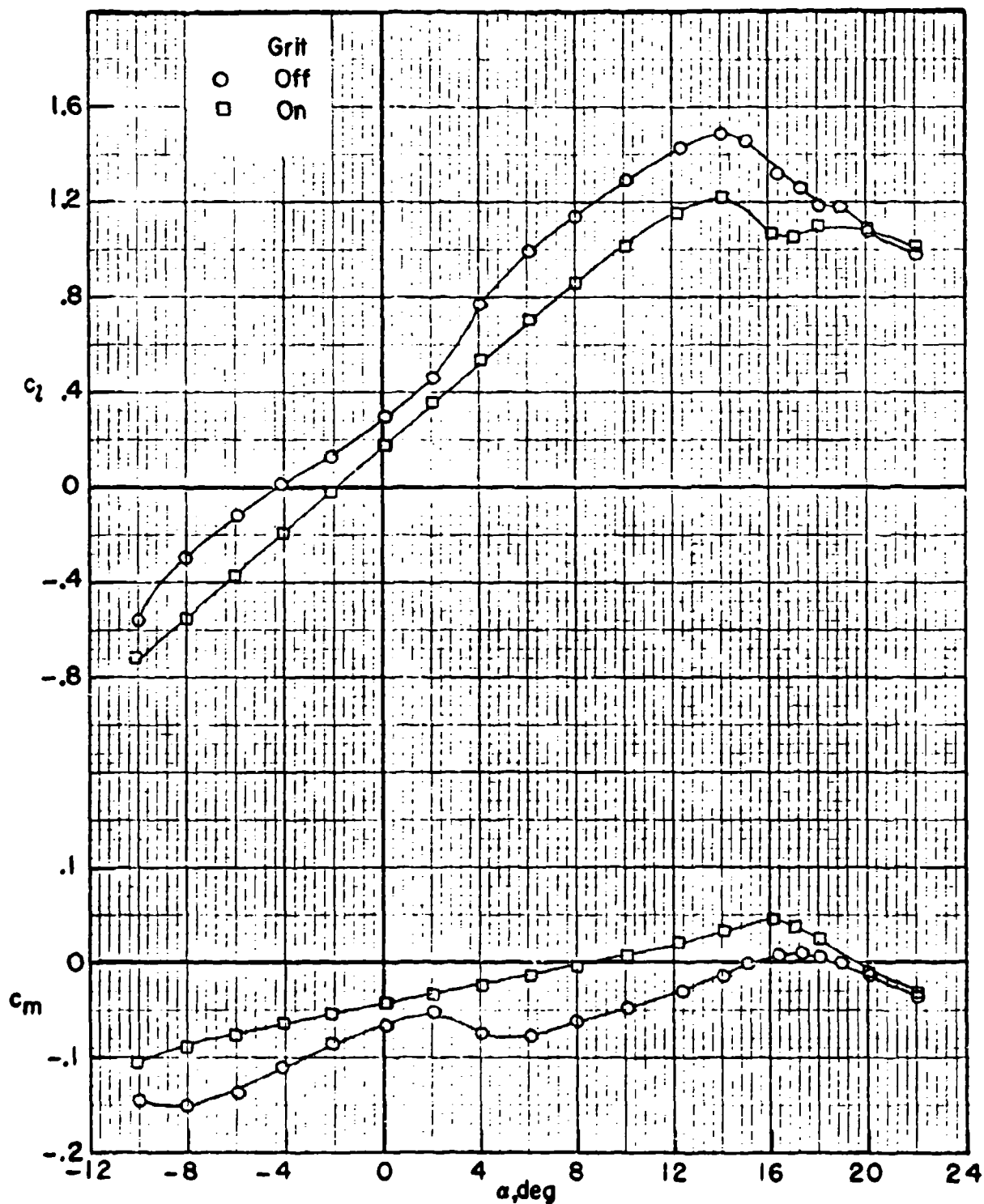
HC144R1070

TWO-DIMENSIONAL SECTION CHARACTERISTICS OF AN 18-PERCENT RVR
AIRFOIL WITH LEADING EDGE FORWARD. $M = 0.26$; $R = 0.94 \times 10^6$



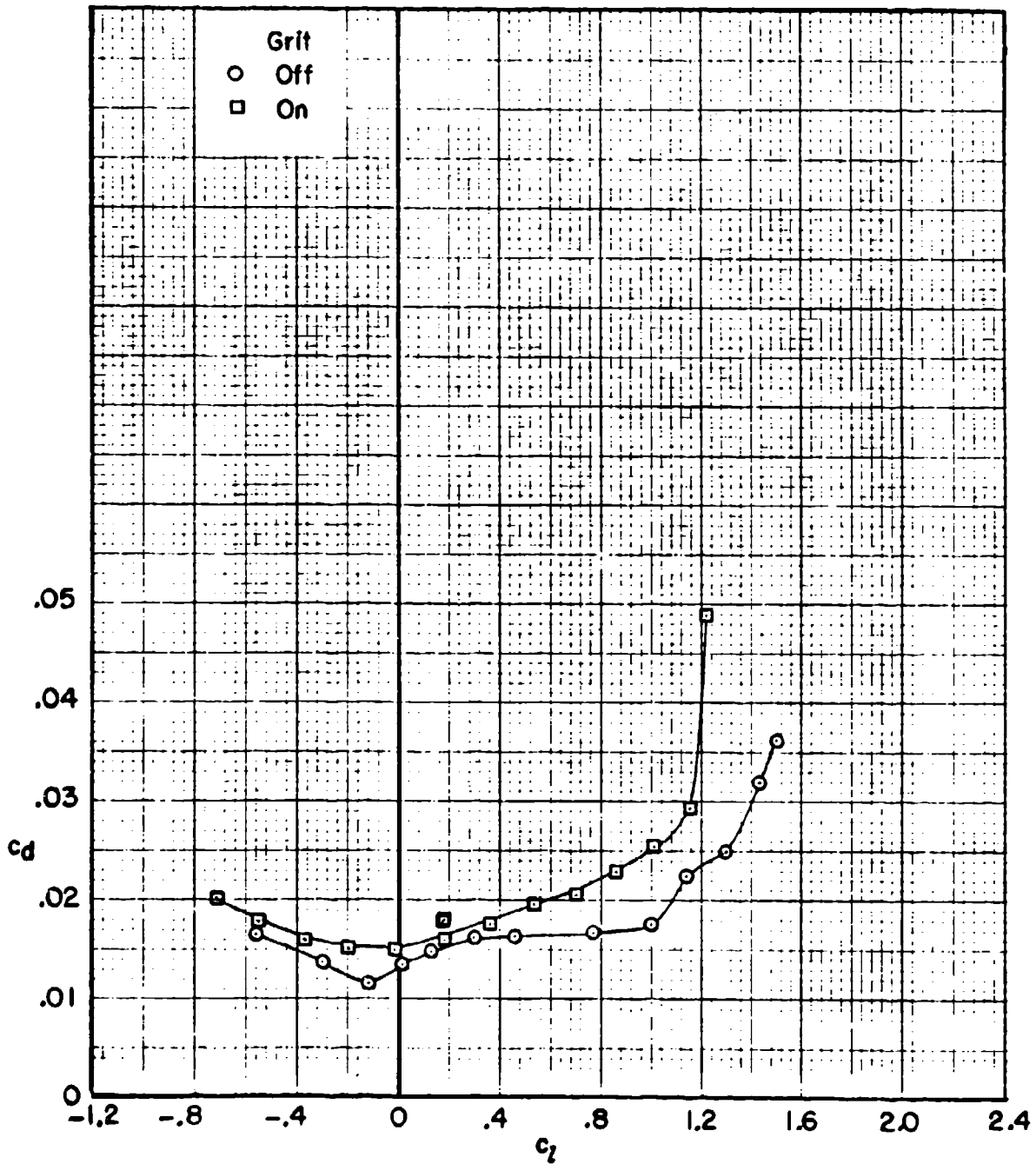
HC144R1070

**TWO-DIMENSIONAL SECTION CHARACTERISTICS OF AN 18-PERCENT RVR
AIRFOIL WITH LEADING EDGE FORWARD. $M = 0.26$; $R = 2.5 \times 10^6$**

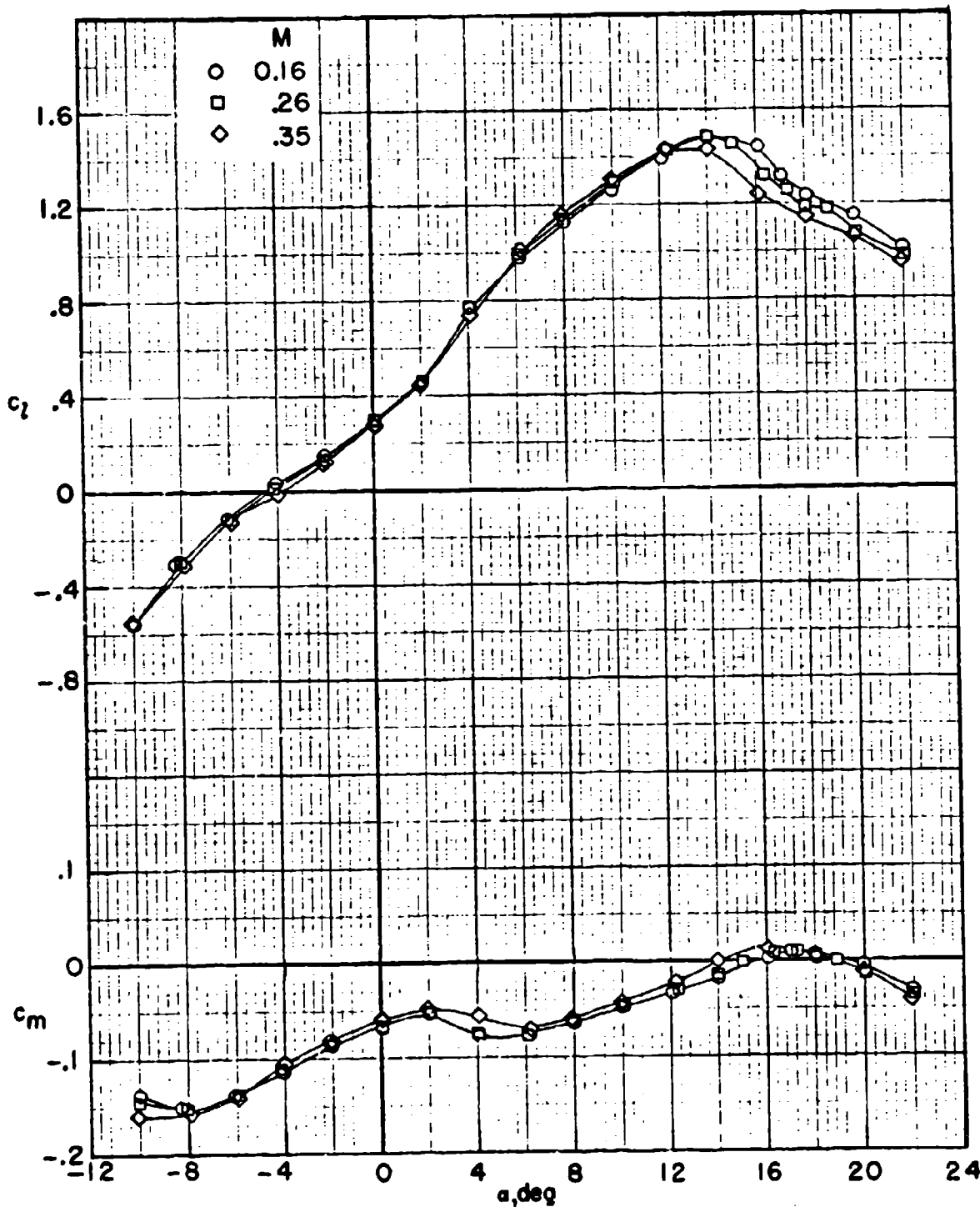


HC144R1070

**TWO-DIMENSIONAL SECTION CHARACTERISTICS OF AN 18-PERCENT RVR
AIRFOIL WITH LEADING EDGE FORWARD. $M = 0.26$; $R = 2.5 \times 10^6$**

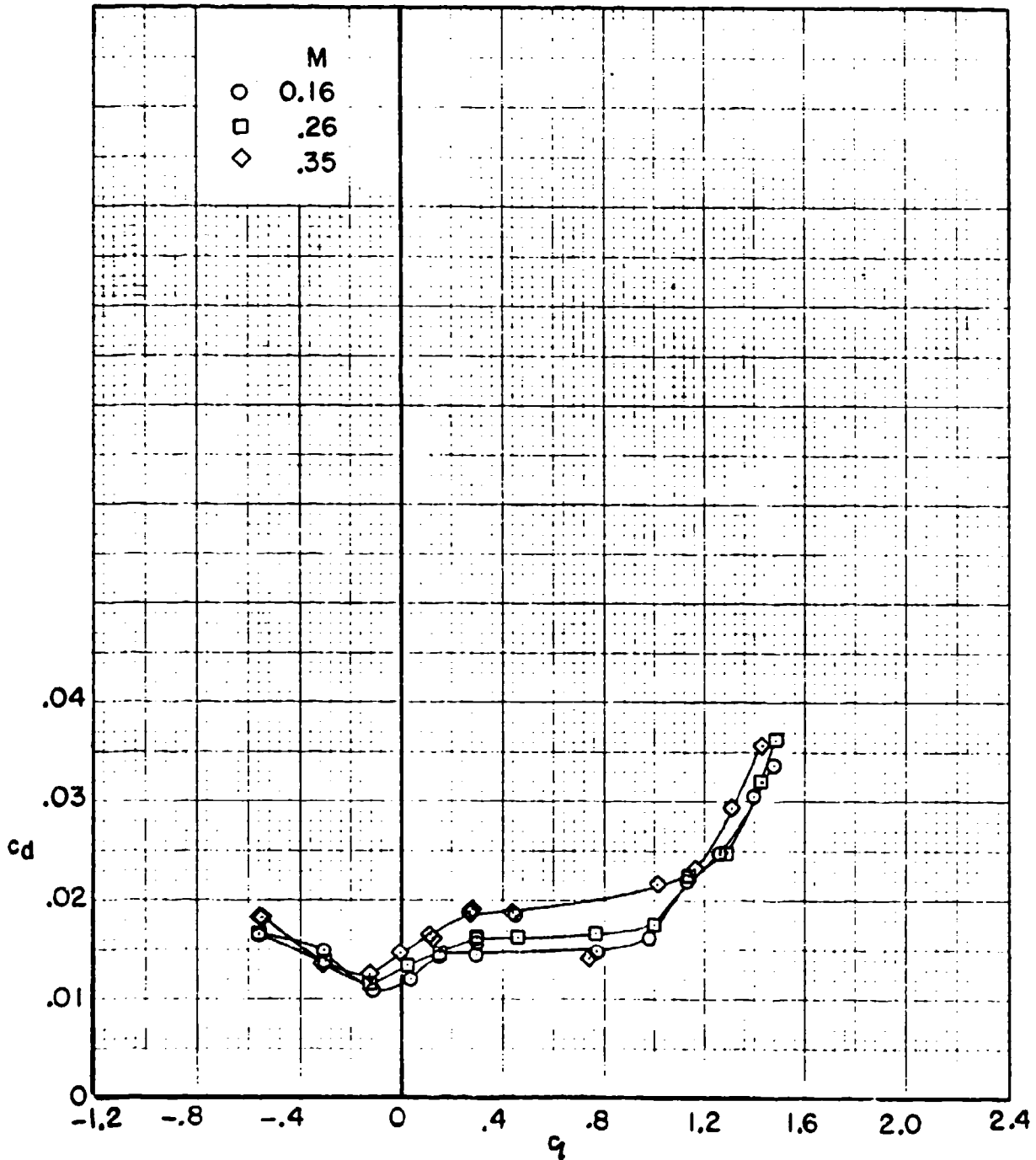


TWO-DIMENSIONAL SECTION CHARACTERISTICS OF AN 18-PERCENT RVR AIRFOIL WITH LEADING EDGE FORWARD. $R = 2.50 \times 10^6$; MODEL SMOOTH



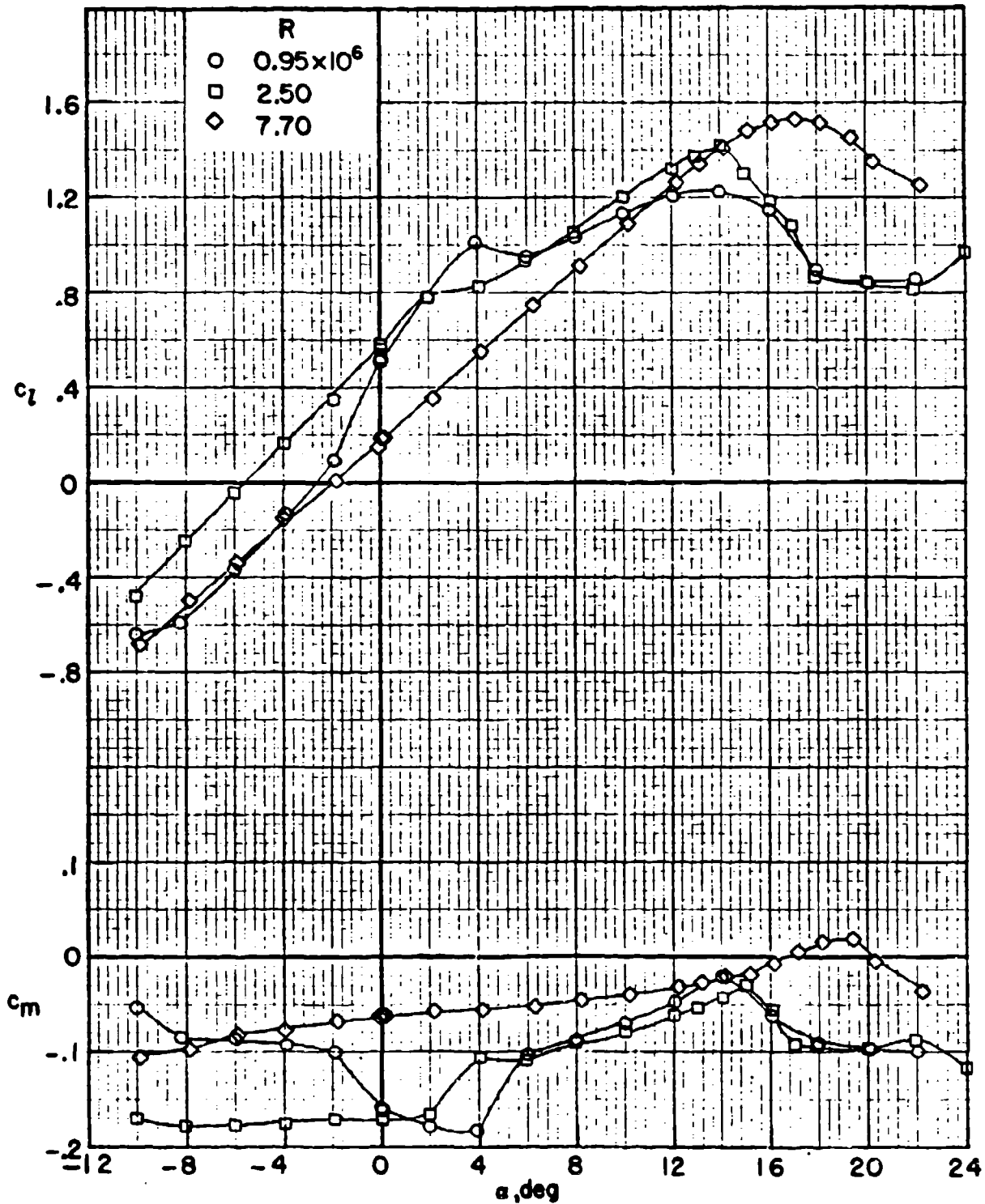
HC144R1070

TWO-DIMENSIONAL SECTION CHARACTERISTICS OF AN 18-PERCENT RVR AIRFOIL WITH LEADING EDGE FORWARD. $R = 2.50 \times 10^6$; MODEL SMOOTH



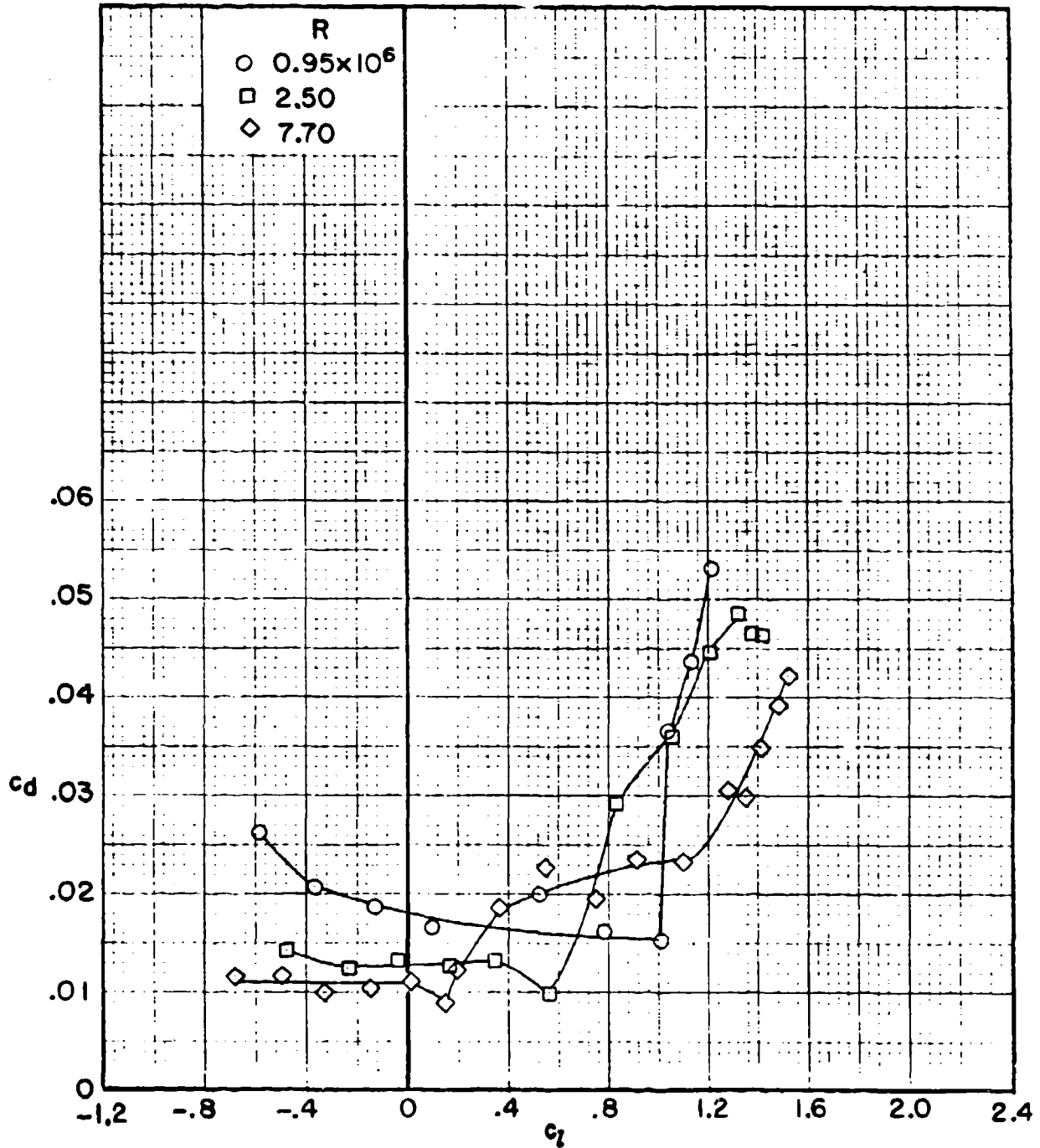
HC144R1070

TWO-DIMENSIONAL SECTION CHARACTERISTICS OF AN 18-PERCENT RVR AIRFOIL WITH TRAILING EDGE FORWARD. $M = 0.26$; MODEL SMOOTH

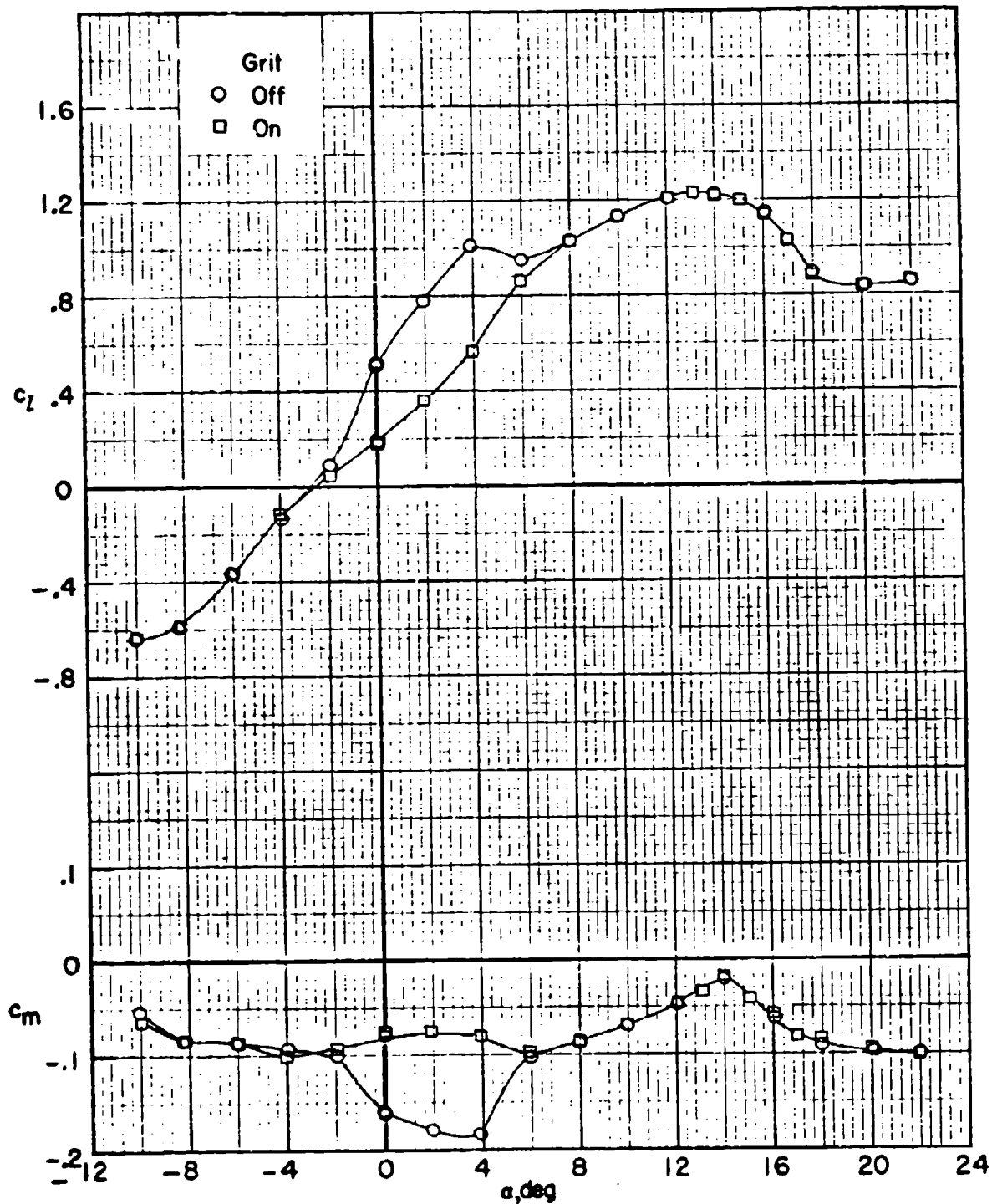


HC144R1070

TWO-DIMENSIONAL SECTION CHARACTERISTICS OF AN 18-PERCENT RVR AIRFOIL WITH TRAILING EDGE FORWARD. $M = 0.26$; MODEL SMOOTH

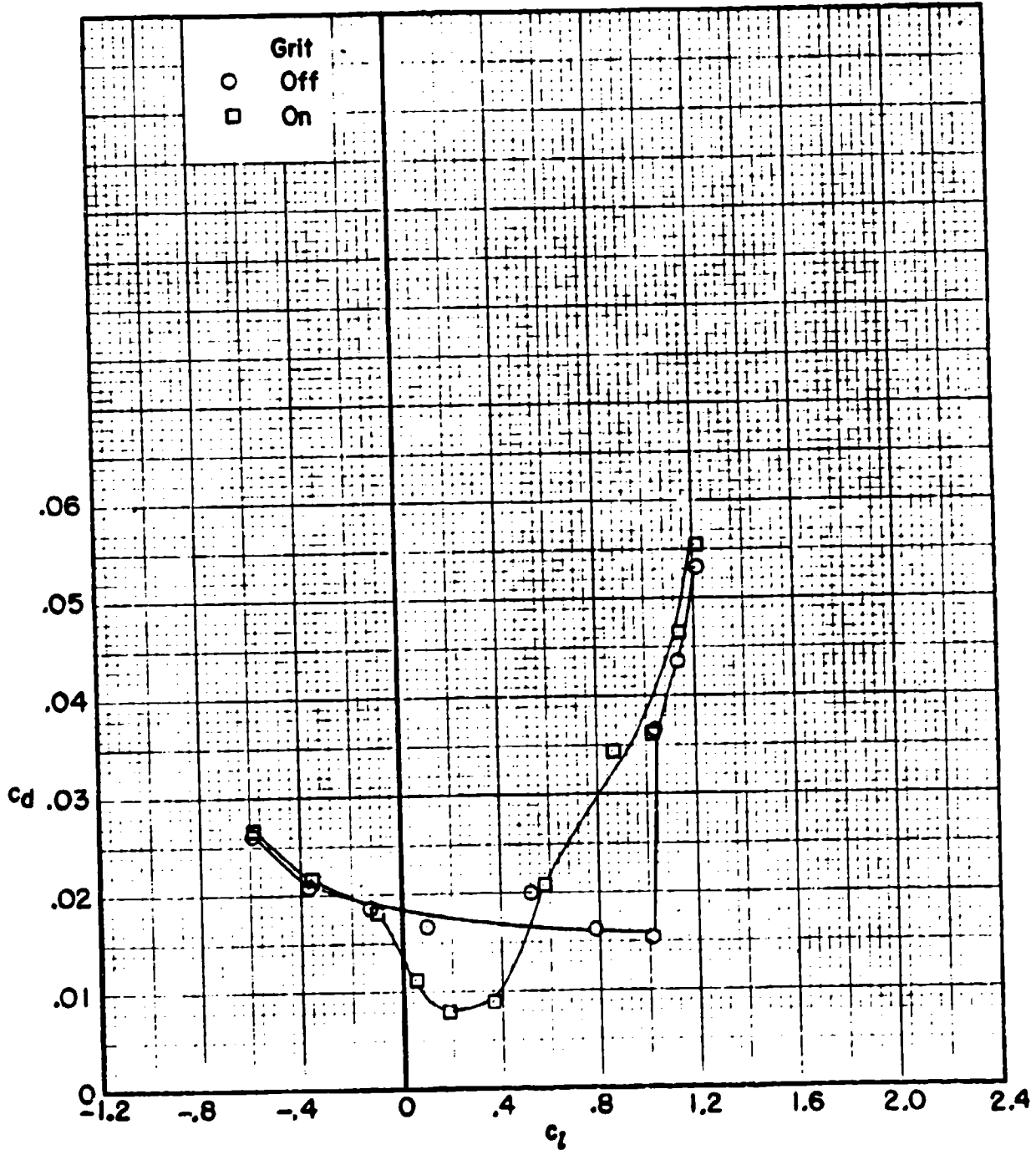


TWO-DIMENSIONAL SECTION CHARACTERISTICS OF AN 18-PERCENT RVR
AIRFOIL WITH TRAILING EDGE FORWARD. $M = 0.26$; $R = 0.95 \times 10^6$

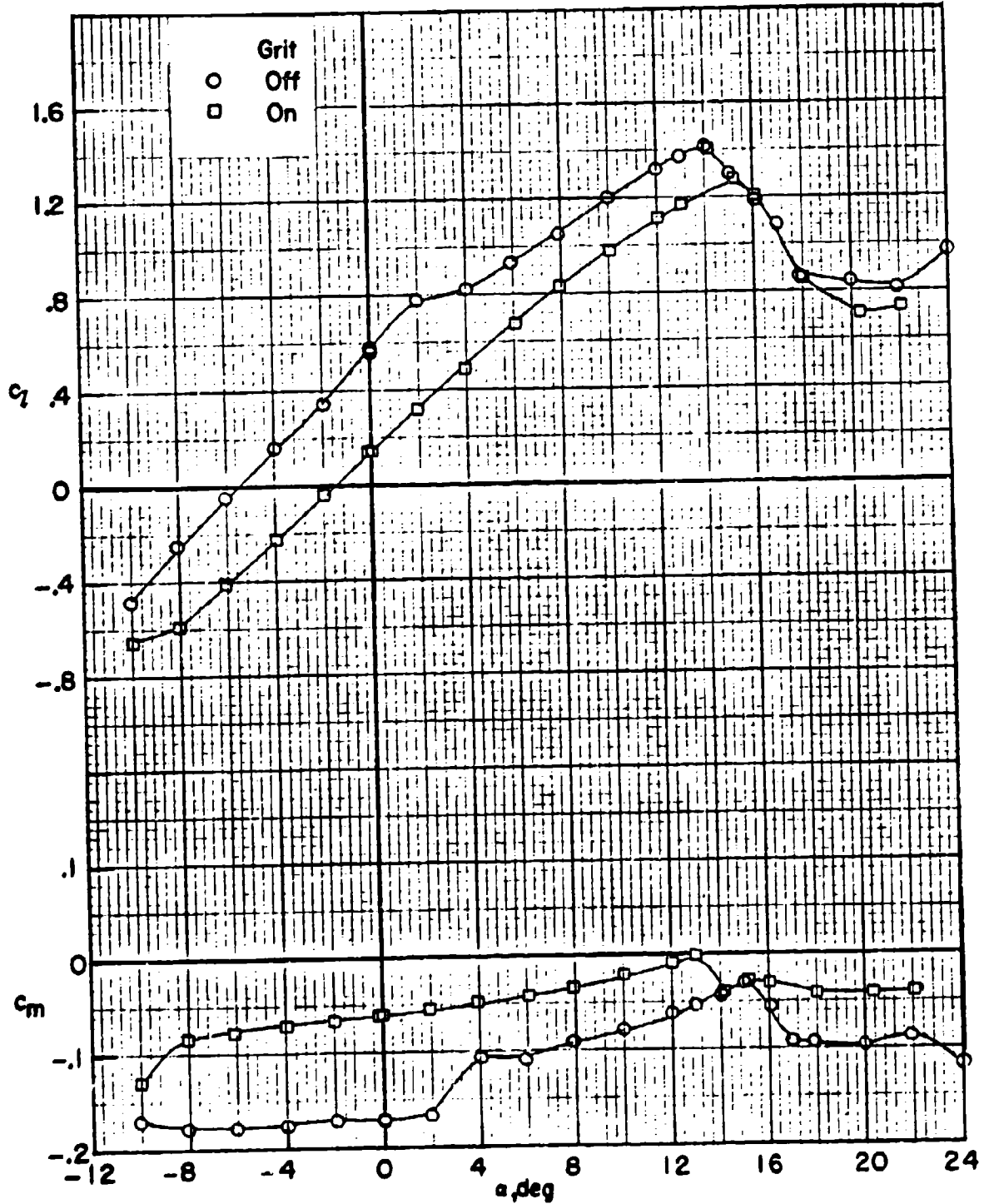


HC144R1070

TWO-DIMENSIONAL SECTION CHARACTERISTICS OF AN 18-PERCENT RVR AIRFOIL WITH TRAILING EDGE FORWARD. $M = 0.26$; $R = 0.95 \times 10^6$

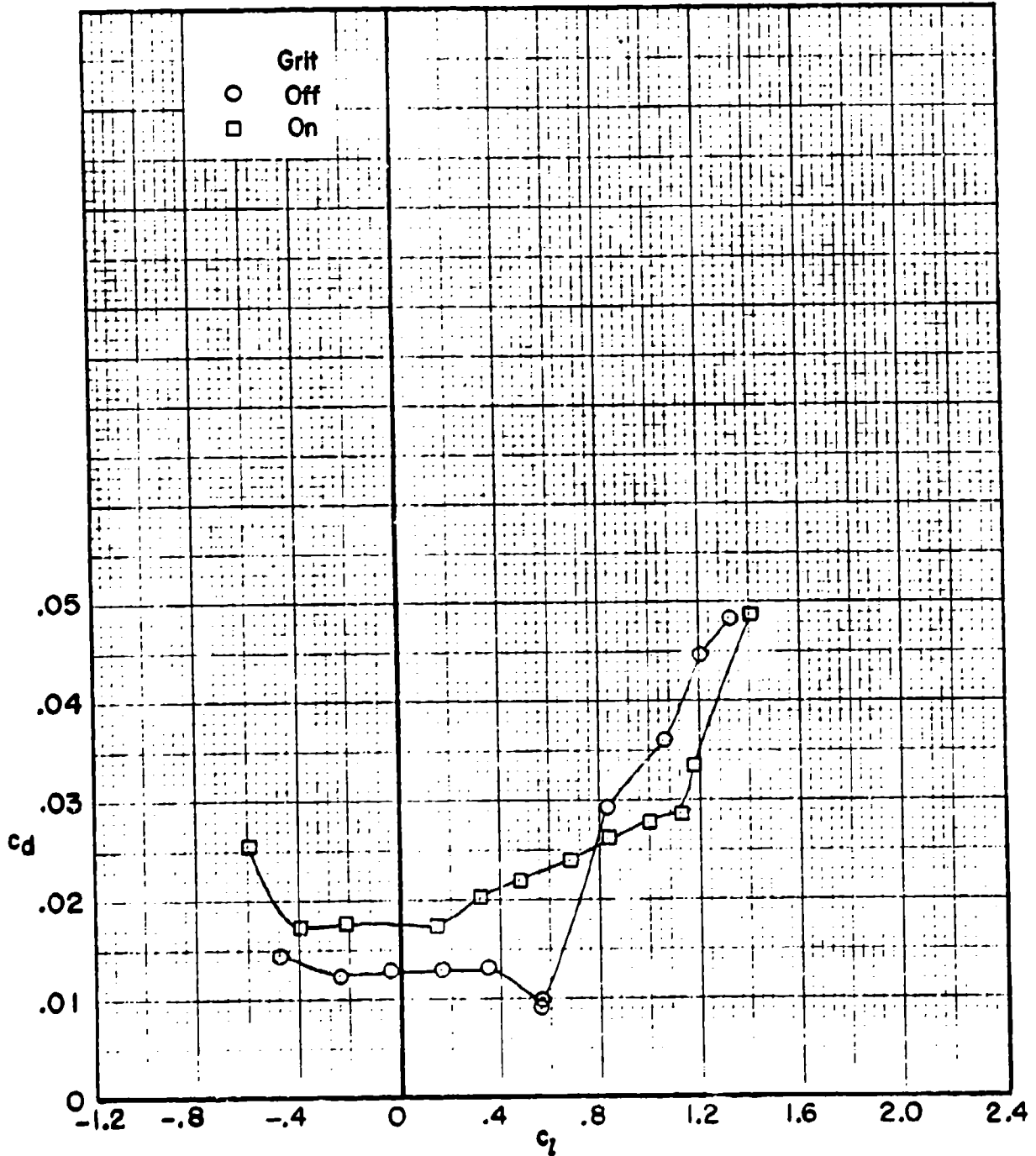


**TWO-DIMENSIONAL SECTION CHARACTERISTICS OF AN 18-PERCENT RVR
AIRFOIL WITH TRAILING EDGE FORWARD. $M = 0.28$; $R = 2.50 \times 10^6$**

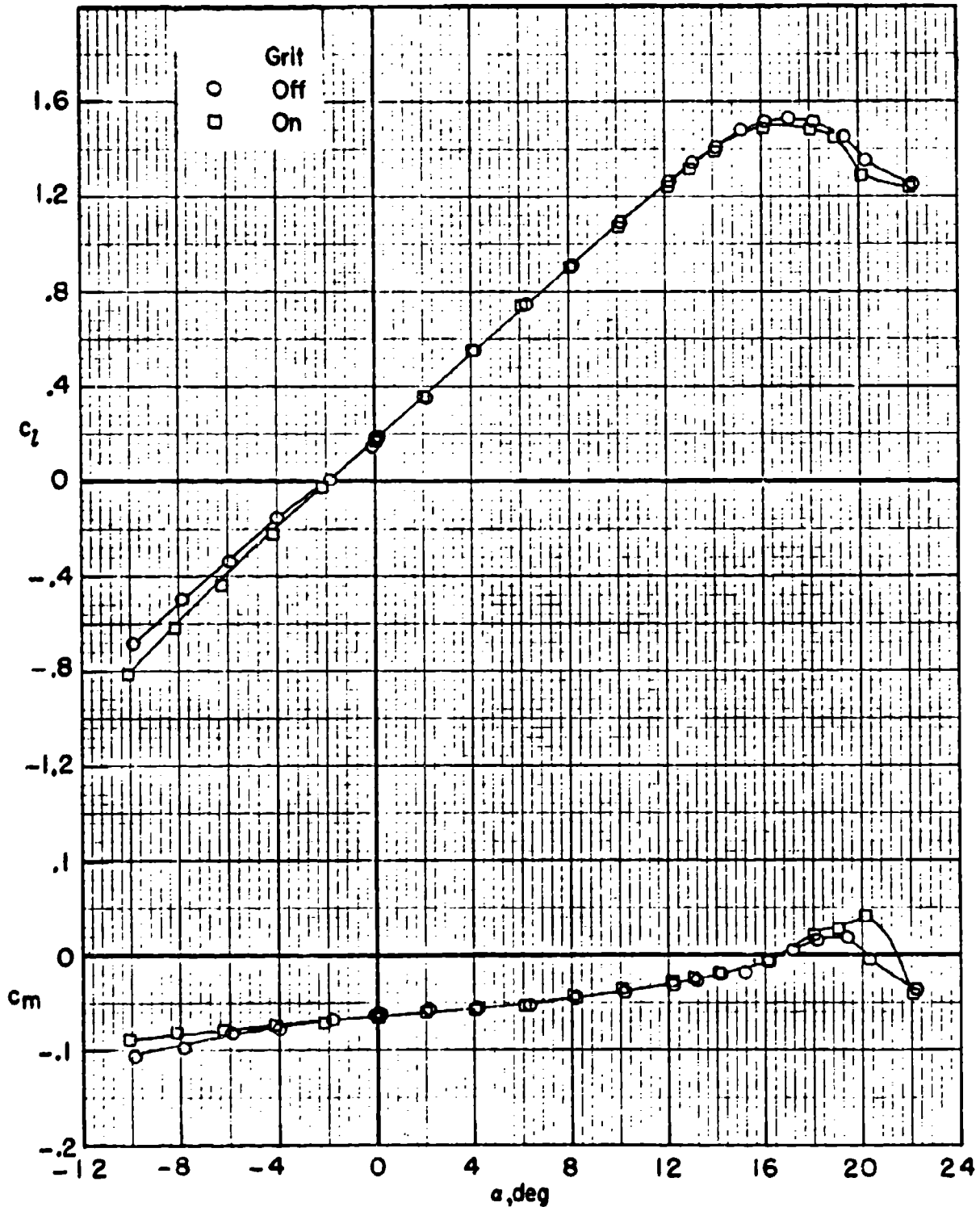


HC144R1070

**TWO-DIMENSIONAL SECTION CHARACTERISTICS OF AN 18-PERCENT RVR
AIRFOIL WITH TRAILING EDGE FORWARD. $M = 0.28$; $R = 2.50 \times 10^6$**

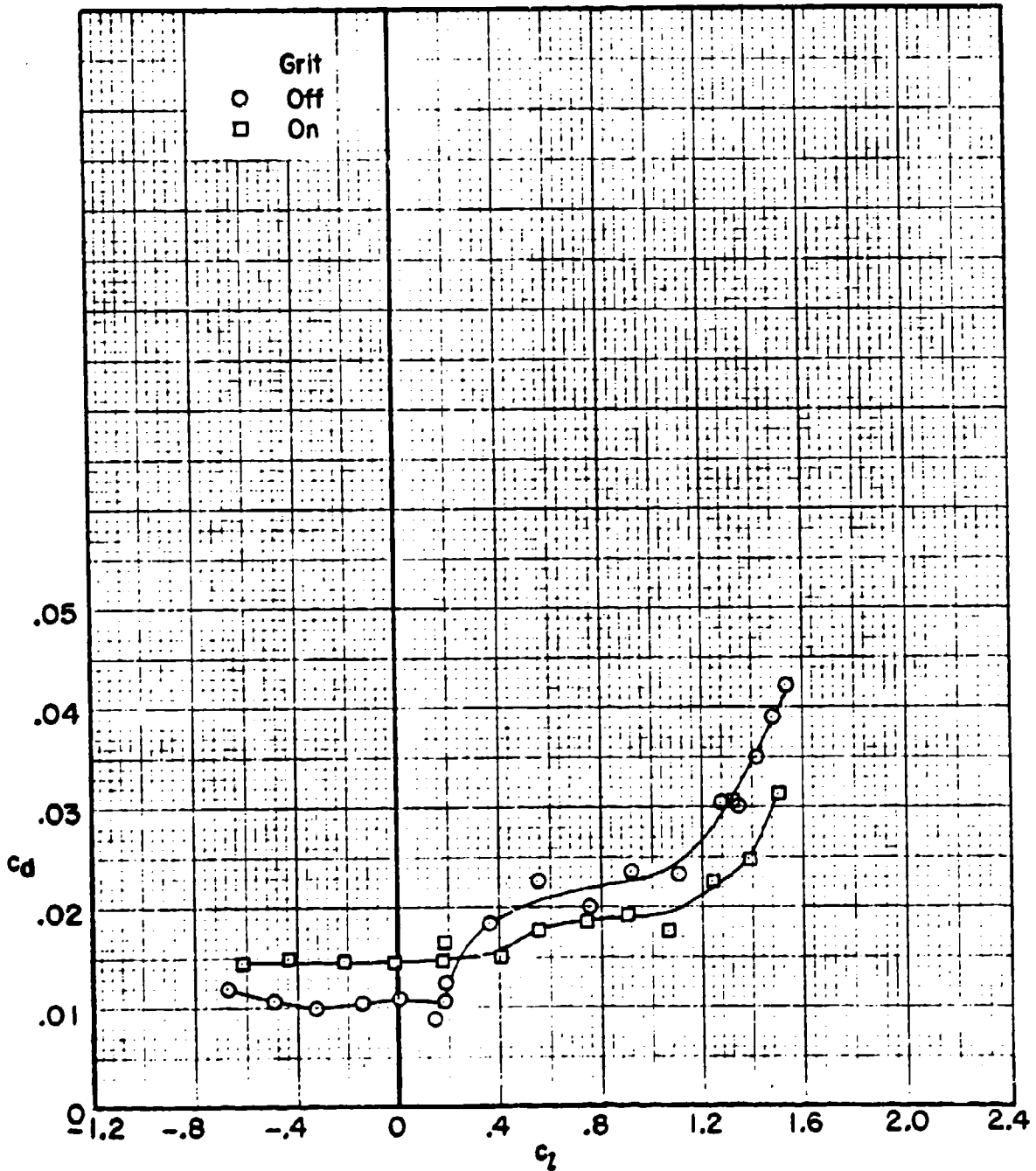


TWO-DIMENSIONAL SECTION CHARACTERISTICS OF AN 18-PERCENT RVR AIRFOIL WITH TRAILING EDGE FORWARD. $M = 0.26$; $R = 7.70 \times 10^6$



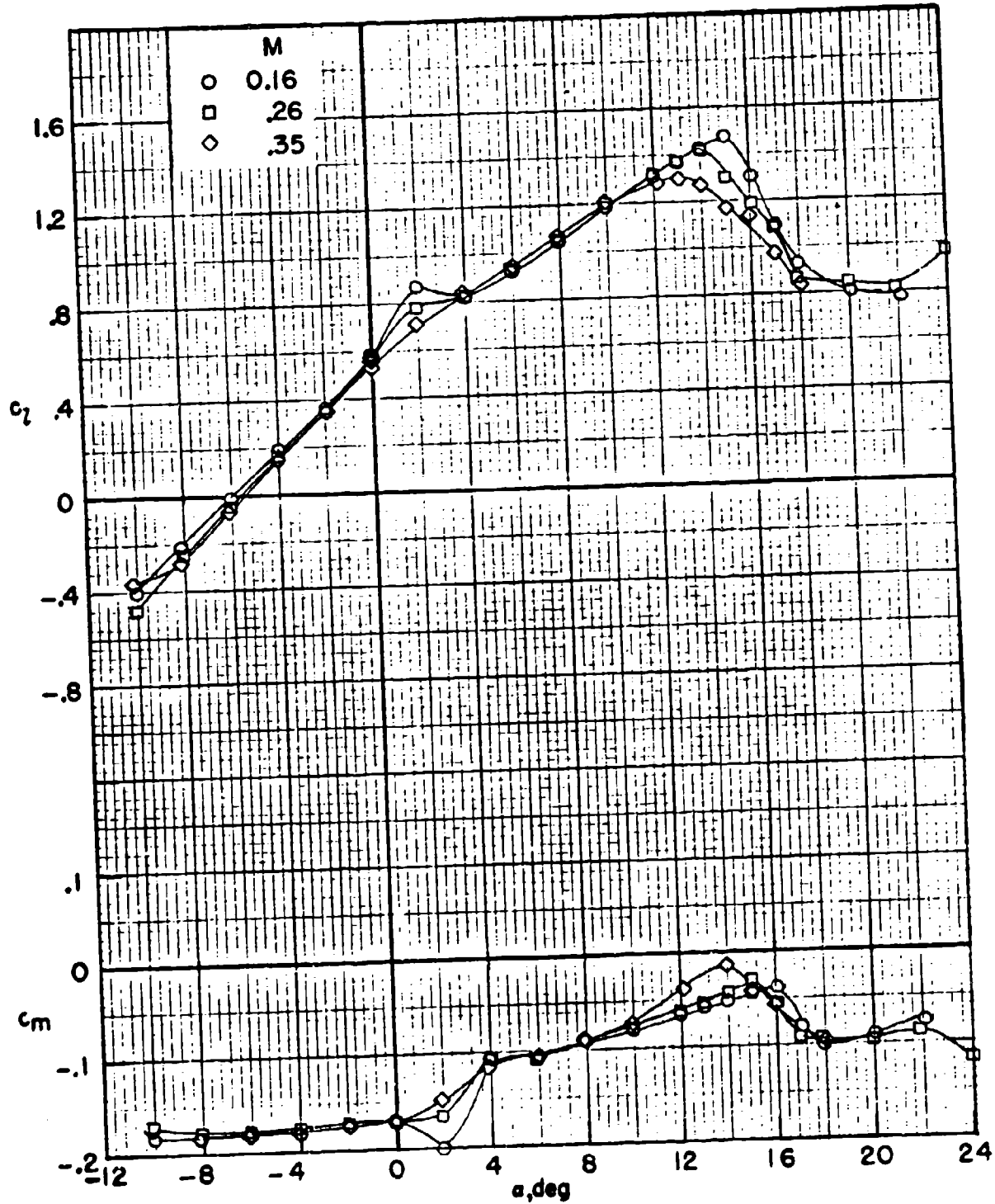
HC144R1070

TWO-DIMENSIONAL SECTION CHARACTERISTICS OF AN 18-PERCENT RVR AIRFOIL WITH TRAILING EDGE FORWARD. $M = 0.26$; $R = 7.70 \times 10^6$

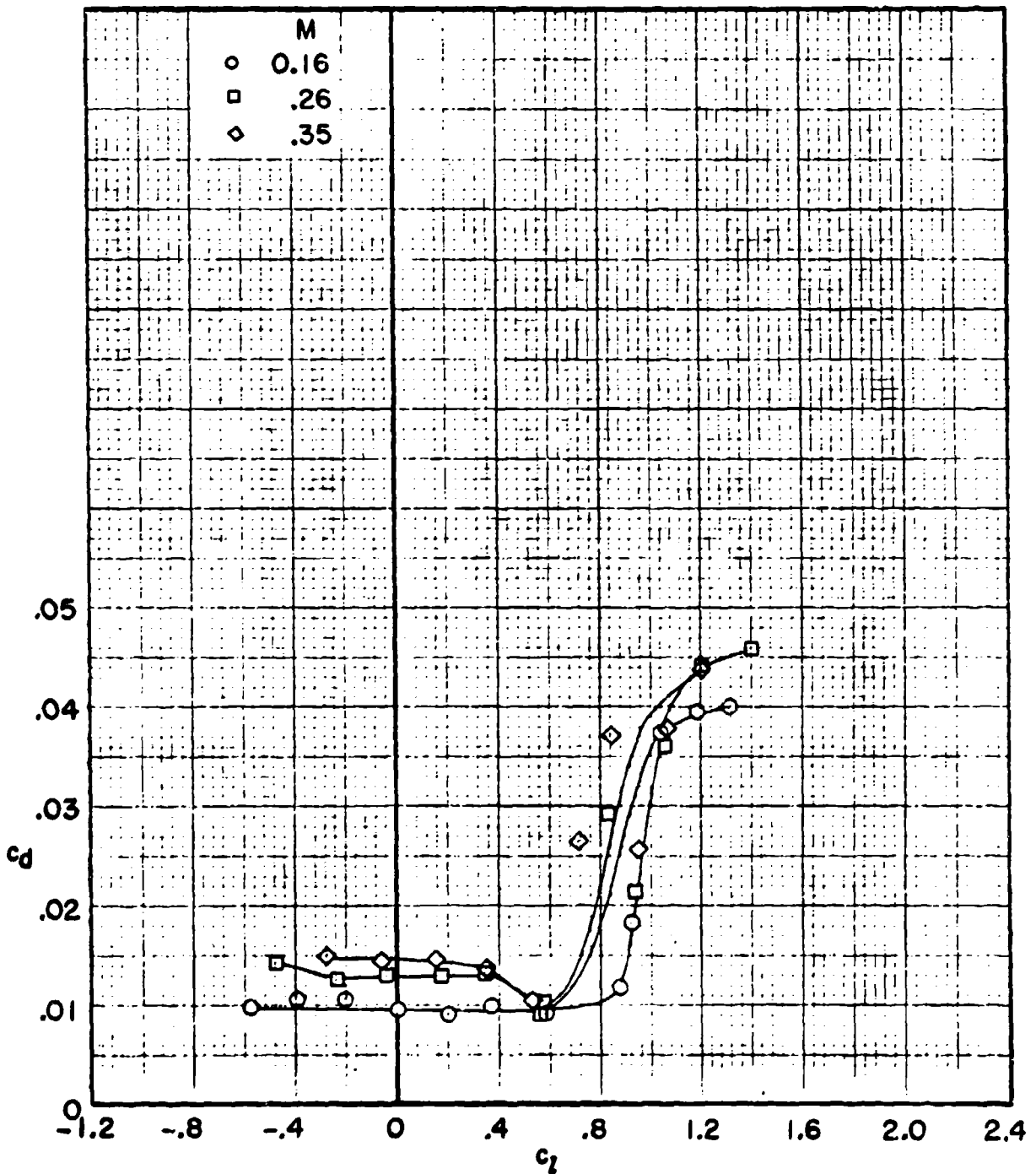


HC144R1070

TWO-DIMENSIONAL SECTION CHARACTERISTICS OF AN 18-PERCENT RVR AIRFOIL WITH TRAILING EDGE FORWARD. $R = 2.50 \times 10^8$; MODEL SMOOTH



TWO-DIMENSIONAL SECTION CHARACTERISTICS OF AN 18-PERCENT RVR AIRFOIL WITH TRAILING EDGE FORWARD. $R = 2.50 \times 10^6$; MODEL SMOOTH



FAIRCHILD
REPUBLIC DIVISION

HC144R1070

This page intentionally left blank.

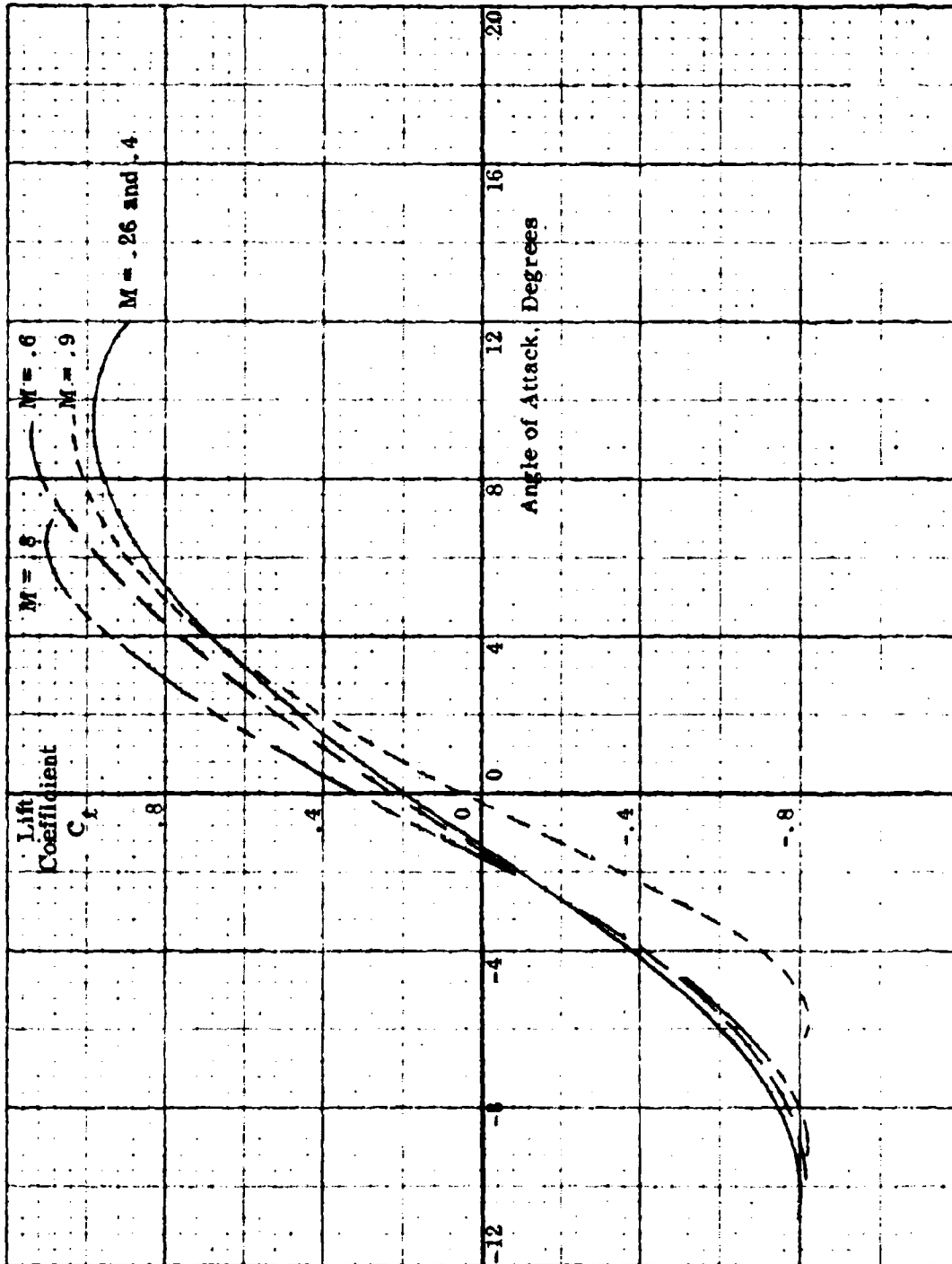
HC144R1070

APPENDIX D

AIRFOIL SECTION DATA

This appendix contains the two sets of airfoil section lift and drag data developed as described in Section 5.1 from the results of the Langley Low Turbulence Pressure Tunnel tests. The first set (Figs D1 through D18) is developed for the Reynolds number range used in the model rotor tests, and the second set (Figs D19 through D36) corresponds to the Reynolds number range of a full scale rotor.

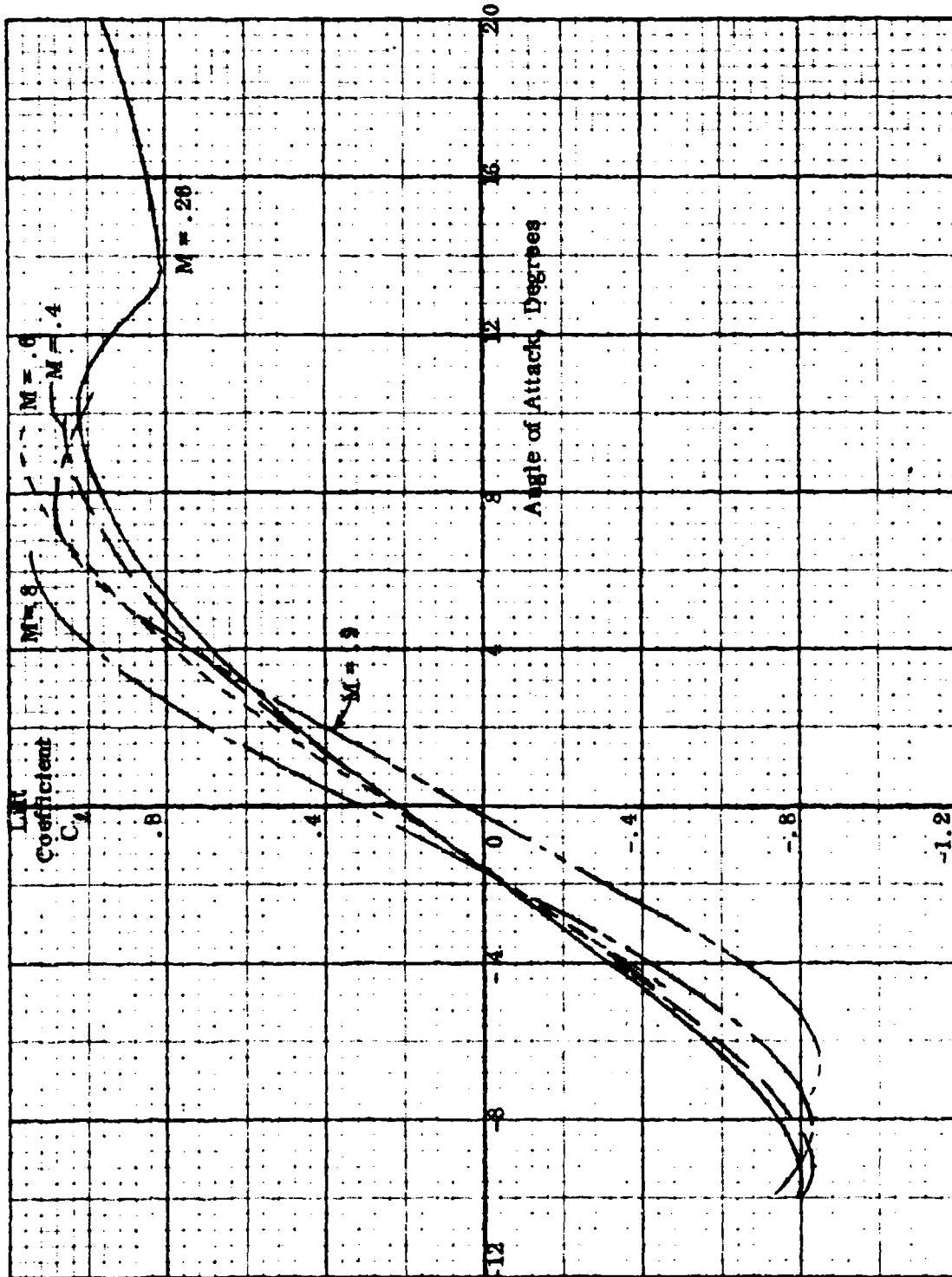
SECTION LIFT COEFFICIENT - 6% AIRFOIL, FORWARD
MODEL REYNOLDS NUMBER



HC144R1070

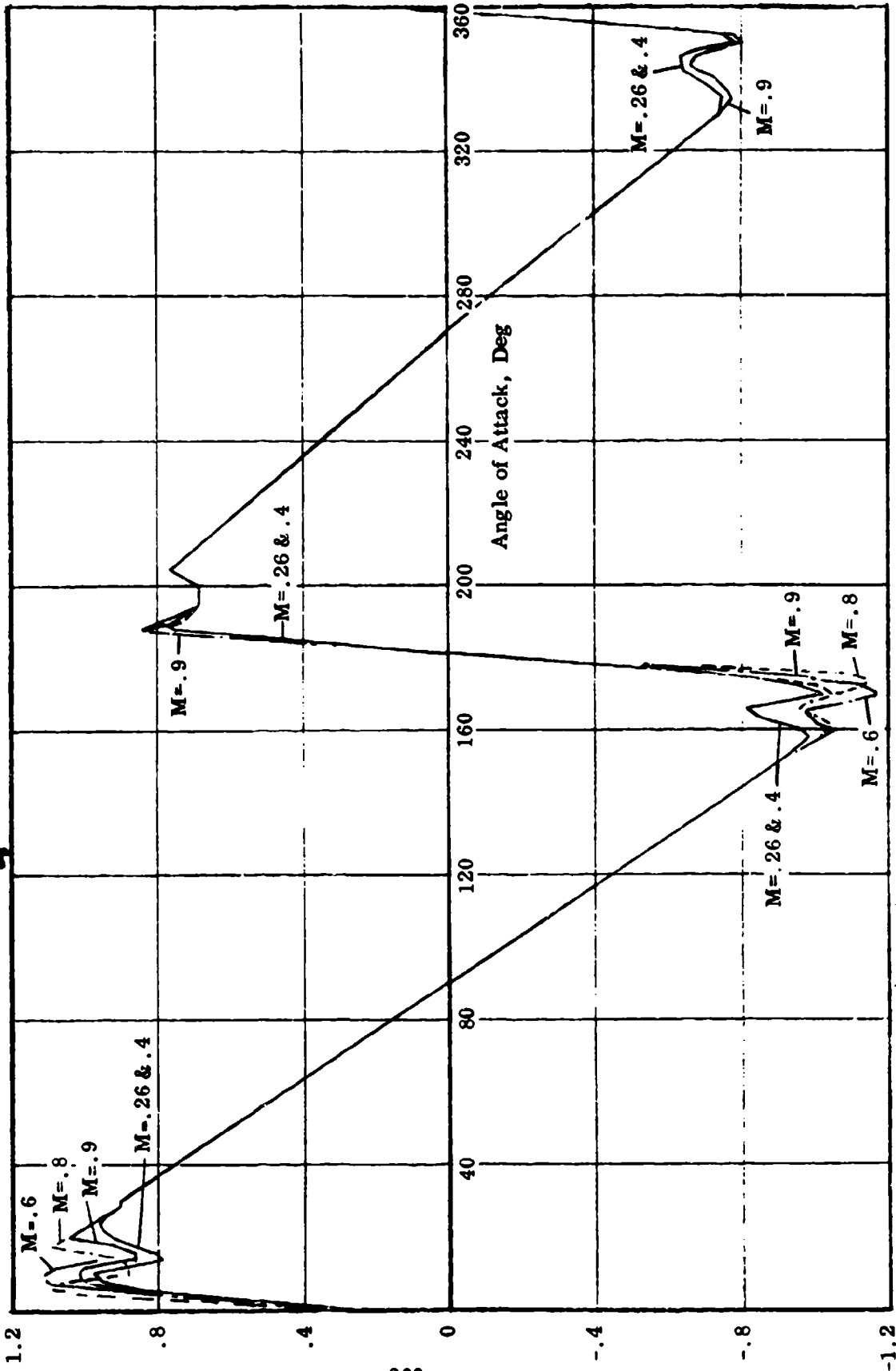
Figure D.2

SECTION LIFT COEFFICIENT -6% AIRFOIL, REVERSE
MODEL REYNOLDS NUMBER

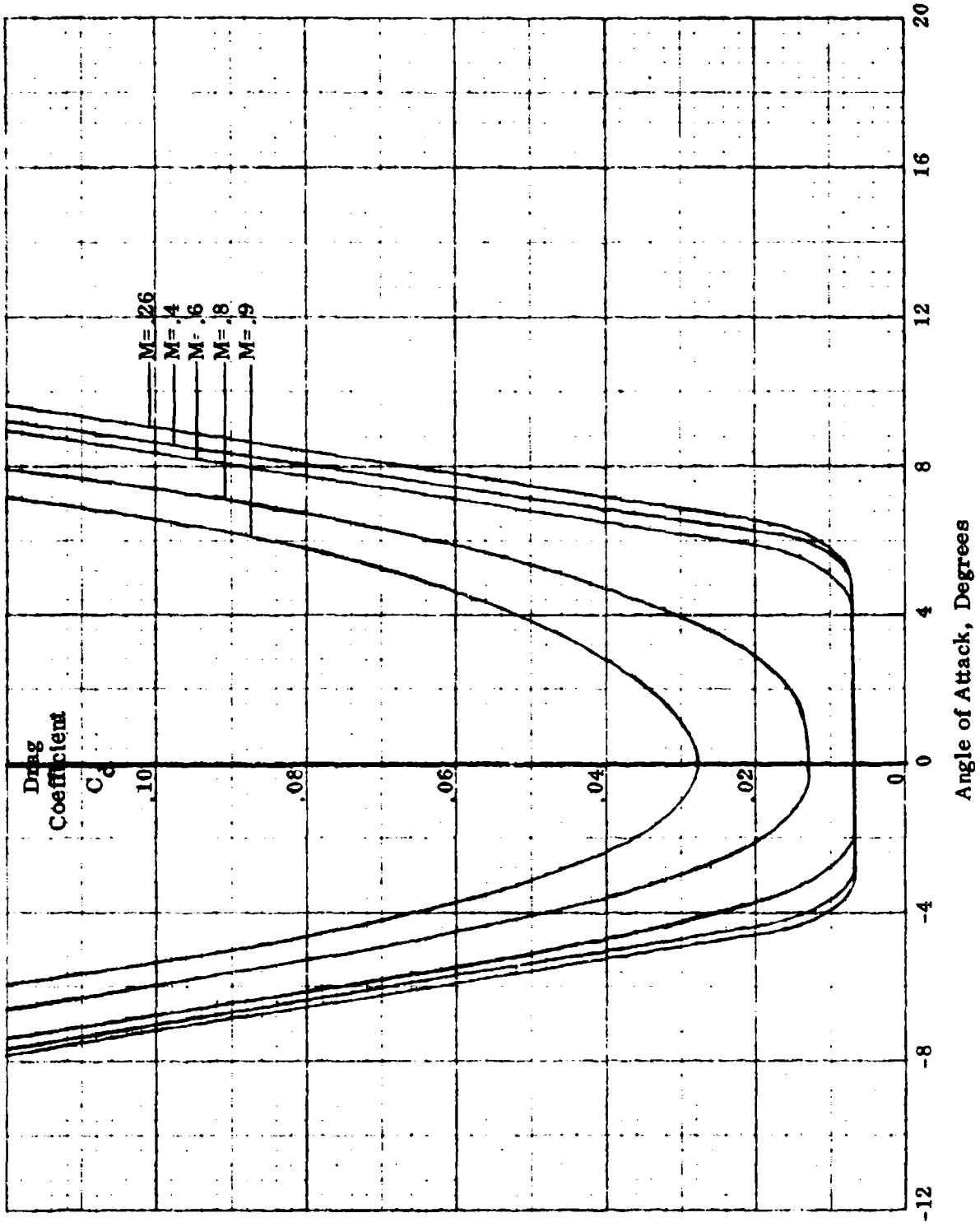


SECTION LIFT COEFFICIENT THROUGH 360° ANGLE OF ATTACK
6% AIRFOIL - MODEL REYNOLDS NUMBER

Lift Coefficient
 C_l



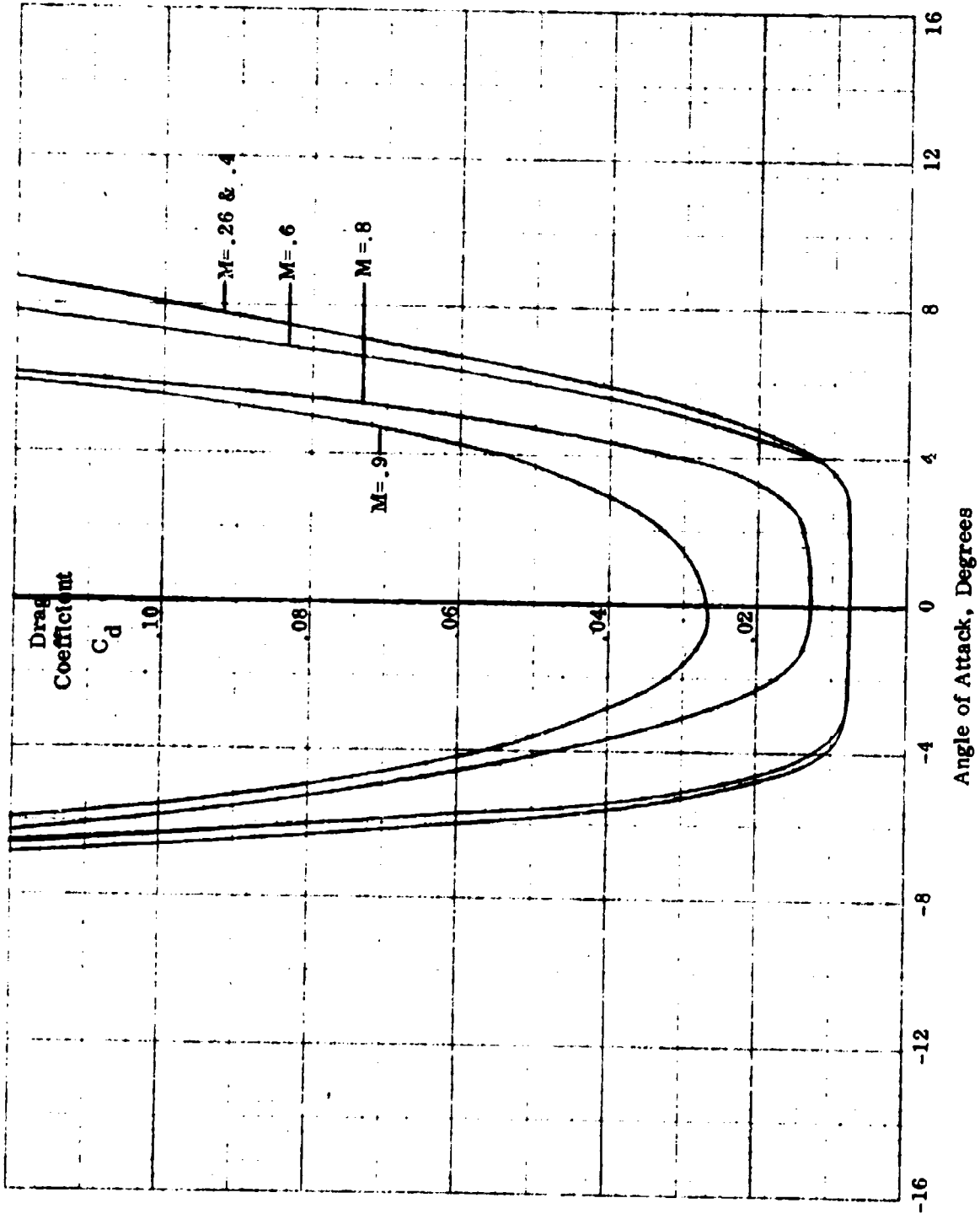
SECTION DRAG COEFFICIENT - 6% AIRFOIL, FORWARD
MODEL REYNOLDS NUMBER



HC144R1070

Figure D.5

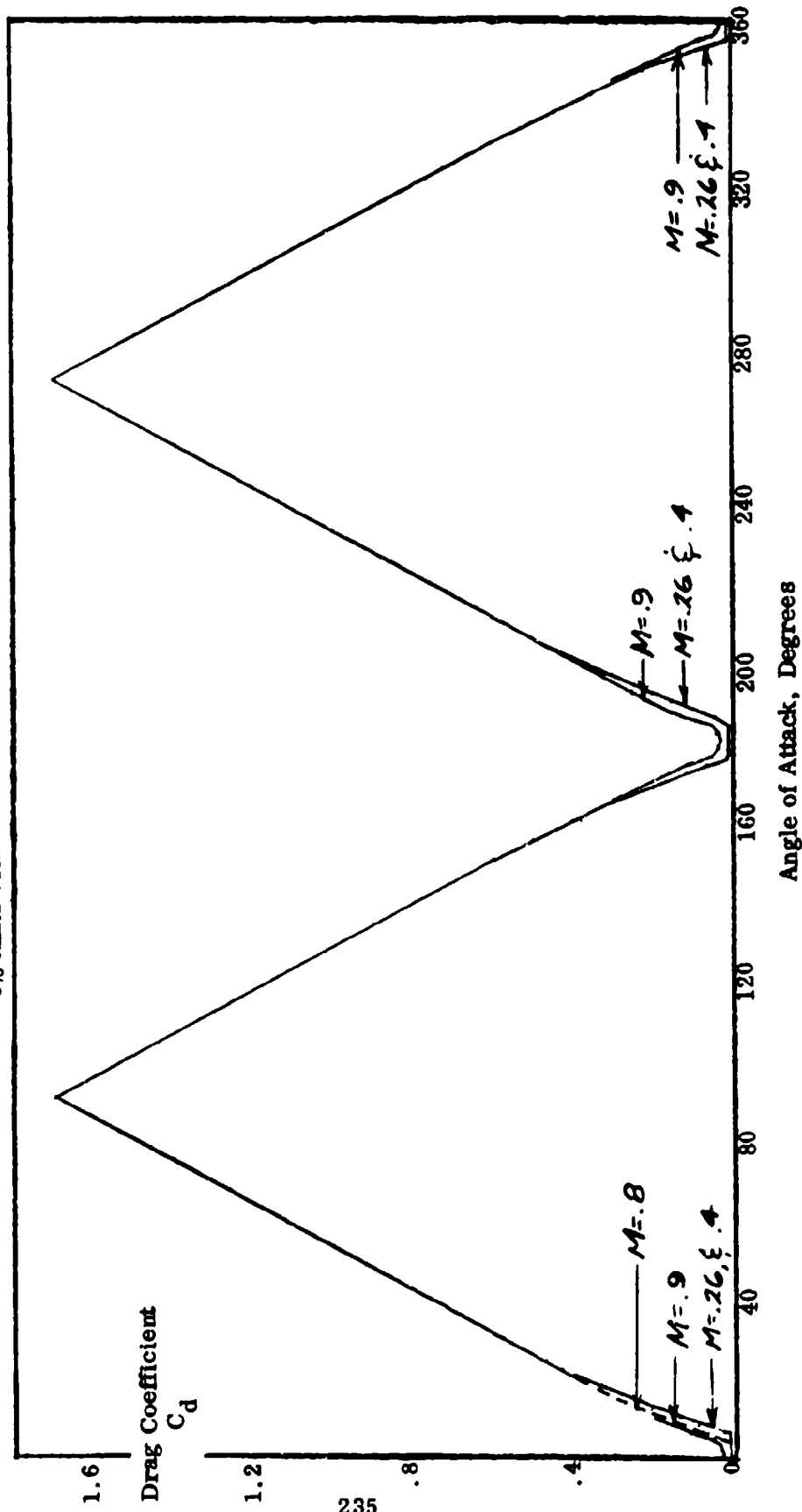
SECTION DRAG COEFFICIENT - 6% AIRFOIL, REVERSE
MODEL REYNOLDS NUMBER



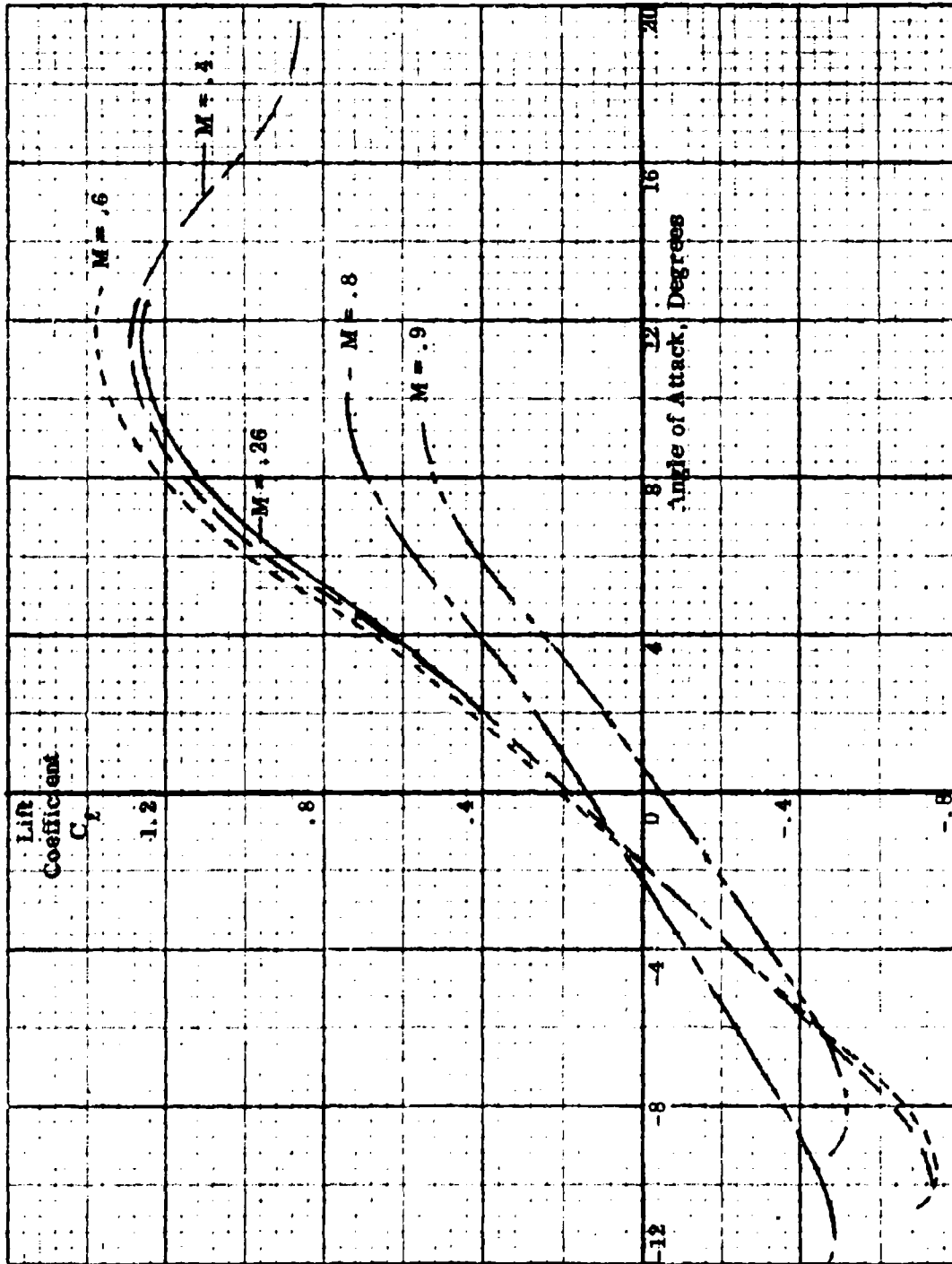
HC144R1070

Figure D.6

SECTION DRAG COEFFICIENT THROUGH 360° ANGLE OF ATTACK
6% AIRFOIL - MODEL REYNOLDS NUMBER



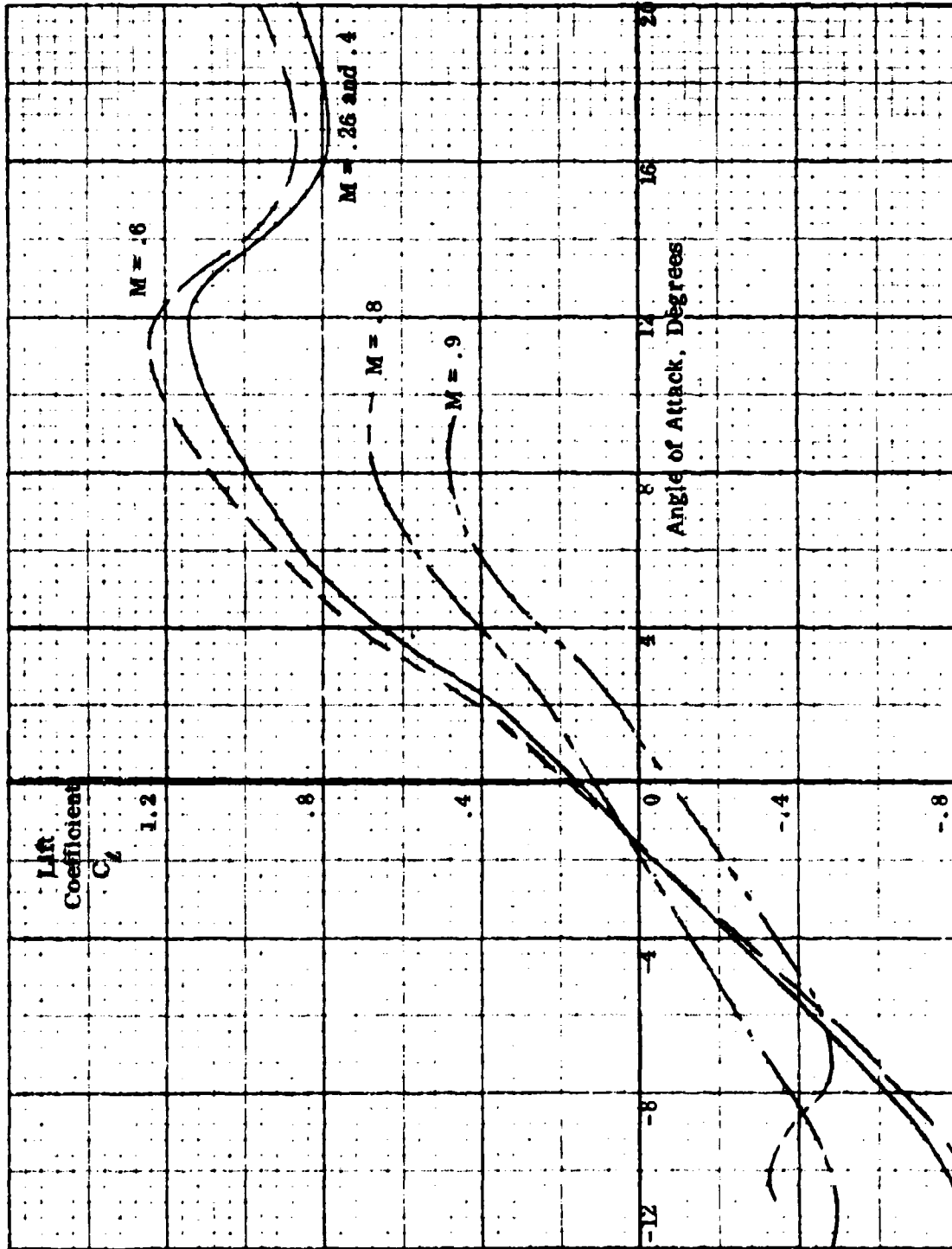
SECTION LIFT COEFFICIENT - 12% AIRFOIL, FORWARD
MODEL REYNOLDS NUMBER



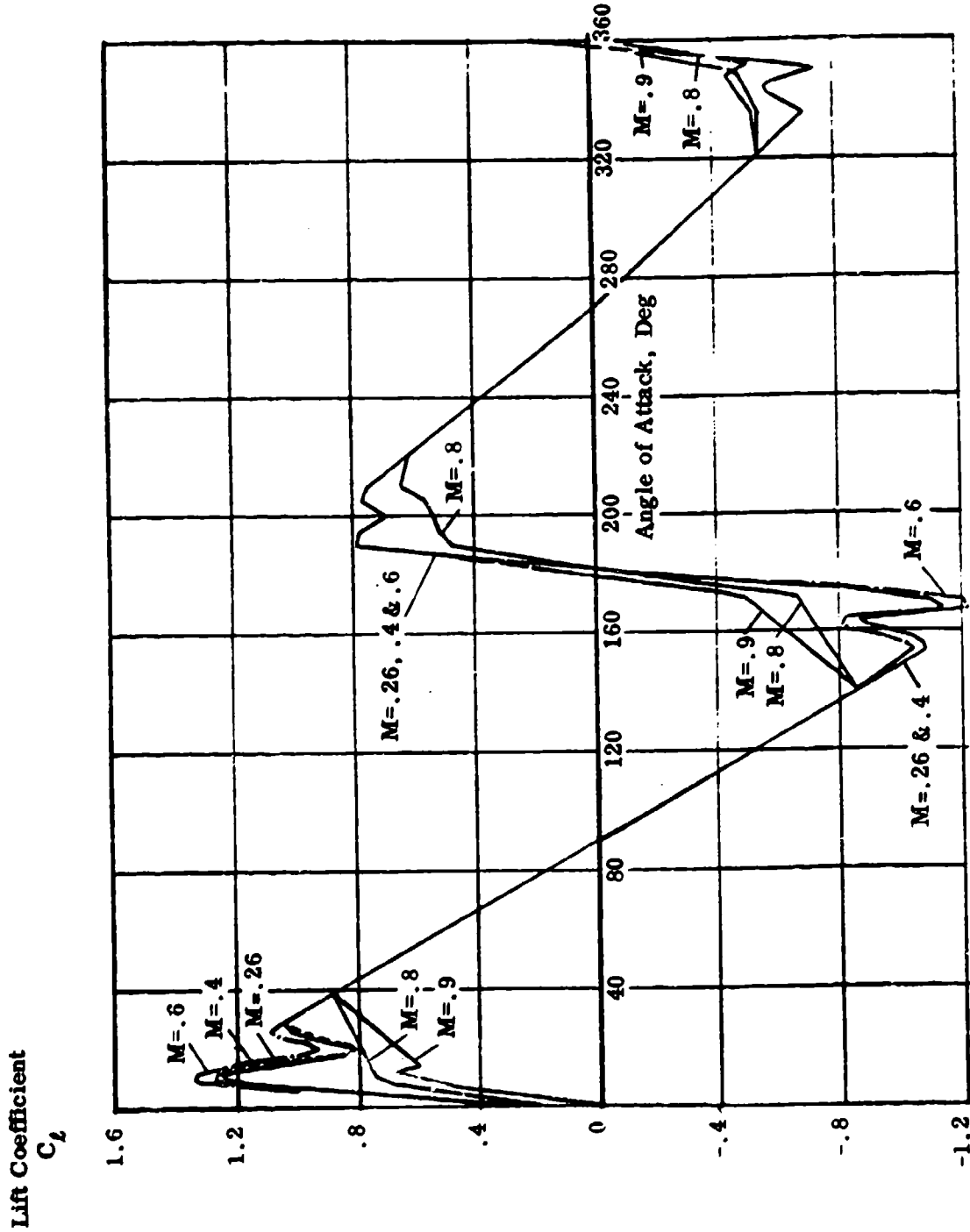
HC144R1070

Figure D. 8

**SECTION LIFT COEFFICIENT - 12% AIRFOIL, REVERSE
MODEL REYNOLDS NUMBER**



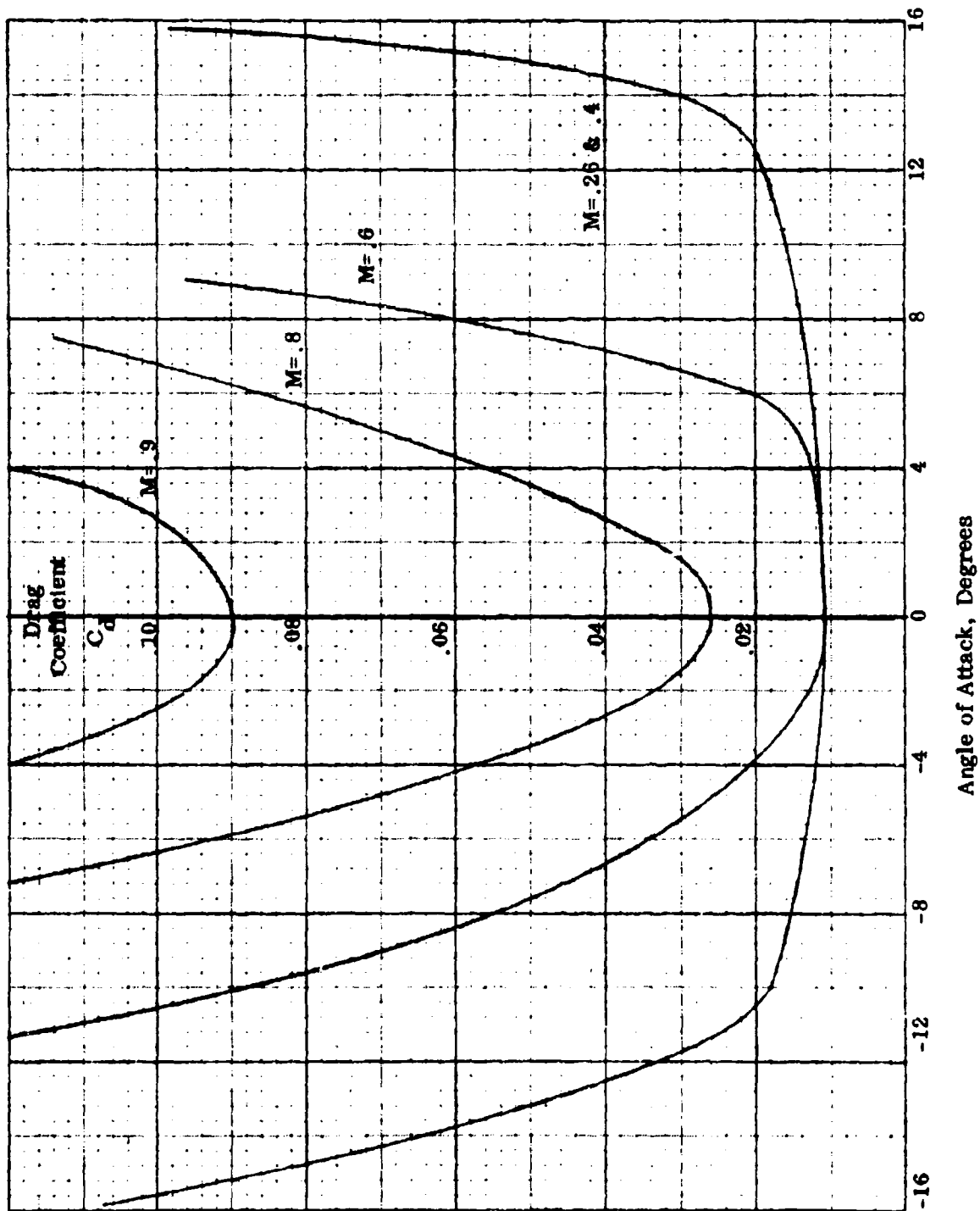
SECTION LIFT COEFFICIENT THROUGH 360° ANGLE OF ATTACK
12% AIRFOIL - MODEL REYNOLDS NUMBER



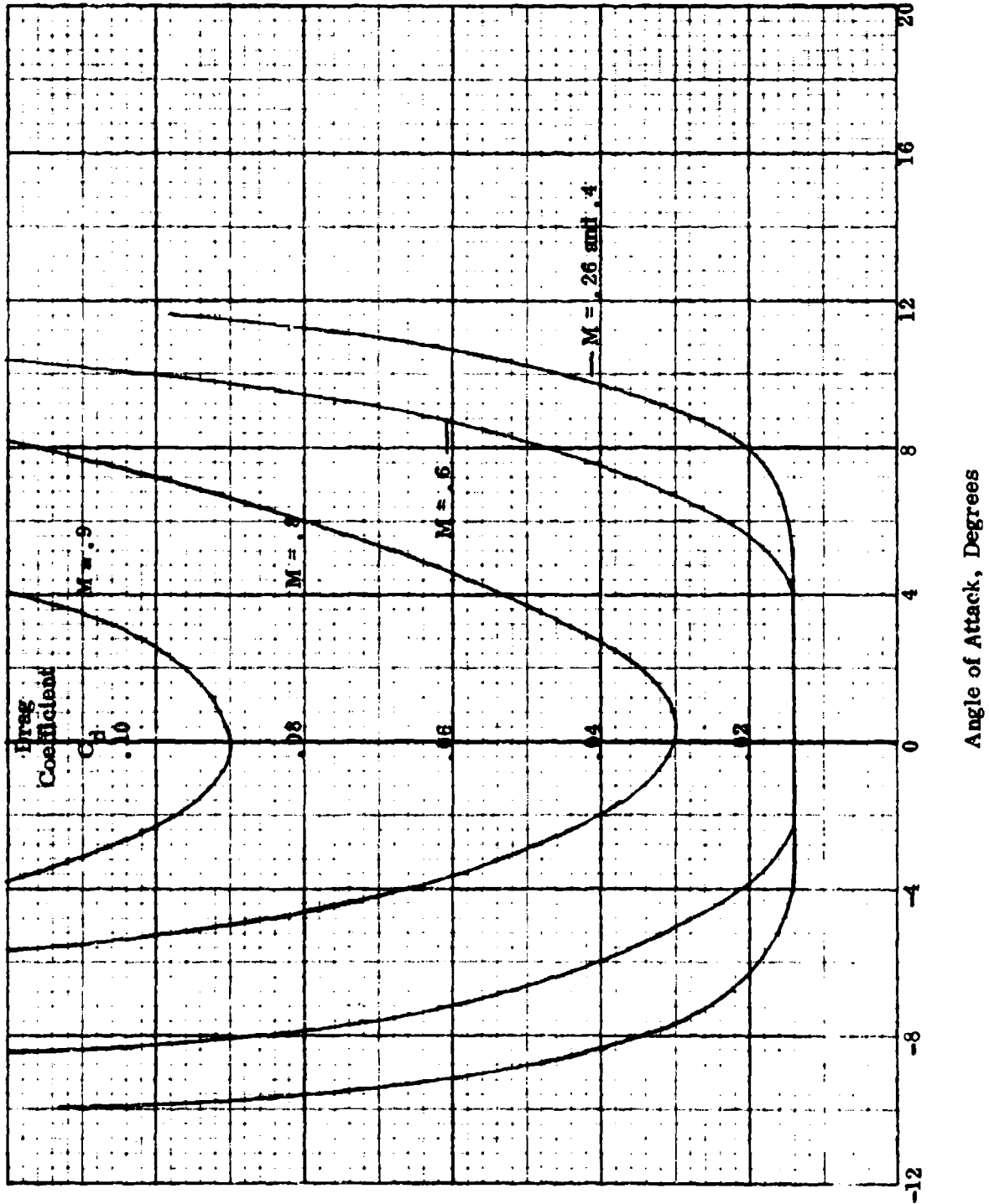
HC144R1070

Figure D. 10

**SECTION DRAG COEFFICIENT - 12% AIRFOIL, FORWARD
MODEL REYNOLDS NUMBER**



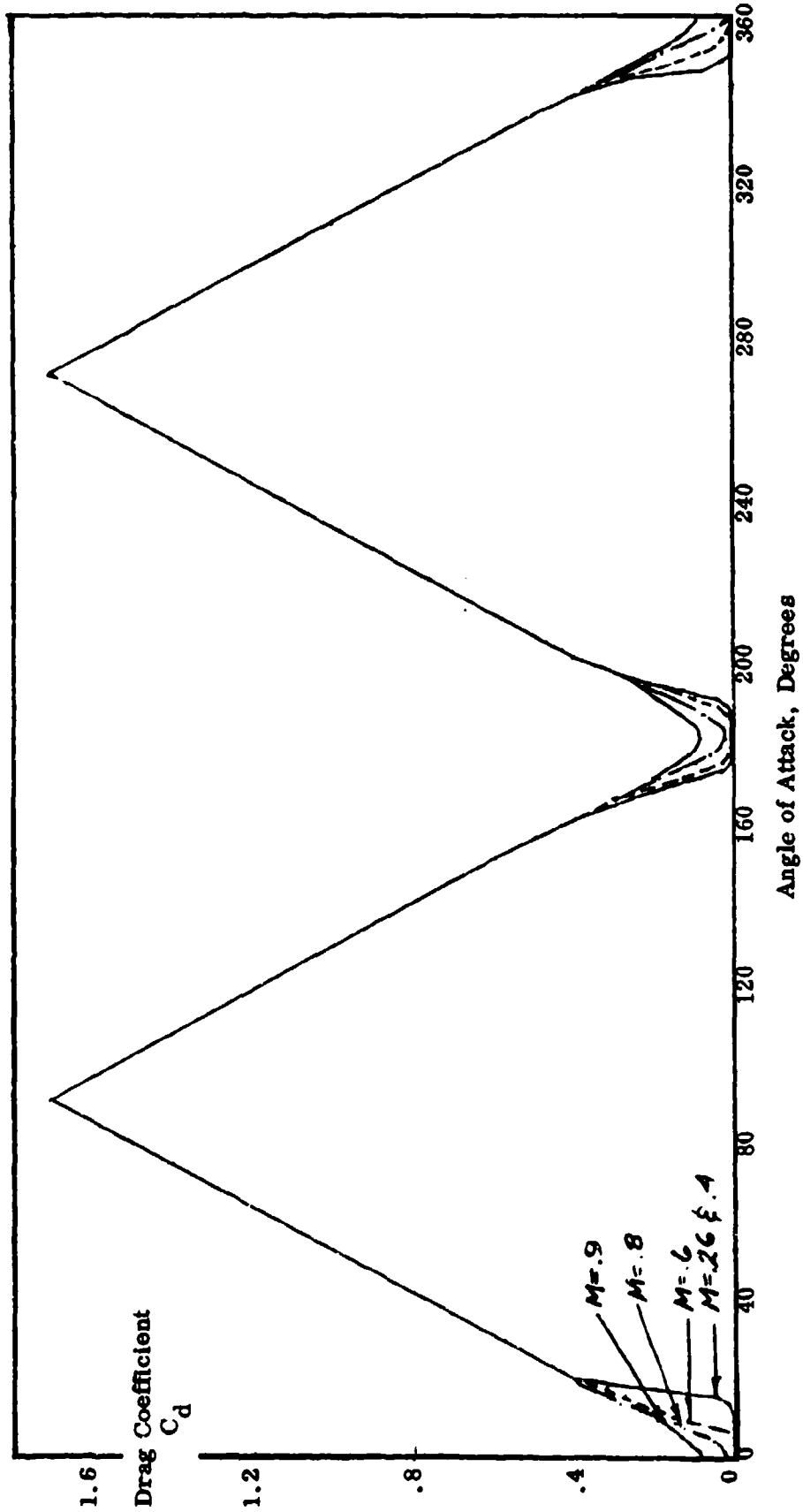
SECTION DRAG COEFFICIENT - 12% AIRFOIL, REVERSE
MODEL REYNOLDS NUMBER



HC144R1070

Figure D.12

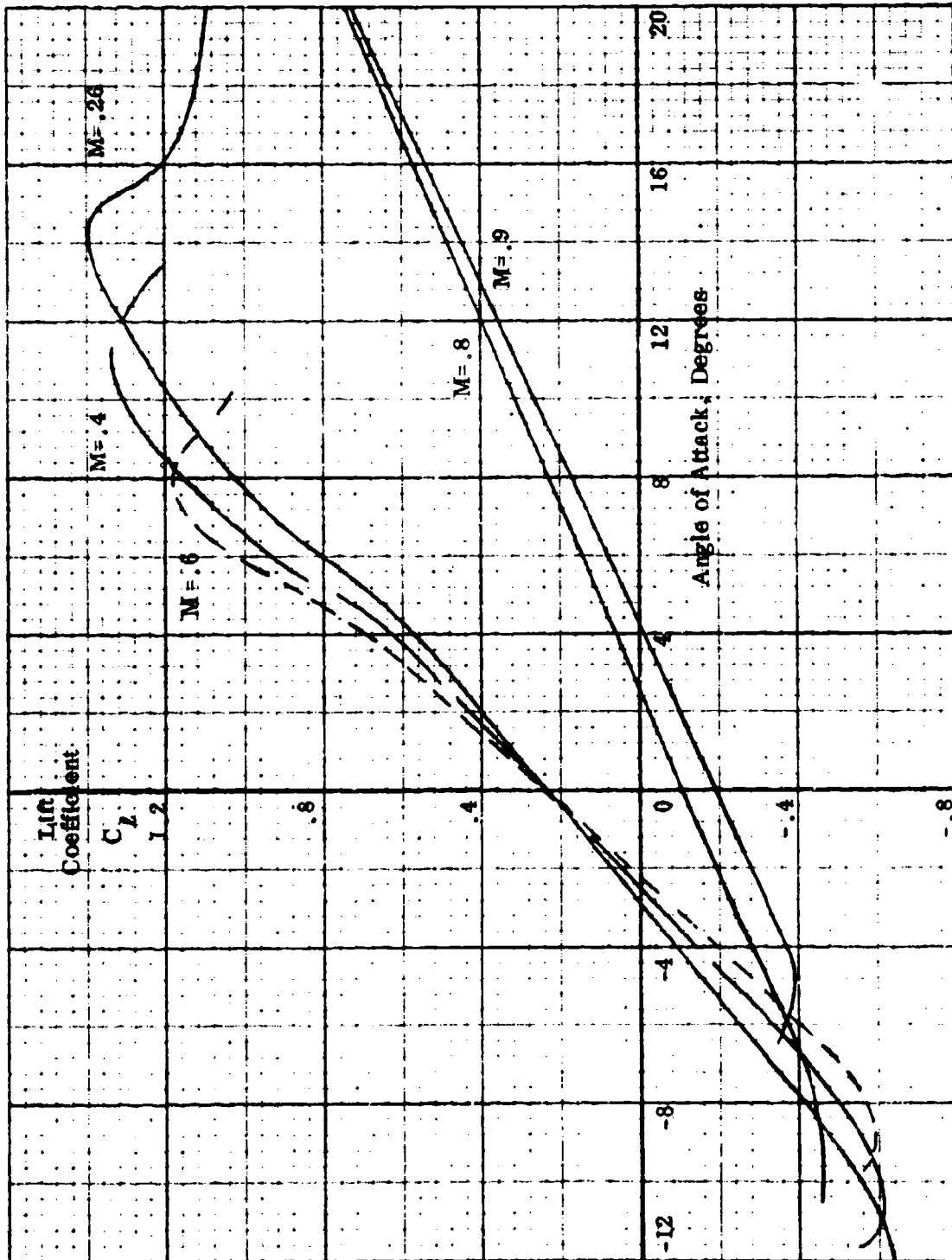
**SECTION DRAG COEFFICIENT THROUGH 360° ANGLE OF ATTACK
12% AIRFOIL - MODEL REYNOLDS NUMBER**



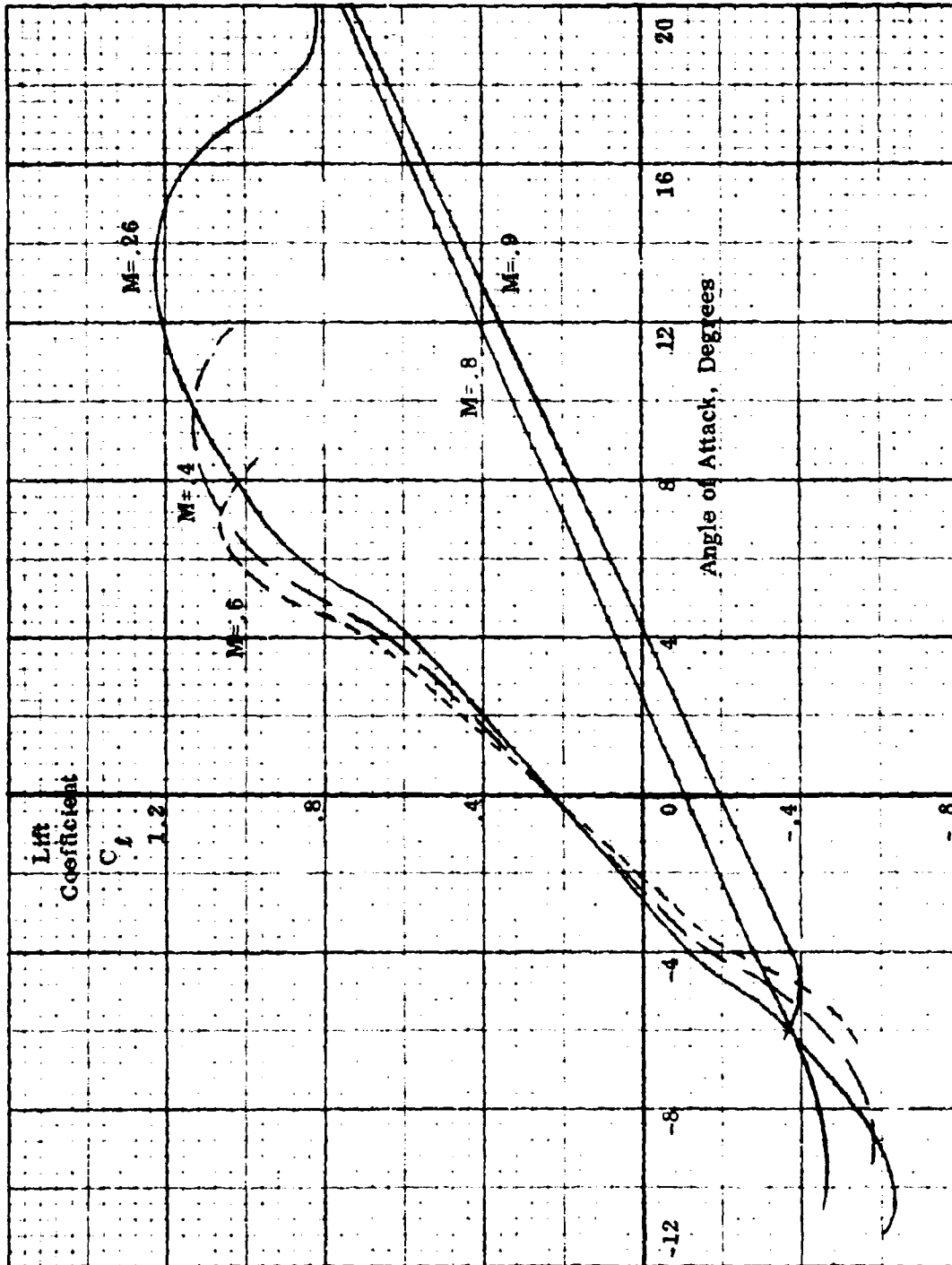
HC144R1070

Figure D.13

SECTION LIFT COEFFICIENT - 18% AIRFOIL, FORWARD
MODEL REYNOLDS NUMBER

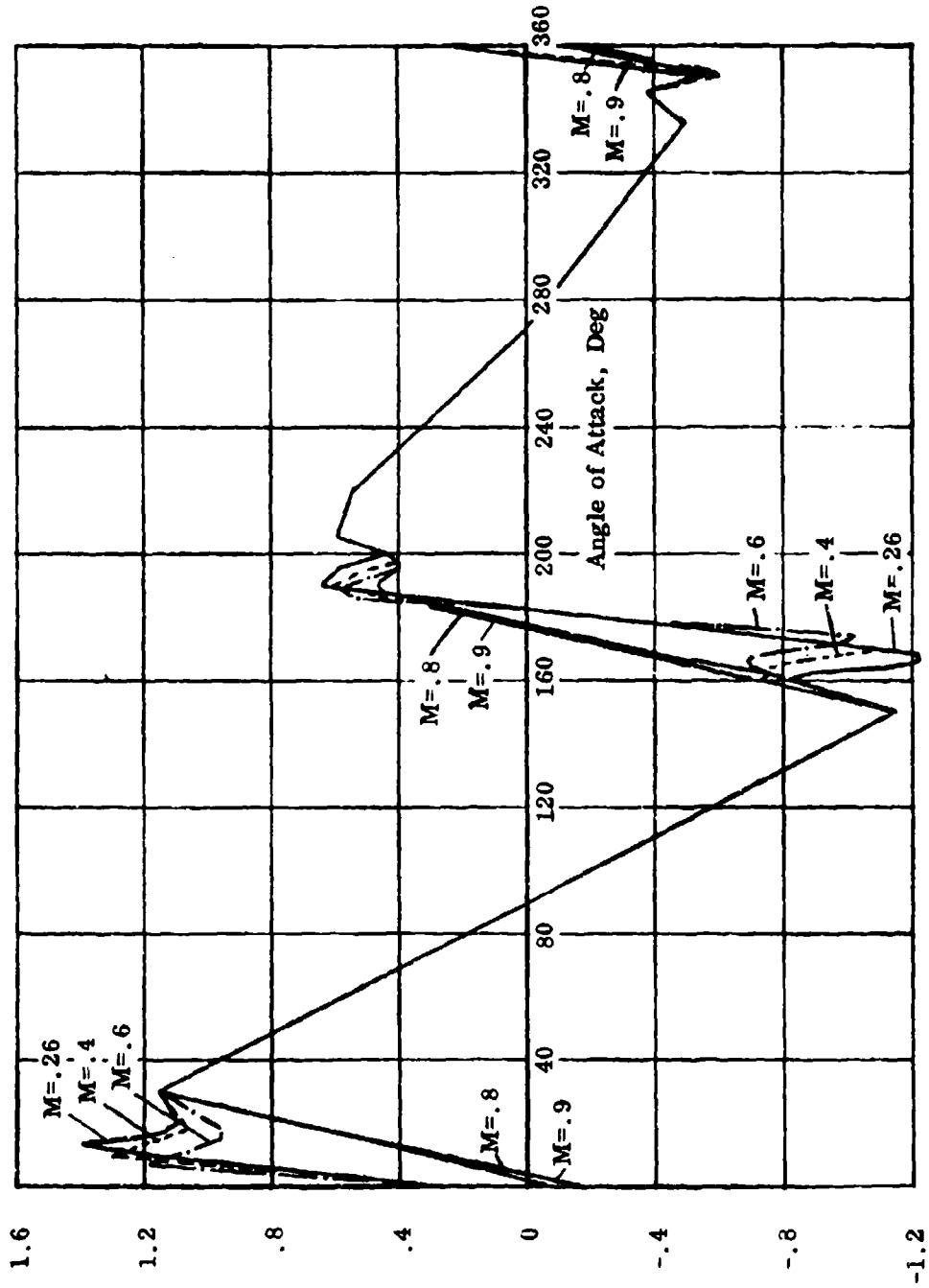


**SECTION LIFT COEFFICIENT - 16% AIRFOIL, REVERSE
MODEL REYNOLDS NUMBER**



SECTION LIFT COEFFICIENT THROUGH 360° ANGLE OF ATTACK
18% AIRFOIL - MODEL REYNOLDS NUMBER

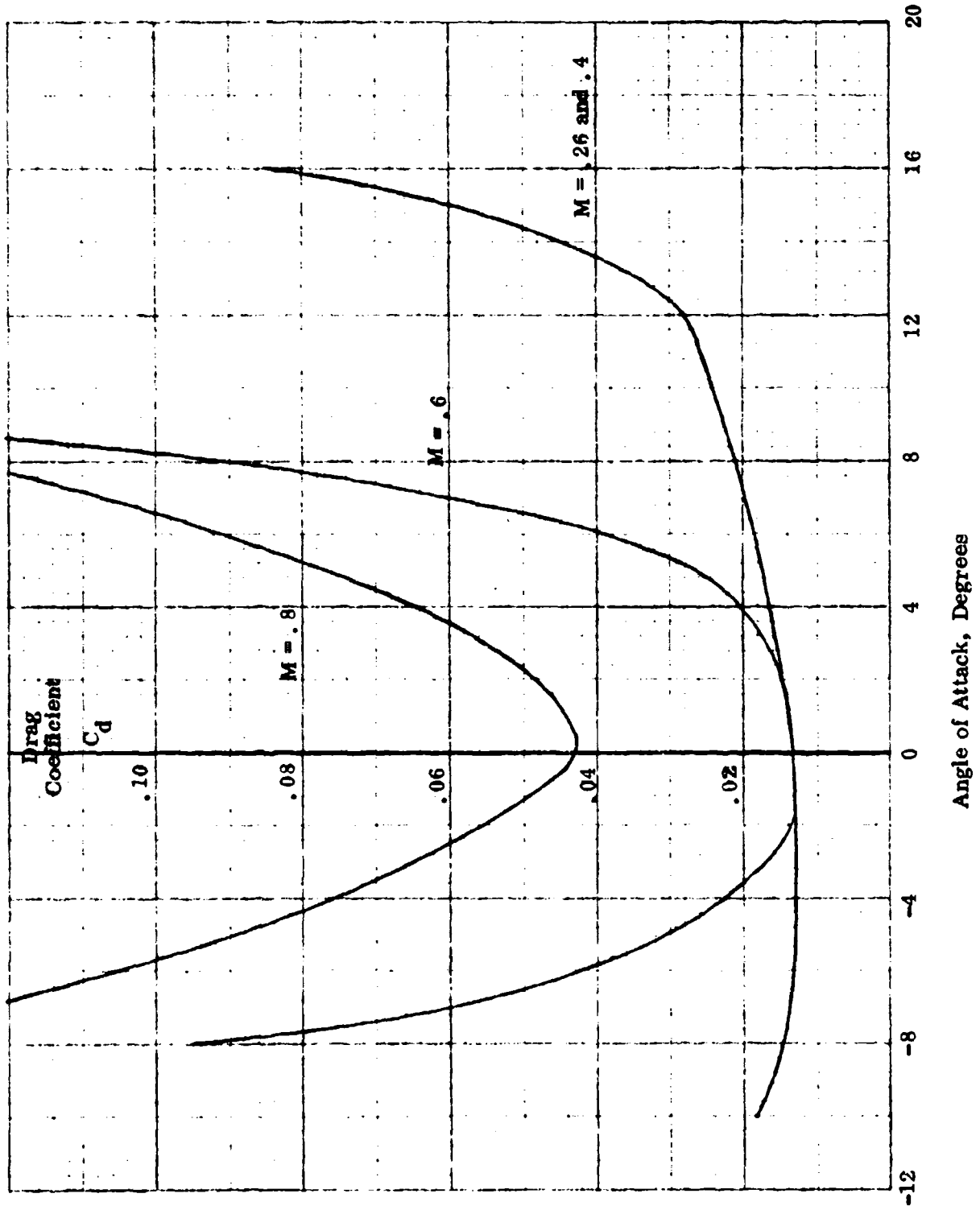
Lift Coefficient
 C_L



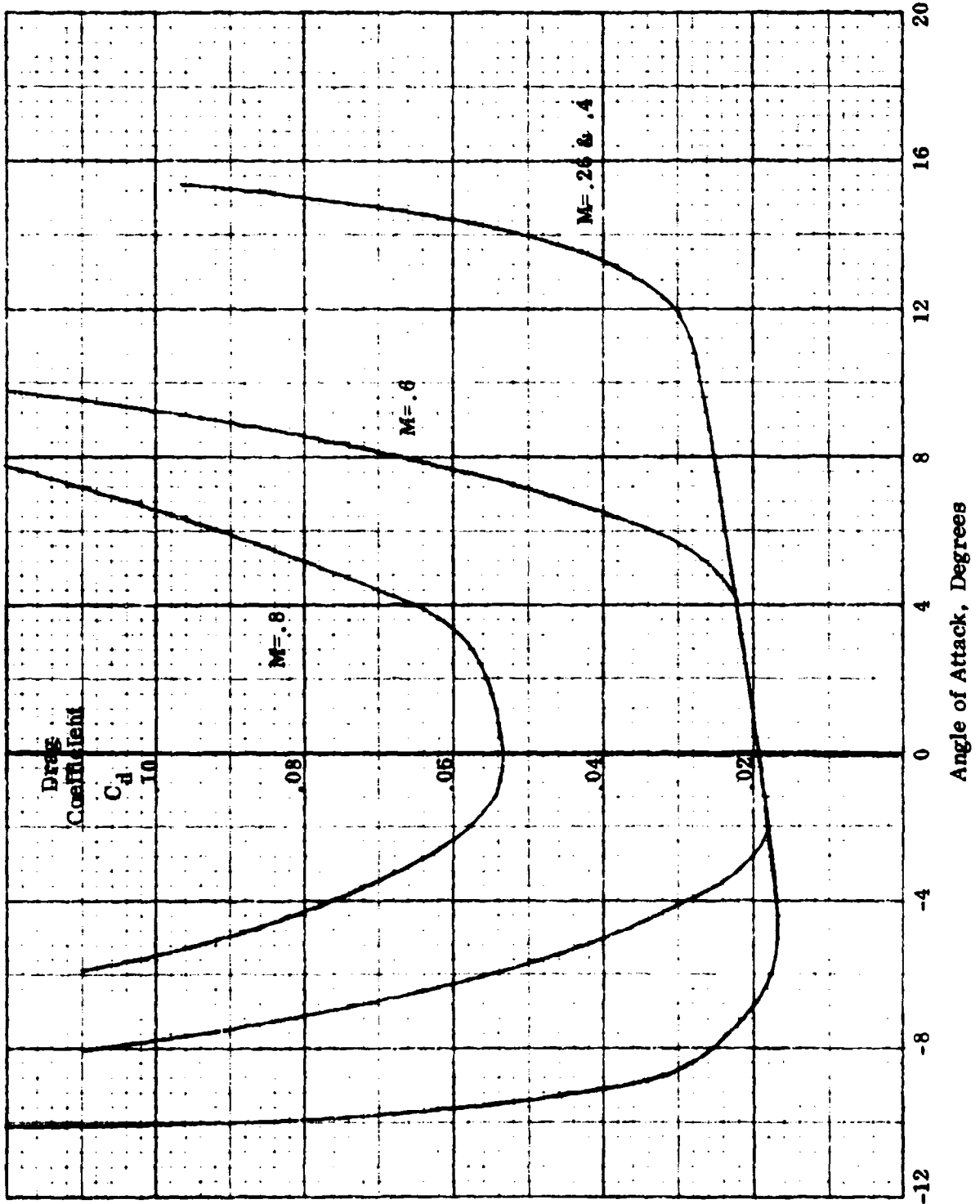
HC144R1070

Figure D.16

SECTION DRAG COEFFICIENT - 18% AIRFOIL, FORWARD
MODEL REYNOLDS NUMBER



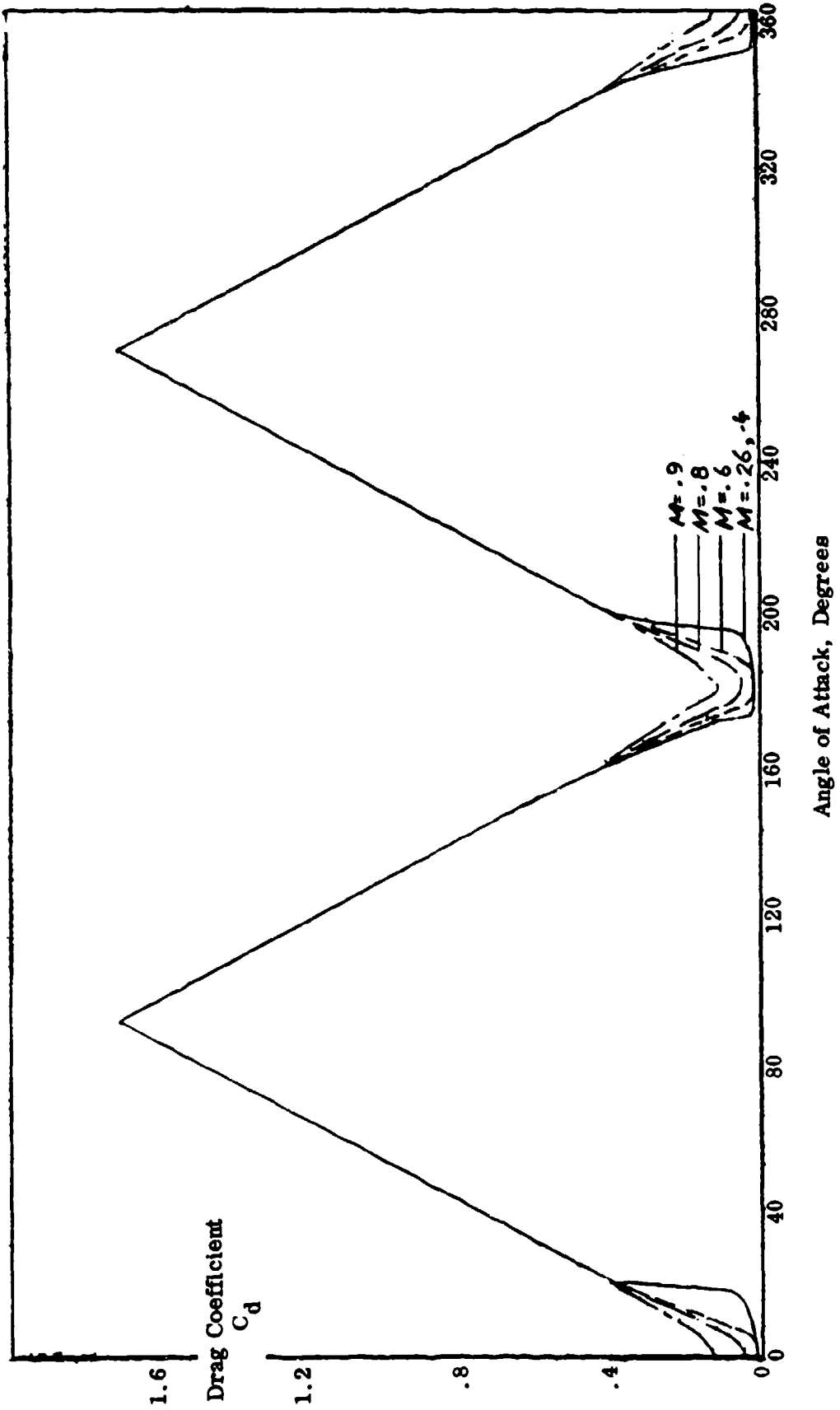
SECTION DRAG COEFFICIENT - 18% AIRFOIL, REVERSE
MODEL REYNOLDS NUMBER



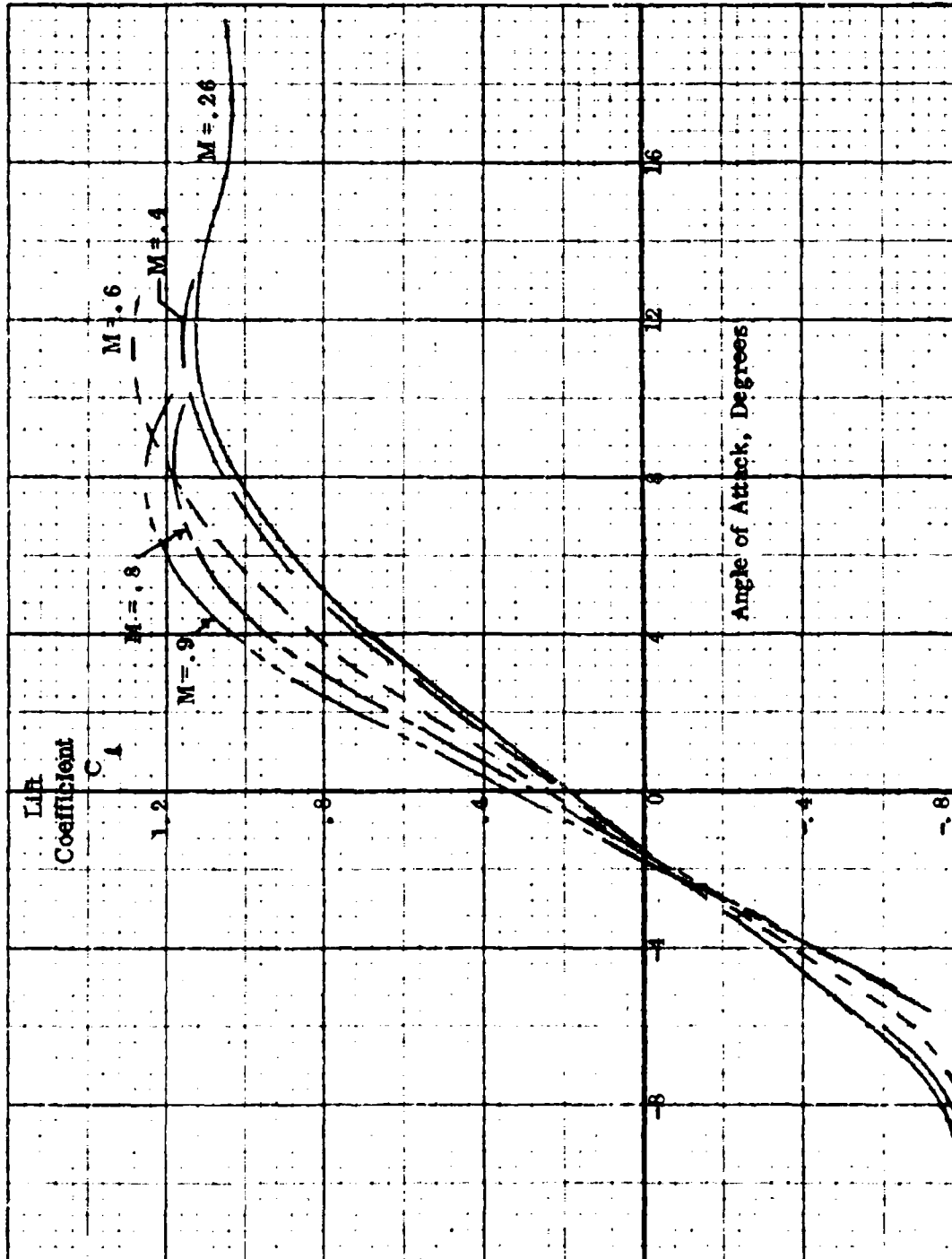
HC144R1070

Figure D. 18

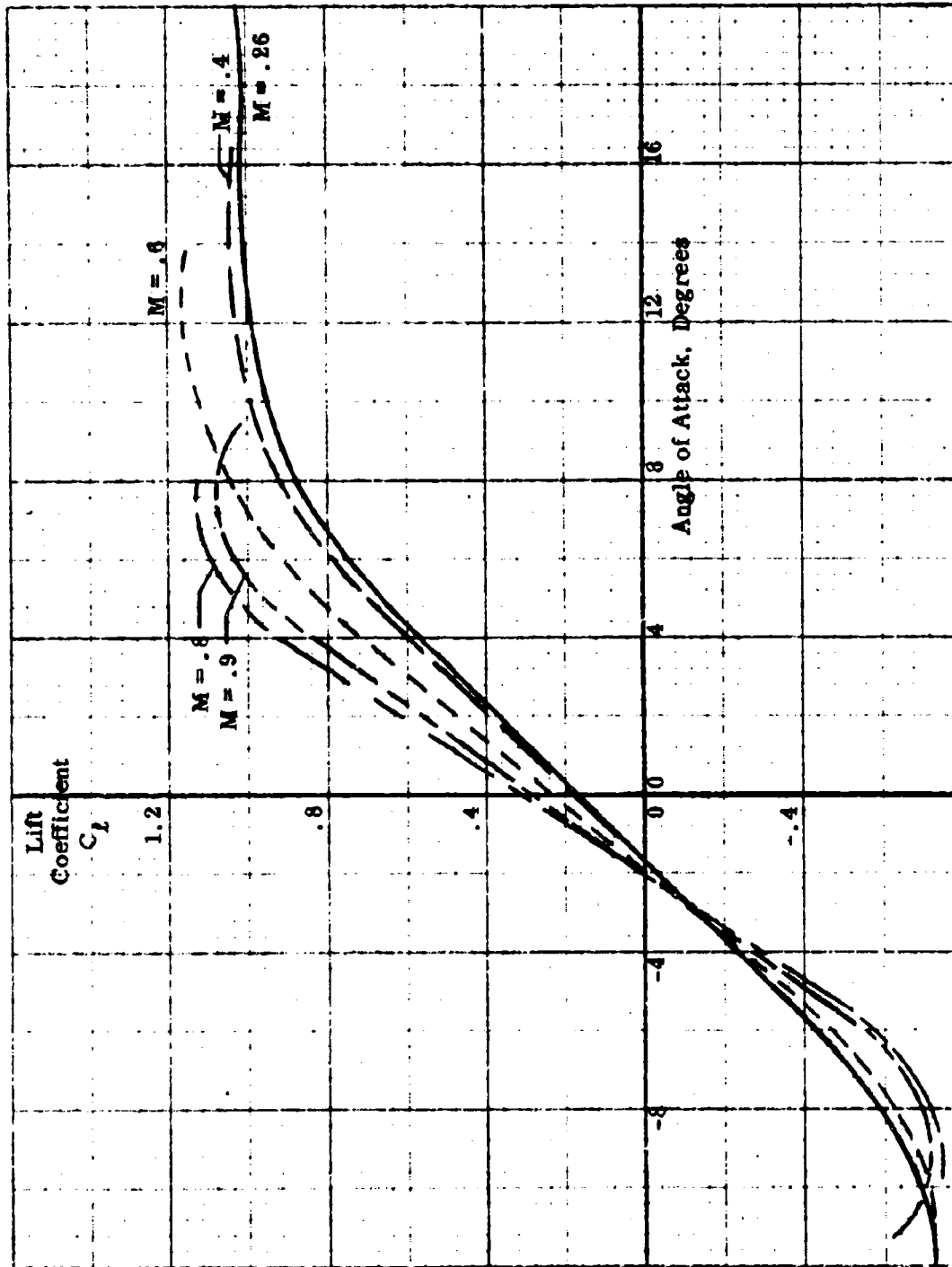
SECTION DRAG COEFFICIENT THROUGH 360° ANGLE OF ATTACK
18% AIRFOIL - MODEL REYNOLDS NUMBER



SECTION LIFT COEFFICIENT - 6% AIRFOIL, FORWARD
FULL SCALE REYNOLDS NUMBER

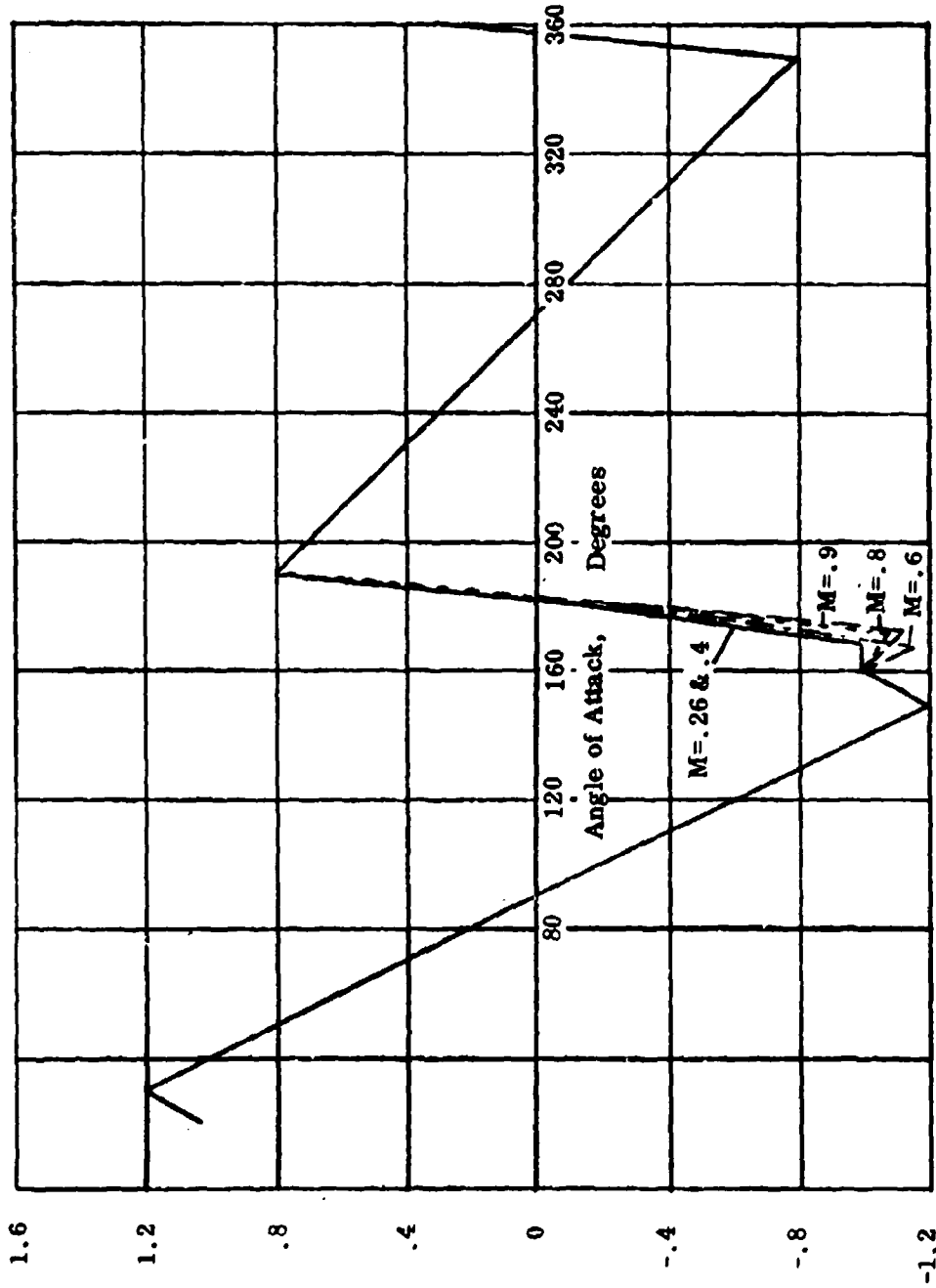


**SECTION LIFT COEFFICIENT - 6% AIRFOIL, REVERSE
FULL SCALE REYNOLDS NUMBER**

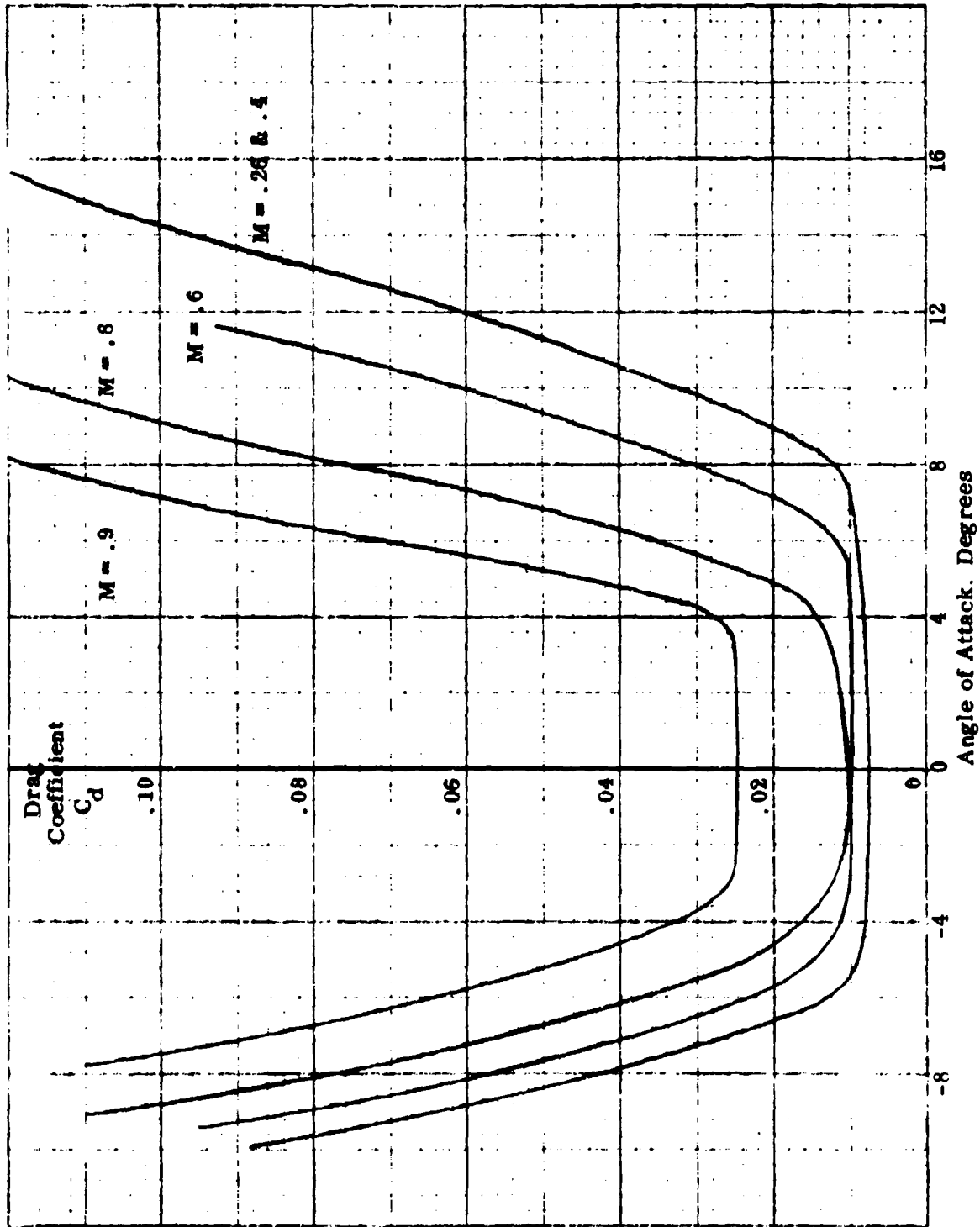


SECTION LIFT COEFFICIENT THROUGH 360° ANGLE OF ATTACK
6% AIRFOIL - FULL SCALE REYNOLDS NUMBER

Lift Coefficient
 C_L



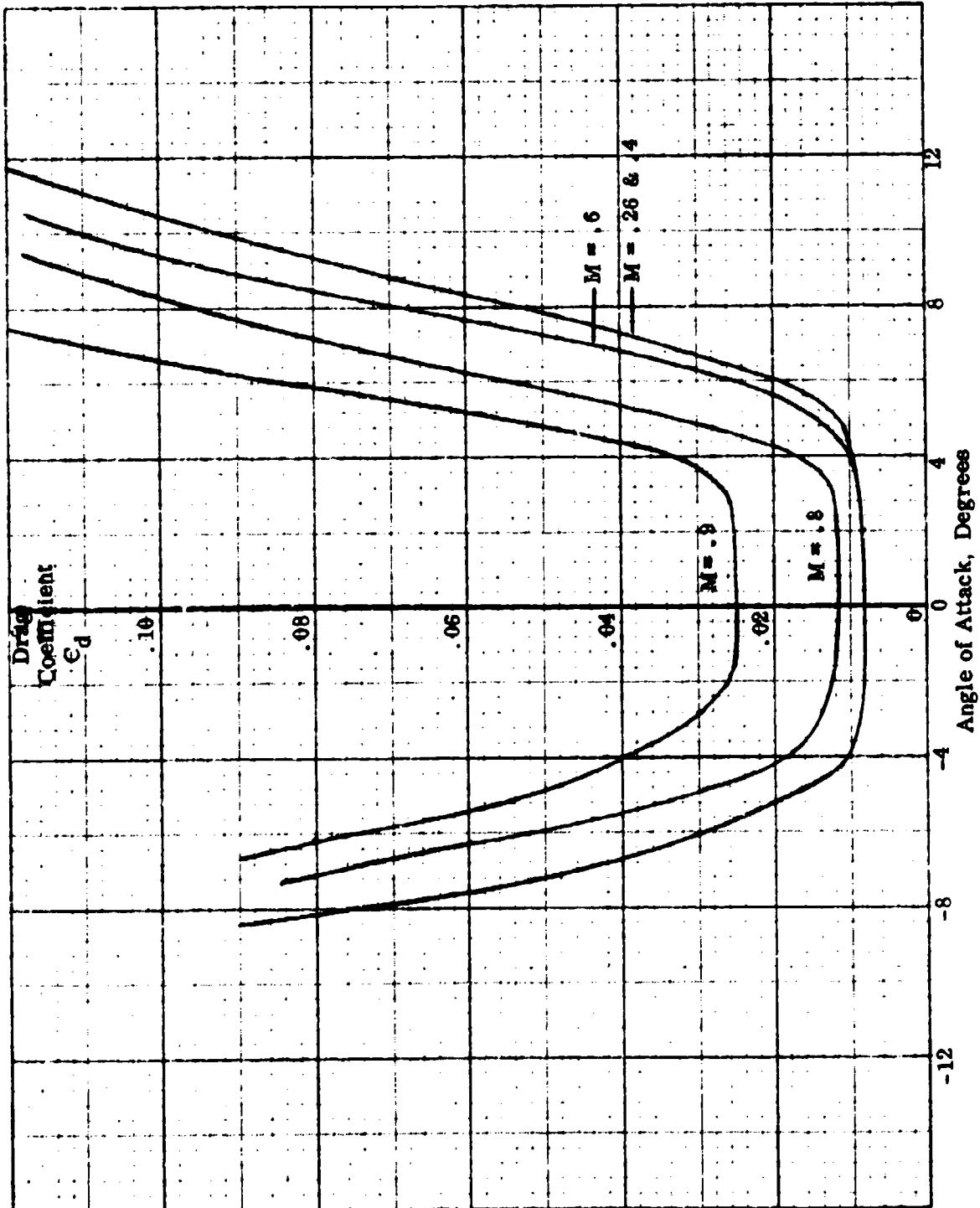
SECTION DRAG COEFFICIENT - 6% AIRFOIL, FORWARD
FULL SCALE REYNOLDS NUMBER



HC144R1070

Figure D.23

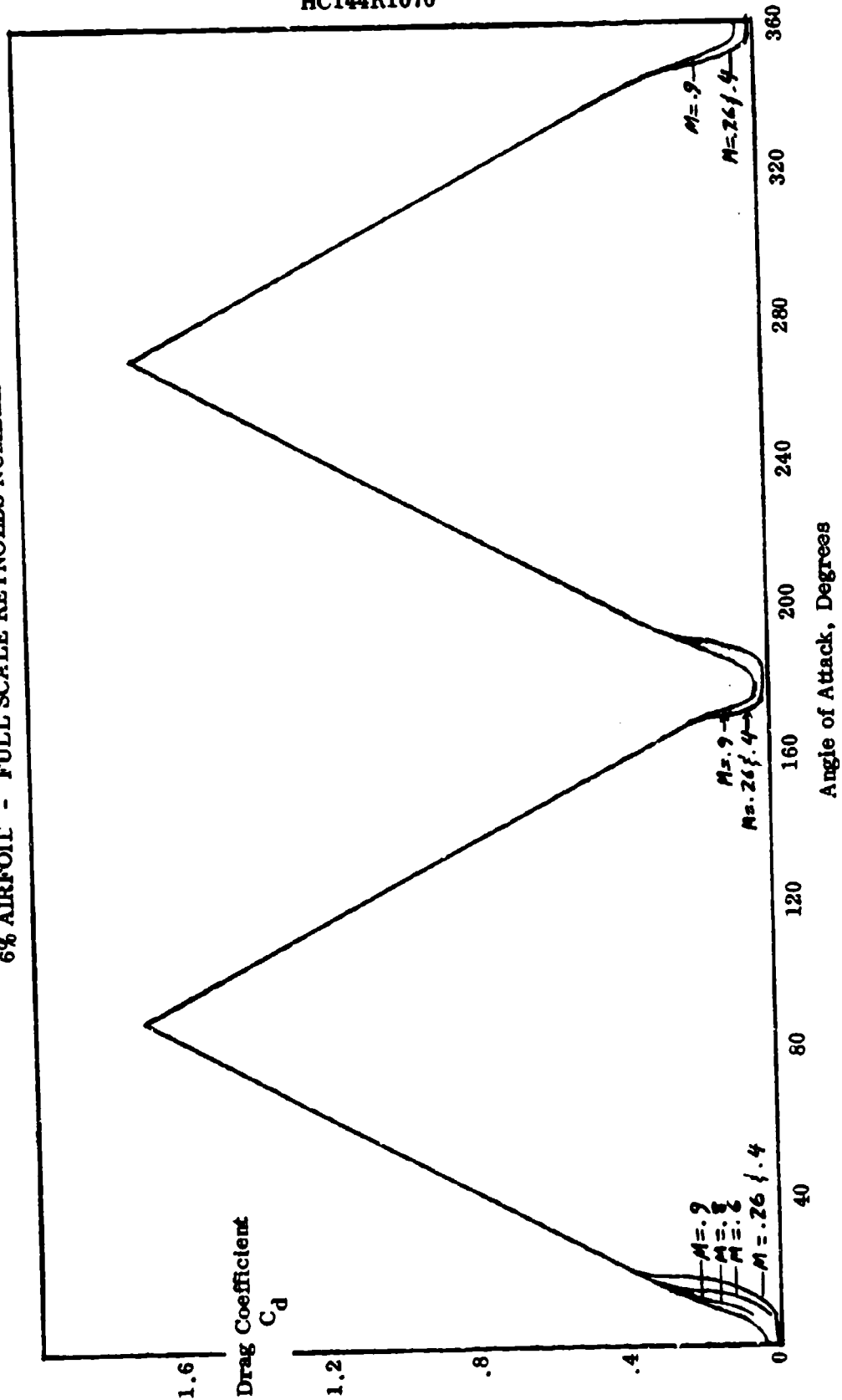
SECTION DRAG COEFFICIENT - 6% AIRFOIL, REVERSE
FULL SCALE REYNOLDS NUMBER



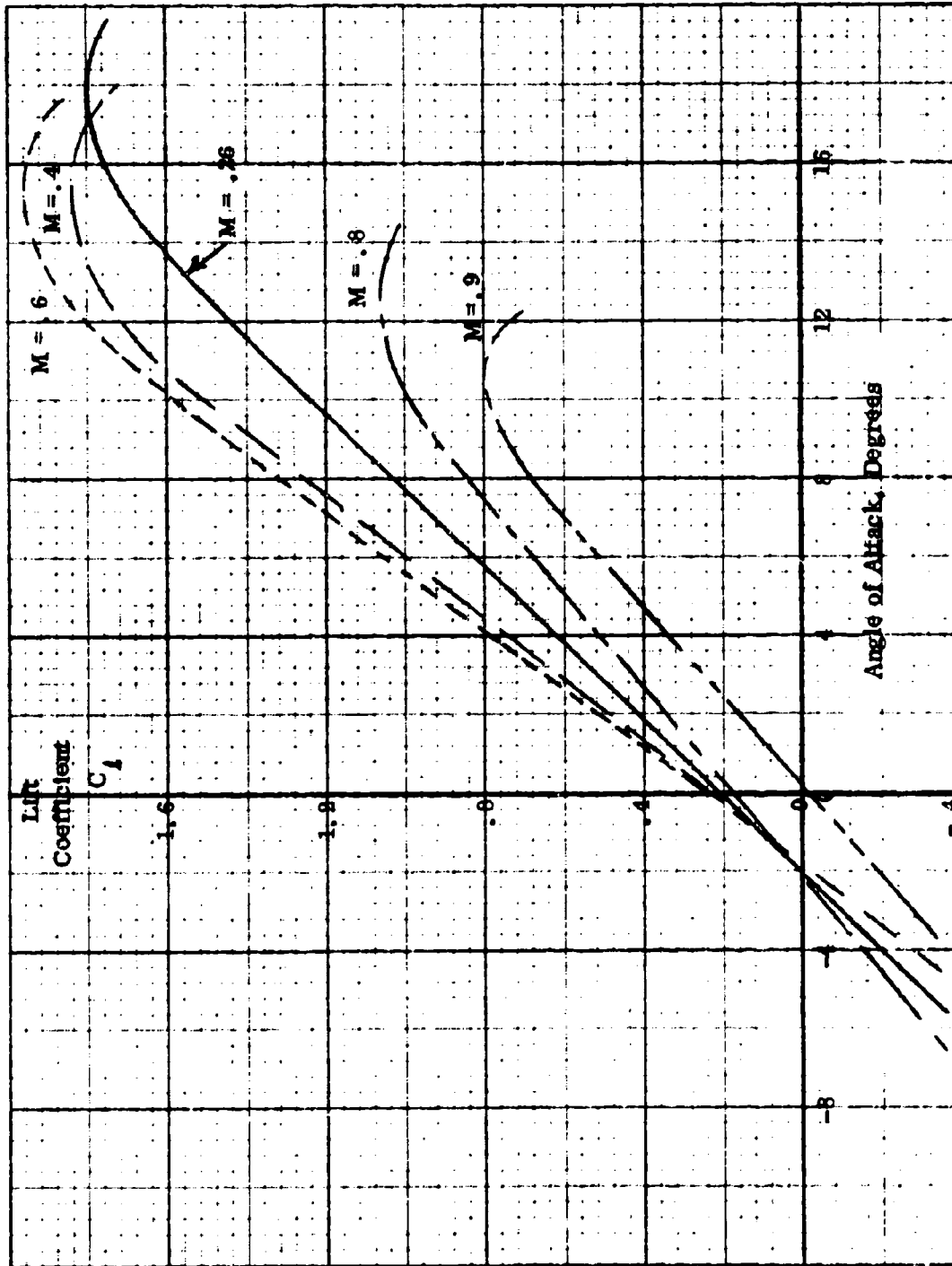
HC144R1070

Figure D.24

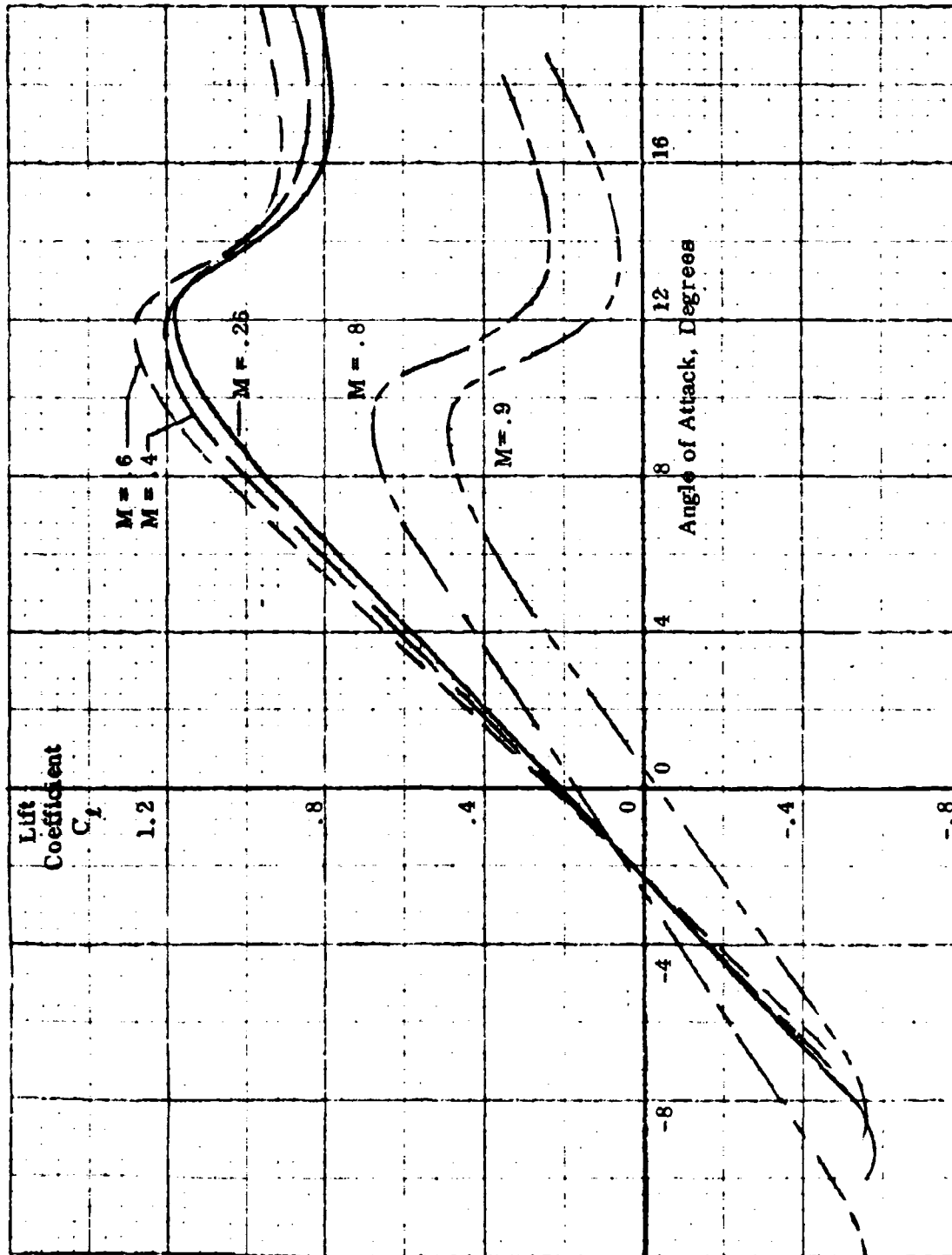
SECTION DRAG COEFFICIENT THROUGH 360° ANGLE OF ATTACK
6% AIRFOIL - FULL SCALE REYNOLDS NUMBER



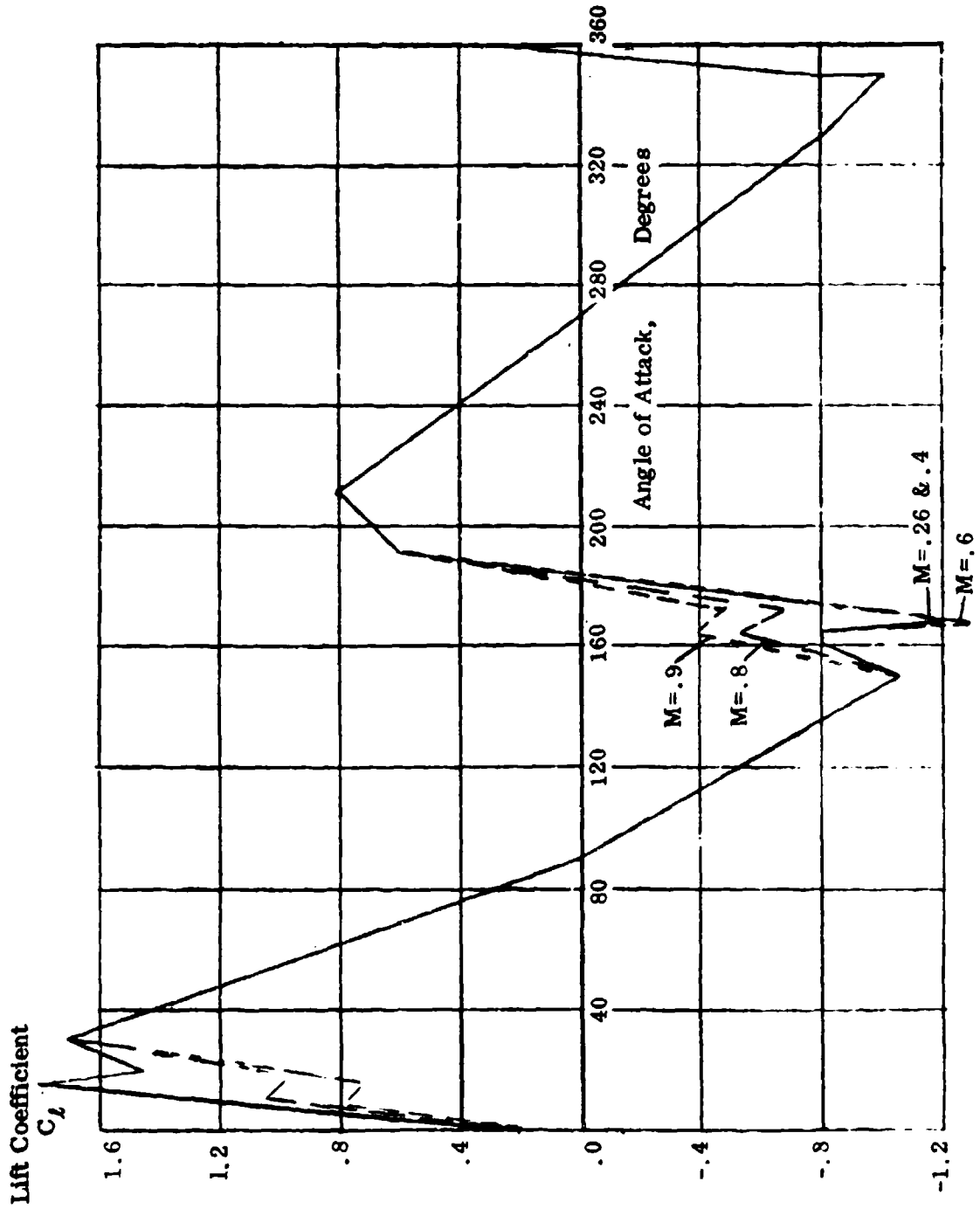
SECTION LIFT COEFFICIENT - 12% AIRFOIL, FORWARD
FULL SCALE REYNOLDS NUMBER



SECTION LIFT COEFFICIENT - 12% AIRFOIL, REVERSE
FULL SCALE REYNOLDS NUMBER



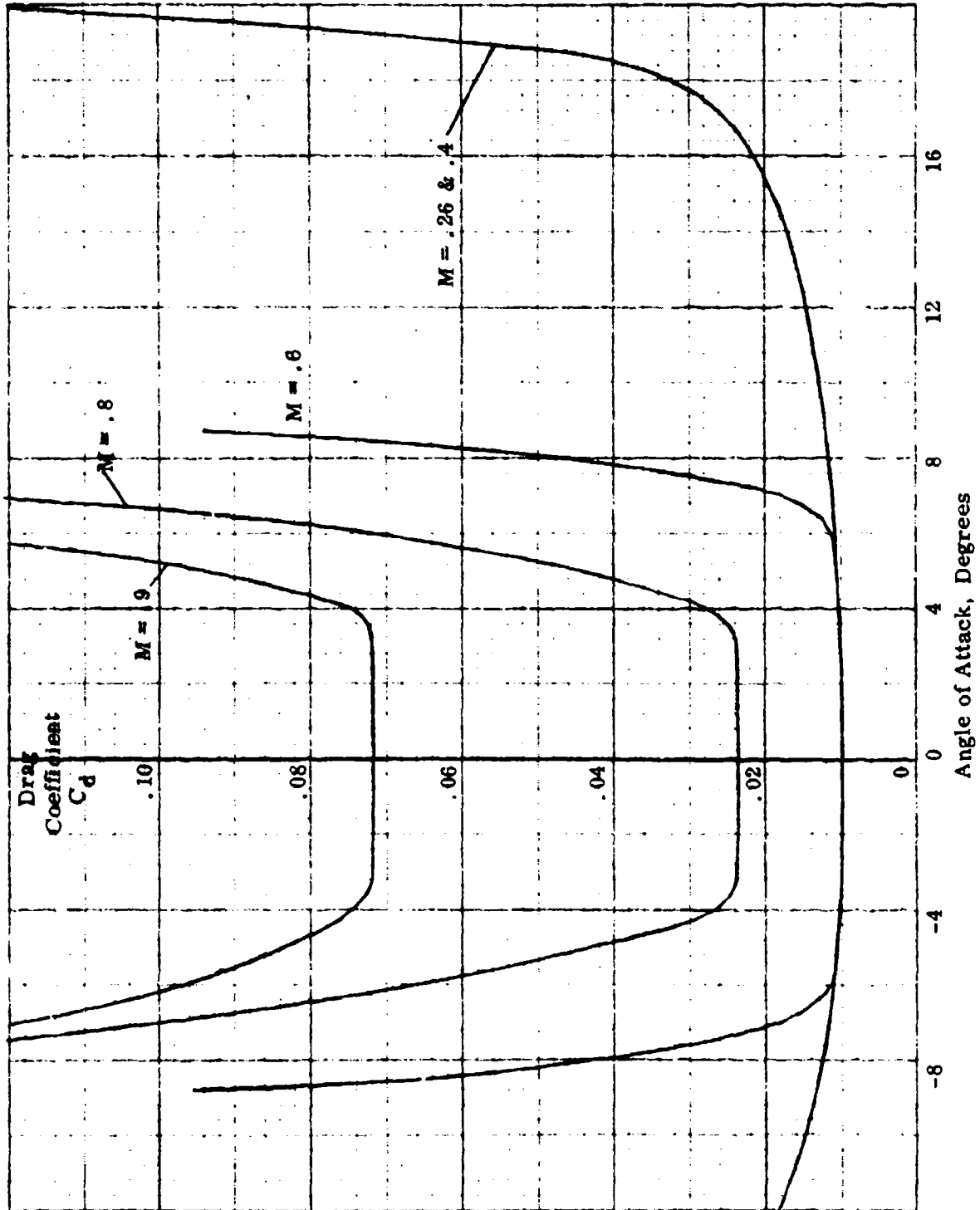
SECTION LIFT COEFFICIENT THROUGH 360° ANGLE OF ATTACK
12% AIRFOIL - FULL SCALE REYNOLDS NUMBER



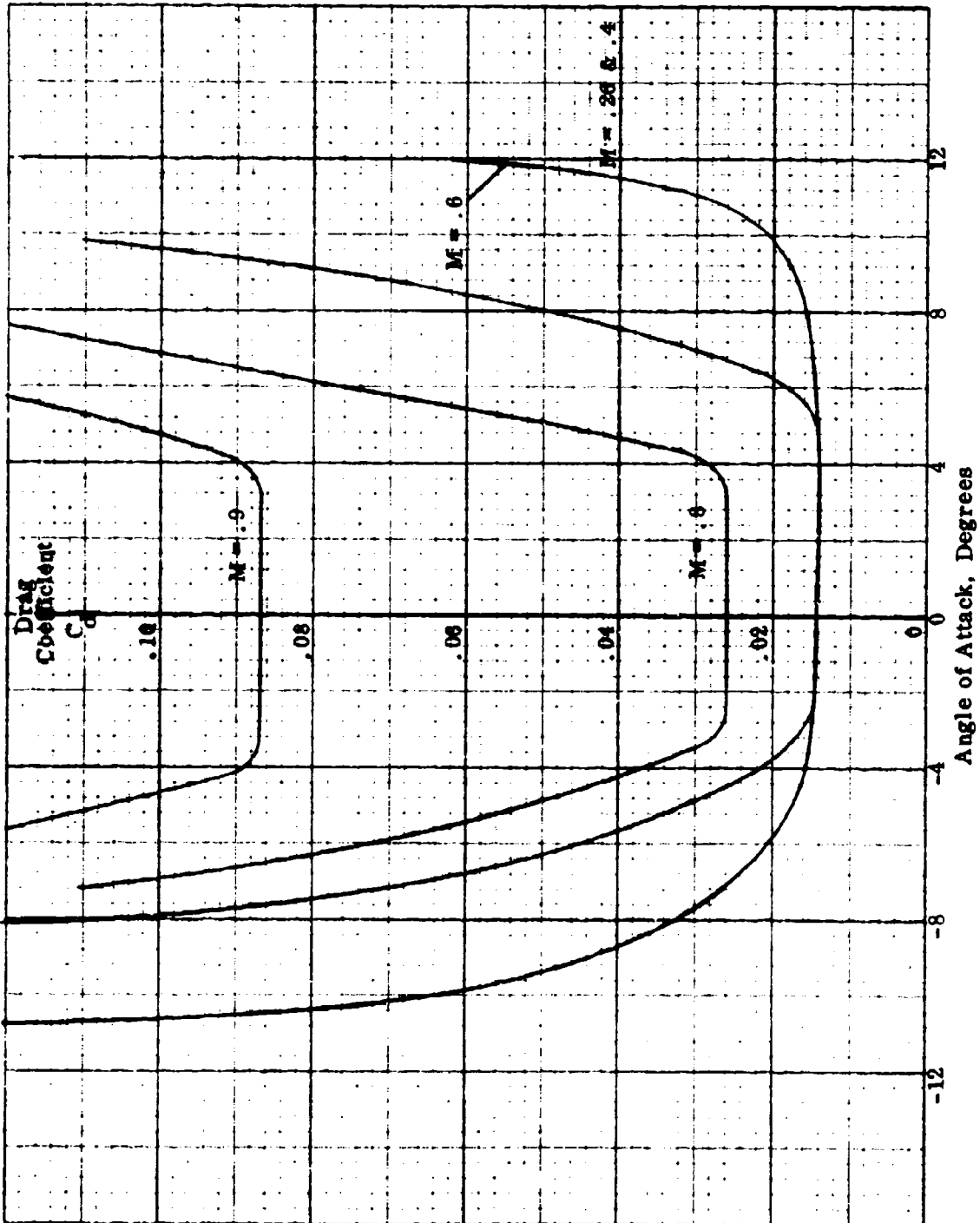
HC144R1070

Figure D. 28

SECTION DRAG COEFFICIENT - 12% AIRFOIL, FORWARD
FULL SCALE REYNOLDS NUMBER



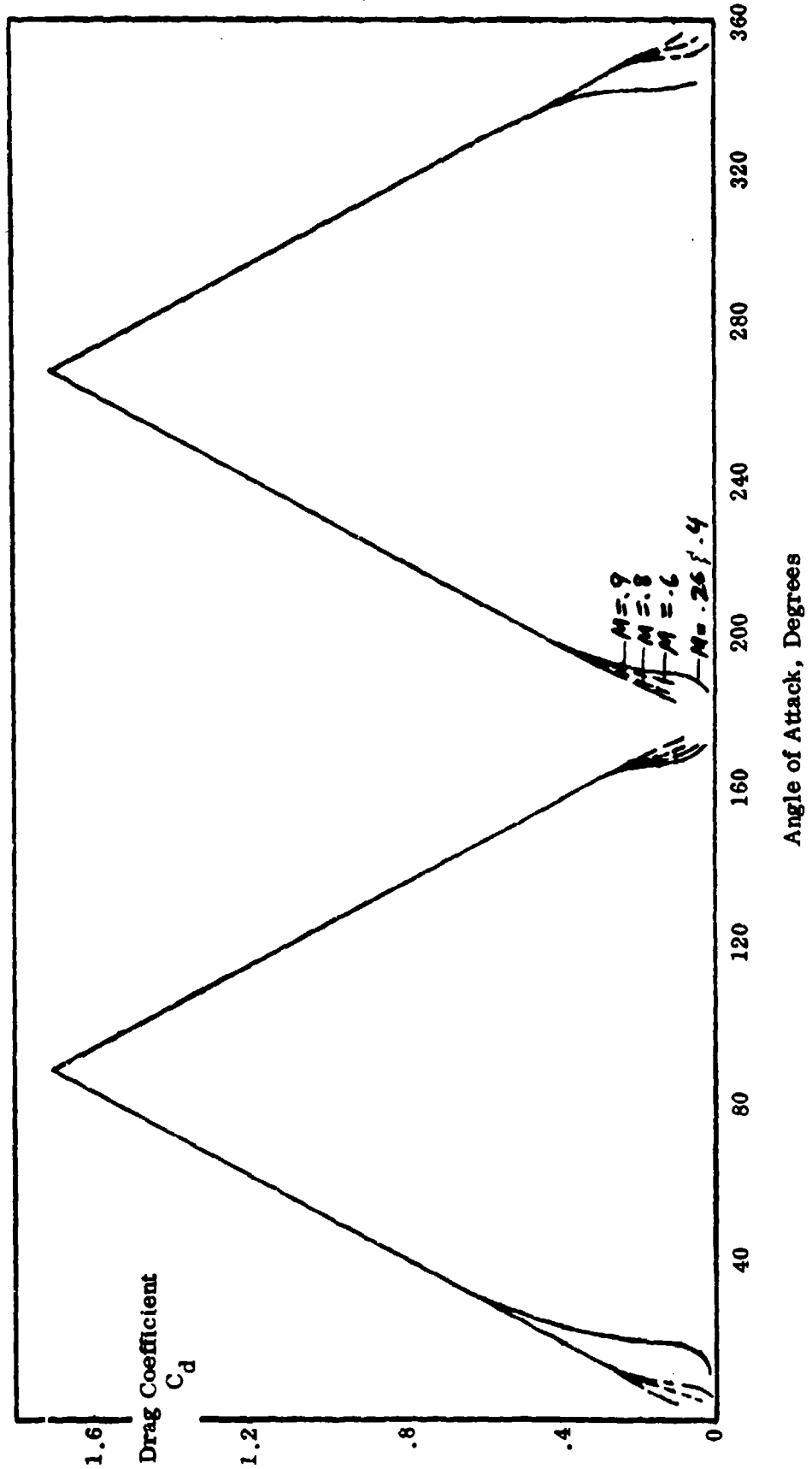
**SECTION DRAG COEFFICIENT - 12% AIRFOIL, REVERSE
FULL SCALE REYNOLDS NUMBER**



HC144R1070

Figure D. 30

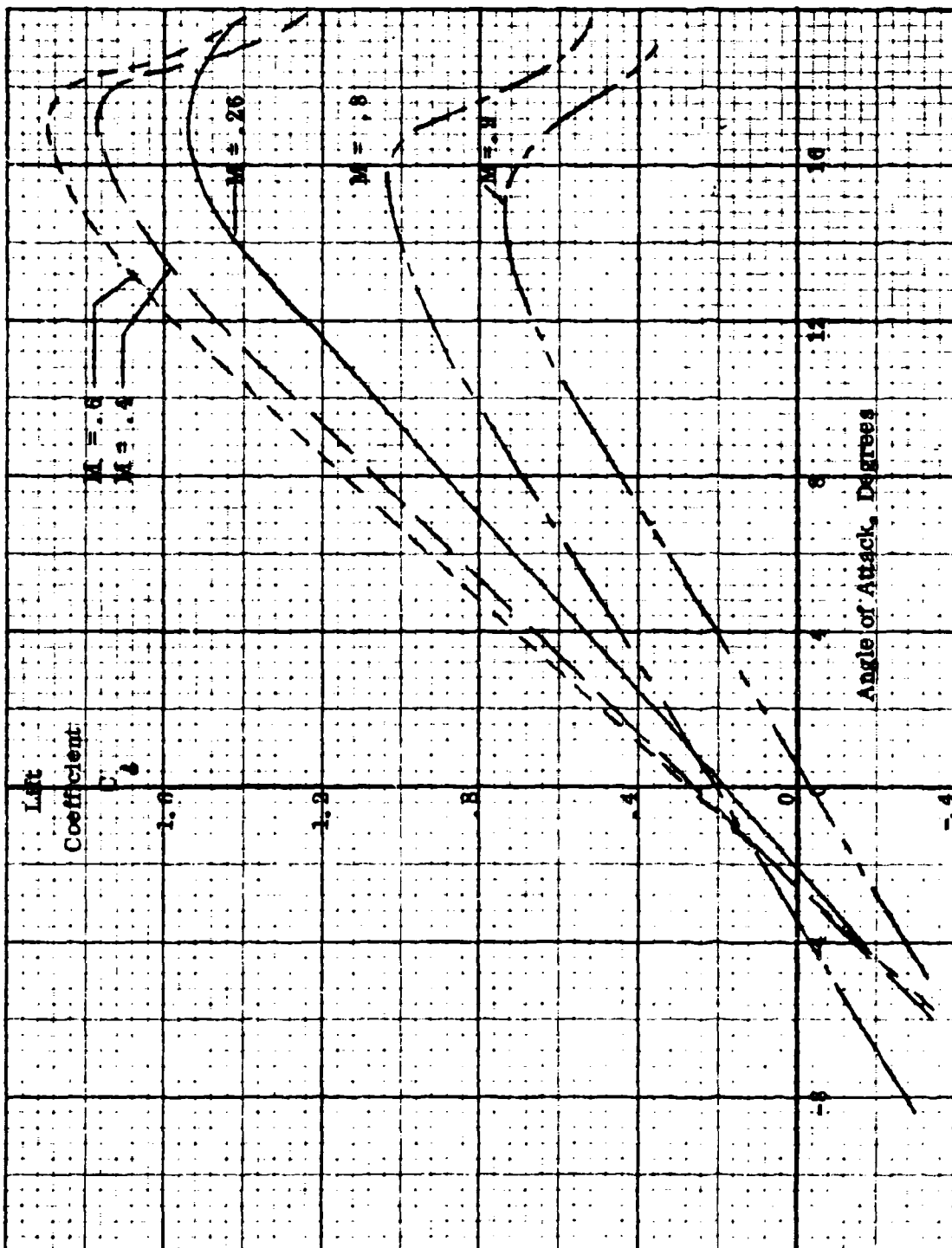
SECTION DRAG COEFFICIENT THROUGH 360° ANGLE OF ATTACK
12% AIRFOIL - FULL SCALE REYNOLDS NUMBER



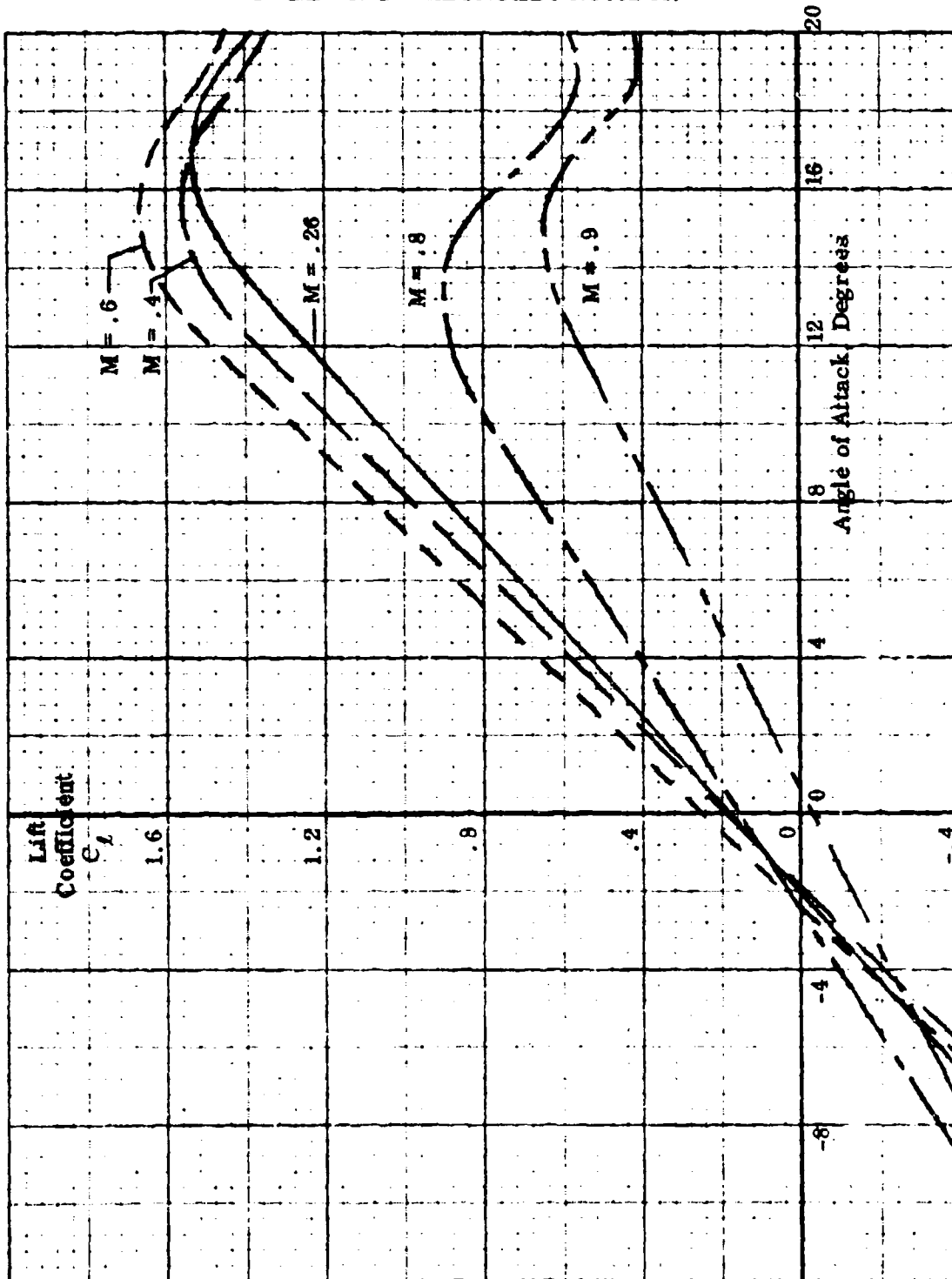
HC144R1070

Figure D. 31

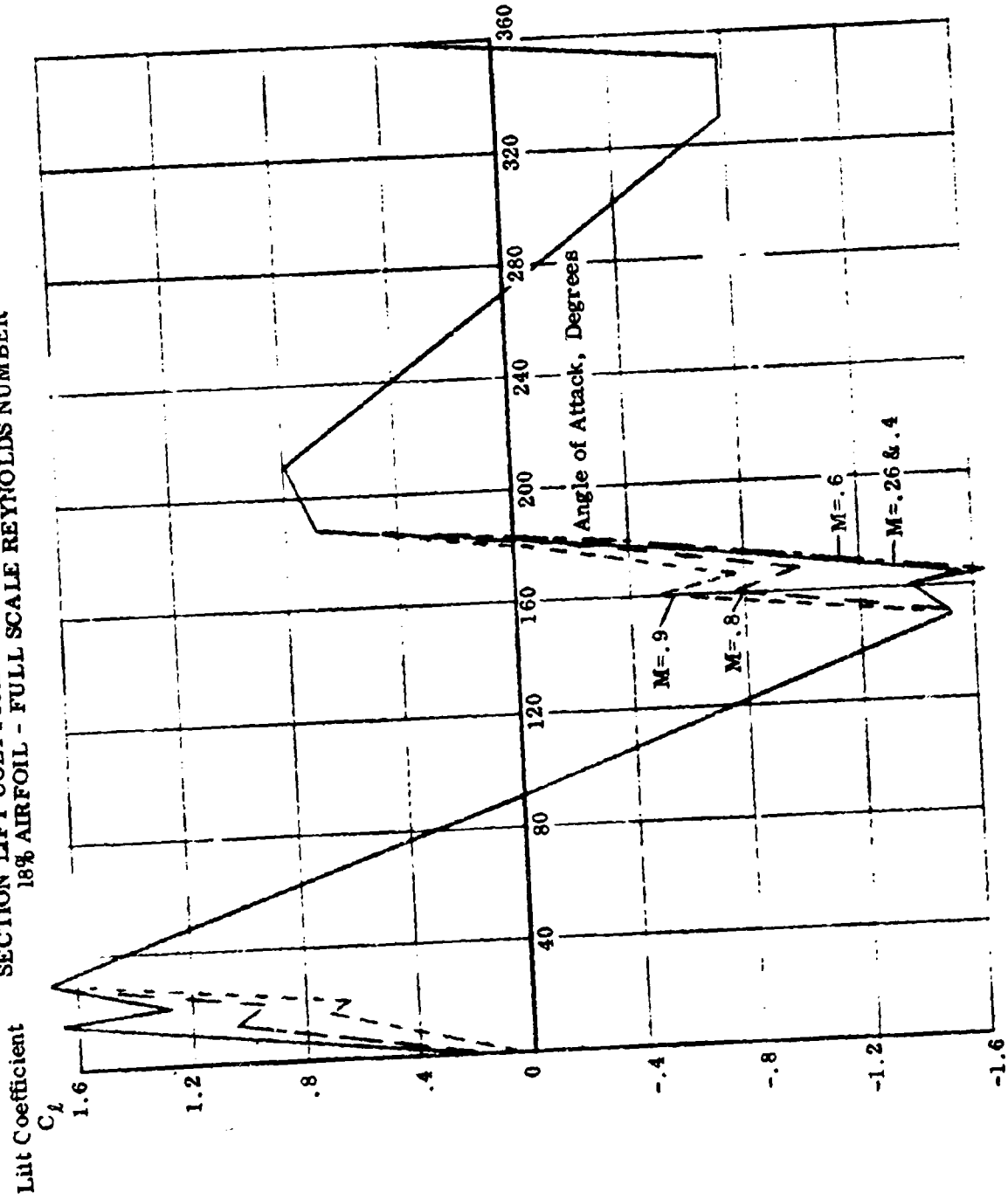
**SECTION LIFT COEFFICIENT - 18% AIRFOIL, FORWARD
FULL SCALE REYNOLDS NUMBER**



SECTION LIFT COEFFICIENT - 18% AIRFOIL, REVERSE
FULL SCALE REYNOLDS NUMBER



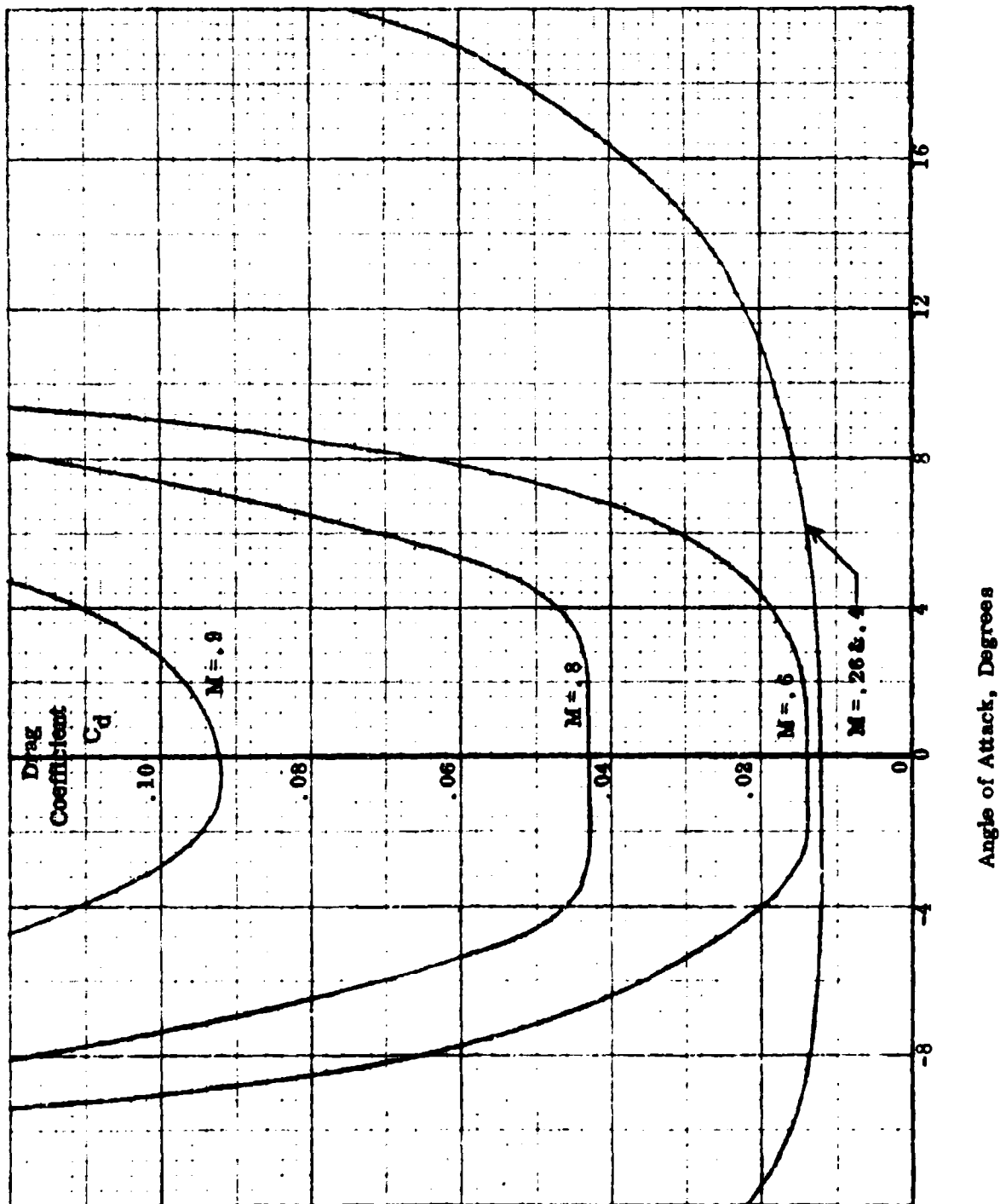
SECTION LIFT COEFFICIENT THROUGH 360° ANGLE OF ATTACK
18% AIRFOIL - FULL SCALE REYNOLDS NUMBER



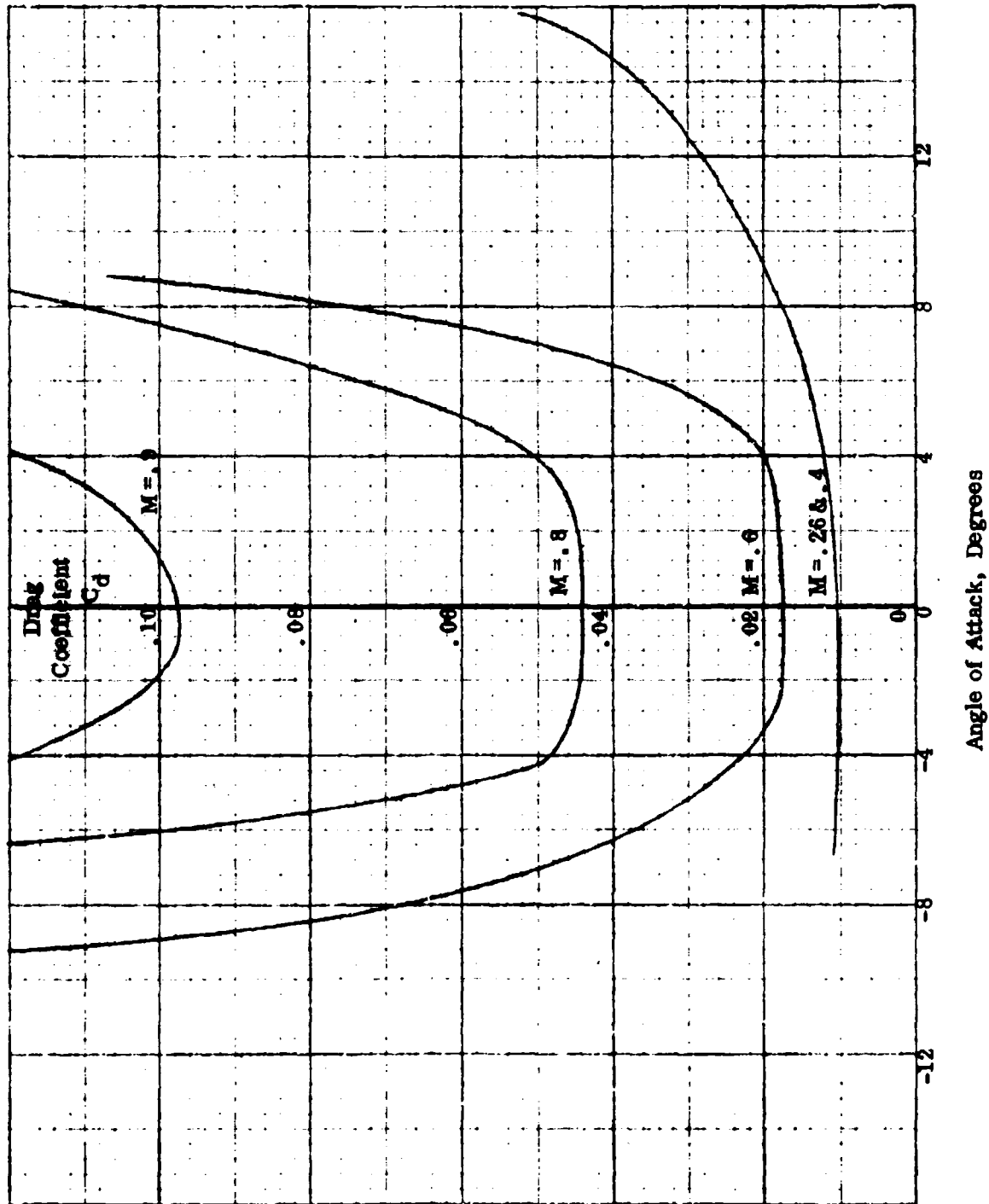
HC144R1070

Figure D. 34

**SECTION DRAG COEFFICIENT - 18% AIRFOIL, FORWARD
FULL SCALE REYNOLDS NUMBER**



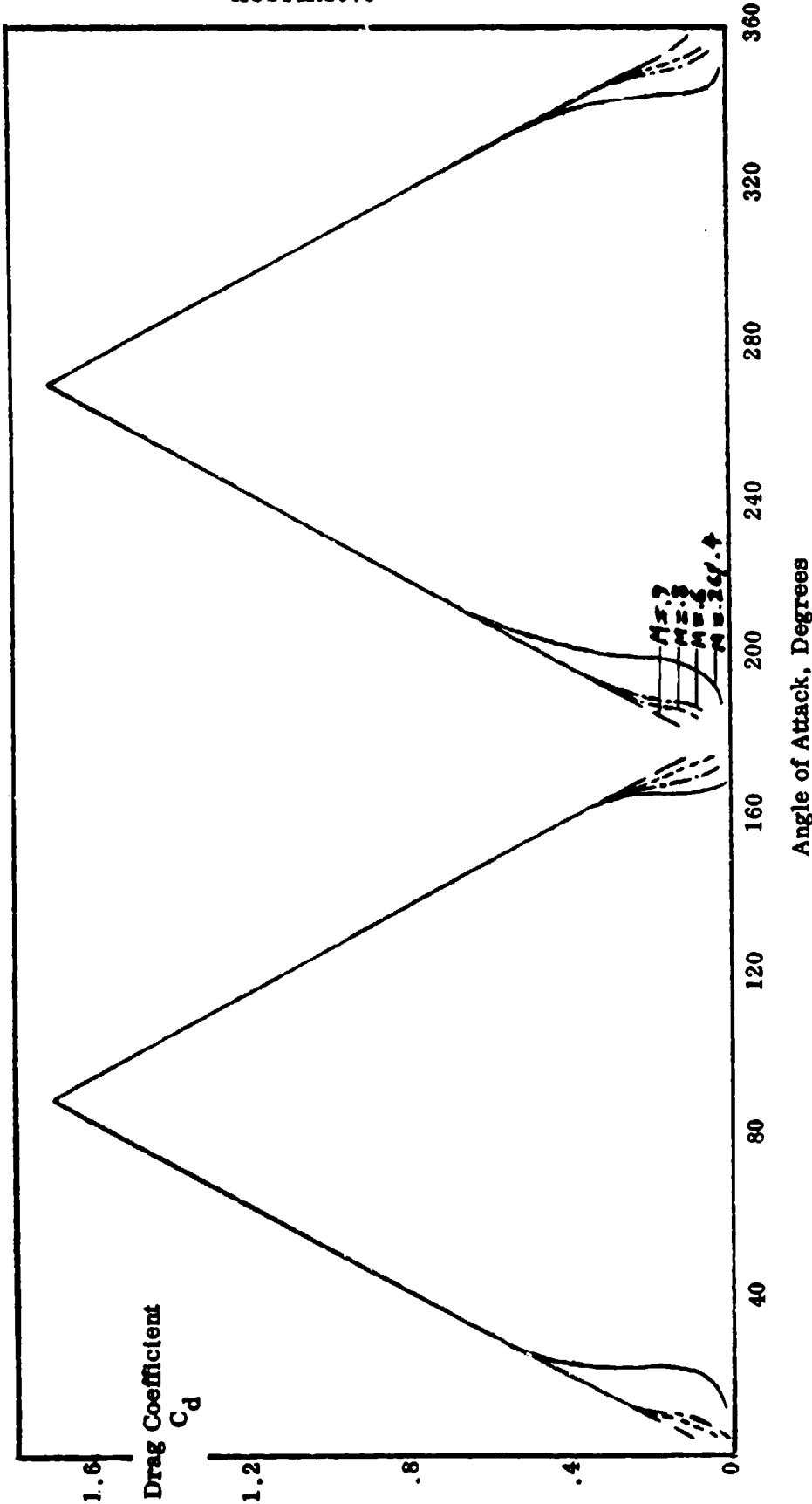
SECTION DRAG COEFFICIENT - 18% AIRFOIL, REVERSE
FULL SCALE REYNOLDS NUMBER



HC144R1070

Figure D. 36

SECTION DRAG COEFFICIENT THROUGH 360° ANGLE OF ATTACK
18% AIRFOIL - FULL SCALE REYNOLDS NUMBER



FAIRCHILD
REPUBLIC DIVISION

HC144R1070

This page intentionally left blank.

Unclassified

Security Classification

DOCUMENT CONTROL DATA - R & D

(Security classification of title, body of abstract and indexing annotation must be entered when the overall report is classified)

1. ORIGINATING ACTIVITY (Corporate author) Fairchild Industries, Inc. Fairchild Republic Company Farmingdale, N. Y. 11735		2a. REPORT SECURITY CLASSIFICATION Unclassified	
		2b. GROUP N/A	
3. REPORT TITLE Model Wind Tunnel Tests of a Reverse Velocity Rotor System			
4. DESCRIPTIVE NOTES (Type of report and inclusive dates) Final Report			
5. AUTHOR(S) (First name, middle initial, last name) J. R. Ewans, T. A. Krauss			
6. REPORT DATE January 31, 1973		7a. TOTAL NO. OF PAGES 280	7b. NO. OF REFS 2
8a. CONTRACT OR GRANT NO. N00019-71-C-0506		8b. ORIGINATOR'S REPORT NUMBER(S) HC144R1070	
b. PROJECT NO			
c.		8d. OTHER REPORT NO(S) (Any other numbers that may be assigned this report)	
d.			
10. DISTRIBUTION STATEMENT This document is subject to special export controls and is transferred to foreign government only for official use of the Naval Air Systems Command, Code 48-32			
11. SUPPLEMENTARY NOTES		12. SPONSORING MILITARY ACTIVITY Naval Air Systems Command Department of the Navy	
13. ABSTRACT A one-seventh scale model reverse velocity rotor system was manufactured and tested with the goal of substantiating the results that had been predicted for this system in previous analytical studies. The 8 ft diameter 4 bladed hydraulically powered model rotor was provided with remote operation of the controls and shaft angle. Tests were conducted in the 12 ft pressure wind tunnel at NASA Ames during June and July 1972. The tests did not cover the whole range of conditions desired, but results were obtained at advance ratios from 0.3 to 2.46 and at tunnel speeds up to 350 knots. Significant results of the tests were the freedom of the rotor from instability, and the ability to trim the rotor laterally and longitudinally under all conditions. Reasonable agreement was found between the measured performance of the model rotor and that predicted using the results of two-dimensional wind tunnel tests made on three reversible airfoil sections of the model rotor blade. It is recommended that further tests be performed with this model to expand the envelope of test conditions, particularly to include testing with two-per-rev control angle input.			

14. KEY WORDS	LINK A		LINK B		LINK C	
	ROLE	WT	ROLE	WT	ROLE	WT
Reverse Velocity Rotor						
Reversible Airfoil-Rotor Blade						
Two per Rev Pitch						
Radial Flow						
Reverse Flow						
Lift to Drag Ratio						
High Advance Ratio						
High Speed Helicopter						
Helicopter Two per Rev Control System Mechanism						
Rotor Blade Stability						
Rotor Control						
Rotor Dynamics						
Model Rotor Wind Tunnel Test						
Airfoil Wind Tunnel Test						
Predicted Rotor Performance						